2009 Atomic, Molecular, Optical Sciences Research Meeting

Airlie Conference Center
Warrenton, Virginia
September 13-16, 2009

U.S. DEPARTMENT OF ENERGY | Office of Science

Office of Basic Energy Sciences
Chemical Sciences, Geosciences & Biosciences Division

Foreword

This volume summarizes the 2009 Research Meeting of the Atomic, Molecular and Optical Sciences (AMOS) Program sponsored by the U. S. Department of Energy (DOE), Office of Basic Energy Sciences (BES), and comprises descriptions of the current research sponsored by the AMOS program. The research meeting is held annually for the DOE laboratory and university principal investigators within the BES AMOS Program to facilitate scientific interchange among the PIs and to promote a sense of program identity.

The BES/AMOS program is vigorous and innovative, and enjoys strong support within the Department of Energy. This is due entirely to our scientists, the outstanding research they perform, and its relevance to DOE missions. FY2009 has been an exciting year for BES and the research community. Forty-six new Energy Frontier Research Centers have been funded, and 95 Single Investigator and Small Group Research proposals have been selected for funding. Also, the first experiments at the Linac Coherent Light Source (LCLS) are to start this month. There are many opportunities for the AMOS community to explore new scientific frontiers that shed light on the DOE mission and the strategic challenges our nation and the world face.

We are deeply indebted to the members of the scientific community who have contributed valuable time toward the review of proposals and programs, either by mail review of grant applications, panel reviews, or on-site reviews of our multi-PI programs. These thorough and thoughtful reviews are central to the continued vitality of the AMOS Program.

We appreciate the privilege of serving in the management of this research program. In carrying out these tasks, we learn from the achievements and share the excitement of the research of the many sponsored scientists and students whose work is summarized in the abstracts published on the following pages. We also appreciate Mark Pederson's coordination of computational resources and interactions with related DOE program offices.

Thanks to the staff of the Oak Ridge Institute for Science and Education, in particular Margaret Lyday, Connie Lansdon, and to the Airlie Conference Center for assisting with the meeting. We also thank Diane Marceau, Robin Felder, and Michaelene Kyler-King in the Chemical Sciences, Biosciences, and Geosciences Division for their indispensable behind-the-scenes efforts in support of the BES/AMOS program. Finally, thanks to Larry Rahn for his expert help in assembling this volume.

Jeffrey L. Krause
Michael P. Casassa
Chemical Sciences, Geosciences and Biosciences Division
Office of Basic Energy Sciences
Department of Energy

Cover Art Courtesy of Diane Marceau
Chemical Sciences, Geosciences and Biosciences Division, Basic Energy Sciences, DOE

This document was produced under contract number DE-AC05-06OR23100 between the U.S. Department of Energy and Oak Ridge Associated Universities.

The research grants and contracts described in this document are supported by the U.S. DOE Office of Science, Office of Basic Energy Sciences, Chemical Sciences, Geosciences and Biosciences Division.

Agenda

2009 Meeting of the Atomic, Molecular and Optical Sciences Program

Office of Basic Energy Sciences
U. S. Department of Energy

Airlie Center, Warrenton, Virginia, September 13-16, 2009

Sunday, September 13

3:00-6:00 pm	**** Registration ****
6:00 pm	**** Reception (No Host) ****
7:00 pm	**** Dinner ****

Monday, September 14

7:30 am	**** Breakfast ****
8:30 am	*Welcome and Introductory Remarks* **Jeff Krause and Eric Rohlfing**, BES/DOE
Session I	Chair: **Nora Berrah**
9:00 am	*Ultrafast Atomic and Molecular Optics at Short Wavelengths* **Henry Kapteyn and Margaret Murnane,** University of Colorado
9:30 am	*Quantum Control of Electron Momenta Using Few-Cycle Attosecond Pulses or Intense Laser Fields* **Tony Starace,** University of Nebraska
10:00 am	*Symmetry Breaking in the Photo Double Ionization of Carbon Dioxide* **Thorsten Weber,** Lawrence Berkeley National Laboratory
10:30 am	**** Break ****
11:00 am	*Applications of the New Femtosecond Undulator Beamline at the Advanced Light Source to Solution-Phase Molecular Dynamics* **Bob Schoenlein,** Lawrence Berkeley National Laboratory
11:30 am	*X-Ray Absorption and Scattering from Laser-Aligned Molecules* **Linda Young,** Argonne National Laboratory
12:00 noon	*First Principles Dynamics of Ultrafast Chemistry* **Todd Martinez,** SLAC National Accelerator Laboratory
12:30 pm	**** Lunch ****

Session II Chair: **Tom Weinacht**

4:00 pm *Combining High Level Ab Initio Calculations with Laser Control of Molecular Dynamics*
Spiridoula Matsika, Temple University

4:30 pm *Controlling Molecular Rotations of Asymmetric Top Molecules: Methods and Applications*
Vinod Kumarappan, Kansas State University

5:00 pm *Isolated attosecond pulse dynamics*
Steve Leone, Lawrence Berkeley National Laboratory

5:30 pm *Update on the Linac Coherent Light Source*
Phil Bucksbaum, SLAC National Accelerator Laboratory

5:45 pm *Update on the Energy Frontier Research Center for Advanced Solar Photophysics*
Rich Schaller, Los Alamos National Laboratory

6:00 pm **** Reception (No Host) ****

6:30 pm **** Dinner ****

Tuesday, September 15

7:30 am **** Breakfast ****

Session III Chair: **Dave DeMille**

8:30 am *Cold and Ultracold Polar Molecules*
Jun Ye, University of Colorado

9:00 am *Experiments in Ultracold Collisions and Ultracold Molecules*
Phil Gould, University of Connecticut

9:30 am *Strongly Anisotropic Bose and Fermi Gases*
John Bohn, University of Colorado

10:00 am *Formation of Ultracold Molecules*
Robin Côté, University of Connecticut

10:30 am **** Break ****

11:00 am *Time-Dependent Treatment of Three-Body Systems in Intense Laser Fields*
Brett Esry, Kansas State University

11:30 am *Physics of Correlated Systems*
Chris Greene, University of Colorado

12:00 noon *Properties of Actinide Ions from Measurements of Rydberg Ion Fine Structure*
Steve Lundeen, Colorado State University

12:30 pm **** Lunch ****

Session IV Chair: **Ali Belkacem**

4:00 pm	*Ultrafast Holographic X-ray Imaging and its Application to Picosecond Ultrasonic Wave Dynamics in Bulk Materials* **Christoph Rose-Petruck,** Brown University
4:30 pm	*Detailed Investigations of Interactions between Ionizing Radiation and Neutral Gases* **Allen Landers,** Auburn University
5:00 pm	*Imaging of Electronic Wave Functions during Chemical Reactions* **Terry Miller,** Ohio State University
5:30 pm	*High Harmonic Generation in Molecules* **Markus Gühr,** SLAC National Accelerator Laboratory
6:00 pm	**** Reception (No Host) ****
6:30 pm	**** Dinner ****

Wednesday, September 16

7:30 am **** Breakfast ****

Session V Chair: **Tom Rescigno**

8:30 am	*Photoionization of Caged Atoms and Molecules* **Ron Phaneuf,** University of Nevada
9:00 am	*Steady-State and Transient Hydrocarbon Production in Graphite by Low Energy Impact of Atomic and Molecular Deuterium Projectiles* **Fred Meyer,** Oak Ridge National Laboratory
9:30 am	*Global Nonresonant Vibrational-Photoelectron Coupling in Molecular Photoionization* **Erwin Poliakoff,** Louisiana State University
10:00 am	**** Break ****
10:30 am	*Electron-Molecular Ion Fragmentations* **Mark Bannister,** Oak Ridge National Laboratory
11:00 am	*Development of Continuous REMPI Detection of the PbF Molecule for Measurement of the Electron's Electric Dipole Moment* **Neil Shafer-Ray,** University of Oklahoma
11:30 am	*Closing Remarks* **Jeff Krause**, BES/DOE
11:45 am	**** Lunch ****

Table of Contents

Laboratory Research Summaries (by institution)

University Research Summaries (by PI)

Laboratory Research Summaries
(by institution)

AMO Physics at Argonne National Laboratory

R. W. Dunford, E. P. Kanter, B. Krässig, R. Santra, S. H. Southworth, L. Young
Argonne National Laboratory, Argonne, IL 60439

dunford@anl.gov, kanter@anl.gov, kraessig@anl.gov, rsantra@anl.gov,
southworth@anl.gov, young@anl.gov

Overview:

Our research focuses on understanding the basic principles underlying combined x-ray and optical interactions over an unprecedented range of intensities. Exploration of the extreme intensity regime for x-ray interactions is a new frontier enabled by the successful turn-on, in April 2009, of the world's first hard x-ray free electron laser, the LCLS (Linac Coherent Light Source). We have been preparing for the exploration of high intensity x-ray interactions by theoretical studies [2,3,19,25]; the latter two form the basis for two experiments scheduled for the first beamtime period between September and December 2009. Understanding the nature of resonant and non-resonant x-ray absorption is an essential first step for prominent applications, such as single biomolecule imaging, that rely on unprecedented x-ray intensities of ~10^{22} W/cm^2. This understanding is best achieved with gas phase targets, where observations can be closely linked with theory.

In addition to the exploration of high intensity x-ray interactions, we also pioneer the *control* of basic x-ray interactions using high intensity optical lasers [1,9,16,26,28]. X-ray and optical interactions are linked through resonant x-ray absorption and with an intense optical field we have demonstrated, in March 2009 at the Advanced Light Source femtosecond x-ray beamline, that it is feasible to induce x-ray transparency via strong-field coherent coupling of core-excited Rydberg states, as previously proposed [26]. The predictive power of theory for the gas phase system, and the ultrafast, reversible nature of the induced transparency allow one to envision engineering applications such as imprinting femtosecond optical pulse shapes and sequences onto 100 picosecond x-ray pulses as available at synchrotron sources.

The use of hard x rays as weakly interacting probes of the dynamics of photoinduced processes represents the third thrust area of our program. This area utilizes traditional laser pump-x-ray probe methodologies to observe ultrafast processes with the aim of achieving joint picosecond and picometer resolution. With an interactive theoretical and experimental effort, we have investigated processes of interest to the ultrafast laser community, e.g. orbital hole dynamics following tunnel ionization [5,24], alignment dynamics in a laser produced plasma [17,30], and laser-induced alignment of molecules [6,10,18,21,22]. The latter represents an important application of AMO techniques to the LCLS goal of single biomolecule imaging, where the unknown orientation of the biomolecule poses a severe problem in image reconstruction. Our more fundamental goal is to understand the nature of laser-induced distortion of the molecular framework using x-ray scattering and spectroscopy techniques. This research is enabled by the tunable, polarized hard x rays at the Advanced Photon Source and drives two exciting advances to existing laser pump/x-ray probe methodologies - higher repetition rate laser excitation methods that can provide up to 6500-fold statistical improvement and 1-picosecond x-ray production. These developments will benefit a broad community including chemistry, condensed matter and materials science.

High-intensity x-ray science at LCLS

We are involved in a number of proposals at LCLS. Below we describe two experimental projects slotted for the September – December 2009 period where Argonne is the lead institution. The two theory projects scout new directions for experiments.

Tracking transient atomic states produced by ultraintense x-ray pulses (E.P. Kanter, B. Krässig, S.T. Pratt, R. Santra, S.H. Southworth, L. Young, J. Bozek[1], L. DiMauro[2], N. Berrah[3], P. Bucksbaum[4], D. R. Reis[4], A. Belkacem[5])

This experiment focuses on understanding the mechanisms of high intensity x-ray absorption using the prototypical neon atom for which extensive calculations have been carried out by members of this team. LCLS provides access to ultraintense x-ray radiation for the first time – and understanding the atomic response to this radiation is of fundamental importance with possible ramifications vis-à-vis biomolecule imaging. At high photon energy, the atomic response is dominated by inner shell photoabsorption. We expect sequential single photon absorption to dominate the FEL-atom interaction with, e.g., six-photon absorption leading to fully-stripped neon [25]. Such processes depend only on the fluence of the radiation. However, with *ultraintense* x-ray radiation (focused intensities of ~10^{18}W/cm^2) one can induce sequential K-shell absorption prior to the intraatomic Auger decay (2.4 fs) to create exotic hollow atom states with high probability. (At low x-ray intensity hollow atoms are formed only indirectly via electron correlation with very low yield.) These processes will exhibit a *nonlinear* FEL intensity dependence. Control of the hollowed electron shell can be achieved by selection of the photon energy.

We plan to track the evolution of the neon atom during its exposure to the focused FEL pulse using electron spectroscopy. Electron spectroscopy will provide distinctive signatures for competing ionization pathways. For example, see Fig. 1 which contrasts the PAP vs the PPA sequence, where P and A signify photo- and Auger electrons, respectively. Each photoabsorption process will provide a unique photoelectron signature and hollow atom formation can be detected both with photoelectron and hypersatellite Auger signatures. In comparison to ion charge state spectroscopy, the precise route to the highly charged ion can be viewed because each step provides an individual electron and all steps are visible in a single shot – as opposed to methods using simple recoil ion imaging where the final ion detected has been buffeted by many photoelectron/Auger emissions.

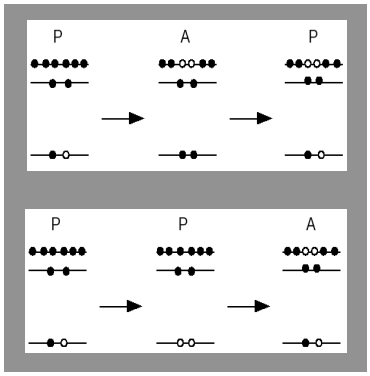

Fig. 1. Competing x-ray multiphoton mechanisms at high x-ray intensity.

Resonant nonlinear x-ray processes at high x-ray intensity (E.P. Kanter, B. Krässig, S.T. Pratt, R. Santra, S.H. Southworth, L. Young, J. Bozek[1], L. DiMauro[2], N. Berrah[3], P. Bucksbaum[4], D. Reis[4])

In this experiment, we will investigate resonant nonlinear x-ray processes in atomic Ne at high x-ray intensity. Atomic neon is a simple target with dipole resonant features, at well-defined energies, within the photon energy range spanned by the LCLS at inception, ~800-2000 eV. Thus, it is a natural choice with which to test theoretical understanding of resonant non-linear x-ray processes. At high photon energies resonant absorption by inner-shell electrons will dominate all x-ray photoprocesses, with cross sections ~100× greater than those for non-resonant valence ionization. On an inner-shell resonance, absorption/stimulated emission cycles (Rabi flopping) will be the dominant photoinduced process. With this in mind, members of this group have calculated modifications to the resonant Auger effect induced by high intensity x-rays [19]. Calculations using the LCLS design parameters (10^{13} photons/pulse, 230 fs pulse duration, 1μm focal diameter) show that the x-ray peak intensity (~10^{18} W/cm^2) is sufficient to induce Rabi oscillations in the 1s-3p transition at 867.1 eV within the 2.4 fs lifetime of 1s vacancy states. Oscillations are predicted to appear in single-shot resonant-Auger-electron line profiles, and averaging over an ensemble of shots produces a distinct broadening of the line profile.

Resonances can be used to enhance x-ray multiphoton processes. At photon energies less than the binding energy of the 1s electron, *resonant* two-photon absorption has a signficantly larger cross section than *non-resonant* two-photon absorption; though both generate the same final state of the system - an atom with a 1s hole plus an *s*- or *d*-wave photoelectron. Capitalizing on this resonance phenomenon, we will study two-photon absorption in neon at 848.6 eV, where, in a simple scenario, the first photon ionizes the Ne 2p electron and the second photon excites the Ne^+ 1s-2p resonance. Ne^+ $1s^{-1}$ *K-LL* Auger electrons will be the signature of this resonant two-photon creation of a 1s hole. This generation of a 2p hole orbital is advantageous for observing/studying the Rabi-cycling phenomenon; the Ne^+ 1s-2p dipole matrix element is 5.6× larger than that for the 1s-3p transition in Ne. We will follow the response of the neon atom on two photon resonance at 848.6 eV as a function of x-ray FEL intensity. At low x-ray intensity, the signature of 1s hole creation will not be present, but as the intensity is raised, the Auger line will appear and then gradually broaden as Rabi-oscillations become important. A laser pump/x-ray probe experiment is also planned where the Ne 2p electron is ionized by an intense optical laser pulse to produce a clean target of Ne^+[2p] from which Ne^+ 1s-2p resonant x-ray absorption processes can be studied. At high x-ray intensities, Rabi oscillations can be studied and at lower x-ray intensities alignment of the Ne^+ 2p hole state can be studied. This laser-pump/x-ray probe experiment is a simple, valuable spatial and timing overlap diagnostic.

X-ray two-photon photoelectron spectroscopy (R. Santra, N. V. Kryzhevoi[6], and L. S. Cederbaum[6])

Photoelectron spectroscopy is an outstanding technique for quantitatively characterizing the electronic structure of matter. Since the energy needed for the removal of an inner-shell electron is characteristic of the atomic species involved, inner-shell ionization using x rays allows one to determine the elemental composition of a sample. Furthermore, there is generally a measurable effect of the molecular environment on the binding

energy of an inner-shell electron. This phenomenon is known as chemical shift. Traditional x-ray photoelectron spectroscopy (XPS) is based on x-ray one-photon absorption. In Ref. [3], we demonstrated that the advent of x-ray free-electron lasers such as the LCLS will enable a novel kind of photoelectron spectroscopy: x-ray two-photon photoelectron spectroscopy (XTPPS). XTPPS is more sensitive to chemical effects and electronic many-body effects than is traditional photoelectron spectroscopy. In order to demonstrate the potential of XTPPS, we calculated the inner-shell single and double ionization spectra of the organic molecule para-aminophenol using many-body Green's function methods. A kinetic model was employed to determine the probability of inner-shell double hole formation in para-aminophenol exposed to an intense, one-femtosecond x-ray pulse. The resulting photoelectron spectrum at a photon energy of 1 keV was calculated. The theoretical work presented in Ref. [3] suggests that x-ray two-photon photoelectron spectroscopy using x-ray free-electron lasers will provide access to electronic-structure information not currently available.

Above threshold ionization in the x-ray regime (H. R. Varma, M. F. Ciappina[7], N. Rohringer[8], and R. Santra)
XTPPS exploits that at high photon energy, each photon absorbed interacts with a different inner-shell electron. A less probable process in the x-ray regime is above-threshold ionization (ATI). In order to understand the nature of ATI in the x-ray regime we studied two-photon ATI using atomic hydrogen as a model system [2]. Within the minimal-coupling formalism of nonrelativistic quantum electrodynamics, two distinct interactions---$\mathbf{A}\cdot\mathbf{p}$ in second order and A^2 in first order---contribute to the two-photon absorption amplitude. In Ref. [2], we assessed the relative importance of these two interactions. We found that above a photon energy of 6.8 keV, the contribution from A^2 to the total two-photon absorption cross section dominates. In this high-energy regime, above-threshold ionization is a nonsequential, purely nondipole process. The studies in Ref. [2] revealed the unexpected failure of the plane-wave model in calculating the two-photon cross section even at very high energies. The plane-wave model underestimates the photon energy at which A^2 becomes dominant by more than two orders of magnitude. We employed rate equations to calculate the probabilities of ionization by Compton scattering, one-photon absorption, and two-photon absorption. These calculations suggest that even at LCLS, at a photon energy of 6.8 keV, the most important mechanism leading to the ionization of atomic hydrogen remains Compton scattering.

[1]LCLS, SLAC, Stanford, CA
[2]Ohio State University, Columbus, OH
[3]Western Michigan University, Kalamazoo, MI
[4]PULSE Center, SLAC, Stanford, CA
[5]LBNL, Berkeley, CA
[6]University of Heidelberg, Heidelberg, Germany
[7]Institute of High Performance Computing, 1 Fusionopolis Way #16-16 Connexis, Singapore 138682
[8]LLNL, Livermore, CA

Control of x-ray interactions with strong laser fields

To date, ultrafast x-ray science has focused on using x-rays as weakly-interacting, linear probes to measure structural changes with atomic spatial resolution on the picosecond to femtosecond timescale. Ultrafast x-ray absorption spectroscopy, with its sensitivity to local electronic and atomic structure, has been used to track light-induced molecular dynamics in solution as well as electronic dynamics in solids. In the gas phase [7,20], our earlier work demonstrated phenomena such as orbital-hole alignment following tunnel ionization [24 and references therein], alignment in laser-produced plasmas [17,31] and controlled x-ray absorption from laser-aligned molecules [21]. All of these examples use light to modify the target system and x-rays to *monitor* the response.

Here we use light for a fundamentally different purpose – to *control* x-ray interactions with matter. We accomplish this by using optical radiation to modify the short-lived core-excited states accessed by x-ray absorption. This laser-induced modification is both ultrafast and reversible – allowing us to realize a femtosecond x-ray transmission switch. Our work is inspired by quantum optics studies of electromagnetically induced transparency at longer wavelengths. We have taken a combined theoretical [9,16,26,28] and experimental [1] approach and the abstract below discusses our experimental demonstration of ultrafast laser-induced transparency in neon performed at the Advanced Light Source Femtosecond Spectroscopy Beamline.

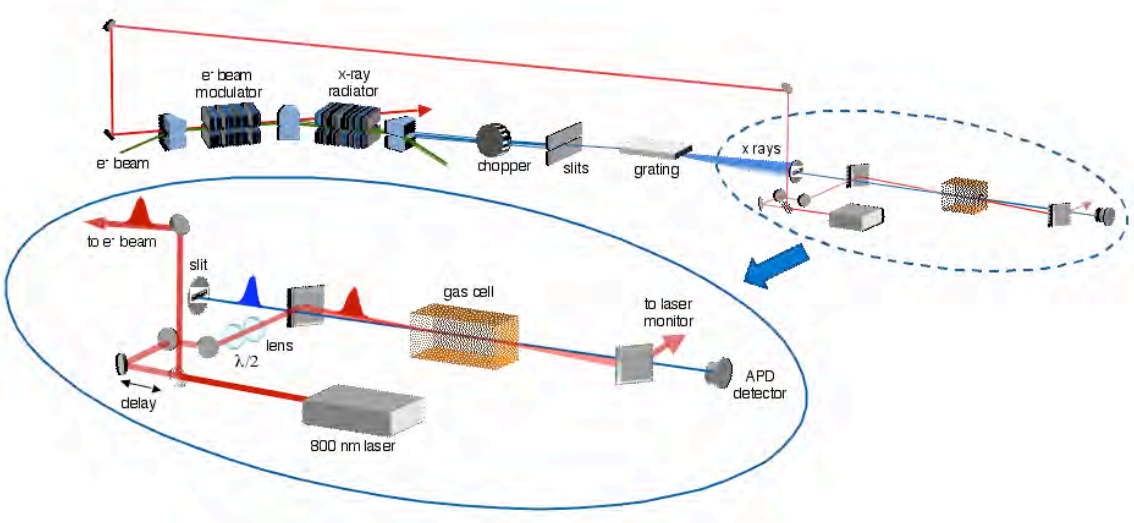

Fig. 2. Femtosecond Spectroscopy Beamline at the Advanced Light Source. Femtosecond x-ray and laser pulses are derived from the same 800 nm laser oscillator to provide x-ray/laser pulse synchronization to better than 100 fs. Inset shows the apparatus used to study ultrashort laser-induced transparency for x rays. Overlapped focused x-ray and laser pulses copropagate through a gas cell. Transmitted x rays are detected by an avalanche photodiode (APD). The x-ray pulses are generated at 1 kHz and the laser pulses at 500 Hz. The x-ray pulses alternately probe the target in the presence and absence of the laser.

Controlling x-rays with light: ultrafast transparency (T.E. Glover[1], M.P. Hertlein[1], S.H. Southworth, T.K. Allison[1], J. van Tilborg[1], E.P. Kanter, B. Krässig, H. R. Varma, B. Rude[1], R. Santra, A. Belkacem[1], and L. Young)

To achieve active optical control of x-ray absorption we explore a new and unique regime of coherent strong coupling between short-lived core-excited states. In this regime, the strong-optical-laser coupling field required to induce Rabi flopping between core-excited states prior to inner shell decay also induces ionization and multilevel mixing on a timescale comparable to a single optical cycle (2.7 fs). Despite these complications, a femtosecond optical pulse is observed to efficiently and reversibly induce transparency in a gaseous medium nominally opaque to x rays, i.e. neon at the 1s→3p resonance at 867.1 eV. An ultrashort transparency window is created which dramatically increases, by a factor of three, the transmission of a femtosecond x-ray probe pulse. This transparency is most efficiently induced when the linearly polarized optical and x-ray pulses are polarized parallel to one another (See Fig. 3). Theoretical simulations for gas-phase neon, displayed in Fig. 3, were shown to have excellent predictive power.

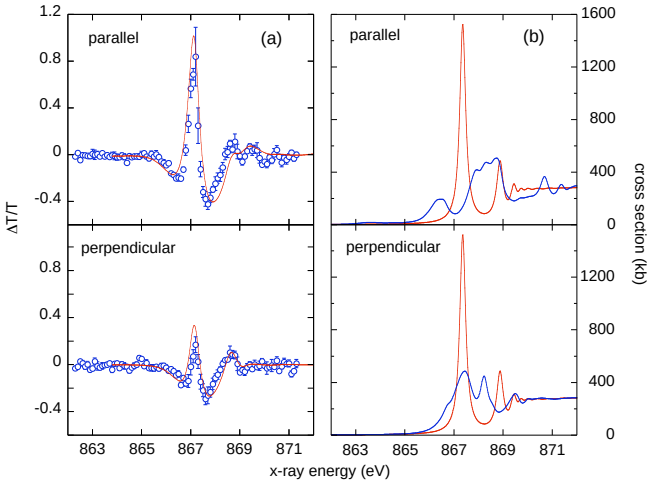

Fig. 3. (a) Changes in x-ray transmission spectrum of neon due to the presence of a laser-dressing field of ~10^{13} W/cm^2 intensity for parallel $\boldsymbol{\varepsilon}_L \| \boldsymbol{\varepsilon}_X$ (upper) and perpendicular $\boldsymbol{\varepsilon}_L \perp \boldsymbol{\varepsilon}_X$ (lower) configurations. Red solid line: theoretical simulations with *no adjustable parameters* of the propagation of an x-ray pulse through the laser-dressed neon gas. Experimental conditions were measured *in situ*. (b) *Ab initio* x-ray absorption cross sections for neon with no laser (red) and with an 800 nm dressing laser beam at 10^{13} W/cm^2 (blue).

Based upon this predictive power, one may proceed to applications – e.g. to imprint ultrafast laser pulse sequences onto long x-ray pulses as available at synchrotron sources [26]. Indeed, one can imagine using multiple optical control pulses in multicomponent media to achieve spectral and temporal control over a wide x-ray bandwidth. Since the dominant decay mechanism is intra-atomic, extension of optical control of x-ray absorption to condensed phase and molecular systems may also be feasible. Furthermore, the ability to optically control x-ray absorption on the ultrafast timescale may allow the exciting prospect of tuning the relative importance of absorption and scattering. Quantum control in the x-ray regime has been demonstrated here for a weak x-ray probe. The next frontier includes the use of intense free-electron lasers for nonlinear x-ray spectroscopy and experiments where x-rays are used as both control and probe pulses.

[1]Lawrence Berkeley National Laboratory, Berkeley, CA

Ultrafast x-ray probes of photoinduced dynamics

Third-generation synchrotron radiation facilities such as Argonne's Advanced Photon Source (APS) deliver tunable, polarized x rays with high photon flux and a pulse duration of about 100 ps. This pulse duration imposes a restriction on the kind of dynamical processes that may be studied or exploited at a third-generation synchrotron radiation facility. For processes on the appropriate timescale, the APS, with an average flux equal to that of the LCLS, is an outstanding weakly interacting probe of structure and dynamics – with excellent stability, user-controlled tunability, and ease of access. Understanding the structure of *adiabatically* aligned molecules represents one area where the x-ray pulse length does not hamper experiments. Abstracts below describe work toward this scientific goal and other x-ray probe studies of ultrafast laser-induced dynamics. In addition, developments to efficiently use the entire APS flux for laser pump/x-ray probe studies with high repetition rate lasers and to shorten the pulse duration to 1 ps are described.

X-ray scattering from laser-aligned molecules (S.H. Southworth, R.W. Dunford, P. J. Ho, E. P. Kanter, B. Krässig, J. J. Lin,[1] A. M. March, R. Santra, D. Starodub,[2] L. Young) In the presence of a strong nonresonant linearly polarized laser field, molecules align due to interaction of the laser electric field vector with the molecular anisotropic polarizability. The alignment process is of intrinsic interest and of interest in applications to spectroscopy and photophysics, quantum control, high-harmonic generation, chemical reactivity, liquids and solvation, and x-ray structural determination. Molecular alignment is normally probed by additional laser pulses that dissociatively ionize the molecule within an ion spectrometer that projects the fragments onto a position-sensitive detector and displays asymmetric fragmentation patterns. Our approach is different; we employ an x-ray microprobe of an ensemble of aligned molecules, as shown in Fig 4.

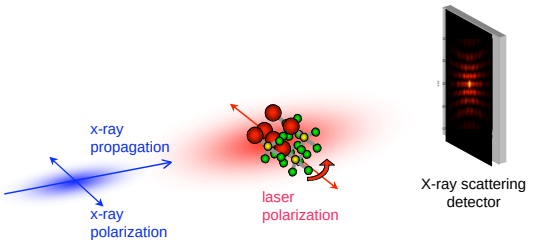

Fig.4. Schematic of x-ray probe of laser-aligned molecules. Pulsed non-resonant laser fields are required to produce the field strength necessary to align small molecules quasiadiabatically. Microfocused x-ray pulses probe a region of a high degree of alignment. Control over the molecular axis is provided by the laser polarization.

A resonant x-ray absorption probe of quasiadiabatically aligned bromotrifluoromethane molecules was demonstrated both experimentally and theoretically in Ref. [21]. The next natural step is to consider elastic x-ray scattering. Theoretical and calculational studies of x-ray scattering by laser-aligned molecules are presented in Refs. [6,10]. Our experimental program makes use of monochromatic x rays at Sector 7 of the Advanced Photon Source (APS) and broad-band x rays at Sector 14 of the APS. Both beamlines include 800-nm, 1-kHz laser systems synchronized with the x-ray pulses for pump-probe experiments.

We have developed a molecular-beam target chamber and related instrumentation for spatially and temporally overlapping microfocused laser and x-ray pulses at Sector 7. Since this beamline provides monochromatic x rays, the instrument has been used primarily for resonant x-ray absorption spectroscopy of laser-ionized and laser-aligned atoms and molecules [4,17,21,24,31]. However, the target chamber was also used in the past year to develop and test instruments and methods needed for x-ray scattering from laser-aligned molecules. First, experience was gained in using large-area, position-sensitive detectors to record x rays scattered from a cw molecular beam. Second, a heated, 1-kHz pulsed valve was used to produce a molecular beam of p-dibromobenzene seeded in high-pressure helium for rotational cooling. Para-dibromobenzene has a high anisotropic polarizability, and the technical goal is to produce a rotationally-cooled molecular beam that is well suited for laser alignment.

A new target chamber is being developed for x-ray scattering from laser-aligned molecules using the high-flux (~10^{10} x rays/pulse), pink-beam ($\Delta E/E$ ~2%) x rays at Sector 14. This beamline and endstation are optimized for time-resolved x-ray scattering studies of laser-pumped crystalline targets, e.g., for biomolecular or materials research. We will replace the crystalline targets with laser-aligned molecular beams and record diffraction patterns to compare with theory [6,10]. Our initial goal is to record x-ray scattering patterns from a skimmed, cooled, laser-aligned molecular beam of p-dibromobenzene. Long-term goals include experimental and calculational studies of strong-field-laser-induced distortion of molecular geometries. We will focus on relatively small molecules for basic studies of the physical processes, but the results will be relevant to the much anticipated experiments at x-ray free-electron lasers to investigate non-crystalline biomolecules and nano-particles. In addition, the techniques developed at the APS may provide an alternative approach to free-electron lasers for structural studies of non-crystalline materials.

X-ray scattering from impulsively aligned molecules (P.J. Ho, M.R. Miller, R. Santra)

In previous theoretical and experimental work, we focused on resonant x-ray absorption [18,21,22] and elastic x-ray scattering [10] by small, adiabatically aligned molecules. In the adiabatic alignment regime, it is possible to ensure that the alignment duration is comparable to the x-ray pulse duration. However, in this alignment regime, the molecules are aligned only when the strong alignment field is present. Alternatively, a short, intense laser pulse may be employed to create a spatially aligned molecular sample that persists after the laser pulse is over. In Ref. [6], we theoretically investigated whether this impulsive molecular alignment technique may be

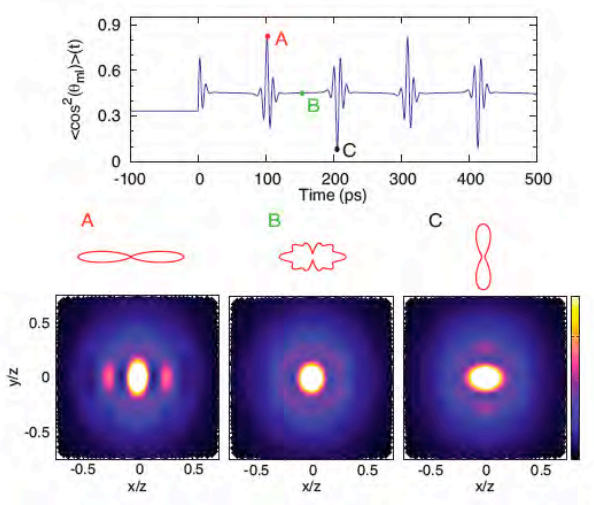

Fig 5. Simulated ultrafast x-ray diffraction imaging of bromine molecules at 1K kicked by a horizontally polarized 50-fs laser pulse, centered at t=0 with a peak intensity of 3 × 10^{13} W/cm^2.

exploited for experiments using x-ray pulses from a third-generation synchrotron radiation facility. Using a linear rigid rotor model, the alignment dynamics of model molecular systems with systematically increasing size were calculated utilizing both a quantum density matrix formalism and a classical ensemble method. For each system, the alignment dynamics obtained for a 95-ps laser were compared to those obtained for a 10-ps laser pulse. The average degree of alignment after the laser pulse, as calculated quantum mechanically, increases with the size of the molecule. This effect was quantitatively reproduced by the classical calculations. The average degree of impulsive alignment was found to be high enough to induce a pronounced linear dichroism in resonant x-ray absorption using the intense 100-ps x-ray pulses currently available at the APS. However, for structural studies based on elastic x-ray scattering, bright x-ray pulses with a duration of 1 ps or shorter will be required in order to make full use of impulsive molecular alignment. This can be seen in Fig. 5 where the x-ray scattering patterns are shown for bromine molecules excited with 50 fs laser pulses. Currently, we are collaborating with Dilano Saldin and Abbas Ourmazd (University of Wisconsin, Milwaukee) on extracting molecular-structure information from x-ray scattering patterns of laser-aligned symmetric-rotor molecules.

High-repetition-rate laser and x-ray experiments (L. Young, L. Chen,[3] E. Kanter, B. Krässig, S. Southworth, D. Tiede,[3] B. Adams,[4] D. Arms,[4] K. Attenkofer,[4] E. Dufresne,[4] Y. Li,[4] D. Walko,[4] J. Wang,[4] A. M. March, A. Stickrath,[3] D. Yost,[5] T. Schibli,[5] J. Ye[5])
There is typically a large mismatch in repetition rates between the lasers (1-5 kHz) and x rays (6.5 MHz at the Advanced Photon Source) used for pump/probe experiments at synchrotron-radiation facilities. The mismatch is due to the need in many experiments to generate laser pulses of sufficient energy (~1-5 mJ/pulse), and therefore low rep-rate amplifiers are needed for typical average powers of ~1-5 W. For example, pulse energies of ~1-5 mJ are needed to produce sufficient densities of laser-aligned molecules or to produce sufficient energies of 2nd - 4th harmonics for near-UV excitation of solvated molecules. Consequently, synchrotron x rays are not efficiently utilized, and data rates are far lower than they could be with higher rep-rate lasers. A potential solution to the rep-rate limitation is to use passive enhancement cavities as pioneered by the JILA group [R. J. Jones *et al.*, Phys. Rev. Lett. **94**, 193201 (2005)] to enhance intra-cavity pulse energies by factors as high as ~600. High rep-rate μJ pulses can then be increased to the required mJ regime. Our collaboration has initiated a research program to develop high rep-rate laser techniques for efficient utilization of x rays at the APS. The possible 6500x statistical gain will pave the way toward high precision x ray absorption spectroscopies for gas phase systems.

The heart of the project is presently a 10-W average power, 1064 nm laser that operates over the 50 kHz - 6.5 MHz rep rate range with either 10 ps or 130 ps pulses. The laser was purchased through Argonne LDRD funding, and that funding has also been used to hire two postdoctoral researchers, Anne Marie March and Andrew Stickrath, to develop the high rep-rate techniques and perform first experiments at the APS. Our collaboration includes beamline scientists, laser scientists, and researchers with diverse interests in time-resolved x-ray science, including atomic, molecular, chemical dynamics, materials science, and applied science. In the past year, the basic laser system has been installed and augmented by components needed for locking to the 352 MHz RF system at

APS and for pulse picking and phase-control synchronization of the laser and x-ray pulses. A dedicated data acquisition system was also developed that will work smoothly with other EPICS-based network-control systems at the APS, e.g., beamline control and data acquisition systems.
As a feasibility test, a simple passive cavity was locked to the laser pulses. The optics and controls needed for a working passive cavity are being developed and tested at JILA, and that system will soon be combined with the laser at Argonne. In addition, components and methods are being developed for implementation of the first high-rep-rate experiments on gas-phase molecules and production of 2nd and 3rd harmonic radiation for molecular charge-transfer excitation in fast-flow liquid jets.

Picosecond x rays at the Advanced Photon Source (B. Krässig, R.W. Dunford, E.P. Kanter, S.H. Southworth, L. Young, Solar Energy Conversion Group, APS staff)
Efforts are underway to shorten the duration of the x-ray pulses produced at Argonne's Advanced Photon Source by a factor of 100 down to about 1 picosecond. This complex project has been named the Short Pulse X ray project (SPX). This will enable researchers from a variety of different fields to study the time evolution of their dynamically evolving samples on an atomic scale. The bunch shortening will be achieved by rotating the electron bunch in its phase space using a set of deflecting RF cavities, a scheme developed by Zholents et al. [Nucl. Instrum. Meth. A **425**, 385 (1999)]. In this scheme the bunch rotation induced by the first cavity is reversed by the second, leaving the beam characteristics outside the section between the two deflecting cavities unaffected. This rf-deflection scheme works well only on high energy storage rings of large diameter.

This past year the decision was made to pursue only the high repetition rate version of the SPX, which requires superconducting rf cavities. In view of this, in collaboration with Jefferson Lab, there has been successful testing of a prototypical single-cell superconducting rf cavity led by Ali Nassiri of the Accelerator Operations Group. The technical challenge is to create a compact multicell deflection cavity with the requisite voltage gradient (>4 MV/m) that occupies a small fraction of a straight section in the APS storage ring. In addition, SPX implementation and the required R&D has become an integral part of the APS Renewal Document. The AMO group will be involved in developing science drivers and beamline design for the SPX.

A simple cross-correlation technique between infrared and hard x-ray pulses (B. Krässig, R.W. Dunford, E. C. Landahl[6], S.H. Southworth, L. Young)
In Ref. [4] we report a gas phase technique to establish the temporal overlap of ultrafast infrared laser and hard x-ray pulses. The technique uses tunnel ionization of a closed shell atom in the strong field focus of an infrared laser beam to open a distinct x-ray absorption resonance channel with a clear fluorescence signature. This process has an intrinsic response of a few femtoseconds and is nondestructive to the two photon beams. It provides a step-functionlike cross-correlation result. The details of the transient provide a diagnostic of the temporal overlap of the two pulses.

Multichannel coherence in strong-field ionization (N. Rohringer[7] and R. Santra)
Atomic and molecular ions generated by a strong optical laser pulse are not in general in the electronic ground state. The density matrix for such ions is characterized by the

electronic quantum-state populations and by the coherences among the electronic quantum states. Nonvanishing coherences signal the presence of coherent electronic wave-packet dynamics in the laser-generated ions. For noble-gas atoms heavier than helium, the most important channels populated via strong-field ionization are the outer-valence single-hole states with a total angular momentum of j=3/2 or j=1/2. Complete ion quantum state populations, i.e., the diagonal elements of the ion density matrix in the ion eigenstate basis, were determined experimentally and theoretically in Refs. [27] (Xe) and [24] (Kr). An important question is whether the ion density matrix has, in fact, any nonzero off-diagonal elements. Are there any coherences? In order to answer this question, we have developed in Ref. [5] a time-dependent multichannel theory of strong-field ionization. We derived the ion density matrix and expressed the hole density in terms of the elements of the ion density matrix. Our wave-packet calculations demonstrated that neon ions generated in a strong optical field (800 nm) are almost perfectly coherent. In strong-field-generated xenon ions, however, the coherence is substantially suppressed. We are currently collaborating with Steve Leone (University of California, Berkeley) and Ferenc Krausz (Max Planck Institute for Quantum Optics, Garching) to determine, experimentally and theoretically, the complete ion density matrix, including coherences, of strong-field-generated Kr ions.

[1]Academia Sinica, Taipei, Taiwan 10617
[2]Arizona State University, Tempe, Arizona
[3]Chemical Sciences and Engineering Division, Argonne National Laboratory
[4]X-Ray Science Division, Argonne National Laboratory
[5]JILA, University of Colorado, Boulder, Colorado
[6]De Paul University, Chicago, IL
[7]Lawrence Livermore National Laboratory, Livermore, CA

Publications (2007-2009)

[1] T.E. Glover, M.P. Hertlein, S.H. Southworth, T.K. Allison, J. van Tilborg, E.P. Kanter, B. Krässig, H. R. Varma, B. Rude, R. Santra, A. Belkacem[1], and L. Young. "Controlling x-rays with light: ultrafast transparency", submitted (2009).

[2] H. R. Varma, M. F. Ciappina, N. Rohringer, and R. Santra, "Above-threshold ionization in the x-ray regime," submitted (2009).

[3] R. Santra, N. V. Kryzhevoi, and L. S. Cederbaum, "X-ray two-photon photoelectron spectroscopy: A theoretical study of inner-shell spectra of the organic para-aminophenol molecule," Phys. Rev. Lett. **103**, 013002 (2009).

[4] B. Krässig, R.W. Dunford, E. P. Kanter, E. C. Landahl, S.H. Southworth, and L. Young, "A simple cross-correlation technique between infrared and hard x-ray pulses," Applied Physics Letters **94**, 171113 (2009).

[5] N. Rohringer and R. Santra, "Multichannel coherence in strong-field ionization," Phys. Rev. A **79**, 053402 (2009).

[6] P. J. Ho, M. R. Miller, and R. Santra, "Field-free molecular alignment for studies using x-ray pulses from a synchrotron radiation source," J. Chem. Phys. **130**, 154310 (2009).

[7] L. Young, R. W. Dunford, E. P. Kanter, B. Krässig, R. Santra, S. H. Southworth, "Strong-field control of x-ray processes," In *Pushing the Frontiers of Atomic Physics: Proceedings of the XXI International Conference on Atomic Physics*, R. Côté, P.L. Gould, M. Rozman and W.W. Smith, Eds., World Scientific Publishing Co., NJ, Singapore (2009), p. 344-353.

[8] R. Santra, "Concepts in x-ray physics," J. Phys. B **42**, 023001 (2009).

[9] H. R. Varma, L. Pan, D. Beck, and R. Santra, "X-ray absorption near-edge structure of laser-dressed neon," Phys. Rev. A **78**, 065401 (2008).

[10] P. J. Ho and R. Santra, "Theory of x-ray diffraction from laser-aligned symmetric-top molecules," Phys. Rev. A **78**, 053409 (2008).

[11] A. S. Sandhu, E. Gagnon, R. Santra, V. Sharma, W. Li, P. Ho, P. Ranitovic, C. L. Cocke, M. M. Murnane, and H. C. Kapteyn, "Observing the creation of electronic Feshbach resonances in soft x-ray-induced O_2 dissociation," Science **322**, 1081 (2008).

[12] I. A. Sulai, Q. Wu, M. Bishof, G. W. F. Drake, Z.-T. Lu, P. Mueller, and R. Santra, "Hyperfine suppression of $2\ ^3S_1 - 3\ ^3P_J$ transitions in ^{3}He," Phys. Rev. Lett. **101**, 173001 (2008).

[13] L. Young, C. Buth, R.W. Dunford, P. Ho, E.P. Kanter, B. Krässig, E.R. Peterson, N. Rohringer, R. Santra, and S.H. Southworth. "Using strong electromagnetic fields to control x-ray processes" Proceedings of the Pan-American Advanced Studies Institute, Buzios, Brazil 2008, in press Revista Mexicana de Fisica.

[14] C. Buth, R. Santra, and L. Young. "Refraction and absorption of x-rays by laser-dressed atoms," Proceedings of the Pan-American Advanced Studies Institute, Buzios, Brazil, 2008, in press Revista Mexicana de Fisica.

[15] P. Ho and R. Santra, "Theory of x-ray diffraction by laser-aligned molecules," Proceedings of the Pan-American Advanced Studies Institute, Buzios, Brazil, 2008, in press Revista Mexicana de Fisica.

[16] C. Buth and R. Santra, "X-ray refractive index of laser-dressed atoms," Phys. Rev. A **78**, 043409 (2008).

[17] E. P. Kanter, R. Santra, C. Hoehr, E. R. Peterson, J. Rudati, D. A. Arms, E. M. Dufresne, R. W. Dunford, D. L. Ederer, B. Kraessig, E. C. Landahl, S. H. Southworth, and L. Young, "Characterization of the spatiotemporal evolution of laser-generated plasmas," J. Appl. Phys. **104**, 073307 (2008).

[18] C. Buth and R. Santra, "Rotational molecular dynamics of laser-manipulated bromotrifluoromethane studied by x-ray absorption," J. Chem. Phys. **129**, 134312 (2008).

[19] N. Rohringer and R. Santra, "Resonant Auger effect at high x-ray intensity," Phys. Rev. A **77**, 053404 (2008).

[20] R. Santra, R. W. Dunford, E. P. Kanter, B. Kraessig, S. H. Southworth, and L. Young, "Strong-field control of x-ray processes," Advances in Atomic, Molecular, and Optical Physics **56**, 219 (2008).

[21] E. R. Peterson, C. Buth, D. A. Arms, R. W. Dunford, E. P. Kanter, B. Kraessig, E. C. Landahl, S. T. Pratt, R. Santra, S. H. Southworth, and L. Young, "An x-ray probe of laser-aligned molecules," Appl. Phys. Lett. **92**, 094106 (2008).

[22] C. Buth and R. Santra, "Theory of x-ray absorption by laser-aligned symmetric-top molecules," Phys. Rev. A **77**, 013413 (2008).

[23] R. Santra, C. Buth, E. R. Peterson, R. W. Dunford, E. P. Kanter, B. Kraessig, S. H. Southworth, and L. Young, "Strong-field control of x-ray absorption," J. Phys.: Conference Series **88**, 012052 (2007).

[24] S. H. Southworth, D. A. Arms, E. M. Dufresne, R. W. Dunford, D. L. Ederer, C. Höhr, E. P. Kanter, B. Kraessig, E. C. Landahl, E. R. Peterson, J. Rudati, R. Santra, D. A. Walko, and L. Young, "K-edge x-ray absorption spectroscopy of laser-generated Kr^{+} and Kr^{2+}," Phys. Rev. A **76**, 043421 (2007).

[25] N. Rohringer and R. Santra, “X-ray nonlinear optical processes using a self-amplified spontaneous emission free-electron laser,” Phys. Rev. A **76**, 033416 (2007).

[26] C. Buth, R. Santra, and L. Young, “Electromagnetically induced transparency for x rays,” Phys. Rev. Lett. **98**, 253001 (2007).

[27] Z.-H. Loh, M. Khalil, R. E. Correa, R. Santra, C. Buth, and S. R. Leone, “Quantum state-resolved probing of strong-field-ionized xenon atoms using femtosecond high-order harmonic transient absorption spectroscopy,” Phys. Rev. Lett. **98**, 143601 (2007).

[28] C. Buth and R. Santra, “Theory of x-ray absorption by laser-dressed atoms,” Phys. Rev. A **75**, 033412 (2007).

[29], M. de Jonge, C. Tran, C.T. Chantler, Z. Barnea, B.B. Dhal, D. Paterson, E.P. Kanter, S.H. Southworth, L. Young, M.A. Beno, J. A. Linton and G. Jennings, “Measurement of the x-ray mass attenuation coefficient and determination of the imaginary component of the atomic form factor of tin in the energy range of 29-60 keV,” Physical Review A **75**, 032702 (2007).

[30] C. Höhr, E.R. Peterson, E.C. Landahl, D. A. Walko, R.W. Dunford, E.P. Kanter, and L. Young, “A simple short-range point-focusing spatial filter for time-resolved x-ray fluorescence” Synchrotron Radiation Instrumentation: Ninth International Conference on Synchrotron Radiation Instrumentation, AIP Conference Proceedings **879**, 1226-1229 (2007).

[31] C. Höhr, E. R. Peterson, N. Rohringer, J. Rudati, D. A. Arms, E. M. Dufresne, R. W. Dunford, D. L. Ederer, E. P. Kanter, B. Kraessig, E. C. Landahl, R. Santra, S. H. Southworth, and L. Young, “Alignment dynamics in a laser-produced plasma,” Phys. Rev. A **75**, 011403(R) (2007).

J.R. MACDONALD LABORATORY - OVERVIEW 2009

The J.R. Macdonald Laboratory focuses on the interaction of intense-laser pulses with matter. The targets include neutral single atoms and molecules in the gas phase, single ions in our accelerator beams, trapped atoms in our MOTRIMS systems, and nanostructures. In addition we pursue several outside collaborations at other facilities and with other groups (e.g., ALS, ALLS, Århus, Auburn University, University of Colorado, Columbia University, FLASH, LCLS, Max-Planck Institutes for Quantum Optics (MPQ) and Kernphysik (MPI-K), Sao Carlos, Tokyo, Weizmann Institute of Science, and others). Most of our laser work is associated with one or more of the following themes[1]:

1) **Attosecond physics:** The ultimate goal of this work is to follow, in real time, electronic motion in atoms and molecules. We have characterized the temporal shape of single attosecond pulses generated by the generalized double optical gating (GDOG) method – 260 as pulses. We have employed these pulses to control and monitor electron dynamics in He atoms. Using an attosecond pulse train in an EUV/infrared pump-probe scheme we have explored He and D_2 targets. The quantitative re-scattering theory for high energy above-threshold-ionization electrons and high-harmonic generation has been developed and applied both to determine the target and electron wave-packet properties as well as to retrieve the laser field parameters.

2) **Time-resolved dynamics of heavy-particle motion in neutral molecules:** We have continued our studies on the time evolution of heavy particle motion in simple molecules, such as N_2 and CO, following excitation by an ultrashort laser pulse. For example, we have demonstrated the impact of the time delay on the competition between asymmetric and symmetric charge breakup of N_2^{4+}. On the theory side, this involves including nuclear vibration and rotation in addition to the electron excitation as part of the quest for a more complete theoretical description of atoms and molecules in strong fields. For example, we have studied imaging the ro-vibrational nuclear dynamics of small molecules in strong laser fields.

3) **Control:** Methods for controlling the motion of heavy particles in small molecules continue to be developed. Theoretically, the ability to control the dissociation of molecules (e.g., H_2^+) into different final channels has been investigated by the application of pulse pairs or carrier-envelop phase (CEP) control. Experimentally, we have localized the electron on a specific nucleus of a dissociating D_2^+ in a two-color experiment on D_2 using the phase as a control knob. We have completed the development of a 3D VMI imaging setup for studies of molecular alignment and orientation, and initiated first measurements. The MOTRIMS technique has been used to study photoassociation with excitation (PAE) of Rb_2 with the goal of enhancing this process by shaping the spectral phase.

4) **Studies involving simultaneous use of laser and accelerators:** We have continued our investigations of the ionization and dissociation of molecular-ion beams from our ECR source, which was recently replaced by a new permanent magnet ECR. We have focused this year on the simple polyatomic molecule, H_3^+, and its isotopologues, while continuing our work on H_2^+ and other diatomic molecules. For example, we have demonstrated that vibrational trapping – predicted by aligned-molecule calculations – vanishes if nuclear rotation is included in the

[1]Details of the projects are provided in the individual contributions of the PIs: *I. Ben-Itzhak, Z. Chang, C.L. Cocke, B.D. DePaola, B.D. Esry, V. Kumarappan, C.D. Lin, I.V. Litvinyuk and U. Thumm*.

calculations. Instead, the reduced dissociation probability is due to the fact that the vibrational dipole matrix elements are smaller – this explanation was also verified experimentally.

5) **Photons from the KLS interacting with solids and clusters:** The study of electron dynamics in photo-ionization and excitation of nanotubes has been conducted in collaboration with Professor T. Heinz from Columbia University. Theoretical investigation of attosecond time-resolved photoelectron spectroscopy of metal surfaces has been carried out.

In addition to the laser related research, we are conducting some collision studies using our high and low energy accelerators. Some of this work is conducted in collaboration with visiting scientists (for example, S. Lundeen, J. Shinpaugh & L. Toburen, E. Wells).

Finally, it is hard to summarize this year without mentioning the Attosecond Physics meeting that we will be hosting in late July 2009 and the recent hire of *Matthias Kling* as an assistant professor in our department. We are confident that this hire will strengthen our attosecond physics efforts.

Structure and Dynamics of Atoms, Ions, Molecules, and Surfaces:
Molecular Dynamics with Ion and Laser Beams

Itzik Ben-Itzhak, J. R. Macdonald Laboratory, Kansas State University
Manhattan, Ks 66506; ibi@phys.ksu.edu

The goal of this part of the JRML program is to study the different mechanisms for molecular fragmentation initiated by ultrashort intense laser pulses or following fast or slow collisions. To that end we typically use molecular ion beams as the subject of our studies and have a close collaboration between theory and experiment[1]*. Examples of our recent work are given below.*

Benchmark measurements of H_3^+ nonlinear dynamics in intense ultrashort laser pulses, *J. McKenna, A.M. Sayler, B. Gaire, Nora G. Johnson, K.D. Carnes, B.D. Esry, and I. Ben-Itzhak*

The H_3^+ molecule is the simplest polyatomic molecule. It has a unique triangular geometry and is expected to play a major role on the road to a better understanding of complex molecules in intense ultrashort laser pulses. It is just at the edge of what one can expect theory to handle, and our goal is to present first benchmark measurements of this fundamental system.

Extensive laser studies of the hydrogen molecule and molecular ion [1,Pub. #13] provide the basis for our understanding of diatomic molecules in intense ultrafast laser pulses. One expects that H_3^+ studies will lead to better understanding of polyatomic molecules in intense fields because it may become possible to treat this non-perturbative system theoretically in the near future. However, H_3^+ has eluded experimentalists until recently, and even using intensities on the order of 10^{16} W/cm^2 – normally sufficient to at least dissociate a molecule – did not generate any detectable breakup signal.

Using the high detection efficiency of our coincidence 3D momentum imaging technique [2,Pub. #3,10,13,14] we have managed to study the dissociation and ionization of D_3^+ – we favor D_3^+ over H_3^+ to avoid the HD^+ contaminant present in the latter beam. Our initial measurements of D_3^+ fragmentation in intense ultrafast laser pulses provide detailed information about the different breakup channels and their intensity dependence as shown in Fig.1(Left). Moreover, kinetic energy release (KER) and angular distributions of two-body and three-body breakup (the latter are shown in the right panel of Fig. 1) were also obtained.

First, the intensity dependence, shown in Fig. 1(Left), indicates that two-body breakup dominates the dissociation of D_3^+ in the laser pulses used in our studies. This differs significantly from dissociation of neutral H_3 following dissociative recombination, i.e. $H_3^+ + e^- \rightarrow H + H + H$, [3,4]. Second, single ionization is dominated by two-body breakup at low intensities while three-body breakup takes over for intensities above about 3×10^{15} W/cm^2. Qualitatively, this can be understood by looking at the potential energy surfaces (PES) of the transient D_3^{2+} (calculated by Esry who solved the Born-Oppenheimer equation in three-dimensions using B-splines, and shown in the inset of Fig. 1(Left)). Dissociation on the ground state mainly leads to $D^+ + D_2^+$, while in contrast the excited electronic state leads solely to $D^+ + D^+ + D$. As the laser intensity increases the excited state population increases thus leading to three-body breakup domination.

Arguably the most insightful information on D_3^+ breakup is provided by the alignment, θ, and orientation, χ, dependence of the molecular plane relative to the laser polarization (see definitions in Fig. 1(right)). These are determined from the momenta vectors of the three fragments measured in our 3D imaging scheme. Both single and double ionization are more likely when the laser polarization is within the molecular plane, i.e. θ=90°. This is consistent

[1]Some of our studies are done in collaboration with *Z. Chang's* group, *C.W. Fehrenbach,* and others.

with the MO-ADK theory [5], which predicts a higher tunneling-ionization rate in the direction that that wave function extends further – that is within the molecular plane for the H_3^+ molecule. What is not clear yet is why single and double ionization follow a similar angular dependence, specifically $\sin^3\theta$. The orientation dependence for double ionization exhibits peaks every 60°, i.e. every time a deuteron is dissociating along the electric field (recall that the field flips direction periodically within the laser pulse). This also can be explained by the fact that the electronic wave function extends further along these directions than in between the nuclei in the H_3^+ triangular configuration. However, in contrast to the similarity in alignment, single ionization shows a completely different orientation than double ionization. The dominant feature is aligned with the polarization, i.e. D fragments prefer to dissociate along the field. In addition, a weaker breakup feature appears at χ=90°, which becomes larger for the longer 40 fs pulses. This indicates that more complex dynamics are responsible for the orientation effect. This project was presented as invited talks at ICOMP 2008 and at DAMOP 2009 – the latter by my post doc., Jarlath McKenna, and a first manuscript has been submitted [Pub. #20].

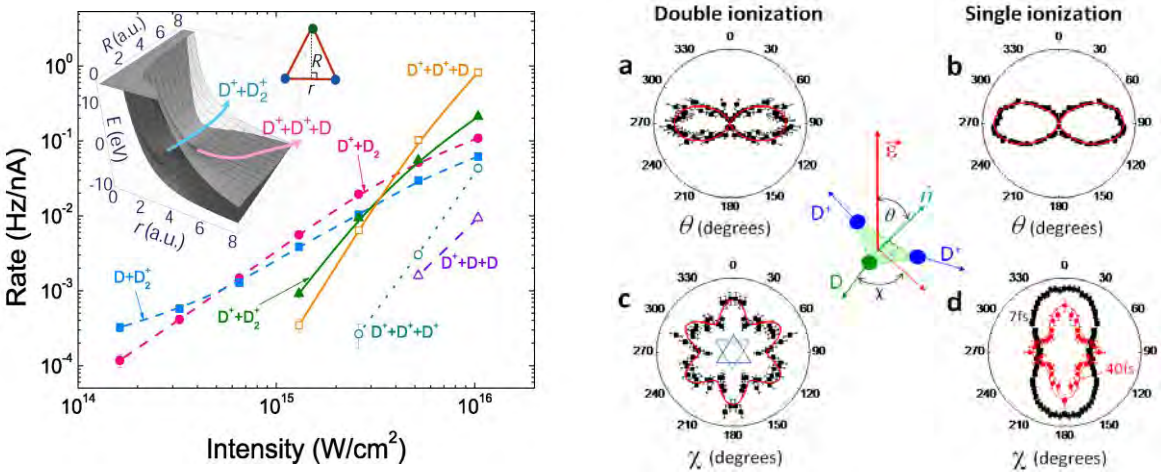

Figure 1. *Left*: Normalized rates for D_3^+ fragmentation channels as a function of laser intensity using 7 fs, 790 nm laser pulses. The rates have been normalized to the ion beam current of ~5 nA. The inset shows cuts of the lowest two potential energy surfaces calculated for D_3^{2+}, where R and r are defined by the diagram.. *Right*: (a,b) The alignment, θ, of the normal vector to the molecular plane relative to the laser polarization – see inset for definitions (θ > 180° is mirrored to complete the polar plot): (a) Double ionization and (b) single ionization, for 7 fs, 10^{16} W/cm^2 laser pulses. The fits to the data are $\sin^3\theta$ angular distributions. (c,d) The orientation, χ, of the velocity vector of the D^+ and D fragments of double and single ionization, respectively, relative to the projection of the laser polarization within the molecular plane (for large fields within the molecular plane, i.e., 60°< θ <120°): (c) Double ionization for 7 fs pulses, and (d) single ionization for 7 fs and 40 fs pulses. The error bars show the statistical error of the data.

Intense short pulse laser-induced ionization and dissociation of molecular-ion beams – *J. McKenna, A.M. Sayler, P.Q. Wang, B. Gaire, Nora G. Johnson, M. Zohrabi, E. Parke, M. Leonard, K.D. Carnes, F. Anis, J.J. Hua, B.D. Esry, I. Ben-Itzhak*

The goal for these projects was to extend our knowledge of H_2^+ and apply it to more complex molecules in intense ultrafast laser pulses.

Studies of the benchmark H_2^+ and H_2 molecules provide the foundation for our understanding of the behavior of diatomic and somewhat more complex molecules in intense ultrashort laser pulses. To extend this knowledge base, we explored enhanced ionization in both these targets in collaboration with Lew Cocke's group (Pub. #12). We also studied dissociation and ionization of

HD^+ in 395 & 790 nm pulses (Pub. #19), and in particular the role of the HD^+ permanent dipole (Pub. #17). Taking advantage of our improved energy resolution we have studied the KER shift as a function of the sign of the pulse chirp, revisited the vibrational suppression in H_2^+ dissociation, and found clear evidence for the elusive zero-photon dissociation mechanism [6]. In addition, we studied the formation of metastable D* fragments from a neutral D_2 target exposed to intense laser fields. All these projects benefited from the strong collaboration with the theory group of Esry.

Armed with better understanding of the benchmark systems above, we explored more complex molecules. For example, we identified dissociation paths leading to very high KER in N_2^+ beam targets (pub #11). We conducted a study of multiple ionization of N_2^+, O_2^+, CO^+ and NO^+, showing that these molecules tend to stretch between consecutive ionization steps, i.e. they follow a stairstep mechanism (Pub. #18). We also investigated an electronic and vibrationally cold CO^{2+} target – a two-level system undergoing perpendicular transitions. For this unique target we observe bond softening and 2-photon above threshold dissociation peaks, nicely separated by the photon energy.

In addition to our laser studies, we have conducted a few ion-molecule collision experiments [see, for example, Pub. #15,16]. We have also finished upgrading our molecular dissociation imaging setup – a project that was the topic of the M.Sc. Thesis of my student, *Nora G. Johnson* – and initiated studies of collisions of a few keV molecular ion beams with atomic targets. For example, at present we are investigating $HeD^+ + He$ collisions.

Future plans: We will continue interrogating H_2^+ beams with laser pulses, in particular exploring the effect of a two-color field, and then begin pump-probe experiments, which are a challenge due to the low target density of ion beams. We will also continue our studies of more complex molecules such as H_3^+ isotopologues, CO^{2+} etc. We are in the process of improving the collision setup to enable high resolution Q-value measurements and will continue kinematically complete studies of dissociative capture and collision induced dissociation at keV energies.

1. J.H. Posthumus, Rep. Prog. Phys. **67**, 623 (2004); and references therein.
2. I. Ben-Itzhak *et al*. Phys. Rev. Lett. (2005)
3. S. Datz *et al*., Phys. Rev. Lett. 74, 896 (1995).
4. V. Kokoouline, C.H. Greene, and B.D. Esry, Nature **412**, 891 (2001), and references therein.
5. X.M. Tong, Z.X. Zhao, and C.D. Lin, Phys. Rev. A **66**, 033402 (2002).
6. J.H. Posthumus et al., Phys. Rev. Lett. **101**, 233004 (2008); and references therein.

Publications of DOE sponsored research in the last 3 years:

20. "Benchmark measurements of H_3^+ nonlinear dynamics in intense ultrashort laser pulses", J. McKenna, A.M. Sayler, B. Gaire, Nora G. Johnson, K.D. Carnes, B.D. Esry, and I. Ben-Itzhak, Phys. Rev. Lett. (2009) – **hopefully accepted**.
19. J. McKenna, A.M. Sayler, B. Gaire, Nora G. Johnson, E. Parke, K.D. Carnes, B.D. Esry, and I. Ben-Itzhak, "Intense 395nm ultrashort laser-induced dissociation and ionization of an HD^+ beam", Phys. Rev. A (2009) – **accepted**.
18. "Laser-induced multiple ionization of molecular ion beams: N_2^+, CO^+, NO^+, and O_2^+ ", B. Gaire, J. McKenna, Nora G. Johnson, A.M. Sayler, E. Parke, K.D. Carnes, and I. Ben-Itzhak, Phys. Rev. A **79**, 063414 (2009); and Virtual Journal of Ultrafast Science **8** (July 2009), at http://www.vjultrafast.org.
17. "Permanent dipole transitions remain elusive in HD^+ strong-field dissociation", J. McKenna, A.M. Sayler, B. Gaire, Nora G. Johnson, M. Zohrabi, K.D. Carnes, B.D. Esry and I. Ben-Itzhak, J. Phys. B **42**, 121003 (2009) – Fast Track Communication.
16. "Rapid Formation of H_3^+ from ammonia and methane following 4 MeV proton impact", Bethany Jochim, Amy Lueking, Laura Doshier, Sharayah Carey, E. Wells, Eli Parke, M. Leonard, K.D. Carnes, and I. Ben-Itzhak, J. Phys. B **42**, 091002 (2009) – Fast Track Communication.

15. "Bond rearrangement following collisions between fast ions and ammonia or methane", E. Wells, E. Parke, Laura Doshier, Amy Lueking, Bethany Jochim, Sharayah Carey, Mat Leonard, K.D. Carnes, and I. Ben-Itzhak, *Application of Accelerators in Research and Industry*, edited by B.L. Doyle and F.D. McDaniel (AIP press, New York 2009), vol. **1099**, p. 133.
14. "Interrogating molecular-ion beams by ultra-short laser pulses", I. Ben-Itzhak, J. McKenna, A.M. Sayler, B. Gaire, Nora G. Johnson, E. Parke, and K.D. Carnes, *Application of Accelerators in Research and Industry*, edited by B.L. Doyle and F.D. McDaniel (AIP press, New York 2009), vol. **1099**, p. 146.
13. "Molecular ion beams interrogated with ultrashort intense laser pulses", Itzik Ben-Itzhak, *Progress in Ultrafast Intense Laser Science* IV, Series: Springer Series in Chemical Physics, Vol. **91**, edited by *K. Yamanouchi*, *A. Becker* , R. Li, and S.L. Chin (Springer, New York 2009) p. 67 – invited.
12. "Elusive enhanced-ionization structure for H_2^+ in intense ultrashort laser pulses", I. Ben-Itzhak, P.Q. Wang, A.M. Sayler, K.D. Carnes, M. Leonard, B.D. Esry, A.S. Alnaser, B. Ulrich, X.M. Tong, I.V. Litvinyuk, C.M. Maharjan, P. Ranitovic, T. Osipov, S. Ghimire, Z. Chang, and C.L. Cocke, Phys. Rev. A **78**, 063419 (2008); and *Virtual Journal of Ultrafast Science* **8** (January 2009), at http://www.vjultrafast.org.
11. "High kinetic energy release upon dissociation and ionization of N_2^+ beams by intense few-cycle laser pulses", B. Gaire, J. McKenna, A.M. Sayler, Nora G. Johnson, E. Parke, K.D. Carnes, B.D. Esry, and I. Ben-Itzhak, Phys. Rev. A **78**, 033430 (2008); and *Virtual Journal of Ultrafast Science* **10** (October 2008), at http://www.vjultrafast.org.
10. "Enhancing high-order above-threshold dissociation of H_2^+ beams with few-cycle laser pulses", J. McKenna, A.M. Sayler, F. Anis, B. Gaire, Nora G. Johnson, E. Parke, J.J. Hua, H. Mashiko, C.M. Nakamura, E. Moon, Z. Chang, K.D. Carnes, B.D. Esry, and I. Ben-Itzhak, Phys. Rev. Lett. **100**, 133001 (2008); and *Virtual Journal of Ultrafast Science* **7** (May 2008), at http://www.vjultrafast.org.
9. "Measuring the dissociation branching ratio of heteronuclear ND^+", J. McKenna, A.M. Sayler, B. Gaire, Nora G. Johnson, E. Parke, K.D. Carnes, B.D. Esry, and I. Ben-Itzhak, Phys. Rev. A **77**, 063422 (2008).
8. "Soft fragmentation of carbon monoxide by slow highly charged ions", E. Wells, T. Nishide, H. Tawara, K.D. Carnes, and I. Ben-Itzhak, Phys. Rev. A **77**, 064701 (2008).
7. "Ionization and dissociation of molecular ion beams caused by ultrashort intense laser pulses", I. Ben-Itzhak, A.M. Sayler, P.Q. Wang, J. McKenna, B. Gaire, Nora G. Johnson, M. Leonard, E. Parke, K.D. Carnes, F. Anis, and B.D. Esry, Journal of Physics: Conference Series **88**, 012046 (2007).
6. "Determining intensity dependence of ultrashort laser processes through focus *z*-scanning intensity-difference spectra: application to laser-induced dissociation of H_2^+", A.M. Sayler, P.Q. Wang, K.D. Carnes, and I. Ben-Itzhak, J. Phys. B **40**, 4367 (2007).
5. "Picosecond ion pulses from an EN tandem created by a femtosecond Ti:sapphire laser", K.D. Carnes, C.L. Cocke, Z. Chang, I. Ben-Itzhak, H.V. Needham, and A. Rankin, Nucl. Instrum. Methods B **261**, 106 (2007).
4. "Systematic study of charge state and energy dependence of TI to SC ratios for F^{q+} ions incident on He", R. Ünal, P. Richard, I. Ben-Itzhak, C.L. Cocke, M.J. Singh, H. Tawara, and N. Woody, Phys. Rev. A **76**, 012710 (2007).
3. "Determining laser-induced dissociation pathways of multi-electron diatomic molecules: application to the dissociation of O_2^+ by high intensity ultrashort pulses", A.M. Sayler, P.Q. Wang, K.D. Carnes, B.D. Esry, and I. Ben-Itzhak, Phys. Rev. A **75**, 063420 (2007); and *Virtual Journal of Ultrafast Science* 6 (July 2007), at http://www.vjultrafast.org.
2. "Determining the absolute efficiency of a delay line microchannel-plate detector using molecular dissociation", B. Gaire, A.M. Sayler, P.Q. Wang, Nora G. Johnson, M. Leonard, E. Parke, K.D. Carnes, and I. Ben-Itzhak, Rev. Sci. Instrum. **78**, 024503 (2007).
1. "Dissociation of H_2^+ in intense femtosecond laser fields studied by coincidence three-dimensional momentum imaging", P.Q. Wang, A.M. Sayler, K.D. Carnes, J.F. Xia, M.A. Smith, B.D. Esry, and I. Ben-Itzhak, Phys. Rev. A **74**, 043411 (2006); and *Virtual Journal of Ultrafast Science* **5** (November 2006), at http://www.vjultrafast.org.

Characterization and applications of isolated attosecond pulses generated with double optical gating

Zenghu Chang
J. R. Macdonald Laboratory, Department of Physics,
Kansas State University, Manhattan, KS 66506, chang@phys.ksu.edu

The goals of this aspect of the JRML program are (1) to measure the pulse width and phase of the single isolated attosecond pulses generated with a double optical gating, (2) to use the isolated attosecond pulses for studying electron dynamics during the autoionization of helium and for directly measuring field distributions in Bessel beams.

1. Temporal characterization of the isolated attosecond pulses generated with a generalized double optical gating, *Ximao Feng, Steve Gilbertson, Hiroki, Mashiko, Sabih Khan, Mike Chini, He Wang, Yi Wu and Zenghu Chang.*

Isolated attosecond pulses are powerful tools for exploring electron dynamics in matter [1]. We developed a double optical gating (DOG) technique for generating single isolated attosecond pulses with multi-cycle pump lasers [2-6]. The pulse duration and phase of such pulses were measured using the Complete Reconstruction of Attosecond Burst (CRAB) method [7-8]. The double optical gating is a combination of the two-color gating and the polarization gating. The DOG allows a wider gate than the polarization gating, which significantly reduces the depletion of the ground state population. The longest pulses one can use for generating single attosecond pulses with DOG are 10 to 15 fs. To loosen the requirement for the laser pulse duration more, we need to reduce the ground state population depletion from the leading edge of the laser pulse. The idea is to create a polarization gating field with two counter-rotating *elliptically* polarized pulses, which is a generalization of double optical gating (GDOG). In the GDOG case, because the field strength before the gate is lower, 20 fs input laser pulses for argon and 30 fs lasers for neon can still generate isolated attosecond pulses.

In our experiment, the laser field for GDOG was created using birefringent optics as shown in Fig. 1 (a). A linearly polarized pulse from a carrier-envelope phase stabilized laser [9-15] was incident on the first quartz plate, which had its optical axis oriented at 45 degrees with respect to the input polarization. This created two orthogonally polarized pulses with a delay between them. The combination of the second quartz plate and a barium borate (BBO) crystal, with their optical axes set in the plane of the input polarization, act as a quarter waveplate. Finally, a fused silica Brewster window was added. Together they created the required polarization gating field with two counter-rotating *elliptically* polarized pulses. The isolated XUV pulses were measured using the CRAB (Complete Reconstruction of Attosecond Bursts) method based on attosecond streaking. A Mach-Zehnder interferometer configuration shown in Fig. 1 (b) was used to control the temporal and the spatial overlap of the attosecond XUV field and the near infrared (NIR) streaking field. Figures 2(a) and (b) show the experimental and retrieved CRAB traces. Figure 2(c) shows the temporal shape and phase of the 260 as XUV pulse. The frequency marginal comparison shows good agreement as indicated in Fig. 2(d). The minor modulation in the spectrogram comes from the attosecond pre- and post-pulses. However, their intensities were three orders of magnitude lower than the main pulse, as shown in the inset of Fig. 2(c). Here, from the reconstructed streaking field the NIR intensity was estimated to be 2.8×10^{11} W/cm^2 at the second gas target. We have also generated single isolated attosecond pulses with 30 fs amplifier laser pulses.

The generation of isolated attosecond pulses with 20 to 30 fs lasers offers two advantages. First, they are much easier to work with than the fragile $\leq$5 fs lasers used in previous attosecond generation experiments. Second, their energy can be much higher than the few-cycle lasers, which allows the scaling of isolated attosecond pulses to the energy level needed for studying nonlinear phenomena.

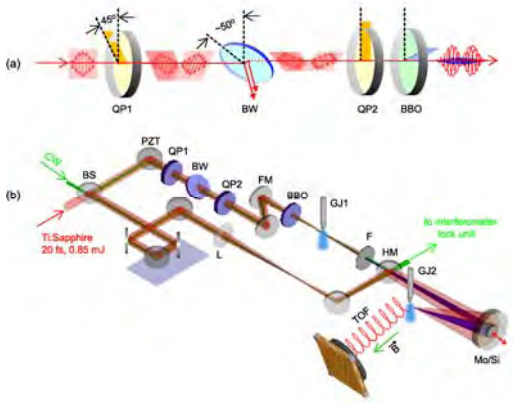

Fig.1 (a) GDOG optics consist of a quartz plate (QP1), a Brewster window (BW), a second quartz plate (QP2) and a BBO crystal. (b) Setup for measuring the single attosecond pulses.

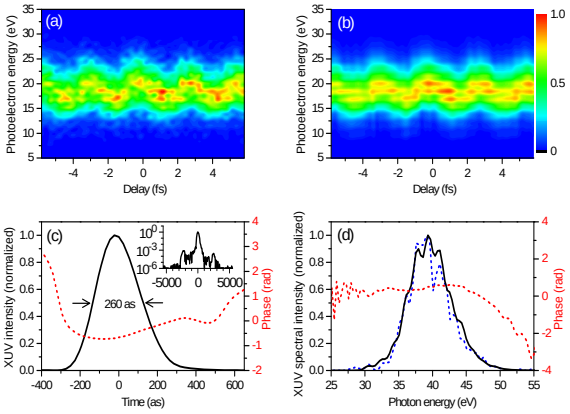

Fig.2 Attosecond XUV pulse generated from argon gas using 20 fs laser pulses. (a) Experimental and (b) Retrieved traces. (c) Retrieved XUV pulse. (d) Measured XUV and the retrieved XUV spectra.

2. Controlling and monitoring electron dynamics in helium atoms. *Steve Gilbertson, Ximao Feng, Michael Chini, Sabih Khan, He Wang, and Zenghu Chang.*

The isolated attosecond pulses generated with a double optical gating allowed us to investigate the much faster electron dynamics in atoms and molecules. Being an atom that has only two electrons, helium is a perfect target for studying correlated electron dynamics. Autoionization is one of the processes dominated by electron-electron interactions. In 1963, it was observed by exciting helium atoms with XUV light from synchrotrons.

When a helium atom in its ground state absorbs an XUV photon with energy of 60.1 eV, a single electron can be emitted leaving the other electron in the ground state of He^+. Alternatively, both electrons can be excited to the 2s2p state. This state can then "autoionize" with one electron returning to the ground state and the other electron being liberated from the atom. The so called "Fano profiles" present in an XUV absorption spectrum from helium is the results of the interference between the direct photoionization channel and the autoionization channel, as depicted in Fig .3. The lifetime of the 2s2p state, estimated from the width of the Fano spectral profile is ~17 fs. Observing the autoionization process in time domain is almost impossible using synchrotron light because its pulse duration is on the picoseconds level.

Recently, we conducted the first experiment on autoionization using isolated attosecond pulses. The scheme is also included in Fig. 3 . An isolated XUV pulse with 136 as duration whose spectrum covers the range from ~30 to 70 eV ionized and doubly excited the helium atom. A 9 fs laser pulse centered at 780 nm also acted on the atom. The intensity of the near infrared (NIR) laser is on the order of $1x10^{12}$ W/cm^2, which is intense enough to ionize the electrons in the 2s2p state before they completely decayed through autoionization. As a result, the contribution from the autoionization to the Fano profile can be controlled by either the laser intensity or the delay between the attosecond excitation pulse and the NIR ionization laser pulse. This allowed us to control the coupling strength of the two channels that interfere or the so called *q* parameter, which was almost impossible to do without using attosecond pulses to start the autoionization process. Thus attosecond pulses make it possible to *control* electron dynamics in atoms. The whole process can be time resolved by streaking the photoelectrons with the NIR laser field.

To observe the controllable autoionization process, we used an interferometric attosecond streak camera that is similar to the one for charactering the attosecond pulses except that detection gas was helium. The attosecond pulses were generated from neon gas with DOG using 1.5 kHz, 9 fs laser pulse centered at 780 nm. The single attosecond pulses were then used to populate the 2s2p resonance in helium. Figure 4(a) shows the spectrogram of the photoelectron from helium as a function of the delay between the attosecond pulse and the IR pulse. The 2s2p autoionization resonance occurs at 35.5 eV in photoelectron energy. When the IR pulse comes first, the resonance is stronger than when it lags behind the XUV pulse. We attribute this to depletion of the autoionization resonance by the IR pulse due to multiphoton ionization. Since the helium atom is in the 2s2p doubly excited state, only 5.2 eV more is required to ionize the atom.

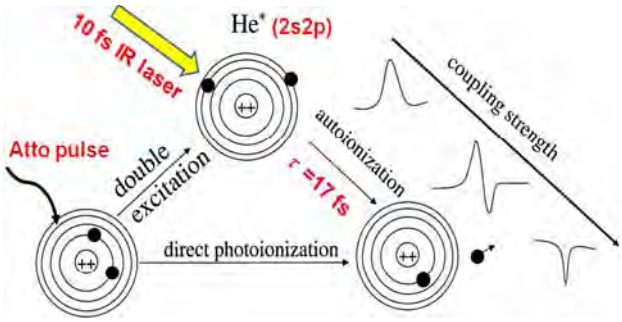

Fig.3 Principle of controlling autoionization of helium. An single isolated XUV pulse starts the process by simultaneously excited the two electrons to the 2s2p state and ionization one of the electrons from the ground state. An intense near infrared 9 fs laser synchronized with the attosecond pulse ionizes the electrons in the 2s2p state before they decay through autoionization. Thus the interference between the two ionization channels is altered.

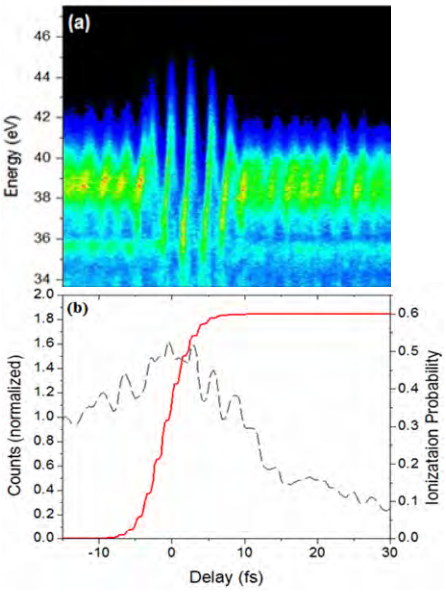

Fig.4 (a) Experimental streaked spectrogram in helium. (b) Calculated ionization probability.

The PPT ionization rate was used to estimate of the depletion of the doubly excited state. The intensity of the IR field was estimated to be ~7 x 10 ^{11} W/cm^2. This yielded a final ionization probability of 0.6 as shown in figure 4(b). Also shown is the total counts integrated over the width of the 2s2p resonance as a function of delay. These results confirms that the coupling strength of the two ionization channels, direct and auto, can be controlled by varying the IR intensity and delay.The experimental results was explained by calculations based on the strong field approximation (SFA). In this model, the XUV attosecond field simultaneously can either excite the two ground state electrons to the 2s2p discrete resonance state, or free one of them to the continuum states. The resonant state then autoionizes into the continuum with decay amplitude given by $\frac{\Gamma}{2}(q-i)e^{-iE_r t-\frac{\Gamma t}{2}}$, where E_r is the resonance energy and Γ is the resonance width. The parameter q indicates the relative probability of excitation to the resonant state and direct photoionization to the continuum. Finally, both the direct photoionized and autoionized electrons propagate in the NIR field. The results agreed well with the experiments.

The isolated attosecond pulses were also used in mapping out the electric field in a femtosecond Bessel beam[16]. We have participated in studying dynamics in molecules (lead by Ben-Itzhak) [17,18], and x-ray lasers (lead by Rocca at Colorado State University) [19]. We also worked on micro-machining using the ultrafast lasers lead by Lei at KSU [20].

PUBLICATIONS (2007-2009) (All publications in 2006 and most of 2007 papers are not included):

1. P. B. Corkum and Z. Chang, "*The attosecond revolution*," Optics and Photonics News **19**, 24 (2008).
2. H. Mashiko, S. Gilbertson, C. Li, S. D. Khan, M. M. Shakya, E. Moon, and Z. Chang, "*Double optical gating of high-order harmonic generation with carrier-envelope phase stabilized lasers*," Phys Rev. Lett. **100**, 103906 (2008).
3. Z. Chang, " *Controlling attosecond pulse generation with a double optical gating*," Phys. Rev. A **76**, 051403(R) (2007).
4. S. Gilbertson, H. Mashiko, C. Li, S. D. Khan, M. M. Shakya, E. Moon, and Z. Chang, ***"****A low-loss, robust setup for double optical gating of high harmonic generation*," Appl. Phys. Lett. **92**, 071109 (2008).
5. H. Mashiko, S. Gilbertson, C. Li, E. Moon, and Z. Chang, "*Optimizing the photon flux of double optical gated high-order harmonic spectra*," Phys. Rev. A **77**, 063423 (2008).
6. S. Gilbertson, H. Mashiko, C. Li, E. Moon, and Z. Chang, "*Effects of laser pulse duration on extreme ultraviolet spectra from double optical gating*," Appl. Phys. Lett. **93**, 111105 (2008).
7. H. Wang, M. Chini, S. D. Khan, S. Chen, S. Gilbertson, X. Feng, H. Mashiko and Z. Chang, "*Practical issues of retrieving isolated attosecond pulses*," J. Phys. B: At. Mol. Opt. Phys. **42**, 134007 (2009).
8. M. Chini, H. Wang, S. D. Khan, S. Chen, and Z. Chang, ***"****Retrieval of Satellite Pulses of Single Isolated Attosecond Pulses*," Appl. Phys. Lett. **94**, 161112 (2009).
9. C. Li, H. Mashiko, H. Wang, E. Moon, S. Gilbertson, and Z. Chang, ***"****Carrier-envelope phase stabilization by controlling compressor grating separation*," Appl. Phys. Lett. **92**, 191114 (2008).
10. Eric Moon, He Wang, Steve Gilbertson, Hiroki Mashiko and Zenghu Chang, "*Carrier-envelope phase stabilization of grating-based chirped-pulse lasers*," Laser and Photonics Reviews, DOI 10.1002/lpor.200810060 (2009).
12. H. Wang, M. Chini, Y. Wu, E. Moon, H. Mashiko and Z. Chang, "*Carrier-envelope phase stabilization of 5 fs, 0.5 mJ, pulses from adaptive phase modulators*," Applied Physics B, DOI 10.1007/s00340-009-3639-0 (2009).
13. H. Wang, E. Moon, M. Chini, H. Mashiko, C. Li, and Z. Chang, " *Coupling between energy and carrier-envelope phase in hollow-core fiber based f-to-2f interferometers*," Optics Express **17**, 12089 (2009).
14. H. Mashiko, C. M. Nakamura, C. Li, E. Moon, H. Wang, J. Tackett, and Zenghu Chang, "*Carrier-envelope phase stabilized 5.6 fs, 1.2 mJ pulses*," Appl. Phys. Lett. **90**, 161114 (2007).
15. H. Wang, Y. Wu, C. Li, H. Mashiko, S. Gilbertson, and Z. Chang, " *Generation of 0.5 mJ, few-cycle laser pulses by an adaptive phase modulator*," Optics Express 16, 14448 (2008).
16. Steve Gilbertson, Ximao Feng, Sabih Khan, Michael Chini, He Wang, Hiroki Mashiko, and Zenghu Chang, " *Direct measurement of an electric field in femtosecond Bessel-Gaussian beams*," Optics Letters34, 2390 (2009) .
17. J. McKenna, A. M. Sayler, F. Anis, B. Gaire, Nora G. Johnson, E. Parke, J. J. Hua, H. Mashiko, C. M. Nakamura, E. Moon, Z. Chang, K. D. Carnes, B. D. Esry, and I. Ben-Itzhak, "*Enhancing high-order above-threshold dissociation of H_2^+ beams with few-cycle laser pulses*," Phys. Rev. Lett. **100,** 133001 (2008).
18. I. Ben-Itzhak, P. Q. Wang, A. M. Sayler, K. D. Carnes, M. Leonard, B. D. Esry, A. S. Alnaser, B. Ulrich, X. M.Tong, I. V. Litvinyuk, C. M. Maharjan, P. Ranitovic, T. Osipov, S. Ghimire, Z. Chang, and C. L. Cocke, "*Elusive enhanced ionization structure for H_2^+ in intense ultrashort laser pulses*," Phys. Rev. A **78,** 063419 (2008).
19. Y. Wang, M. Berrill, F. Pedaci, M.M. Shakya, S. Gilbertson, Z. Chang, E. Granados, B. M. Luther, M. A. Larotonda, J.J. Rocca, "*Measurement of 1 picosecond soft x-ray laser pulses from an injection-seeded plasma amplifier*," Phys. Rev. A **79**, 023810, (2009).
20. S. Lei, S. Devarajan, and Z. Chang, "*A comparative study on the machining performance of textured cutting tools with lubrication*," Int. J. Mechatronics and Manufacturing Systems **2**, 401 (2009).

Structure and Dynamics of Atoms, Ions, Molecules and Surfaces:
Two-color probing of atomic and molecular systems and EUV/IR pump-probe experiments

C.L.Cocke, Physics Department, J.R. Macdonald Laboratory, Kansas State University, Manhattan, KS 66506, cocke@phys.ksu.edu

During the past year we have concentrated at KSU on two projects. We have used two-color (800nm/400nm) beams to investigate left-right asymmetry in the emission of electrons from Xe and the dissociation of H_2 and D_2. We have used a EUV/IR pump-probe setup to continue our investigation of the ionization of He in the presence of an IR field and to investigate the IR induced gerade/ugerade mixing in D_2^+ after the production of this molecule by a EUV pulse. We have continued to pursue collaborations at the ALS and JILA/Univ. of Colorado.

Recent progress:

1.Two-color experiments: *D. Ray, W. Cao, Z.Chen, S.De, H.Machiko, K.P.Singh, P.Ranitovic, I.Znakovskaya, G.G.Paulus, M.F.Kling, C.D.Lin, I.V.Litvinyuk and C.L.Cocke*. We have developed a compact, robust, in-line optical system which converts an 800nm laser beam into a superposition of 800nm and 400nm with adjustable phase between the two colors. Such a field has a controlled left/right asymmetry and allows us to study effects similar to those seen with CEP (carrier-envelope-phase) stabilized beams [1]. We have performed two types of experiment: (1) In collaboration with the group of C.D.Lin we have used theoretical quantitative rescattering modeling of the plateau component of the Xe electron spectrum to deduce, from an experimental spectrum, the intensities of both components of the two-color field and the relative phase. Especially the phase is very reliably extracted from this analysis. A manuscript is in preparation. (2) We have measured the asymmetric emission of $D^+(H^+)$ ions from the fragmentation of $D_2(H_2)$ by such a two-color field [2,3]. A strong dependence of the asymmetry on the ion energy is found. Different dependences of the asymmetry on the phase of the two colors is found in three regions of ion energy release, namely one photon, two photon and rescattering dissociation regions. A sample spectrum is shown in fig. 1. A model calculation carried out by F.He [4,5] and U.Thumm reproduces many of the observed effects. The physical process in play for the rescattering component is similar to that reported with CEP stabilized pulses by Kling et al. [1]; the behavior of the asymmetry in the low ion energy region has not been previously reported. This work has been submitted for publication.

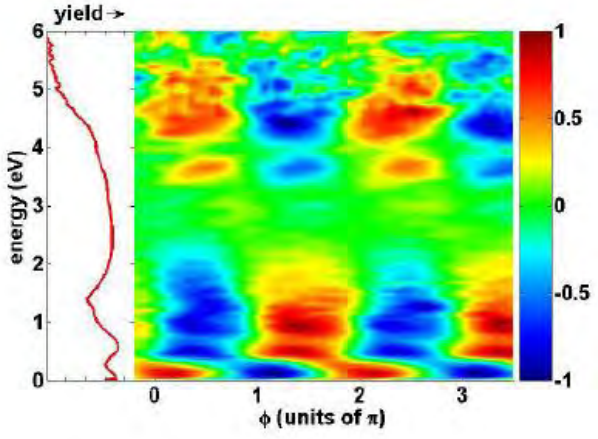

Fig 1. Left/right asymmetry plotted as a density plot for D^+ ions emitted from the application of a two-color field to D_2 molecules, as a function of the phase angle between the two colors and the energy of the emitted ion. Different patterns are seen in one photon (<.03 eV), two photon (0.4-2 eV) and rescattering (4-6 eV) regions.

2. EUV/IR Pump/probe experiments: He. *P.Ranitovic, B.Gramkow, D.Ray, I.Bocharova, H.Mashiko, M.Trachy, S.De, K. Singh, W.Cao, I.Litvinyuk, A.Sandhu, E.Gagnon, M.Murnane, H.Kapteyn, X-M.Tong, C.L.Cocke.* The manipulation in real time of electronic and vibrational wave packets using an EUV pulse from harmonic generation to provoke an electronic excitation or ionization and an IR field to influence the subsequent evolution of the wave function is a common theme in attosecond science. We have set up an apparatus for doing such experiments. This section describes the first of two such experiments performed to date with the apparatus. Pump probe experiments have been carried out using an attosecond pulse train (APT) in the EUV as a pump and a short infrared pulse (~1x10 ^{13} w/cm^2, 50 fs) as a probe. The reaction products are detected in a COLTRIMS geometry, which allows ion-electron coincidences to be measured. The apparatus was described in last year's abstract. The EUV harmonics (11th through 17th) generated from Xe ionize the He in the presence of an IR field. The yield of He^+ ions is measured as a function of the time delay between the IR and the EUV . Sample results are shown in fig. 2.

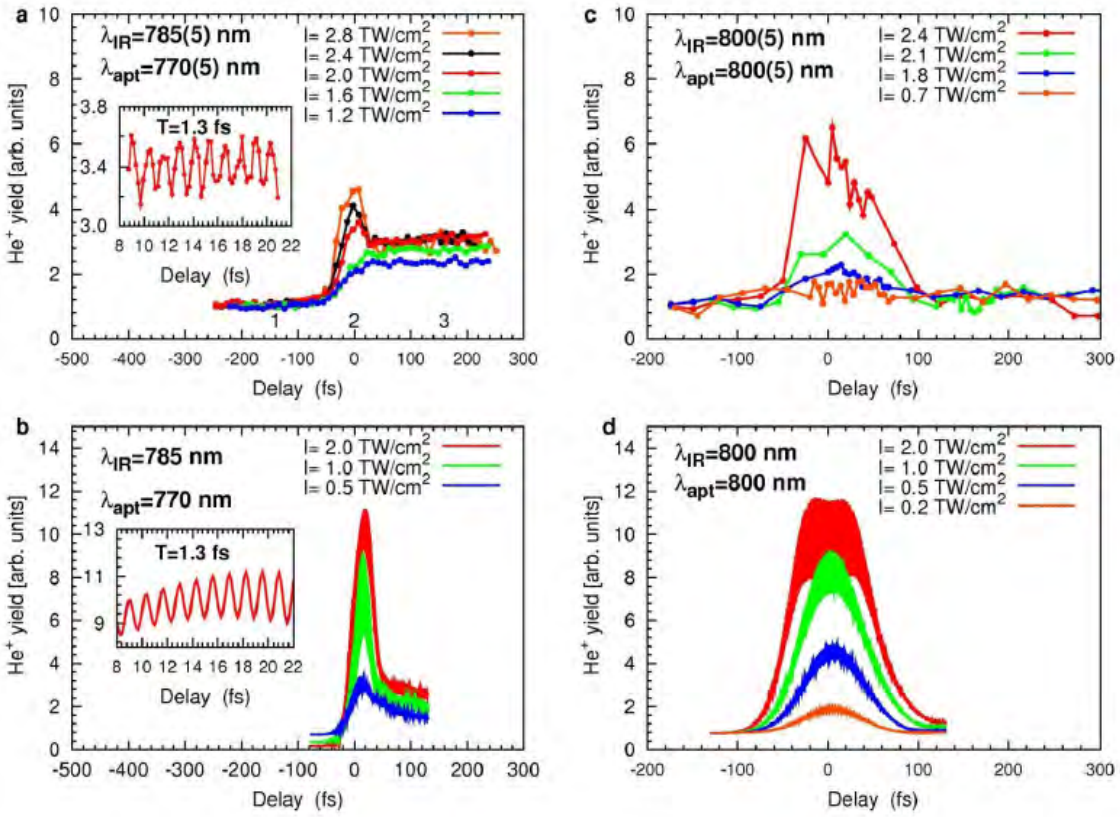

Fig.2. (a,c) The experimental yield of He^+ ions as a function of the time delay between an APT and IR is shown for two different IR wavelengths. If the IR comes first, only the 17th harmonic (relatively weak) can ionize the He. If the IR comes last, for the shorter wavelength IR the 15th harmonic is resonant with the 1s4p state of neutral He and excites it strongly; the 4p electron is then later removed by the IR. In the overlap region, the yield of He^+ depends on the instant of time at which the APT strobes the atom: when the IR field is strong, strong absorption occurs through the broadened 1s4p and 1s2p resonances. This occurs twice per IR cycle[6], giving rise

to an oscillatory yield (see inset) with a periodicity of half the optical period. (b,d)Theoretical calculations corresponding to the experimental data of (a,c).

The experimental results are compared with a solution to the time-dependent Schroedinger equation carried out by X.-M.Tong. Good agreement between theory and experiment is found. The theoretical results show clearly that the He resonances and exact harmonic energies play a crucial role in determining the outcome of the EUV/IR ionization. This work has been submitted for publication.

3. EUV/IR Pump/probe experiments: D_2. *K. P. Singh, W. Cao, P. Ranitovic, S. De, F. He, D. Ray, S. Chen, U. Thumm,A. Becker, M. M. Murnane, H. C. Kapteyn, I. Litvinyuk, C. L. Cocke*. This project is a continuation of the IR/APT work discussed above and was carried out with the same apparatus. In this case, a two-color IR field was used to produce the 11th through 17th harmonics, including both even and odd order to produce one attosecond "strobe" per IR cycle. The yield of D^+ ions from the dissociation of the molecule was measured as a function of the direction of emission of the ions and the relative phase of the IR and APT. The purpose of the experiment was to see if the IR can be used to steer the electronic wave cloud in such a way as to control the left-right location of the electron at the time it becomes localized on one of the two nuclei during the dissociation of the molecule. A similar effect was seen by Kling et al. [5] using CEP locked pulses, with no APT involved. The results are shown in fig. 3, where a clear oscillation of the asymmetry is seen. A model calculation by F.He and U.Thumm shows good agreement with the results. This work has been submitted for publication.

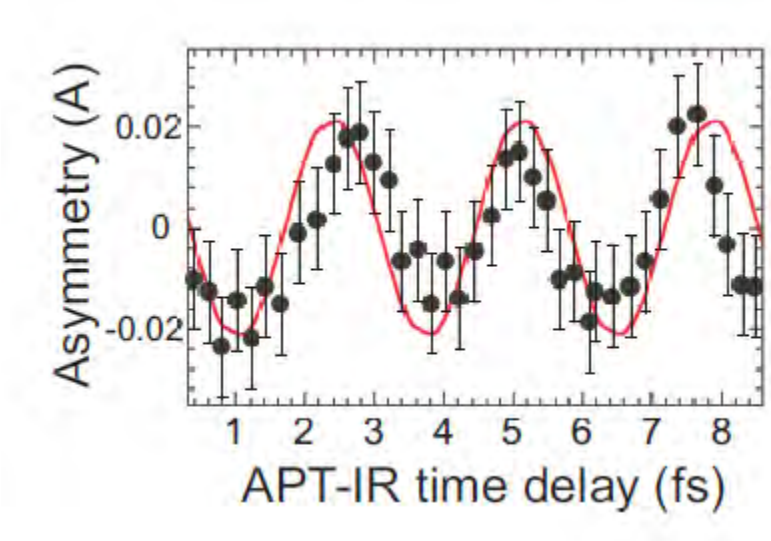

Fig. 3. The asymmetry parameter *A* versus the APT-IR time delay Circles: experimental data, solid line: theory. The data have been smoothed using three-point run-ning average of raw data. The error bars denote the statistical error in total D^+ counts for the averaged data. The positive delays correspond to the APT following the IR pulse.

4. Collaborations: Continuing collaborative work with a large collaboration at the ALS, LBL and with the group of Murnane and Kapteyn at JILA/CU has continued. Publications 2,5 and 6 are collaborative works.

Some publications not previously cited from 2008-2009:

1) "Control of electron localization in molecules using XUV and IR pulses",K. P. Singh, W. Cao, P. Ranitovic, S. De, F. He, D. Ray, S.,Chen, U.Thumm, A. Becker, M. M. Murnane, H. C.Kapteyn, I. Litvinyuk, C. L. Cocke, submitted (2009).

2) "IR-Assisted Ionization of Helium by Attosecond XUV Radiation", P. Ranitovic, Xiao-Min Tong, B. Gramkow, S. De, B. DePaola, K. P. Singh, W. Cao, M. Magrakvelidze, D. Ray, I. Bocharova, H. Mashiko, A. Sandhu, E. Gagnon, M. M. Murnane, H. C. Kapteyn, I. Litvinyuk and C. L. Cocke, submitted (2009).

3) "Ion-energy dependence of asymmetric dissociation of D_2 by a two-color laser field", D. Ray, F. He, W.Cao, S. De, H. Mashiko , P.Ranitovic ,K.P.Singh, I. Znakovskaya, U. Thumm, G.G.Paulus, M.F.Kling, I. Litvinyuk, and C.L. Cocke, submitted (2009).

4) "Photo-double-ionization of H_2 : Two-center interference and its dependence on the internuclear distance", M. S. Schöffler et al., Phys. Rev. A 78,013414 (2008).

5) "Observing the Creation of Electronic Feshbach Resonances in Soft X-ray–Induced O_2 Dissociation", Arvinder S. Sandhu, Etienne Gagnon, Robin Santra, Vandana Sharma, Wen Li, Phay Ho, Predrag Ranitovic, C. Lewis Cocke, Margaret M. Murnane, and Henry C. Kapteyn, *Science* 14, 1081 (2008).

6) "Angular Correlation between Photoelectrons and Auger Electrons from K-Shell Ionization of Neon", A.L. Landers, F. Robicheaux, T. Jahnke, M. Schöffler, T. Osipov, J. Titze, S. Y. Lee, H. Adaniya, M. Hertlein, P. Ranitovic, I. Bocharova, D. Akoury, A. Bhandary, Th. Weber, M. H. Prior, C. L. Cocke, R. Dörner, and A. Belkacem , Phys. Rev. Lett. 102, 223001 (2009)

References:

[1] B. Sheehy *et al.*, *Phys. Rev. Lett.* **74**, 4799 (1995).
[2] M. R. Thompson, *et al., J. Phys. B: At. Mol. Opt. Phys.* **30**, 5755 (1997).
[3] F. He *et al.*, Phys. Rev. Lett **99**, 083002 (2007)
[4] F. He, C. Ruiz, and A. Becker, *J. Phys. B* ***41***, 081003
(2008).
[5] M. F. Kling *et al.*, *Science* **312**, 246 (2006).
[6] P.Johnsson *et al., Phys.Rev.Lett.* **99**, 233001 (2007).

Coherent Control of Ladder Excitation and Photoassociation with Excitation Using Shaped Ultrafast Optical Pulses

B. D. DePaola
J. R. Macdonald Laboratory Department of Physics
Kansas State University
Manhattan, KS 66056
depaola@phys.ksu.edu

Program Scope

This work focusses on using shaped ultrafast optical pulses to (1) resonantly excite an atomic ladder system, and (2) optimally cause photoassociation with excitation. In both of these projects, the focus is on cold ^{87}Rb in a magneto-optical trap (MOT). We do not believe there is any intrinsic value in cold excited Rb in either atomic or molecular form, however it makes an excellent model system for trying to understand the underlying physics in both of these processes.

Ladder Excitation

The process under study here can be represented by

$$Rb\left(5s_{1/2}\right) \rightarrow Rb\left(5p_{3/2}\right) \rightarrow Rb\left(5d_{3/2,5/2}\right) \rightarrow Rb^{+}, \tag{1}$$

where all three transitions come from the same ultrafast laser pulse. The idea is to measure the relative probability of exciting to the $Rb\left(5d_{3/2,5/2}\right)$ states as the spectral phase of the laser pulse is varied. This relative efficiency is determined by measuring the Rb^{+}, which is produced in the same laser pulse through the photoionization of $Rb\left(5d_{3/2,5/2}\right)$. Rb is an ideal candidate for this sort of measurement because all three transition wavelengths are well within the bandwidth of a "standard" Ti:Sapphire laser: The $5s_{1/2} - 5p_{3/2}$ transition is at 780 nm; the $5p_{3/2} - 5d$ transition is at 776 nm; and the photoionization threshold is roughly 1254 nm. The central wavelength of the Kansas Light Source (KLS) system is 790 nm with a bandwidth in excess of 30 nm. Excitation of the Rb system has, of course, been studied before, most notably by the group of Silberberg. [1] In that work, 420 nm radiation from the last step of the $Rb\left(5d_{5/3,3/2}\right) \rightarrow Rb\left(5p_{3/2}\right) \rightarrow Rb\left(5s_{1/2}\right)$ cascade was detected. One advantage of using the ion signal is a much greater detection efficiency.

In one KSU experiment, the relative excitation efficiency was measured as a function of λ_1 and λ_2 for a spectral phase "pulse", approximately described by

$$\phi(\lambda) = \begin{cases} 0 & \lambda \leq \lambda_1 \\ \pi/2 & \lambda_1 < \lambda < \lambda_2 \\ 0 & \lambda \geq \lambda_2, \end{cases} \tag{2}$$

The spectral phase was shaped by a commercial acousto-optic modulator (AOM) based device. Because the temporal length of an optical pulse is limited by the physical length of the AOM crystal,

the infinitely sharp edges described in Eq. 2 was approximated by an error function having a rise of roughly $\pm\pi/2$ over 2 nm. The prediction of second order perturbation theory is that excitation should be enhanced when λ_1 and/or λ_2 coincides with the two resonant wavelengths, 780 nm and 776 nm.

Excitation was also measured as a function of a sinusoidal spectral phase, given by

$$\phi(\lambda) = A \sin\left[2\pi cT\left(\lambda^{-1} - \lambda_0^{-1}\right) + \phi_0\right], \tag{3}$$

where A, T, and ϕ_0 are parameters, and λ_0 is an arbitrary constant, chosen to be at the peak of the spectral intensity of the laser. In these experiments, A was set to π, thus allowing the phase to change over the range of $\pm\pi$.

Photoassociation with Excitation

Photoassociation [2] is the process by which colliding pairs of ultracold atoms are induced to form a molecule by means of a catalysis photon. In the specific case of Rb, the process can be represented by:

$$Rb(5s) + Rb(5s) + \hbar\omega \rightarrow Rb_2(5s, 5p) \rightarrow Rb_2(5s, 5s) + \hbar\omega' \tag{4}$$

Here, ω is the optical frequency of the catalysis photon, and $\hbar\omega'$ is the energy of the photon that is emitted when the excited molecule relaxes to its electronic ground state. In our work we are particularly interested in a special form of photoassociation in which an additional photon brings the molecule to a doubly excited molecular state. [Pub. #1,2] Because this process consists of photoassociation followed by excitation, it is referred to as PAE. In the work described here, the same ultrafast laser pulse that provides the catalysis photon, also excites the molecule to the $Rb_2(5p, 5p)$ manifold, the final step in the PAE process. The $Rb_2(5p, 5p)$ manifold is then probed with a narrow linewidth cw laser which excites to an autoionizing state in the $Rb_2(5p, 4d)$ manifold. [Pub. #2] *The goal of this project is to measure the extent to which shaping the spectral phase of the pulse can enhance the PAE process.* The phases used for coherent ladder excitation were also used here for PAE. In these experiments, it was also found to be advantageous to additionally measure the time between the initiation of the PAE process and the detection of Rb_2^+: The individual states in the $Rb_2(5p, 4d)$ manifold take different amounts of time to autoionize due to the variations in the curvatures of their molecular potentials. Thus, this "incubation time" helps to further distinguish PAE to different states.

Recent Progress

In the case of atomic ladder excitation, the experimental results were in agreement with the second order perturbation calculations. In the case of the $\pi/2$ spectral phase pulse, this means that horizontal and vertical structures were seen centered around λ_1 and λ_2 equalling the resonant transition wavelengths. In the case of the sinusoidal phase of Eq. 3, a contour plot of Rb_2^+ *versus* T and ϕ_0 yielded a diagonal structures, indicating that, for constant $Rb_2(5p, 5p)$ production rates, T and ϕ_0 are linearly related. That is, the argument of the sine in Eq. 3 is constant. This means that the measured slopes of the diagonal structures are directly related to the transition wavelengths *via*:

$$\lambda = \left[\left(-2\pi c \frac{dT}{d\phi_0}\right)^{-1} + \lambda_0^{-1}\right]^{-1}, \tag{5}$$

a result that might actually be interesting were the resonant frequencies of the system unknown. One aspect of this result that actually *is* interesting is that the contrast in the sinusoidal data is

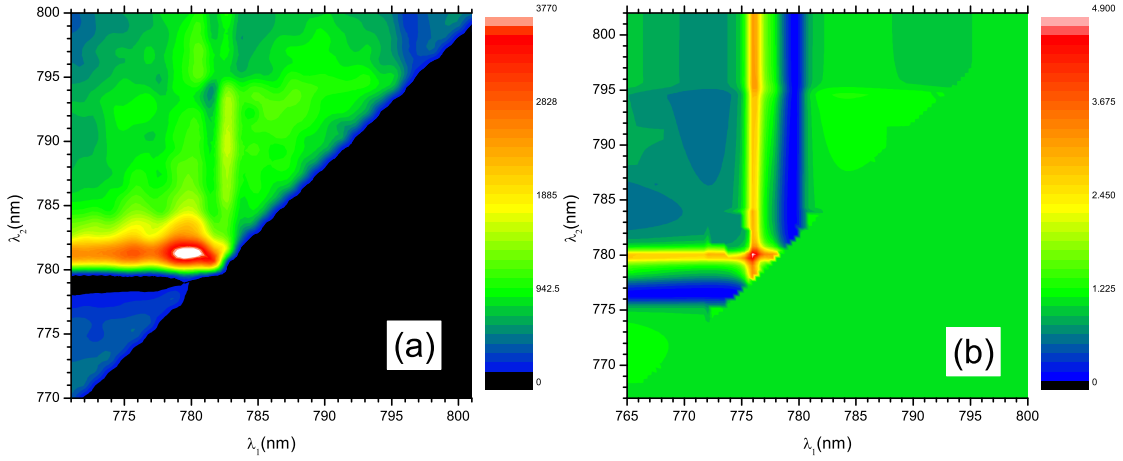

Figure 1: Experimental (a) and theoretical (b) results for the $\pi/2$ spectral phase pulse of Eq. 2. The Rb_2^+ counts are plotted *versus* the wavelengths at which the $\pi/2$ phase changes occur.

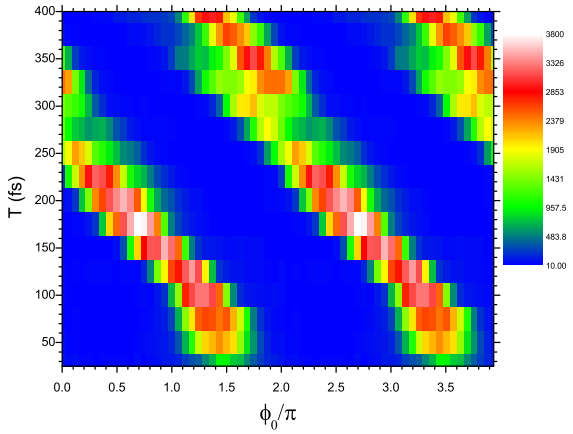

Figure 2: Experimental results for the sinusoidal spectral phase of Eq. 3. The Rb_2^+ counts are plotted *versus* the two parameters ϕ_0 and T. Here, $A = \pi$.

more than an order of magnitude greater than that for the $\pi/2$ pulse data (> 100 compared with ~ 6).

In Figure 1 we show the corresponding measurement (a), and calculation (b) for PAE. In this figure we plot Rb_2^+ counts versus λ_1 andλ_2 for the $\pi/2$ phase pulse of Eq. 2.

While the qualitative agreement between theory and experiment is striking, some quantitative differences remain. It is very likely that these are due to the simplicity of the model, in which the bands of molecular energy levels are approximated by a few discrete levels. Furthermore, these levels are modeled as being independent of internuclear separation. More sophisticated modeling will have to be done before we can say with any confidence that we completely understand the process.

The PAE result for the sinusoidal phase of Eq. 3 is shown in Fig. 2. Here, we plot only the counts from the Rb_2^+ ions that took the longest to arrive at the detector, thus limiting the molecular states that are measured. The same information about PAE is contained in Fig. 2 as in Fig. 1. However, the contrast in the sinusoidal phase data is much greater than in the $\pi/2$ pulse data.

Future Plans

In the future, we will continue our measurements of PAE, and effects of various spectral phases on it. We will also try to improve our modeling of the process by using more realistic potential curves. The measurement of the incubation time of the molecular ions is very important in isolating a single state in a molecular manifold. However, we have no idea what that state is. We will therefore continue our cw PAE measurements [Pub. #1]; by scanning the probe laser, we hope to learn more about the structure of the manifold of autoionizing states.

References

1. N. Dudovich, B. Dayan, S. M. Gallagher-Faeder, and Y. Silberberg, Phys. Rev. Lett. **86**, 47 (2001).

2. K. M. Jones, E. Tiesinga, P. D. Lett, and P. S. Julienne, Rev. Mod. Phys. **78**, 483 (2006).

Recent Publications

1. "Photoassociation in Cold Atoms via Ladder Excitation", M. L. Trachy, G. Veshapidze, M. H. Shah, H. U. Jang, and B. D. DePaola, Phys. Rev. Lett. **99**, 043003 (2007).

2. "Pathway for Two-Color Photoassociative Ionization with Ultrafast Optical Pulses in a Rb Magneto-Optical Trap", G. Veshapidze, M. L. Trachy, H. U. Jang, C. W. Fehrenbach, and B. D. DePaola, Phys. Rev. A **76**, 051401(R) (2007).

3. "An Auto-Incrementing Nanosecond Delay Circuit", H. U. Jang, J. Blieck, G. Veshapidze, M. L. Trachy, and B. D. DePaola, Rev. Sci. Instrum. **78**, 094702 (2007).

4. "MOTRIMS: Magneto-Optical Trap Recoil Ion Momentum Spectroscopy", B. D. DePaola, R. Morgenstern, and N. Andersen, Adv. At. , Mol. , Opt. Phys. **55**, 139-189 (2007).

5. "Measurement of Population Dynamics in Stimulated Raman Adiabatic Passage", M. A. Gearba, H. A. Camp, M. L. Trachy, G. Veshapidze, M. H. Shah, H. U. Jang, and B. D. DePaola, Phys. Rev. A **76**, 013406 (2007).

6. "Model-Independent Measurement of the Excited Fraction in a Magneto-Optical Trap", M. H. Shah, H. A. Camp, M. L. Trachy, G. Veshapidze, M. A. Gearba, and B. D. DePaola, Phys. Rev. A **75**, 053418 (2007).

Time-dependent Treatment of Three-body Systems in Intense Laser Fields

B.D. Esry
J. R. Macdonald Laboratory, Kansas State University, Manhattan, KS 66506
esry@phys.ksu.edu
http://www.phys.ksu.edu/personal/esry

Program Scope

The primary goal of my program is to quantitatively understand the behavior of simple benchmark systems in ultrashort, intense laser pulses. As we gain this understanding, we will work to transfer it to other more complicated systems. In this effort, my group works closely with the experimental groups in the J.R. Macdonald Laboratory, including, in particular, the group of I. Ben-Itzhak.

A second component of my program is to develop novel analytical and numerical tools to (i) more efficiently and more generally treat these systems and (ii) provide rigorous, self-consistent pictures within which their non-perturbative dynamics can be understood. The ultimate goal is to uncover the simplest picture that can explain the most.

1. Carrier-envelope phase effects and coherent control

Recent Progress Beginning with Ref. [1], we have been investigating the impact of the carrier-envelope phase (CEP) of few-cycle pulses on atoms and molecules. The CEP, φ, is defined from the laser's electric field as $\mathcal{E}(t)=\mathcal{E}_0(t)\cos(\omega t+\varphi)$ for some pulse envelope $\mathcal{E}_0(t)$ and carrier frequency ω. We have mainly focused on its consequences for the dissociation of H_2^+ and its isotopes [1,2,P3,P12], although we have recently submitted a study of CEP effects on atomic excitation [3].

In parallel, we have been developing a general theory of CEP effects that allows much to be done analytically [P4,P12,4]. As a consequence, this theory provides a convenient, simple picture within which CEP effects can be understood and simple predictions made without any time-dependent calculation. The essential point is that our picture recasts CEP effects as interference between multiphoton pathways whose relative phases depend on the CEP. In other words, CEP effects are a manifestation of the canonical Brumer-Shapiro control scheme.

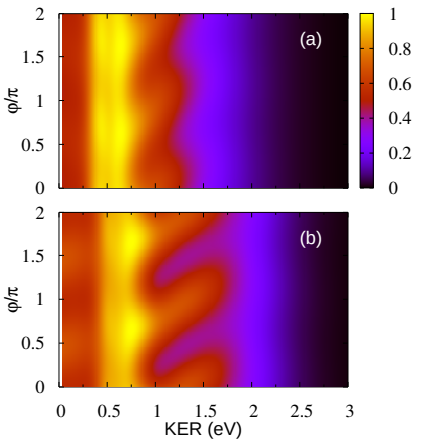

Figure 1: The total dissociation probability $P(E)$ for (a) H_2^+ and (b) D_2^+ in a 5.9 fs, 10^{14} W/cm^2 laser pulse. Each panel is normalized to unity at its overall peak value to facilitate qualitative comparison. (Adapted from [P12]).

Figure 1 shows a typical result for the total dissociation probability of H_2^+ and D_2^+ in a few-cycle pulse, calculated in the standard two-channel ($1s\sigma_g$ and $2p\sigma_u$) approximation that neglected nuclear rotation and constrained the nuclei to motion along the polarization direction [P12]. What is surprising about these is that CEP effects are usually studied as asymmetries. Right-left asymmetries of atomic ionization along the laser polarization is the usual example (see [5], for instance). Figure 1 shows quite strong CEP effects, though, in the *total* dissociation probability, and D_2^+ shows stronger effects than H_2^+. Unfortunately, my student, Fatima Anis, recently performed similar calculations — but including nuclear rotation (see [P6] and [P13] for related details) — and found *no* CEP effect in the total dissociation probability. This would not be the first example of artifacts generated in this common model for H_2^+ that vanished in a more complete calculation [P6,P13,6].

Fortunately, Fatima's calculations show that the dissociation asymmetry we predicted in [P12] survives the addition of nuclear rotation with little modification. For H_2^+ dissociation, "asymmetry" refers to the direction of the proton in the reaction products p+H relative to the laser polarization. In a long pulse, the proton has equal probability to go left and right. But, this symmetry is broken in a short pulse, and the breaking is controlled by the CEP. Figure 2 shows the normalized asymmetry, defined as $P_{\rm Left}$–$P_{\rm Right}/2P_{\rm avg}$, calculated without nuclear rotation [P12]. The normalization factor, $P_{\rm avg}$, is the CEP-averaged dissociation probability.

Based on our general theory of CEP effects [P4,P12], the nuclear wave function for the H_2^+ model above, $\mathbf{F}^T(R,t)=(F_g(R,t),F_u(R,t))$, can be written as

$$\mathbf{F}(R,t) = \sum_{n=-\infty}^{\infty} e^{in\varphi}\mathbf{F}_n(R,t) \qquad (1)$$

using only the fact that the wave function must be periodic in the CEP φ. Our analysis in [P4,P12] shows that the φ-independent components $\mathbf{F}_n(R,t)$ can be thought of as n-photon amplitudes. Projecting $\mathbf{F}(R,t)$ onto the appropriate outgoing-wave scattering states and taking dipole selection rules into account [P12], the asymmetry $\mathcal{A}=P_{\rm Left}-P_{\rm Right}$ can be obtained,

$$\mathcal{A} = 2\sum_{\substack{n\ \text{even}\\ n'\ \text{odd}}} \mathrm{Re}\left(e^{i(n-n')\varphi}e^{i(\delta_g-\delta_u)}\langle gE|F_n\rangle\langle uE|F_{n'}\rangle^*\right), \qquad (2)$$

in terms of the scattering phase shifts $\delta_{g,u}$ and scattering states $|(g,u)E\rangle$. There are several things to note in this expression. First, the only CEP-dependent factors are the exponentials $\exp[i(n–n')\varphi]$; all other factors are CEP-independent. Thus, the only CEP dependence is analytical. Second, the CEP dependence must have periodicity $2\pi/(2m–1)$, m=1,2,3,.... Third, to have any CEP dependence, the amplitudes $\langle(g,u)E|F_n\rangle$ for different photon processes n must contribute at the same energy. It is primarily this requirement that leads to the need for broad bandwidth, intense laser pulses. For $\mathcal{A}(E)$, only the interference between different photon processes of *different* molecular channels is important. One can similarly show that it is the interference between different photon processes in the *same* molecular channel that generates CEP effects in the total dissociation probability in Fig. 1.

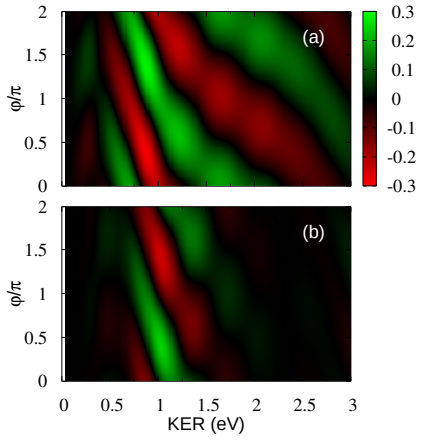

Figure 2: The normalized dissociation asymmetry for (a) H_2^+ and (b) D_2^+ in a 5.9 fs, 10^{14} W/cm^2 laser pulse. (Adapted from [P12]).

We have recently extended this analysis to He in an infrared (IR) pulse overlapped with an attosecond pulse train (APT) [4], showing that the delay τ between the two acts as a control parameter in much the same way as φ above. Analytic expressions for physical observables analogous to Eq. (2) can be derived and provide similar insight. A key conclusion of this analysis is that such IR+APT experiments are very conveniently thought of as multi-color control experiments in the same vein as two-color experiments — and as CEP experiments per the discussion above.

Future Plans We will continue to develop and apply our general theory for CEP effects to both atomic and molecular systems. In particular, since our method can simultaneously treat fields with CEP, two-color delay, and IR+APT delay, we can unify these seemingly distinct kinds of experiments into a single picture. This will be a timely contribution, especially since experiments themselves are already starting to combine such fields (see C.L. Cocke's abstract, for instance). Additionally, we will apply our analysis for He — which is backed up by full-dimensional, two-electron solutions of the time-dependent Schrödinger equation — to the relevant experiments in our Lab (see C.L. Cocke's and Z. Chang's abstracts). We will especially continue to focus on fully understanding the control of H_2^+ via any of the means listed above, an effort which has seen recent progress by I. Ben-Itzhak's group.

2. Vibrational trapping in H_2^+ — or the lack thereof

Recent progress My group collaborates closely with I. Ben-Itzhak's experimental group as can be seen by our many joint publications. This has been an especially fruitful collaboration from our viewpoint as his is one of the few groups that can use an H_2^+ beam as a target for intense laser studies, raising our hopes of a complete theoretical treatment for this benchmark system.

We have, in fact, uncovered new phenomena in this "understood" system. Publication [P7], for instance, is a joint work in which theory is used to show that the H_2^+ states correlating to the n=2 manifold of H play a clear role in the experiment, thus showing a shortcoming of the standard two-channel model. Moreover, we showed there that the nuclear kinetic energy spectrum showed evidence of above-threshold dissociation through these excited states.

In a more recent submission [7], we revisited the rather old notion of vibrational trapping in H_2^+. Vibrational trapping, sometimes called bond-hardening, is a phenomenon which is usually explained in terms of the Floquet potentials and consists of a portion of the vibrational wave function getting trapped in

a light-induced potential well. The primary observable consequence — either theoretically or experimentally — is the reduced dissociation probability for excited vibrational states which is attributed to their being preferentially caught in the well. Vibrational trapping is typically mentioned as an intense-field phenomenon and can be easily seen in a standard two-channel calculation of H_2^+ dissociation in an intense laser. We had explored this phenomenon theoretically to some extent in [P6] and concluded, as others had before (see references in [P6]), that including nuclear rotation essentially eliminates the more extreme form of trapping in which the dissociation probability actually decreases with increasing laser intensity. The higher vibrational states did, however, still show a lower dissociation probability even though one photon was more than enough to dissociate them.

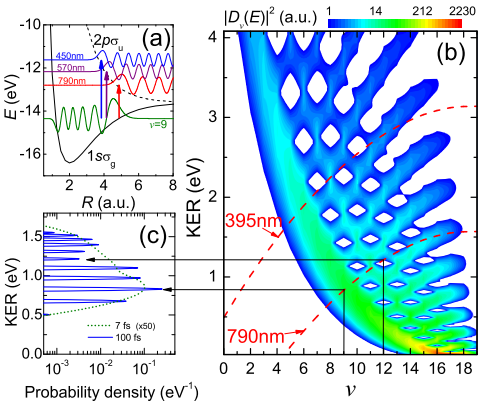

Figure 3: (a) H_2^+ potentials and wave functions. (b) The H_2^+ vibrational dipole matrix elements ($|D_v(E)|^2$). The dashed lines indicate the results for 790 nm and 395 nm photons. (c) Spectrum for H_2^+ dissociation at 790 nm from perturbation theory at 4×10^{10} W/cm^2 for 7 fs and 100 fs pulses, after Franck-Condon averaging the initial vibrational distribution. (Adapted from Ref. [7].)

Figure 3 explains why the higher vibrational states do not dissociate appreciably. As it turns out, the explanation is rather mundane and does not require invoking anything as complicated as the Floquet picture — first-order time-dependent perturbation theory is sufficient. The answer is simply that the vibrational dipole matrix elements are smaller. Figure 3(b) shows the squared dipole matrix elements as a function of initial vibrational states v and final kinetic energy release (KER). As Fig. 3(a) shows schematically, initial and final states with comparable classical turning points will have the largest overlap, and when the energy separating these turning points matches the photon energy something like a resonant condition is achieved. Further, the dipole matrix element oscillates as a function of KER, so that the states whose dissociation is "suppressed" depends on laser wavelength.

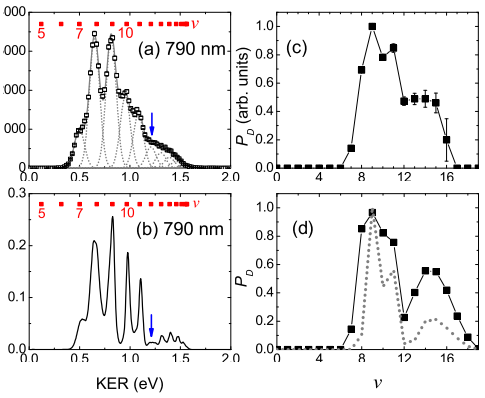

Figure 4: (a) Experimental H_2^+ KER spectrum using a 40 fs, 3×10^{13} W/cm^2 pulse. (b) Nonperturbative theoretical spectrum for a 45 fs, 4×10^{10} W/cm^2 pulse. Ticks for one-photon dissociation from a state v are shown along the top of the panels. The corresponding relative dissociation probabilities P_D from the area of the Gaussian fits in (a) are shown in (c). The equivalent theoretical P_D from (b) are shown in (d), along with perturbative results (dashed line) normalized at v=9. (Adapted from Ref. [7].)

To solidify this explanation and demonstrate its relevance to experiment, I. Ben-Itzhak's group simply measured the dissociation of H_2^+. Since they have sufficient resolution to resolve the vibrational states, we could carry out a farily detailed comparison which is shown in Fig. 4. Similar results and comparisons were made in [7] for 395 nm as well. While not perfect, we believe the agreement in Fig. 4 confirms that the lower dissociation probability of the higher vibrational states of H_2^+ in intense lasers is simply a result of a small dipole matrix element, which can, in turn, be easily understood from the wave functions as in Fig. 3(a). Thus, it does not appear necessary to invoke a multiphoton, intense laser explanation for "vibrational trapping".

Future plans Understanding this benchmark system will continue to be a component of my program. We will proceed along several fronts: revisiting "understood" issues like the example above, trying to identify new phenomena, and working towards a full-dimensional solution of the time-dependent Schrödinger equation. One of my goals is to be able to make a quantitative comparison of theory and experiment for the momentum distribution of p+H.

References

1. V. Roudnev, B.D. Esry, and I. Ben-Itzhak, Phys. Rev. Lett. **93**, 163601 (2004).
2. V. Roudnev and B.D. Esry, Phys. Rev. A **71**, 013411 (2005).
3. F. Anis and B.D. Esry, J. Phys. B (submitted) (2009).
4. J.V. Hernández and B.D. Esry, (in preparation).
5. G.G. Paulus, F. Grasbon, H. Walther, P. Villoresi, M. Nisoli, S. Stagira, E. Priori and S. De Silvestri, Nature **414**, 182 (2001).
6. G.L. Ver Steeg, K. Bartschat, and I. Bray, J. Phys. B **36**, 3325 (2003).
7. J. McKenna, F. Anis, B. Gaire, N.G. Johnson, M. Zohrabi, K.D. Carnes, B.D. Esry, and I. Ben-Itzhak, Phys. Rev. Lett. (submitted) (2009).

Publications of DOE-sponsored research in the last 3 years

P15. "Laser-induced multiphoton dissociation branching ratios for H_2^+ and D_2^+," J.J. Hua and B.D. Esry, Phys. Rev. A (accepted) (2009).

P14. "Permanent dipole transitions remain elusive in HD^+ strong-field dissociation," J. McKenna, A.M. Sayler, B. Gaire, N.G. Johnson, M. Zohrabi, K.D. Carnes, B.D. Esry and I. Ben-Itzhak, J. Phys. B **42**, 121003(FTC)(2009).

P13. "Rotational dynamics of dissociating H_2^+ in a short intense laser pulse," F. Anis, T. Cackowski, and B.D. Esry, J. Phys. B **42**, 091001(FTC) (2009).

P12. "The role of mass in the carrier-envelope phase effect for H_2^+ dissociation," J.J. Hua and B.D. Esry, J. Phys. B **42**, 085601 (2009).

P11. "Elusive enhanced ionization structure for H_2^+ in intense ultrashort laser pulses," I. Ben-Itzhak, P.Q. Wang, A.M. Sayler, K.D. Carnes, M. Leonard, B.D. Esry, A.S. Alnaser, B. Ulrich, X.M. Tong, I.V. Litvinyuk, C.M. Maharjan, P. Ranitovic, T. Osipov, S. Ghimire, Z. Chang, and C.L. Cocke, Phys. Rev. A 78, 063419 (2008).

P10. "Isotopic pulse-length scaling of molecular dissociation in an intense laser field," J.J. Hua and B.D. Esry, Phys. Rev. A 78, 055403 (2008).

P9. "High kinetic energy release upon dissociation and ionization of N_2^+ beams by intense few-cycle laser pulses," B. Gaire, J. McKenna, A.M. Sayler, N.G. Johnson, E. Parke, K.D. Carnes, B.D. Esry, and I. Ben-Itzhak, Phys. Rev. A **78**, 033430 (2008).

P8. "Intensity dependence in the dissociation branching ratio of ND^+ using intense femtosecond laser pulses," J. McKenna, A.M. Sayler, B. Gaire, N.G. Johnson, E. Parke, K.D. Carnes, B.D. Esry, and I. Ben-Itzhak, Phys. Rev. A **77**, 063422 (2008).

P7. "Enhancing high-order above-threshold dissociation of H_2^+ beams with few-cycle laser pulses," J. McKenna, A.M. Sayler, F. Anis, B. Gaire, N.G. Johnson, E. Parke, J.J. Hua, H. Mashiko, C.M. Nakamura, E. Moon, Z. Chang, K.D. Carnes, B.D. Esry, and I. Ben-Itzhak, Phys. Rev. Lett. **100**, 133001 (2008).

P6. "Role of nuclear rotation in dissociation of H_2^+ in a short laser pulse," F. Anis and B.D. Esry, Phys. Rev. A **77**, 033416 (2008).

P5. "Ionization and dissociation of molecular ion beams caused by ultrashort intense laser pulses," I. Ben-Itzhak, A.M. Sayler, P.Q. Wang, J. McKenna, B. Gaire, N.G. Johnson, M. Leonard, E. Parke, K.D. Carnes, F. Anis, and B.D. Esry, J. Phys.: Conf. Ser. **88**, 012046 (2007).

P4. "General theory of carrier-envelope phase effects," V. Roudnev and B.D. Esry, Phys. Rev. Lett. **99**, 220406 (2007).

P3. "HD^+ in a short strong laser pulse: Practical consideration of the observability of carrier-envelope phase effects," V. Roudnev and B.D. Esry, Phys. Rev. A **76**, 023403 (2007).

P2. "Determining laser induced dissociation pathways of multi-electron diatomic molecules: application to the dissociation of O_2^+ by high intensity ultrashort pulses," A.M. Sayler, P.Q. Wang, K.D. Carnes, B.D. Esry, and I. Ben-Itzhak, Phys. Rev. A **75**, 063420 (2007).

P1. "Dissociation of H_2^+ in intense femtosecond laser field studied by coincidence 3D momentum imaging," P.Q. Wang, A.M. Sayler, K.D. Carnes, J.F. Xia, M.A. Smith, B.D. Esry, and I. Ben-Itzhak, Phys. Rev. A **74**, 043411 (2006).

Controlling molecular rotations of asymmetric top molecules: methods and applications

V. Kumarappan
James R. Macdonald Laboratory, Department of Physics
Kansas State University, Manhattan, KS 66506
vinod@phys.ksu.edu

1 Program Scope

The goal of this part of the JRML research program is to develop better methods of aligning and orienting polyatomic molecules, particularly for ultrafast AMO experiments. At this point, we are still in the process of setting up the experiments, and in the following we'll describe progress made so far.

2 Recent Progress

2.1 kHz VMI setup: *Xiaoming Ren and Vinod Kumarappan*

The importance of keeping the rotational temperature of the molecular as low as possible is now widely appreciated [1], and our goal is to get it as low as possible. We also want to be able to run the experiment as rapidly as is technically feasible, particularly in view of the fact that the shared laser system in JRML is available only 3-4 days a month. These two requirements set the parameters for the design of our new velocity map imaging spectrometer which we will use for alignment and orientation experiments.

Since lab space became available in Nov 2008, we have built a high resolution, 1 kHz velocity map imaging spectrometer [2] for aligning molecular targets at ∼1 K rotational temperature. The heart of this setup is a kHz Even-Lavie valve [3]. This miniaturized solenoid valve operates at repetition rates of up to 1 kHz with a gas pulse duration of ∼10 μs, which allows operation with up to 100 bar of stagnation pressure for the adiabatic expansion. We use helium as the buffer gas, and seed less than ∼0.1% of the target molecule in this high density flow. The result of the high pressure adiabatic expansion out of the 100 μm nozzle is a target with rotational temperatures in the ∼1 K range.

If the heart of the setup is the cold molecule source, the brain is the data acquisition system. We analyze the light distribution produced by each individual ion/electron hit on the micro-channel plate/phosphor screen detector to determine its centroid. This gives us sub-pixel resolution for each ion hit, and also provides an excellent measure of saturation since we can quantify the number of overlapping hits on the detector. In order to achieve this, we acquire images of the phosphor screen that every laser shot using a fast CMOS camera (Basler A504k, 1000 fps at 500×500 pixels). The P47 phosphor itself has a decay lifetime of 120 ns, and camera exposure is gated to 50 μs. The images are analyzed in real-time on a dual quad-core workstation using a parallel image processing algorithm, which finds the centroid of the light produced by each ion hit. By analyzing the shape and size of the light distribution, the algorithm also separates most partially overlapped hits and tags those that can be identified as overlapping hits but cannot be separated. We can detect 50-100 hits per laser shot without any

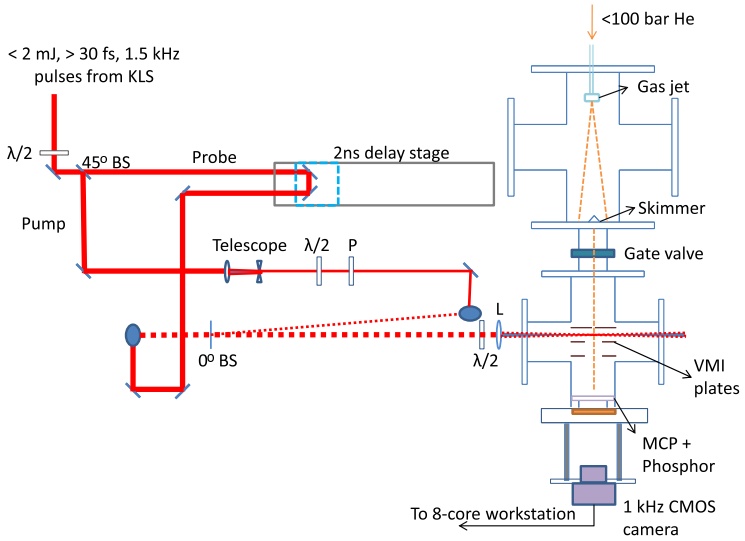

Figure 1: *The experimental setup. The abbreviation used are P for polarizer, BS for beam-splitter, λ/2 for half-wave plate, and L for 35 cm focal length lens.*

significant image saturation effects. The end product is a high resolution, high data rate, high dynamic range (limited only by the total acquisition time available) spectrometer well suited for our experiments.

We measured the non-adiabatic alignment of iodobenzene as a test of the setup, shown in Figure 1. Figure 2 shows the measured time-evolution of $\langle cos^2\theta_{2D}\rangle$, where θ_{2D} is the angle the location of an ion hit makes with respect to the alignment axis on the 2D detector. Note that this angle is not the same as the Euler angle θ that describes the orientation of the molecule with the laser polarization, but it does provide a convenient measurement of the degree of alignment. The pump was polarized in the plane of the detector, and the probe perpendicular to it. This geometry minimizes the the influence of probe-selectivity on the measured distribution. The degree of alignment is comparable with published data [4], providing indirect evidence that the molecular target is as cold as expected.

2.2 3D Velocity Map Imaging: *Xiaoming Ren, Varun Makhija and Vinod Kumarappan*

VMI is widely used in AMO experiments because of its ease of implementation and rapid rate of data acquisition when compared to other imaging techniques like COLTRIMS. It does suffer from one significant limitation - the measurements are 2D projections of 3D velocity distributions. A standard VMI setup limits us to either 2D measurements, as was used the iodobenzene measurements, or to distributions that are cylindrically symmetric with the axis of symmetry in the plane of the detector. In the latter case, Abel inversion is used to reconstruct the full 3D velocity distribution. But the requirement of cylindrical symmetry for Abel inversion is quite restrictive, disallowing the use of elliptical polarization or any combination of linear polarizations not along the same direction in a multi-pulse experiment.

We have developed a tomographic method to overcome this limitation [5]. As is well-known in medical imaging [8], an arbitrary 3D function can be reconstructed from a sufficient number of 2D projections along different directions on any 2D plane using the inverse Radon transform. In the case of a laser-VMI experiment, which projects the 3D velocity distribution of charged particles onto a 2D detector, the axis of projection can be changed by simultaneously rotating all the polarization vectors involved in a experiment using a half-wave plate. A filtered back-

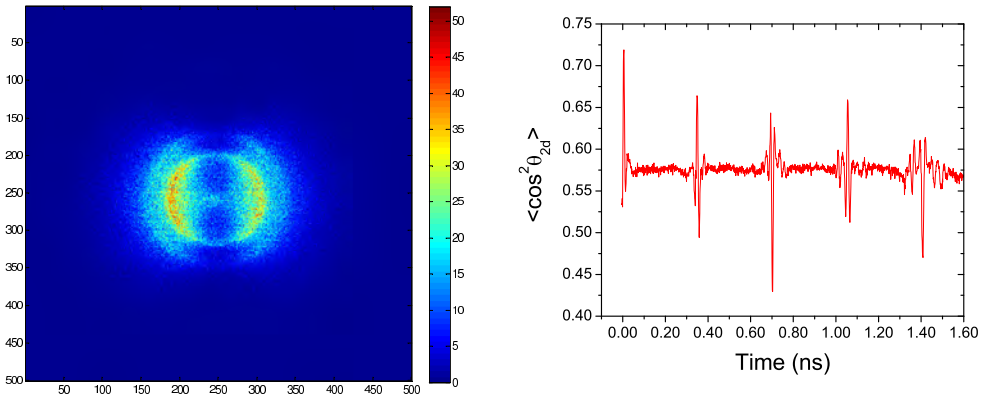

Figure 2: *A typical velocity map image of I^+ ions from iodobenzene is shown. The two rings correspond to singly and doubly-charged Coulomb explosion partner to the I^+ ions. In this case, the molecules are not aligned, and the Coulomb explosion beam is horizontally polarized. The image shows the directional selectivity of the probe process. $\langle cos^2\theta_{2D}\rangle$ shown in the graph is measured with the probe polarized perpendicular to the detector, so that the probe does not favor any direction in the plane of the detector.*

projection algorithm (or any of a variety of other algorithms available) can then be used to reconstruct the 3D distribution. This method is completely general and does not place any restrictions on the symmetry of the distribution.

Figure 3 shows representative slices of 3D velocity distributions of I^+ fragments from aligned iodobenzene. After aligning the molecules as described in the previous section, we produce I^+ ions using the probe pulse which is polarized perpendicular to the pump pulse. Clearly, the recontrcuted velocity distribution does not possess cylindrical symmetry – it reflects both the angular distribution of the molecules and the angular selectivity of the probe beam.

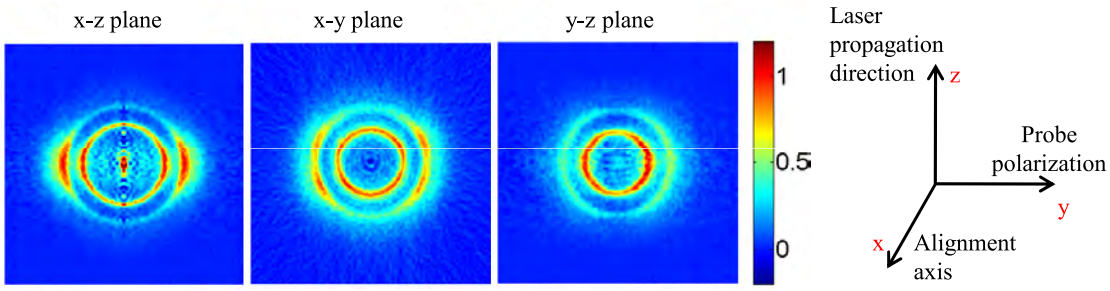

Figure 3: *Three representative slices (at y=0, z=40, and x=40, respectively. The total 3D volume is 360×360×360 voxels.) of the 3D velocity distribution of I^+ fragments from aligned iodobenzene molecules ($\langle cos^2\theta_{2D}\rangle = 0.68$). The geometry is given by the coordinate axes on the right. The distribution is not cylindrically symmetric since the pump and probe polarizations are perpendicular to each other.*

3 Future Plans

We have installed a magnetic shield around the VMI spectrometer to enable us to measure photoelectron angular distributions from aligned molecules. A polarization pulse shaper will be added soon, with the goal of measuring and optimizing field-free 3D alignment of asymmetric

top molecules. We are working on an optical method for measuring 3D alignment so that a genetic algorithm can converge in a reasonable amount of time. Two groups have shown this year [9, 10] that a state-selected target is essential for orienting molecules, and we will add a state-selector in the next few months. This will allow us to orient asymmetric tops in laser-field-free conditions.

4 Publications and conference contributions from DOE sponsored research:

1. "Tomographic measurement of 3D ion velocity distributions from rotationally cold molecules using a kHz VMI spectrometer", Xiaoming Ren, Varun Makhija, and Vinod Kumarappan, contributed poster, Second International Conference on Attosecond Physics, Manhattan, KS (2009).

References

[1] V. Kumarappan, C. Z. Bisgaard, S. S. Viftrup, L. Holmegaard, and H. Stapelfeldt, "Role of rotational temperature in adiabatic molecular alignment", J. Chem. Phys. **125**, 7 (2006).

[2] Andre T. J. B. Eppink and David H. Parker, "Velocity map imaging of ions and electrons using electrostatic lenses: Application in photoelectron and photofragment ion imaging of molecular oxygen", Review of Scientific Instruments **68**, 3477-3484 (1997).

[3] U. Even, J. Jortner, D. Noy, N. Lavie, and C. Cossart-Magos, "Cooling of large molecules below 1 K and He clusters formation", J. Chem. Phys. **112**, 8068-8071 (2000).

[4] L. Holmegaard, S. S. Viftrup, V. Kumarappan, C. Z. Bisgaard, H. Stapelfeldt, E. Hamilton, and T. Seideman, "Control of rotational wave-packet dynamics in asymmetric top molecules", Phys. Rev. A **75**, 4 (2007).

[5] To the best of our knowledge, our work, [6] and [7] were all carried out independently.

[6] M. Wollenhaupt, M. Krug, J. Khler, T. Bayer, C. Sarpe-Tudoran, and T. Baumert, "Three-dimensional tomographic reconstruction of ultrashort free electron wave packets", Applied Physics B: Lasers and Optics **95**, 647-651 (2009).

[7] C. Smeenk, L. Arissian, A. Staudte, D. M. Villeneuve, and P. B. Corkum, "Tomographic reconstruction of the 3D momentum distribution in velocity map imaging experiment", contributed poster, Second International Conference on Attosecond Physics, Manhattan, KS, 2009.

[8] See, for instance, A. C. Kak and M. Stanley, "Principles of Advanced Tomographic Imaging", IEEE Press, New York, 1988.

[9] Lotte Holmegaard, Jens H. Nielsen, Iftach Nevo, Henrik Stapelfeldt, Frank Filsinger, Jochen Kupper, and Gerard Meijer, "Laser-Induced Alignment and Orientation of Quantum-State-Selected Large Molecule", Physical Review Letters **102**, 023001-4 (2009).

[10] Omair Ghafur, Arnaud Rouzee, Arjan Gijsbertsen, Wing Kiu Siu, Steven Stolte, and Marc J. J. Vrakking, "Impulsive orientation and alignment of quantum-state-selected NO molecules", Nature Physics **5**, 289-293 (2009).

Interactions of intense lasers with atoms and molecules and dynamic chemical Imaging

C. D. Lin
J. R. Macdonald Laboratory, Kansas State University
Manhattan, KS 66506
e-mail: cdlin@phys.ksu.edu

Program Scope:
We investigate the interaction of intense laser pulses with atoms and molecules. In the last year we have carefully established the validity of the recently developed quantitative rescattering theory (QRS) for high-order harmonic generation (HHG) and high-energy ATI (HATI) electron momentum spectra. Using the QRS, we (i) obtained HHG spectra from aligned molecules, (ii) extracted elastic differential scattering cross sections of electron-ion collisions from HATI spectra, and (iii) extracted laser parameters for few-cycle pulses from HATI spectra. We thus have established the theoretical foundation for using few-cycle infrared lasers for dynamic chemical imaging of a transient molecule.

Introduction
When an atom or molecule is exposed to an intense infrared laser pulse, an electron which was released earlier may be driven back by the laser field to recollide with the parent ion. The collisions of electrons with the ion may result in high-order harmonic generation (HHG) or the emission of high-energy above-threshold-ionization (HATI) electrons. These HHG and HATI spectra contain information on the structure of the target. If such structural information can be extracted, then infrared lasers can be used for dynamic chemical imaging with temporal resolution down to a few femtoseconds.

In the last year, we have fully established the quantitative rescattering theory (QRS) which shows that photo-recombination cross sections can be extracted from the HHG spectra, and elastic differential cross sections (DCS) between electrons and ions can be extracted from the HATI spectra, respectively. In the meanwhile, we also showed that experimental HATI spectra, combined with the QRS, allows an accurate and fast fully non-optical method of retrieving laser parameters. In this report, we summarized the main conclusions achieved since last report and outline the projects to be undertaken in the coming year.

Quantitative rescattering theory (QRS) for HATI electrons induced by lasers
Recent progress
We have fully documented the QRS theory for HATI electrons in paper #A3. The idea and approximations behind the QRS, test of the theory against results from solving the time-dependent Schrodinger Equation (TDSE), against experimental results, the dependence of HATI spectra on the target, the wavelength and intensity of the laser used, have all been carefully examined. In the meanwhile, in paper #A4, it was shown that high-energy photoelectron spectra for different targets can all be attributed to their difference in the elastic differential scattering cross sections, between the returning electrons and the parent ion, thus clarifying the role of target structure in the photoelectron spectra generated by the lasers.

Using the QRS, we also can extract elastic differential cross sections. This has been demonstrated using photoelectron spectra generated by long laser pulses (about 100fs) for Ne, Ar, Kr and Xe atoms, see paper #A5. The extracted elastic scattering cross sections are in good agreement with those calculated from theory. To test the imaging idea, we further used the

theoretically calculated DCS as input, and confirmed that we can retrieve the target atom structure where the atom is described by a model potential. The result of this work is reported in paper #A10. It shows that even with a limited range of energies typically covered by the returning electrons generated by the laser, the retrieval of the structure of simple atoms is quite accurate. This work is a first direct demonstration that accurate structure of the target can be probed using infrared lasers. The QRS theory plays a very important role here since it shows that the DCS can be extracted without the need of knowing accurate parameters of the laser used and the DCS extracted should be independent of laser's wavelength, peak intensity and the carrier-envelope-phase of the few-cycle pulses.

Ongoing projects and future plan

We are extending the QRS to study HATI spectra from aligned molecules. Due to the increasing degrees of freedom for molecular targets the calculations will be more time consuming. Furthermore we need to make sure that differential scattering cross sections by free electrons with aligned molecular ions are accurately calculated. This will require the careful interaction with our collaborator, Dr. Robert Lucchese, in the coming year.

QRS Theory and retrieval of laser parameters from HATI spectra

Recent progress

Since calculations of HATI spectra using the QRS are thousands times faster than solving TDSE numerically but of comparable accuracy as TDSE, the QRS theory can be easily applied to obtain electron spectra that can be directly compared to experiments, where one has to consider electrons generated from the whole focal volume of the laser pulse. Since the DCS is independent of laser's peak intensity, laser focus volume effect is included in the volume-integrated returning electron wave packet. By analyzing the experimental electron energy spectra for detectors on the "right" and the "left" of the laser's polarization, and comparing with spectra simulated using the QRS, we were able to retrieve accurate carrier-envelope-phase (CEP), the peak intensity and pulse duration of phase-stabilized few-cycle pulses. These results were reported in papers #A6 and #A7.

Very recently we have improved this method such that it can be applied to single-shot measurements. It relies on measuring HATI electron momentum spectra for each single shot and the method has been applied to single-shot data taken at MPI, Garching, where 4500 single-shot data were recorded [Nature Phys. 5, 357 (2009)] . Our new method allows us to retrieve the peak laser intensity, pulse duration and the CEP of each shot, quickly. Using this method to tag the CEP of each single shot, it is possible to study the CEP effect for laser pulses where the CEP's are not stabilized. This is important since even for phase-stabilized pulses the variation of CEP from shot to shot is still about 20^{o} or more, while our method shows that in single-shot measurement the CEP is accurate to better than about 3^{o}. Moreover, CEP stabilization cannot be done for longer wavelength lasers yet and for experiments at very high peak intensities. Using CEP-tagging, the study of the waveform dependence of laser-matter interaction can be extended to beams where phase stabilization is not yet possible.

Ongoing projects and future plan

The new CEP retrieval method for determining laser parameters is very powerful. We hope to collaborate with experimentalists such that they will adopt the method and determine the CEP for each shot themselves. Currently we are also testing this method in two-color experiments. In these experiments, for example, using 800 nm laser to generate the 2^{nd} harmonic, then recombine 800nm and 400nm pulses with varying time delay, the combined beam, if the relative phase of the two colors are varied continuously, deals with physics issues that are similar to the study of

CEP dependence in few-cycle pulses. The present retrieval method will allow accurate determination of the relative phase between the two colors.

QRS Theory and HHG spectra from aligned molecules

Recent progress

In the last year, we have extended the QRS so that both the amplitude and phase of high-order harmonics can be calculated. We first applied the method to atomic systems where accurate results can be obtained from solving the TDSE. The validity of the QRS for atoms was reported in Paper #A11. Since our major interest is HHG in molecular systems, we need to use photo-recombination cross sections, or equivalently, photoionization amplitude and phase, of molecules. This is a highly specialized area. Thus we sought help from Dr. Robert Lucchese, and has since successfully generated transition dipole amplitude and phase using his computer codes. From these data, using the QRS, we were able to calculate accurate HHG spectra from aligned molecules. Initial results obtained for CO_2 molecules for emitted HHG polarized along the direction of the laser polarization direction have been reported, see Paper #A2. In the meanwhile, a long write-up, detailing the QRS theory for HHG has been published, see Paper #A1. In these two papers, we have shown that the QRS indeed can explain HHG spectra from partially aligned molecules, when compared to experimental results reported from a number of different laboratories. We thus established that HHG spectra provide an alternative method for studying molecular frame photoionization cross sections which are difficult to perform using standard synchrotron radiations.

We have also made an initial study of the macroscopic propagation effect of HHG in a dilute medium using the single-atom dipole moment calculated from the QRS. In Paper #A9 we showed that the QRS is valid for such dilute medium and thus photoionization cross sections and phases can be extracted from the experimental HHG spectra.

Ongoing projects and future plan

The QRS provides a quantitative theory for calculating HHG spectra without introducing additional arbitrary approximations. Thus calculations can be directly compared to experiments. Since in many experiments some of the experimental parameters, such as the peak laser intensity and temperature of the gas jet, are not accurately determined, using QRS, calculations can be carried out by adjusting these parameters until the theory achieves better agreement with experiments. This is possible since QRS calculations are very fast after the photoionization dipole amplitudes and phases are available. Currently the QRS theory is being applied to study the relative contributions of HHG from outermost vs. from inner orbitals, for N_2 and CO_2. The former has been studied experimentally at Stanford and latter at NRC, Canada. We are also studying the polarization of HHG measured for these two molecules, which will be compared to data from JILA. Study of HHG from a truly dynamic system will begin in the later part of the coming year.

Attosecond Physics

In the last two years we have not devoted much effort on attosecond physics experiments so we were able to focus on the development of the QRS theory. Experiments using attosecond pump and infrared probe beams are beginning to emerge recently. Electron spectra using He targets from such experiments have appeared recently. The interpretation of these experiments so far has relied on solving the TDSE which often does not provide a clear interpretation of the origin of the observed features. We will begin to look into problems associated with this type of experiments and hope to be able to find alternative approaches where interpretation can be more transparent.

Publications (16 papers published between January 2007- December 2008 are not listed)
Published papers

A1. Anh-Thu Le, R.R. Lucchese, S. Tonzani, T. Morishita, C.D. Lin, " Quantitative rescattering theory for high-order harmonic generation from molecules", Phys. Rev. A80, 013401 (2009).

A2. A. T. Le, R. R. Lucchese, M. T. lee and C. D. Lin, "Probing molecular frame photoionization via laser generated high-order harmonics from aligned molecules", Phys. Rev. Lett. 102, 203001 (2009).

A3. Zhangji n Chen, A. T. Le, T. Morishita a nd C. D. Lin," Quantitative rescattering theory for laser-induced high-energy plateau photoelectron spectra", Phys. Rev. A. 79, 033409 (2009).

A4. Z. J. Chen, A. T. Le, Toru Morishita, and C. D. Lin, "Origin of species dependence of high-energy plateau photoelectron spectra", J. Phys B (fast track communications), J. Phys. B42, 061001 (2009).

A5. T. Morishita, M. Okunishi, K. Shimada, G. Prumper, Z. J. Chen, S. Watanabe, K. Ueda, and C. D. Lin, " Retrieval of experimental differential electron-ion elastic scattering cross sections from high-energy ATI spectra of rare gas atoms by infrared lasers", J. Phys. B. 42, 105205 (2009).

A6. S. Micheau, Z. J. Chen, A. T. Le, J. Rauschenberger, M. F. Kling and C. D. Lin, "Accurate retrieval of t arget structure and laser parameters of few-cy cle pulses from photoelectron momentum spectra", Phys. Rev. Lett. **102**, 073001 (2009).

A7. Sam uel Micheau, Zhangjin Chen, Toru Mo rishita, Anh-Th u Le and C. D. Lin, "Robust carrier-envelope phase retrieval of few-cycle laser pulses fro m high-energy photoelectron spectra in the above-threshold ionization of atoms", J. Phys. B42, 065402 (2009).

A8. Samuel Micheau, Zhangjin Chen, Toru Morishita, Anh-Thu Le and C. D. Lin, "Quantitative rescattering theory for non-sequential double ionization of atoms by intense laser pulses", Phys. Rev. **A79**, 013417 (2009)

A9. Cheng Jin, A. T. Le and C. D. Lin, "Retrieval of target photo-recombination cross sections from high-order harmonics generated in a macroscopic medium", Phys. Rev. A79, 053413 (2009).

A10. Junliang Xu, Hsiao-Ling Zhou, Zhangjin Chen and C. D. Lin, "Genetic-algorithm implementation of atomic potential reconstruction from differential electron scattering cross sections", Phys. Rev. A79, 052508 (2009).

A11. T. Le, Toru Morishita, and C. D. Lin, "Extraction of the species-dependent dipole amplitude and phase from high-order harmonic spectra in rare gas atoms ", Phys. Rev. A78, 023814 (2008).

B. Papers submitted for publication

B1. Zhangjin Chen, T. Wittmann and C. D. Lin, "A robust all-non-optical method for the characterization of single-shot few-cycle laser pulses", submitted to Phys. Rev. Lett.

Structure and Dynamics of Atoms, Ions, Molecules and Surfaces:
Atomic Physics with Ion Beams, Lasers and Synchrotron Radiation

I.V. Litvinyuk, Physics Department, J.R. Macdonald Laboratory, Kansas State University, Manhattan, KS 66506, ivl@phys.ksu.edu

1. Time-resolved dynamics of heavy-particle motion in neutral molecules and molecular ions

Our goal is to study and understand the physics of ultrafast processes involving the motion of nuclei associated with the rotation, vibration, rearrangement and dissociation of molecules and molecular ions. We apply pump-probe techniques in combination with COLTRIMS detection to study the dynamics of nuclear motion as it takes place in real time with the ultimate goal of recovering the time-dependent molecular structure and orientation — making a "molecular movie".

Recent progress:

1.1 Pump-probe studies of nuclear dynamics in N_2, O_2 and CO using few-cycle pulses and Coulomb explosion as a probe, *I. Bocharova, M. Magrakvelidze, S. De, D. Ray, C.L. Cocke and I.V. Litvinyuk.* We use a pair of intense few-cycle (8 fs) pulses with variable delay to im age all nuclear dynam ics in m ulti-electron diatom ic mol ecules following interaction with an ultrashor t pump pulse. Such interaction results in produc tion of various charge/e xcited states, both bound and dissociative. COLTRIMS technique allows us to select a specific final charg e state and to plot kinetic energy release (KER) and angular distributions of the fragm ents as a function of pump-probe delay. From KER time dependence we can id entify specific interm ediate states of molecular ions and follow their tim e evolu tion. W e also m odel nuclear m otion in those molecular ions num erically, using their known el ectronic potentials within a one-dim ensional quantum wavepacket model. The model reprodu ces well our experim ental time-dependent KER spectra for all studied molecules. The behavior o f those m olecules differs due to their different electronic structure. Though only io nic fragm ents are detected in these experim ents, the results can also reveal interesting electron dynamics, as described below.

1.1.a Real-time dynamics of electron localization observed in dissociating N_2^{3+}. In thi s particular experiment, we measured dependence of yields and kinetic energies for symmetric N^{2+} + N^{2+} (2,2) and asymme tric N^{3+} + N^{+} (3,1) dissociation channels of N_2^{4+} on time delay between few-cycle 800 nm pump and probe pulses. The pump pulse produces a dissociating molecular tri-cation from which the tim e-delayed probe pulse removes the fourth electron. That results in either (2,2) or (3,1) final dissociation channel. We observe that the asymmetric (3,1) channel is produced only for delays of up to 20 fs and completely suppressed for longer delays. The symmetric (2,2) channel is efficiently produced for all studied delays. W e interpret that observation as an indication that th e unpaired electron in dissociating N_2^{3+} is com pletely localized on one of th e ions after 20 fs. After this localization is completes, the probe pulse can only further ionize N^{+} as the other ion (N^{2+}) has a m uch higher ionizatio n potential. Ours is the first d irect tim e-resolved m easurement of th is electron loc alization, which p lays a n im portant part in the mechanism of charge-resonant enhanced ionization (CREI).

1.2 Dynamic field-free orientation of heteronuclear molecules (CO and NO) induced by two-color femtosecond laser pulses, *S. De, I. Znakovskaya, D. Ray, I. Bocharova, M. Magrakvelidze, F. Anis, B.D. Esry, C.L. Cocke, M. Kling and I.V. Litvinyuk.* In collaboration with MPQ Garching, we conducted at JRML an extensive series of experiments on rotational dynamics induced in heteronuclear diatomic molecules by field-asymmetric femtosecond laser pulses. The pump pulses were produced by combining fundamental 800 nm frequency with its second harmonic (400 nm). For certain relative phases such ($\omega+2\omega$) pulses break inversion symmetry of electric field and generate coherent rotational wavepackets containing both odd and even J-states. In heteronuclear molecules such wavepackets result in periodically reviving field-free macroscopic orientation. We detected orientation by Coulomb exploding the molecules with one-color (800 nm) pulses and measuring fragment angular distributions with VMI. We were able to produced oriented ensembles in both CO and NO in field-free conditions. Model calculations for CO reproduce well our experiments and suggest that orientation in CO is due to its asymmetric hyperpolarizability, rather than its permanent dipole moment. Ours is the first successful experiment having produced field-free molecular orientation.

Future plans: We started to use our new velocity map imaging (VMI) detector instead of COLTRIMS in our pump-probe dynamics studies. While we do lose coincidence information, with VMI much improved count rates allow us to explore much longer delay ranges (tens of picoseconds) within our limited experimental time. We have already observed vibrational and rotational revivals in nitrogen. We will continue to study longer time dynamics in diatomics. With heteronuclear diatomics we will continue working on two-color laser orientation.

2. Strong-field ionization of molecules studied by COLTRIMS

This aspect is directed towards understanding dynamics and mechanisms of single, double and multiple ionization of molecules by intense femtosecond laser pulses. To achieve that, we measure coincidence momentum spectra of resulting ion fragments (and sometimes also electrons) for different pulse ellipticities, durations and peak intensities. The experiments were conducted at JRML, as well as (in collaboration with INRS-Quebec and University of Waterloo) at the Advanced Laser Light Source (ALLS) in Montreal.

Recent progress:

2.1 Alignment dependence of tunneling ionization of D_2 measured in randomly oriented molecules with circularly polarized pulses, *M. Magrakvelidze, S. De, I. Bocharova, H. Feng, U. Thumm and I.V. Litvinyuk.* In this experiment at JRML we employed electron-ion coincidence momentum spectroscopy to measure the relative angle between an emitted electron and a deuteron resulting from field dissociation of the molecular ion produced by a circularly polarized pulse. We deduced the angular dependence of the molecular ionization probability without having to align the molecules first. We determined that with 50 fs pulses of 1850 nm wavelength and 2×10^{14} W/cm^2 intensity neutral D_2 molecules are 1.15 times more likely to be ionized when the laser electric field is parallel to the molecular axis than for the perpendicular orientation, in excellent agreement with our ab initio theoretical model. Our results also agree with predictions of the molecular Ammosov-Delone-Krainov (mo- ADK) theory, as well as those of a similar experiment performed with 800 nm pulses of comparable intensity and duration on H_2 molecules.

2.2 Electron recollission processes in H_2 and D_2 studied with few-cycle laser pulses, *I. Bocharova, F. Legare, J. Sanderson and I.V. Litvinyuk.* In this ALLS collaboration we studied electron recollision processes induced in D_2 by nonlinear interaction with 800 nm few-cycle laser pulses using coincidence ion momentum imaging. We took advantage of 5 kHz repetition rate and ultra-short duration (6 fs) of the ALLS beamline to study ionization of hydrogen at very low intensities (down to 1×10^{14} W/cm^2). We show that sequential double ionization is suppressed at intensities below 2×10^{14} W/cm^2 and the inelastic rescattering processes (recollision induced electronic excitation and double ionization) become dominant and can be carefully investigated as a function of laser intensity and ellipticity. We experimentally confirm that non-sequential double ionization (NSDI) arises from recollision-induced electronic excitation of D_2^+ $^2\Sigma_g^+$ state followed within sub-cycle time scale by field ionization.

2.3 Dynamics of Coulomb explosion in CO_2 studied by triple-coincidence ion momentum imaging, *I. Bocharova, J. Sanderson, F. Legare and I.V. Litvinyuk.* In this ALLS collaboration we studied dynamics of laser-induced Coulomb explosion of CO_2 by full triple-coincidence momentum resolved detection of resulting ion fragments. From the coincidence momentum data we can reconstruct molecular geometry immediately before explosion. We observe the dynamics of Coulomb explosion by comparing reconstructed CO_2 geometries for different Ti:Sapphire laser pulse durations (at the same intensity) ranging from few cycles (7 fs) to 200 fs. We conclude that for longer pulse durations (ε100 fs) Coulomb explosion proceeds through the enhanced ionization mechanism taking place at the critical O-O distance of 8 a.u., similarly to well known charge-resonance enhanced ionization (CREI) in H_2.

Future plans: We are planning to take advantage of our newly acquired expertise in molecular orientation to measure angular dependence of ionization rates for heteronuclear diatomics. Further, we will use VMI to measure angular resolved electron ATI spectra for aligned and oriented molecules to uncover single ionization mechanisms. We are also planning to extend hydrogen rescattering experiments to few-cycle pulses at longer wavelengths, taking advantage of the newly developed source at ALLS. We have already completed a series of experiments with 1300 nm few-cycle pulses, and are planning siilar studies at 1500 nm and 1800 nm. With CO_2 we are planning to conduct a real pump-probe dynamics experiment with consequent full time-dependent molecular structure reconstruction.

Publications in 2008-2009:

7. *"Angular dependence of the strong-field ionization measured in randomly oriented hydrogen molecules"*, Maia Magrakvelidze, Feng He, Sankar De, Irina Bocharova, Dipanwita Ray, Uwe Thumm, I. V. Litvinyuk, Phys. Rev. A **79**, 033408 (2009)

6. *"Quantum-beat imaging of the nuclear dynamics in D2+: Dependence of bond softening and bond hardening on laser intensity, wavelength, and pulse duration"*, Maia Magrakvelidze, Feng He, Thomas Niederhausen, Igor V. Litvinyuk, Uwe Thumm, Phys. Rev. A **79**, 033410 (2009)

5. *"Elusive enhanced ionization structure for H2+ in intense ultrashort laser pulses"*I. Ben-Itzhak, P. Q. Wang, A. M. Sayler, K. D. Carnes, M. Leonard, B. D. Esry, A. S. Alnaser, B. Ulrich, X. M. Tong, I. V. Litvinyuk, C. M. Maharjan, P. Ranitovic, T. Osipov, S. Ghimire, Z. Chang, C. L. Cocke Phys. Rev. A **78**, 063419 (2008)

4. *"Wavelength-dependent study of strong-field Coulomb explosion of hydrogen"*, I V Litvinyuk, A S Alnaser, D Comtois, D Ray, A T Hasan, J-C Kieffer, D M Villeneuve, New J. Phys. **10**, 83011 (2008)

3. *"Direct Coulomb-explosion imaging of coherent nuclear dynamics induced by few-cycle laser pulses in light and heavy hydrogen"*, I. A. Bocharova, H. Mashiko, M. Magrakvelidze, D. Ray, P. Ranitovic, C. L. Cocke, I. V. Litvinyuk, Phys. Rev. A **77**, 53407 (2008)

2. *"Large-Angle Electron Diffraction Structure in Laser-Induced Rescattering from Rare Gases"* D. Ray, B. Ulrich, I. Bocharova, C. Maharjan, P. Ranitovic, B. Gramkow, M. Magrakvelidze, S. De, I. V. Litvinyuk, A. T. Le, T. Morishita, C. D. Lin, G. G. Paulus, C. L. Cocke, Phys. Rev. Lett. **100**, 143002 (2008)

1. *"Strong-field non-sequential double ionization: wavelength dependence of ion momentum distributions for neon and argon"*, A S Alnaser, D Comtois, A T Hasan, D M Villeneuve, J-C Kieffer. I V Litvinyuk, J. Phys. B **41**, 31001 (2008)

Structure and Dynamics of Atoms, Ions, Molecules and Surfaces: Atomic Physics with Ion Beams, Lasers and Synchrotron Radiation

Uwe Thumm, J.R. Macdonald Laboratory, Kansas State University
Manhattan, KS 66506 thumm@phys.ksu.edu

1. Laser-molecule interactions

Project scope: We seek to develop numerical and analytical tools to i) efficiently predict the effects of strong laser fields on the bound and free electronic and nuclear dynamics in small molecules and ii) to fully image the laser-controlled nuclear dynamics.

Recent progress: We continued our investigations of the dissociation and ionization of $H_2^{(+)}$ and $D_2^{(+)}$ in short intense laser pulses. We investigated the possibility of controlling the electronic motion in dissociating D_2^+ and studied the controlled manipulation of bound vibrational wave packets with a sequence of short control laser pulses. We introduced a quantum-beat imaging technique that allows vibrational and rotational beat frequencies, ro-vibrational couplings, molecular potential curves, and the nodal structure of nuclear wave functions to be derived from either measured kinetic-energy-release (KER) spectra or numerical probability densities.

Example 1: Controlling and stopping the nuclear motion in D_2^+ with laser pulses (with Thomas Niederhausen and Fernando Martin). We investigated the bound vibrational and dissociation dynamics of D_2^+ [1,2] in short intense laser pulses by applying wave-packet propagation methods.

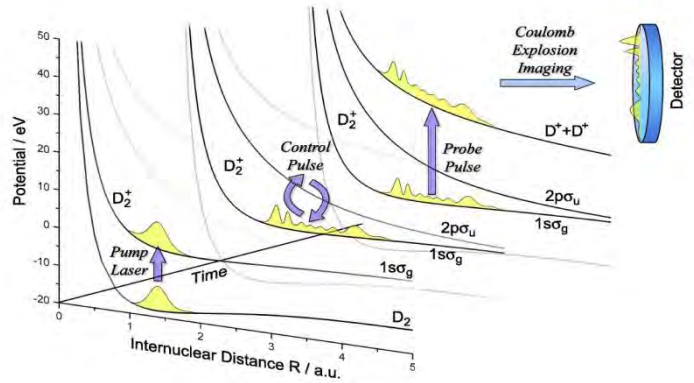

Fig. 1. Ionization of D_2 (v=0) by a pump pulse, followed by the modification of the vibrational wave packet on the D_2^+ $1s\sigma_g^+$ potential curve by a control pulse, and the final destructive analysis via Coulomb explosion imaging by a probe pulse.

Based on new full 3D calculations, we examined the possibility of manipulating the vibrational-state decomposition of bound vibrational wave packets with a sequence of up to eight of control laser pulses at minimal dissociative loss (Fig. 1).

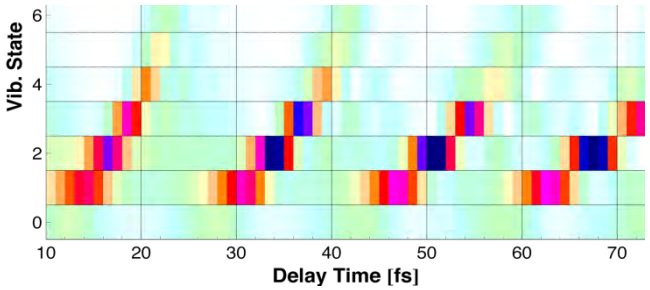

Fig. 2. Stationary vibrational state composition of an initial Franck-Condon nuclear wave packet in D_2^+ after exposure to a 6fs 0.1 PW/cm^2 Gaussian control pulse as a function of the control-pulse delay.

We found that such a sequence of short control pulses can effectively steer the nuclear motion in D_2^+ molecular ions and, depending on the control-pulse delays, even stop a moving nuclear wave packet to produce an excited stationary vibrational state (Fig.2).

Future plans: Control schemes for quenching moving ro-vibrational wave packets into stationary states using a sequence of standardized control pulses will be further examined. Note that the quality of this Raman–control mechanism can be tested experimentally by Coulomb-explosion imaging, i.e., by identifying the nodal structure of the surviving vibrational state in the kinetic energy release (KER) spectrum of the molecular fragments.

Example 2: Strong-field modulated diffraction effects in the correlated electronic-nuclear motion in dissociating molecular ions (with Feng He and Andreas Becker). We have studied the electronic motion inside dissociating H_2^+ molecules that are exposed to a fs IR laser pulse. The sensitive dependence of the correlated electronic-nuclear motion can be explained in terms of the diffractive electronic momentum distribution of the dissociating molecule. This distribution is dynamically modulated by the nuclear motion and periodically shifted in the oscillating IR electric field. Depending on the IR laser intensity, the direction of the electronic motion can follow or oppose the IR laser electric force. Our interpretation of this effect in terms of a Wigner phase-space distribution [3] is based on the passage of electronic flux through diffractive "momentum gates" of the two-center system that may or may not allow the electron to transfer to the other nucleus. It reveals that the oscillating vector potential of IR laser field periodically shifts these gates, directiong the electron through different gates at different laser intensities.

Future plans: We intend to further investigate the control - at a sub-fs time scale - of the internuclear electronic dynamics in small molecules using XUV and IR pulses and pulse trains [4] of variable shapes [5], delays, center frequencies, and intensities.

Example 3: Imaging the ro-vibrational nuclear dynamics of small molecules in strong laser fields (with Maia Magrakvelidze, Thomas Niederhausen, Bernold Feuerstein, Martin Winter, and Rüdiger Schmidt). We investigated the extent to which measured time-dependent fragment KER spectra and calculated nuclear probability densities can reveal 1) transition frequencies between stationary vibrational states, 2) stationary rotational states and ro-vibrational (RV) couplings, 3) the nodal structure of stationary rotational and vibrational states, 4) field-free and laser-field-dressed adiabatic electronic potential curves of the molecular ion, and 5) the progression of decoherence induced by random interactions with the environment [2,6-8].

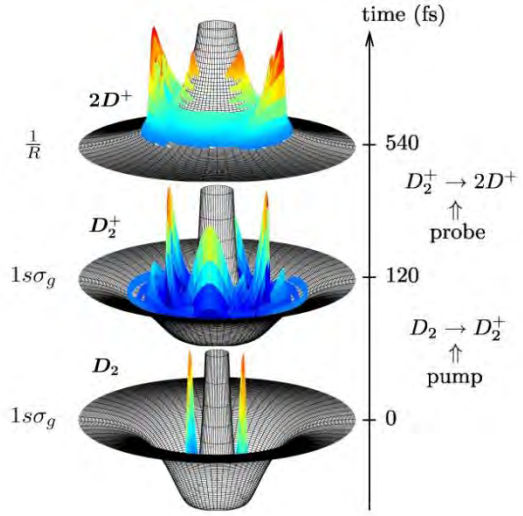

Fig. 3. Snapshots of the calculated time evolution of a RV wave packet in $D_2^{0,+,2+}$.
At t=0 a pump laser pulse ionizes D_2 and excites the initial RV wave packet from the $1s\sigma_g$, $v=0$ state in D_2 (bottom graph) to the $1s\sigma_g$ state of D_2^+ where it evolves, continuously changing its distribution in R and θ.
Middle graph: probability density of the wave packet in D_2^+ at t=120 fs. Ionization by a probe laser pulse after a delay of, e.g., τ=540 fs projects the wave packet onto the repulsive potential surface of the $2D^+$-system (top graph), leading to fragmentation by CE.
Measurement of the KER of the D^+ fragments as a function of τ enables the characterization of the wave packet dynamics in terms of R- and θ-dependent spectra.

Our imaging method is based on the Fourier transformation, w(R, θ, f), over finite samplig times T, of the time-, internuclear distance (R)-, and molecular orientation (θ)- dependent probability density w(R, θ, t) of the D_2^+ nuclear wave packet [7,8]. Applied to numerically propagated D_2^+ RV wavepackets, it allows us to simulate novel experiments that record a time series of pump-probe-delay (τ)-dependent KER spectra by Coulomb-explosion mapping for $0 < \tau < T$. Our numerical results for vibrational wave packets [2,6,7] demonstrate that the obtained two-dimensional R-dependent power spectra enable the comprehensive characterization of the wave-

packet dynamics and directly visualize the laser-modified molecular potential curves in intense, including `bond softening' and `bond hardening' processes [2]. The harmonic time-series analysis leads to a general scheme for the full reconstruction, up to an overall phase, of the initial wave packet based on measured KER spectra [7].

Including rotation of the molecular ion (Fig. 3) [8], beat frequencies that correspond to a vibrational transition $v \rightarrow v'$ are split into multiple lines due to rotational-vibrational coupling. These lines represent individual angular-momentum contributions to the ro-vibrational wave packet (Fig. 4).

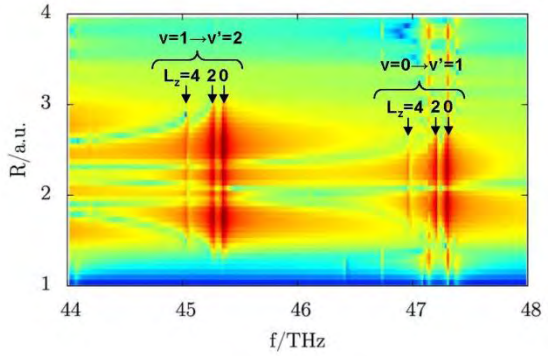

Fig. 4. Angle-integrated power spectra for D_2^+, $|\int d\theta\, w(R,\theta,f)|^2$, as a function of the beat frequency f andde internuclear distance R. Due to ro-vibrational couplings, lines for the same vibrational transition and different angular momenta L_z do not coincide. Vibrational transitions at larger L_z appear at lower frequencies.

Future plans: We intend to simulate the extent to which the quantum-beat analysis of measured time-dependent fragment KER spectra can quantify the laser-modulated ro-vibrational structure of H_2^+ and other diatomic molecules. Extending this technique to more complicated polyatomic molecular systems and reaction complexes may enable the investigation of molecular dynamics across the (field-modified) potential barrier along a particular reaction coordinate, and, thus, provide a basis for novel multidimensional optical-control schemes for chemical reactions. We further envision to apply this method to quantify the progression of decoherence in the nuclear motion based on a time series of KER spectra [7].

2. <u>Attosecond time-resolved photoelectron spectroscopy of metal surfaces</u> (with Chang-hua Zhang)

Project scope: We attempt to model the time-resolved photo-electron emission and Auger decay in pump-probe and streaking experiments with complex targets, such as clusters, carbon nanotubes, and surfaces.

Recent progress: In a recent experiment [9], an attosecond extreme XUV light pulse is used to release electrons from either bound core levels or delocalized conduction-band states. The released electrons get exposed to the same IR probe pulse, that was also used to generate the XUV pulse via harmonic generation. The two laser pulses are thus synchronized with a precisely adjustable time delay τ, and the measured asymptotic photoelectron kinetic energy E depends on τ. By varying τ, a tomographic image of the time-resolved photo-electron kinetic energy distribution $P(E,\tau)$ can be recorded. For tungsten surfaces a relative delay of 110 ± 70 as was measured [9] between the detection of electrons that are photoemitted by absorption of a single XUV photon from 4f-core and conduction-band levels. We calculated the energy-resolved spectra $P_{cb}(E, \tau)$ and $P_{4f}(E, \tau)$ for the two groups of photoelectrons as a function of τ. The comparison of experiment [9] and theory [10] shows that our IR pulse modulation of the photoelectron kinetic energy agrees with the experiment. In order to find the temporal shift between our calculated spectra for streaked photoemission from 4f-core and conduction-band levels, we examined their center-of-energies $E_{CM}(\tau)$ and find agreement with the measured relative delay (Fig. 5).

Future plans: (1) We intend to include diffraction effects during the propagation of photoelectrons inside the solid. **(2)** For XUV pulses that are of the order of or longer than the IR period, illumination of an adsorbate-covered metal surface with an XUV and a delayed IR laser pulse results in sidebands in the photoelectron spectra.We have started a detailed analysis of such measured [11] sideband spectra, and are able [12] to reproduce the measured relative side band heights (SBH). The SBHs parameterize the delay between the photoemitted core-level electrons and Auger electrons.

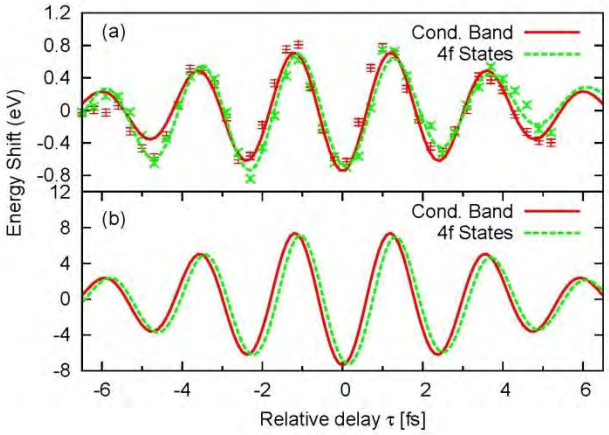

Fig. 5. Streaked photo-emission from conduction-band and 4f-core levels of a W (110) surface: E_{CM} as a function of the delay between the XUV and IR pulse. (a): Experimental results [9]. The damped sinusoidal curves are fits to the raw experimental data. (b): Calculated results [10] showing a relative shift of 110 as between the two groups of electrons. Energies for the 4f photoelectrons are multiplied by a factor 2.5 in (a) and 1.1 in (b).

[1] *Controlled vibrational quenching of nuclear wave packets in D_2^+*, T. Niederhausen and U. Thumm, Phys. Rev. A **77**, 013407 (2008).

[2] *Quantum-beat imaging of the nuclear dynamics in D_2^+: Dependence of bond softening and bond hardening on laser intensity, wavelength, and pulse duration*, M. Magrakvelidze, F. He, T. Niederhausen, I. V. Litvinyuk, and U. Thumm, Phys. Rev. A 79, 033410 (2009).

[3] *Strong-field modulated diffraction effects in the correlated electronic-nuclear motion in dissociating H_2^+*, F. He, A. Becker, and U. Thumm, Phys. Rev. Lett. 101, 213002 (2008).

[4] *Control of electron localization in molecules using XUV and IR pulses*, K. P. Singh, W. Cao, P. Ranitovic, S. De, F. He, D. Ray, S. Chen, U. Thumm, A. Becker, M. M. Murnane, H. C. Kapteyn, I. Litvinyuk, C. L. Cocke, Phys. Rev. Lett., in preparation (2009).

[5] *Ion-energy dependence of asymmetric dissociation of D2 by a two-color laser field,* D. Ray, F. He, S. De, W.Cao, H. Mashiko, P.Ranitovic, K.P.Singh, I. Znakovskaya, U. Thumm, G.G.Paulus, M.F.Kling, I. Litvinyuk, and C.L. Cocke, Phys. Rev. Lett., submitted (2009).

[6] *Towards a complete characterization of molecular dynamics in ultra-short laser fields*, B. Feuerstein, T. Ergler, A. Rudenko, K. Zrost, C.D. Schroeder, R. Moshammer, J.Ullrich, T. Niederhausen, and U. Thumm, Phys. Rev. Lett. **99**, 153002 (2007).

[7] *Time-series analysis of vibrational nuclear wave packet dynamics in D_2^+*, U. Thumm, T. Niederhausen, and B. Feuerstein, Phys. Rev. A **77**, 063401 (2008).

[8] *Multidimensional quantum-beat spectroscopy: towards the complete temporal and spatial resolution of the nuclear dynamics in small molecules*, M. Winter, R. Schmidt, and U. Thumm, Phys. Rev. Lett., submitted (2009).

[9] A. L. Cavalieri *et al*., Nature **449**, 1029 (2007).

[10] *Attosecond photoelectron spectroscopy of metal surfaces*, C.-H. Zhang and U. Thumm, Phys. Rev. Lett. 102, 123601 (2009).

[11] L. Miaja-Avila *et al.*, Phys. Rev. Lett. **101**, 046101 (2008)

[12] *Laser-assisted photoemission from adsorbate-covered metal surfaces: time-resolved core-hole relaxation from sideband profiles,* C.-H. Zhang and U. Thumm, Phys. Rev. A, submitted (2009).

Other DoE-sponsored publications (2006-2009):

Capture and ionization in laser-assisted proton–hydrogen collisions, T. Niederhausen and U. Thumm, Phys. Rev. A **73**, 041404(R) (2006).

Neutralization of H^- near vicinal metal surfaces, B. Obreshkov and U. Thumm, Phys. Rev. A **74**, 012901 (2006).

Step-up vs. step-down scattering asymmetry in the neutralization of H^- on free-electron vivinal surfaces, B. Obreshkov and U. Thumm, Surf. Sci. **601**, 622 (2007).

Non-resonant formation of H^- near unreconstructed Si(100) surfaces, B. Obreshkov and U. Thumm, Phys. Rev. A **76**, 052902 (2007).

Angular dependence of the strong-field ionization of randomly oriented hydrogen molecules, M. Magrakvelidze, F. He, S. De, I. Bocharova, D. Ray, I. Litvinyuk, and U. Thumm, Phys. Rev. A 79, 033408 (2009).

Engineered Electronic and Magnetic Interactions in Nanocrystal Quantum Dots

Victor I. Klimov

Chemistry Division, C-PCS, MS-J567, Los Alamos National Laboratory
Los Alamos, New Mexico 87545, klimov@lanl.gov, http://quantumdot.lanl.gov

1. Program Scope

Using semiconductor nanocrystals (NCs) one can produce extremely strong spatial confinement of electronic excitations not accessible with other types of nanostructures. Because of spatial constraints imposed on electron and hole wavefunctions, electronic energies in NCs are directly dependent upon their dimensions, which is known as the quantum-size effect. This effect has been a powerful tool for controlling spectral responses of NCs and enabling potential applications such as multicolor labeling, optical amplification, and low-cost lighting. In addition to spectral tunability, strong spatial confinement results in a significant enhancement of carrier-carrier interactions that lead to a number of novel physical phenomena including large splitting of electronic states induced by electron-hole (e-h) exchange coupling, ultrafast mutiexciton decay via Auger recombination, high-efficiency intraband relaxation via e-h energy transfer, and direct generation of multiple excitons by single absorbed photons via carrier multiplication. Understanding the fundamental physics of electronic and magnetic interactions under conditions of extreme quantum confinement and the development of methods for controlling these interactions represent the major thrusts of this project. Research topics studied here include single-exciton optical gain using engineered exciton-exciton interactions, tunable magnetic exchange with paramagnetic ions in core/shell heterostructures, and Auger recombination and carrier multiplication in NCs of direct- and indirect-gap materials. In addition to their fundamental significance, these studies are relevant to a number of emerging applications of NCs in areas such as low-threshold lasing, solar-energy conversion, and magneto-optical imaging.

2. Recent Progress

During the past year, our work in this project focused on studies of exchange interactions in Mn-doped core-shell structures, single-NC magnetic-field spectroscopy of band-edge states in CdSe quantum dots, comparative studies of Auger recombination in direct- and indirect-gap semiconductors, pressure-dependent studies of multiexciton dynamics in PbSe NCs, and optical gain studies of "giant" NCs comprising small CdSe cores overcoated with thick CdS shells. During 2007-09, our work resulted in 23 peer-reviewed publications including reports in *Nature* and *Nature Mater.*, feature articles in *Annu. Rev. Phys. Chem.* and *Acc. Chem. Res.*, 4 *Phys. Rev. Letters*, 3 *J. Am. Chem. Soc.* papers, 4 *Nano Letters*, 3 *Phys. Rev. B* articles, etc. The studies conducted in this project were presented in 38 invited conference talks and numerous university seminars. Below, we provide a description of two pieces of our work in which we deal with Auger effects in NCs of direct- and indirect-gap semiconductors [1] and exchange interactions in engineered core-shell Mn-doped NCs [2]. In our Auger studies, we observe a very unusual trend, namely a *universal size-dependent scaling* of multiexciton decay rates across a wide range of NC systems (including direct- and indirect-gap materials). In our studies of magnetically doped NCs, we demonstrate for the first time that exchange interactions in nanostructures can be tuned not only in *size* but also in *sign*.

2.1 Universal size-dependent trends in Auger recombination in NCs of direct- and indirect-gap semiconductors. In bulk direct-gap materials, Auger decay is a three-particle process wherein the e-h recombination energy is transferred to the third carrier. Because of combined requirements of energy and translational momentum conservation, this process exhibits a thermally activated behavior and is characterized by a rate (r_A) that scales as $r_A \propto \exp(-E_A/k_BT)$], where E_A is the activation threshold, which is directly proportional to the energy gap, E_g. In indirect-gap bulk materials, carriers involved in Auger recombination are separated in $\boldsymbol{k}$-space. In this case, Auger decay occurs with appreciable efficiencies only with participation of momentum-conserving phonons. While involvement of phonons removes the activation barrier, it leads to a significant reduction of the decay rate because such Auger recombination is a higher-order, four-particle process. For example, direct-gap InAs and indirect-gap Ge, exhibit room-temperature Auger constants that differ by five orders

of magnitude ($1.1\text{x}10^{-26}$ cm^6s^{-1} [81] vs. $1.1\text{x}10^{-31}$ cm^6s^{-1}, respectively), despite a relatively small difference in energy gaps (0.35 eV and 0.66 eV, respectively).

The strong spatial confinement that is characteristic of ultrasmall semiconductor NCs, leads to relaxation of translational momentum conservation, which should diminish the distinction between direct- and indirect-gap semiconductors with regard to the Auger processes. To analyze the effect of arrangement of energy bands in ***k***-space on Auger recombination, we have performed a comparison of multiexciton decay rates in NCs of indirect-gap (Ge) and direct-gap (InAs, PbSe, and CdSe) semiconductors.

Carrier recombination dynamics were monitored using transient absorption (TA) pump-probe spectroscopy, in which the absorption changes associated with non-equilibrium carriers injected by a sub-100 fs pump pulse were probed with a second variably delayed pulse. In the case of direct-gap NCs, the probe wavelength is tuned to the lowest-energy 1S absorption feature to monitor carrier-induced band-edge bleaching. Because of the small oscillator strength of inter-band (valence-to-conduction band) transitions, indirect-gap NCs do not exhibit band-edge bleaching but rather show a structureless photoinduced absorption due to intra-band transitions. Since the strength of these transitions increases with decreasing energy, photoinduced absorption is typically probed in the infrared (IR) (we used 1100 nm in our measurements of Ge NCs).

From TA dynamics measured as a function of pump intensity, we determine Auger decay times of biexciton states (τ_2), and then, use them to calculate effective Auger constants $C_{NC}=V_0^2(8\tau_2)^{-1}$ (V_0 is the NC volume). Remarkably, despite a vast difference in electronic structures of the bulk solids (especially when one compares direct- and indirect-gap materials), the Auger constants in same-size NCs of different compositions (Ge, PbSe, InAs, and CdSe) are similar. Further, they show a universal cubic size dependence described approximately by $C_{NC} = \beta R^3$ (R is the NC radius). The numerical pre-factor in this expression (β) varies by less than an order of magnitude (from 0.4×10^{-9} cm^3s^{-1} for CdSe NCs to 2.3×10^{-9} cm^3s^{-1} for Ge NCs) depending on composition, which is in sharp contrast to several orders of magnitude spread in Auger constants in the corresponding bulk materials.

A close correspondence in Auger constants and multiexciton decay rates observed for similarly sized NCs of different compositions indicates that the key parameter, which defines Auger rates in these materials, is NC size rather than the energy gap or electronic structure details. These observations can be rationalized by confinement-induced relaxation of momentum conservation, which removes the activation barrier in Auger decay in NCs of direct-gap semiconductors and eliminates the need for a momentum-conserving phonon in indirect-gap NCs. Thus, this effect may smear out the difference between materials with different energy gaps (E_g would normally determine the height of the activation barrier) or different arrangements of energy bands in ***k***-space.

2.2 Tunable exchange interactions in Mn-doped core/shell NCs. Traditionally, embedding paramagnetic atoms into low-dimensional semiconductor structures requires molecular-beam epitaxy or chemical vapor deposition techniques. There now exists a rich variety of "diluted magnetic semiconductor" (DMS) quantum wells, superlattices, and hetero-interfaces, with recent work demonstrating magnetic doping of epitaxially-grown "zero-dimensional" quantum dots. In parallel however, advances in colloidal chemistry have recently allowed magnetic doping of semiconductor NCs providing an alternative and potentially lower-cost route towards magnetically active quantum dots. With a view towards enhancing carrier-paramagnetic atom spin interactions, colloidal NCs typically generate stronger spatial confinement of electronic wavefunctions compared to their epitaxial counterparts, which is thought to enhance *sp-d* exchange coupling even for a single magnetic dopant atom.

Central to the efforts in DMS nanomaterials is a drive to control the interaction strength between carriers (electrons and holes) and the embedded magnetic atoms. In this context, colloidal NCs provide great flexibility through growth-controlled "engineering" of electron and hole wavefunctions in individual NCs. In our recent work [2], we have demonstrated a widely tunable magnetic *sp-d* exchange interaction between electron-hole excitations (excitons) and paramagnetic manganese ions using "inverted" core/shell NCs composed of Mn^{2+}-doped ZnSe cores that are over-coated with undoped (i.e., nonmagnetic) shells of narrower-gap CdSe.

Four series of ZnSe/CdSe NCs were grown, each having ZnSe cores of radius $r \cong 17$ Å. Within each series the CdSe shell thickness, *h*, systematically increases from 0 - 8 Å. Two series used nonmagnetic (undoped) "reference" cores, and two used Mn^{2+}-doped cores. Elemental analysis of pyridine-washed magnetic cores indicates ~2 Mn^{2+} ions per core, on average. Paramagnetic resonance studies indicate that the Mn^{2+} reside primarily within the ZnSe core, for all *h*. Low-temperature optical studies of magnetic circular dichroism in this nanostructures reveal giant Zeeman spin-splittings between the spin ±1 band-edge excitons that, surprisingly, are tunable both in magnitude *and in sign*. Effective exciton *g*-factors are controllably tuned from -200 to +30 solely

by increasing the CdSe shell thickness, demonstrating that strong quantum confinement and wavefunction engineering in core/shell NC materials can be used to manipulate carrier–Mn^{2+} wavefunction overlap and the *sp-d* exchange parameters themselves.

Our observations strongly suggest that the sign of the electron-Mn^{2+} exchange constant, α, in NCs is opposite to that in bulk materials. We believe that this effect results from a confinement induced admixture of *p*-type valence band symmetry into the electron's Bloch wavefunction, causing a negative kinetic-exchange contribution to α that increases with confinement energy (hole exchange constant, β, remains largely unaffected, being already dominated by kinetic exchange). Such a possibility has been indeed expected based on recent theories of DMS quantum wells, however, prior to our studies this effect has never been observed experimentally.

3. Future Plans

In our future work, we plan to explore two topics: *single-exciton gain* through giant exciotn-exciton repulsion in IR emitting type-II NCs and *"visualization" of single spins* in individual magnetically doped NCs.

3.1 Single-exciton optical gain in IR using exciton-exciton repulsion in type-II NCs. So far, optical gain in the IR spectral range with colloidal nanostructures has been only demonstrated for NCs of lead salts such as PbSe and PbS. These materials, however, are characterized by a high, eight-fold degeneracy of the lowest-energy emitting states, which results in high optical gain thresholds that corresponds to excitation of at least 4 excitons per NC on average. This high exciton multiplicity leads to very short gain lifetimes (~10 ps) because of rapid shortening of the Auger time constants with the number of excitons. This greatly complicates applications of these materials in practical lasing technologies.

As we discussed in refs. 19 - 23, type-II heterostructures can demonstrate optical gain in the single-exciton regime, for which the population-inversion lifetime is limited not by Auger decay but by the much slower intrinsic radiative recombination. In our work, we will focus on the synthesis and spectroscopic characterization of type-II NCs with IR emission energies. We will explore material systems such as PbSe/CdS and CdSe/CdTe that exhibit type-II alignment of energy states in the bulk form. The ultimate goal of this work will be the demonstration of optical gain and amplified spontaneous emission in the IR due to single-exciton states.

3.2 Detection of single magnetic spins in semiconductor NCs. Motivated by our recent progress in doping NCs with magnetic Mn ions [2] and also by our advances in spectrally- and polarization-resolved microscopy of single NCs [3], we propose to develop optical techniques to measure the magnetization of *single* Mn spins that have been doped into NCs. This approach will exploit the well-known *exchange coupling* in DMSs such as $Zn_{1-x}Mn_xSe$ or $Cd_{1-x}Mn_xSe$, wherein the spin orientation of embedded Mn atoms dramatically influences the semiconductor's band-edge radiative transitions.

To detect the spin state of a single Mn ion, it is necessary that we selectively measure photoluminescence (PL) from an individual NC. This will be achieved using established techniques for single-NC microscopy (already in regular use in our laboratories). It further requires that in synthesized structures, the NC emission energy is lower than the energy of the internal Mn transition (2.13 eV). The latter situation can be realized using, for example, Mn-doped CdSe NCs of large sizes. Additionally, we will explore the use of inverted core-shell structures based on ZnSe and CdSe. This approach will take advantage of previous techniques for incorporation of Mn into ZnSe NCs and the growth of high-quality ZnSe(core)/CdSe(shell) structures [2]. As has been demonstrated previously, the emission energy for these structures can extend to 1.8 eV, which is below the energy of the internal Mn transition. Core-shell NCs will also provide an interesting opportunity for controlling strength of the exchange interaction of NC quantum-confined states with Mn ions by tuning the spatial distributions of electronic wave functions.

The interaction of the Mn atom with electrons and holes (generated by photoexcitation) is expected to yield a PL spectrum consisting of 6 *discrete* peaks, each peak corresponding to the radiative recombination of spin 1 electron-hole pairs (excitons) that have interacted with a *specific* spin state of the Mn atom. The intensity distribution and energy splitting of the observed PL peaks will reveal the probability of the Mn spin being in that specific quantum-mechanical state, and the energy splitting between the peaks reveals the strength of the exchange coupling.

4. Publications (2007 - 2009)

1. Robel, R. Gresback, U. Kortshagen, R. D. Schaller, V. I. Klimov, Universal size-dependent trends in Auger recombination in direct- and indirect-gap semiconductor nanocrystals, *Phys. Rev. Lett.*, **102**, 177404 (2009)
2. D. Bussian, M. Ying, S. A. Crooker, M. Brynda, A. L. Efros, V. I. Klimov, Tunable magnetic interactions in manganese-doped inverted core/shell ZnSe/CdSe nanocrystals, *Nature Mater.* **8**, 35 (2009)
3. H. Htoon, S. A. Crooker, M. Furis, S. Jeong, Al. L. Efros, V. I. Klimov Anomalous circular polarization of photoluminescence spectra of individual CdSe nanocrystals in an applied magnetic field, *Phys. Rev. Lett*. **102**, 017402 (2009)
4. F. Garca-Santamara, Y. Chen, J. Vela, R. D. Schaller, J. A. Hollingsworth and V. I. Klimov, Suppressed Auger recombination in "giant" nanocrystals boosts optical gain performance, *Nano Lett*. DOI: 10.1021/nl901681d (2009).
5. J. Joo, J. M. Pietryga, J. A. McGuire, S.-H. Jeon, D. J. Williams, H.-L. Wang and V. I. Klimov, A reduction pathway in the synthesis of PbSe nanocrystal quantum dots, *J. Am. Chem. Soc.* DOI: 10.1021/ja903445f (2009)
6. D. C. Lee, J. M. Pietryga, I. Robel, D. J. Werder, R. D. Schaller, V. I. Klimov, Colloidal Synthesis of infrared-emitting germanium nanocrystals *J. Am. Chem. Soc.* (*Communication*) **131**, 3436 (2009)
7. D. Bussian, A. Malko, H. Htoon, Y. Chen, V. I. Klimov, J. A. Hollingsworth, Quantum optics with nanocrystal quantum dots in solution: Quantitative study of clustering, *J. Phys. Chem.* **113**, no. 6, 2241 (2009)
8. J. A. McGuire, J. Joo, J. M. Pietryga, R. D. Schaller, and V. I. Klimov, New aspects of carrier multiplication in semiconductor nanocrystals, *Acc. Chem. Res.* **41**, 1810 (2008)
9. J. Vela, B. S. Prall, P. Rastogi, D. J. Werder, J. L. Casson, D. J. Williams, V. I Kimov, J. A. Hollingsworth, Sensitization and protection of lanthanide ion emission in In2O3:Eu nanocrystal quantum dots, *J. Phys. Chem. C* **112**, 20246 (2008).
10. B.Q. Sun, A.T. Findikoglu, M. Sykora, D.J. Werder, and V.I. Klimov, Hybrid photovoltaics based on semiconductor nanocrystals and amorphous silicon, *Nano Lett.* **9**, 1235 (2009)
11. M. Durach, A. Rusian, V. I. Klimov, M. I. Stockman, Nanoplasmonic renormalization and enhancement of Coulomb interactions, *New J. Phys.* **10**, 105011 (2008)
12. J. M. Pietryga, K. K. Zhuravlev, M. Whitehead, V. I. Klimov, R. D. Schaller, Evidence for barrierless Auger recombination in PbSe nanocrystals: A pressure-dependent study of transient optical absorption, *Phys. Rev. Lett.* **101**, 217401 (2008)
13. M. Sykora, L. Mangolini, R. D. Schaller, U. Kortshagen, D. Jurbergs, and V. I. Klimov, Size-dependent intrinsic radiative decay rates of silicon nanocrystals at large confinement energies, *Phys. Rev. Lett*. **100**, 067401 (2008).
14. V. I. Klimov, J. A. McGuire, R. Schaller, and V. I. Rupasov, Scaling of multiexciton lifetimes in semiconductor nanocrystals, *Phys. Rev. B* **77**, 195324 (2008).
15. H. Htoon, M. Furis, S. A. Crooker, S. Jeong, V. I. Klimov, Linearly-polarized 'fine structure' of the bright exciton state in individual CdSe nanocrystal quantum dots, *Phys. Rev. B* **77**, 035328 (2008)
16. R. D. Schaller, J. M. Pietryga, and V. I. Klimov, Carrier multiplication in InAs nanocrystal quantum dots with an onset defined by the energy conservation limit, *Nano Lett.* **7**, 3469 (2007)
17. V. I. Rupasov and V. I. Klimov, Carrier multiplication in semiconductor nanocrystals via intraband optical transitions involving virtual biexciton states, *Phys. Rev. B* **76**, 125321 (2007).
18. X. Jiang, R. D. Schaller, S. B. Lee, J. M. Pietryga, V. I. Klimov, and A. A. Zakhidov, PbSe nanocrystal/conducting polymer solar cells with an infrared response to 2 micron, *J. Mat. Res.* **22**, 8, 2204 (2007)
19. V. I. Klimov, S. A. Ivanov, J. Nanda, M. Achermann, I. Bezel, J. A. McGuire, and A. Piryatinski, Single-exciton optical gain in semiconductor nanocrystals, *Nature* **447**, 441 (2007).
20. A. Piryatinski, S. A. Ivanov, S. Tretiak, and V. I. Klimov, Effect of quantum and dielectric confinement on the exciton-exciton interaction energy in type II core/shell semiconductor nanocrystals, *Nano Lett.* **7**, 108 (2007)
21. V. I. Klimov, Spectral and dynamical properties of multiexcitons in semiconductor nanocrystals, *Annu. Rev. Phys. Chem.* **58**, 635 (2007).
22. J. Nanda, S. A. Ivanov, J. Nanda, M. Achermann, I. Bezel, A. Piryatinski, V. I. Klimov Light Amplification in the single-exciton regime using exciton-exciton repulsion in type-II nanocrystal quantum dots, *J. Phys. Chem. B* **111**, 15382 (2007).
23. S. A. Ivanov, A. Piryatinski, J. Nanda, S. Tretiak, D. Werder, V. I. Klimov, Type-II core/shell CdS/ZnSe nanocrystals: Synthesis, electronic structures, and spectroscopic properties, *J. Am. Chem. Soc.* **129**, 11708 (2007).

Atomic, Molecular and Optical Sciences at LBNL

A. Belkacem, C. W. McCurdy, T. N. Rescigno and T. Weber

Chemical Sciences Division, Lawrence Berkeley National Laboratory, Berkeley, CA 94720

Email: abelkacem@lbl.gov, cwmccurdy@lbl.gov, tnrescigno@lbl.gov, tweber@lbl.gov

Objective and Scope

The AMOS program at LBNL is aimed at understanding the structure and dynamics of atoms and molecules using photons and electrons as probes. The experimental and theoretical efforts are strongly linked and are designed to work together to break new ground and provide basic knowledge that is central to the programmatic goals of the Department of Energy. The current emphasis of the program is in three major areas with important connections and overlap: inner-shell photo-ionization and multiple-ionization of atoms and small molecules; low-energy electron impact and dissociative electron attachment of molecules; and time-resolved studies of atomic processes using a combination of femtosecond X-rays and femtosecond laser pulses. This latter part of the program is folded in the overall research program in the Ultrafast X-ray Science Laboratory (UXSL).

The experimental component at the Advanced Light Source makes use of the Cold Target Recoil Ion Momentum Spectrometer (COLTRIMS) to advance the description of the final states and mechanisms of the production of these final states in collisions among photons, electrons and molecules. Parallel to this experimental effort, the theory component of the program focuses on the development of new methods for solving multiple photo-ionization of atoms and molecules. This project seeks to develop theoretical and computational methods for treating electron processes that are currently beyond the grasp of first principles methods, either because of the complexity of the targets or the intrinsic complexity of the processes themselves. This dual and tightly linked approach of experiment and theory is key to break new ground and solve the problem of photo double-ionization of small molecules and unravel unambiguously electron correlation effects.

Inner-Shell Photoionization and Dissociative Electron Attachment of Small Molecules

Ali Belkacem and Thorsten Weber

Chemical Sciences Division, Lawrence Berkeley National Laboratory, Berkeley, CA 94720

Email: abelkacem@lbl.gov, tweber@lbl.gov

Objective and Scope

This program is focused on studying photon and electron impact ionization, excitation and dissociation of small molecules and atoms. The first part of this project deals with the interaction of soft x-rays with atoms and simple molecules by seeking new insight into atomic and molecular dynamics and electron correlation effects. These studies are designed to test advanced theoretical treatments by achieving a new level of completeness in the distribution of the momenta and/or internal states of the products and their correlations. The second part of this project deals with the interaction of low-energy electrons with small molecules with particular emphasis on Dissociative Electron Attachment (DEA). Both studies are strongly linked to our AMO theoretical studies led by C.W. McCurdy and T. Rescigno and are designed to break new ground and provide basic knowledge that is central to the programmatic goals of BES in electron-driven chemistry. Both experimental studies (photon and electron impact) make use of the powerful COLd Target Ion Momentum Spectroscopy (COLTRIMS) method to achieve a high level of completeness in the measurements.

Momentum imaging of the photo double ionization of the ethylene molecule.

Direct photo double ionization is a process that arises essentially because of the electron correlation. The signature of the electron correlation can be seen in the angular dstributions of the two ejected electrons in the molecular frame system. Ethylene (C_2H_4) is chosen as the ideal system to probe electron correlation in a relatively small molecule containing a single π bond. We subjected ethylene molecules to VUV radiation near the double ionization threshold in order to unravel the electron correlation and subsequent molecular dynamics. As a result of double photoionization, three distinct dissociation channels were observed: a symmetric break-up channel ($CH_2^+ + CH_2^+$), a deprotonation channel ($H^+ + C_2H_3^+$) and an asymmetric break-up ($H_2^+ + C_2H_2^+$). We performed the experiment at a photon energy of 40 eV, approximately 10 eV above the double photo ionization threshold. In each of the dissociation channels we observe at least two separate pathways that led to the products. In the vertical transition, the difference between the photon energy and the sum energy of the two ejected electrons defines where on the energy potential of the di-cation the system lands. Comparing to the very limited theoretical potential energy curves found in the literature we conclude that the third excited state (singlet S_3) is the dominant channel for symmetric break up. In particular two-conical intersections and one-avoided crossing led to the sophisticated manifold of dissociation pathways originiting from S_3 to eventually dissociate through the di-cation ground state S_1. It is quite surprising that no direct population of the S_1 ground state of the di-cation was observed in this experiment (no stable or dissociating S_1). All

channels originate from excited states of the di-cation. This absence of the dicationic ground state is tentatively attributed to having a negligible Franck-Condon overlap in the torsional mode when a transition takes place from the planar neutral ground state to the twisted dicationic ground state. The partial and complete differential cross sections were obtained for the symmetric break-up channel. The single differential cross section for the major channel (starting at S_3) and minor channel (starting at S_2) showed marked differences. In the minor channel pathway (S_2) the single differential cross section showed surprising structures, which could indicate the presence of resonant processes involving autoionizing states. The multi-differential cross section and in particular the angle of emission of the electrons relative to each other in the molecular frame exhibit a very strong electron correlation. Despite the complexity of the system under study several similarities to double photoionization of the hydrogen molecule were observed.

Photo and Auger electron angular distributions of fixed-in-space CO_2.

We performed the first kinematically complete experiment of carbon 1s photoionization of CO_2 including Auger decay and the fragmentation. The experiment was performed at the Advanced Light Source using a COLTRIMS technique. By coincident measurements of carbon (1s) photoelectrons and ion fragments using synchrotron light at several energies above the C(1s) threshold, we determine photoelectron angular distributions as well as Auger electron angular distributions with full solid angle in the molecular fixed frame. We confirm recent unexpected results showing an asymmetry of the photoelectron angular distribution along the molecular axis after ionization of the carbon 1s orbital. This observation is surprising because the carbon dioxide molecule is linear with the carbon atom placed between the oxygen atoms. The carbon 1s orbital is almost spherical-symmetric and diffraction of the electron wave at the oxygen atoms located at equal distance to the center of the wave should produce a symmetric electron angular distribution with respect to the center of mass. In this experiment we do not only confirm the asymmetry but in addition we give a direct experimental support of a mechanism proposed by theory colleagues McCurdy and Rescigno. In the vibrational ground state the nuclear wave function is symmetric. However the measurement of a single photoionization event at an individual molecule can find the molecule at asymmetric bond length. In such a case, the symmetry is broken by different C-O bond lengths on each side of the center, and the subsequent Auger decay makes it more likely for the longer bond to break. Different internuclear distances at the instant of Auger decay lead to different nuclear kinetic energy releases (KER). As a consequence the asymmetry should vary with the KER, which is what we observe. Our high resolution measurements revealed new details in the molecular-fixed frame photoelectron angular distribution and showed for the first time CO_2 Auger electron angular distributions in that frame. We observe a clear link between Auger and photo electron angular distributions due to post-collision interaction.

Kinematically complete experimental study of the dissociation pathways of the singly ionized CO molecule.

We studied the dissociation of the singly ionized carbon monoxide molecule, followed by subsequent autoionization of O^*, by detecting for the first time all four final fragments ($C^+ + O^+ + 2e$) in coincidence. In this experiment the supersonic jet of carbon monoxide was illuminated by the 43 eV x-ray beam at the Advanced Light Source. Although some direct double ionization of CO molecule was observed, the energetics dictated that most

of the registered events must be attributed to single ionization followed by an autoionization in the atomic state of the oxygen. The energy of the slow electron is constant and independent of the first electron energy or of the nuclear kinetic energy release (KER) which is a clear signature of autoionization. The molecular dissociation of CO^+ ion followed by autoionization of the oxygen has been observed before. In this study we performed the most kinematically complete experiment where by simultaneously measuring the vector momenta of all particles we were able to extract the KER of the reaction together with the energies and complete angular distributions of photo-electron and autoionization electron in the body-fixed molecular frame. The study of these detailed angular distributions as a function of polarization and KER reveal a surprising dissociation dynamics. Comparison with theoretical calculations by colleagues Rescigno and Orel shine light on the molecular states involved in the initial process of photo-ionization. We observe a strong correlation between the angle of emission of the photo-electron and the angle of emission of the autoionization electron despite the fact that autoionization takes place in the atomic oxygen when the molecule has already fully dissociated. Further studies both experimental and theoretical are on-going to understand the origin of this unique photo and autoionization electron correlation.

Dissociative electron attachment to water molecules: imaging of the dissociation dynamics of the water anion.

A Coltrims spectrometer has been modified for measuring the angular dependence and kinetic energy release of negative ion fragments arising from dissociative electron attachment to water and heavy water molecules. The resonant attachment of a low energy electron to a water molecule occurs via three metastable electronic states of the H_2O anion, whose vertical transition energies determine the incident electron energy at which attachment occurs. Following the electron attachment a competition between autodetachment of the electron and very fast molecular dynamics that keeps the electron attached to the nuclei takes place. This fast dynamics is key in converting electronic energy to nuclear motion. The dissociation of the three resonance states of the anion ($^2B_1$, $^2A_1$ and $^2B_2$) involves complicated polyatomic dynamics involving conical intersection and, perhaps Renner-Teller effects, and occurs in several interesting ways. The angular dependence of dissociative attachment depends both on the entrance amplitude and the more complicated nuclear dynamics of the anion transient state. We find that the attachment of the electron to the molecule is exquisitely sensitive to the orientation of the molecule with respect to the incoming electron. The measured angular distributions of the anion fragments (O^- or H^-) confirm quite well the concept of entrance amplitude and the unique angular selectivity of electron attachment for each resonance.

Future Plans

We plan to continue application of the COLTRIMS approach to achieve complete descriptions of the single photon double ionization of CO and its analogs. Of particular interest is an in-depth study of the “photo-autoionization” electron correlation and entanglement. Our earlier observations of the isomerization of acetylene to the vinylidene configuration forms a basis for possible further studies of this phenomena perhaps using deuterated acetylene to alter the relative time scales of molecular rotation and the dissociation dynamics. We plan to continue using our new “electron impact Coltrims” to study dissociation electron attachment to some biologically relevant molecules.

Recent Publications

D. Akoury, K. Kreidi, T. Jahnke, Th. Weber, A. Staudte, M. Schoeffler, N. Neumann, J. Titze, L. Ph. H. Schmidt, A. Czasch, O. Jagutzki, R.A. Costa Fraga, R.E. Grisenti, R. Diez Muino, N.A. Cherepkov, S.K. Semenov, P. Ranitovic, C.L. Cocke, T. Osipov, H. Adaniya, J.C. Thompson, M.H. Prior, A. Belkacem, A. L. Landers, H. Schmidt-Boecking, R. Doerner, "*The simplest double slit: Interference and Entanglement in double photoionization of H_2*", Science **318**, 949 (2007).

M.S. Schoeffler, J. Titze, N. Petridis, T. Jahnke, K. Cole, L.Ph.H. Schmidt, A. Czasch, D. Akoury, O. Jagutzki, J.B. Williams, N.A. Cherepkov, S.K. Semenov, C.W. McCurdy, T.N. Rescigno, C.L. Cocke, T. Osipov, S. Lee, M.H. Prior, A. Belkacem, A.L. Landers, H. Schmidt-Boecking, Th. Weber, R. Doerner, "*Utrafast probing of core hole localization in N_2*", Science 320, 920 (2008).

F. Martin, J. Fernandez, T. Havermeier, L. Foucar, Th. Weber, K. Kreidi, M. Schoeffler, L. Schmidt, T. Jahnke, O. Jagutzki, A. Czasch, E.P. Benis, T. Osipov, A. Landers, A. Belkacem, M.H. Prior, H. Schmidt-Boecking, C.L. Cocke, R. Doerner, "*Single photon-induced symmetry breaking of H_2 Dissociation*", Science **315**, 629 (2007).

K. Kreidi, D. Akoury, T. Jahnke, Th. Weber, A. Staudte, M. Schoeffler, N. Neumann, J. Titze, L. Ph. H. Schmidt, A. Czasch, O. Jagutzki, R.A. Costa fraga, R.E. Grisenti, M. Smolarski, P. Ranitovic, C.L. Cocke, T. Osipov, H. Adaniya, J.C. Thompson, M.H. Prior, A. Belkacem, A. Landers, H. Schmidt-Boecking, R. Doerner, "*Interference in the collective electron momentum in double photoionization of H_2*", Phys. Rev. Lett. 100, 133005 (2008)

T. Osipov, T.N. Rescigno, Th. Weber, S. Miyabe, T. Jahnke, A.S. Alnaser, M.P. Hertlein, O. Jagutzki, L. Ph. Schmidt, M. Schoeffler, L. Foucar, S. Schoessler, T. Havermeier, M. Odenweller, S. Voss, B. Feinberg, A.L. Landers, M.H. Prior, R. Doerner, C.L. Cocke, A. Belkacem, "*Fragmentation pathways for selected electronic states of the acetylene dication*", J. Phys. B: At. Mol. Opt. Phys. 41, 091001 (2008)

M. Schoeffler, K. Kreidi, D. Akoury, T. Jahnke, Th. Weber, A. Staudte, N. Neumann, J. Titze, L. Ph. H. Schmidt, A. Czasch, O. Jagutzki, R.A. Costa Fraga, R.E. Grisenti, R. Diez Muino, N.A. Cherepkov, S.K. Semenov, P. Ranitovic, C.L. Cocke, T. Osipov, H. Adaniya, J.C. Thompson, M.H. Prior, A. Belkacem, A.L. Landers, H. Schmidt-Boecking, R. Doerner, "*Photo double ionization of H2: Two-center interference and its dependence on the internuclear distance*", Phys. Rev. A 78, 013414 (2008)

A.L. Landers, F. Robicheaux, T. Jahnke, M. Schoeffler, T. Osipov, J. Titze, S.Y. Lee, H. Adaniya, M. Hertlein, P. Ranitovic, I. Bocharova, D. Akoury, A. Bhandary, Th. Weber, M.H. Prior, C.L. Cocke, R. Doerner and A. Belkacem, "*Angular correlation between photoelectrons and Auger electrons from K-shell ionization of neon"*, Phys. Rev. Lett. 102, 223001 (2009).

F. Sturm, M. Schoeffler, S. Lee, T. Osipov, S. Kirschner, N. Neumann, H.-K. Kim, B. Rudek, J. Williams, J. Daughhetee, C.L. Cocke, K. Ueda, A. Landers, Th. Weber, M.H. Prior, A. Belkacem, and R. Doerner. "*Photo and Auger electron angular distributions of fixed-in-space CO2",* Accepted for publication in PRA (2009).

Electron-Atom and Electron-Molecule Collision Processes

T. N. Rescigno and C. W. McCurdy
Chemical Sciences, Lawrence Berkeley National Laboratory, Berkeley, CA 94720
tnrescigno@lbl.gov, cwmccurdy@lbl.gov

Program Scope: This project seeks to develop theoretical and computational methods for treating electron processes that are important in electron-driven chemistry and physics and that are currently beyond the grasp of first principles methods, either because of the complexity of the targets or the intrinsic complexity of the processes themselves. A major focus is the development of new methods for solving multiple photoionization and electron-impact ionization of atoms and molecules. New methods are also being developed and applied for treating low-energy electron collisions with polyatomic molecules and clusters. A state-of-the-art approach is used to treat multidimensional nuclear dynamics in polyatomic systems during resonant electron collisions and predict channeling of electronic energy into vibrational excitation and dissociation.

Recent Progress and Future Plans:

Exterior complex scaling (ECS) continues to provide the computational framework for our studies of strongly correlated processes that involve several electrons in the continuum. We have used this methodology with some success in studies of two-photon double ionization of helium (refs. 7,13,16). Experiments underway at FLASH aimed at studying two-photon double ionization of homonuclear diatomics have prompted us to extend our 2 hν-DPI studies to molecular hydrogen. We have completed a preliminary study (ref. 22) which focused on calculating the fully differential cross section at 30 eV photon energy for equal-energy sharing of the ejected electrons. Although the results for H_2 showed some of the trends observed earlier for helium, such as a general preference for back-to-back electron escape, the calculations reveal significant molecular effects. We find significant differences in both the shape and magnitude of the differential cross sections for photon polarization parallel and perpendicular to the molecular axis. We also find that the propensity for back-to-back ejection, which is greatest when one electron is aligned with the polarization vector, decreases as the angle between one electron and the polarization vector increases. These initial studies were carried out for a single internuclear distance. However, we expect the effects of nuclear motion to be significant in both real and virtual sequential absorption where one photon is absorbed and the nuclei can move before the second photon is absorbed. These effects, as well as results for other energy-sharings, will be the subject of future studies.

The onset of Young's two-slit interference effects in single photoionization (or double photoionization at extreme unequal energy sharing) of homonuclear diatomics is expected when the De Broglie wavelength of the ejected electron is comparable to the internuclear distance. The interpretation of these effects can be obscured by the use of circularly polarized, as we showed in our studies of H_2 double ionization at high energies, which was published in *Physical Review Letters* (ref. 17). We have followed this study with a systematic comparison (ref. 19) of two-center effects in the photoionization of H_2^+, H_2 and Li_2^+ using circularly polarized light. The results show that, in general, the calculated angular distributions for circularly polarized

Li_2^+ photoelectron angular distributions at 52 eV photon energy for (top to bottom) parallel, pependicular and circular polarization.

light are very similar to those obtained by averaging the corresponding angular distributions for parallel and perpendicular linearly polarized light, implying that coherence between the corresponding Σ_u^+ and Π_u amplitudes is barely responsible for the shape of the angular distributions.

The treatment of molecular ionization dynamics beyond the Born-Oppenheimer approximation, which may be a key issue in interpreting ultrafast experiments on molecules using X-ray pulses, requires not only fast, accurate and efficient computational methods, but also the proper choice of coordinate systems. To this end, we have continued our development of an ECS-based, finite-element, discrete variable method in prolate spheroidal coordinates, which are the natural choice of coordinates for diatomic targets. The viability of this approach was demonstrated with calculations on the bound and continuum wave functions and photoionization amplitudes for H_2^+. This problem was formulated using both time-independent (ref. 20) and time-dependent (ref. 24) techniques and we demonstrated that essentially exact numerical results could be obtained far more efficiently than what could be achieved using conventional single-center expansion methods. The extension to many-electron diatomic targets, however, requires efficient treatment of the electron-electron repulsion. This problem has also been solved by using an efficient Poisson equation treatment of the electron-electron repulsion based on a multipole representation of $1/r_{12}$ in prolate spheroidal coordinates. We have applied this methodology to double ionization of H_2 with remarkable success. The results are currently being prepared for publication. We believe that the speed and accuracy of this approach will pave the way for a full treatment of H_2 DPI beyond the Born-Oppenheimer approximation.

Recent experiments on carbon 1s ionization from CO_2 showed several striking features, namely, a weak but definite asymmetry in the body-frame photoelectron angular distributions with respect to $O^+ + CO^+$ fragment ions and a rapid change in the shape of the angular distributions over a very narrow energy range. The former finding was surprising since the electron is being ejected from the central carbon in the linear, symmetric molecule. In our recently published theoretical study of this problem (ref. 23), we showed that the asymmetry could be explained without invoking a breakdown of the two-step model for core-level photoioniztion or an unlikely post-collision interaction, but rather by a proper accounting of asymmetric vibrational motion along with reasonable assumptions about the nuclear dissociation dynamics. Our theoretical angular distributions, computed using the complex Kohn variational method, are in good agreement with experiment. We were also able to explain the rapid change in the angular distributions to an energy-dependent destructive interference between partial waves.

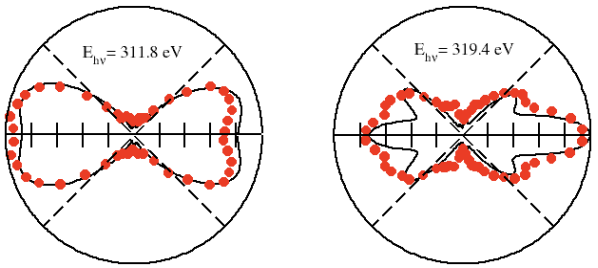

Molecular-frame photoelectron angular distributions for C 1s ejection from CO_2. Small but definite asymmetry seen in experiment is reproduced in theoretical calculations.

Inner-valence photoionization of CO at energies below the vertical threshold for direct double ionization can produce unstable singly charged CO^+ ions that dissociate to C+ plus an autoionizing O* atom that then emits a second electron at very large internuclear separations.

Although this "indirect double ionization" process in CO has been extensively studied, much of that work has focused on identification of the atomic autoionizing states which are, but relatively less is known about the character of the singly ionized states initially produced. With a view toward interpreting the results of recent ALS experiments on CO, which for the first time measure the energies, body-frame angular distributions of both Auger and photo-electrons and the associated kinetic energy releases, we have undertaken a theoretical study of this problem. The results of large-scale electronic structure calculations reveal a dissociative CO^+ state that is produced by removal of a CO 3σ(oxygen 2s) electron. This state rapidly changes character as the internuclear separation increases, undergoing several avoided crossings before correlating with $C^+(^2P) + O^*(2p^3(^2P)3s,^3P$. The identification of this state was further confirmed by carrying out photoionization calculations for CO 3σ ionization and computing body-frame photoelectron angular distributions, which were found to be in good agreement with the measured quantities. We are currently preparing the results of this joint theoretical/experimental study for publication.

Publications (2007-2009):

A. T. N. Rescigno, Wim Vanroose, D. A. Horner, F. Martín and C. W. McCurdy , "First Principles Study of Double Photoionization of H_2 Using Exterior Complex Scaling", *J. Elec. Spectros., Rel. Phenom.* **161**, 85 (2007).

B. D. A. Horner, W. Vanroose, T. N. Rescigno, F. Martin and C. W. McCurdy, Role of Nuclear Motion in Double Ionization of Molecular Hydrogen by a Single Photon, *Phys. Rev. Lett.* **98**, 073001 (2007).

C. D. J. Haxton , C. W. McCurdy and T. N. Rescigno Dissociative Electron Attachment to the H_2O molecule I: Complex-valued Potential Energy Surfaces for the $^2B_1$, $^2A_1$ and $^2B_2$ Metastable States of the Water Anion, *Phys. Rev. A.* **75,** 012710 (2007).

D. D. J. Haxton, T. N. Rescigno and C. W. McCurdy, Dissociative Electron Attachment to the H_2O molecule II: Nuclear Dynamics on Coupled Electronic Surfaces Within the Local Complex Potential Model, *Phys. Rev. A.* **75,** 012711 (2007).

E. F. L. Yip, D. A. Horner, C. W. McCurdy and T. N. Rescigno, Single and Triple Differential Cross Sections for Double Photoionization of H^-, *Phys. Rev. A.* **75**, 042715 (2007).

F. D. J. Haxton, C. W. McCurdy and T. N. Rescigno, Comment on "A Wave Packet Method for Treating Nuclear Dynamics on Complex Potentials" , *J. Phys. B* **40**, 1461 (2007).

G. D. A. Horner, F. Morales, T. N. Rescigno, F. Martin and C. W. McCurdy, Two-Photon Double Ionization of Helium Above and Below the Threshold for Sequential Ionization, *Phys. Rev. A* **76**, 030701(R) (2007)

H. T. N. Rescigno, C. W. McCurdy, D. J. Haxton, C. S. Trevisan and A. E. Orel, Nuclear Dynamics in Resonant Electron Collisions with Small Polyatomic Molecules, *J. Phys. Conference Series* **88**, 012011 (2007).

I. K. Houfek, T. N. Rescigno and C. W. McCurdy, Probing the Nonlocal Approximation to Resonant Collisions of Electrons with Diatomic Molecules, *Phys. Rev. A* **77**, 012710 (2008).

J. M. S. Schoeffler, J. Titze, N. Petridis,T. Jahnke, D. Akoury, K. Cole, L. Ph. H. Schmidt, A. Czasch, O. Jagutzki, N. A. Cherepkov, S. K. Semenov, C. W. McCurdy, T. N. Rescigno, C. L. Cocke, T. Osipov, S. Lee, M. H. Prior, A. Belkacem, A. Lander, H. Schmidt-Boecking, Th. Weber, and R. Doerner, Ultrafast probing of core hole localization in N_2, Science **320,** 920 (2008)

K. T. Osipov, T. N. Rescigno, T. Weber, S.Miyabe, T.Jahnke, A. Alnaser, M. Hertlein, O. Jagutzki, L. Schmidt, M. Schoeffler, L. Foucar, S. Schoessler, T. Havermeier, M. Odenweller, S. Voss, B. Feinberg, A. Landers, M. Prior, R. Doerner, C. L. Cocke and A. Belkacem, Fragmentation Pathways for Selected Electronic States of the Acetylene Dication, *J. Phys. B* **41**, 091001 (2008)

L. P. L. Bartlett, A. T. Stelbovics, T. N. Rescigno and C. W. McCurdy, "Application of Exterior Complex Scaling to Positron-Hydrogen Collisions Including Rearrangement", *Phys. Rev. A* **77**, 032710 (2008).

M. D. A. Horner, T. N. Rescigno and C. W. McCurdy, Decoding sequential vs non-sequential two-photon double ionization of helium using nuclear recoil, *Phys. Rev. A.* **77**, 030703(R) (2008).

N. L. Campbell, M. Brunger and T. N. Rescigno, "Carbon dioxide electron cooling rates in the atmospheres of Mars and Venus", *J. Geophys. Res.-Planets* **113**, 2008JE003099 (2008).

O. F. L. Yip, C. W. McCurdy and T. N. Rescigno, "A hybrid Gaussian-discrete variable representation approach to molecular continuum processes II: application to photoionization of diatomic Li_2^+ ", *Phys. Rev. A* **78**, 023405 (2008).

P. D. A. Horner, T. N. Rescigno and C. W. McCurdy , "Triple Differential Cross sections and Nuclear Recoil in Two-Photon Double Ionization of Helium", *Phys. Rev. A* **78**, 043416 (2008).

Q. D. A. Horner, S. Miyabe, T. N. Rescigno , C. W. McCurdy, F. Morales and F. Martin, "Classical Two-Slit Interference Effects in Photo-double Ionization of Molecular Hydrogen at High Energies", *Phys. Rev. Lett.* **101**, 183002 (2008).

R. D. J. Haxton, T. N. Rescigno and C. W. McCurdy, "Three-body breakup in dissociative electron attachment to the water molecule", Phys. Rev. A **78**, 040702(R) (2008).

S. J. Fernández, F. L. Yip, T. N. Rescigno, C. W. McCurdy and F. Martín, "Two-center effects in one-photon single ionization of H_2^+, H_2 and Li_2^+ with circularly polarized light", Phys. Rev. A **79**, 043409 (2009).

T. L. Tao, C. W.McCurdy and T. N. Rescigno, "Grid-based methods for diatomic quantum scattering problems: a finite-element, discrete variable representation in prolate spheroidal coordinates", Phys. Rev. A **79**, 012719 (2009).

U. A. Palacios, T. N. Rescigno and C. W. McCurdy, "Time-dependent treatment of two-photon resonant single and double ionization of helium by ultrashort laser pulses" , Phys. Rev. A **79**, 033402 (2009).

V. F. Morales, F. Martin, D. A. Horner, T. N. Rescigno and C. W. McCurdy, "Two-photon double ionization of H_2 at 30 eV using Exterior Complex Scaling", J. Phys. B **42**, 134013 (2009).

W. S. Miyabe, C. W. McCurdy, A. E. Orel and T. N. Rescigno, "Theoretical study of asymmetric molecular-frame photoelectron angular distributions for C 1s photoejection from CO_2 ", Phys. Rev. A **79**, 053401 (2009).

X. L. Tao, C. W. McCurdy and T. N. Rescigno, "Grid-based methods for diatomic quantum scattering problems II: Time-dependent treatment of single- and two-photon ionization of H_2^+ ", Phys. Rev. A **80**, 013401 (2009).

Ultrafast X-ray Science Laboratory

C. William McCurdy (Director), Ali Belkacem, Oliver Gessner, Martin Head-Gordon, Stephen Leone, Daniel Neumark, Robert W. Schoenlein, Thorsten Weber

Chemical Sciences, Lawrence Berkeley National Laboratory, Berkeley, CA 94720

CWMcCurdy@lbl.gov, ABelkacem@lbl.gov, OGessner@lbl.gov, MHead-Gordon@lbl.gov, SRLeone@lbl.gov, DMNeumark@lbl.gov, RWSchoenlein@lbl.gov, TWeber@lbl.gov

Program Scope: This program seeks to bridge the gap between the development of ultrafast X-ray sources and their application to understand processes in chemistry and atomic and molecular physics that occur on both the femtosecond and attosecond time scales. Current projects include: (1) The construction and application of high harmonic generation sources in chemical physics, (2) Applications of a new ultrafast X-ray science facility at the Advanced Light Source at LBNL to solution-phase molecular dynamics, (3) Time-resolved studies and non-linear interaction of femtosecond x-rays with atoms and molecules, (4) Theory and computation treating the dynamics of two active electrons atoms and molecules in intense short pulses, as well as the development of tractable theoretical methods for treating molecular excited states of large molecules to elucidate their ultrafast dynamics, and (5) Advanced attosecond pulse techniques in studies of atomic and molecular dynamics.

Recent Progress and Future Plans:

1. Soft X-ray high harmonic generation and applications in chemical physics

This part of the laboratory is based on a set of high repetition rate femtosecond VUV pulse sources. It will provide light pulses in the VUV- and soft X-ray regime with pulse durations on the sub-40 fs timescale and repetition rates up to 3 kHz. The sources will be complemented by state-of-the-art photoelectron and photoion detection schemes and a high resolution transient absorption setup. The sources are based on HHG with an IR fundamental in gaseous media. The driving IR laser provides pulses of 25 fs duration at 3 kHz repetition rate with pulse energies up to 5 mJ. After separation from the fundamental, a narrow band of high harmonic photon energies is selected by means of filters, multilayer mirrors, and gratings. The first beamline providing ultrashort pulses at 23.7 eV photon energy is operational. A second, capillary-based femtosecond VUV pulse source has produced first light beyond 140 eV photon energy.

The first experiments focus on the ionization dynamics of pure and doped Helium droplets. An existing experimental setup consisting of a Helium cluster source and a velocity-map-imaging photoelectron spectrometer, has been modified to record femtosecond time-resolved photoelectron energy- and angular-distributions. Synchrotron based studies have revealed the emission of extremely slow (<1 meV) electrons by Helium droplets that are excited ~1 eV below the atomic Helium ionization threshold. Furthermore, the photoelectron spectra of doped Helium droplets show a rich structure that depends on the photon energy and cluster size. A series of femtosecond time-resolved VUV-pump IR-probe photoelectron imaging experiments has revealed an unexpected abundance of relaxation processes which indicate an important role of atomic and molecular Rydberg states in the electronic de-excitation pathways. First evidence for

an intra-droplet electronic decay has been revealed. Currently a state-of-the-art momentum-resolving ion spectrometer is being installed to gain a more complete picture of the potentially rich nuclear dynamics initiated by the electronic excitation.

Ultimately, the high-repetition high harmonics source will be equipped with 3 beam lines in order to make optimum use of the femtosecond driving laser. Photoelectron-photoion coincidence imaging experiments and transient X-ray absorption experiments will be installed at the additional beam lines. We will generate and utilize femtosecond soft X-ray pulses with photon energies reaching the water window (290eV-540eV). Finally, the investigator team is applying for time at the LCLS to study inner shell ionization of field-ionized rare gas atoms.

2. Applications of the new femtosecond undulator beamline at the Advanced Light Source to solution-phase molecular dynamics

The objective of this research program is to advance our understanding of solution-phase molecular dynamics using ultrafast x-rays as time-resolved probes of the evolving electronic and atomic structure of solvated molecules. Two new beamlines have been constructed at the Advanced Light Source, with the capability for generating ~200 fs x-ray pulses from 200 eV to 10 keV. We have also developed a new capability for transmission XAS studies of thin liquid samples in the soft x-ray range, based on a novel Si_3N_4 cell design with controllable thickness <1 μm.

Present research is focused on charge-transfer processes in solvated transition-metal complexes, which are of fundamental interest due to the strong interaction between electronic and molecular structure. In particular, Fe^{II} complexes exhibit strong coupling between structural dynamics, charge-transfer, and spin-state interconversions. We previously reported the first time-resolved EXAFS measurement of the atomic structural dynamics associated with the Fe^{II} spin-crossover transition, showing the dilation of the Fe-N bond distance by ~0.2 Å within 70 ps of photoexcitation into the $MLCT^1$ state. This year we have focused on understanding the evolution of the valence electronic structure, and the influence of the ligand field dynamics on the Fe *3d* electrons, using time-resolved XANES measurements at the Fe L-edge. Our recent picosecond results show a clear 1.7 eV dynamic shift in the Fe-L_3 absorption edge with the ultrafast formation of the high-spin state. This reflects the evolution of the ligand-field splitting, and is the first time-resolved solution-phase transmission spectra ever recorded in the soft x-ray region. Preliminary femtosecond x-ray studies show these dynamics evolving on a 200 fs time scale.

A second area of focus is on the structural dynamics of liquid water following coherent vibrational excitation of the O-H stretch (in collaboration with A. Lindenberg et al. at Stanford). Time-resolved results at the O K-edge show distinct changes in the near-edge spectral region that are indicative of a transient temperature rise of 10K following laser excitation and rapid thermalization of vibrational energy. The rapid heating at constant volume creates an increase in internal pressure, ~8MPa, which is manifest by spectral changes that are distinct from those induced by temperature alone. Femtosecond studies of hydrogen bond dynamics are presently underway.

An important goal is to apply time-resolved X-ray techniques to understand the structural dynamics of more complicated reactions in a solvent environment. Future research will focus on charge-transfer, and ligand dynamics in bi-transition-metal

complexes and porphyrins, as well as reaction dynamics of solvated halide molecules.

3. Time-resolved studies and non-linear interaction of femtosecond x-rays with atoms and molecules:

An extension of non-linear processes to the XUV spectral region was until recently considered unfeasible due to a lack of sufficiently intense short-wavelength radiation sources. In recent years, higher-order harmonic generation has reached intensities high enough as to induce two or three photon ionization processes. The design and construction of our intense XUV source is based on scaling-up in energy of the loose focusing high harmonic generation scheme. The first application of this intense source high harmonics is to study the isomerization of ethylene ($C_2H_4^+$) leading to the formation of the ethylidene configuration (CH_3CH^+). Application of a VUV pump (20-24 eV) and NIR probe (800 nm) resulted in ethylene cation isomerization in ethylidene with subsequent fragmentation to CH_3^+ and CH^+, which occurred favorably if the IR probe was applied 80 fs after EUV excitation. The ethylidene configuration is found to be transient with a lifetime of ~ 60 fs. This configuration is predicted by theory as a transient state that connects an excited electronic state to the ground state of the cation. Furthermore we developed a state-of-the-art split-mirror capability that enables x-ray pump and x-ray probe studies of molecular systems. As a first application we performed a 5^{th} harmonic pump 5^{th} harmonic probe to study the dynamics and the coupling of electronic and nuclear degrees of freedom in the V and Z states of neutral ethylene. This study is being extended to 5^{th} harmonic pump and 19^{th} harmonic probe of the same system. In collaboration with the Argonne National Laboratory AMO group we performed a first gas phase experiment at the ALS femtosecond beamline using an experimental set up build by the two groups. In this transmission measurement experiment the collaboration performed the first transient laser induced transparency of x-rays interacting with the K-shell of neon.

The construction of the new Momentum Imaging Spectroscopy for TimE Resovled Studies (MISTERS) apparatus began in the second half of 2008. Currently the main chamber together with the two-stage supersonic gas jet-dump and the second stage of the target preparation chamber are mounted and sit on a custom made moveable frame, which also holds the gas jet manifold. The rail system for the spectrometer-sledge and the sledge itself are in place; the spectrometer electrodes are machined as well. A mechanical in-vacuum xyz-tip-tilt stage has been developed and built for steering the back-focusing mirror (or split mirror stage). The first crucial parts for an effective two-stage differential pumping stage were designed and ordered. Assembling and mounting the first stage of the target preparation chamber is scheduled for Fall 2009; first vacuum test will start right afterwards. Once finished, the setup will be optimized for two-photon double ionization of helium atoms and hydrogen molecules using the high harmonics sources of the UXSL. We intend to measure one ion and one electron in coincidence in order to get access to key values like the momentum vector of the di-electron in the case of helium and the kinetic energy release (KER) in the photo ionization of hydrogen molecules. This will enable us to distinguish between sequential and non-sequential processes and understand the mechanisms behind them.

4. Theory and computation

We are developing and applying computational methods that will allow the accurate treatment of multiple ionization of atoms and molecules by short pulses in the VUV and soft X-ray regimes. We have extended our numerical methods based on the finite-element discrete variable representation to the essentially exact time-dependent treatment of two electron atoms in a radiation field, including the rigorous extraction of the amplitudes for ionization from these wave packets and separation of single and double ionization probabilities [12, 13]. These developments have been applied to short pulse single and double ionization of helium and have showed new effects that appear only for subfemtosecond pulses [14]. Most recently we have found an intrinsically two-electron interference phenomenon in which subfemtosecond UV pulses can be used to probe spin entanglement directly [15]. Applications to pump/probe investigations of correlation in the doubly excited states of helium are in progress using a new time propagation scheme that involves simultaneous explicit and implicit steps. The extension of the these methods to many-electron atoms and molecules is being accomplished by the construction of orbitals from our DVR basis functions and the development of new multiconfiguration time-dependent Hartree Fock methods for double ionization using prolate spheroidal coordinates for the treatment of general diatomics.

We are also developing tractable theories for molecular excited states, including bright and dark states and their intersections. A new quasidegenerate perturbation theory building upon single excitation CI has been formulated, implemented and tested [16]. It is self-interaction-free, and efficient enough to apply to systems in the 50-100 atom regime. The analytical gradient of this model has been formulated and implemented which opens the way for exploring potential energy surfaces [17]. Additionally, we have formulated new spin-flip model that can properly treat low-lying dark excited states that have large double excitation contributions [18], with computational cost that is proportional to single excitation CI, as well as a new double spin flip method [19] that can properly treat systems with 4 strongly correlated electrons. Work in progress includes further spin-flip methods, and calculations of excited states of helium clusters to complement experimental efforts.

5. Attosecond atomic and molecular science

Isolated attosecond pulses are produced by the process of high harmonic generation using few-cycle 800 nm carrier-envelope-phase (CEP) stabilized driver pulses. With appropriate focusing of the 800 nm pulses into the Ne target gas, a new method of ionization gating, phase match control of the high harmonic output generates isolated attosecond pulses that are wavelength tunable. Isolated attosecond pulses are produced in this case on the leading edge of the driver pulse, and tuning is achieved by selecting where on the leading edge the attosecond pulse is created by varying the CEP. Streak field detection of direct ionization processes in Ne or SF_6 reveals the isolated nature of the attosecond pulses and provides a direct measure of the contrast ratio of the isolated pulses. This is accomplished by measuring the electron momentum distribution for two CEP values that are 180 degrees out of phase. In this case the contrast is measured to be approximately 3:1 for the main attosecond pulse:neighboring secondary attosecond pulse. Based on the measurements, the isolated attosecond pulse is presently limited to 400-500

attoseconds by the limited bandwidth of the reflective optics used for separation of the isolated attosecond pulse.

New experiments are performed on the fragmentation dynamics of SF_6 by measuring the ion fragment pathways both with and without an 800 nm applied field. Mass spectra reveal a multitude of product ions when SF_6 is excited with the 100 eV attosecond pulses. These include S^+, SF_2^{++}, SF_4^{++}, SF_4^+, SF_5^+, among many product ions. Each product branch is markedly manipulated by the application of the 800 nm field. For example, the S^+ and SF^+ branches can be diminished, while the SF_2^{++} and SF^{++} branches can be increased, by the overlap of the few cycle 800 nm pulse over the first few fs of the fragmentation. Longer time alterations in the product branches are also observed. Work is in progress to determine the mechanism of the changes in product branching pathways, whether that may be a mechanism such as field-induced potential surface crossings, tunnel ionization, or multiphoton excitation by the 800 nm field. The initial experiments suggest that an electronic manipulation of the pathways following the isolated attosecond pulse that ejects one or two electrons is likely.

Publications, by Subject Area (2007-2009)

1. Christer Z. Bisgaard, Owen J. Clarkin, Guorong Wu, Anthony M. D. Lee, Oliver Geßner, Carl C. Hayden, Albert Stolow, "Time-Resolved Molecular Frame Dynamics of Fixed-in-Space CS_2 Molecules", Science **323**, 1464 (2009).
2. M. Khalil, M.A. Marcus, A.L. Smeigh, J.K. McCusker, H.H.W. Chong, and R.W. Schoenlein, "Picosecond x-ray absorption spectroscopy of photochemical transient species in solution," in **Ultrafast Phenomena XV**, Springer Series in Chemical Physics , **88**, P. Corkum, D. Jonas, D. Miller, A.M. Weiner, Eds., Springer-Verlag, (2007).
3. N. Huse, H. Wen, D. Nordlund, E. Szilagyi, D. Daranciang, T.A. Miller, A. Nilsson, R.W. Schoenlein, and A.M. Lindenberg, "Probing the hydrogen-bond network of water via time-resolved soft x ray spectroscopy," *Phys. Chem. Chem. Phys*., **11**, 3951–3957 (2009) – cover article.
4. N. Huse, M. Khalil, T.-K. Kim, A.L. Smeigh, L. Jamula, J.K. McCusker, and R.W. Schoenlein, "Probing reaction dynamics of transition-metal complexes in solution via time-resolved x-ray spectroscopy," *J. Phys. Conf*., **148**, 012043 (2009).
5. N. Huse, T.-K. Kim, M. Khalil, L. Jamula, J.K. McCusker, and R.W. Schoenlein, "Probing reaction dynamics of transition-metal complexes in solution via time-resolved soft x-ray spectroscopy," in **Ultrafast Phenomena XVI**, Springer Series in Chemical Physics, **92**, P. Corkum, S. De Silvestri, K.A. Nelson, E. Riedle, R.W. Schoenlein, Eds., Springer-Verlag, (2009).
6. H. Wen, N. Huse, R.W. Schoenlein, and A.M. Lindenberg, "Ultrafast conversions between distinct hydrogen bond structures in water observed by femtosecond x-ray spectroscopy," submitted *PNAS*, (2009).
7. N. Huse, T.-K. Kim, L. Jamula, J.K. McCusker, F.M.F. de Groot, and R.W. Schoenlein, "Direct Observation of Transient Ligand-Field Changes in Transition Metal Complexes via Time-Resolved Soft X-ray Spectroscopy," submitted *Nature Chem*., (2009).
8. J. van Tilborg, T.K. Allison, T.W. Wright, M.P> Hertlein, R.W. Falcone, Y. Liu, H. Merdji and A. Belkacem, "Femtosecond isomerization dynamics in the ethylene cation measured in an EUV-pump NIR probe configuration", J. Phys. B: At. Mol. Opt. Phys. **42** (2009) 081002.

9. T.K. Allison, J. van Tilborg, T.W. Wright, M.P. Hertlein, R.W. Falcone, and A. Belkacem, "Separation of high order harmonics with fluoride windows", Optics Express **17**, (2009) 8941.

10. Y.M. Rhee and M. Head-Gordon, "Scaled second order perturbation corrections to configuration interaction singles: efficient and reliable excitation energy methods", J. Phys. Chem. A **111**, 5314 (2007).

11. C. C. Wang, O. Kornilov, O. Gessner, J. H. Kim, D. S. Peterka, and D. M. Neumark, "Photoelectron Imaging of Helium Droplets Doped with Xe and Kr Atoms", J. Phys. Chem. A, *in press* (2008).

12. A. Palacios, C. W. McCurdy and T. N. Rescigno, Extracting Amplitudes for Single and Double Ionization from a Time-Dependent Wavepacket, *Phys. Rev. A* **76**, 043420 (2007).

13. A. Palacios, T. N. Rescigno and C. W. McCurdy, Cross Sections for Short-Pulse Single and Double Ionization of Helium, *Phys. Rev. A* **77**, 032716 (2008).

14. A. Palacios, T. N. Rescigno and C. W. McCurdy, "Time-dependent treatment of two-photon resonant single and double ionization of helium by ultrashort laser pulses" , Phys. Rev. A **79**, 033402 (2009).

15. A. Palacios, T. N. Rescigno and C. W. McCurdy, "Two-electron time-delay interference in atomic double ionization by attosecond pulses," Phys. Rev. Letts. (submitted).

16. D. Casanova, Y.M. Rhee and M. Head-Gordon, "Quasidegenerate scaled opposite spin second order perturbation corrections to single excitation configuration interaction", J. Chem. Phys. 128, 164106 (2008)

17. Y.M. Rhee and M. Head-Gordon, "Quartic-scaling analytical gradient of quasidegenerate scaled opposite spin second order perturbation corrections to single excitation configuration interaction", J. Chem. Theor. Comput. 5, 1224-1236 (2009).

18. D. Casanova and M. Head-Gordon, "The spin-flip extended single excitation configuration interaction method", J. Chem. Phys. 129, 064104 (2008).

19. D. Casanova, L.V. Slipchenko, A.I. Krylov, and M. Head-Gordon, "Double spin-flip approach within equation-of-motion coupled cluster and configuration interaction formalisms: Theory, implementation and examples" J. Chem. Phys. 130, 044103 (2009).

20. A. Jullien, T. Pfeifer, M. J. Abel, P. M. Nagel, J. Bell, D. M. Neumark, and S. R.Leone, "Ionization phase-match gating for wavelength-tunable isolated attosecond pulse generation," Appl. Phys. B **93**, 433 (2008).

21. T. Pfeifer, M. J. Abel, P. M. Nagel, A. Jullien, Z.-H. Loh, M. J. Bell, D. M. Neumark, and S. R. Leone, "Time-resolved spectroscopy of attosecond quantum dynamics," Chem. Phys. Lett. **463**, 11 (2008).

22. M. J. Abel, T. Pfeifer, A. Jullien, P. M. Nagel, M. J. Bell, D. M. Neumark, and S. R.Leone, "Carrier-envelope phase-dependent quantum interferences in multiphoton ionization," J. Phys. B: At. Mol. Opt. Phys. **42**, 075601 (2009).

23. T. Pfeifer, M. J. Abel, P. M. Nagel, W. Boutu, M. J. Bell, Y. Liu, D. M. Neumark,and S. R. Leone, "Measurement and optimization of isolated attosecond pulsecontrast," Opt. Lett. (in press) (2009).

24. M. J. Abel, T. Pfeifer, P. M. Nagel, W. Boutu, M. J. Bell, C. P. Steiner, D. M.Neumark, and S. R. Leone, "Isolated attosecond pulses from ionization gating of high harmonic emission," Chem. Phys. (submitted).

ATOMIC AND MOLECULAR PHYSICS RESEARCH
AT
OAK RIDGE NATIONAL LABORATORY

David R. Schultz, Group Leader, Atomic Physics
[schultzd@ornl.gov]
ORNL, Physics Division, P.O. Box 2008
Oak Ridge, TN 37831-6372

Principal Investigators

M. E. Bannister, S. Deng,* P. R. Harris,* C. C. Havener, J. H. Macek,
F. W. Meyer, C. O. Reinhold, D. R. Schultz, and C. R. Vane

*Postdoctoral Fellow

The OBES atomic physics program at ORNL has as its overarching goal the understanding of states and interactions of atomic-scale matter. These atomic-scale systems are composed of multiply charged ions, charged and neutral molecules, atoms, atomic ions, electrons, solids, and surfaces. Particular species and interactions are chosen for study based on their relevance to gaseous or plasma environments of basic energy science interest such as those in fusion energy, gas phase chemistry, and plasma processing. Towards this end, the program has developed and operates the Multicharged Ion Research Facility (MIRF) which has recently undergone a broad, multi-year upgrade. Work is also performed as needed at other facilities such as ORNL's Holifield Radioactive Ion Beam Facility (HRIBF) and the CRYRING heavy-ion storage ring in Stockholm. Closely coordinated theoretical activities support this work as well as provide leadership in complementary or synergistic research.

Steady-State and Transient Hydrocarbon Production in Graphite by Low-Energy Impact of Atomic and Molecular Deuterium Projectiles – *F. W. Meyer, P. R. Harris, and H. Zhang*

Ion-surface interactions play an essential role in many applications ranging from semiconductor device technology to magnetic fusion. The plasma- material interface is a critical bottleneck in fusion power conversion. A recent panel report to the Fusion Energy Sciences Advisory Committee (FESAC)[1] found that 4 of the top 5 critical knowledge gaps for fusion involve the Plasma-Materials Interface (PMI). Just completed fusion community REsearch NEeds Workshops (RENEW)[2] have recommended new PMI research programs and facilities to *advance the science and technology of plasma-surface interactions*.

In line with these recommendations, we have continued this past year our studies of the interactions of slow H or D ions with carbon based surfaces. Our measurements focus on the energy region below the physical sputtering threshold (<50 eV) where chemical sputtering is the main mechanism for material erosion. This energy region is also the anticipated particle energy regime of the ITER divertor.[3] Due to the high D^+ currents obtainable with our ECR ion source, and the highly efficient beam deceleration optics employed at the entrance to our floating scattering chamber, we were able to perform measurements at energies as low as 5 eV/D, and were thus able to have good overlap with the energies accessible to molecular dynamics (MD) simulations carried out in parallel with our measurements.[4,5]

Using a quadrupole mass spectrometry approach in conjunction with calibrated hydrocarbon leaks, we have obtained production yields of methyl, methane and heavier hydrocarbons for deuterium atomic and molecular ions incident on ATJ graphite, HOPG, and a-C:D thin films in the energy range 5–250 eV/D. The yields were determined at sufficient accumulated ion beam fluences that steady-state conditions were reached. By summing the different hydrocarbon yields,

estimates could be obtained of the total erosion of graphite by chemical sputtering processes, which dominate at low energies, i.e., below the physical sputtering threshold. These estimates also permitted comparison with ellipsometry and total mass loss measurements.

One focus of the measurements was comparison of chemical sputtering yields for atomic and molecular species of the same velocity, as a test of the commonly made assumption of identical sputtering yields when normalized to the number of D atoms in the incident projectiles. In our QMS measurements, we found projectile dependent yields below ~60 eV/D, where the D^+ projectile had the smallest yields and D_3^+ projectiles had the largest yields. The effect increased with decreasing energy and amounted to about a factor of two at 10 eV/D. At higher energies, where immediate dissociation of incident molecular projectiles is highly probable, the observed yields for equivelocity incident atomic and molecular ions are the same, as was noted in previous work.[6]

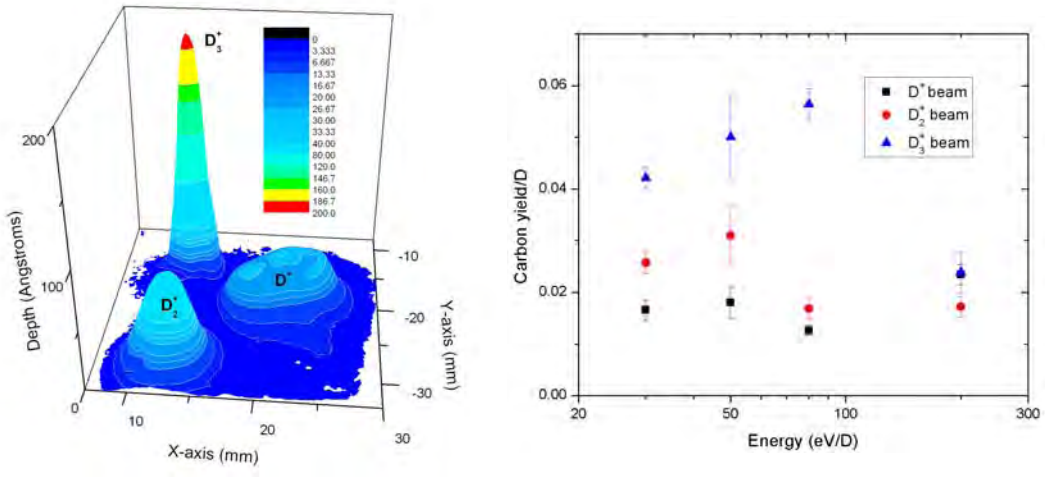

Figure 1. (left) Ellipsometry scan of thin film a-C:D sample irradiated by 30 eV/D D^+, D_2^+, and D_3^+ beams to fluences of 1-2 x 10^{18} D/cm^2. (right) Total C yields/D for equivelocity atomic and molecular D projectiles incident on a-C:D at 30, 50, 80, and 200 eV/D.

Interestingly, the molecular vs. atomic size effect is also evident in recently completed total erosion measurements of a-C:D thin films. For these measurements, the thin film was exposed to equal velocity D^+, D_2^+, and D_3^+ beams to fluences of 1-2 x 10^{18} D/cm^2. From 2-D ellipsometry scans and the known thin film density, the total C removal could be determined. Normalization to the integrated number of incident D projectiles, obtained from simple beam current intergration multiplied by the number of D atoms per incident projectile (1, 2, or 3 for D^+, D_2^+, or D_3^+, respectively) gives the total C yield per D. Figure 1 shows typical craters produced by atomic and molecular beam irradiation, together with a summary of the measured yields. As can be seen from the figure, while there is no observed difference between the different projectiles at the highest energy of 200 eV/D, as expected, significant differences are observed at all the investigated lower energies, which range from a factor of 2 to almost 5. These differences are much more pronounced than the differences seen in our QMS measurements for atomic vs. molecular projectiles. The reason for this more pronounced effect is presently not understood, and will be the subject of further investigation.

In addition to steady-state chemical sputtering yields, we have studied[7] transient hydrocarbon ejection and hydrogen (deuterium) re-emission from pre-loaded graphite surfaces immediately

after the start of beam irradiation. When the surfaces were prepared by irradiation to saturation with lower energy deuterium beams, transient hydrocarbon emission and re-emission of D_2 significantly larger than steady-state values were observed, which exponentially decayed as a function of beam fluence. The initial peak heights are related to the starting hydrocarbon and deuterium densities in the prepared sample, while the exponential decay constants provide information on the hydrocarbon kinetic release and deuterium de-trapping cross sections. Figure 2 shows typical transients, and Table 1 summarizes the deuterium re-emission and kinetic hydrocarbon ejection cross sections deduced from the transient measurements. Interestingly, the kinetic ejection cross sections for 80 eV/D incident energy atomic and molecular projectiles show a similar ordering as the total C yields shown in Figure 1, while at the higher energy (150 eV/D), the cross sections, particularly for the heavier C_2D_x hydrocarbons, are closer in agreement. The implications of these cross section trends on the total sputtering yields are presently being studied, as is the evidence suggested in the last two rows of Table 1 that the prepared surface may in fact depend on the nature of the incident projectile.

Table 1: Summary of cross sections deduced from the exponential decay constants fitted to the transient mass signals shown in Figure 2 (uncertainties in parentheses).

Ions	**Energy** (eV/D)	**Preparing species** (20 eV/D)	**Cross section /D** (10^{-17}cm^2)			
			D_2	**CD_4**	**C_2D_2**	**C_2D_4**
D	80	D		2.6 (0.8)	2.3 (0.7)	1.9 (0.6)
D_2	80 D	$_2$		4.4 (1.0)	3.1 (1.0)	2.6 (0.7)
D_3	80 D	$_3$	12 (3.5)	6.8 (2.0)	4.1 (1.2)	4.8 (1.4)
D	150	D	6.3 (1.9)	3.7 (1.1)	2.9 (0.9)	3.9 (1.2)
D_2	150 D	$_2$	15 (5)	13 (4.0)	5.4 (1.6)	7.9 (2.4)
D_3	150 D	$_3$	7.4 (2.2)	8.4 (2.5)	4.0 (1.2)	5.8 (1.7)
D	80 D	$_2$		4.7 (1.4)	3.8 (1.2)	7.2 (2.2)
D	150 D	$_2$	21 (6)	8.8 (2.7)	5.0 (1.5)	7.6 (2.3)

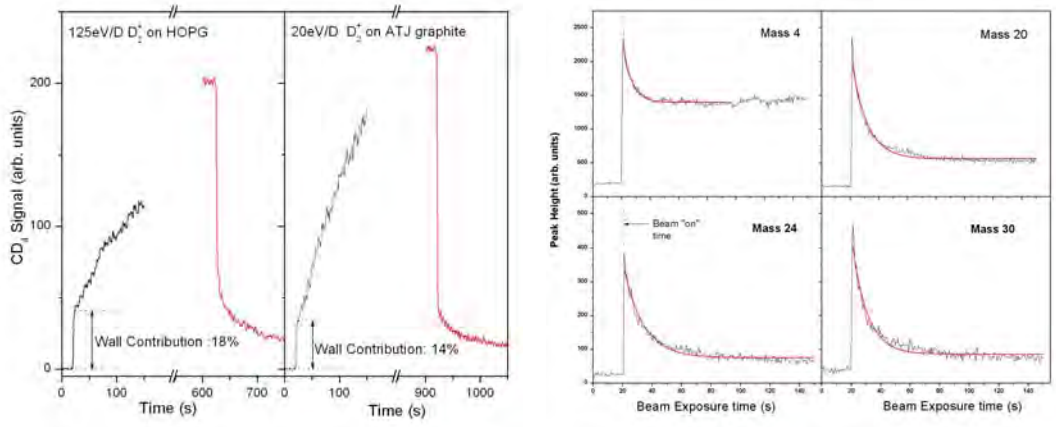

Figure 2: (left) CD_4 transient response to D_2^+ beam incident on virgin graphite samples; (right) mass transients due to re-emission of D_2 and kinetic ejection of CD_4, C_2D_2, and C_2D_4 induced by 150 eV D^+ incident on ATJ graphite prepared by high fluence 20 eV/D D^+, D_2^+ or D_3^+ exposure. Note exponential decay fits in red.

To obtain further insights into these intriguing differences, we are exploring the use of XPS and UV Raman spectroscopy to examine the chemical/structural modifications occurring during atomic and molecular D beam exposure. From the valence band region of the XPS spectra, beam induced modification of C-C bonding will be explored, while UV Raman spectroscopy will provide information on the extent of sp^3 hybridization induced by exposure beam to the various beams.

1. *Priorities, Gaps and Opportunities: Towards a Long-Range Strategic Plan for Magnetic Fusion Energy*, FESAC Report, DOE/SC-0102 (2007).
2. Links: U.S. DOE ReNeW Workshop, Bethesda MD, June 8-12 (2009); Preliminary Executive Summary;Thrust 10: Executive Summary
3. G. Federici, Phys. Scr. **T124,** 1 (2006).
4. L. I. Vergara, F. W. Meyer, H. F. Krause, P. Träskelin, K. Nordlund, and E. Salonen, J. Nucl. Mater. **357**, 9 (2006).
5. P. S. Krstic, C. O. Reinhold, and S. J. Stuart, New J. Phys. **9**, 209 (2007).
6. M. Balden and J. Roth, J. Nucl. Mater. **280**, 39 (2000).
7. H. Zhang and F. W. Meyer, *Proceedings,18th International Conference on Plasma Surface Interactions, Toledo, Spain, May 25-30, 2008*, J. Nucl. Mater. **390-391**, 127 (2009)

Low-Energy Molecular Ion Collisions Using Merged-Beams – *C. C. Havener*

$(H_2\text{-}H)^+$ is the most fundamental ion-molecule two-electron system. The temporary complex which is formed during charge transfer (CT) of $H_2^+ + H$ proceeds through dynamically coupled electronic, vibrational, and rotational degrees of freedom. Despite the fundamental nature of the $(H_2 - H)^+$ system, most of the collisional theoretical data remains untested[1-3] due to sparse experimental investigations. Interestingly enough, huge discrepancies have persisted over the last two decades in the measured and calculated total cross section for $H^+ + H_2$ collisions[2] and the measurements related to $H_2^+ + H$ were limited to higher collision energies.[4] Knowledge of CT for H_2^+ on H is necessary for modeling of such plasmas as found in the cold divertor plasma regions of a fusion tokamak or interstellar clouds where the main constituents are H, H^+, and H-molecules.

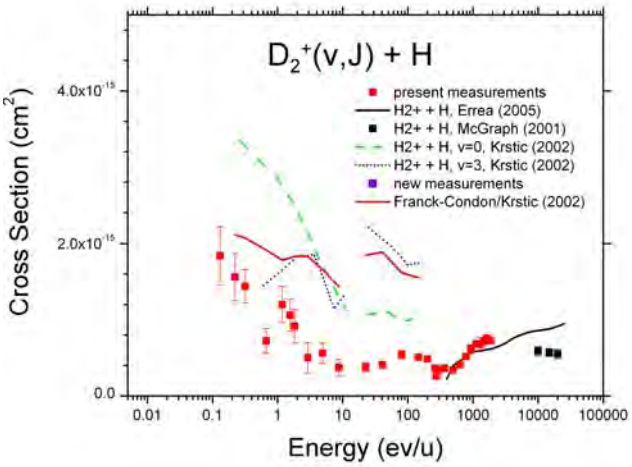

Figure 1. Present merged-beam measurements for $D_2^+ + H$ compared to other measurements at high energy and to theory for $H_2^+ + H$. The low-energy theory includes CT with nuclear substitution for v = 0, 3 and a Franck-Condon distribution of initial vibrational states of H_2^+ summed over all final vibrational states.

The ion-atom merged-beams apparatus at MIRF has been upgraded[5] to accept high-velocity beams from the 250-kV High-Voltage Platform and is now able to access low-energy collisions with a variety of molecular ions on H from keV/u to meV/u. This new capability allows theory to be benchmarked at keV/u energies, where the vibrational modes of the initial molecular ion can be considered frozen, to eV/u energies where the vibrational energies are critical but rotational modes are "frozen," and to meV/u energies where all modes are important. At low energies CT for $H_2^+ + H$ can also involve nuclear substitution where the proton from the atomic target may be interchanged with one of the protons in the molecular ion. By using the isotopic system $D_2^+ + H$, the CT cross section without nuclear substitution has been measured this last year from keV/u to meV/u collision energies by observing the H^+ products.[6]

Our present merged-beam measurements for $D_2^+ + H$ are compared to other measurements at high energy and to theory for $H_2^+ + H$ in Figure 1. The collision is ro-vibrationally frozen at high energy where our measurements are seen to be in good agreement with McGraph's measurements[4] and also with Errea's calculations.[3] Clearly, pure CT and dissociative CT dominate this energy range. CT through nuclear substitution could not take place as the relative motion is too fast. So should be the case at intermediate energy (20 – 200eV/u). At intermediate and low energy, calculations are presented for the initial vibrational state of v = 0, v = 3 and a Franck-Condon distribution[7] summed over all possible final vibrational states. At the intermediate energy, the theoretical approach considers the motion of the projectile classically but treats the vibrational and electronic states in a quantum way.[1] Clearly our measurements indicate that the predictions are too high by about a factor of two.

At the lower energy (0.2 eV/u – 10 eV/u), the collision times are long enough to sample vibrational or even rotational modes and there may be a significant contribution from nuclear substitution included in the calculations but excluded in the measurements. Calculations use the infinite-order sudden approximation (IOSA) freezing the target rotation,[1] and show the general structure seen in our measurements. The energy shifts between our measurements and the theoretical calculations are expected as D_2^+, D_2, and H_2^+, H_2 are dynamically different. Presently we are extending the measurements below 0.1 eV/u where rotational and vibrational states could lead to significant structure in the cross section. One might expect that the total cross section should continue to increase at lower energies due to expected Langevin behavior as has been seen in merged-beams measurements of CT for atomic ions with H.[8]

1. P. Krstic, Phys. Rev. A **66**, 042717 (2002).
2. D. W. Savin *et al.*, Astrophys. J. Lett. 606, L167 (2004); Erratum: Astrophys. J. Lett. 607, L147 (2004).
3. L. F. Errea *et al.*, Nucl. Instrum. Methods Phys. Res. B **235**, 362 (2005).
4. C. McGraph, Phys. Rev. A **64**, 062712 (2001).
5. C. C. Havener *et al.*, Nucl. Instrum. Methods Phys. Res. B **261**, 129 (2007).
6. V. Andrianarijaona, J. J. Rada, R. Rejoub, and C. C. Havener, to be published in *Proceedings, XXVI ICPEAC, Kalamazoo, MI, July 22-28, 2009*.
7. Z. Amitay *et al.*, Phys. Rev. A **60,** 3769 (1999).
8. C. C. Havener *et al.*, *Proceedings, 20th International Conf. on the Application of Accelerators in Research and Industry*, Am. Inst. Phys. Conf. Proc. **1099**, 150 (2009).

Electron-Molecular Ion Interactions – *M. E. Bannister, C. R. Vane, and S. Deng*

The first Grand Challenge identified in a recent report to Basic Energy Sciences involves the control of materials processes at the level of electrons. Electron-driven fragmentation of molecular ions provides a testable platform for investigating and fully developing our

understanding of the mechanisms involved in electronic energy redistribution in many-body quantum mechanical systems, and is important from a fundamental point of view. These dissociative processes are also important practically in that electron-ion collisions are in general ubiquitous in plasmas and molecular ions can represent significant populations in low to moderate temperature plasmas. Neutral and charged radicals formed in dissociation of molecules in these plasmas represent some of the most highly reactive components in initiating and driving further chemical reaction pathways in a wide variety of environments, such as the divertor and edge regions in fusion reactors, plasma enhanced chemical vapor deposition reactors, and environments where chemistries are driven by secondary electron cascades, for example in the upper atmosphere of the earth, and cooler regions of the solar or other stellar atmospheres. It is absolutely critical to know the rates, branching fractions, and other kinematical parameters of the various possible relevant collision processes in order to correctly model these environments.

Dissociative Excitation and Ionization: Measurements of cross sections for electron-impact dissociative excitation (DE) and dissociative ionization (DI) of molecular ions have continued using the MIRF crossed-beams apparatus.[1] In coordination with our dissociative recombination (DR) investigations of di-hydride ions, we have continued a systematic study of the DE and DI channels for these ions. Experiments, during this period, included measurements on heavy-fragment ion channels of BD_2^+. Above the DI threshold, the magnitude of the cross sections for dissociation of BD_2^+ ions forming BD^+ fragments are very close to those measured previously for the XD^+ fragment produced by dissociation of XD_2^+ (X = C, N, O, and F). In the DE-only portion of the cross section, a large, broad peak is observed in the 7–15-eV range, similar to but somewhat larger than that seen for the $CH_2^+ \rightarrow CH^+$ cross section.[2] This peak is thought to be the result of excitations to bound electronic states lying above the dissociation limit, but further insight from experiments and theory is needed to verify this. For the XH^+/XD^+ fragment channel in DE/DI of di-hydrides XH_2^+/XD_2^+ (X = B, C, N, O, and F), it was found that the scaling[3] given before as a function of the interaction energy E divided by the dissociation threshold E_{th} still holds for energies greater than $4E_{th}$. This scaling does not hold as well for the X^+ fragment channel. However, the $BD_2^+ \rightarrow B^+$ results did continue the trend that the cross section decreases for the $XD_2^+ \rightarrow X^+$ channel as the electronegativity of X increases for X = B, C, N, O, and F. However, only for the BD_2^+ system does the cross section for the X^+ fragment channel exceed that of the XH^+/XD^+ fragment channel.

Final measurements have also been completed for the dissociation of CD_3^+ producing the CD_2^+ fragment ion.[4] Above the DI threshold, the cross section for this channel was found to follow the scaling noted above. At lower energies, a large peak was measured in the 10–15-eV range, reminiscent of the peaks observed in the $DCO^+ \rightarrow CO^+$ and $CH_2^+ \rightarrow CH^+$ data.[2,5] Measurements for DE/DI of N_2D^+ for the N_2^+, ND^+, and N^+ fragment channels exhibited sharp peaks in the DE region for two of the channels (N_2^+ and ND^+).

The dissociation experiments discussed above used molecular ions produced by the ORNL MIRF Caprice ECR ion source,[6] but other cooler sources will also be used in order to understand the role of electronic and ro-vibrational excited states. A second ion source, a hot-filament Colutron ion source, is presently online and expected to produce fewer excited molecular ions. An even colder pulsed ion source, very similar to the one used for measurements[7] on the dissociative recombination of rotationally cold H_3^+ ions at CRYRING, is under development for use at the ORNL MIRF. Additionally, work continues on a similar supersonic source that uses a piezoelectric mechanism for more reliable pulsed valve operation. With this range of ion sources, one can study dissociation with both well-characterized cold sources and with hotter sources that better approximate the excited state populations in plasma environments found in applications such as fusion, plasma processing, and aeronomy. Another source being implemented for the study of electron-molecular ion interactions is an electrospray ionization source that will produce ions from large, fragile biomolecules such as nucleotides and peptides,

allowing us to probe the fundamental mechanisms of fragmentation in very complex molecular systems.

Dissociative Recombination: Studies of molecular ion neutralization processes in our ongoing collaboration with the group of Mats Larsson and Richard Thomas at Stockholm University are in the midst of transition because of the impending move of the CRYRING heavy ion storage ring to Germany and the opening of the University of Stockholm Double ElectroStatic Ion Ring ExpEriment (DESIREE), which should come on line in 2010-11. DESIREE will afford an expansion of capabilities to studies of more complex (heavier) molecular ion systems involved in a variety of charge transfer dissociation processes, with ions stored and prepared in a cryogenic environment.

1. M. E. Bannister, H. F. Krause, C. R. Vane *et al.*, Phys. Rev. A **68**, 042714 (2003).
2. C. R. Vane, E. M. Bahati, M. E. Bannister, and R. D. Thomas, Phys. Rev. A **75**, 052715 (2007).
3. M. E. Bannister *et al.*, in *Atomic Processes in Plasmas*, edited by J. D. Gillaspy, J. J. Curry, and W. L. Wiese (AIP Press, Melville, NY, 2007), pp. 197-205.
4. E. M. Bahati, M. Fogle, C. R. Vane, M. E. Bannister et al., Phys. Rev. A **79**, 052703 (2009).
5 E. M. Bahati, R. D. Thomas, C. R. Vane, and M. E. Bannister, J. Phys. B **38**, 1645 (2005).
6. F. W. Meyer, in *Trapping Highly Charged Ions: Fundamentals and Applications*, edited by J. Gillaspy (Nova Science, Huntington, NY, 1997), p. 117.
7. B. J. McCall *et al.*, Nature **422**, 500 (2003).

Molecular Ion Interactions (ICCE Trap Developments) – *C. R. Vane, M. E. Bannister, S. Deng, and C. C. Havener*

An Ion Cooling and Characterization Endstation (the MIRF ICCE Trap) has recently been developed and commissioned at the ORNL MIRF. It was designed to provide a variety of enhanced experimental capabilities for studies of the interactions of electrons with complex atomic and molecular systems, specifically to enable more nearly state-specific measurements of a number of dissociation processes involving the electron-driven breakup of heavy molecular ions. Development of the ICCE trap apparatus is in direct support of our mission goal of establishing experimental capabilities necessary for state-selectively producing and manipulating atomic and molecular ions to implement studies of a broad range of plasma relevant ion-interactions in as controlled a manner as possible. Interpretation of measurements of multi-fragment dissociation of complex molecular and cluster ion systems requires increased levels of control over the internal state populations of the reacting partners, as well as highly detailed and complete information from analysis and detection systems. To provide these capabilities, we have designed and constructed an electrostatic reflecting ion beam linear trap of the *Zajfman* design[1,2] as an experimental endstation on the MIRF high-energy beamline that will enable stored cooling and state characterization of molecular ions of essentially any mass.

Pulses of ions are injected from the side through a pulsed parallel plate 13 ^{o} deflector into a 1.5-meter-long electrostatic-mirror trap. The side-injection design, a first for linear electrostatic traps, was chosen to avoid the necessity of fast (< 1 μs) switching of the high-voltage mirror electrodes. This design permits storage of the highest energy ion beams possible, thus taking advantage of the kinematic emission of dissociation fragments, making their detection as efficient as possible. This ultrahigh vacuum, all electrostatic device permits effective long-term (seconds) storage of high-energy ion beams where excited internal states decay by radiative cooling.

Stored ion beams are produced in several ion sources, including a permanent-magnet ECR ion source mounted on the MIRF high-voltage platform for 'hot' atomic and molecular ions, and a pulsed, supersonic expansion discharge source for internally 'cold' molecular ions (CMIS),

being mounted on a stand-alone 10-kV isolated cab inet. As noted above for electron-m olecular ion studies, the CMIS design [3] has been used a CRYRING, and is capable of providing a ne arly completely v ibrational gr ound-state p opulation of light m olecular ions. For stored ion measurements with more fragile, very heavy molecular ions and cluster ions, an electrospray ion source (ESI) is also being mounted on the 10-kV platform.

The complete ion cooling and characterization endstation (ICCE trap) consists of an ultra-high vacuu m transport beam line and cham bers with co mputer controlled, fast-reaction electrostatic deflection and focusing e lements, a f ully electrostatic 38-mm diameter mirror trapping s ystem, and a c rossed bea m, low-energy (5 –100 eV), high-curren t electron target [4] located midway between the trap m irrors. The a pparatus is instrumented with a num ber of beam diagnostic and product characterization components, including two imaging detectors for velocity analysis of neutral frag ments arising from fragmentation of the trapped molecular ions, either by collisions with gas at oms (collisional dissociation (CD) and dissociative electron cap ture (DEC)), or with the electrons (dissociative exc itation or ionization (DE, DI), and less likely , dissociative r ecombination (DR)). The ion trap pre sently operates at roo m t emperature with vacuum at ~1 -2 x 1 0^{-10} Torr and ion inte rnal state cooling proceeding through radiative decay is thermodynamically lim ited to 300 ^{o} K. Next y ear, we will install an overall copper liner cooled to <70^{o} K using commercial stirling cryocoolers, and c onnect one of the mirrors and its shroud to a 4^{o} K helium cryocooler.

Initial work is concentrating on t rapping and cooling of O_2^+ and then ozone ions, and on m easurements of DE C fro m resid ual gas (primarily H_2) a nd electron im pact dissoc iation (DE, DI, an d DR) as fu nctions of electron energy f or various trapping/coo ling tim es. These results will be co mpared with our prior O_3^+ DR measurements at CRYRING,[5] that indicated almost co mplete 3-body dissociation at zero electron energy , form ing predom inantly electronically excited O (^{3}P and ^{1}D) frag ment ato ms. As a t est, be ams of 10-keV O_2^+ ions from the high-voltage platform ECR ion sour ce have been tuned int o the ICCE trap, stored and co oled for seconds, and neutral O and O_2 products from 10-eV electron co llisions were imaged in the detectors. Figure 1 displays a recently measured 10-keV O_2^+ ion population lifetime curve, taken from detect ed rates of n eutral frag ment em issions as a function of trapp ing tim e. Fu ture improvements of appro ximately one order of m agnitude to trapping times of tens of second s are anticipated with improved vacuum from cryogenic cooling, and from reduction of magnetic fields along the tra p axis with a m odified Hel mholtz coil arrangem ent. Measurements of O_3^+ wi ll be followed by a si milar stu dy involving electron-i nduced dissocia tion of several specifi c, much heavier bio-molecular ions that demonstrate the same preference for three-body breakup.

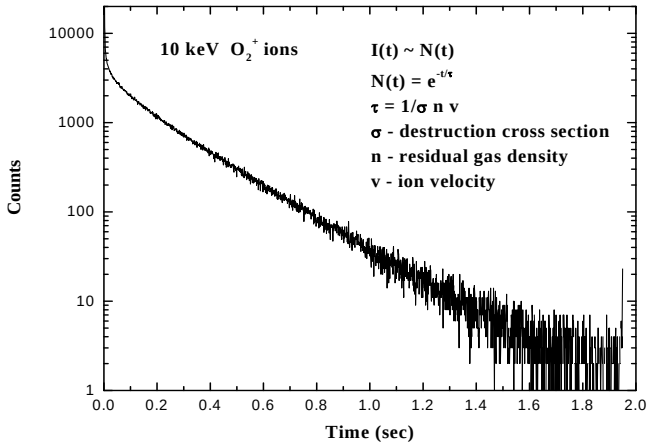

Figure 1. Storage lifetime plot for 10-keV O_2^+ ions in the ICCE Trap.

1. O. Heber *et al.,* Rev. Sci. Instrum. **76**, 013104 (2005).
2. H. F. Krause *et al.*, AIP Conf. Proc. **576** (AIP, New York 1994), pp. 126-129.
3. B. J. McCall *et al.,* J. Phys.: Conf. Ser. **4,** 92 (2005); Nature **422**, 500 (2003).
4. P. D. Witte, PhD Thesis, University of Heidelberg (2002)**.**
5. V. Zhaunerchyk *et al.,* Phys. Rev. A **77**, 022704 (2008).

Manipulation and Decoherence of Rydberg Wavepackets – *C. O. Reinhold*

Atoms in Rydberg states with large values of princi pal quantum num ber (n>300) pro vide a valuable laboratory in which to control quantum states of mesoscopic size (~micrometers). These giants can be manipulated using tailored sequences of el ectric pulses f rom co mmercial programmable pulse generators whos e strengths are co mparable to the Coulom b ele ctric f ields (~mV/cm) and whose time scales are shorter tha n the clas sical orbital period of the ato m (~nanoseconds). Our recent work demonstrates the remarkable level of time-resolved control and imaging of the electronic s tates that can be achieved. [1] One practical li mitation for manipulating Rydberg atoms i s that th ey are extre mely frag ile objects and can be easily altered by their environment. This happens because high-n Rydberg atoms have exceedingly small level spacings and spurious electric noise effectively broa dens t he quantum frequency sp ectrum. Electron wavepackets in near-circular orbits [2] provide an excellent starting point to combat decoherence since the electron stays far from the nucleus where large energy transfers can take place. We have shown that the quantum co herence of very high-n (n~305) Rydberg wavepackets traveling alo ng nearly circular orbits can be maintained on microsecond time scales corresponding to hundreds of classical orbi tal periods. [3] This large sp atio-temporal coherence is unprecedented for electr onic degrees of fr eedom involving a large ensem ble (~100) of quantum states. Our protocol for producing circular wavepackets leads to temporal interferences of spatially separated Schrödinger cat-like wavepackets and we are currently working on protocols for measuring and controlling the phase of the cat states. Because quantum thr ee-dimensional calculations ne ar n=300 are not feasible, we employ a hybrid quantum –classical traj ectory m ethod to si mulate the experi mental wave packet d ynamics. The crossover fro m qua ntum to classical dy namics can be studied experimentally by adding a controlled am ount of noi se in the form of random fluctuations of the electromagnetic pulses an d study ing the rate of de coherence as a function of the "strength" or "color" of noise. Noise might also be introduc ed experimentally b y addi ng a dilute gas of particles into the experimental cha mber. In the long term w e w ould like to extend the present techniques to engineer two-electron wavepackets involving distant electrons in two interacting Rydberg atoms and planetary atoms. This work is performed in collaboration with the groups of F.B. Dunnin g (Rice University) and J. Burgdorf er and S. Yoshida (Vienna University of Technology).

1. F. B. Dunning, J. J. Mestayer, C. O. Reinhold, S. Yoshida, and J. Burgdörfer, *Topical Review*, J. Phys. B **42**, 022001 (2009).
2. C. O. Reinhold, S. Yoshida, J. Burgdorfer, J. J. Mestay er, B. Wyker, J. C. L ancaster, and F. B. Dunning, Phys. Rev. A **78**, 063413 (2008).
3. C. O. Reinhold, S. Yoshida, J. Burgdörfer, B. Wyker, J. J. Mestayer, and F. B. Dunning, *Fast Track Communication*, J. Phys. B **42**, 091003 (2009).

Molecular Dynamics Simulations of Chemical Sputtering – *C. O. Reinhold and P. S. Krstic*

Physical and chem ical pr ocesses resulting fro m th e interaction of hydrogen isotopes wit h surfaces ar e of significant i mportance within th e fusion co mmunity as they provide a cri tical bottleneck in power conversion. These interacti ons lead to surface ero sion and particle

deposition, which degrades fusion perf ormance. Co nsiderable information on sputtering yields is available in the literatu re at high-i mpact energies of im pinging pa rticles (above ~50 eV) where the interactions can be modeled using two-body potentials such as those in the TRIM code. In contrast, little is known for low-impact ener gies where chemical processes do minate. Low-energy experiments are very difficult to perform, and measured sputtering yields are very scarce. In an attempt to bridge the ga p of data, we have undertaken a series of simulations for 1–30- eV H, D, and T atoms and molecules impacting carbon[1-3] using the available experimental data above 15 eV for validation. Thi s work is done paralle l to experim ents at ORNL by Fred Mey er and co-workers. We perfor m molecular dynam ics (MD) si mulations using many-body Reactive Empirical Bond Order (REBO) potentials for atoms and m olecules im pacting on a l arge simulation ce ll of a few-thousand atom s representing the surface. Some of the calculated y ields of selected hydrocarbon molecules can be directl y validated with experim ent. In addition, the simulations provide extensive predictions at lo w en ergies a s w ell as for the e ntire spectru m of ejected parti cles.[1] We ha ve recently shown that the individual y ields of molecules change dramatically as the surfaces undergo cumulative bombardment. The latter sequentially breaks and passivates bonds and leads to the for mation of stable hy drocarbon term inal m oieties that are collisionally detached. We have shown that the large y ields of saturated hydrocarbons ty pically observed in experiments are not the result of single i mpacts but rather the consequence of multiple cumulative i mpacts. We are currently investigating the isotope dependence of surface erosion (i.e., H, D, or T im pact). We have f ound that the chemistry at the interface is not too sensitive to the mass of the im pinging atom s (i.e., num ber of term inal m oieties produced by cum ulative bom bardment at the interface). However t he sputtering yields increas e considerably for increasin g projectile mass. We are also studying the sensitivity of the results with respect to the many-body interaction potentials used in the si mulations.[2] Due to co mputing time constraints, m ost of our simulations have been perfor med u sing the si mplest potentials. However, we are regularly improving them to extend their applicability range. In the longer term, we plan to e xtend our sim ulations to address the interest within the fusion c ommunity to stud y materials different fro m p ure carbon such as mixed materials including C, W, Li, and H. This work is performed in collaboration S. Stuart (Clemson University).

1. P. S. Krstic, C. O. Reinhold, and S. J. Stuart, J. Appl. Phys. **104**, 103308 (2008).
2. C. O. Reinhold, P. S. Krstic, and S. J. S tuart, Nucl. Instrum. Methods Phys. Res. B **267**, 691 (2009).

Development of Theoretical Methods for Atomic and Molecular Collisions – *D. R. Schultz, S. Yu. Ovchinnikov, J. B. Sternberg, and J. H. Macek*

Plasma science applications, such as fusion ener gy, material processing, and the che mistry of the upper atm osphere, co ntinue to necessit ate and drive the st udy of atomic and molecular collisions. Further more, co ntrol of atomic-scal e dy namics, ultraf ast phenom ena, and em ergent behavior fro m co mplex sy stems provide strong m otivation to st udy such ato mic and molecular interactions as fundamental test beds. T hese re search areas in turn dem and the development of theoretical methods to either reach new levels of accuracy for fundam ental sy stems or novel completeness for complex systems. Over the past year projects have been undertaken along these lines including the following.

Following our recent developm ent o f the so-call ed regularized, lattice, time-dependent Schrodinger equation (RLTDSE) method,[1] we have uncovered an unexpected presence and role of vortices in atomic collisions.[2,3] The RLTDSE method is an adaptation of the approach we have developed and used over the past decade to describe atom ic collisions by directly solving the underlying dynamics using a lattice-based co mputational approach, allowing t he dynamics to be followed to asymptotically large distances for the first time. Vort ices are usually associated with

systems containing large numbers of particles. However, of particular topical interest are those formed within atomic-scale wave functions and observed in macroscopic systems such as super fluids and quantum condensates. Our RLTDSE calculations (Figure 1) have uncovered them in the electronic wave function describing the prototypical quantum system consisting of a single electron in the field of two moving protons. In particular, we have shown how vortices appear in this system, rotate around the nuclei, and interact, thereby transferring angular momentum from nuclear to electronic motions, casting new light on how angular momentum is transferred in atomic-scale interactions. The method has also allowed us to demonstrate that certain vortices persist up to macroscopic distances in the ejected electron spectrum and may thus be observable.

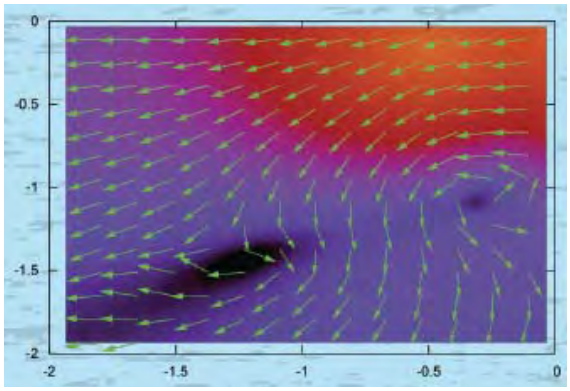

Figure. 1. Density plot of the electronic wave function at an inter-nuclear separation of 5 a.u. in scaled coordinates (q_x,q_z) for a single electron in the field of two protons. Arrows represent the electronic probability current, showing the formation of vortices along nodal lines. All of the coordinates are scaled by R, and the coordinate axis q_z is parallel to the approaching proton's initial velocity.

We have also sought to explore how vortices in atomic wave functions could be produced in a controlled manner and manipulated. To that end, we have calculated the response of an atomic wave function to one or a series of ultrafast electric field pulses. The result is that vortices are created, interact, and follow predictable trajectories. In work to be published, it will be shown that such pulse control of vortices produced in low-lying states of atoms provides a fertile ground to explore quantum control, somewhat in analogy to the manipulation of Rydberg wavepackets with electric pulses.[4]

1. T.-G. Lee, S. Yu. Ovchinnikov, J. Sternberg, V. Chupryna, D. R. Schultz, and J. H. Macek, Phys. Rev. A **76**, 050701(R) (2007).
2. J. H. Macek, J. B. Sternberg, S. Yu. Ovchinnikov, T.-G. Lee, and D. R. Schultz, Phys. Rev. Lett. **102**, 134201 (2009).
3. S. Y. Ovchinnikov, J. H. Macek, J. S. Sternberg, T.-G. Lee, and D. R. Schultz, [Invited] Proceedings, *20th International Conf. on the Application of Accelerators in Research and Industry*, Am. Inst. Phys. Conf. Proc. **1099**, 164 (2009).
4. F. B. Dunning, J. J. Meysayer, C. O. Reinhold, S. Yoshida, and J. Burgdorfer, *Topical Review*, J. Phys. B **42**, 022001 (2009).

References to Publications of DOE Sponsored Research from 2007-2009 (descending order)

Year 2009 Publications

"Chemical Sputtering, Surface Damage ad Modification of Graphite by Low Energy Impact of Atomic and Molecular Deuterium Projectiles," F. W. Meyer, H. Zhang, P. R. Harris, H. M. Meyer, III, and M. J. Lance, Proc. 31st Symposium on Applied Surface Analysis, Santa Cruz, CA., Apr. 22-24 (2009).

"Steady-State and Transient Hydrocarbon Production in Graphite by Low Energy Impact of Atomic and Molecular Deuterium Projectiles," H. Zhang and F.W. Meyer, J. Nucl. Mat. **390–391**, 127 (2009).

"Resonant Ionization Laser Ion Source for Radioactive Ion Beams," Y. Liu, J. R. Beene, T. Gottwald, C. C. Havener, C. Mattolat, J. Lassen, K. Wendt, and C. R. Vane, *20th International Conf. on the Application of Accelerators in Research and Industry*, Am. Inst. Phys. Conf. Proc. **1099**, 141 (2009).

"Electron-Impact Dissociation of CD_3^+ and CH_3^+ Ions Producing CD_2^+, CH^+, and C^+ Fragment Ions," E. M. Bahati, M. Fogle, C. R. Vane, M. E. Bannister, R. D. Thomas, and V. Zhaunerchyk, Phys. Rev. A **79**, 052703 (2009).

"Isotope Effects in Low Energy Ion-Atom Collision," C. C. Havener, D. G. Seely, J. D. Thomas, and T. J. Kvale," *20th International Conf. on the Application of Accelerators in Research and Industry*, Am. Inst. Phys. Conf. Proc. **1099**, 150 (2009).

"Production, Characterization, and Measurement of H(D) Beams on the ORNL Merged-Beams Experiment," J. D. Thomas, T. J. Kvale, S.M. Z. Strasser, D. G. Seely, and C. C. Havener, *20th International Conf. on the Application of Accelerators in Research and Industry*, Am. Inst. Phys. Conf. Proc. **1099**, 154 (2009).

"Production of Long-Lived H_2^-, HD^-, and D_2^- during Grazing Scattering Collisions of H_2^+, H_3^+, D_2^+, D_3^+, and D_2H^+ Ions with KBr, KCl, and LiF Surfaces," D. G. Seely, F. W. Meyer, H. Zhang, and C. C. Havener, *20th International Conf. on the Application of Accelerators in Research and Industry*, Am. Inst. Phys. Conf. Proc. **1099**, 159 (2009).

"Evolution of Quantum Systems from Microscopic to Macroscopic Scales," S. Yu Ovchinnikov, J. H. Macek, J. S. Sternberg, T.-G. Lee, and D. R. Schultz, *20th International Conf. on the Application of Accelerators in Research and Industry*, Am. Inst. Phys. Conf. Proc. **1099**, 164 (2009).

"Low-Energy Grazing Ion-Scattering from Alkali-Halide Surfaces: A Novel Approach to C-14 Detection," F. W. Meyer, E. Galutschek, and M. Hotchkis," *20th International Conf. on the Application of Accelerators in Research and Industry*, Am. Inst. Phys. Conf. Proc. **1099**, 308 (2009).

"High-Energy Laser-Accelerated Electron Beams for Long-Range Interrogation," N. J. Cunningham, S. Banerjee, V. Ramanathan, N. Powers, N. Chandler-Smith, R. Vane, D. Schultz, S. Pozzi, S. Clarke, J. Beene, and D. Umstadter, *20th International Conf. on the Application of Accelerators in Research and Industry*, Am. Inst. Phys. Conf. Proc. **1099**, 638 (2009).

"Efficient Isobar Suppression by Photodetachment in the RF Quadrupole Ion Cooler," Y. Liu, C. C. Havener, T. L. Lewis, A. Galindo-Uribarri, and J. R. Beene, *20th International Conf. on the Application of Accelerators in Research and Industry*, Am. Inst. Phys. Conf. Proc. **1099**, 737 (2009).

"Large Scale Quantum Coherence of Nearly Circular Wavepackets," C. O. Reinhold, S. Yoshida, J. Burgdörfer, B. Wyker, J. J. Mestayer, and F. B. Dunning, *Fast Track Communication*, J. Phys B **42**, 091003 (2009).

"Transfer of Rovibrational Energies in Hydrogen Plasma-Carbon Surface Interactions," P. S. Krstic, E. M. Hollmann, C. O. Reinhold, S. J. Stuart, R. P. Doerner, D. Nishijima, and A. Yu. Pigarov, J. Nucl. Materials **390-391**, 88 (2009).

"Creation of Non-Dispersive Bohr-Like Wavepackets," J. J. Mestayer, B. Wyker, F. B. Dunning, S. Yoshida, C. O. Reinhold, and J. Burgdorfer, Phys. Rev. A **79**, 033417 (2009).

"Hydrogen Reflection in Low-Energy Collisions with Amorphous Carbon," C. O. Reinhold, P. S. Krstic, and S. J. Stuart, Nucl. Instrum. Meth. Phys. Res. B **267**, 691 (2009).

"Plasma-Surface Interactions of Hydrogenated Carbon," P. S. Krstic, C. O. Reinhold, and S. J. Stuart, Nucl. Instrum. Meth. Phys. Res. B **267**, 704 (2009).

"Engineering Atomic Rydberg States with Pulsed Electric Fields," F. B. Dunning, J. J. Mestayer, C. O. Reinhold, S. Yoshida, and J. Burgdörfer, *Topical Review*, J. Phys. B **42**, 022001 (2009).

"Origin Evolution and Imaging of Vortices in Atomic Processes," J. H. Macek, J. B. Sternberg, S. Yu. Ovchinnikov, T.-G. Lee, and D. R. Schultz, Phys. Rev. Lett. **102**, 134201 (2009).

Year 2008 publications

"Attosecond Time Delays in Heavy-Ion Induced Fission Measured by Crystal Blocking," J. U. Anderson, J. Chevallier, J. S. Foster, S. A. Karamian, C. R. Vane, J. R. Beene, A. Galindo-Uribarri, J. Gomez del Campo, C. J. Gross, H. F. Krause, E. Padilla-Rodal, D. C. Radford, D. Shapira, C. Broude, F. Malaguti, and A. Uguzzoni, Phys. Rev. C 78, 064609 (2008).

"Rotating Dual-Wire Beam Profile Monitor Optimized for Use in Merged-Beams Experiments," D. G. Seely, H. Bruhns, D. W. Savin, T. J. Kvale, E. Galutschek, H. Aliabadi, and C. C. Havener, Nucl. Instrum. Methods Phys. Res. **585**, 69 (2008).

"Chemical Sputtering and Surface Damage by Low-Energy Atomic and Molecular Hydrogen and Deuterium Projectiles," F. W. Meyer, H. Zhang, M. J. Lance, and H. F. Krause, Vacuum **82**, 880 (2008).

"Surface Modification and Chemical Sputtering of Graphite Induced by Low-Energy Atomic and Molecular Deuterium Ions," H. Zhang, F. W. Meyer, H. M. Meyer III, M. J. Lance, Vacuum **82**, 1285 (2008).

"Electron-Impact Ionization of Be-like C III, N IV, and O V," M. R. Fogle, E. Bahati Musafiri, M. E. Bannister, C. R. Vane, S. D. Loch, M. S. Pindzola, C. P. Ballance, R. D. Thomas, V. Zhaunerchyk, P. Bryans, W. Mitthumsiri, and D. W. Savin, Astrophys. J. Suppl. Ser. **175**, 543 (2008).

"Dissociative Recombination of BH_2^+: The Dominance of Two-Body Breakup and an Understanding of the Fragmentation," V. Zhaunerchyk, E. Vigren, W. Geppert, M. Hamberg, M. Danielsson, M. Kaminska, M. Larsson, R. D. Thomas, E. Bahati Musafiri, and C. R. Vane, Phys. Rev. A **78**, 024701 (2008).

"Dissociative Recombination Dynamics of the Ozone Cation," V. Zhaunerchyk, W. Geppert, F. Österdahl, M. Larsson, R. D. Thomas, E. Bahati Musafiri, M. E. Bannister, M. R. Fogle, and C. R. Vane, Phys. Rev. A **77**, 022704 (2008).

"Tailoring Very-High-n Circular Wavepackets," C. O. Reinhold, S. Yoshida, J. Burgdorfer, J. J. Mestayer, B. Wyker, J. C. Lancaster, and F. B. Dunning, Phys. Rev. A **78**, 063413 (2008).

"Energy and Angle Spectra of Sputtered Particles for Low-Energy Deuterium Impact of Carbon," P. S. Krstic, C. O. Reinhold, and S. J. Stuart, J. Appl. Phys. **104**, 103308 (2008).

"Measurement and Modeling of Hydrogen Molecule Ro-Vibrational Accommodation on Graphite", E. M. Hollmann, P. S. Krstic, R. P. Doerner, D. Nishijima, A. Yu. Pigarov, C. O. Reinhold, and S. J. Stuart, Plasma Phys. Control. Fusion **50**, 102001 (2008).

"Extracting Irreversible Dephasing Rates from Electric Dipole Echoes in Rydberg Stark Wavepackets", S. Yoshida, C. O. Reinhold, J. Burgdorfer, W. Zhao, J. J. Mestayer, J. C. Lancaster, and F. B. Dunning, Phys. Rev. A **78**, 063414 (2008).

"Realization of Localized Bohr-like Wavepackets," J. J. Mestayer, B. Wyker, J. C. Lancaster, F. B. Dunning, C. O. Reinhold, S. Yoshida, and J. Burgdörfer, Phys. Rev. Lett. **100**, 243004 (2008).

"Occupation of Fine-Structure States in Electron Capture and Transport," M. Seliger, C. O. Reinhold, T. Minami, D. R. Schultz, S. Yoshida, J. Burgdörfer, E. Lamour, J.-P. Rozet, and D. Vernhet, Phys. Rev. A **77**, 042713 (2008).

"Total and State-Selective Charge Transfer in He^{2+} + H Collisions," T. Minami, T.-G. Lee, M. S. Pindzola, and D. R. Schultz," J. Phys. B **41**, 134201 (2008).

"Time-Dependent Lattice Methods for Ion-Atom Collisions in Cartesian and Cylindrical Coordinate Systems," M. S. Pindzola and D.R. Schultz, Phys. Rev. A **77**, 014701 (2008).

"Transferring Rydberg Wavepackets between Islands across the Chaotic Sea," S. Yoshida, C. O. Reinhold, J. Burgdörfer, J. J. Mestayer, J. C. Lancaster, and F. B. Dunning, Phys. Rev. A **77**, 013411 (2008).

"Low-Energy Charge Transfer for Collisions of Si^{3+} with Atomic Hydrogen," H. Bruhns, H. Kreckel, D. W. Savin, D. G. Seely, and C. C. Havener, Phys. Rev. A **77**, 064702 (2008).

Year 2007 publications

"Ion Atom Merged-Beams Experiments," C. C. Havener, E. Galutschek, R. Rejoub, and D. G. Seely, Nucl. Instrum. Methods Phys. Res. B **261**, 129 (2007).

"Three-Step Resonant Photoionization Spectroscopy of Ni and Ge: Ionization Potential and Odd-Parity Rydberg Levels," T. Kessler, K. Bruck, C. Baktash, J. R. Beene, C. Geppert, C. C. Havener, H. F. Krause, Y. Liu, D. R. Schultz, D. W. Stracener, C. R. Vane, and K. Wendt, J. Phys. B **40**, 4413 (2007).

"The ORNL Single-Pass Ion-Atom Merged-Beam Experiment," C. C. Havener, [Invited] *Proceedings, 2nd International Workshop on Electrostatic Storage Devices, July 17-21, 2007, Stockholm, Sweden*.

"Experiments on Interactions of Electrons with Molecular Ions in Fusion and Astrophysical Plasmas," M. E. Bannister, H. Aliabadi, E. Bahati Musafiri, M. R. Fogle, P. S. Krstic, C. R. Vane,

A. Ehlerding, W. Geppert, F. Hellberg, V. Zhaunerchyk, M. Larsson, and R. D. Thomas, Book Chapter - *Atomic Processes in Plasmas: The 15th International Conference on Atomic Processes in Plasmas;* AIP Conf. Proceedings **926**, 195-205 (2007).

"Low-Energy Electron Capture by Ne^{2+} Ions from H(D)," B. Seredyuk, H. Bruhns, D. W. Savin, D. G. Seely, H. Aliabadi, E. Galutschek, and C. C. Havener, Phys. Rev. A **75**, 054701 (2007).

"Quantum and Classical Transport of Excited States of Ions, " C. O. Reinhold, M. Seliger, T. Minami, D. R. Schultz, J. Burgdörfer, E. Lamour, J.-P. Rozet, and D. Vernhet, Nucl. Instrum. Methods Phys. Res. B **261**, 125 (2007).

"Angular Distribution of Ions Transmitted by an Anodic Nanocapillary Array," H. F. Krause, C. R. Vane, F. W. Meyer, and H. M. Christen, *Proceedings, 13th International Conference on the Physics of Highly Charged Ions, Belfast, Northern Ireland, UK*, J. Phys.: Conf. Ser. **58**, 323 (2007).

"Electron-Impact Ionization of Be-like, C^{2+}, N^{3+}, and O^{4+}," M. E. Bannister, E. Bahati Musafiri, C. P. Balance, M. R. Fole, S. D. Loch, W. Mitthumsiri, M. S. Pindzola, D. W. Savin, R. D. Thomas, C. R. Vane, and V. Zhaunerchyk, *Proceedings, XXV International Conference on Photonic, Electronic and Atomic Collisions, Freiburg, Germany, July 25-31, 2007*, Vol. I, Fr131.

"Dissociative Excitation of Diatomic and Polyatomic Molecular Ions Producing Heavy Fragment Ions," M. E. Bannister, E. Bahati Musafiri, M. R. Fogle, P. S. Krstic, M. Larsson, R. D. Thomas, C. R. Vane, and V. Zhaunerchyk, *Proceedings, Abstracts of Conributed Papers, XXV International Conference on Photonic, Electronic and Atomic Collisions, Freiburg, Germany, July 25-31, 2007.*

"Electron-Impact Dissociation of CH_2^+ Ions: Measurement of CH^+ and C^+ Fragment Ions," C. R. Vane, E. Bahati Musafiri, M. E. Bannister, and R. D. Thomas, Phys. Rev. A **75**, 052715 (2007).

"Atomic Collisions at Ultrarelativistic Energies," C. R. Vane and H. F. Krause, Nucl. Instrum. Methods Phys. Res. B **261**, 244 (2007).

"Three-Body Breakup in Dissociative Recombination of the Covalent Triatomic Molecular Ion O_3^+," V. Zhaunerchyk, W. D. Geppert, M. Larsson, R. D. Thomas, E. Bahati, M. E. Bannister, M. R. Fogle, C. R. Vane, and F. Österdahl, Phys. Rev. Lett. **98**, 223201 (2007).

"Ions Transmitted through an Anodic Nanocapillary Array," H. F. Krause, C. R. Vane, and F. W. Meyer, Phys. Rev. A **75**, 042901 (2007).

"The New ORNL Multicharged Ion Research Facility Floating Beamline," F. W. Meyer, M. R. Fogle, and J. W. Hale, *Proceedings, 22nd Particle Accelerator Conference (PAC'07), Albuquerque, NM, June 25-29, 2007*.

"Merged-Beams Measurements of Absolute Cross Sections for Electron-Impact Excitation of S^{4+} ($3s^2\ ^1S \rightarrow 3s3p\ ^1P$) and S^{5+}($3s\ ^2S \rightarrow 3p\ ^2P$)," B. Wallbank, M. E. Bannister, H. F. Krause, Y.-S. Chung, A.C.H. Smith, N. Djuric, and G. H. Dunn, Phys. Rev. A **75**, 052703 (2007).

"Low-Energy Chemical Sputtering of ATJ Graphite by Atomic and Molecular Deuterium Ions," F. W. Meyer, P. S. Krstic, L. I. Vergara, H. F. Krause, C. O. Reinhold, and S. J. Stuart, Phys. Scr. **T128**, 50 (2007).

"Chemical Sputtering of Room Temperature AT J Graphite and HOPG by Slow Atomic and Molecular Ions," F. W. Meyer, H. Z hang, L. I. Vergara, and H. F. Krause, Nucl. Instrum . Methods Phys. Res. B **258**, 264 (2007).

"Chemical Sputtering from Amorphous Carbon under Bombardment by Deuterium Atoms and Molecules," P. S. Krstic, C. O. Reinhold, and S. J. Stuart, New J. Phys. **9**, 219 (2007).

"Regge Oscillations in Electron-Atom Elastic Cross Sections," D. Sokolovski, Z. Felfli, S. Yu. Ovchinnikov, J. H. Macek, and A. Z. Msezane, Phys. Rev. A **76**, 1 (2007).

"Transporting Rydberg Electron Wavepackets with Chirped Trains of Pulses," J. J. Mestayer, W. Zhao, J. C. Lancaster, F. B. Dunning, C. O. Reinhold, S. Yoshida, and J. Burgdörfer, Phys. Rev. Lett. **99**, 183003 (2007).

"Electric Dipole Echoes in Rydberg Atoms," S. Yoshida, C. O. Reinhold, J. Burgdörfer, W. Zhao, J. J. Mestayer, J. C. Lancaster, and F. B. Dunning, Phys. Rev. Lett. **98**, 203004 (2007).

"Quantum Treatment of Continuum Electrons in the Fields of Moving Charges," T.-G. Lee, S. Yu. Ovchinnikov, J. Sternberg, V. Chupryna, D. R. Schultz, and J. H. Macek, Phys. Rev. A **76**, 050701 (2007).

"The Time-Dependent Close-Coupling Method for Atomic and Molecular Collision Processes," M. S. Pindzola, F. Robicheaux, S. D. Loch, J. C. Berengut, T. Topcu, J. Colgan, M. Foster, D. C. Griffin, C. P. Ballance, D. R. Schultz, T. Minami, N. R. Badnell, M. C. Witthoeft, D. R. Plante, D. M. Mitnik, J. A. Ludlow, and U. Kleiman, J. Phys. B **40**, R39 (2007).

"Electric Dipole Echoes and Noise-Induced Decoherence," J. J. Mestayer, W. Zhao, J. C. Lancaster, F. B. Dunning, C. O. Reinhold, S. Yoshida, and J. Burgdörfer, J. Phys. Conf. Ser. **88**, 012055 (2007).

"Open Quantum System Approach in Multiple Atomic Collisions in Solids and Gases," C. O. Reinhold, M. Seliger, T. Minami, S. Yoshida, J. Burgdörfer, J. J. Mestayer, W. Zhao, J. C. Lancaster, and F. B. Dunning, J. Phys. Conf. Ser. **88**, 012030 (2007).

"Low-Energy Chemical Sputtering of ATJ Graphite by Atomic and Molecular D Ions," F. W. Meyer, P. S. Krstic, L. I. Vergara, H. F. Krause, C. O. Reinhold, and S. J. Stuart, Phys. Scr. **T128**, 50 (2007).

"Time Scales of Chemical Sputtering of Carbon," C. O. Reinhold, P. S. Krstic, and S. J. Stuart, Nucl. Instrum. Methods Phys. Res. B **258**, 274 (2007).

"Chemical Sputtering by Impact of Excited Molecules," P. S. Krstic, C. O. Reinhold, and S. J. Stuart, Europhys. Lett. **77**, 33002 (2007).

"Numerical Study of Charge Transfer in $H^+ + He^+$ and $He^{2+} + Li^{2+}$ Collisions," T. Minami, M.S. Pindzola, T.-G. Lee, and D. R. Schultz, " J. Phys. B **40**, 3629 (2007).

"Capture and Transport of Electronic States of Fast Ions Penetrating Solids: An Open Quantum System Approach with Sinks and Sources," M. Seliger, C. O. Reinhold, T. Minami, D. R. Schultz, M. S. Pindzola, S. Yoshida, J. Burgdörfer, E. Lamour, J.-P. Rozet, and D. Vernhet, Phys. Rev. A **75**, 032714 (2007).

"Dephasing of Stark Wavepackets Induced b y Co lored Noise," S. Yoshida, C. O. Reinhold, J. Burgdörfer, W. Zhao, J. J. Mestay er, J. C. Lancaster, and F. B . Dunning, Phy s. Rev. A **75**, 013414 (2007).

"Methane Production b y Deuterium Im pact at Carbon S urfaces," S. J. Stu art, P. S. Krstic, T. A. Embry, and C. O. Reinhold, Nucl. Instrum. Methods Phys. Res. B **255**, 202 (2007).

The PULSE Institute for Ultrafast Energy Science at SLAC

Y. Acremann, M. Bogan, P.H. Bucksbaum (Director), K. Gaffney, M. Gühr, A. Lindenberg, T. Martinez, D. Reis (Deputy Director), J. Stohr, SLAC National Accelerator Laboratory, phb@slac.stanford.edu

PULSE Vision Statement: A laser science revolution is underway now at the SLAC National Accelerator Laboratory. The Linac Coherent Light Source, LCLS, has already exceeded its main design goal with the steady production of millijoule energy, 100 femtosecond pulses of 1.5 Å x rays. This is a billion times more brilliant than any other laboratory source of x rays. This new class of x-ray sources will revolutionize many areas of science by making it possible for the first time to see atomic scale structures and simultaneously track atomic motions of the underlying nanoscale processes of energy conversion and transport.

The PULSE mission is to advance the frontiers of ultrafast science at SLAC with particular emphasis on discovery and Grand Challenge energy-related research enabled by LCLS. The PULSE Institute initiates and leads multidisciplinary collaborative research programs in studies of atoms, molecules, and nanometer-scale systems, where motion and energy transfer occurs on picosecond, femtosecond, and attosecond time scales. Ultrafast energy research at PULSE combines the disciplines of atomic and molecular physics, ultrafast chemistry and biochemistry, ultrafast condensed matter and materials science, ultrafast x-ray science, nanoscale x-ray imaging science, and the enabling science for next-generation ultrafast light and electron sources. Our metrics of success are the level of the ultrafast science challenges we address, and our progress toward and impact on their solution.

PULSE research utilizes the capabilities of LCLS, but also goes beyond this. For example, PULSE has a vigorous program on high harmonics generation and associated measurement techniques for atoms and molecules on the sub-femtosecond timescale. We are also developing the applications of ultrafast pulsed sources of relativistic electrons both in the laboratory and at the SLAC FACET facility, for research in materials and chemical science. PULSE research extends to the research floor of the SPEAR3 synchrotron at SLAC, where ultrafast lasers can create transient conditions that are probed by synchrotron radiation. Finally, PULSE develops frontier research that makes use of technologies such as ultrafast imaging of biological and nanoscale materials, and ultrafast x-ray studies of matter in extreme environments. Our aim is to establish the leadership of SLAC research in these areas to solve fundamental challenges in basic energy science.

PULSE Core Research Strengths: PULSE brings together world-leading research strengths and unique facilities in several areas, providing the expertise and resources to tackle frontier energy research problems:

- **Ultrafast Nanomagnetism. (Stöhr, Acremann, Lindenberg):** PULSE has world-leading efforts on the study of magnetic dynamics on the nanometer and sub-picosecond scale.
- **Atomic and Chemical Dynamics. (Bucksbaum, Gaffney, Gühr, Martinez):** The recent addition of the Martinez theory group, together with our strength in harmonics sources and the opportunities of LCLS, gives PULSE a central position in the study and the control of excited state molecular dynamics.
- **Ultrafast Materials Science. (Lindenberg, Reis, Nilsson):** The study of rapid processes in materials is a broad area of strength at PULSE, with the materials science engineering group of Lindenberg, condensed matter physics of Reis, and interfacial catalysis science of Nilsson.
- **Ultrafast Source Science. (Reis, Lindenberg, Bucksbaum, Acremann, Stöhr, Bogan):** Most PULSE senior investigators have made impressive contributions in this area, and LCLS is providing new opportunities with the PULSE contributions to the SXR, CXI, XPP, and AMO instruments.
- **Nanoscale & Biomolecular Imaging. (Bogan, Gühr, Bucksbaum, Stöhr, Acremann):** PULSE is developing non-periodic imaging techniques for LCLS, and also extending this concept to aligned molecules, holography for magnetism, and several other areas.
- **SLAC facilities (LCLS, SSRL, FACET, PULSE Institute Building):** The PULSE Institute building will provide 18000sf of laboratory and office space, to enable us to develop close collaborations in important ultrafast areas such as time-resolved photoemission, time-resolved x-ray scattering, support for ultrafast

biological imaging, and multidimensional spectroscopy. PULSE also takes advantage of our proximity to SSRL and to LCLS to build strong SLAC core facilities in laser science and accelerator science. The facilities are described in greater detail in the Facilities sections of each subtask.

- **Stanford:** The major educational, physical research, engineering research, and medical research activities at Stanford provide strong support for all of our activities in PULSE. Stanford is also helping us build an international ultrafast x-ray research community for LCLS by supporting our annual Ultrafast X-ray Summer School.

- **Organization Chart for the PULSE Institute:**

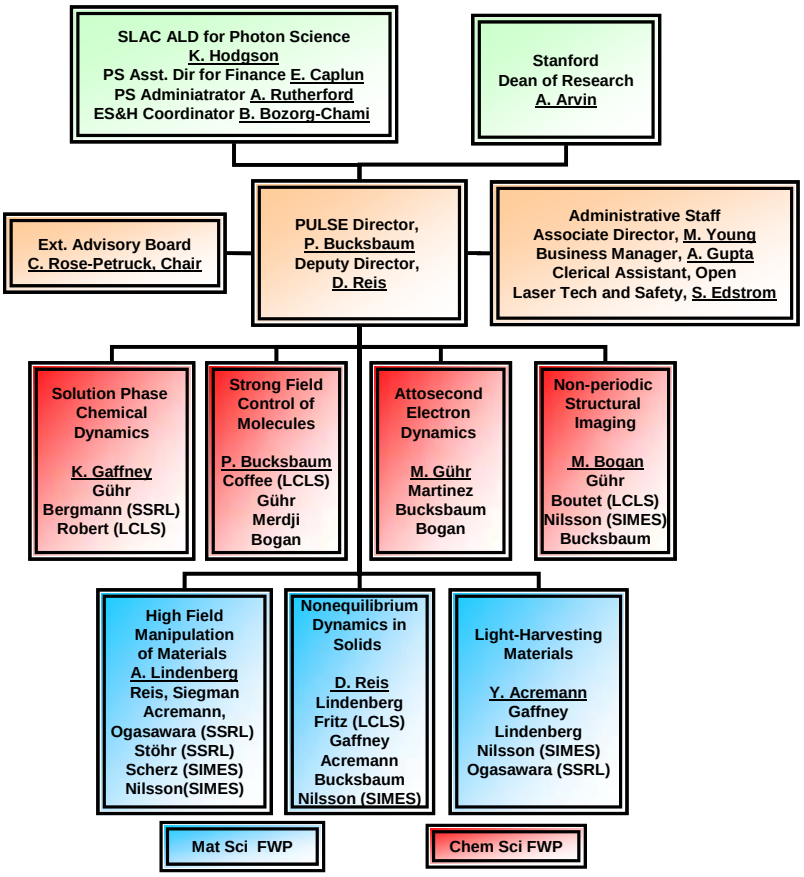

Organization chart for PULSE. Subtasks show Task Leaders (underlined) and Key Personnel.

Program Enhancements and Innovations over the Next Three Years:

PULSE is in its initial period of significant growth. The next three years offer compelling rich opportunities to develop our young Institute.

- **LCLS begins user operations in September 2009**, and there is a critical need for PULSE participation in commissioning and in early experiments, as well as general activities to build an LCLS user community. The laser is already working beyond its specifications, and that means that new research opportunities must now be captured to realize its potential for groundbreaking science.

- **PULSE is moving into a newly renovated institute building** starting In June 2009, which will eventually provide 18,000 sf of laboratory and office space designed for work in ultrafast laser materials science, chemistry, AMO Physics, and biochemistry. Optimal utilization of this space is essential for PULSE, SLAC, and BES. This proposal is sized to fit that new space.

- **PULSE has recruited major new research groups** in the area of ultrafast x-ray scattering (D. Reis) and chemical dynamics theory (T. Martinez). These provide greatly expanded opportunities for frontier work in ultrafast science.
- **The Department of Energy Office of Basic Energy Science is coordinating its basic research to meet the next decade's Grand Challenges in energy and climate change.** PULSE staff is eager to respond to this challenge. We have realigned our research areas accordingly. We have applied for a SISGR to start energy-related collaborative activities, and we have also secured LDRD funding to seed theory in this area. This current renewal requests that we be allowed to align our young Institute with this important BES mission.

Subtasks in PULSE: PULSE has refocused its research divisions to focus on BES frontier energy science, LCLS-based research, and SLAC-based ultrafast science. Seven research subtasks for this purpose have been defined, whose relationship to the former PULSE tasks is listed below the respective funding summaries. The Chemical Science programs are described in further detail in separate abstracts.

Tasks supported by the Chemical Sciences FWP: These tasks are aimed at the control and imaging of chemical dynamics, from electrons in small molecules to atoms in clusters. The emphasis is on grand challenges for energy science. The proposed research utilizes our core strengths in molecular theory (Martinez), ultrafast spectroscopy (Gaffney), quantum control (Bucksbaum) and strong field AMO physics (Gühr and Bucksbaum). The imaging expertise in PULSE includes biological imaging (Bogan) with laser manipulation of targets for imaging (Bucksbaum) and our special abilities to capture and image ultrafast processes as they happen. Tasks in this area utilize the PULSE Institute building as well as SPEAR3 and the LCLS AMO, CXI, and XPP end stations. Subtasks:

- **Attosecond Coherent Electron Dynamics (ATO)** (formerly Subtask E.2.a) Task Leader Markus Gühr. (co-leader P. Bucksbaum) This task studies the fastest timescales in chemical physics involved with electron correlation, and nonradiative chemical processes, connecting LCLS research to the new field of attophysics.
- **Strong Fields in Molecules (SFA)** (formerly Subtask E.2.b) Task Leader Phil Bucksbaum. This task incorporates and extends strong-field quantum control to LCLS experiments in molecular dynamics and molecular imaging. Strong field effects in atoms and molecules can be studied using ultrafast x rays, or employed to create targets for x-ray imaging. In addition, LCLS is itself the world's first source of coherent volt/Ångstrom fields of x-ray radiation. A separate component of this program in ultrafast x-ray scattering is in the Nonequilibrium Dynamics in Solids task.
- **Solution-Phase Chemical Dynamics (SPC)** (formerly Subtask E.3) Task Leader Kelly Gaffney. This task explores ultrafast chemical processes in solutions, utilizing LCLS, synchrotrons, and the PULSE labs. Emphasis is on the ultrafast dynamics of energy conversion in chemistry.
- **Nonperiodic Imaging (NPI)** (formerly Subtask E.4) Task Leader Michael Bogan. This task studies nonperiodic nanoscale imaging, one of the greatest new opportunities for LCLS. The frontier science questions under study range from nanobiology to aerosol chemistry to combustion.

Tasks supported by the Materials Sciences FWP: From magnetism to melting, PULSE has assembled one of the strongest research teams in the US for ultrafast studies of condensed matter. Many of the roadblocks to efficient and low cost utilization or conversion of light energy involve electron dynamics in the initial picoseconds following photoabsorption, in materials driven from equilibrium. We will use the imaging capabilities of x-ray scattering, in real space and in k-space, to understand how structural and spin domains are formed, destroyed, and altered on the nanometer and femtosecond scale. We will utilize many of the special facilities on the SLAC site, including most of the LCLS instruments, the SPEAR3 synchrotron, and the new FACET facility. Subtasks:

- **High Field Manipulation of Materials (FMM)** (formerly Subtask D.2.a, and parts of D.2.b-d and D.3.b Task Leader Aaron Lindenberg. The goal here is to explore the interaction of intense ultrashort fields with

matter, develop mechanisms for all-optical manipulation of charges, spins, and atoms, and to simultaneously watch these processes occur with atomic-scale resolution probes.

- **Nonequilibrium Dynamics in Solids (NQS)** (formerly Subtask D.3.a and part of E.2.b) Task Leader David Reis. Ultrafast x rays can track nonequilibrium dynamics in solids with atomic-scale resolution in time and space and with atomic specificity. LCLS is a unique tool for these studies.
- **Ultrafast Processes in Light Harvesting Materials (LHM)** (formerly parts of D.2.b-d and D.3.b) Task Leader Yves Acremann. Ultrafast x-ray and optical techniques can probe the dynamics of charge separation, charge transport, and charge transfer in a variety of light harvesting materials, including organic semiconductors, colloidal nanomaterials, and complex alloys.

Outreach: The Ultrafast X-ray Summer School is a five day residential program hosted annually by PULSE. The goal is to disseminate information and train students and post-docs on new opportunities in ultrafast science, particularly using X-ray Free Electron Lasers. Lectures are presented by expert scientists in this exciting new field. The attendees are expected to participate in the discussions and to prepare a mock beamtime proposal poster with input from the instrument scientists for the Linac Coherent Light Source. The living expenses and travel for the lecturers in the school and the reception and coffee break refreshments are paid by the student registration and a supplement from the Stanford Dean of Research. The PULSE Central Management budget only pays for the staff time involved. This year's Ultrafast X-ray Summer School is co-directed by PULSE Deputy Director David Reis and PULSE Research Scientist Hamed Merdji.

PULSE maintains a **visitors program** to enable researchers from around the world to work in our center. These visitors are extremely valuable to the PULSE primary research program. Visitors are given an office, access to PULSE laboratories and institute services, and some expense reimbursement, according to SLAC rules. PULSE extends to them the Stanford designation of Visiting Scientist or Visiting Professor (in line with their rank at their home institution), which entitles them to access to the Stanford Housing Office and the use of the Stanford Library. The budget for this program is relatively modest, particularly when one considers that a senior investigator with major talents and established abilities can be associated as a sabbatical visitor for a year, for less than the cost of a Postdoc. In 2009-2010 the sabbatical visitors are Steve Durbin (Purdue), Ken Schaffer and Mette Gaarde (LSU) and Jon Marangos (Imperial). Future visits are also planned by Roseanne Sension (Michigan). We expect numerous shorter visits associated with our collaborations on LCLS experiments.

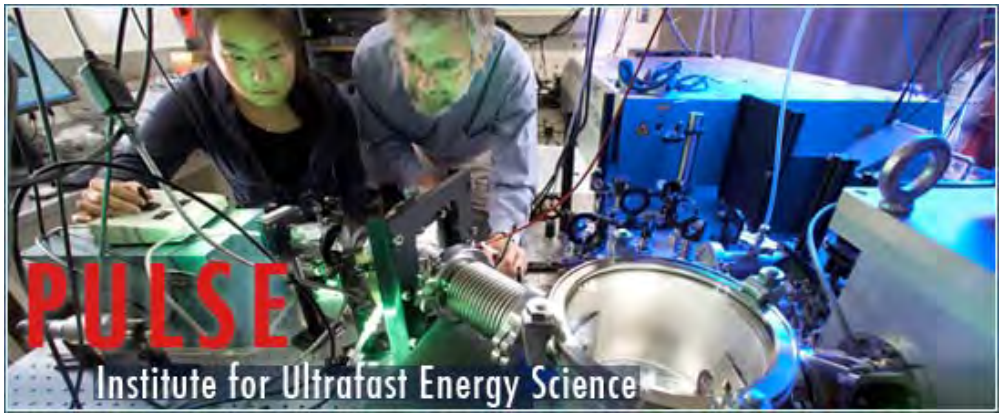

Find out more: http://pulse.slac.stanford.edu

Non-Periodic Imaging

Principle Investigator: Mike Bogan
Stanford PULSE Institute for Ultrafast Energy Science, SLAC National Accelerator Laboratory,
2575 Sand Hill Rd MS 59, Menlo Park, CA 94025, email: mbogan@slac.stanford.edu

PROGRAM SCOPE: Biology is nature's nanotechnology, and is dominated by non-periodic structures that transform, store and transport energy and information. We have pioneered a revolutionary approach to view this nanoscale world. Our single particle coherent lensless imaging with ultrafast soft x-ray free-electron-lasers (FELs) has revealed nanoscale structure before x-ray damage occurs (Fig 1). The Non-Periodic Imaging program, task E.4 at the PULSE Institute for Ultrafast Energy Science, is part of an international collaboration whose goal is to perform coherent imaging of non-periodic structures using x-ray FELs, such as the Linac Coherent Light Source (LCLS). LCLS will extend our resolution, already achieved at the soft-X-ray FEL at DESY, by more than an order of magnitude. *The experimental opportunities of non-periodic imaging (NPI) with LCLS are enormous.*

Coherent diffraction imaging is elegant in its experimental simplicity: a coherent x-ray beam illuminates the sample and the far-field diffraction pattern of the object is recorded on an area detector. These measured diffraction intensities are proportional to the modulus squared of the wave amplitude (scattering amplitude) exiting the object. An inversion of the diffraction pattern to an image in real space requires the retrieval of the diffraction pattern phases. This can be achieved by iterative transform algorithms if the object is isolated and the diffraction pattern intensities are adequately sampled (an approach known as oversampling). Our shrinkwrap algorithm is particularly robust and practical. The algorithm reconstructs images ab initio which overcomes the difficulty of requiring knowledge of the high-resolution shape of the diffracting object. Coherent diffraction imaging overcomes the restrictions of limited-resolution x-ray lenses, offering a means to produce images of general non-crystalline objects at a resolution only limited in principle by the x-ray wavelength and by radiation-induced changes of the sample during exposure. While we are primarily motivated to image biological macromolecules, the general imaging techniques, diagnostics, optics, sample manipulation, and understanding of materials behavior in intense x-ray fields, are of fundamental importance to ultrafast x-ray science and cut across all areas of research of PULSE.

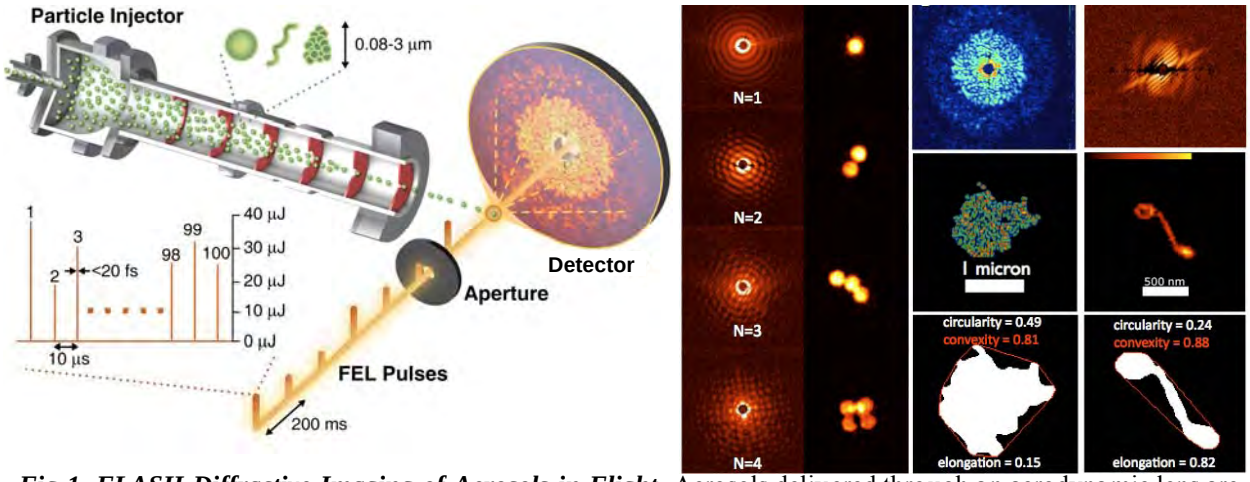

Fig 1. FLASH Diffractive Imaging of Aerosols in Flight. Aerosols delivered through an aerodynamic lens are steered into the interaction region. FLASH is operated in multi-bunch mode. Upon coincident arrival of a particle and x-ray pulse with readout of an x-ray sensitive area detector, a diffraction pattern containing particle structural information is recorded. **Examples**: Left: Diffraction patterns of single and aggregated 250 nm diameter spheres, where N equals the number of particles in the aggregate. The second column shows images of reconstructed electron density solved using ESPRESSO. Right: The diffraction pattern (top), reconstructed electron density (middle), and binary convex hull image (bottom) of an aggregate particle comprised of 88 nm spheres and a single carbon nanofiber.

Achieving the goal of coherent diffractive imaging of a single particle requires extensive technical and theoretical advances. This will be achieved through a combination of simulation and experiments. The experiments will be carried out at synchrotron sources and the currently operational soft-x-ray FEL at DESY called FLASH. We will also perform the first NPI experiments at LCLS during our awarded beamtime in late 2009. This systematic series of diffraction experiments will grow in complexity as we progress and will include studies of well-characterized single particle aerosol standards, water droplets, gas phase molecules and (bio)materials supported by membranes. As we develop the fundamental science behind NPI with hard x-rays, we will establish LCLS as one the most powerful tools in aerosol science and nanotechnology, provide critical early insights into single particle diffraction, and help unravel the mystery of the structure of water. We will also begin exploring a complementary non-destructive NPI technique, ultrafast electron holography, which can image electric and magnetic fields of thin materials on a sub-nm scale with sub-10-fs resolution.

Our technical experience in coherent imaging experiments and FLASH results currently guide the development of the coherent x-ray imaging (CXI) endstation scheduled for operation at LCLS in 2011, as well as other experiments where high-resolution structural information is acquired. The theoretical models and simulations of the interaction of particles in intense XFEL beams will be compared and tested with short-pulse coherent imaging, holographic, and scattering experiments at FLASH and LCLS. This program will be complemented with the experimental investigation of aerosol nano-engineering methods and nanoscale template design to deliver encapsulated biomolecules to the FEL and optimize diffraction pattern acquisition. Another component of the project is the development of laser alignment of molecules and particles using intense near-IR lasers that will be done in conjunction with other efforts at PULSE. New efforts complementing the existing components of the non-periodic imaging program will be initiated, including studies of the structure of water and the development of ultrafast electron holography.

RECENT PROGRESS: The recent realization of the FLASH soft x-ray free electron laser (FEL) provided the first opportunity to experimentally verify "diffract and destroy" science. ***Our team has pioneered the experimental methods in FLASH diffractive imaging*** (Fig 1). Extending our experiments to the hard x-rays of LCLS promises to revolutionize structural biology, aerosol science, and characterization of essentially all nanomaterials by allowing a diffraction pattern to be recorded from non-periodically structured materials, potentially as small as a single molecule.

We have continued our ambitious effort to define the capabilities of ultrafast x-ray lasers for non-periodic structural imaging and now the task is primarily housed in the *Ultrafast Aerosol Science and Biomacromolecular Dynamics Laboratory* in PULSE. FY2009 marked the transition of the task E4 leadership to staff scientist Mike Bogan, arriving from the ultrafast bioimaging group lead by Henry Chapman at LLNL. Following subtask leader Bogan and collaborator's demonstrations of ultrafast single-shot diffraction imaging at FLASH during 2006/2007, the Non-Periodic Imaging scientific program was expanded even further in 2008/2009 into several areas including (i) the first successful substrate-free diffraction imaging of single particles at FLASH; (ii) ultrafast diffraction imaging of nanoscale dynamics initiated by an optical pump laser; (iii) the first FLASH diffraction imaging of a cell using a new method called massively parallel x-ray holography, and (iv) experimental verification of tampers for arresting sample explosion.

Predictions suggest the high photon fluences (~10^{12} photons/pulse) and ultrashort pulse lengths required for NPI can be significantly relaxed, if the sample is surrounded by a sacrificial tamper layer. The tamper dampens the Coulomb explosion by providing a bath of photo-induced free electrons to the sample, and arresting the hydrodynamic expansion of the sample through inertial confinement. Our recent FLASH results show that the sample lifetime can be extended to several picoseconds under these conditions. The results also indicate that tampering could produce atomic resolution in "diffract and destroy" experiments at LCLS. For biological imaging, water is likely to be the ideal tamper material. In April 2009 we performed, with our collaborators, the first tests of an in-vacuum water droplet dispenser for preparing and delivering hydrated biological materials at FLASH.

We have established that iterative transform phase retrieval techniques can be used for direct imaging of individual 0.25-2 μm diameter particles illuminated by 13.5 nm FLASH pulses using the single resultant diffraction pattern alone. Experiments are performed using a re-entrant differentially pumped aerodynamic lens stack that delivers the aerosols generated at atmospheric pressure to our x-ray detector system that surrounds the particle beam/x-ray interaction region (Fig 1). To calibrate our soft x-ray camera for single particle diffraction, a test aerosol of polystyrene spheres is generated using an electrospray operated in Taylor cone-mode. This 'particle injector' is the prototype for the LCLS CXI endstation injector.

We recently performed the highest resolution single particle x-ray diffractive imaging experiment yet. We interpreted aerosol morphology to 35 nm resolution using the electron densities reconstructed from single-shot diffraction patterns collected from aerosols in flight at FLASH. Example diffraction patterns collected from a single 250 nm diameter sphere and aggregates with N = 2, 3, 4 are shown in Fig 1. The coherent illumination of multiple spheres results in interference fringes in part defined by the number of spheres in the aggregate, their relative orientation to each other and orientation of the aggregate to the x-ray pulse. The electron density of each aggregate was reconstructed to 35 nm resolution using iterative phase retrieval with the ESPRESSO algorithm [S. Marchesini, arXiv:0809.2006v1]. As N increases, increasingly complex coherent speckles modulate the scattered signal and encode the locations of the spheres in the aggregate. For example, Figure 1 shows a diffraction pattern collected from a large aggregate of 88 nm spheres. This aggregate was about 1 μm in diameter and was not spherical. The aggregate particle was unique, existed for less than two milliseconds in vacuum and, based on previous time-resolved x-ray diffractive imaging experiments, was completely destroyed just picoseconds after the x-ray pulse interacted with the particle. Though for these reasons its 3D structure cannot be obtained by proposed methods for diffraction patterns collected from identical objects, the retrieved 2D structure provides valuable information on particle morphology, not accessible by other means.

Morphological information can be extracted from this single-shot diffraction pattern of a unique object by applying morphological analysis methods utilized in electron microscopy to the reconstructed electron density (Fig. 1, bottom row). Potential exists to extract additional degrees of morphological information from unique particles *in situ* using proposed tomographic femtosecond diffractive imaging methods[36], but these are currently unavailable. This paradigm shift in the imaging of single aerosol particles has allowed us to identify entirely unexplored applications of ultrafast lasers in aerosol science[35]. Ultrafast snapshots of aerosol morphology and single particle pump-probe experiments will be the two key experiments we will use to define this new realm of the ultrafast in aerosol science.

In FY2009,

FUTURE PLANS: ***We aim to apply our FLASH experimental expertise to help pioneer non-periodic imaging at LCLS.*** We must address some very basic questions about single particle diffraction at LCLS: *What is the practical limit of detection for single particle diffraction? What resolution can be achieved?* To answer these questions, known structures must be probed in a systematic manner and the sample damage dynamics must be measured.

Expected Progress in FY2010: Significant effort will be directed toward moving into and equipping our new lab space at SLAC. We plan to recruit, train, and retain outstanding young talent necessary to support the rapidly growing coherent diffraction imaging of non-periodic structures program at PULSE. Our experimental efforts will concentrate on our first experiments at LCLS in Dec 2009 and potentially in Mar-June 2009, emphasizing imaging of nanomaterials, nanocrystals, cells, viruses and biomolecules.

Expected Progress in FY2011: We will continue our experimental campaign at LCLS, performing the first single particle diffraction experiments with hard x-rays at the XPP endstation. We will utilize our experience from FLASH and early LCLS experiments to work in conjunction with LCLS staff to field the LCLS CXI instrument. We will continue to develop the particle beam generation, trapping, manipulation and diagnostics instrumentation necessary to perform any experiments utilizing laser interactions with single particles. We plan to undertake time-resolved imaging studies of the LCLS- matter interaction and

perform LCLS imaging of aligned nanoparticles.

COLLABORATIONS: This work is done with colleagues fr om SLAC, Stanford, LL NL, Uppsala, LBNL, Arizona State University, TU Berlin, Max Planck Biomedical Heidelberg, and CFEL@DESY.

SELECTED PUBLICATIONS FROM DOE SPONSORED RESEARCH IN 2006-2009:

1. Bogan, M; Boutet, S; Chapman, H.; Barty, A; *et al.*: FLASH diffractive imaging of aerosols in flight, ***Nano Letters***, **2009**, submitted.
2. Hau-Riege, S.P., S. Boutet, A. Barty, Bajt, S.; *et al.*: Arresting sample explosion for single particle X-ray imaging", ***Nature Physics***, **2009**, submitted.
3. Bogan, M.; Starodub, D.; Decorwin-Martin, P.; *et al.* Single Particle Diffraction at FLASH, *Proceedings of the 23rd Particle Accelerator Conference, Vancouver, Canada, May 9th, **2009***.
4. Bogan, M**.,** S. Boutet, "In situ 2D ultrafast x-ray microscopy of aerosols", Record of Invention, March, **2009**.
5. Marchesini, S.; Boutet, S.; Sakdinawat, A.; Bogan, M.; *et al.*: Massively parallel X-ray holography, ***Nature Photonics,*** **2008**, 2, 560-563.
6. Bergh, M; Huldt, G; Timneanu, N; Maia, F; Hajdu, J: Feasibility of imaging living cells at subnanometer resolutions by ultrafast X-ray diffraction. ***Quar. Rev. Biophys.*** **2008**, **41,** 181-204.
7. Benner, W; Bogan, M.; *et al.:* Nondestructive characterization and alignment of aerodynamically focused particle beams by single particle charge detection, ***J. Aerosol Sci.,*** **2008**, 39 917-928.
8. Boutet, S; Bogan, M.; *et al.:* Ultrafast soft x-ray scattering of spherical polystyrene nanoparticles, ***J. Electron Spectrosc. Rel. Phenom.,*** **2008**, 166-167, 65-73.
9. Barty, A., Boutet, S., Bogan, M.J., *et al.:* Ultrafast single-shot diffraction imaging of nanoscale dynamics. ***Nature Photonics,*** **2008,** 2, 415-419.
10. Chapman, H., S. Bajt, A. Barty, W. Benner, M. Bogan; *et al.*: Coherent Imaging at FLASH *Proceedings of the 9th Intl. Conf. on X-ray Microscopy, Zurich, Switzerland, July 21-25th, **2008***.
11. Hajdu, J., Maia, F.: Clarity through a keyhole. ***Nature Physics,*** **2008,** 4, 351-353.
12. Bogan M., *et al.*: Single particle X-ray diffractive imaging. ***Nano Letters,*** **2008,** 8, 310-316.
13. Bajt, S., Chapman, H., Spiller, E. *et al.*: A camera for coherent diffractive imaging and holography with a soft-X-ray free electron laser. ***Applied Optics,*** **2008,** 47, 1673-1683.
14. Gabrysch, M., Marklund, E., Hajdu, J., et al.: Formation of secondary electron cascades in single-crystalline plasma-deposited diamond upon exposure to femtosecond x-ray pulses, ***J. Appl. Phys.,*** **2008**, 103, 064909.
15. Andersson I. *et al* Structure and function of Rubisco.***Plant Physiol. Biochem,*** **2008,** 46, 275-291.
16. Andersson, I. Catalysis and regulation in Rubisco. ***J. Exp. Bot.,*** **2008,** 59, 1555-1558.
17. H.N. Chapman, S.P. Hau-Riege, M. Bogan, *et al.:* Femtosecond time-delay X-ray holography. ***Nature,*** **2007,** 448, 676–679.
18. Bogan, M, Benner, H., *et al.* "Aerosol sample preparation methods for X-ray diffractive imaging: Size-selected nanoparticles on silicon nitride foils," ***J. Aerosol Sci.,*** **2007,** 38, 1119-1128.
19. S.P. Hau-Riege, H.N. Chapman, J. Krzywinski, *et al.* "Interaction of nanometer-scale multilayer structures with x-ray free-electron laser pulses," ***Phys Rev. Lett.,*** **2007,** 98 145502.
20. Bogan, M.; Benner, WH.; Frank, M.; Chapman, HN.; Woods B.; Boutet, S.; Hajdu, J. "Method and apparatus for x-ray imaging of free nanoscale biomaterials" Record of Invention: **2007**.
21. Hau-Riege, S.; London, R.; Bogan, M. *et al.* "Damage-resistant single-pulse optics for x-ray free electron lasers", Damage to VUV, EUV, and X-ray Optics, Proc. SPIE Vol. 6586, 65860T, **2007**.
22. K. Gaffney and H.N. Chapman, "Imaging Atomic Structure and Dynamics with Ultrafast X-ray Scattering," ***Science,*** **2007,** 316, 1444-1448.
23. Chapman, H.; Hau-Riege, S.; Bogan, M.; Bajt, S.; *et al.* Femtosecond time-delay X-ray holography, ***Nature***, **448**, 676-679.
24. Chapman, H.N; A. Barty, M.J. Bogan**,** S. Boutet, Femtosecond diffractive imaging with a soft-x-ray free-electron laser, ***Nature Physics***, **2006, 2**, 839-843.

High harmonic generation in molecules

Markus Gühr and Philip H. Bucksbaum
Stanford PULSE Institute, Stanford Linear Accelerator Center, Menlo Park, CA 94025
and Physics Department, Stanford University, Stanford, CA 94305, mguehr@slac.stanford.edu

Scope

The goal of this task is to understand the relation of high harmonic spectra to electronic structure in atoms and molecules on the attosecond time scale. We observe atomic and molecule electronic structure and dynamics in strong fields through measurements of the amplitude and phase of high harmonics. This year we have studied the field-dependent shift of the Ar Cooper minimum through experiments and simulations of the atom and its field dressed continuum states. The experiments require an accurately calibrated harmonic spectrometer, which we accomplish via laser induced plasma emission. We have also studied the influence of multiple orbitals on harmonic generation in molecules, and intend to use this to observe electron dynamics during non-adiabatic processes.

Recent Progress

B. K. McFarland, J. P. Farrell, L. Spector, P. H. Bucksbaum and M. Gühr

a) Strong field Cooper minima

Using the example of atomic Ar, we show that high harmonic generation (HHG) amplitude and phase are subject to Cooper minima seen in photoionization [1]. The vacuum ultraviolet (VUV) photoionization of Ar causes population transfer from the 3P electronic ground state of Ar to the d or s continuum states which is described by the photoionization dipole matrix element. In the recombination step of HHG an electronic dipole transition between the continuum states and the electronic ground state results in the emission of VUV radiation. Recombination is described by the complex conjugate of the photoionization dipole element. Thus any information obtained from photoionization or absorption spectroscopy can in principle be applied to the HHG spectrum [2-4]. The Cooper minimum results from the nodal structure of an electronic ground state, which results in a sign change in the dipole matrix element as a function of the continuum state energy. Due to the sign change the excitation or recombination amplitude must go to zero at a particular energy, commonly referred to as the Cooper minimum. The matrix element sign change is reflected by a change in the phase of the emitted dipole in HHG. Thus HHG contains detailed structural information.

We measure the harmonic amplitude and the VUV absorption spectrum of argon with a VUV spectrometer calibrated using plasma emission lines of various rare gases. Both spectra show a minimum in the expected range consistent with the Cooper minimum, however the HHG minimum is shifted to higher energies. We measure the Ar harmonic phase in an interferometric experiment using N_2 HHG as a reference. The measured π phase shift of the Ar harmonics around the HHG minimum fully confirms the Cooper minimum interpretation. In contrast to [2-4], we explain the shift between absorption and HHG Cooper minimum by the strong laser field acting on the Ar continuum during recombination. We calculate the Stark shift of the continuum states under the influence of this strong laser electric field. Only the uphill states contribute to recombination events in our case, and the corresponding matrix elements show a blue shift in agreement with experimental findings. In particular, the Cooper minimum shifts to higher photon energies for increasing field. To show this trend, we performed a trajectory dependent study of the Cooper minimum position.

Figure 1 A) shows HHG spectra of Ar after the HHG beam had passed through an aperture prior to the spectrometer grating. Harmonic radiation corresponding to short trajectories is preferentially phase matched on axis whereas the long trajectories emit radiation in a ring like structure off-axis. With an almost closed aperture, the short trajectories are pronounced, and the signal is rather weak compared to the open aperture case. This indicates that the long trajectory radiation is dominant for the open aperture case. The Cooper minimum is shifted from harmonic 35 for short trajectories to harmonic 33 for long trajectories. Figure 1 B) shows the field under which the trajectories in the Cooper minimum region collide with the ion. For long trajectories the field is lower than for short trajectories, leading to a weaker field-induced shift of the Cooper minimum for long compared to short trajectories.

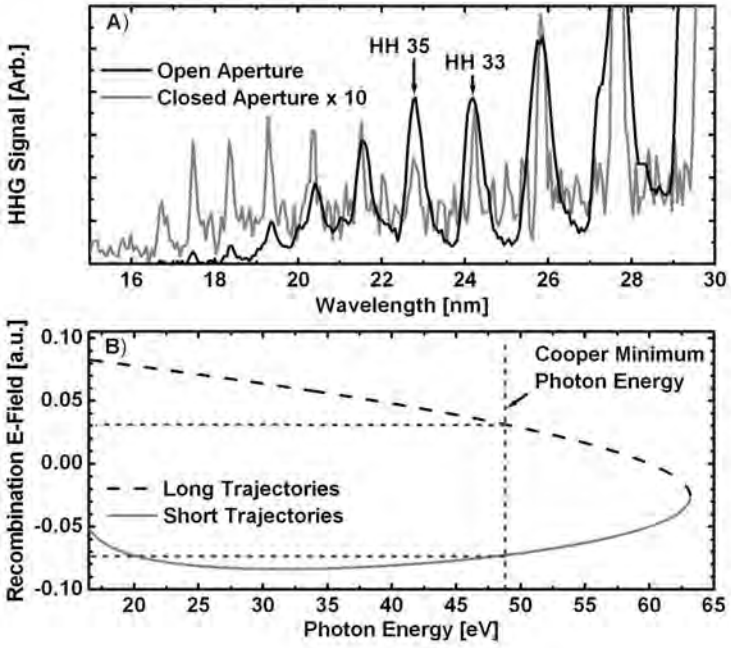

Figure 1: A) High harmonic spectra for Ar with a closed aperture in the spectrometer passing mainly harmonics originating from short trajectories (grey curve) and open aperture passing mainly harmonics originating from long trajectories (black curve). Note the difference in the signal by a factor of 10..The position of the photoabsorption Cooper minimum lies at 26nm corresponding to the 31st harmonic in our plot. B) Electric field as a function of photon energy radiated upon recombination by short trajectory electrons (grey) and long trajectory electrons (dashed black). For a particular photon energy, the electric field upon recombination is always higher for short trajectories compared to the long ones

b) Plasma calibration of HHG spectra

The calibration of VUV spectrometer for HHG spectroscopy is usually performed with metal filter absorption edges which cut away part of the harmonic spectrum or by directly counting harmonics assuming that they are integer multiples of the fundamental quantum energy. A fundamental problem in using harmonics for calibration purposes lies in the extreme sensitivity of the harmonic wavelength to the fundamental pulse parameters and to phase matching. The fundamental laser chirp, duration and the HHG phase matching influence the harmonic wavelength; shifts in wavelength of half an odd harmonic are not unusual.

We implemented a simple calibration method using plasma emission lines in an HHG spectroscopy set-up. We show that lines emitted by a laser-generated plasma of rare gases and molecular nitrogen can be conveniently used to calibrate harmonic spectrometers. The plasma generation and HHG use the same laser beam geometry. The intensity conditions for plasma generation and HHG emission are different. In an HHG setup with optimized phase matching, efficient plasma emission is hindered. We implement a short focus geometry for this purpose and change the gas target position with respect to the laser focus to switch between a calibration mode, where the plasma lines are intense and the harmonics are relatively weak, and an HHG mode, where the plasma lines are weak and the harmonics are strong. To change between the modes, no re-alignment of the laser is needed.

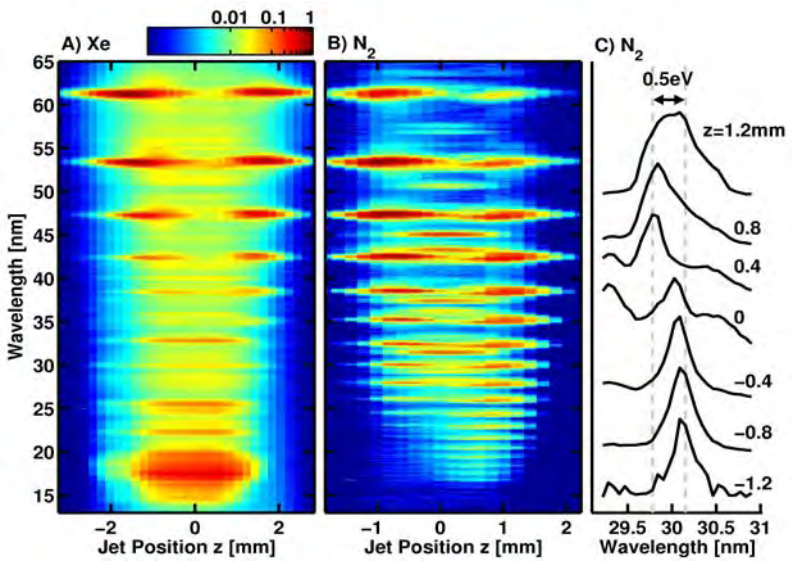

Figure 2: a) VUV emission spectrum of Xe in a focused 30 fs, 800 nm laser pulse as a function of gas jet position with respect to the laser focus. The z-axis is along the laser propagation direction. Harmonic emission is visible for jet positions before and after the laser focus (z=0), whereas sharp plasma emission lines appear around the focus. B) Same for N_2. c) The wavelength of the 27th harmonic shifts as a function of jet position, which makes it unsuitable for calibration purposes.

Figure 2 A and B show the VUV signal as a function of gas jet position along the laser propagation direction for Xe and N_2 respectively. The position z=0 corresponds to the laser focus. Before and after the focus a regular harmonic pattern appears, corresponding to the laser harmonics. At the focus, the harmonics are suppressed and plasma line emission dominates. The documented plasma lines are used to calibrate the spectrometer wavelength. Figure 2C demonstrates the shift in wavelength of the 27th harmonic as the jet scans through the focus.

c) Harmonic generation from multiple orbitals

Up to now, the modelling and interpretation of HHG has always assumed that only the highest occupied orbital can be ionized and thus contribute to HHG. However, at least two orbitals need to be observable in order to deduce electron dynamics because the quantum representation of motion is a coherent superposition of several orbitals. We found multi-orbital effects in HHG for nitrogen molecules and attributed the spectral signatures in the high harmonic spectrum to the highest occupied molecular orbital (HOMO) and the next lower bound orbital, the HOMO-1. We used the control over the molecular alignment with respect to the strong laser field in order to prepare the different orbital contributions.

The methodology of multi-orbital HHG is currently being developed to follow more complicated electronic dynamics in molecules with HHG spectroscopy. Over the past few months, we have been setting up a new high harmonic generator and spectrometer that can be used with any kind of (corrosive) molecules without any damage to the pumping system and optics.

Future Plans

M. Gühr and P. H. Bucksbaum

a) Chemical imaging

We will use our experience in multi-orbital HHG to follow molecular electronic dynamics after photoexcitation. Dynamics occurring at so-called conical intersections (CI) is very interesting in this context. The conical intersections are crucial for biological processes such as light harvesting, primary visual processes and UV stabilization of DNA and for chemical processes in the earth's atmosphere. It is possible to excite a wave packet by an ultrafast laser pulse such that it explores the potential landscape of the excited state and reaches the conical intersection, where it can change its electronic state. We want to monitor this multiple state electronic dynamics using high harmonic generation on photo-excited molecules.

b) Electron correlation

The electro n-electron correlati on effects, which are neg lected in the Hartree-Fock (HF) approximation, are expected to be highlight ed at the attosecond tim e scale. Around each individual electron, the density of other electrons is re duced by both exchange and Coulom b interactions (correlation hole). The "instant" removal of an electron will lead to charge migration dynamics aim ed at filling this ho le. In o ther wo rds, the charge ho le created on the neu tral molecular ground state is not an eigenstate of the ionic system, leading to a coherent superposition of cationic states. The attosecond time scale of the electron dynamics is determined by the energy differences am ong the excited cationi c states. W e plan to directly m onitor the charge migration in the tim e domain, giving us in sight into electron co rrelation. This involves spectroscopy with VUV laser sources and LCLS laser pulses.

References

[1] J. W. Cooper, Phys. Rev. **128**, 681 (1962).
[2] A. T. Le, T. Morishita and C. D. Lin, Phys. Rev. A **78**, 023814 (2008)
[3] S. Minemoto, T. Um egaki, Y. Oguchi, T. Mo rishita, A.-T.Le, S. Watanabe, and H. Sakai, Phys. Rev. A **78**, 061402 (2008).
[4] H. J. Worner, H. Niikura, J. B. Bertrand, P. B. Corkum, and D. M. Villeneuv e, Phys. Rev. Lett. **102**, 103901 (2009)

Publications over the past 3 years

1) J. P. Farrell, B. K. McFarland, P. H. Buck sbaum, and M. Gühr, Calibration of a high harm onic spectrometer by laser induced plasma emission, submitted (2009)
2) B. K. McFarland, J.P. Farre ll, P. H. Bucksbaum and M. Gühr, High harm onic phase of nitrogen, submitted (2009)
3) J.P. Farrell, B. K. McFarland, M. Gühr, and P. H. Bucksbaum , Relation of high harm onic spectra to electronic structure in N_2, submitted (2009)
4) M. Gühr, B. K. McFarland, J.P. Farrell and P. H. Bucksbaum, High harmonic generation from multiple molecular orbitals of N_2, Ultrafast Phenomena XVI, Springer (2008)
5) B. K. McFarland, J.P. Farrell, P. H. Buck sbaum and Markus Gühr, High Harm onic Generation from multiple orbitals, Science **322**, 1232 (2008)
6) M. Fushitani, M. Bargheer, M. Gühr, H. Ibrahim and N. Sc hwentner, Control of Chrom ophore to Bath Coupling by Interferometry , J. Phys. B: At. Mol. Opt. Phys. **41**, 074913 (2008)
7) H. Ibrahim, M. Gühr and N. Sc hwnenter, Valence transitions of Br_2 in Ar matrices: Interaction with the lattice and predissociation, J. Chem. Phys. **128**, 064504 (2008)
8) M. Gühr, Coherent Dynam ics of Halogen Molecules in Rar e Gas Solids, in Cohere nt Vibrational Dyna mics, Eds.: S. De Silvestri, G. Cerullo and G. Lanzani, Taylor and Francis (2008)
9) M. Gühr, B. K. McF arland, J. P. Farrell and P. H. Bucksbaum , High harm onic generation on N_2 and CO_2 beyond the two point model, J. Phys. B: At. Mol. Opt. Phys., **40**, 3745-3755 (2007)
10) M. Gühr, M. Bargheer, M. Fushitani, T. Kilj unen and N. Schwentner, Ultrafast dynam ics of halogens in rare gas solids, Phys. Chem. Chem. Phys, **9**, 779-801, (2007)
11) Philip Bucksbaum, The future of attosecond spectroscopy, Science **317**, 766 (2007)

Strong Field Control of Coherence in Molecules and Solids

Philip H. Bucksbaum, Ryan Coffee, and David Reis, Stanford PULSE Institute for Ultrafast Energy Science, SLAC National Accelerator Laboratory, Menlo Park, CA 94025

This is subtask E2b of PULSE, and has been renamed "Strong Field Control of Molecules" (SFA) in the renewal. Our efforts are directed towards investigations of strong-field induced coherent processes in atoms and molecules that are of value as either LCLS experiments or ultrafast x-ray diagnostics. This year we added the related project of ultrafast hard x-ray studies of coherently excited phonons in solids, with the addition of David Reis to PULSE. We also made considerable progress in several other areas: formation of coherent transient alignment in molecules; studies of short wavelength electronic coherences; and a proposal approved for our first studies of strong field processes using LCLS. We have proposed to move a substantial portion of the condensed matter portion of this program to the DMSE FWP in FY10-12.

Recent Progress:

Multi-pulse Molecular Alignment *James Cryan, Ryan N. Coffee, and Phil H. Bucksbaum* We have demonstrated transient alignment in room temperature nitrogen, which exceeds the ionization-limited single pulse alignment and approaches the maximum theoretical value. We employ eight equally spaced ultra-fast laser pulses with an optimal separation to take advantage of periodic revivals of an ensemble of quantum rigid rotors. Each successive pulse increases the transient alignment $\langle\cos^2(\theta(t))\rangle$ and also moves the rotational population away from thermal equilibrium. By comparing our data to quantum simulations, we determine experimental values of $\langle\cos^2(\theta(t))\rangle$,

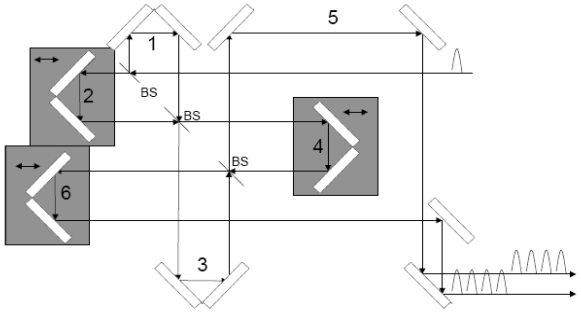

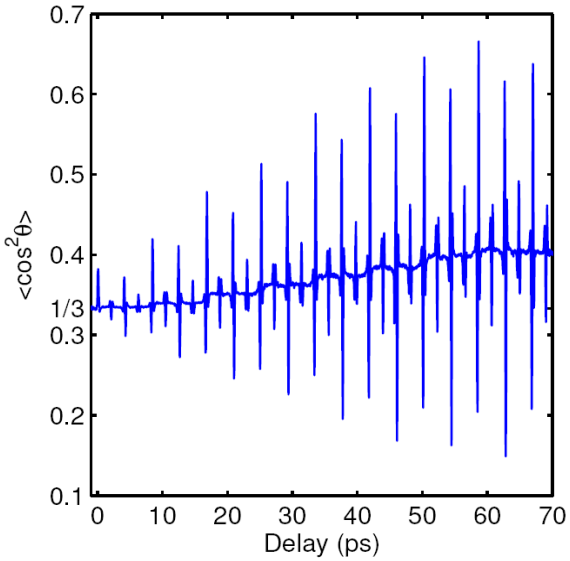

the J-state distributions, and functional dependancies of the alignment features.

Figure 1: Left: The multiple pulse alignment of molecules is based on a nested interferometer design shown above left. This produces eight equally spaced pulses. The length difference between arms is such that the spacing between pulses is approximately 8.4 ps. This is the rotational period 1/2B, where B is the rotational constant for molecular nitrogen. **Right:** Our multiple pulse technique uses a train of pulses acting at the 'quantum echo' of the initial pulse, i.e. when the density matrix $\rho(t)$ returns to the value it has immediately after the initial impulse. This time is slightly in advance of the maximum alignment, formally when $\partial^2\langle\cos^2(\theta(t))\rangle/\partial t^2=0$. This technique not only produces a high field-free transient alignment, but also exhibits a sizable time-averaged population alignment $\langle\langle\cos^2(\theta(t))\rangle\rangle_t$, shown in the figure above as the rising baseline.

Longitudinal alignment: *Doug Broege. Ryan Coffee, Phil Bucksbaum* Strong fields can be employed at LCLS and in other applications to produce true three-dimensional alignment. An important step along this path is the demonstration and control of longitudinal alignment, that is alignment along the direction perpendicular to the laser polarization. This year we demonstrated the alignment of diatomic molecules along the direction of laser propagation in a field free environment, carried out with the use of a circularly polarized 800nm ultrafast laser on atmospheric and dry diatomic nitrogen. The wavepacket created with this field exhibits both transient and time averaged alignment along the laser propagation vector. Measurement of these features were performed interferometrically with a pair of co-propagating 400nm pulses. Additional measurements of birefringence were taken to ensure all wavepacket features were azimuthally symmetric within the plane of polarization. Along with traditional impulsive alignment, this technique allows for 3 dimensional control of molecular alignment without the need for a crossed beam geometry.

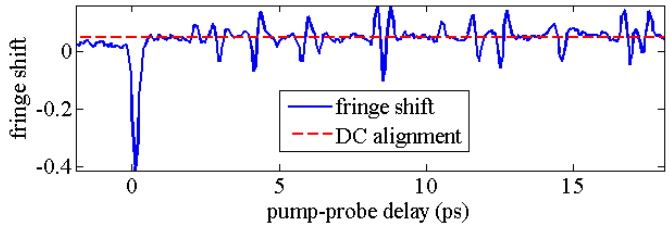

Figure 2. The position of the fringes (camera pixels) resulting from the interference between the two probe beams as a function of pump-probe delay (ps). Fringe position is directly related to the index of refraction of the sample, which is composed of both atmospheric oxygen and nitrogen. Sign convention is chosen so that a positive signal indicates a decrease in index of refraction, which implies alignment along the quantization axis. This plot shows that the rotational wavepackets created exhibit both coherent alignment at revivals and a continuous population related alignment. The dotted line shows an increase in time averaged alignment.

Energy relaxation in Solids: *David Reis* A portion of our program involves the study of ultrafast energy relaxation processes in condensed matter following femtosecond laser excitation. In order to meet our scientific goals, we are developing new methodologies for probing structure on the picosecond (ps) and femtoseconds (fs) time-scale at synchrotron (APS) and linac based sources (SPPS and we are working towards LCLS). Over the past several years, we have concentrated on diffraction from long-wavelength phonons; however, x-ray scattering has the potential for probing phonons throughout the Brillouin zone. In the past year we have made progress on two fronts: **a.** probing the unfolding of superlattice phonons into high wavevector bulk modes and **b.** probing momentum resolved anharomonic decay of phonons. This year we are starting two new labs in the PULSE institute at SLAC, one for optical pump-probe studies and the other to develop a table-top high-repetition-rate ps x-ray source. We are also collaborating on several LCLS experiments and commissioning as well as continuing to make use of the APS and now SSRL.

a. unfolded phonons. An ultrafast laser pulse generates high frequency folded acoustic modes in a semiconductor superlattice (InGaAs/InAlAs) and a ps x-ray probe detects their propagation across the SL into the substrate. When these phonons propagate across the boundary, they unfold to become very high frequency and high wavevector acoustic modes. These modes are of particular interest because they play an important role in heat transport as well as have nanoscale wavelength, but there is almost a complete lack of coherent near monochromatic sources and detectors of these phonons (Trigo 2008).

b. x-ray diffuse scattering to probe phonon decay. Experiments on InP, which has an unusually long-lived LO phonon, were carried out at the BioCARS beamline of the APS with ~ 1010 photons per pulse at 15 keV. Figure 3(a) shows the static temperature diffuse scattering at room temperature

of a (001) oriented InP single crystal at near grazing incidence. The probe covers many Brillouin zones, represented by the mesh-like pattern superimposed on this image. Photo-excitation with an intense laser pulse perturbs the equilibrium TDS image and produces a differential signal (Fig. 3 b - d). The data show a complex redistribution of the intensity that suggests the presence of a transient non-equilibrium population (Fig. 3 e - g) persisting up to a few hundred ps. Interestingly it appears that the transverse modes continue to increase in population several hundreds of ps after excitation while other modes are cooling.

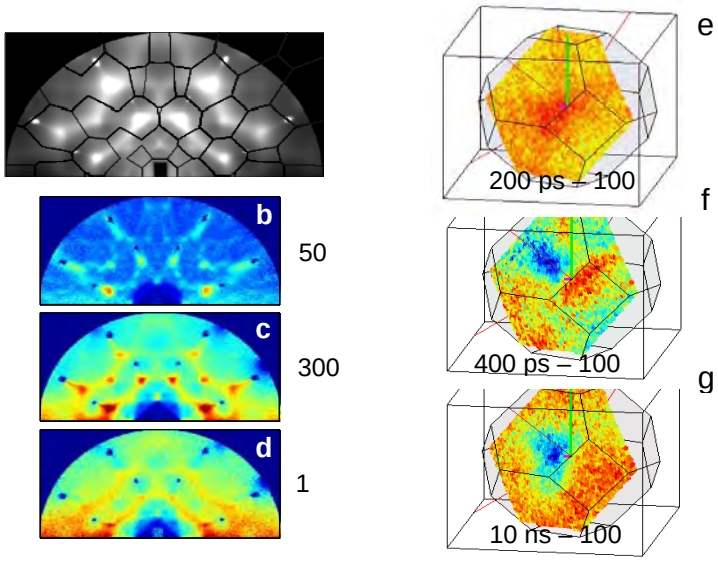

Figure 3: (a) room temperature thermal diffuse scattering image of (001) oriented InP near grazing incidence with 15 keV x-ray photons. Time-resolved images after laser excitation at (b) t = 50 ps, (c) t = 400 ps and (d) t = 1 ns. (e) – (g) difference of the images at different time delays plotted inside the first Brillouin zone. For clarity only one of the Brillouin zones shown in (a) is displayed.

Future work:

Xray Multiple Ionization of Impulsively Aligned Molecules: *Ryan Coffee, Markus Guehr, Phil Bucksbaum, John Bozek, Christian Buth, Marcus Hertlein, Ali Belkacem, Nora Berrah, Linda Young, Lou DiMauro, Hamed Merdji, Janos Hajdu* The LCLS free-electron x-ray laser will be the first coherent radiation source that is capable of saturating K-shell photoionization for elements in the second row of the periodic table. This creates the opportunity for the first time to study novel multiple core-hole processes in atoms and molecules. We have been granted time in the first round of AMO experiments in FY10, to use the very high fields of the LCLS to create core vacancies in both atoms in a diatomic molecule, and study the Auger relaxation of this novel correlated system. This double core-hole state has a strong effect on the angle and energy of Auger emission which we will study by impulsively aligning the molecules prior to their photoionization. This is particularly interesting for ultrafast physics since the relaxation involves time scales of a few femtoseconds or less.

Light-induced coherent structure in molecules: *Ryan Coffee, Todd Martinez, Phil Bucksbaum, others* A number of important quantum dynamical properties in chemical physics can be simulated and controlled using strong fields to coherently excite molecules. We will initiate a combined theory and experimental program to study these. An important example is the light-induced conical intersection, which is produced when a strong coupling field is used to add a controlled additional degree of freedom to a molecule. Another example is the use of controlled laser fields to induce angstrom-scale structure in motional wave packets in molecules. The ultrashort x-ray pulses of LCLS could be an extremely useful tool to study these.

1. Broege, D., R.N. Coffee, and P.H. Bucksbaum, 2008a, "Strong-field impulsive alignment in the presence of high temperatures and large centrifugal distortion," Phys. Rev. A, **78**, 035401.

2. Broege, D., R.N. Coffee, and P.H. Bucksbaum, “Longitudinal Alignment,” 2009, in preparation.
3. Broege, D., R.N. Coffee, and P.H. Bucksbaum, 2008b, “Impulsive alignment of hot, centrifugally distorted molecules,” CLEO/QELS08, ISBN: 978-1-55752-859-9.
4. Coffee, R.N., J.P. Cryan, P.H. Bucksbaum, 2009, “Impulsive alignment of N2 with a train of 8 pulses,” Proceedings CLEO/IQEC09.
5. Coffee, R.N., P.H. Bucksbaum, L. Fang, and G.N. Gibson, 2007, “Direct dissociation and laser modulated pre-dissociation of N_2^+,” CLEO/QELS 2007, OSA: 1-55752-834-9.
6. Cryan, J., P.H. Bucksbaum, and R.N. Coffee, 2009, “Field-free alignment in repetitively kicked nitrogen gas,” submitted for publication.
7. Douglas Broege, Ryan Coffee, Philip Bucksbaum, “Strong field impulsive alignment in the presence of high temperatures and large centrifugal distortion,” Bull. Am. Phys. Soc. 53, No. 7, DAMOP Abstract: K6.00004 (2008)
8. Ravasio, D. Gauthier, F. R. N. C. Maia, M. Billon, J-P. Caumes, D. Garzella, M. Ge´le´oc, O. Gobert, J-F. Hergott, A-M. Pena, H. Perez, B. Carre´, E. Bourhis, J. Gierak, A. Madouri, D. Mailly, B. Schiedt, M. Fajardo, J. Gautier, P. Zeitoun, P. H. Bucksbaum, J. Hajdu, and H. Merdji, “Single-Shot Diffractive Imaging with a Table-Top Femtosecond Soft X-Ray Laser-Harmonics Source,” Phys. Rev. Letters, in press.
9. Hillyard, P.B., D. A. Reis, and K. J. Gaffney. Carrier-induced disordering dynamics in InSb studied with density functional perturbation theory. Physical Review B (Condensed Matter and Materials Physics), 77(19):195213, 2008.
10. Lindenberg, A., S. Engemann, K. J. Gaffney, K. Sokolowski-Tinten, J. Larsson, P. B. Hillyard, D. A. Reis, D. M. Fritz, J. Arthur, R. A. Akre, M. J. George, A. Deb, P. H. Bucksbaum, J. Hajdu, D. A. Meyer, M. Nicoul, C. Blome, T. Tschentscher, A. L. Cavalieri, R. W. Falcone, S. H. Lee, R. Pahl, J. Rudati, P. H. Fuoss, A. J. Nelson, P. Krejcik, D. P. Siddons, P. Lorazo, and J. B. Hastings. X-ray diffuse scattering measurements of nucleation dynamics at femtosecond resolution. Physical Review Letters, 100(13):135502, 2008.
11. Reis, D.A.,. Squeezing more out of ultrafast x-ray measurements. Physics, 2:33, Apr 2009.
12. Sheu, Y. M., S. H. Lee, J. K. Wahlstrand, D. A. Walko, E. C. Landahl, D. A. Arms, M. Reason, R. S. Goldman, and D. A. Reis. Thermal transport in a semiconductor heterostructure measured by time-resolved x-ray diffraction. Physical Review B (Condensed Matter and Materials Physics), 78(4):045317, 2008.
13. Stoica, V. A., Y.-M. Sheu, D. A. Reis, and R. Clarke. Wideband detection of transient solid-state dynamics using ultrafast fiber lasers and asynchronous optical sampling. Opt. Express, 16(4):2322–2335, 2008.
14. Trigo, M., Y. M. Sheu, D. A. Arms, J. Chen, S. Ghimire, R. S. Goldman, E. Landahl, R. Merlin, E. Peterson, M. Reason, and D. A. Reis. Probing unfolded acoustic phonons with x rays. Physical Review Letters, 101(2):025505, 2008.
15. Lings, B., J. S. Wark, M. F. DeCamp, D. A. Reis, and S. Fahy. Simulations of time-resolved x-ray diffraction in laue geometry. J. Phys.: Condens. Matter, 18:9231–9244, 2006.
16. Fritz, D. M., D. A. Reis, et al.. Ultrafast bond softening in bismuth: Mapping a solid’s interatomic potential with x-rays. Science, 315:633–636, February 2 2007.
17. Hillyard, P. B., K. J. Gaffney, et. al. , Carrier-density-dependent lattice stability in insb. Physical Review Letters, 98(12):125501, 2007.
18. Murray, E. D., S. Fahy, D. Prendergast, T. Ogitsu, D. M. Fritz, and D. A. Reis. Phonon dispersion relations and softening in photoexcited bismuth from first principles. Phys. Rev. B, 75:184301, 2007.
19. Reis, D. A. , K. J. Gaffney, G. H. Gilmer, and B. Torralva. Ultrafast dynamics of laser-excited solids. MRS bulletin, 31:601–606, 2006.
20. Reis, D. A. and A. M. Lindenberg. Ultrafast x-ray scattering in solids. In M. Cardona and R. Merlin, editors, Light Scattering in Solids IX. Springer-Verlag, , 2006.

Solution Phase Chemical Dynamics

Principal Investigator: Kelly J. Gaffney
PULSE Institute, Photon Science, SLAC,
Stanford University, Menlo Park, CA 94025
Telephone: (650) 926-2382
Fax: (650) 926-4100
Email: kgaffney@slac.stanford.edu

I. Program Scope: The initial stages of efficient photochemical reactions invariably occur on the femtosecond (fs) to picosecond (ps) time scale. Identifying the mechanisms for directed and efficient channeling of solar energy to chemical energy will be a principle objective of this research sub-task. The effective conversion of light to chemical energy necessitates directing the energy flow, which requires the suppression of the thermodynamic driving force to convert the light energy to heat and re-establish equilibrium. The effectiveness of molecular photo-catalysts depends critically on the excited state electronic structure and dynamics. Preserving the harvested energy within the electronic degrees of freedom represents a critical step to efficient light harvesting and depends intimately on the complex interplay between electronic and nuclear motion. While the investigation of non-adiabatic dynamics has been widely pursued with time resolved optical spectroscopy, the complexity of the phenomena and dual influence of nuclear and electronic arrangement on these optical signals has made unambiguous interpretation of experimental data unusual. We propose to disentangle this coupled evolution of the electrons and nuclei by probing the molecular structure with ultrafast x-ray scattering and the electronic structure with ultrafast x-ray spectroscopy.

We will also investigate equilibrium chemical dynamics. The assembly and conformation of soft-matter depends critically on non-covalent interactions. These interactions, such as ion pairing, hydrogen bonding, and van der Waals attractions contribute to the assembly of nanostructures in a broad range of chemical and materials science applications as well. While the formation and folding of nanometer complexes generally involves the formation of numerous non-covalent interactions, the intrinsic interactions are generally well defined local interactions: hydrogen bond formation, ion pairing, and higher-order electrostatic interactions. We propose to study the thermal dynamics of H-bonding and ion pairing dynamics with the objective of generating a molecular-scale, mechanistic understanding conformational dynamics in solution. We will investigate these conformational dynamics with time resolved vibrational spectroscopy, x-ray photon correlation spectroscopy, and molecular dynamics simulations.

II. Scientific Progress:

***Photochemistry of bimetallic photo-catalysts*:** We have initiated femtosecond resolution pump-probe measurements of the bi-metallic d^8-d^8 coordination complex Ir_2[1,8-diisocyano-menthane]$_4$. Our initial measurements have pumped the system at 590 nm and probed the transient response throughout the visible. These initial results appear in **Fig. 1**. The signal peaked around 600 nm corresponds to the ground state bleach and the stimulated emission at very small time delays. The signal peaked at 710 nm corresponds to the stimulated emission signal. **Figure 1(B)** shows the time dependent pump-probe signal at 730 nm and 650 nm, roughly corresponding to the inner and outer turning points on the excited state potential. The oscillatory pattern are clear p out of phase, as expected and show strong evidence for two vibrational modes being strongly coupled to the electronic excitation. Fourier transformation of the signals show vibrational frequencies of 80 and 120 cm^{-1}. One of these modes should possess a strong metal-metal stretching component, since the equilibrium Ir-Ir bond length in the excited state should be roughly 0.5 Å shorter than the ground state configuration excited at 590 nm.

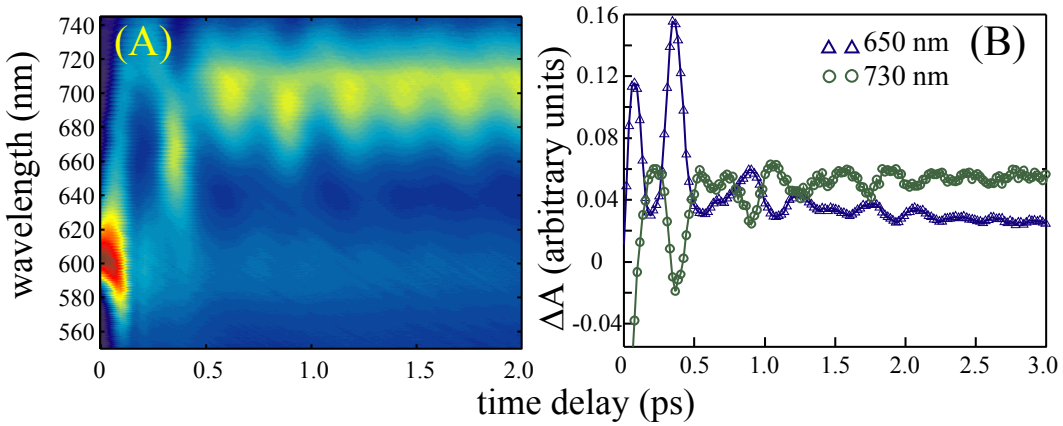

Fig. 1: (A) Femtosecond transient absorption spectrum measured for Ir_2[1,8-diisocyanomenthane]$_4$ using a photoexcitation at 590 nm. The signal centered at 710 nm corresponds to the stimulated emission from the excited state and the strong oscillations in the spectrum result from coherent metal-metal vibrational dynamics in the excited state. (B) Time dependent change in absorption induced by excitation at 590 nm and probed at 650 nm and 730 nm. These probe wavelengths roughly correspond to the wavelengths that stimulate emission from the excited state potential back to the ground state potential at the turning points of the excited state potential. The anti-correlation of the oscillatory pattern supports this conclusion.

These preliminary results demonstrate that we will be able to learn a significant amount about the excited state dynamics of the bi-metallic photo- catalysts with optical pump-probe measurements and also gives us confidence that these materials will be emendable to time resolved x-ray scattering measurements.

***Atomic resolution mapping of the excited state electronic structure of Cu_2O with time-resolved soft x-Ray absorption spectroscopy*:** Soft x-ray absorption spectroscopy (XAS) has many attributes that make it a powerful tool for investigating electronic structure. Of particular significance, the electronic structure can be interrogated with atomic specificity, so that the electronic structure can be decomposed into specific atomic contributions. While widely utilized to characterize the ground state structure of materials, we have used XAS to characterize the excited electronic state properties of cuprous oxide (Cu_2O), a widely studied transition metal oxide semiconductor utilized in photovoltaic and photo-electrochemical applications.

We have used time resolved XAS to characterize the effect of optically generated electronic excited states on chemical bonding in Cu_2O. A shift of the absorption edges to lower energy represents the dominant effect of valence carrier excitation. While the valence excitation shifts the Cu L_3-edge and the O K-edge spectra, there is no integral change in x-ray absorption at either edge. This lack of an integrated change in the Cu L_3-edge and the O K-edge provides strong evidence that the Cu 3 *d* and O 2 *p* orbital contributions to the conduction band edge strongly resemble the orbital contributions to the valence band edge. This demonstrates the ability of time resolved x-ray spectroscopy to characterize the chemical bonding in excited states.

***Attosecond electron dynamics in transition metal complexes investigated with resonant inelastic hard x-ray scattering*:** The excitation of matter with light can lead to the emission of photons with characteristic energies indicative of the electronic and vibrational properties of the excited sample. When the incident radiation resonantly excites a transition in the irradiated material, the emitted light can result from coherent (one-step) inelastic scattering leading to a resonance Raman signal or from incoherent, sequential absorption and emission (two-step) of light leading to a fluorescence signal. We use the simultaneous appearance of these different signals in resonant inelastic light scattering to extract information about the excited state dynamics from the intrinsic time delay in the fluorescence decay channel.

Prior soft x-ray resonant inelastic x-ray scattering (RIXS) studies have extracted information about the attosecond (as) and femtosecond (fs) evolution of core-excited states using core-hole clock spectroscopy. The core-hole clock technique utilizes the sensitivity of the Auger electron or the x-ray emission spectrum to dynamics that occur prior to core-hole decay. Since 3d transition metal K-shell core-holes decay on the femtosecond to sub-femtosecond time scale, hard x-ray RIXS will be almost exclusively sensitive to attosecond electronic dynamics. For the coordination compounds we have investigated, we attribute these excited state decoherence dynamics to electron transfer from metal 4*p* electronic states to predominantly ligand-derived electronic states.

Raman scattering signals can be clearly distinguished from fluorescence signals since they result in emission signals that disperse linearly with incidence photon energy, while the fluorescence spectrum is incident energy independent. The core-hole clock technique allows the rate of excited state dynamics to be extracted from the relative integrated intensity of the characteristic fluorescence, I_f, and Raman, I_R, signals and the core-hole lifetime, τ. We determine the charge transfer times, τ_{CT}, from τ, I_R, and I_f, $\tau_{CT} = \frac{I_R}{I_f}\tau$.

We have measured the Mn and Fe 1*s*3*p* RIXS spectra of $RbMnFe(CN)_6$ and $K_3Mn(CN)_6$. These two species make for a compelling demonstration of the sensitivity of RIXS to electron dynamics because they possess very similar atomic structure, but very different chemical environments. For the Prussian blue analog, $RbMnFe(CN)_6$, the nitrogen end of the cyanide coordinates the manganese atom, while in $K_3Mn(CN)_6$ the carbon end of the cyanide coordinates the manganese atom. The nitrogen ligation in the Prussian blue analogue generates a weak ligand field and a high-spin ground electronic state for the Mn ions. The carbon ligation in $K_3Mn(CN)_6$ generates the standard strong ligand field associated with cyanide and a low-spin ground electronic state. A similar strong field exists for the Fe in $RbMnFe(CN)_6$.

Experimentally, we observe that Raman scattering dominates for the weak ligand field manganese in $RbMnFe(CN)_6$, while fluorescence scattering dominates for the strong ligand field manganese in $K_3Mn(CN)_6$. The results for strong ligand field Fe in $RbMnFe(CN)_6$ strongly resemble the results for the strong ligand field Mn in $K_3Mn(CN)_6$. Using the core-hole clock method, we extract electron transfer times of ~0.2 fs from excited-state Mn and Fe 4*p* orbitals to ligand dominated orbitals for atoms in strong field chemical environments and ~0.9 fs for Mn in a weak ligand [$RbMnFe(CN)_6$].

***Hydrogen bond dynamics in aqueous ionic solutions*:** Aqueous ionic solutions lubricate the chemical machinery of natural and biological systems. While the unique and incompletely understood properties of water receive significant and justified attention, natural and biological processes also depend critically on the ionic species present in solution (Ball, 2008). A full description of ionic solutions requires not only a detailed understanding of the dynamics and structure of water in- and out-side the first ionic solvation shell, but also a clear understanding of the inter-conversion mechanism and dynamics for these two populations of water molecules.

We have used multidimensional vibrational spectroscopy (2DIR) and Car-Parrinello molecular dynamics (CPMD) simulations to investigate the hydrogen bond (H-bond) structural dynamics in aqueous 6 M sodium perchlorate ($NaClO_4$) solutions (Park, 2009). Aqueous perchlorate solutions provide an excellent system for studying H-bond exchange dynamics because the donation of a H-bond from a given deuterated hydroxyl group (OD) to another water molecule or a perchlorate ion leads to spectroscopically distinct OD stretch frequency. 2DIR monitors the H-bond exchange by observing the time dependent growth in the off-diagonal signal in the 2DIR spectra, as shown in **Fig. 3**. The rise in off-diagonal signal occurs with a 6 ps time constant, similar to the time constant for molecular rotation measured with polarization-resolved pump-probe measurements.

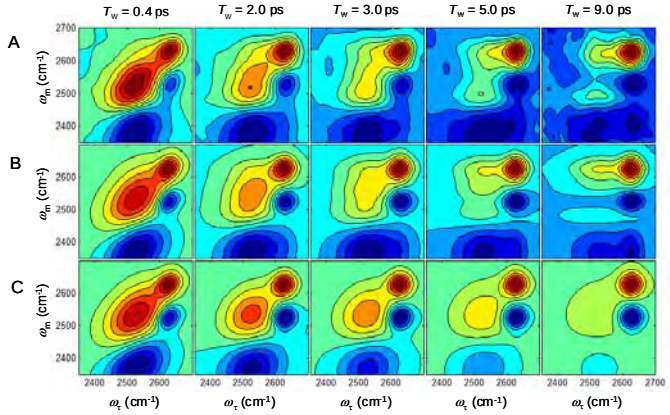

Fig. 3: Multidimensional vibrational spectra for a series of time delays. The rise in off-diagonal signal with increasing time delay results from H-bond exchange with a 6 ps time constant. (A) Experimental spectra, (B) calculated spectra, including two-species kinetic exchange, and (C) calculated spectra without H-bond exchange. Clearly, H-bond ex-change must be included to accurately reproduce the experi-mental spectra.

This indicates that molecular rotation and H-bond exchange occur via large angle jumps, as seen Laage and Hynes in computer simulations.

The CPMD simulations performed on aqueous 6 M $NaClO_4$ solution clearly demonstrate that water molecules organize into two radially and angularly distinct structurally sub-shells within the first solvation shell of the perchlorate anion, with one sub-shell possessing the majority of the water molecules that donate H-bonds to perchlorate anions and the other sub-shell possessing predominantly water molecules that donate two H-bonds to other water molecules. The CPMD simulations also demonstrate that the molecular exchange between these two structurally distinct sub-shells proceeds more slowly than the H-bond exchange between the two spectrally distinct H-bond configurations. We interpret this to indicate that orientational motions predominantly dictate the rate of H-bond exchange, while translational diffusion must occur to complete the molecular exchange between the two structurally distinct sub-shells around the perchlorate anions. The 2DIR measurements observe the H-bond exchange between the spectrally distinct H-bond configurations, but the lifetime of the hydroxyl stretch precludes the observation of the slower molecular exchange. Our 2DIR experiments and CPMD simulations demonstrate that orientational motions predominantly equilibrate water molecules within their local solvation sub-shells, but the full molecular equilibration within the first solvation shell around the perchlorate anion necessitates translational motion.

Publications:

1. Ultrafast Dynamics of Laser-Excited Solids: D.A. Reis, K.J. Gaffney, G.H. Gilmer, D. Torralva, *Mat. Res. Soc. Bull.* **31**, 1 (2006).
2. Ultrafast Bond Softening in Bismuth: Mapping a Solid's Interatomic Potential with X-rays: D.M. Fritz, *et al. Science* **315**, 633 (2007).
3. Carrier Density Dependent Lattice Stability in InSb: P.B. Hillyard, *et al. Phys. Rev. Lett.* **98**, 125501 (2007).
4. Imaging Atomic Structure and Dynamics with Ultrafast X-ray Scattering: K.J. Gaffney, H.N. Chapman, *Science* **316**, 1444 (2007).
5. X-ray Diffuse Scattering Measurements of Nucleation Dynamics at Femtosecond Resolution: A.M. Lindenberg, *et al.Phys. Rev. Lett.* **100**, 135502 (2008).
6. Ultrafast Carrier Induced Disordering in InSb Studied with Density Functional Perturbation Theory: P.H. Hillyard, D.A. Reis, K.J. Gaffney, *Phys. Rev. B* **77**, 195213 (2008).
7. Efficient Multiple Exciton Generation Observed in Colloidal PbSe Quantum Dots with Temporally and Spectrally Resolved Intraband Excitation: M. Ji, S. Park, S.T. Connor, T. Mokari, Y. Cui, K.J. Gaffney, *Nano. Lett.* **9**, 1217 (2009).
8. Ultrafast Dynamics of Hydrogen Bond Exchange in Aqueous Ionic Solutions: S. Park, M. Odelius, K.J. Gaffney, *J. Phys. Chem. B.* **113**, 7825 (2009).

First Principles Dynamics of Ultrafast Chemistry

Todd J. Martínez
SLAC National Accelerator Laboratory, Menlo Park, CA 94025

Abstract: The *ab initio* multiple spawning method has been developed as a means of describing ultrafast chemistry on multiple excited states from first principles, solving the electronic and nuclear Schrödinger equations simultaneously. Applications to date have treated laser-induced excitation as an instantaneous event. Here, we describe new improvements to the method which allow for the direct modeling of the excitation event, opening the door to modeling of optimal control type experiments with non-transform-limited excitation pulses. This includes an "optimal" spawning algorithm that determines the location of new nuclear basis functions using direct optimization[1] and explicit incorporation of the laser field into the time-dependent Hamiltonian. We also extend the method to allow for strong laser fields and the concomitant modification of the Born-Oppenheimer surfaces. Applications of the method to high harmonic generation, time-resolved photoelectron spectroscopy, and optimal control will be presented.

[1] S. Yang and T. J. Martínez, **Advances in the Theory of Atomic and Molecular Systems**, Ed. P. Piecuch, Springer, in press.

University Research Summaries
(by PI)

Probing Complexity using the ALS and the LCLS

Nora Berrah
Physics Department, Western Michigan University, Kalamazoo, MI 49008
e-mail:nora.berrah@wmich.edu

Program Scope

The objective of our research program is to investigate complexity through *fundamental interactions between photons and gas-phase systems* to advance our understanding of correlated and many body phenomena. Our research investigations probe multi-electron interactions, the dynamics of interacting few body quantum systems and energy transfer processes from electromagnetic radiation. Most of our work is carried out in a strong partnership with theorists.

Our current interests include: 1) The study of non linear and strong field phenomena in the x-ray regime using the linac coherent light source (LCLS), the first x-ray ultra-fast free electron laser (FEL) facility at the SLAC National Laboratory. Our investigations will focus on atoms, molecules and clusters to understand ultrafast and ultra-intense phenomena. 2) The study of correlated processes in select molecules, clusters and their anions using advanced techniques with vuv-soft x-rays from the Advanced Light Source (ALS) at Lawrence Berkeley Laboratory. We present here results completed and in progress this past year and plans for the immediate future.

Recent Progress

1) X-Ray Non-Linear Physics Studies of Molecules with Intense Ultrafast LCLS Pulses

The LCLS *started lasing* in April 2009 and is scheduled to provide beam time to users in September, 2009. My team will be contributing to the commissioning of the LCLS AMO instrument this summer. Furthermore, we are scheduled to carry out some of the first AMO experiments this fall. The present instrument consists of five electron time-of-flight (TOF) spectrometers and an ion imaging detector to measure the electron angular distribution and the ion charged states resulting from the ionization of atoms, molecules and clusters with the X-ray FEL. Specifically, we will carry out non-linear studies in N_2 and CO molecules as a function of focused x-ray laser intensity. We will study multiple and multi-photon ionization focusing on the measurements of Auger electrons subsequent to the ionization with 800 eV intense LCLS photons.

2) Emergence of Valence Band Structure and Autoionization Resonances in Rare-Gas Clusters

The formation of electronic band structure by the valence-shell of Ar, Kr, and Xe clusters was studied for various cluster sizes using angle-resolved photoelectron spectroscopy. Our system allows us to probe selectively either the cluster surface or cluster bulk since the e-TOFs provide very good electron kinetic energy resolution. Different widths of the fine-structure components in the cluster spectra are attributed to a splitting of the outermost $p_{3/2}$ levels due to valence-orbital overlap between neighboring atoms. Photoelectron angular distributions from the cluster differ from the atomic cases and vary substantially for different bands. Our measurements have shown

unambiguously for the first time the evolution of the electronic structure with increasing cluster size. Our data demonstrate clearly the changes of the valence band structure in the transition from a condensed-phase monolayer to the bulk [1,2].

We have also measured the photoionization of argon clusters in the Ar 3s→np Rydberg resonance region. For the first time, partial photoelectron yields and photoelectron angular distributions for the two spin–orbit components in argon clusters are reported as a function of the photon energy. The angular distributions of cluster photoelectrons differ substantially from the atomic ones. It allows, moreover, the identification of bulk and surface resonances [3].

3. Molecular-Frame Angular Distributions of Resonant CO:C (*1s*) Auger Electrons

Measurements of molecular-frame electron angular distributions (MFAD) allow access to an unprecedented level of detailed information, such as phases of photoelectron waves, localization of charge, core hole double-slit interference and photoelectron diffractions which are hidden in conventional gas-phase electron spectroscopy due to the random orientation of the molecules. Most of these studies to date have focused on photoelectrons. However, our team has used a novel methodology to determine for the first time the molecular-frame angular distributions of resonantly excited CO:C (*1s*) Auger electrons.

The molecular frame is the natural reference frame for the study of molecules and their interaction with electromagnetic radiation or charged particles. In order to experimentally determine MFAD the molecules have to be ''fixed'' in space, which can be realized by applying the angle-resolved photoelectron-photoion coincidence technique [a]. Although most of these studies have focused on photoelectrons, Auger electrons provide complementary information on the electronic structure and the anisotropy of atoms, molecules, and solids after the initial excitation. Because of their element and sites specificity, Auger electrons are often used as a probe for the atomic environment in large molecules and solids. In the case of resonant excitation, the focus of our work, they represent the only way (apart from fluorescence) to obtain information since no other electron is emitted. From a theoretical point of view, understanding the MFADs is probably the most demanding open question in molecular Auger spectroscopy.

There is no report on MFADs of resonant Auger electrons probably because the high kinetic energy of Auger electrons combined with the necessary high kinetic energy resolution does not allow detection in the full 4π solid angle. The determination of Auger electron MFAD is substantially more challenging and time consuming than the measurement of photoelectron MFADs [b,c]. Recently, in collaboration with the Sendai group, we used a newly developed analytical framework, allowing full three-dimensional MFADs from measurements of electrons at only two angles in combination with 4π momentum-resolved ion detection [4]. This novel approach makes high-resolution measurements of Auger electron MFADs considerably more convenient and feasible as demonstrated in our subsequent work [5,6].

Our experiment [4] was performed at the ALS Beamline 4.0.1 in the two-bunch mode. Our apparatus consists of a coincidence system that employs a momentum imaging spectrometer with two electron time-of-flight (TOF) analyzers mounted in the plane perpendicular to the light propagation direction, at 0° and 54.7° with respect to the horizontal. The uniqueness of our coincidence system lies in the fact that we have vey good electron kinetic energy resolution.

Specifically, our investigation was focused on elucidating the assignment of two main groups, "*h*" and "*i*" from the resonant Auger spectrum subsequent to the resonantly excited CO:C ($1s$)→ π^* Auger electrons [4]. For the selected geometry, the MFADs of the ''*h*'' and ''*i*'' groups show distinct differences. In particular, the MFAD of group '' *h*'' displays a strong asymmetry with a preferential emission of the electrons along the direction of the carbon atom, while the MFAD of group '' *i*'' is more isotropic and has a large fraction of its total intensity in the plane perpendicular to the molecular axis. The different shapes of the MFADs are well reproduced by ab initio calculations in the one-center approach. They provide an unambiguous assignment of group ''*h*'' to two states, $3\ ^2\Pi$ and $4\ ^2\Pi$, which have almost identical MFADs. Group ''*i*'' appears in the energy region where the calculations predict transitions to the $5\ ^2\Pi$ and $1\ ^2\Phi$ states.

In conclusion, our findings points to very different angular distributions for two closely ing electron spectator groups, both of which could be identified through the comparison with theoretical predictions [4]. Our calculations based on a one-center approach [d] are able to withstand the most stringent test of reproducing well the experimental angular distributions, and furthermore predict that the sum of all Auger transitions is strongly focused toward the carbon atom.

4. Multi-User Movable Ion Beamline

We have successfully and completely commissioned a movable ion beamline (MIPB) that allows the photoionization study of positive and negative ions in the merged beam geometry. This instrument complement the existing excellent ion-photon beamline (IPB) facility fixed at the ALS beamline 10.0.1. The MIPB has been used using photons from beamline 8 that enable deep core-shell ionization in molecules and clusters. We have carried out experiments in C_2^- and C_4^- and plan to continue the investigation of the carbon chain. The instrument is available for any users to exploit the capabilities of any ALS beam lines, specifically below 9 eV and above 340 eV photon energies not available on BL10.0.1.

Future Plans.

The principal areas of investigation planned for the coming year are:
1) We plan to carry out LCLS based experiments and analyze the resulting data. **2)** We plan to continue the data analysis of the Coulomb explosion investigations of large molecules and clusters using the ALS. **3)** We plan to continue the photodetachment experiments in the carbon anions cluster chain using the MIPB. **4)** We plan to carry out the analysis of the experiments conducted on the valence and K-shell photodetachment of C_{60}^- conducted this spring with the IPB in collaboration with the UNR and Giessen groups.

References

[a] E. Shigemasa et al., Phys. Rev. Lett. 74, 359 (1995), F. Heiser et al., Phys. Rev. Lett. 79, 2435 (1997); R. Dorner et al., Phys. Rev. Lett. 81, 5776 (1998); P. Downie et al., Phys. Rev. Lett. 82, 2864 (1999).
[b] A. K. Edwards et al., Phys. Rev. A 55, 4269 (1997).
[c] Th. Weber et al., Phys. Rev. Lett. 90, 153003 (2003).
[d] R. F. Fink, S. L. Sorensen, and A. Naves de Brito, J. Chem.Phys. 112, 6666 (2000) .

Publications from DOE Sponsored Research

1. D. Rolles, H. Zhang, Z. D. Pešić, J. D. Bozek,and N. Berrah " Emergence of Band Structure in Valence Photoemission from Rare Gas Clusters" Chem. Phys. Lett. 468, 148 (2009).

2. N. Berrah, D. Rolles, Z. D. Pesic, M. Hoener, H. Zhang, A. Aguilar, R. C. Bilodeau, E. Red, J. D. Bozek, E. Kukk, R. Dies Muino and G. Abajo, "Probing free Xe clusters from within" Euro.Phys. J. Special Topics (EPJ) ST, **169,** 59 (2009).

3. H. Zhang, D. Rolles, J.D. Bozek R. Bilodeau and N. Berrah, " Photoionization of argon clusters in th e Ar 3s→np Rydberg resonance region", *J. Phys. B: At. Mol. Opt. Phys.*, **42,** 105103, (2009).

4. D. Rolles, G. Prumper, H. Fukuzawa, X.-J. Liu, Z. D. Pesic, R. F. Fink, A. N. Grum-Grzhimailo, I. Dumitriu, N. Berrah, and K. Ueda, Molecular-Frame Angular Distributions of Resonant CO:C(1s) Auger Electrons, Phys. Rev. Lett. **101**, 263002 (2008).

5. G. Prumper, H. Fukuzawa,D. Rolles, K. Sakai, K. Prince, J. Harries, Y. Tamenori, N. Berrah, and K. Ueda, "Is CO C 1*s* Auger Electron Emission Affected by the Photoelectron? Phys. Rev. Lett. **101**, 233202 (2008)

6. G Prümper, D Rolles, H Fukuzawa, X J Liu, Z Pešić, I Dumitriu, R R Lucchese, K Ueda and N. Berra h, "Measurements of molecular-frame Auger electron angular distributions at the CO C $1s^{-1}$ $2\pi^*$ resonance with high energy resolution", *J. Phys. B: At. Mol. Opt. Phys.* **41,** 215101 (2008).

7. Z. Pesic, D. Rolles, R.C. Bilodeau, I. Dimitriu and N. Berrah, "Th ree-Body Fra gmentation o f CO $_2^{2+}$ upon K-shell Photoionization", Phys Rev A. Phys. Rev. A **78**, 051401 (2008) (rapid C.)

8. H. Zhang, D. Rolles, J.D. Bozek,B. Rude, R. C. Bilodeau and N. Berrah" Angular distributions of inner shell photoelectrons from rare-gas clusters", Phys. Rev. A **78**, 063201 (2008).

9. M. Wiedenhoeft, A. A. Wills, X. Fen g, S. Canton, J. Viefh aus, T. Go rczyca, U.Beck er, and N. Berrah "Exc hange and PCI effects on Angular Distribution in Xe $4d_{5/2}$" J. Phys. B . **41** 095202, (2008).

10. N. Berrah, J. D. Bo zek, R. C. Bilo deau G. D. Ac kerman, "Inner-S hell Phot odetachment and Fragmentation of small clusters B_2^-, B_3^-", Phys. Rev. A. **76**, 042709 (2007).

11. G. Turri, B. Lohmann, B. Langer, G. Snell, U. B ecker and N. B errah, "Spin p olarization of the Ar^* $2p^{-1}{}_{1/2}4s$, and $2p^{-1}{}_{1/2}3d$ Auger decay" J. Phys. B **40**, 3453 (2007).

12. N. Berrah , R.C. Bilodeau, I. Dumitriu, J.D. Bozek,G.D. Ackerman, O. T. Zatsarinny and T. W. Gorczyca "Sh ape res onances i n K-sh ell phot odetachment of B^-: Experi ment and The ory" Phys. Rev. A **76,** 032713 (2007).

13. L . F. DiMauro, J. Arthur, N. Berrah, J. Bozek, J. N. Galayda and J. Hastings,**"**Progress report on the LCLS XFEL at SLAC"**, .** *Phys.: Conf. Ser.* **88**, 012058 (2007).

14. D. Rolles, Z. D. Pešić, H. Zhang,, R. C. Bilodeau, J. D. Bozek, and N. Berrah, "Size effects in van der Waals clusters studied by spin and angle-resolved electron spectroscopy and multi-coincidence ion imaging" *J. Phys.: Conf. Ser.* **88** 012003, (2007).

15. E. Sok ell, A. A. Wills, M. Wiendenhoeft, X. Feng, D. R olles an d N. Berrah, "Inner-shell photoionization of molecules using a two-dimensional imaging technique" *J. Phys.: Conf. Ser.* **88** 012007 (2007).

16. D. R olles, H. Zhang, A . Wills, R . B ilodeau, E . K ukk B . R ude, G . Ac kerman, J. B ozek an d N. Berrah "Size e ffects in Van der Waals clusters using angle resolved photoelectron spectroscopy, Phys. Rev. A, Rap Com. **75**, 032101(R) (2007).

17. D. Rolles , Z. D. Peši ć, M. Perri, R. Bilodeau, G. Ackerman, B. Rude, D. Kilcoyne, J. D. Bozek, and N. Berrah "A velocity map imaging spectrometer for electron-ion and ion-i on coincidenc e experiments with synchrotron radiation, Nucl. Instr. and Meth. **B 261**, 170 (2007).

18. Z. D. Pešić, D. Rolles, M. Perri, R. C. Bilodeau, G. D. Ackerman, B. S. Rude, A. L. D. Kilcoyne, J. D. B ozek, a nd N. B errah, "St udies of M olecular F ragmentation usi ng Vel ocity M ap Im aging Spectrometer and Synchrotron Radiation", J. Elect. Spec. and Rela. Phen, **155**, 155 (2007)

19. D. Cubaynes, H-L Zhou, N. Berrah, J-M. Bizau, J. D. Bozek, S. Canton, S. Diehl, X-Y Han, A. Hibbert, E. T. Kenn edy, S. T. Man son, L. VoKy, F. Wuilleumier, "Dyn amical an d relativ istics effects in experimental and theoretical studies of i nner-shell photoionization of sodium", J P hys B **40**, F121 (2007).

Strongly Anisotropic Bose and Fermi Gases

Principal Investigator
John Bohn
JILA, UCB 440
University of Colorado
Boulder, CO 80309
Phone (303) 492-5426
Email bohn@murphy.colorado.edu

Program Scope

This program focuses on the fundamental properties of dilute quantum degenerate gases whose constituent particles possess dipole moments. It is concerned with the implications of the dipole-dipole interactions on the structure, dynamics, and control of these gases, as well as their ability to provide prototypes for novel condensed matter systems and potentially useful materials. The properties of the gas are tunable to a high degree, by varying such quantities as the density of the gas, the orientation of the dipoles, the scattering length of the constituents, and the anisotropy of the trap in which they are held.

Recent Progress

We continue our investigations into the structure and stability of dipolar Bose-Einstein condensates. These matters get to the heart of the novelty of dipolar particles, namely, their anisotropic interparticle interactions, which are either repulsive or attractive depending on the relative orientation of the particles. An unusual consequence of this anisotropy, known for some time now, is the existence of excitations analogous to the roton mode in superfluid helium. In helium, this excitation determines many properties of the gas, including the velocity below which the fluid flows without resistance, as well as the features of correlated motion of the atoms in the fluid. We are developing the theory of how these excitations play out in realistic experimental circumstances for dipoles.

In dipolar BEC, the roton-like excitations offer far more variety than in helium, inasmuch as their properties can be tuned via both the strength of the dipole moment and the anisotropy of the trap. Moreover, when the excited roton mode becomes degenerate with the ground state, an instability occurs that can cause collapse of the BEC into local density fluctuations. Carefully characterizing these fluctuations and the ensuing collapse is important for understanding how far the gas can be pushed in the quest for new physics or even device applications.

We have characterized this kind of collapse, both for non-rotating condensates and those containing vortex states. The roton modes, like harmonic oscillator modes, are characterized by their radial and angular nodal patterns in pancake-shaped trapping potentials. The collapse can lay bare this nodal structure, which is in turn related to the density profile of the BEC before collapse. Experiments that deliberately trigger a collapse, therefore, can serve as

probes of the novel dipole-generated structure. We have modeled the time-dependent collapse of these structures, as would pertain to realistic experimental circumstances for a BEC of chromium (see Figure). The corresponding experiments are being carried out in the Pfau group in Stuttgart.

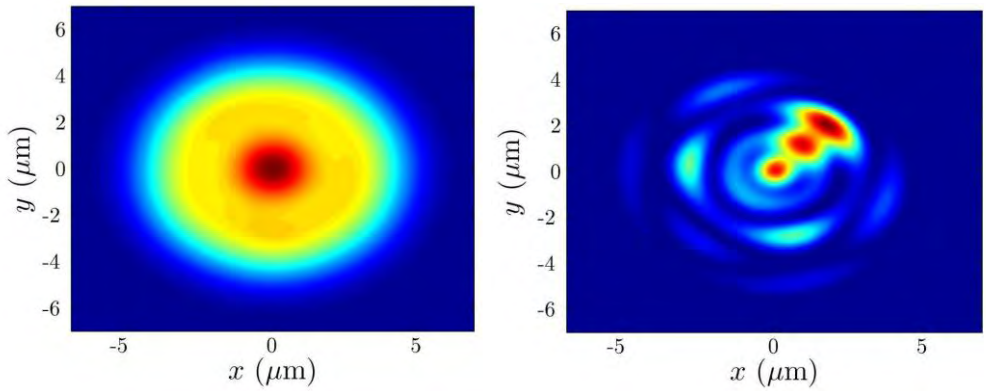

Figure. Density profiles for dipolar BEC's that have undergone collapse, as viewed "looking down" on the BEC from the polarization axis. Red is high density, blue is low. In the left panel, collapse was triggered via radial roton modes, while in the right panel the rotons have angular nodes. This kind of imaging can reveal the unique features arising from anisotropic interactions in the gas.

This dipolar BEC work is performed by fourth-year graduate student Ryan Wilson. Additionally, this year saw the publication of the final results from the thesis of former DOE-supported graduate student Daniele Bortolotti, on the physics of an ultracold mixture of bosons and fermions. This work laid out the appropriate mean-field theory of such a mixture, including the capacity of the atoms to join into molecules near a Fano-Feshbach resonance. Intriguingly, this work showed that the mean-field theory is not adequate for the description of this fascinating system, in the sense that it is for boson-boson mixtures. Nevertheless, the theory presents an essential touchstone that all future theories must build from.

Future Plans

Thus far the entire field of dipolar BEC has been concerned with particles polarized perpendicular to the plane in which they are confined, hence preserving cylindrical symmetry. Recently we have begun to explore the situation where the polarization is tilted with respect to this plane. In this case the superfluid velocity itself is anisotropic, with consequences that have yet to be appreciated. Also, we are looking toward a certain class of polar molecules with extremely low polarizabilities. Because they are polarized in a very weak field, the field generated by the dipoles themselves can be comparable to the applied field, thus coupling the internal and motional states of the particles. Both these unusual

attributes – anisotropic superfluidity and quantum dielectric properties -- demand exploration to investigate novel properties of dipolar materials.

DOE-supported publication in the past three years

Stability of Fermionic Feshbach Molecules in a Bose-Fermi Mixture
A. V. Avdeenkov, D. C. E. Bortolotti, and J. L. Bohn, Phys. Rev. A **74**, 012709 (2006).

Bogoliubov modes of a dipolar condensate in a cylindrical trap
S. Ronen, D. C. E. Bortolotti, and J. L. Bohn, Phys, Rev. A **74**, 013623 (2006).

Dipolar Bose-Einstein Condensates with Dipole-Dependent Scattering Length
S. Ronen, D. C. E. Bortolotti, D. Blume, and J. L. Bohn, Phys. Rev. A **74**, 033611 (2006).

Scattering Length Instability in Dipolar Bose Gases
D. C. E. Bortolotti, S. Ronen, J. L. Bohn, and D. Blume, Phys. Rev. Lett. **97**, 160402 (2006).

Radial and Angular Rotons in Trapped Dipolar Gases
S. Ronen, D. C. E. Bortolotti, and J. L. Bohn, Phys. Rev. Lett. **98**, 030406 (2007).

Pseudo-potential Treatment of Two Aligned Dipoles Under External Harmonic Confinement
K. Kanjilal, J. L. Bohn, and D. Blume, Phys. Rev. A **75**, 052705 (2007).

Manifestations of the Roton Mode in Dipolar Bose-Einstein Condensates
R. M. Wilson, S. Ronen, J. L. Bohn, and H. Pu, Phys. Rev. Lett. **100**, 245302 (2008).

Generalized Mean-Field Approach to a Resonant Bose-Fermi Mixture
D. C. E. Bortolotti, A. V. Avdeenkov, and J. L. Bohn, Phys. Rev. A **78**, 063612 (2008).

Stability and Excitations of a Dipolar Bose-Einstein Condensate with a Vortex
R. M. Wilson, S. Ronen, and J. L. Bohn, Phys. Rev. A **79**, 013621 (2008).

How Does a Dipolar Bose-Einstein Condensate Collapse?
J. L. Bohn, R. M. Wilson, and S. Ronen, Proceedings of the 17th International Laser Physics Conference, published in Laser Physics **19**, 547 (2009).

Angular Collapse of Dipolar Bose-Einstein Condensates
R. M. Wilson, S. Ronen, and J. L. Bohn, Phys. Rev. A (accepted, 2009).

Atomic and Molecular Physics in Strong Fields

Shih-I Chu
Department of Chemistry, University of Kansas
Lawrence, Kansas 66045
E-mail: sichu@ku.edu

Program Scope

In this research program, we address the fundamental physics of the interaction of atoms and molecules with intense ultrashort laser fields. The main objectives are to develop new theoretical formalisms and accurate computational methods for *ab initio* nonperturbative investigations of multiphoton quantum dynamics and very high-order nonlinear optical processes of one-, two-, and many-electron quantum systems in intense laser fields, taking into account detailed electronic structure information and many-body electron-correlated effects. Particular attention will be paid to the exploration of the effects of electron correlation on high-harmonic generation (HHG) and multiphoton ionization (MPI) processes, time-frequency spectrum, and coherent control of HHG processes for the development of tabletop x-ray laser light sources, and for the exploration of attosecond AMO processes, etc.

Recent Progress

1. *Ab initio* Theoretical Investigation of the Frequency Comb Structure and Coherence in the VUV-XUV Regimes via High-Order Harmonic Generation: From Atomic H to Rare Gas Atoms

In the last few years, femtosecond laser-based optical frequency combs have led to remarkable advancements in ultrafast science [1], high-precision optical frequency measurement and synthesis [2], and enabled optical atomic clocks [3]. As a universal optical frequency comb synthesizer, this method provides a direct link between optical and microwave frequencies. More recently, there is substantial experimental interest in the exploration of the feasibility of generating frequency comb in the extreme ultraviolet (xuv) and vacuum ultraviolet (vuv) regimes at a repetition frequency of more than 100 MHz via high-order harmonic generation (HHG) [4,5]. At such a repetition rate, the mode spacing of the frequency comb is large enough for high-resolution spectroscopy. However, there are currently experimental difficulties in the realization of the frequency comb structure within each high harmonic, with the exception of the third-order harmonic case [5].

To advance this field, we have recently presented the first fully *ab initio* quantum investigation of the frequency comb structure and coherence within each order of the high-order harmonic generation spectrum in the high-frequency vuv-xuv regime [6]. The HHG spectrum of atomic H driven by a train of equal-spacing short laser pulses is calculated by propagating the time-dependent Schrödinger equation (TDSE) accurately and efficiently by means of the time-dependent generalized pseudospectral (TDGPS) method [7]. We explore the comb structure and coherence by varying the laser pulse separation τ, the number of pulses N, and the laser intensity. We found that a nested comb structure appears within each of the harmonics, ranging from the first harmonic all the way to the cutoff harmonic, and this global pattern persists regardless of the values of τ and N used and even in the presence of appreciable ionization.

More recently, we have extended the study to the rare gas atoms by means of *self-interaction-free* time-dependent density functional theory (TDDFT) [8]. We found that it is essential to include the dynamical electron correlation for the quantitative exploration of the strong-field MPI, HHG, and frequency comb structure and coherence. We explore in detail the temporal coherence and robustness of the comb structure by varying τ, N, the phase difference between pulses, and the laser intensity. We found that the frequency comb structure and coherence are preserved in each harmonic regardless of the values of τ and N used for the case of weak and medium strong incident laser-pulse trains. However, under

superstrong fields, nonuniform and substantial ionization takes place during each pulse, jeopardizing the temporal coherence of the emitted frequency comb modes.

2. Exploration of Coherent Control of Multiphoton Resonance Dynamics in Intense Frequency-Comb Laser Fields: Many-Mode Floquet Theoretical Approach

We generalize the many-mode Floquet theorem (MMFT) [9, 10] for the nonperturbative investigation of multiphoton resonance dynamics driven by intense frequency-comb laser fields [11]. The frequency comb structure generated by a train of short laser pulses can be exactly represented by a combination of the main frequency and the repetition frequency. MMFT allows non-perturbative and exact treatment of the interaction of a quantum system with the frequency-comb laser fields. We explore multiphoton resonance processes between a two-level system and frequency-comb laser. We found that the multiphoton processes can be coherently controlled by tuning the laser parameters such as the carrier-envelope phase (CEP) shift. In particular, high-order harmonic generation shows immense (many-orders-of magnitude) enhancement by tuning the CEP shift, due to simultaneous multiphoton resonances [11].

3. Coherent Control of a Single Attosecond XUV Pulse by Few-Cycle Intense Laser Pulses

We perform *ab initio* quantum and classical explorations of the production and control of a single attosecond pulse by using intense few-cycle laser pulses as the driving field [12]. The time-frequency characteristics of the attosecond xuv pulse are analyzed in detail by means of the wavelet transform of the time-dependent induced dipole. To better understand the physical processes, we also perform classical trajectory simulation of the strong-field electron dynamics and electron returning energy map. We found that the quantum and classical results provide complementary information regarding the underlying mechanisms responsible for the production of the coherent attosecond pulse. For few-cycle (5 fs) driving pulses, it is shown that the emission of the consecutive harmonics in the super continuum cutoff regime can be synchronized and locked in phase resulting in the production of a coherent attosecond pulse. Moreover, the time profile of the attosecond pulses can be controlled by tuning the carrier envelope phase.

4. Effect of Electron Correlation on High-Order-Harmonic Generation of Helium Atoms in Intense Laser Fields

Recently we have developed a *time-dependent generalized pseudospectral* (TDGPS) approach in hyperspherical coordinates for fully *ab initio* and nonperturbative treatment of high-order harmonic generation (HHG) processes of two-electron atomic systems in intense laser fields [13]. The procedure is applied to a detailed investigation of HHG processes of helium atoms in ultrashort laser pulses at a KrF wavelength of 248.6 nm. The six-dimensional coupled hyperspherical-adiabatic-channel equations are discretized and solved efficiently and accurately by means of the TDGPS method. The effects of electron correlation and doubly excited states on HHG are explored in detail. A HHG peak with Fano line profile is identified which can be attributed to a broad resonance of doubly excited states [13].

5. Extension of High-order Harmonic Generation Cutoff via Coherent Control of Intense Few-Cycle Chirped Laser Pulses

We present an *ab initio* quantum exploration of the HHG cutoff extension mechanisms controlled by a few cycle *chirped* laser pulse [14]. It is shown that significant cutoff extension can be achieved through the optimization of the chirping rate parameters. Furthermore the time duration of the emitted attosecond bursts produced by the chirped laser pulse is significantly reduced from that of the chirp-free laser pulses.

6. Precision Study of the Orientation Effects in MPI/HHG of H_2^+ in Intense Laser Fields

Recently we have developed a TDGPS method for accurate and efficient treatment of the time-dependent Schrödinger equation (TDSE) of two-center diatomic molecules systems in prolate spheroidal coordinates [15]. The method is applied to a fully *ab initio* 3D study of the orientation effects in MPI and

HHG of H_2^+ subject to intense laser pulses. The calculations were performed for the ground and two first excited electronic states of H_2^+ at the internuclear separation $R = 2.0$ a.u. The dependence of MPI and HHG behavior on the orientation angle is analyzed. We found that orientation effects are strongly affected by the symmetry of the wave function and the corresponding distribution of the electron density. While the anisotropy of MPI and HHG is rather weak for the $1\sigma_g$ state, both processes are suppressed at the orientation angle 90° for the $1\sigma_u$ state and at the angle 0° for the $1\pi_u$ state. We discuss the multiphoton resonance and two-center interference effects in the HHG spectra which can lead both to enhancement and suppression of the harmonic generation [15].

7. Above-Threshold-Ionization Spectra from Core Region of Time-Dependent Wave Packet: A New *ab initio* Time-Dependent Approach

Recently the phenomenon of multiphoton above-threshold ionization (ATI) and investigations of resulting electron distributions attracted much new interest. This is related to advances in laser technology which made possible generation of ultrashort and intense laser pulses. For such pulses, the absolute or carrier-envelope phase (CEP) plays an important role and properties of the ejected electrons momentum (or energy–angular) distributions differ significantly from those for long pulses. Recent experiments were able to measure high-resolution fully differential data on ATI of noble gases. Thus accurate theoretical description of the electron distributions becomes an important and timely task.

In a recent work, we develop a new method for accurate treatment of TDSE and electron energy and angular distributions after above-threshold multiphoton ionization [16]. The procedure does not require propagation of the wave packet at large distances, making use of the wave function in the core region. It is based on the extension of the Kramers–Henneberger picture of the ionization process while the final expressions involve the wave function in the laboratory frame only. The approach is illustrated by a case study of above-threshold ionization of the hydrogen atom subject to intense laser pulses. The ejected electron energy and angle distributions have been calculated and analyzed. We explore the electron spectrum dependence on the duration of the laser pulse and carrier-envelope phase [16].

8. Role of the Electronic Structure and Multi-electron Response in the MPI and HHG Processes of Diatomic Molecules in Intense Laser Fields

Recently we have continued the development of *self-interaction-free* time-dependent density functional theory (TDDFT) [17,18] for accurate and efficient treatment of strong-field AMO physics, taking into account both electron correlations and detailed electronic structure. Given below is a brief summary of the most recent progress.

There have been much current experimental and theoretical interests in the study of strong-field molecular ionization and HHG. Most theoretical studies in the recent past are based on approximate models such as the ADK model, strong-field approximation, etc. The effects of detailed electronic structure and multi-electron responses are often ignored. Although these models have some partial success in weaker field processes, they cannot provide an overall consistent picture of the ionization and HHG behavior of different molecules.

We have recently further developed the *self-interaction-free* TDDFT [17,18] for nonperturbative investigation of the ionization mechanisms as well as the HHG power spectra of homonuclear (N_2, O_2, and F_2) and heteronuclear (CO) diatomic molecules in intense ultrashort lasers [19]. A *time-dependent two-center generalized pseudospectral method* in prolate spheroidal coordinates is developed for accurate and efficient treatment of the TDDFT equations in space and time. Our studies reveal several intriguing behaviors of the nonlinear responses of molecules to intense laser fields: (a) It is found that detailed electron structure and correlated multielectron responses are important factors for the determination of the strong-field ionization behavior. Further, it is not adequate to use only the HOMO for the description of the ionization behavior since the inner valence electrons can also make significant or even dominant

contributions. Finally, the ionization potential (IP) is laser-intensity and frequency dependent and it is also not the only major factor determining the molecular ionization rates. (b) We predict substantially different nonlinear optical response behaviors for homonuclear (N_2) and heteronuclear (CO) diatomic molecules, despite the fact that CO has only a very small permanent dipole moment. In particular, we found that the MPI rate for CO is higher than that of N_2. Furthermore, while laser excitation of the homonuclear N_2 molecule can generate only odd harmonics, both even and odd harmonics can be produced from the heteronuclear CO molecule [19].

More recently, we have extended the TDDFT approach for the study of the effect of correlated multielectron responses on the multiphoton ionization (MPI) of diatomic molecules N_2, O_2, and F_2 in intense short laser pulses with arbitrary molecular orientation [20]. We show that the contributions of inner molecular orbitals to the total MPI probability can be significant or even dominant over the HOMO, depending upon detailed electronic structure and symmetry, laser field intensity, and orientation angle.

Future Research Plans

In addition to continuing the ongoing researches discussed above, we plan to initiate the following several new project directions: (a) Exploration of 3D orientation dependent MPI/HHG and ATI processes of diatomic molecules in intense laser pulses. (b) Development of TDGPS method and extension of self-interaction-free TDDFT to triatomic molecular systems [21] for the study of the MPI mechanisms and HHG phenomena in strong fields. (c) Development of time-dependent *localized* Hartree-Fock (LHF)-DFT method for the study of singly, doubly, and triply excited states of Rydberg atoms and ions, inner shell excitations [22], as well as photoionization of atomic excited states [23]. (d) Coherent control of rescattering and attosecond phenomena in strong fields.

References Cited (* Publications supported by the DOE program in the period of 2006-2009.)

[1] M. Hentschel *et al.*, Nature (London) **414**, 509 (2001); M. Drescher *et al.*, Science **291**, 1923 (2001).
[2] M. Fischer *et al.*, Phys. Rev. Lett. **92**, 230802 (2004); H. S. Margolis *et al.*, Science **306**, 1355 (2004).
[3] M. Takamoto *et al.*, Nature (London) **435**, 321 (2005); S. A. Diddams *et al.*, Science **293**, 825 (2001).
[4] C. Gohle, *et al.*, Nature (London) **436**, 234 (2005).
[5] R. J. Jones, *et al.*, Rev. Lett. **94**, 193201 (2005).
*[6] J. J. Carrera, S. K. Son, and S. I. Chu, Phys. Rev. A **77**, 031401(R) (2008).
[7] X. M. Tong and S. I. Chu, Chem. Phys. **217**, 119 (1997).
*[8] J. J. Carrera and S. I. Chu, Phys. Rev. A **79**, 063410 (2009).
[9] T. S. Ho, S. I. Chu, and J. V. Tietz, Chem. Phys. Lett. **96**, 464 (1983); T. S. Ho and S. I. Chu, Phys. Rev. A **31**, 659 (1985).
[10] S. I. Chu and D. A. Telnov, Phys. Rep. **390**, 1-131 (2004).
*[11] S.-K. Son and S. I. Chu, Phys. Rev. A **77**, 063406 (2008).
*[12] J. Carrera, X. M. Tong, and S. I. Chu, Phys. Rev. A **74**, 023404 (2006).
*[13] X. X. Guan, X. M. Tong, and S. I. Chu, Phys. Rev. A **73**, 023406 (2006).
*[14] J. Carrera and S. I. Chu, Phys. Rev. A **75**, 033807 (2007).
*[15] D. A. Telnov and S. I. Chu, Phys. Rev. A **76**, 043412 (2007).
*[16] D. Telnov and S. I. Chu, Phys. Rev. *A* **79**, 043421 (2009).
[17] X. Chu and S. I. Chu, Phys. Rev. A**70**, 061402 (R) (2004).
*[18] S. I. Chu, J. Chem. Phys. **123**, 062207 (2005). (Invited review article)
*[19] J. Heslar, J. Carrera, D. Telnov, and S. I. Chu, Int. J. Quantum Chem. **107**, 3159 (2007).
*[20] D. Telnov and S. I. Chu, Phys. Rev. A**79**, 041401(R) (2009).
*[21] S. K. Son and S. I. Chu, Phys. Rev. A (in press).
*[22] Z.Y. Zhou and S. I. Chu, Phys. Rev. A**75**, 014501 (2007).
*[23] Z. Y. Zhou and S. I. Chu, Phys. Rev. A**79**, 053412 (2009).

Formation of Ultracold Molecules

Robin Côté

Department of Physics, U-3046
University of Connecticut
2152 Hillside Road
Storrs, Connecticut 06269

Phone: (860) 486-4912
Fax: (860) 486-3346
e-mail: rcote@phys.uconn.edu
URL: http://www.physics.uconn.edu/∼rcote

Program Scope

Current experimental efforts to obtain ultracold molecules (*e.g.*, photoassociation (PA), buffer gas cooling, or Stark deceleration) raise a number of important issues that require theoretical investigations and explicit calculations.

This Research Program covers interconnected topics related to the formation of ultracold molecules. We propose to investigate schemes to form ultracold molecules, such as homonuclear dimers (alkali or alkaline earth) using stimulated and spontaneous processes. We will also study heteronuclear molecules, in particular those with large dipole moments like alkali hydrides or some bi-alkali dimers (e.g. LiCs or LiRb). In addition, we will investigate the enhancement of the formation rate via Feshbach resonances, paying special attention to quantum degenerate atomic gases. Finally, we will explore the possible formation of a new and exotic type of molecules, namely ultralong-range Rydberg molecules.

Recent Progress

Since the start of this Program (August 1st 2005), we have worked on several projects. We limit ourselves to work published over the last three years (since 2006).

• Formation of polar molecules

We explored the formation of alkali hydrides from one- and two-photon photoassociative processes. We found that the one-photon formation rate for LiH and NaH in their $X^1\Sigma^+$ ground electronic state is sizable in the upper ro-vibrational states $|v'', J = 1\rangle$; assuming conservative values for the atom densities (10^{12} cm^{-3}), temperature (1 mK), laser intensity (1000 W/cm^2), and the volume illuminated by it (10^{-6} cm^3), the rate coefficients are of the order 3×10^{-13} cm^3/s, leading to about 30,000 molecules per second [1]. We also found that all of those molecules would populate a narow distribution of J-states in the $v'' = 0$ vibrational level by spontaneous emission cascading; the momentum transfer due to the photon emission is not large enough for remove the molecules from traps deeper than 10 μK or so. In the two-photon case, we calculated the formation rate of LiH into the singlet ground state via the $B^1\Pi$ excited state. This excited electronic state has only three bound levels (in the $J = 1$ manifold) and a fairly good overlap with the $X^1\Sigma^+$ ground electronic state. We found rate coefficients about 1000 times larger [2]. However, the constraints brought by the possibility of back-stimulation from a bound state to the continuum limits these larger rates to values of the same order as the single photon process via an excited state [2].

More recently, we also explored the formation of LiH molecules in the $a^2\Sigma^+$ electronic state [3]. It is predicted to support one ro-vibrational level, leading to a sample in a pure single ro-vibrational state. We found that very large rate coefficients ca be obtained by using the $b^3\Pi$ excited state, which supports only five or six bound levels. Because of the extreme spatial extension of their last "lobe", the wave functions of the two uppermost bound levels have large overlap with the $(v = 0, J = 0)$ bound level of $a^3\sigma^+$, leading to branching ratios ranging from 1% to 90%. This property implies that large amounts of LiH molecules could be produced in a single quan tum state, a prerequisite to study degenerate molecular gases [3].

• Homonuclear molecules

We analyzed results from two-photon photoassociative spectroscopy of the least-bound vibrational level ($v = 62$) of the $X^1\Sigma_g^+$ state of the $^{88}Sr_2$ dimer [4]. By combining measurements of the binding energy with an accurate short range potential and calculated van der Waals coefficients, we were able to determine the s-wave scattering length $a_{88} = -1.46a_0$. We also modeled the observed Autler-Townes resonance splittings. Through mass scaling, we determined the scattering lengths for all other isotopic combinations. These measurements provide confirmation of atomic structure calculations for alkaline-earth atoms and provide valuable input for future experiments with ultracold strontium.

We suggested and analyzed a technique for efficient and robust creation of dense ultracold molecular ensembles in their ground rovibrational state [5]. In this approach, a molecule is brought to the ground state through a series of intermediate vibrational states via a multistate chainwise stimulated Raman adiabatic passage technique. We studied the influence of the intermediate states decay on the transfer process and suggested an approach that minimizes the population of these states, resulting in a maximal transfer efficiency. As an example, we analyzed the formation of $^{87}Rb_2$ starting from an initial Feshbach molecular state and taking into account major decay mechanisms due to inelastic atom-molecule and molecule-molecule collisions. Numerical analysis suggests a transfer efficiency $> 90\%$, even in the presence of strong collisional relaxation as are present in a high density atomic gas.

• Rydberg-Rydberg interactions

We began working on the Rydberg-Rydberg interactions to explain some spectral features observed in ^{85}Rb experiments. We calculated the long-range molecular potentials between two atoms in $70p$ in Hund's case (c), by diagonalization of an interaction matrix. We included the effect of fine structure, and showed how the strong ℓ-mixing due to long-range Rydberg-Rydberg interactions can lead to resonances in excitation spectra. Such resonances were first reported in S.M. Farooqi *et al.*, Phys. Rev. Lett. **91** 183002, where single UV photon excitations from the $5s$ ground state occurred at energies corresponding to normally forbidden transitions or very far detuned from the atomic energies. We modeled a resonance correlated to the $69p_{3/2} + 71p_{3/2}$ asymptote by including the contribution of various symmetries: the lineshape is reproduced within the experimental uncertainties [6]. More recently, we extended this work to the case of strong resonances observed near the $69d + 70s$ asymptote [7]. We found that our theoretical results are in good agreement with the observations of our colleagues at UConn.

• Degenreate Fermi gas

In [8], we worked on the spectroscopic signature of Cooper pairs in a degenerate Fermi gas, namely ^6Li. We calculated two-photon Raman spectra for fermionic atoms with interactions described by a single-mode mean-field BCS-BEC crossover theory. By comparing calculated spectra of interacting and non-interacting systems, we found that interactions lead to the appearance of correlated atomic pair signal - due to Cooper pairs; splitting of peaks in the spectroscopic signal - due to the gap in fermionic dispersion; and attenuation of signal - due to the partial conversion of fermions into the corresponding single-mode dimer. By exploring the behavior of these features, on can obtain quantitative estimates of the BCS parameters from the spectra, such as the value of the gap as well as the number of Cooper pairs.

• Influence of Feshbach resonances on formation rates

We have started to investigate the formation of molecules using photoassociation of atoms in the vicinity of Feshbach resonances. In our initial work [9], we calculated the rate coefficients to form

singlet molecules of LiNa using this Feshbach Optimized Photoassociation (FOPA) mechanism, and found that they increase by 10^{3-4} when compared to the off-resonance rate coefficients. We also gave a simple analytical expression relating the rate coefficient to the off-resonance rate coefficient and parameters of the resonance (such as its position and width).

We expanded this work to take into account the effect of saturation on the rate coefficient [10]. We computed rate coefficients and showed that new double-minima features would appear at large laser intensity near the resonance. We compared our theoretical results with recent experimental measurements, and found an extremely good agreement without any adjustable parameters.

We combined this idea of FOPA with our previous work using STIRAP [11]. We showed that it is possible to enhance the Rabi frequency between the continuum and an intermediate state so that the efficient transfer of a pair of atoms directly from the continuum into the ro-vibrational ground state becomes achievable with moderate laser intensities and pulse durations. This approach opens interesting perspectives, since it does not require degenerate gases to work efficiently.

Finally, we also explored the role of Feshbach resonance and spin-orbit coupling in the formation of ultracold LiCs molecules [12]. We analyzed the experimental data of our co-workers, and found that even in the case of unpolarized atomic spin states (*i.e.* a mixture of all m_f states), hyperfine coupling can modify the formation rate measurably.

Future Plans

In the coming year, we plan to continue the alkali hydride work. We also will extend this work to other polar molecules relevant to the experimental community, such as LiCs, LiRb, LiK, etc. We also plan to continue our work on FOPA, by expanding our treatment to the time domain.

We expect to carry more calculations on Rydberg-Rydberg interactions and explore the possibility of forming metastable long-range doubly-excited Rydberg molecules as well as the experimental signature to be expected.

Publications sponsored by DOE

1. E. Juarros, P. Pellegrini, K. Kirby, and R. Côté, *One-photon-assisted formation of ultracold polar molecules.* Phys. Rev. A **73**, 041403(R) (2006).

2. E. Juarros, K. Kirby, and R. Côté, *Laser-assisted Ultracold Lithium-hydride Molecule Formation: Stimulated vs. Spontaneous Emission.* J. Phys. B **39**, S965 (2006).

3. E. Juarros, K. Kirby, and R. Côté, *Formation of ultracold molecules in a single pure state: LiH in* $a^3\Sigma^+$. In preparation.

4. Y.N. Martinez de Escobar, P.G. Mickelson, P. Pellegrini, S.B. Nagel, A. Traverso, M. Yan, R. Côté, and T.C. Killian, *Two-photon photoassociative spectroscopy of ultracold* ^{88}Sr. Phys. Rev. A **78**, 062708 (2008).

5. E. Kuznetsova, P. Pellegrini, R. Côté, M.D. Lukin, and S.F. Yelin, *Formation of deeply bound molecules via adiabatic passage.* Phys. Rev. A **78**, 021402(R) (2008).

6. J. Stanojevic, R. Côté, D. Tong, S.M. Farooqi, E.E. Eyler, and P.L. Gould, *Long-range Rydberg-Rydberg interactions and molecular resonances.* Eur. Phys. J. D **40**, 3 (2006).

7. J. Stanojevic, R. Côté, D. Tong, S.M. Farooqi, E.E. Eyler, and P.L. Gould, *Long-range potentials and* $(n?1)d + ns$ *molecular resonances in an ultracold Rydberg gas.* Phys. Rev. A **78**, 052709 (2008).

8. M. Koštrun and R. Côté, *Two-color spectroscopy of fermions in mean-field BCS-BEC crossover theory.* Phys. Rev. A **73**, 041607(R) (2006).

9. P. Pellegrini,, M. Gacesa, and R. Côté, *Giant formation rates of ultracold molecules via Feshbach Optimized Photoassociation.* Phys. Rev. Lett. **101**, 053201 (2008).

10. P. Pellegrini, and R. Côté, *Probing the unitarity limit at low laser intensities.* New J. Phys. **11**, 055047 (2009).

11. E. Kuznetsova, M. Gacesa, P. Pellegrini, S.F. Yelin, and R. Côté, *Efficient formation of ground state ultracold molecules via STIRAP from the continuum at a Feshbach resonance.* New J. Phys. **11**, 055028 (2009).

12. J. Deiglmayr, A. Grochola, M. Repp, R. Wester, M. Weidemüller, O. Dulieu, P. Pellegrini, and R. Côté, *Influence of a Feshbach resonance on the photoassociation of LiCs.* New J. Phys. **11**, 055034 (2009).

Optical Two-Dimensional Spectroscopy of Disordered Semiconductor Quantum Wells and Quantum Dots

Steven T. Cundiff
JILA, University of Colorado and NIST, Boulder, CO 80309-0440
cundiff@jila.colorado.edu

July 24, 2009

Program Scope: The goal of this program is to implement optical 2-dimensional Fourier transform spectroscopy and apply it to electronic excitations, including excitons, in semiconductors. Specifically of interest are quantum wells that exhibit disorder due to well width fluctuations and quantum dots. In both cases, 2-D spectroscopy will provide information regarding coupling among excitonic localization sites.

Progress: During the last year, we have demonstrated the use of our new apparatus to observe two-quantum coherences in semiconductor quantum wells. In addition to seeing the expected two-quantum coherences between the ground state and the biexcition state, we also see them between the ground state and many-body states. We have also performed a detailed study of the polarization dependence of the real part of the two-dimensional Fourier transform (2DFT) spectra of quantum wells. We have also made to important technique advances. The first is a method of determining the overall phase of the 2DFT spectra using the interference pattern formed by the excitation beams. The second advance is the development of phase cycling techniques to cancel scattered light from the excitation beams that creates a noise background.

The coherent response of excitons in semiconductor quantum wells (QWs) is strongly dependent on the excitation conditions and material properties, such as polarization configuration and inhomogeneous broadening due to well-width fluctuations. Contributions to the light-matter interactions include the excitons themselves, the formation of excitonic "molecules," or biexcitons, and the many-body interactions of these states [1]. The interplay of these contributions has been explored though intensity- and polarization-dependent transient four-wave mixing (TFWM) studies. The latter result in changes in the dephasing time, the temporal profile of the emission, and a phase shift of the beats. Explanations of these results vary and include inhomogeneity or exciton-exciton interactions, such as exciton-exciton exchange, excitation-induced dephasing (EID), local-field corrections, and excitation-induced shift (EIS). Many authors have attributed the polarization dependence to biexcitons and their subsequent interactions.

We used 2DFT spectroscopy to separate and isolate the competing intra-actions and interactions of the excitons and biexcitons, which are strongly polarization dependent [L]. Through a quantitative comparison of the magnitude of 2DFT data and the line shape in the phase-resolved spectra, the selection rules were exploited to demonstrate the suppression of either many-body or biexcitonic effects in the coherent response. Clear indications of the associated contributions are observed in the 2DFT spectra, whereas they had only previously been inferred in TFWM experiments. Many-body interactions are observed for most excitation conditions as strong population and coherent coupling peaks, and as dispersive line shapes in the real part of the 2DFT spectra. When many-body interactions are suppressed however, the exciton and biexciton contributions are similar in strength and the off-diagonal coupling peaks nearly vanish.

One of the hallmarks of many-body interactions was the appearance of a signal for "negative" delay in two-pulse TFWM experiments. For an ensemble of non-interacting two-level systems, there is no signal for negative delay. These signals can be phenomenologically described as arising from local field effects, EID, biexcitonic effects or EIS. While the early work was motivated by explaining the negative delay signal, these effects also contribute, indeed dominate, for positive delay. TFWM could not reliably distinguish between these phenomena, an ambiguity resolved by 2DFT spectroscopy [A,E]. The 2D extension of this technique for molecular vibrations was proposed [2, 3] and observed [4, 5]. Its sensitivity to two exciton correlations in semiconductors was demonstrated in simulations [6, 7].

We measured 2DFT spectra for the pulse sequence that corresponds to the "negative" delay case in a two-pulse TFWM experiment. In two-pulse TFWM, the sample is excited by two pulses, $E_1(t-\tau)$ and $E_2(t)$ with wavevectors $\mathbf{k}_1$ and $\mathbf{k}_2$, respectively. Their interaction produces a signal $E_s \propto E_1^* E_2 E_2$ in the direction $\mathbf{k}_s = 2\mathbf{k}_2 - \mathbf{k}_1$ where the delay between the excitation pulses is defined to be positive if the conjugated pulse, E_1, arrives before pulse E_2. Thus "negative" delay means that the conjugated field arrives last. When the conjugated pulse arrives last in 2DFT spectroscopy, two-quantum coherences can be observed [4, 5]. Theory has shown that 2DFT spectra for this pulse ordering are very sensitive to two-exciton correlations [6, 7]. For excitonic resonances in semiconductors, we observe two-quantum coherences due to many-body effects in addition to those due to biexcitons, which were expected [8, 9]. By measuring the real part of the two-quantum coherences 1, as opposed to the magnitude as was done previously [9], we are able to resolve the different contributions and confirm that the dominant one is due to many-body interactions. The polarization of the excitation fields can be used to suppress the biexciton contribution, isolating the many-body effects. The results agree well with theory from the Mukamel group. These results have been submitted for publication.

2DFT spectroscopy can be implemented in a variety of geometries, which have varying success separating phase contributions from the signal and phase offsets associated with the pump beams or heterodyning interferometers. Obtaining this global phase allows extraction of the real and imaginary components of the 2DFT spectrum. The global phase is associated only with the third-order response function of the material, and is independent of the phase of the excitation pulses or the phase of any additional heterodyning pulses. The importance of this has been demonstrated with respect to finding absorptive lineshapes of vibrational correlations in molecules and in the many-body interactions of semiconductor excitons.

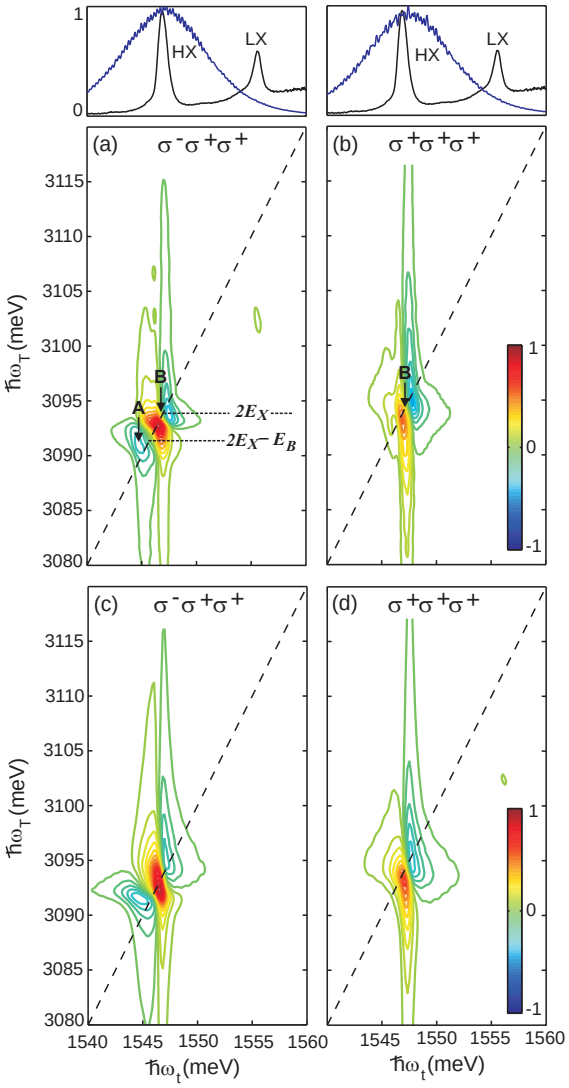

Figure 1: (Color) 2D two-quantum spectra of GaAs quantum wells at different polarizations. (a) Experimental spectra obtained using cross-circular ($\sigma^-\sigma^+\sigma^+$) polarization and (b) using co-circular ($\sigma^+\sigma^+\sigma^+$) polarization. The laser excitation shown above with the absorbance spectra is resonant with HX energy, therefore only the HX peak can be observed. E_X is the exciton energy, and E_B is the biexciton binding energy. (c) and (d) show simulations using the same polarizations.

For non-collinear phase-matching 2DFT experiments, correctly "phasing" the spectra has been achieved by matching the complex TFWM spectrum to the spectrally resolved transient absorption (SRTA), recorded in an auxiliary yet in situ measurement. The method requires using the two-beam, pump-probe geometry to mimic the exact excitation condition used in the 2DFT measurement, a criterion that is especially strict for semiconductor spectroscopy. However, mimicking these conditions exactly can be tricky since the geometry is different. Moreover, at low excitation densities matching the weak SRTA and complex TFWM spectra can lead to significant errors. Furthermore, SRTA cannot be measured to phase certain cases of 2DFT spectra; namely, cross-polarization and some virtual-echo techniques.

We developed a method for acquisition of the global phase for non-collinear 2DFT experiments without relying

on a SRTA measurement [J]. Instead, an all-optical measurement is demonstrated, which is based on using spatial interference patterns at the sample position combined with SI measurements. These demonstrations are performed on 2DFT spectra of semiconductor excitons in multiple quantum wells (MQWs). First, the samples are excited by suitably strong, co-linear polarized pump beams, where the SRTA measurement can provide good comparison to the all-optical scheme proposed. Secondly, a cross-linear polarized excitation case is presented where no such comparison is possible.

Phase cycling has been used in multidimensional NMR and collinear optical 2DFT spectroscopy to extract signals and remove noise, interference effects or multiple-quantum contributions. It is therefore useful for non-collinear experiments that suffer from a low signal-to-noise ratio. Some situations may be dominated by noise source such as pump scatter, which emanates from the same location as the TFWM signal. In 2DFT spectra, pump scatter is observed along the diagonal of the single-quantum spectra, because the pump is only self-coherent, i.e. only correlated when $\omega_t = \omega_\tau$. This is not an issue for two-quantum spectra, because the Fourier transform yields a different spectral range, without pump scatter. In the single-quantum 2DFT spectra, cycling the phase of the excitation pulses during a 2DFT scan suppresses the noise along the diagonal.

In NMR spectroscopy phase alternative pulse sequences (PAPS) are used, where the relative phase of the two RF pulses switches between in phase and out of phase every time step in a scan. Incorrectly phased artifacts in the detected signal then cancel when the Fourier transform is performed, leaving only the signal in the two-dimensional spectrum. The optical analogy of PAPS employed here records and averages two spectral interferograms that have nearly identical time delay and a controlled phase shift between two pairs of beams, thus allowing the incorrectly phased noise to cancel when averaged. An example is for an adjustment of the second time period T, such that the phase that is cycles is proportional to $\phi_T = n\pi + \omega_T T$, where the first term is toggled between $o\pi$ and 1π for every time step along axis τ. Our implementation of this algorithm strongly suppresses diagonal streaks in the 2DFT spectra. More complex phase cycling schemes can be used to remove the scatter from all pump pulses.

Future Plans: We are currently using the phase cycling technique to obtained improved 2DFT spectra from quantum dots formed in thin quantum wells due to fluctuations in the interfaces. Last year, we showed 2D spectra from this sample, however the neither the instrument resolution nor signal-to-noise ratio were sufficient to extract significant physics from these spectra. We have improved the resolution by inserting a relay lens to better match the CCD camera to the spectrograph. The signal-to-noise issue has been solved by using phase-cycling.

Our preliminary data show no signs of coherent coupling between the quantum dots. The homogeneous linewidth can be determined from the spectra. By varying the temperature, we can determine the role of phonon scattering in the homogeneous linewidth. Varying the excitation power will reveal the contribution from carrier-carrier scattering. We also expect to be able to see relaxation between the quantum dots by varying the delay T. Relaxation between dots could occur to phonon-assisted tunneling or activation out of the dot at higher temperatures.

Publication during the last 3 years from this project:

A. X. Li, T. Zhang, C.N. Borca, and S.T. Cundiff, "Many-Body Interactions in Semiconductors Probed by Optical Two-Dimensional Fourier Transform Spectroscopy," Phys. Rev. Lett. **96**, 057406 (2006).

B. I. Kuznetsova, P. Thomas, T. Meier, T. Zhang, X. Li, R.P. Mirin, S.T. Cundiff, "Signatures of many-particle correlations in two-dimensional Fourier-transform spectra of semiconductor nanostructures," Sol. State Commun. **142**, 154 (2007).

C. A. G. V. Spivey and S. T. Cundiff, "Inhomogeneous dephasing of heavy-hole and light-hole exciton coherences in GaAs quantum wells," J. Opt. Soc. Am. B **24**, 664 (2007).

D. L. Yang, I. V. Schweigert, S. T. Cundiff, and S. Mukamel, "Two-dimensional optical spectroscopy of excitons in semiconductor quantum wells: Liouville-space pathway analysis," Phys. Rev. B **75**, 125302 (2007).

E. T. Zhang, I. Kuznetsova, T. Meier, X. Li, R.P. Mirin, P. Thomas and S.T. Cundiff, "Polarization-dependent optical 2D Fourier transform spectroscopy of semiconductors," Proc. Nat. Acad. Sci. **104**, 14227 (2007).

F. I. Kuznetsova, T. Meier, S.T. Cundiff, and P. Thomas, "Determination of homogeneous and inhomogeneous broadening in semiconductor nanostructures by two-dimensional Fourier-transform optical spectroscopy," Phys. Rev. B **76**, 153301 (2007).

G. A. G. V. Spivey, C. N. Borca and S. T. Cundiff, "Correlation coefficient for dephasing of light-hole excitons and heavy-hole excitons in GaAs quantum wells," Solid State Commun. **145**, 303 (2008).

H. I. Kuznetsova, P. Thomas, T. Meier, T. Zhang, and S. T. Cundiff,"Determination of homogeneous and inhomogeneous broadenings of quantum-well excitons by 2DFTS: An experiment-theory comparison," to appear in Physica Status Solidi (c) (2008).

I. L. Yang, T. Zhang, A.D. Bristow, S.T. Cundiff and S. Mukamel, "Isolating excitonic Raman coherence in semiconductors using two-dimensional correlation spectroscopy," J. Chem. Phys. **129**, 234711 (2008).

J. A.D. Bristow, D. Karaiskaj, X. Dai and S.T. Cundiff, "All-optical retrieval of the global phase for two-dimensional Fourier-transform spectroscopy," Opt. Express **16**, 18017 (2008).

K. X. Li, T. Zhang, S. Mukamel, R.P. Mirin and S.T. Cundiff, "Investigation of Electronic Coupling in Semiconductor Double Quantum Wells using Optical Two-dimensional Fourier Transform Spectroscopy," Sol. State Commun. **149**, 361-366 (2008).

L. A.D. Bristow, D. Karaiskaj, X. Dai, R.P. Mirin and S.T. Cundiff, "Polarization dependence of semiconductor exciton and biexciton contributions to phase-resolved optical two-dimensional Fourier-transform spectra," Phys. Rev. B **79**, 161305(R) (2009).

M. S.T. Cundiff, T. Zhang, A.D. Bristow, Denis Karaiskaj and X.Dai, "Optical Two-Dimensional Fourier Transform Spectroscopy of Semiconductor Quantum Wells," to appear in Acct. Chem. Res., doi:10.1021/ar9000636 (2009).

N. A.D. Bristow, D. Karaiskaj, X. Dai, T. Zhang, C Carlsson, K.R. Hagen, R. Jimenez and S.T. Cundiff, "A Versatile Ultra-Stable Platform for Optical Multidimensional Fourier-Transform Spectroscopy," accepted for publication in Rev. Sci. Instr. (2009).

References

[1] S. T. Cundiff, "Coherent Spectroscopy of Semiconductors," Opt. Express **16**, 4639–4664 (2008).

[2] W. Zhang, V. Chernyak, and S. Mukamel, "Multidimensional Femtosecond Correlation Spectroscopies of Electronic and Vibrational Excitons," J. Chem. Phys. **110**, 5011–5028 (1999).

[3] A. Tortschanoff and S. Mukamel, J. Chem. Phys. **110**, 5007–5022 (2002).

[4] E. Fulmer, P. Mukherjee, A. Krummel, and M. Zanni, "A pulse sequence for directly measuring the anharmonicities of coupled vibrations: Two-quantum two-dimensional infrared spectroscopy," J. Chem. Phys. **120**, 8067–8078 (2004).

[5] S. Sul, D. Karaiskaj, Y. Jiang, and N.-H. Ge, "Conformations of N-acetyl-L-prolinamide by two-dimensional infrared spectroscopy," J. Phys. Chem. B **110**, 19,891–19,905 (2006).

[6] L. Yang and S. Mukamel, "Two-dimensional correlation spectroscopy of two-exciton resonances in semiconductor quantum wells," Phys. Rev. Lett. **100**, 057,402 (2008).

[7] L. Yang and S. Mukamel, "Revealing exciton-exciton couplings in semiconductors using multidimensional four-wave mixing signals," Phys. Rev. B **77**, 075,335 (2008).

[8] K. B. Ferrio and D. G. Steel, "Observation of the ultrafast two-photon coherent biexciton oscillation in a GaAs/$Al_xGa_{1-x}As$ multiple quantum well," Phys. Rev. B **54**, R5231–R5234 (1996).

[9] K. W. Stone, K. Gundogdu, D. B. Turner, X. Li, S. T. Cundiff, and K. A. Nelson, "Two-quantum 2D FT electronic spectroscopy of biexcitons in GaAs quantum wells," Science **324**, 1169–1173 (2009).

July 2009

Theoretical Investigations of Atomic Collision Physics

A. Dalgarno
Harvard-Smithsonian Center for Astrophysics
Cambridge, MA 02138
adalgarno@cfa.harvard.edu

We have constructed a methodology with which we can present a detailed description of the thermalization of initially energetic atoms traversing a cold atomic gas. The methodology also applies to the opposite case in which the atoms are initially cold and the bath gas is warm. In response to an inquiry from Claudio Cesar and Paolo Crivelli we have applied it to simulate an experiment they are designing that involves cold hydrogen atoms evolving in a warm neon gas. We calculated the H-Ne interaction potential taking care to achieve an accuracy sufficient to reproduce the van der Waals force at large internuclear distances. Our earlier studies had demonstrated that thermalization occurs through a sequence of scatterings at small angles that are controlled by the long range interactions. We then calculated the differential collision cross section which determines the kernel of the linear Boltzmann equation. The Boltzmann equation was solved by numerical integration for a range of initial conditions. The results supported the proposed experiment. We are continuing to explore the thermalization process including the case in which inelastic energy loss can occur and in which chemical reactions can occur. Experimental data on the evolving velocity distribution of energetic metastable oxygen atoms in molecular nitrogen are available.

There is a growing interest in examining ultracold systems involving positive ions and an experiment has been reported by Grier et al. who employed a dual ion-atom trap to measure charge transfer in collisions at ultralow energies of ytterbium ions Yb^+ with neutral ytterbium atoms Yb of a different isotopic composition. Because of the different isotope shifts of the ions and the atoms there is a small energy difference. It has large consequences at ultralow energies, including the failure of the Born-Oppenheimer approximation to distinguish between the isotopes so that the Born-Oppenheimer potential curves and wave functions do not separate to the correct limits. We believe we have solved the problem with a procedure that is a simple practical extension of the theory. Other methods have been suggested but seem difficult to apply for other than HD^+. We have carried out calculations for the two isotopes of Li^+ in Li for which the isotope shifts are known. Calculations for Ytterbium are in progress. We have also investigated resonance charge transfer for which the ion and atom isotopes are identical. The scattering lengths are sensitive to the reduced masses of the isotopic pairs. We have found an interesting approximate relationship between the Langevin expression for charge transfer and the scattering lengths. We propose to examine its validity for other cases such as Strontium.

The calculation of the Born-Oppenheimer interaction potentials to sufficient accuracy is a demanding task, at large internuclear distances, especially as the charge transfer cross sections depend on the difference between scattering in the gerade and ungerade states and in conventional variational methods the cancellation is extreme. There is a more subtle problem in that it is easier to achieve high accuracy for one of the two participating states than the other which enhances the error in determining the difference. The problem is most severe at large distances where the difference is decreasing exponentially. Because the difference is small it

should be possible to use some kind of perturbation theory and calculate the difference directly. There is a formula, attributed to Holstein and Herring that expresses the difference in terms of an integral over the median plane through the midpoint of the internuclear axis joining an ion to its neutral parent.

The integrand contains the polarized wave function of the electron that undergoes charge transfer. We have used an extension method in inverse powers of the internuclear distance R to evaluate the polarized wave functions for Li_2^+, Na_2^+, Rb_2^+ and Cs_2^+.

Rydberg atoms are sensitive probes of their environment and to exploit their potential reliable estimates of their interaction strengths are needed. Accurate information is needed to understand experiments involving ultracold spin-polarized hydrogen in Bose-Einstein Condensates and phenomena like photoassociation and ultracold plasmas. Quantitative calculations are important also as a means of identifying the molecular states which can be challenging if the states are found as a product of diagonalization methods. Surprising little is known about the details though important discoveries have been made by extensions of Fermi's original analysis. For hydrogen atoms the long range interactions have been obtained for ground state atoms interacting with excited Rydberg atoms with principal quantum up to n=3. We have now extended the principal quantum number to n=10. A special perturbation theory was needed and the resulting potential curves are extremely complicated. However as a function of n there are simplifying features.

Spin-polarized atoms and molecules are valuable in many areas of physics. However they are ordinarily created in a buffer gas in which collisions can lead to spin depolarization and to frequency shifts. The fundamental microscopic processes that give rise to spin depolarization are spin exchange and spin relaxation. Spin exchange transfers spin polarization from one atom to another and spin relaxation results in a loss of polarization due to the interaction of the electron spin with the orbital angular momentum of the collision complex. We are attempting to develop a comprehensive understanding of these processes and to predict their rates for the alkali metal atoms in a gas of ^{3}He. Spin exchange in binary collisions occurs through the Fermi contact hyperfine interaction of the valence electron of the alkali metal with the nuclear spin of ^{3}He.The strength of the interaction is proportional to the electron spin density of the atom-He complex at the helium nucleus. Compared to the free metal atom, the electron density is enhanced by the exchange interaction of the valence electron with the ^{3}He core. An atomic model has been constructed based on this physical picture. The interaction may be calculated directly using quantum chemistry methods and this we have done for Li-He which has only five electrons. Special care was needed to obtain reliable values of the spin density close to the nucleus. For the heavier atoms we adopted the atomic model. To estimate the enhancement factors for them we calculated the frequency shifts and matched them to experiment. The frequency shifts depend on the interaction potentials. These were available for Na and K but not Rb. For Rb we carried out ab initio calculations. The empirical enhancement factors obtained are respectively 2.0, 1.85 and 1.83 for Na, K and Rb. For Li we calculated an averaged value of 2.5. The calculated temperature dependence of the spin exchange rates is steeper than the measured rates for Na, K and Rb, a difference that is surely due to the use of the atomic model, as suggested by the results for Li.

The hyperfine constant of the alkali-metal atom is affected by the approach of the helium atom causing pressure-dependent frequency shifts of hyperfine levels. They have been observed in experiments with vapour cells. Happer and his collaborators have used perturbation theory to

estimate the variation with internuclear distance of the hyperfine interaction strength and we followed their approach. The case of Li-He is simple enough that for it we were able to carry through a direct quantum mechanical calculation which confirmed the accuracy of the perturbation method. The hyperfine pressure shift is large and negative at small nuclear separations but because of the repulsive nature of the interatomic potential the small R region makes little contribution to the overall pressure shift. For similar reasons the pressure shifts for the heavier alkali metal atoms are small despite the greater magnitude of the interaction strengths. Collisions at ultracold temperatures are of special interest for applications in magnetic trapping and evaporative cooling. We have computed the spin-exchange rate coefficients as a function of energy in a magnetic field of 1 G .Small variations in the form of the Fermi contact interaction can lead to large changes in the spin-exchange cross sections. The ratios of the rate constants for diffusion and inelastic scattering are very large. Our calculations ignore the anisotropic component of the hyperfine interaction and these ratios may change when we include it but we expect them to remain large.

Spin relaxation for which there is no change in the nuclear spin state of ^{3}He is driven by a spin-rotation coupling and a change of magnetic quantum number of plus or minus 1 can result in a collision with He. We used a model introduced by Walker, Thywissen and Happer and applied it to K atoms. The rate coefficient is negligible at low temperatures but increases rapidly above 10K to values of order 10(-17)cm3s^{-1} at 600K in a magnetic field of 2 Tesla. A more accurate calculation of the coupling constant is desirable. It can be carried out though it involves the evaluation of the spin-orbit interaction and non-adiabatic coupling to electronically excited molecular states.

We are interested in controlling the behavior of dipolar molecules that have both electric and magnetic dipoles in the presence of electric and magnetic fields. We have carried out elaborate calculations of the scattering of OH molecules. OH is an important constituent in astrophysical and atmospheric environments. More generally doublet pi molecules may provide tests of physics beyond the standard model. The quantum mechanical formalism for collisions of doublet pi molecules in the absence of external fields has been worked out by Alexander and we have extended it to examine the influence of fields on the structure and on collisions with helium. We find that electric fields of less than 15 kV/cm greatly enhance the probability for Stark relaxation. The total cross sections are dominated by elastic scattering and increase smoothly with decreasing energy. They give limited evidence of rapid variations near excitation thresholds and disagree with recent experiments. Further analysis is warranted.

Publications 2007-2009

E. Abrahamsson, R.V. Krems and A. Dalgarno, Fine Structure Excitation of OI and CI by Impact with Atomic Hydrogen, ApJ 654, 1171, 2007.

Xi Chu, Alexander Dalgarno and Gerrit C. Groenenboom, Dynamic polarizabilities of rare-earth-metal atoms and dispersion coefficients for their interaction with helium atoms Phys. Rev. A. 75, 032723, 2007.

P. Zhang, V. Kharchenko and A. Dalgarno, Thermalization of supertherm al N(^{4}S) atoms in He and Ar gases, Molec. Phys. 105, 1487, 2007.

G. C. Groenenboom , X. Chu and R.V. Krem s, Electronic An isotropy between Open She ll Atoms in First and Second Order Perturbation Theory, J. Chem. Phys.126 204306, 2007.

B.C. Shepler, B. H. Yang, T. J. Dhilip Kum ar, P.C. Stancil, J. M. Bowm an, N. Balakrishnan, P. Zhang, E. Bodo, and A. Dalgarno, L ow Energy H+CO Scattering Revisited: CO Rotational Excitation with New Potential Surfaces, A&A 475, L15-L18, 2007.

P. Zhang and A. Dalgarno Static Dipole Pola rizability of Ytterbium, J. Phys. Chem . A, 111 , 12471, 2007.

P. Zhang, V. Kharchenko, A. Dalgarno, Y. Matsumi, T. Nakayama and K. Takahashi, Approach to Thermal Equilibrium in Atomic Collisions, Phys. Rev. Lett. 100, 103001, 2008.

E. Bodo, P. Zhang and A. Dalgarno, Ultraco ld Ion-Atom Collis ions: near Resonant Charg e Exchange, New J. Phys. 10, 033024, 2008.

P. Zhang and A. Dalgarno, Long-Range Interactions of Ytterbium Atoms, Molec. Phys., 106, 1525, 2008.

P. Zhang, V. Kharchenko, A. Dalgarno, Y. Matsumi, T. Nakayama and K. Takahashi, Approach to Thermal Equilibrium in Atomic Collisions, Phys. Rev. Lett. 100, 103001, 2008.

E. Bodo, P. Zhang and A. Dalgarno, Ultraco ld Ion-Atom Collis ions: near Resonant Charg e Exchange, New J. Phys. 10, 033024, 2008.

P. Zhang and A. Dalgarno, Long-Range Interacti ons of Ytterbium Atoms, Molec. Phys. 106, 1525, 2008.

D. Vrinceanu and A. Dalgarno, L ong-range In teraction between Ground and Excited State Hydrogen Atoms, J. Phys. B At. Mol. Opt. Phys. 41, 215202, 2008.

T. V. Tscherbul, P. Z hang, H. R. Sadeghpour, N. Brahm s, Y. S. Au J. M. Doyle and A. Dalgarno, Collision-induced Spin Depolari zation of Alkali-M etal Atoms in Cold ^{3}He Gas, Phys. Rev. A 78, 060703R 2008.

T. V. Tscherbul, G. C. Groenenboom, R. V. Krems and A. Dalgarno, Dynam ics of OH(^{2}II)-He Collisions In Combined Electric and Magnetic Fields, Faraday Discuss. in press 2009.

M. J. Jamieson, A. Dalgarno, M. Aym ar and J. Tharam el, A Study of Exchange Interactions in Alkali and Molecu lar Ion Dimers with Applic ation to Charge Transfer in Cold Cs, J. Phys B.: At. Mol. Phys. in press 2009.

S. Bovino, P. Zhang, V. Kharchenko and A. Dalgarno, Trapping Hydrogen Atoms from a Neon-Gas Matrix: A Theoretical Simulation, J. Chem. Phys. in press 2009.

Z. Pavlovich, T. V. Tscherbul, H. R . Sade ghpour, G. C. Groenenboom and A. Dalgarno, Cold Collisions of OH(^{2}II) Molecules with He Atom s in External Fields, J. Phys. Chem . A in press 2009.

Production and trapping of ultracold polar molecules

D. DeMille
Physics Department, Yale University, P.O. Box 208120, New Haven, CT 06520
e-mail: david.demille@yale.edu

Program scope: The goal of our project is to produce and trap polar molecules in the ultracold regime. Once achieved, a variety of novel physical effects associated with the low temperatures and/or the polar nature of the molecules should be observable. We will build on recent results from our group, in which we form and trap ultracold RbCs. We plan to transfer the vibrationally excited molecules currently trapped into their absolute internal ground state and then study the resulting sample of polar molecules. We will investigate a variety of techniques for creating, manipulating and probing this sample, including methods for "distilling" a pure ground-state sample, imaging detection, continuous accumulation of ground state-molecules, etc. Once in place, we will study chemical reactions at ultracold temperatures.

Our group has pioneered techniques to produce and state-selectively detect ultracold heteronuclear molecules. These methods yielded RbCs molecules at translational temperatures $T < 100$ μK, in any of several desired rovibronic states—including the absolute ground state, where RbCs has a substantial electric dipole moment. Our method for producing ultracold, ground state RbCs consists of several steps. In the first step, laser-cooled and trapped Rb and Cs atoms are bound together into an electronically excited state, via the process known as photoassociation (PA).[1] These states decay rapidly into a few, weakly bound vibrational levels in the ground electronic state manifold.[2] By proper choice of the PA resonance, we form metastable molecules exclusively in the $a\ ^3\Sigma^+$ level. We also demonstrated the ability to transfer population from these high vibrational levels, into the lowest vibronic states $X\ ^1\Sigma^+(v=0,1)$ of RbCs [3] using a laser "pump-dump" scheme. Two sequential laser pulses drove population first "upward" into an electronically excited level, then "downward" into the vibronic ground state. In these initial experiments, the vibronic ground- state molecules were spread over a small number (2-4) of the lowest rotational levels, determined by the finite spectral resolution of the pump/dump lasers. We state-selectively detect ground-state molecules with a two-step, resonantly-enhanced multiphoton ionization process (1+1 REMPI) followed by time-of-flight mass spectroscopy.[4]

In more recent work, we have incorporated a CO_2-laser based 1D optical lattice into our experiments. This makes it possible to trap and accumulate vibrationally-excited RbCs molecules as they are formed. (Previously, the molecules were not subject to the magneto-optic trapping forces that held the atoms.) In this optical trap, we have demonstrated the ability to hold the precursor Rb and Cs atoms with long lifetimes ($\gtrsim$5 s). We also have the ability to selectively remove either atomic species by resonant push-beams. We measure molecule number in individual states, using the same methods as earlier. We used these capabilities to measure inelastic (trap loss) cross-sections for individual RbCs vibrational levels on both Rb and Cs atoms in the ultracold regime.[5] We also developed a simple theoretical model for these collisions which matches our data reasonably well. We hope to observe molecule-molecule collisions in the near future, once molecular densities are fully optimized.

We are now preparing to transfer this sample of trapped molecules to their absolute internal ground state. In this X(v=0, J= 0) state the molecules should be immune to all (two-body)

inelastic collisional loss processes, and should also possess a sizeable dipole moment (~1.3 D). To accomplish this, we plan to use an improved version of the method we demonstrated earlier for producing (untrapped) ground-state molecules. A pair of lasers, tuned to the same transitions as used before, will again be used for the transfer. However, here we plan to use a coherent (STIRAP, STimulated Raman Adiabatic Passage) process rather than the incoherent, stepwise method as before. Use of STIRAP is made possible by the small size of our sample and the resulting high Rabi frequencies attainable by tight focusing of single-mode diode lasers. We estimate transfer efficiencies of ~80% should be possible even with "standard" lasers (~0.5 MHz linewidth).

We have carefully considered limitations on STIRAP due to details of the molecular levels due to e.g. hyperfine and rotational structure. We find that high efficiency of ground-state molecule production almost certainly requires full control of all degrees of freedom, including nuclear spins. This analysis was deepened and informed by our recent experiments studying the level structure of deeply-bound Cs_2 ground-state molecules.[6] To address this issue, we now optically pump our trapped atoms to spin-stretched states, and plan to use appropriate laser polarizations and transitions to remain in a stretched state throughout the PA and STIRAP processes. Identification of the correct transitions requires knowledge of the hyperfine structure in each electronic level of the process, and we will use the first STIRAP laser to measure this structure in sufficient detail. A similar technique has now been demonstrated for producing ultracold trapped KRb molecules by the JILA group,[7] validating our basic approach.

Once we have demonstrated the STIRAP transfer to the ground state, we plan to develop a variety of techniques for manipulating and studying this sample. Among the first questions will be the collisional stability of the ground-state molecules. Of particular concern in our approach is loss due to collisions with residual, vibrationally excited molecules. We plan to selectively re-introduce Cs atoms to the trap to address this problem: based on our measurements of "maximal" (i.e., unitarity-limited) inelastic cross-sections for the vibrationally excited molecules, it appears viable to use a high-density Cs cloud as a "scrubber" to eliminate the troublesome species. We note that RbCs + Cs collisions (with both species in their absolute lowest hyperfine sublevel) have no two-body inelastic channel energetically available,[8] so that Cs should not be able to cause loss of the desired ground-state molecules. We also plan to study inelastic loss of RbCs in excited hyperfine sublevels due to collisions with Rb, to see if the surprising large loss rates observed by the JILA group in KRb + Rb collisions of this type[9] are also present here.

Compared to the recent KRb work at JILA, a novel feature of our current system is the REMPI detection system, which should make it possible to state-selectively detect the products of ultracold chemical reactions in our sample. Based on the recent results from JILA,[9] we anticipate that RbCs + Rb samples will rapidly react to form Cs + Rb_2, and we plan to map out the resulting internal state distribution of the outgoing products. In addition, in pure samples of ground state RbCs, chemical reactions are energetically forbidden; however, the reaction barrier can be overcome by vibrationally exciting the molecules with another STIRAP step.

We also plan to develop methods for imaging detection of the ground- state RbCs molecules. This is far more difficult than for atoms, because of the lack of cycling optical transitions. However, the experience of the community studying quantum-degenerate atomic gases makes it plain that imaging detection is a tool so powerful it must be maintained. Here we plan to build on our experience with REMPI detection, and replace our simple channeltron detector with an imaging ion detection setup (microchannel plate + phosphor screen + fiber optic image conduit + CCD camera).[10] Once this method is established, we can effectively study the variety of

interesting two-body and m any-body physics associated with polar m olecules. These include phenomena such as ultra-long rang e "field-linked" states of pol ar m olecules in an external electric field,[11] extraordinarily large ($\sim 10^8$ Å^2) elastic collision rates with nontrivial dependence on the strength of a polarizing electric field and th e attendant possibility of evaporative cooling,[12,13] many-body states such as liquid-crystal-like chains[14] or dipolar crystals;[15] etc.

References

[1]A.J. Kerman *et al.*, Phys. Rev. Lett. **92**, 033004 (2004).

[2]T. Bergeman *et al.*, Eur. Phys. J. D **31**, 179 (2004).

[3]J.M. Sage, S. Sainis, T. Bergeman, and D. DeMille, Phys. Rev. Lett. **94**, 203001 (2005).

[4]A.J. Kerman *et al.*, Phys. Rev. Lett **92**, 153001 (2004).

[5] Eric R. Hudson, Nathan B. Gilfoy, S. Kotochigova, Jeremy M. Sage, and D. DeMille. Inelastic collisions of ultracold heteronuclear molecules in an optical trap. Phys. Rev. Lett. **100,** 203201 (2008). [DOE SUPPORTED]

[6] D. DeMille, S. Sainis, J. Sage, T. Bergeman, S. Kotochigova, and E. Tiesinga. Enhanced sensitivity to variation of me/mp in molecular spectra. Phys. Rev. Lett. **100**, 043202 (2008). [DOE SUPPORTED]

[7] K.-K. Ni *et al.*, Science **322**, 231 (2008).

[8] C.E. Fellows *et al*., J. Mol. Spectrosc. **197,** 19 (1999); J.Y. Seto *et al.*, J. Chem. Phys. **113**, 3067 (2000); C. Amiot and O. Dulieu, J. Chem. Phys. **117**, 5155 (2002).

[9] J. Ye and D. Jin, private communication (2009).

[10] D.W. Chandler and P.L. Houston, J. Chem. Phys. **87**, 1445 (1987); A.J.R. Heck and D.W. Chandler, Annu. Rev. Phys. Chem. **46**, 335 (1995).

[11]A.V. Avdeenkov and J. L. Bohn, Phys. Rev. Lett. **90**, 043006 (2003); A.V. Avdeenkov, D.C.E. Bortolotti and J.L. Bohn, Phys. Rev. A **69**, 012710 (2004).

[12]D. DeMille, D.R. Glenn, and J. Petricka, Eur. Phys. J. D **31**, 275 (2004).

[13]M. Kajita, Eur. Phys. J. D **20**, 55 (2002); C. Ticknor, Phys. Rev. A **76**, 052703 (2007).

[14] D.-W. Wang, M.D. Lukin, and E. Demler, Phys. Rev. Lett. **97**, 180413 (2006).

[15] H. P. Buechler *et al.*, Phys. Rev. Lett. **98**, 060404 (2007).

ATTOSECOND AND ULTRA-FAST X-RAY SCIENCE

Louis F. DiMauro
Department of Physics
The Ohio State University
Columbus, OH 43210
dimauro@mps.ohio-state.edu
co-PI: Pierre Agostini (OSU Physics)

1.1 PROJECT SCOPE

This document describes the BES funded pr oject (grant #: DE-FG02-04ER15614) entitled "Attosecond & Ultra-Fast X-ray Science" at The Ohio St ate University (OSU). Over the past few y ears, we have developed the tools, skills and me trology necessary to conduct the propose d attosecond experiments. Progress over the past y ear includes (1) mea surement of the wavel ength dependence of th e attochirp, (2) construction and commissioning of an attosecond beamline/end-station for RABBITT phase measurements for attosecond science and (3) design and commissioning of a 2π magnetic bottle electron spectrometer for use at OSU and the AMOS end-station at the LCLS XFEL at SLAC.

The original proposal outl ines an experim ental program designed to stud y high harmonic generation in gases and attosecond synthesis using long wavelengt h laser sources. The objective is to explore the scaling of the intense laser-ato m interaction and provide a potential path towards the production of *light pulses with both the time-scale and the length-scale each approaching atomic dimension*. In other words, the formation of kilovolt x-rays bursts with attosecond (10^{-18} s) duration.

Over the pas t y ear we ha ve perfor med both experimental and theoretical stu dies that ver ify the efficacy of this approach. The n ear future will see the applications of these advances for investigating electron dynamics.

1.2 PROGRESS IN FY09

Spectrally resolved high harmonic radiation generated by driving wavelengths of 0.8 μm, 1.3 μm and 2 μm. The high har monics fr om various inert gases we re explored using different fundamental wavelengths. The 2 μm observations were particularly im portant since the uniq ue scaling strateg y discussed in the proposal exploits the behavior of a n atom in long wavelength ($\lambda > 1$ μm) fields. For example, our 2 μm measurements estab lish that high harm onic generation in argon extends t o a photon energy of 220 eV, validating the scaled phy sics. The findings of these studies are su mmarized in Fig. 1 and have been published in Nature Physics in 2008.

Measurement of the wavelength dependence of the attochirp. The above stud y established that long wavelength f undamental fields can generate a higher p hoton energ y cutoff in t he spectru m. However, the critical information needed for com plete description of an attosecond pulse is t he phase o f the different spectral components. In absence of complete characterization, the minimal information set is the relative phase betwe en the adjacent har monic orders. V arious methods based on two-color photoionization have been developed for spectral phase measurements.

In order to gain some initial insight into the spectral phase of the high harmonic spectrum we adopted an all-optical method introduced by Dudovich *et al.* [1]. In this measurement, harmonics are generated using a two-color field composed of an intense fundamental field (ω) and a weak 2ω field. The 2ω field is derived using 2nd harmonic generation in a standard nonlinear crystal and sufficiently weak not to cause HHG alone. The two colors have a defined phase relationship that is controlled by introducing a differential optical path length. The spectrum is composed of intense odd-order (H39-H61) harmonics and weaker even-orders (H40-H62). The phase information is obtained by analyzing the relative phase shift in the oscillating amplitude between successive even harmonics orders.

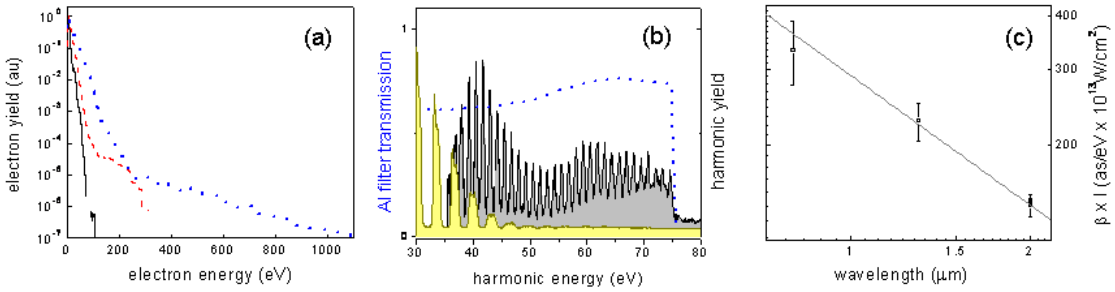

Figure 1: A compilation of experimental results achieved over the last two years that unequivocally establish the impact that longer wavelength fundamental fields have on the production of both high-energy (a) electrons, (b) photons and (c) the production of attosecond pulses. Both plots (a) and (b) verify the λ^2-scaling prediction of the quasi-classical model for increasing the electron and photon energy. Furthermore, measurements show that although the harmonic production efficiency for a single atom decreases with longer wavelength, favorable phase-matching conditions are achievable. Plot (c) shows the scaling of the attochirp derived from our spectral phase measurements. The solid line is the λ^{-1} decrease in the atto chirp predicted by both quasi-classical and quantum analysis, in agreement with our measurement.

We have used this method to measure the spectral phase of the high harmonic comb at three different fundamental wavelengths (0.8 μm, 1.3 μm and 2 μm) and on two different inert gas atoms (argon and xenon). This is the first experimental measurement of the attochirp as a function of fundamental wavelength. This work has been published in Physical review Letters in 2009.

Figure 2 shows that result of our analysis of the attochirp for argon atoms at 0.8 μm and 2 μm. The comparison is performed at constant intensity. Figure 2(a) shows the interpolated recombination time (phase) derived from the all-optical measurement plotted as a function of frequency (harmonic order). The figure is essentially a dispersion plot, and for the two wavelengths shown the dispersion is positive. The attribute to note is that the slope is smaller for the 2 μm fundamental field than 0.8 μm field, e.g. less dispersion. This was the critical feature predicted by us and now has been experimentally verified: longer wavelength fundamental fields produce inherently shorter attosecond burst. Figures 2(b) and (c) are the attosecond pulses reconstructed from the measured phase and amplitude. The results verify the reduction in pulse duration at 2 μm compared to 0.8 μm. Note, the all-optical measurement retrieves the phase in the generation gas source and thus any external dispersion management cannot be measured but the figures does show (red line) the ultimate duration expect with metal filter compensation. A more precise measurement will be performed with the RABBITT method, described in the next section.

The results of these measurements are compiled in the Fig. 1(c). The plot shows the measured attochirp as a function of fundamental field wavelength and the λ^{-1}-scaling predicted by the quasi-classical model. The salient point is that longer wavelength fundamental fields produce inherently shorter attosecond bursts, as well as higher photon energy.

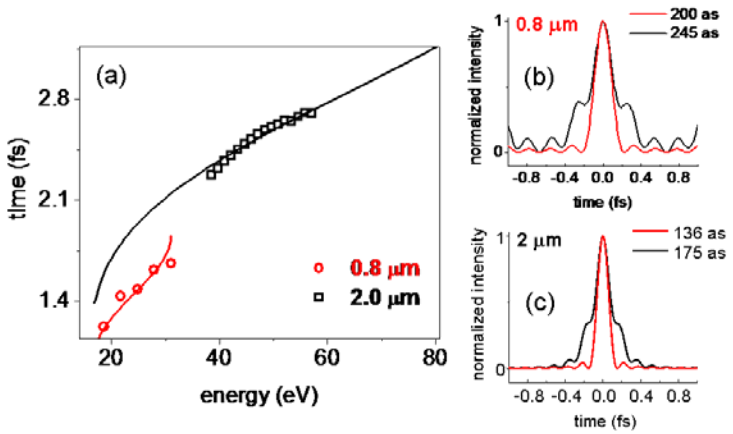

Figure 2: The wavelength dependence of the attochirp. Plot (a) is the emission time as a function of harmonic order for 0.8 μm (red circles) and 2 μm (black squares) fundamental fields at constant intensity. Plots (b) and (c) are the reconstructed pulses (black line) using the phases in (a).

OSU attosecond beamline/end-station for RABBITT measurements. The RABBITT method [2], developed by Agostini and collaborators, is a more direct and reliable measurement of the spectral phase. This method was used to measure the first attosecond pulses. The method is a two-color, pump-probe interferometric technique based on photoionization. The spectral phase is directly extracted from the experiment.

The OSU attosecond beamline/end-station is capable of conducting RABBITT measurements, among other. The apparatus is now complete and preliminary photoelectron harmonic investigations are underway. The apparatus consists of three vacuum chambers (left to right in Fig. 3): harmonic generation source, XUV focusing and electron spectrometer. The optical system is contained within the vacuum chambers and has automated opto-mechanical interferometric stability with attosecond precision.

In the harmonic source chamber, high harmonics are generated in by a high density gas jet interacting with an intense (10^{14} W/cm^2) laser pulse. The size of the harmonic source chamber is sufficient to support a variety of optical geometries and different wavelength (0.8-2 μm) operation. A RABBITT probe beam is derived by splitting a small fraction (~5 %) of the fundamental beam.

The differential pumped XUV focusing chamber allows spectral and spatial filtering and contains a toroidal mirror for focusing the harmonic beam and a spherical mirror for focusing the RABBITT probe beam. Both the focused harmonic and probe beams spatially overlap in the UHV 2π-electron spectrometer chamber. The electron spectrometer is a 2π-magnetic bottle design with a 1.1 meter flight tube. This design provides efficient electron collection (2π-angular acceptance) and excellent energy resolution (2-3 %) over a large energy range for the RABBITT measurement. A suitable inert gas atom is leaked into the electron spectrometer for the RABBITT measurement and the attosecond pump-probe delay is introduced by a delay line located in the harmonic source chamber. The electron spectrometer was designed and constructed by a graduate student (Chris Roedig) and has been tested. This spectrometer is the prototype for a similar instrument constructed at OSU for the initial experiments at the LCLS XFEL in collaboration with Dr. John Bozek (SLAC). The LCLS spectrometer is scheduled for delivery to SLAC at the end of July 2009.

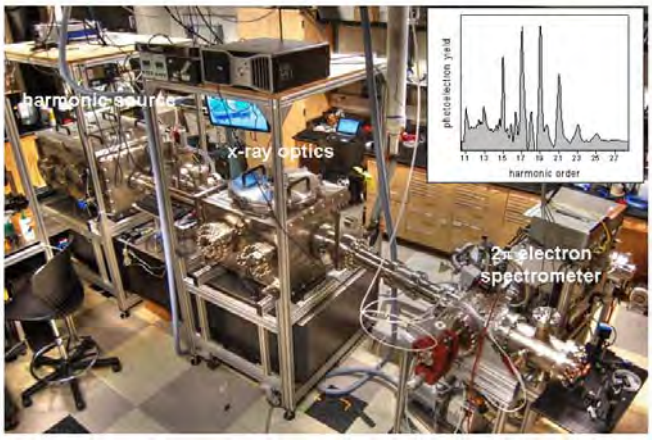

Figure 3: Photography of the OSU attosecond beamline/end-station. The current end-station is for gas-phase studies using the OSU designed 2π-magnetic bottle electron energy spectrometer. The beamline is designed to support different end-stations. The inset shows an initial photoelectron energy spectrum produced by ionizing argon atoms with high harmonics produced by the beamline.

1.3 Proposed Studies in FY10

The following is a brief description of experimental plans in FY10:

1. Finish characterization of the OSU attosecond beamline/end-station apparatus.
2. Begin RABBITT measurements on argon using 0.8 μm, 1.3 μm and 2 μm fundamental fields.
3. Begin FROG measurements using the Keldysh scaled systems and compare to current theoretical models of strong-field harmonic generation.

1.4 References Cited

[1] N. Dudovich *et al.*, Nature Phys. **2**, 781 (2006).

[2] P. Paul *et al.*, Science **292**, 1689 (2001).

1.5 Publication Resulting from this Grant

1. L. F. DiMauro, J. Arthur, N. Berrah, J. Bozek, J. N. Galayda and J. Hastings, "Progress Report on the LCLS XFEL at SLAC", J. Phys. **88**, 012058 (2007).
2. P. Colosimo *et al.*, "Scaling strong-field interactions towards the classical limit", Nature Phys. **4**, 386 (2008).
3. O. Guyetand *et al.*, "Complete Momentum Analysis of Multi-Photon Photo-Double Ionization of Xenon by XUV and Infrared Photons", J. Phys. B **41**, 065601 (2008).
4. P. Agostini and L. F. DiMauro, "Atoms in high intensity mid-infrared pulses", Contemp. Phys. **49**, 179 (2008).
5. G. Doumy *et al.*, "Attosecond Synchronization of High Harmonics from Mid-Infrared Drivers", Phys. Rev. Lett. **102**, 093002 (2009).
6. G. Doumy *et al.*, "The Frontiers of Attosecond Physics", in Proceedings of the International Conference on Atomic Physics, (World Scientific Press, Singapore, 2009) 333-343.
7. T. Auguste et al., "Driving-Frequency Scaling of High Harmonic Quantum Paths", Phys. Rev. A, in review.

IMAGING OF ELECTRONIC WAVE FUNCTIONS DURING CHEMICAL REACTIONS

Louis F. DiMauro
Department of Physics
The Ohio State University
Columbus, OH 43210
dimauro@mps.ohio-state.edu
co-PI: Pierre Agostini (OSU Physics) and Terry A. Miller (OSU Chemistry)

1.1 PROJECT SCOPE

Understanding chemistry at its most fundamental level requires the ability to visualize the electrons that form chemical bonds and ultimately the capacity to control the creation and destruction of these bonds. Femtochemistry provided the way to "clock" the nuclear dynamics of reactant molecules on the 10-100's femtosecond (10^{-15} s) time-scale. However, chemical mechanisms involve the movement of electrons around the (nuclear) structure of the molecule. Once the electrons move the nuclei adjust along the resulting potential energy surface causing the chemical reaction to occur. Experimentally clocking and imaging this initial electron "movement" is unfulfilled and has been identified as one of the five grand challenges for advancing the future of energy research by a DOE/BES report. This project directly addresses this challenge by "watching" and "clocking" the electron motion during a chemical bond breaking. The program exploits the strong-field scaling at long wavelength for (1) the realization of attosecond (10^{-18} s) bursts of XUV light (the electronic "clock") and (2) the tomographic imaging of the molecular wave function (the detector to "watch"). The approach builds on the pioneering work of the NRC group in Canada that utilizes the sub-cycle process responsible for the production of attosecond pulses itself, for producing a "static" image of the HOMO for aligned N_2 molecules. Given the inherent ultra-fast time scale of the process the method could, in principle, record the orbital's evolution during the creation or destruction of a chemical bond.

1.2 PROGRESS IN FY09

The wavelength scaling of strong field interactions. In connection with our DOE-funded project on attosecond generation (DE-FG02-04ER15614), we have verified the efficacy of λ^2-scaling for increasing the cutoff energy for electrons and harmonics [*1*] and the λ^{-1}-scaling decrease in the attochirp [*2*]. These studies enabled the development of the tools needed to address the aims of this proposal and established the impact that longer wavelength fundamental fields on the production of both high-energy (a) electrons, (b) photons and (c) the formation of shorter attosecond pulses.

Test of the Keldysh picture using low binding energy systems. Investigations using cesium atoms as a weakly bound system prototype for future imaging studies on NO excited states have been conducted to examine whether tunnel ionization can be realized using long wavelength fields. Our experiments are studying both the photoelectron energy (PES) and harmonic spectral distributions resulting from the interaction of Cs with intense 100 fs, 3.6 μm pulses. The results are consistent with non-perturbative tunnel ionization and the Keldysh picture of scaled dynamics.

High harmonics generated from aligned molecules. In our experiment, 30-50 fs light pulses from a 1-3 kilohertz repetition rate laser system interacts with a *cw*-gas jet expansion of N_2. The experiment is performed using two temporally delayed linearly polarized pulses: (1) a weak ($<10^{13}$ W/cm^2), 0.8 μm *pump* pulse impulsively aligns the molecule and (2) a delayed intense laser *probe* pulse drives ionization and harmonic generation. The relative delay, intensity and polarization of both pulses can be independently varied. The lower inset in Fig. 1(a) and (b) shows the first half-revival of the N_2 rotational wave packet near 4-5 ps after the pump pulse. The ordinate is the ratio of the integrated harmonic yield for aligned versus unaligned signal for parallel polarized pump and probe pulses. The alignment plot

shows the usual characteristics, an increase around 4.1 ps corresponding to harmonic generation from N_2 that are strongly aligned along the probe's polarization axis while the minimum at 4.5 ps corresponds to the N_2 molecules being anti-aligned. The 0.8 μm probe experiments presented in Fig. 1(a) have conditions and results similar to those reported by Itatani *et al.* [*3*]. In this case, the shortest deBroglie wavelength is 1.5 Å (3 *a.u.*) determined by the 70 eV cutoff energy (maximum order 45 th-order). Fig. 1(b) shows the similar experiment except using a ~170 TW/cm^2, 1.3 μm probe pulse for generating the harmonics while the wavelength of the aligning pump pulse is maintained at 0.8 μm. A typical high harmonic spectrum is shown in the upper inset in Fig. 1(b); the 75 eV cutoff energy is instrumental. The actual measured harmonic cutoff is 100 eV. Under these conditions the deBroglie wavelength is 1.05 Å corresponding to a 30% increase in resolution over the 0.8 μm experiment.

The tomographic reconstruction of N_2 molecules. The procedure for the tomographic reconstruction using the 0.8 μm and 1.3 μm high harmonic data shown in Fig. 1 is now functional and the initial results for the nitrogen HOMO are shown in Fig. 2(e) and (f).

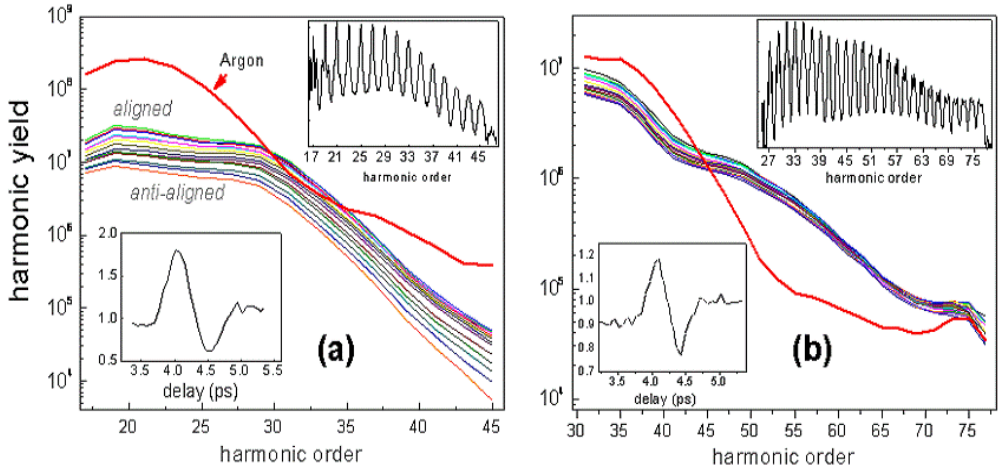

Figure 1: High harmonic generation from aligned N_2 using (a) 0.8 μm and (b) 1.3 μm probe pulses. The bottom insets show the first rotational half revival plotted as the integrated harmonic signal as a function of delay from the 0.8 μm aligning pulse. The top insets show a typical odd-order harmonic comb for the two respective probe wavelengths. The solid lines depict the dependence of harmonic spectrum (integrated over a peak) on the molecular alignment as the relative polarization is varied in 5° steps.

The steps of the reconstruction procedure are similar to that Ref. [*3*] i.e. a 2D inverse Fourier transform obtained from the 2D Fourier transform of the dipole moment obtained by successive 1D transforms and application of the Fourier slice theorem. For contrast, the orbital reconstructed by the NRC group [*3*] and those calculated by Le *et al.* [*4*] are also shown. The latter is a pure theoretical study, the orbital is reconstructed from the harmonics distributions from aligned molecules calculated using the Lewenstein model. The calculated distributions at 0.8 μm and 1.2 μm thus mimic the "experimental" data for the reconstruction. The procedure involves, besides the Fourier manipulation, the measurement of a reference harmonic spectrum from a spherically symmetric system with a similar ionization potential, e.g. Ar and N_2, and the knowledge of a spectral phase shift of the harmonics. An approximate value for the latter can be derived, as in Ref. [*3*], from the two-center model using an inter-nuclear distance of R= 1.1 Å for N_2, or determined from a separate experiment using the all-optical or RABBITT methods proposed here. Using the value for the phase-shift reported in Ref. [*3*] the reconstruction shown in Fig. 2(e) for a 0.8 μm driver appears to have a structure similar to that obtained by Le *et al* [*4*] (Fig. 2[a]). Both lack spatial precision compared to the exact HOMO orbital (Fig. 2[c]). On the other hand, the reconstructed orbital (Fig. 2[d]) of Itatani *et al.* [*3*] reproduces more accurately the *ab-initio* orbital. It should be noted additionally that the shortest deBroglie wavelength at 0.8 μm is 1.5 Å while the features in Fig. 3(d) seem more resolved. Clearly, this raises issues concerning the uniqueness of the orbital reconstruction that our

program strives to address. Among these issues are the question of the harmonic polarization, and that of the experimental determination of the actual harmonic spectral phase. In our experiments the harmonic polarization was not measured.

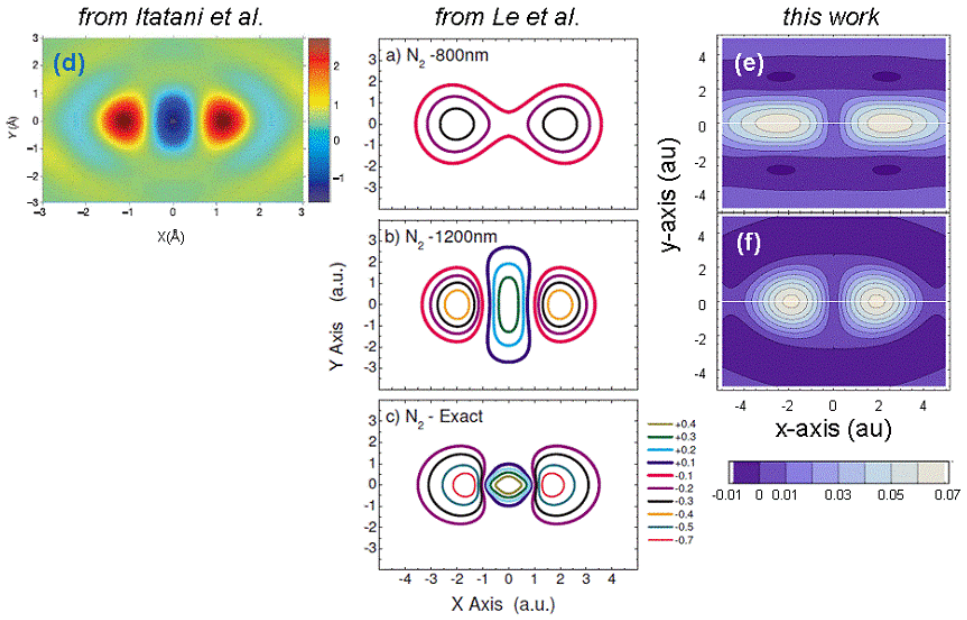

Figure 2: A comparison of the N_2 HOMO reconstruction for different fundamental wavelengths from different groups. Reconstructions are produced at (e) 0.8 μm and (f) 1.3 μm using the harmonic data reported in this proposal while plot (d) is the original work of Itatani *et al.* [3] at 0.8 μm. Plots (a) and (b) are from the theoretical analysis of Le *et al.* [4] at 0.8μm and 1.2 μm, respectively and (c) is the *ab-initio* calculation. Note, that the scale in (a) is Angstrom while the others are in atomic units.

Attosecond beamline/end station. The general design philosophy is to maintain interferometric stability in the pump-probe geometry for RABBITT measurements and transmission into the soft x-ray (0.5 keV) regime. The RABBITT method is a direct and reliable method for measuring the spectral phase required for the tomography. A brief description of this apparatus can be found in this book under the abstract entitled "Attosecond and Ultra-Fast X-ray Science".

Harmonics from liquid phase systems. It is obviously interesting to know if ultra-fast strong field techniques could be applied to condensed phases, where the vast majority of chemical processes occur. We have initiated exploratory investigations using long wavelength fundamental fields for evaluating the feasibility for strong-field processes, e.g. high harmonic generation, as a condensed phase probe. In the experiment, a wire guided fluid jet is used to create thin (100 μm) flowing sample. A 100 fs, 3.7 μm fundamental pulse with a maximum intensity (in vacuum) of ~10^{14} W/cm^2 is focused into the fluid sheet. The radiation emitted along the forward direction is analyzed in an optical spectrometer equipped with an intensified CCD. Under these conditions, odd-order harmonic combs are observed extending to the 13-order. The spectral behavior at these long wavelengths is very different than all previous reports at near-visible wavelengths. The initial emphasis has been on contrasting the harmonics from both water and heavy water and their behavior as a function of wavelength and intensity. The results of these studies have been submitted for publication in Optics Express.

1.3 Proposed Studies in FY10

We are planning a specific series of experiments designed to advance our methods towards more chemically relevant systems and to understand the accuracy for orbital reconstruction from both an experimentally and theoretically perspective. The studies proposed in the renewal include:

- Improve the experimental precision for tomography by developing a better supersonic nozzle source.
- Measure the molecular harmonic phases using the RABBITT technique.
- Extend the imaging experiments to 2 μm fundamental fields.
- Begin studies on other molecular candidates:
  - CO_2 is an excellent triatomic candidate and will test the validity of the two center model.
  - NO molecule is an open-shell species with a permanent dipole moment.
- Extent the tomographic procedure to excited states, e.g. NO.
- Imaging of a dissociative state of ICN to move one more step closer to the "final frontier" of monitoring the changing molecular orbitals that define a chemical bond, as it breaks.
- A systemic study of harmonic generated using *intense* 4 μm light for a series of condensed phase liquids including perproteo and perdeutero versions of water, hexane and isopropanol, as well as, in liquids like CCl_4.
- Investigating electron diffraction from unaligned molecules in the tunneling regime. In complement to the tomography method, the structure of the HOMO can be retrieved from the diffraction of the returning electron wave packet.

1.4 References Cited

1. P. Colosimo *et al.*, Nature Phys. **4**, 386-389 (2008).
2. G. Doumy *et al.*, Phys. Rev. Lett. **102**, 093002 (2009).
3. J. Itatani *et al.*, Nature **432**, 867 (2004).
4. V.-H. Le, A.-T. Le, R.-H. Xie and C. D. Lin, Phys. Rev. A **76**, 013414 (2007).

1.5 Publication Resulting from this Grant

1. "Scaling Strong-Field Interactions towards the Classical Limit", P. Colosimo *et al.*, Nat. Phys. **4**, 386-389 (2008).
2. "Atoms in High Intensity Mid-Infrared Pulses", P. Agostini and L. F. DiMauro, Contemp. Phys. **49**, 179-197 (2008).
3. "Attosecond Synchronization of High Harmonics from Mid-Infrared Drivers", G. Doumy *et al.*, Phys. Rev. Lett. **102**, 093002 (2009).
4. "The Frontiers of Attosecond Physics", G. Doumy *et al.*, in Proceedings of the International Conference on Atomic Physics [ICAP 2009] (World Scientific Press, Singapore, 2009), 333-343.
5. "High Order Harmonics from Mid-Infrared Drivers for Attosecond Physics", G. Doumy *et al.*, in the Proceedings of Atomic Processes in Plasmas [APiP 2009] (American Institute of Physics, New York, 2009), in press.
6. "Harmonic generation from the near-resonant excitation of liquid H_2O and D_2O from an intense mid-infrared laser", A. DiChiara, E. Sistrunk, T. A. Miller, P. Agostini and L. F. DiMauro, Opt. Exp., in review.

Other Relevant Publications

1. "Progress Report on the LCLS XFEL at SLAC", L. F. DiMauro *et al.*, J. Phys. **88**, 012058 (2007).
2. "Interrogating Molecules", G. Doumy and L. F. DiMauro, Science **322**, 1194-1195 (2008).

High Intensity Femtosecond XUV Pulse Interactions with Atomic Clusters

Project DE-FG02-03ER15406

Progress Report to Dr. Jeff Krause - 8/10/09

Principal Investigator:
Todd Ditmire
The Texas Center for High Intensity Laser Science
Department of Physics
University of Texas at Austin, MS C1600, Austin, TX 78712
Phone: 512-471-3296
e-mail: tditmire@physics.utexas.edu

Collaborators: J. W. Keto, B. Murphy and K. Hoffman

Program Scope:

The nature of the interactions between high intensity, ultrafast, near infrared laser pulses and atomic clusters of a few hundred to a few thousand atoms has come under study by a number of groups world wide. Such studies have found some rather unexpected results, including the striking finding that these interactions appear to be more energetic than interactions with either single atoms or solid density plasmas and that clusters explode with substantial energy when irradiated by an intense laser. Under this phase of BES funding we have extended investigation in this interesting avenue of high field interactions by undertaking a study of the interactions of intense extreme ultraviolet (XUV) pulses with atomic clusters. These experiments have been designed to look toward high intensity cluster interaction experiments on the Linac Coherent Light Source (LCLS) under development at SLAC. The goal of our program is to extend experiments on the explosion of clusters irradiated at 800 nm to the short wavelength regime (10 to 100 nm). The clusters studied range from a few hundred to a few hundred thousand atoms per cluster (ie diameters of 1-30 nm). Our studies with XUV light are designed to illuminate the mechanisms for intense pulse interactions in the regime of high intensity but low ponderomotive energy by measurement of electron and ion spectra. This regime of interaction is very different from interactions of intense IR pulses with clusters where the laser ponderomotive potential is significantly greater than the binding potential of electrons in the cluster. With our XUV studies we are studying cluster explosions the low ponderomotive potential, high intensity short wavelength conditions expected in the focus of the LCLS beam.

We have been conducting these studies by converting a high-energy (1 J) femtosecond laser to the short wavelength region through high order harmonic generation. These harmonics are focused into a cluster jet and the ion and electrons ejected are analyzed by time-of-flight methods. We have been studying van der Waals noble gas clusters and have begin studies of metallic clusters in the past year. This most recent experimental effort is being conducted with an eye toward understanding the consequences of irradiating metal clusters chosen such that the intense XUV pulse rests at a wavelength that coincides with the giant plasma resonance of the cluster.

Progress During the Past Year

During the second year of this project, we concluded a campaign of experiments using our femtosecond laser-driven high harmonic source beamline constructed in the first year of funding. In this campaign we concentrated on studies of XUV driven explosions of Xe clusters as these are easy to produce and have been well studied by our group and others when irradiated by intense IR pulses. During this most recent third

year we moved to studies of other clusters of lower Z, including Ar. We observe some significant differences in the characteristics of XUV explosions between Xe and Ar.

We produce intense XUV pulses through the process of high order harmonic generation (HHG). An illustration of the beam line is shown in figure 1. Production of harmonic radiation is accomplished by loosely focusing with a MgF f/60 lens the compressed output of the 20 TW, 40 fs THOR Ti:sapphire laser into a jet of argon at 200 psi. We separated the harmonics from the IR by imaging an annular beam mask in the infrared beam before the focusing lens onto an aperture after the focus, taking advantage of the fact that the XUV harmonics have substantially less divergence than the infrared beam. This allows the removal of most of the infrared radiation. To reject scattered infrared light and to pass high harmonics with the energies between 15 eV and 73 eV an additional a 200 nm thin Al filter was used. To select a single XUV harmonic we then employed a specially designed Sc/Si short focal length multilayer mirror optimized for the 21st harmonic at 32.5 eV (38.1 nm) at close to normal incidence. The harmonic focus was characterized by a scanning knife edge measurement and an AXUV-10 diode (IRD Inc.). These data showed that we were able to produce an 8μm spot with the 38 nm pulse, yielding a a focal intensity of ~ 10^{11} W/cm^2 assuming an XUV pulse duration of 20 fs. These harmonics were then focused into the plume of a second, low density cluster jet. This cluster interaction region was located in a separated vacuum chamber. A Wiley McLaren time-of -flight (TOF) spectrometer was used to extract positive ions after photo ionization of the Xe clusters.

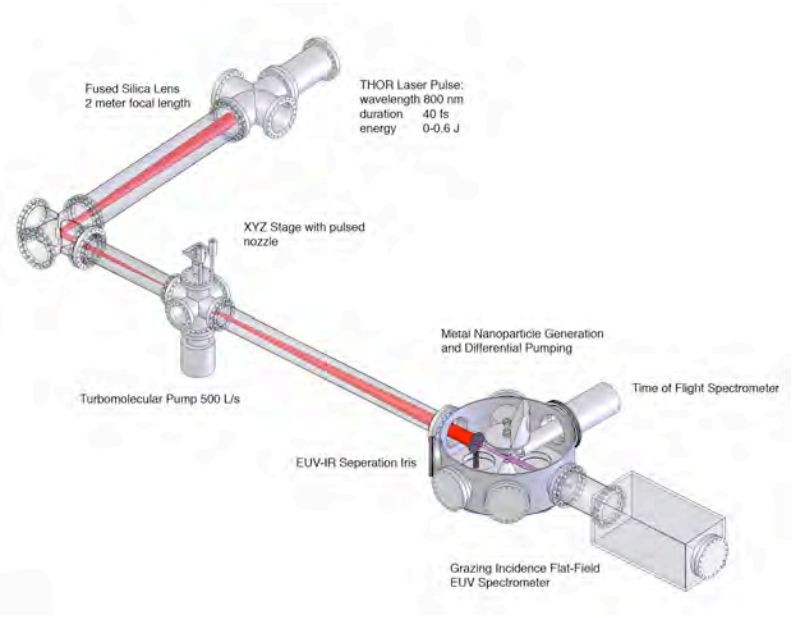

Figure 1: Schematic and specs of the HHG cluster beamline on the THOR 20 TW laser

Our initial experiments in Xe clusters (reported in our 2008 report) showed evidence for production of Xe charge states up to Xe^{8+} and ion energy spectra characteristic of the explosion of a moderate temperature plasma with electron temperature of ~8 eV. From these data we concluded that a Xe nanoplasma was formed in large (~10,000 atom) Xe clusters when irradiated by our 38 nm pulses, and that plasma continuum lowering created conditions in the nanoplasma that allowed single photon photoionization of Xe to at least 5+. We observed no evidence for a Coulomb explosion (which one might expect in a cluster which has been stripped of many of its electrons.)

We expected a similar behavior when we irradiated large Ar clusters. However, our recent data on Ar exhibits evidence for a combination of Coulomb explosion and hydrodynamic expansion. Figure 2

reproduces time-of-flight (TOF) data taken from the irradiation of Ar clusters by the 38 nm harmonic pulse. The average size of the Ar clusters in these data is 7000 atoms. We observe Ar charge states up to Ar^{3+}. These charge states are consistent with sequential single photon ionization of the Ar ions, potentially aided by continuum lowering in the cluster during ionization. Unlike Xe TOF spectra, which exhibit a series of broadened peaks at each ion charge species centered on the expected arrival time, the Ar TOF peaks exhibit a strong peak at an early time and a weaker wing at late time. This peak splitting is usually associated with fast ions ejected in the focal region toward and away from the detector.

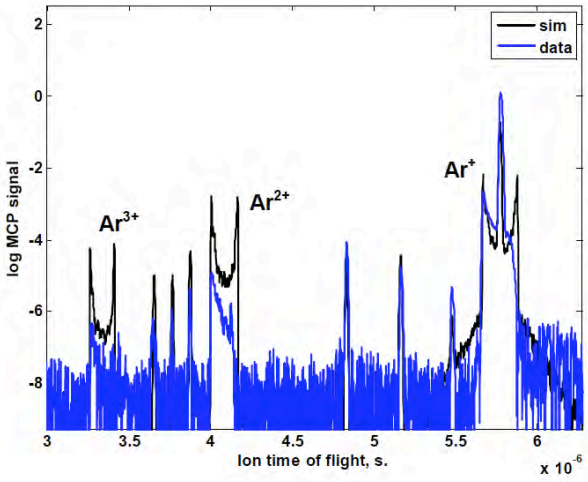

Figure 2: Time-of-flight spectrum of Ar clusters (with average size of 7000 atoms) irradiated by 38 nm pulses at intensity of ~ 10^{12} W/cm^2. The blue curve is the observed data and the black curve is the result of a Monte Carlo simulation of the cluster explosions.

This structure is best illustrated in figure 3 where the Ar^+ peak is expanded. Here it can be seen that the TOF peak has a low ion energy central feature centered on the expected arrival time of singly charged Ar bracketed by "wings" at early and late time. The late time wing is suppressed with respect to the early time peak, which we attribute to the fact that the acceptance of ions ejected away from the TOF detector is lower than those ejected toward the detector. The nature of this unique TOF structure is still under investigation, however we conjecture that the low ion energy feature results from the hydrodynamic expansion of a cold Ar nanoplasma and the high energy ion "wings" may result from the Coulomb explosion of ions near the surface of the Ar cluster. To explore this possibility we conducted Monte Carlo simulations of Ar clusters that were partially ionized by an XUV pulse so that an outer layer of ions are ejected by Coulomb explosion and the remainder explode hydrodynamically. The results of one such simulation are shown as a black curve in figure 2 and 3. This simulation shows qualitatively similar structure as that found in our data.

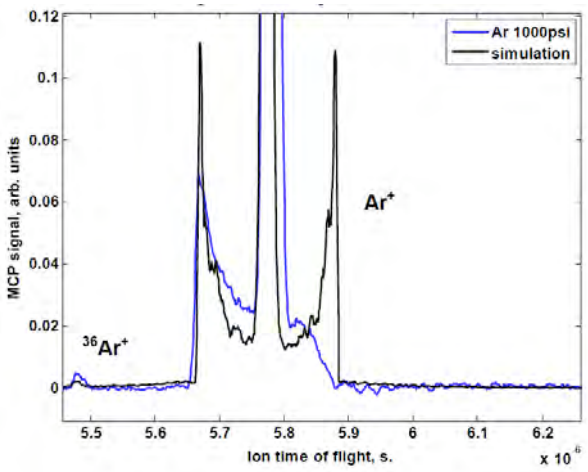

Figure 3: Time-of-flight spectrum of the Ar^+ peak from the data of figure 2. This illustrates the presence of a low energy ion peak in the center of the feature (attributed to an expanding Ar nanoplasma) surrounded by "wings" which represent higher energy ions ejected toward and away from the TOF detector (attributed to Coulomb explosion).

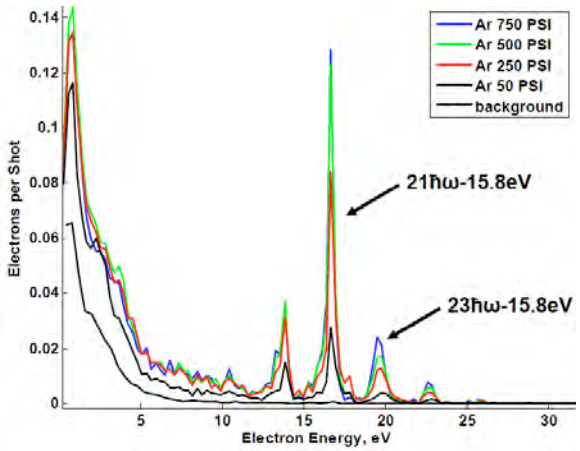

Figure 4: Electron energy spectrum from the irradiation of Ar clusters with our intense 38 nm pulses. We observe electrons characteristic of the photo-ionization of Ar by the 21st harmonic as well as a feature of low energy electrons that we attribute to electrons ejected by the Ar nanoplasma.

We have also investigated the electron spectra from the ionization of these Ar clusters at 38 nm. One such series of spectra from varying Ar cluster size (achieved by varying the gas jet backing pressure) is reproduced in figure 4. These spectra exhibit a clear photo-ionization peak from the 21st harmonic (bracketed by peaks from the 19th and 23rd harmonics which are partially passed by the bandwidth of our XUV multi-layer mirror.) In addition to this photo-ionization peak, we observe a cold electron feature with electrons of energy 1-5 eV. This cold feature may result from the formation of an Ar nanoplasma.

Future Research Plans

Our future plans will now shift to the study of mixed species clusters, such as methane. The explosions of clusters such as methane in intense XUV fields is of interest because these more closely approximate the organic based large molecular targets that will ultimately be studied at the LCLS. We have also begun study of solid material clusters irradiated at 38 nm. We have completed the fabrication of an add-on chamber that allows us to create metal clusters via the laser ablation of micro-particles technique [1]. We have started by investigating Ag clusters, which exhibit interesting absorption resonances at around 20-30 eV attributed to giant collective plasma resonance of both s and d electrons. To date, we have been trouble-shooting the Ag cluster jet and are working to avoid particle aggregation. We intend to acquire Ag cluster data irradiated at 38 nm this fall.

Refereed papers published on work supported by this grant during the past three years;
- those from previous one year are starred (*)

1*) B. F. Murphy, K. Hoffmann, B. Erk, N. Kandidai, J. Keto, and T. Ditmire, "Studies of Exploding Noble Gas Clusters Irradiated by Intense Femtosecond Pulses of Extreme Ultraviolet Light" *Phys. Rev. A*, submitted.

2*) A. P. Higginbotham, O. Semonin, S. Bruce, C. Chan, M. Maindi, T. D. Donnelly, M. Maurer, W. Bang, I. Churina, J. Osterholz, I. Kim, A. C. Bernstein, and T. Ditmire, " Generation of Mie size microdroplet aerosols with applications in laser-driven fusion experiments", *Rev. Sci. Instr.* **80**, 063503 (2009).

3*) B. F. Murphy, K. Hoffmann, A. Belilopetski, J. Keto, and T. Ditmire, "Explosion of Xenon Clusters Driven by Intense Femtosecond Pulses of Extreme Ultraviolet Light" *Phys. Rev. Lett.* **101**, 203401 (2008).

4) S. Kneip, B. I. Cho , D. R. Symes, H. A. Sumeruk, G. Dyer, I. V. Churina, A. V. Belolipetski, A.S. Henig, T. D. Donnelly, and T. Ditmire "K-shell Spectroscopy of Plasmas Created by Intense Laser Irradiation of Micron-scale Cone and Sphere Targets" *J. High Energy Density Physics.* **4**, 41 (2008).

5) D. R. Symes, M. Hohenberger, A. Henig, and T. Ditmire, "Anisotropic Explosions of Hydrogen Clusters under Intense Femtosecond Laser Irradiation" *Phys. Rev. Lett.* **98**, 123401 (2007).

6) B. Shim, G. Hays, R. Zgadzaj, T. Ditmire, and M. C. Downer, "Enhanced harmonic generation from expanding clusters" *Phys. Rev. Lett.* **98**, 123902 (2007).

7) H. A. Sumeruk, S. Kneip, D. R. Symes, I. V. Churina, A. V. Belolipetski, T. D. Donnelly, and T. Ditmire, "Control of Strong-Laser-Field Coupling to Electrons in Solid Targets with Wavelength-Scale Spheres" *Phys. Rev. Lett.* **98**, 045001 (2007).

8) H. A. Sumeruk, S. Kneip, D. R. Symes, I. V. Churina, A. V. Belolipetski, G. Dyer, J. Landry, G. Bansal, A. Bernstein, T. D. Donnelly, A. Karmakar, A. Pukhov and T. Ditmire "Hot Electron and X-ray Production from Intense Laser Irradiation of Wavelength-scale Polystyrene Spheres" *Phys. Plas.* **14**, 062704 (2007).

9) D. R. Symes, J. Osterhoff, R. Fäustlin, M. Maurer, A. C. Bernstein, A. S. Moore, E. T. Gumbrell, A. D. Edens, R. A. Smith, and T. Ditmire "Production of periodically modulated laser driven blast waves in a clustering gas", *J. of High Energy Density Phys.* **3**, 353 (2007).

10) M. Hohenberger, D. R. Symes, K. W. Madison, A. Sumeruk, and T. Ditmire, "Dynamic Acceleration Effects in Explosions of Laser Irradiated Heteronuclear Clusters", *Phys. Rev. Lett.* **95**, 195003 (2005).

11) F. Buersgens, K. W. Madison, D. R. Symes, R. Hartke, J. Osterhoff, W. Grigsby, G. Dyer and T. Ditmire , "Angular distribution of neutrons from deuterated cluster explosions driven by fs-laser pulses", *Phys. Rev. E*, **74**, 016403 (2006)

[1] W.T. Nichols, D.E. Henneke, G. Malyavanatham, M.F. Becker†, J.R. Brock, and J.W. Keto, and H. D. Glicksman, "Large scale production of nanocrystals by laser ablation of aerosols of microparticles," *Appl. Phys. Lett.* **78**, 1128 (2001).

Expected Unexpended Funds

We anticipate that there will be no ($0) unexpended funds from this grant for the grant period ending 10/31/09

Number of Students and Post Docs Supported

Students: 2 (Brendan Murphy, Benjamin Erk)

Post Docs: 2 (Kay Hoffman, partial, Harnan Quevedo, partial)

Ultracold Molecules: Physics in the Quantum Regime

John Doyle
Harvard University
17 Oxford Street
Cambridge MA 02138
doyle@physics.harvard.edu

1. Program Scope

Our research encompasses a unified approach to the trapping of both atoms and molecules. Our goal is to extend our work with CaH to NH and approach the ultracold regime. Our plan is to trap and cool NH molecules loaded directly from a molecular beam, and measure elastic and inelastic collisional cross sections. Cooling to the ultracold regime will be attempted. We note that as part of this work, we are continuing to develop an important trapping technique, buffer-gas loading. This method was invented in our lab and is able to cool large numbers of atoms and molecules.

2. Recent Progress

Milestones for this project include (x indicates complete):

x–spectroscopic detection of ground-state NH molecules via LIF
x–production of NH in a pulsed beam
x–spectroscopic detection of ground-state NH molecules via absorption
x–injection of NH beam into cryogenic buffer gas (including LIF and absorption detection)
x–realization of 4 T deep trap run in vacuum
x–injection of NH molecules into cryogenic trapping region
x–loading of NH molecules into cryogenic buffer gas with 4 T deep trap
x–trapping of NH
x–measurement of spin-relaxation rate of NH with He
x–removal of buffer gas after trapping of NH
o–measurement of elastic and inelastic cross sections
o–evaporative cooling
o–measurement of ultracold cross sections
o–study cold chemical reactions
o–prepare metastable NH for field studies
o–introduce new molecules into system for further studies

NH, like many of the diatomic hydrides, has several advantages for molecular trapping including large rotational constant and relatively simple energy level structure. Some of the several key questions before us when this project began were: Could we produce enough NH using a pulsed beam? Is it possible to introduce a large number of NH molecules into a buffer gas? Would the light collection efficiency be enough for us to adequately detect fluorescence from NH? Could we get absorption spectroscopy to work so that absolute number measurements could be performed? Could we achieve initial loading of NH into the magnetic trap? Will the spin relaxation rates with helium be low enough for us to remove the buffer gas? We have now answered these questions, all to the positive. In addition, we have added something very new to the technical arsenal, co-trapping of N with NH.

There are important questions left. For example, will the NH-NH or NH-N collision rates be adequate for evaporative cooling or sympathetic cooling into the ultracold regime? What will

be the nature of an ultracold dense sample of heteronuclear molecules. Specifically, what about the hydrides, with their large rotational constants? We have recently made progress answering these questions. These questions are still partially open and answering them are some of the stated long-term goals of this work.

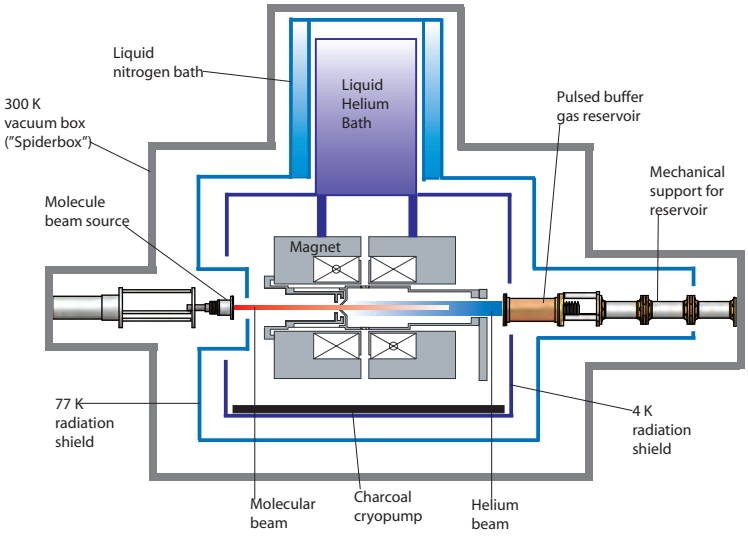

Figure 1: Schematic of current molecule trapping apparatus. The NH molecules and N atoms travel into the trapping region from the molecular beam source, where they are thermalized with the buffer gas and trapped. Simultaneous detection of NH and N is done spectroscopically.

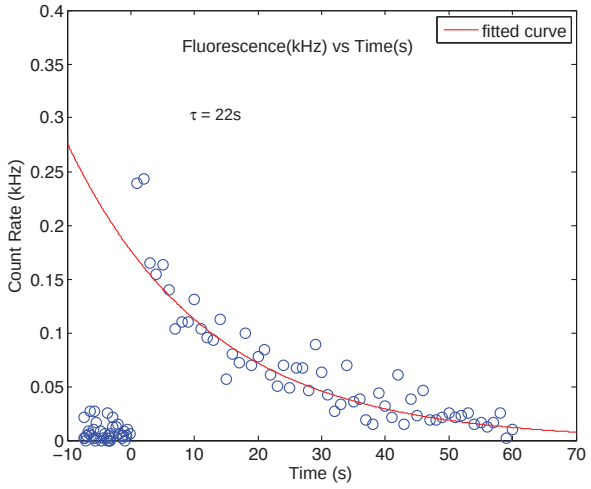

Figure 2: Plot of measured NH lifetime in our magnetic trap. This represents a factor of 20 increase in our trapped molecule lifetime over last years work.

Summary of Status of Project

The heart of the apparatus is a beam machine that we use to produce pulsed NH – alone or in combination with atomic N – in a beam (see figure 1). (Figure 3 shows a photo of the internals of the apparatus.) We have used two types of sources successfully, an "RF Plasma Source (CW)" and a "Glow Discharge Source (Pulsed)". The plasma source is a commercial source used typically in MBE machines. The design of the pulsed source is based on the production of OH via DC discharge as executed by Nesbitt.

This beam is directed toward our trapping magnet, inside of which is a cryogenic buffer-gas cell. This cell can be cooled to as low as 500 mK by a He^3 refrigerator. An entrance orifice of a few mm in diameter to allow the beam of NH to enter the cell. In a new addition to our apparatus, at the opposite end is a much larger orifice that allows for a new cold pulsed beam of helium to enter. The idea is that the helium pulse arrives simultaneously with the NH/N pulse, thermalizes the N/NH (leading to trapping), and then quickly exits. Thus, buffer-gas cooling and trapping of the NH and/or N takes place.

The basic experimental procedure is as follows. The source beam is directed toward the trap for times from about 10-100 ms. This long pulse beam travels about 10 cm to the face of the cell where some portion enter through the orifice and into the cell. The NH and/or N are then cooled by the buffer gas to their ground state by the helium resident in the cell. In our latest experiments we have been using fluorescence and absorption spectroscopy to detect the NH in the trapping region and pulsed TALIF to detect atomic N. We have been able to observe trapped NH molecules and N for many seconds, see figure 2 for new long times for trapped NH. With such long trap lifetimes we are able to make measurements of key spin relaxation cross sections of NH and compare with theory. This was published as *Magnetic Trapping and Zeeman Relaxation of NH*, W.C. Campbell, E. Tsikata, H. Lu, L.D. van Buuren, and J.M. Doyle, Physical Review Letters, **98**, 213001 (2007) and *Mechanism of Collisional Spin Relaxation in* $^3\Sigma$ *Molecules*, W.C. Campbell, T.V. Tscherbul, Hsin-I Lu, E. Tsikata, R.V. Krems, and J.M. Doyle, Physical Review Letters **102** 013003 (2009).

3. Future Plans

We continue on our program of trapping of NH with N. The next step is to measure N-NH cross-sections. Using our new long lifetime of trapped NH, we have already taken preliminary data on N-NH spin relaxation collisional cross sections. This will naturally lead to attempting evaporative/sympathetic cooling. It is our hope to increase the number of trapped N atoms to make this regime even more accessible. We also may take an approach that incorporates a dilution refrigerator that can reach lower temperatures than our current He^3 fridge.

Figure 3:

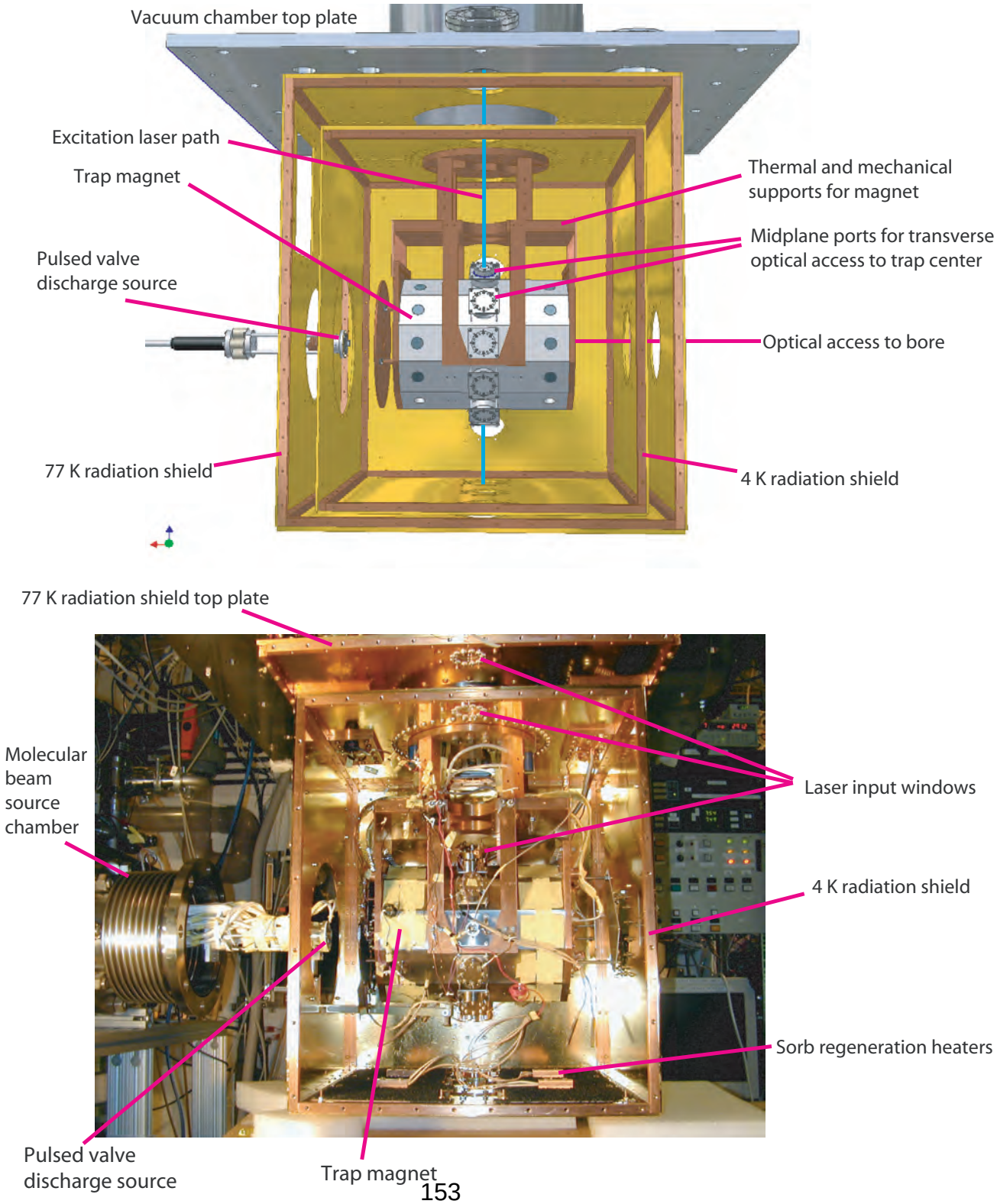
Vacuum chamber top plate
Excitation laser path
Trap magnet
Thermal and mechanical supports for magnet
Midplane ports for transverse optical access to trap center
Pulsed valve discharge source
Optical access to bore
77 K radiation shield
4 K radiation shield
77 K radiation shield top plate
Molecular beam source chamber
Laser input windows
4 K radiation shield
Sorb regeneration heaters
Pulsed valve discharge source
Trap magnet

Atomic Electrons in Strong Radiation Fields

J. H. Eberly
Department of Physics and Astronomy
University of Rochester, Rochester, NY 14627
eberly@pas.rochester.edu

July 24, 2009

Scope: Electron Correlation under Strong Laser Fields

We are interested to understand how very intense laser light couples to multi-electron atoms and molecules. Theoretical study faces substantial challenges in this domain. These arise from the fully phase-coherent character as well as the short-time nature of femtosecond-scale laser pulses in the case that the Coulomb forces among electrons and the nucleus are nearly matched in strength by the laser's electric field force. An important additional challenge arises when there is a need to account accurately for more than one dynamically active electron, as there is in situations of recent experimental activity.

During 2007-08, using very large ensembles of classical multi-electron trajectories, we built on earlier results [1, 2, 3, 4, 5, 6] from studies of two, three and four active atomic electrons in strong time-dependent and phase-coherent fields. We made, for example, what we believe are still the only direct comparisons [7] to experimental momentum distribution data obtained in multiphoton triple ionization [8], with good matches achieved.

Recent Progress #1: Elliptical Polarization Structures in Multiphoton Double Ionization

Many questions remain unsettled regarding strong-field multi-electron ionization, and one that is completely open concerns polarization. Almost all near-optical-frequency double ionization experiments have been carried out with linearly polarized light. The familiar three-step recollision picture suggests dramatically lower ion yield under elliptical or circular polarization, because the return trajectory is much less likely to encounter the atomic core, and this was quickly affirmed experimentally [9]. Double ionization was nevertheless soon reported even with circular or near-circular polarization in studies of atomic magnesium [10] and of several molecules [11].

The lack of cylindrical symmetry puts the case of high-field multiple ionization in elliptically polarized fields beyond the reach of essentially all quantum mechanical calculations. This includes solutions of the time dependent Schrödinger equation as well as applications of the so-called strong field approximation (SFA) [12, 13]. However, with two- and three-dimensional classical-trajectory ensembles, a different theoretical avenue is open. It is reasonably expected to be viable to the

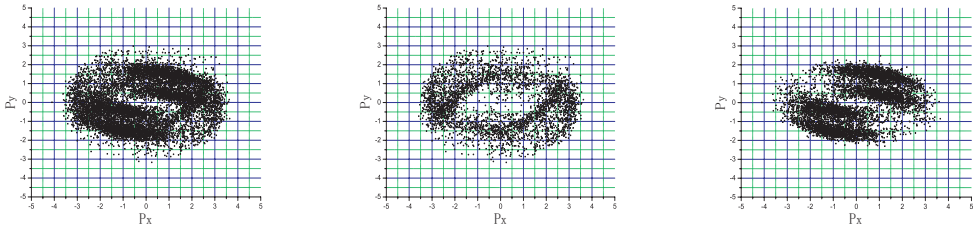

Figure 1: Under elliptical polarization, the ion momentum distribution of DI (left) can be cleanly divided into the momentum distribution of NSDI (center) and the momentum distribution of SDI (right). The ellipticity used here is 0.5, and I = 0.6 PW/cm^2.

extent that electron-laser physics competes strongly with electron-orbital physics in the strong-field domain. We have taken this approach and have derived predictions for double ionization momentum distributions for a full range of ellipticities. Our results significantly extend findings reported by Shvetsov-Shilovski, et al. [14]

With classical trajectories available, the past history of every successful ionization event can be known in all details. Such "back analysis" [15] provides great insight. In the case of double ionization under elliptical polarization a surprising and very clear distinction emerges [16] between non-sequential double ionization (NSDI) and sequential double ionization (SDI), as shown in the ion momentum distributions in Fig. 1. The distinct patterns in the polarization plane show that SDI and NSDI are separated cleanly by their different responses along the major and minor axes of polarization. The theoretical data was obtained at an intensity high enough to include both SDI and NSDI. We observed that in linear polarization about 10% of the single ionizations are converted to SDI events, and this appears consistent with 1d reports obtained from phase space analysis by the Uzer group [17].

More directly relevant to potential experimental work, we observed [18] the suggestion of structure in distributions of ion momentum along the polarization minor axis, as shown in Fig. 2. The peaks have been reproduced in subsequent calculations, and analytic expressions are now available that predict them [16]. Extensions are being actively pursued.

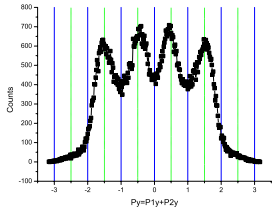

Figure 2: Four-peak structure predicted for distribution of ion momentum along the polarization minor axis from double ionization in a 10 cycle pulse with peak intensity I = 0.6 PW/cm^2 and $\lambda \approx$ 800nm for ellipticity ε = 0.5.

Recent Progress #2: Comparitive Theoretical Overview

A second project is the completion of an overview of the domain of high field ionization physics, focusing on theoretical understanding of multi-electron processes. It is well known that there is

no orderly theory in the high field domain, in the sense that there is no well-defined procedure that provides increasingly better approximations, because there is no single small parameter serving as an analog to the fine structure constant. Instead, there are three or four theoretical approaches with differing heuristic bases in use. An invitation to provide a Colloquium style article for Rev. Mod. Phys. that would assess this situation has led to a cooperative effort with contributions so far from participants from Argonne, Berlin, Rochester and Wuhan [19]. The intention is to compare theoretical results to experimental findings with the goal of determining the ranges of validity and utility of the different approaches in current use.

Future Plans

The extension of the classical approach to 2d and 3d has opened the domain of elliptical polarization to study, and that topic will be pursued.

More speculative work will involve the degree of quantum state entanglement between electrons, i.e., non-local entanglement rather than the local entanglement of atomic orbitals. This raises important questions about issues of specifically quantum complexity under extreme conditions, and the dynamics of entanglement. A fraction of our effort going forward will be devoted to an examination of questions related to this, and connections have recently been established between work underway at the University of Sherbrooke [20] and our previously published work in cooperation with the Fedorov group in the General Physics Institute in Moscow [21].

We continue to value our cooperation on multi-electron strong-field effects with the group of Prof. S.L. Haan at Calvin College [22].

Acknowledgment

Publications marked with *** in the listing below have been supported by DOE Grant DE-FG02-05ER15713.

References

[1] Phay J. Ho, R. Panfili, S. L. Haan and J. H. Eberly, *Phys. Rev. Lett.* **94**, 093002 (2005).

[2] Phay J. Ho, *Phys. Rev. A* **74**, 045401 (2005).

[3] ***Phay J. Ho and J.H. Eberly, *Phys. Rev. Lett.* **95**, 193002 (2005).

[4] ***Phay J. Ho and J.H. Eberly, *Phys. Rev. Lett.* **97**, 083001 (2006).

[5] ***S.L. Haan, L. Breen, A. Karim, and J. H. Eberly, *Phys. Rev. Lett.* **97**, 103008 (2006) [also selected for Virtual Journal of Ultrafast Science].

[6] ***P.J. Ho, Ph.D. Dissertation, University of Rochester (2007).

[7] ***Phay J. Ho and J. H. Eberly, *Optics Expr.* **15**, 1845-1850 (2007).

[8] K. Zrost, A. Rudenko, Th. Ergler, B. Feuerstein, V. L. B. de Jesus, C. D. Schröter, R. Moshammer and J. Ullrich, *J. Phys. B* **39**, S371 (2006).

[9] P. Dietrich, et al., *Phys. Rev. A* **50**, 3585(R), (1994).

[10] G. D. Gillen et al., *Phys. Rev. A* **64**, 043413 (2001).

[11] C. Guo and G. N. Gibson, *Phys. Rev. A* **63**, 040701(R)(2001); C. Guo et al., *Phys. Rev. A* **58**, R4271 (1998).

[12] See the review in W. Becker and H. Rottke, Contemporary Physics **49**, 199 (2008).

[13] For very early high-field calculations for single ionization under elliptical polarization, see A.M. Perelomov, V.S. Popov, and M.V. Terent'ev, Zh. Eksp. Teor. Fiz. **50**, 1393 (1965) [Sov. Phys. JETP **23**, 924 (1965)].

[14] N. I. Shvetsov-Shilovski et al., *Phys. Rev. A* **77**, 063405 (2008).

[15] For an early application, see R. Panfili, S.L. Haan and J.H. Eberly, *Phys. Rev. Lett.* **89**, 113001 (2002).

[16] ***X. Wang and J.H. Eberly, arXiv:0905.3915 (2009).

[17] An alternative classical approach, via phase space techniques, has recently been described: F. Mauger, C. Chandre and T. Uzer, *Phys. Rev. Lett.* **102**, 173002 (2009).

[18] ***X. Wang and J.H. Eberly, Laser Phys. **19**, 1518 (2009).

[19] ***Phay J. Ho, X. Liu, W. Becker, and J.H. Eberly, *Rev. Mod. Phys.* in preparation.

[20] S. Chelkowski, paper presented at Quantum Optics VII, Zakopane, Poland, June 2009.

[21] M.V. Fedorov, M.A. Efremov, P.A. Volkov and J.H. Eberly, *J. Phys. B* **39**, S467-S483 (2006).

[22] ***S.L. Haan, L. Breen, A. Karim and J.H. Eberly, *Optics Expr.* **15**, 767 (2007).

Reaction Imaging and the Molecular Coulomb Continuum

Department of Energy 2009-2010

James M Feagin
Department of Physics
California State University–Fullerton
Fullerton CA 92834
jfeagin@fullerton.edu

Remarkable advances in atom interferometry and ion trapping afford detailed study of quantum interferences in systems with relatively few parameters that can be tracked from quantum towards mesoscopic limits. Although trapped-ion and atom interferometry have proven over the past decade to be powerful tools for establishing quantum control, the essential system entanglements have been achieved almost exclusively with scattered photons. There thus remains fundamental interest in demonstrating analogous levels of entanglement and control using scattered electrons and ions, however, the experiments remain difficult due to the intrinsically short deBroglie wavelengths involved. Nevertheless, relevant progress has been recently achieved in experiments by Th. Weber, R. Dörner, A. Belkacem, and coworkers at the LBNL ALS involving the photo double ionization of molecular hydrogen.[1] In particular, two-center electron diffaction has been observed with which-path marking via entanglement with the ion pair. These and related experiments in this country and internationally involving atom and molecule fragmentation promote a new generation of reaction-imaging physics and strongly motivate our work here.

Two-Center Interferometry

For the past few years, we have been working to develop a robust, albeit approximate, framework for describing two-center interferometry readily adaptable to either photon or charged-particle scattering.[2,3,4] We have thus formulated an impulse-approximation description that allows one to track the relatively sluggish external center-of-mass motion of the target atoms and ions and thereby ensure momentum conservation explicitly while describing the excitation of the target's internal states. These projects continue to link to our more conventional longtime work in the AMO field of collective Coulomb excitations,[5,6] although we have been particularly interested recently in characterizing the resulting entanglements among the recoiling reaction fragments and the scattered particle.

Electron-Pair Excitations

Along with these interests, but for much lower energies of the ejected electron pairs, we have revisited our description of *molecular* photo double ionization based closely on an analogous

---

[1] D. Akoury et al., Science **318**, 949 (2007).
[2] J. M. Feagin, Phys. Rev. A**69**, 062103 (2004). *This work was highlighted in the June 2004 issue of the Virtual Journal of Quantum Information, vjquantuminfo.org, published by the APS and the AIP as an edited compilation of frontier research.*
[3] J. M. Feagin, Phys. Rev. A **73**, 022108 (2006)
[4] R. S. Utter and J. M. Feagin, Phys. Rev. A **75**, 062105 (2007). *This work was highlighted in the June 2007 issue of the Virtual Journal of Quantum Information, vjquantuminfo.org. Utter was a CSUF masters degree student.*
[5] A. Knapp et al., J. Phys. B: At. Mol. Opt. Phys. **35**, L521 (2002). (*Feagin is a coauthor.*)
[6] Th. Weber et al., Phys. Rev. Lett. **92**, 163001 (2004) and references therein. (*Feagin is a coauthor.*)

double-ionization model we established for helium.[7] This lowest-order *helium-like* approximation based on ${}^1P^o$ outgoing molecular electron pairs has the advantage of providing approximate dynamical quantum numbers and propensity rules[8] for excitation of particular molecular fragmentation angular distributions. This description and its predictions were recently studied in detail by A. Huetz and T. Reddish and coworkers in Paris in photo double ionization experiments on H_2 with 4π detection of both the ion and electron pairs. While they found the model to represent well their coplanar angular distributions, they also identified '*frozen-correlation*' configurations for which the model unmistakably fails with one electron observed perpendicular to the plane of the other and the photon polarization.[9] Their observations were a follow-on to somewhat earlier experiments at the ALS by Th. Weber, R. Dörner, A. Belkacem, and coworkers.[10]

Parallel to these experimental achievements, the community has seen decisive advancement in the *ab initio* computation of Coulomb few-body fragmentation, in particular from two groups, T. Rescigno, W. McCurdy, and coworkers at LBNL[11] using a time-*independent* close-coupling approach, and J. Colgan, M. Pindzola and F. Robicheaux at Los Alamos and Auburn[12] using a time-*dependent* close-coupling approach. Their abundant 'virtual data' are in excellent agreement in both magnitude and angular distribution with a wide variety of experimentally measured cross sections. Their results for the 'frozen-correlation' distributions observed by Huetz and Reddish are shown in Fig. 1, and when folded over the experimental angular acceptances agree well with experiment. Their achievements have set milestones in the computational study of the Coulomb continuum.

Analysis of the close-coupling results, albeit in distributions of one-electron angular momenta, show evidence for contributions to the fragmentation from higher electron-pair angular

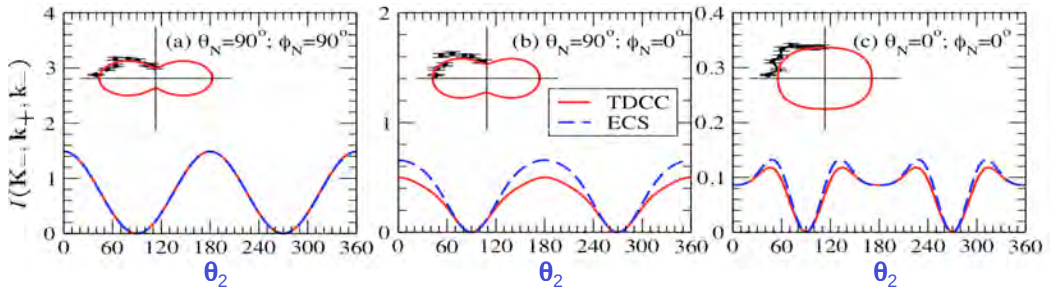

FIG. 1: Ionized electron-pair angular distributions from Colgan et al.[12] computed for photo double ionization of H_2 for 25 eV electron pairs and equal energy sharing and for three orientations θ_N, ϕ_N of the ion-pair relative momentum direction $\mathbf{K}_-$ with respect to a Lab z axis along the photon polarization $\hat{\epsilon}$. Here, the momentum direction $\mathbf{k}_1$ of one electron is fixed perpendicular to $\mathbf{k}_2$ of the other and the $\hat{\epsilon}, \mathbf{K}_-$ plane with $\theta_1 = 90°, \phi_1 = 90°$ and $\cos\theta_2 = \hat{\epsilon} \cdot \hat{\mathbf{k}}_2$. TDCC refers to the work of Colgan and coworkers, while ECS refers to the work of McCurdy and Rescigno and coworkers.[11] The minor differences in the two sets of results are convergence related and have been resolved. The polar-plot insets show a folded comparison with the experimental measurements of Huetz, Reddish and coworkers.[9]

---

[7] T. J. Reddish and J. M. Feagin, J. Phys. B: At. Mol. Opt. Phys. **32**, 2473 (1999); J. M. Feagin, J. Phys. B: At. Mol. Opt. Phys. **31**, L729 (1998).
[8] M. Walter, J. S. Briggs and J. M. Feagin, J. Phys. B: At. Mol. Opt. Phys. **33**, 2907 (2000).
[9] M. Gisselbrecht et al., Phys. Rev. Lett. **96**, 153001 (2006).
[10] Th. Weber et al., Nature (London) **431**, 437 (2004).
[11] W. Vanroose, F. Martin, T. N. Rescigno, and C. W. McCurdy, Phys. Rev. A**70**, 050703 (R) (2004); Science **310**, 1787 (2005).
[12] J. Colgan, M. S. Pindzola and F. Robicheaux, J. Phys. B: At. Mol. Opt. Phys. **37**, L377 (2004); Phys. Rev. Lett. **98**, 153001 (2007).

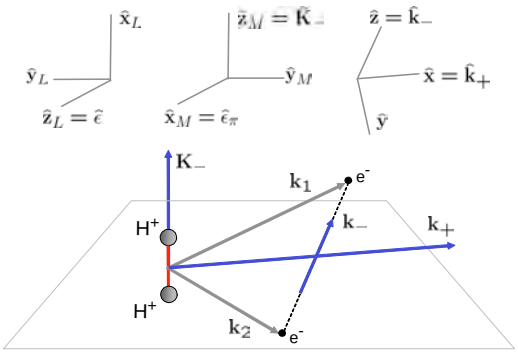

FIG. 2: Rotating $\mathbf{k}_1, \mathbf{k}_2$ plane of an ejected electron pair following the photo fragmentation of molecular hydrogen. Here, $\mathbf{k}_+ = \mathbf{k}_1 + \mathbf{k}_2$ and $\mathbf{k}_- = (\mathbf{k}_1 - \mathbf{k}_2)/2$ refer to the electron pair, and $\mathbf{K}_- = (\mathbf{K}_1 - \mathbf{K}_2)/2$ to the ion pair. The top three insets illustrate our three frames of reference used. Left to right: laboratory, molecular, electron-pair.

momenta. We have thus begun a collaboration this past year with J. Colgan, A. Huetz, and T. Reddish to generalize the helium-like molecular description to higher *total* angular momentum of the electron-pair. In the molecular ground state, the electron-pair total angular momentum $\mathbf{L} = \mathbf{l}_1 + \mathbf{l}_2$ is not a good quantum number, so the helium-like dipole selection rule ${}^1S^e \to {}^1P^o$ generalizes to ${}^1S^e, {}^1P^e, {}^1D^e, \ldots \to {}^1P^o, {}^1D^o, {}^1F^o, \ldots$ (the exchange and parity dipole selection rules remain the same). Based on our longtime experience with electron-pair excitations in helium and H^-, it turns out to be advantageous—perhaps surprisingly so—to define states of total L by quantizing rotations of the momentum plane of the electron pair based on a z axis along their relative momentum direction $\mathbf{k}_- = (\mathbf{k}_1 - \mathbf{k}_2)/2$. One thus introduces symmetric-top wavefunctions $\tilde{D}^L_{Mm}(\hat{\mathbf{k}}_-)$ defined by projections $\hbar m = \mathbf{L} \cdot \hat{\mathbf{k}}_-$ and $\hbar M = \mathbf{L} \cdot \hat{\mathbf{z}}_M$, where $\hat{\mathbf{z}}_M$ is a *molecular-frame* z axis, which we take to be along the ion-pair relative momentum direction $\mathbf{K}_-$.

As depicted in Fig. 3, we have thus found that superpositions of just three molecule symmetrized electron-pair states, ${}^1P^o + {}^1D^o + {}^1F^o$, give a remarkably robust description of the molecular fragmentation distributions including the anomalous out-of-plane *frozen-correlation* configurations.[13] We also find that molecules require special axial-vector geometries in the

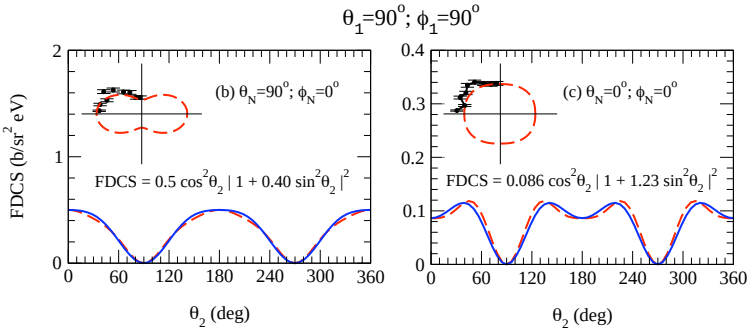

FIG. 3: Fits (solid curves) based on a three-state superposition ${}^1P_{\lambda=1} + {}^1D_{\lambda=1} + {}^1F_{\lambda=1}$ to the H_2 photo double ionization cross sections in Figs. 1b and 1c. Here, the dashed curves show the TDCC result from Fig. 1.

---

[13] J. M. Feagin, J. Colgan, A. Huetz, and T. J. Reddish, Phys. Rev. Lett. **103**, 033002 (2009).

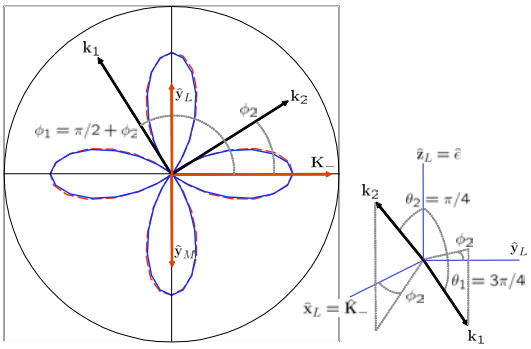

FIG. 4: An electron-pair angular distribution for fixed $\hat{\mathbf{k}}_1 \cdot \hat{\mathbf{k}}_2$ looking down a z_L axis along $\hat{\epsilon}$ onto the $\hat{\mathbf{x}}_L = \hat{\mathbf{K}}_-, \hat{\mathbf{y}}_L$ plane as a function of the azimuthal orientation ϕ_2 of the pair. Here, $\mathbf{k}_2$ and $\mathbf{k}_1$ are oriented above and below, respectively, the $\hat{\mathbf{K}}_-, \hat{\mathbf{y}}_L$ plane (cf. 3D inset) with fixed polar angles $\theta_2 = \pi/4$ and $\theta_1 = \pi - \theta_2$ while varying ϕ_2 along with $\phi_1 = \phi_2 + \pi/2$. The solid four-lobe curve is the resulting $\cos^2 2\phi_2$ distribution predicted from the axial-vector contributions, arbitrarily scaled to a TDCC calculation shown with the dashed curve. The circle radius equals 0.03 b/sr^{2}eV.

momenta of the outgoing electron-pair, which are not seen in atoms, and in Fig. 4 we present evidence for them in the fragmentation cross section. Our electron-pair states may thus prove useful in boosting convergence in numerical computations as well as in modeling a variety of proposed double ionization experiments with complex molecules and solids.[14]

We thus continue our ongoing DOE work to extract basic understanding and quantum control of few-body microscopic systems based on our long-time experience with more conventional studies of correlated electrons and ions. Although our efforts are theoretical, our interests have been strongly motivated by the very recent surge in and success of experiments involving few-body molecular fragmentation and the 4π imaging of all the fragments. We accordingly continue two parallel efforts with (i) emphasis on *reaction imaging* while (ii) pursuing longtime work on *collective Coulomb excitations*.

Recent Publications

Electron-Pair Excitations and the Molecular Coulomb Continuum, J. M. Feagin, J. Colgan, A. Huetz, and T. J. Reddish, Phys. Rev. Lett. **103**, 033002 (2009).

Electron Pairs in the Molecular Coulomb Continuum, J. M. Feagin, Invited Talk to the International Symposium on $(e, 2e)$, Double Photoionization, and Related Topics, Lexington, KY, July (2009).

Trapped-Ion Realization of Einstein's Recoiling-Slit Experiment, R. S. Utter and J. M. Feagin, Phys. Rev. A **75**, 062105 (2007). (**Utter** *was a CSUF masters degree student. This work was highlighted in the June 2007 issue of the Virtual Journal of Quantum Information,* vjquantuminfo.org.)

Two-Center Interferometry and Decoherence Effects, J. M. Feagin, Phys. Rev. A **73**, 022108 (2006).

Hardy Nonlocality via Few-Body Fragmentation Imaging, J. M. Feagin, Phys. Rev. A**69**, 062103 (2004). (*This work was highlighted in the June 2004 issue of the Virtual Journal of Quantum Information,* vjquantuminfo.org.)

Fully Differential Cross Sections for Photo Double Ionization of Fixed-in-Space D_2, Th. Weber et al. Phys. Rev. Lett. **92**, 163001 (2004). (*Feagin is a coauthor.*)

[14] Th. Weber, private communication.

Studies of Autoionizing States Relevant to Dielectronic Recombination

T.F. Gallagher
Department of Physics
University of Virginia
P.O. Box 400714
Charlottesville, VA 22904-4714
tfg@virginia.edu

This research program is focused on the doubly excited autoionizing states of alkaline earth atoms. The direct relevance to the Department of Energy is that a systematic study of autoionization allows us to understand the reverse process, dielectronic recombination (DR), the recombination of ions and electrons via intermediate autoionizing states. DR provides an efficient recombination mechanism for high temperature electrons in both laboratory and astrophysical plasmas,[1-3] and it is important in fusion plasmas because the captured electrons lead to radiative power loss. The most important pathway for DR is through the autoionizing Rydberg states converging to the lowest lying excited states of the parent ion. As a result, DR rates are profoundly influenced by very small electric and magnetic fields, both of which are often present in a plasma.[4] In addition, DR exhibits the same physics as found in other contexts, notably zero kinetic energy electron (ZEKE) spectroscopy[5] and fluorescence yield spectroscopy.[6] More generally, the multichannel nature of two electron alkaline earth atoms presents physics similar to that found in other systems.

During the past year we have worked on several projects. The first is multiphoton assisted recombination in the presence of a microwave field. Specifically, we have recently published a report of an experiment in which we observed DR from a continuum of finite bandwidth in a 38 GHz microwave field.[7,8] As the continuum of finite bandwidth we used the broad Ba $6p_{3/2}11d$ state which straddles the Ba^+ $6p_{1/2}$ limit. If we excite the broad Ba $6p_{3/2}11d$ state to an energy below the Ba^+ $6p_{1/2}$ limit with the laser in the absence of a microwave field the process

$$\text{Ba } 6p_{3/2}11\text{d} \rightarrow \text{Ba } 6p_{1/2}\, nd \rightarrow \text{Ba } 6s\, nd + h\nu \qquad (1)$$

Occurs. However, if we excite the atoms above the limit the process

$$\text{Ba } 6p_{3/2}11d \rightarrow \text{Ba } 6p_{1/2}\, \varepsilon d \qquad (2)$$

and autoionization into other continua occur, and there is no DR. In the presence of the 38 GHz microwave field we are able to observe DR even though the laser is tuned 20 cm^{-1} (600GHz) above the Ba^+ $6p_{1/2}$ limit. What is surprising about this result is that the ponderomotive energy in a 50V/cm 38GHz field is only $0.15\,cm^{-1}$, and using the simpleman's model, often used to describe above threshold ionization (ATI), we would expect to see microwave assisted recombination at energies up to three times the ponderomotive energy above the Ba^+ $6p_{1/2}$ limit.[9] We have suggested that the reason why so much energy can be removed from the electron is that while it is created in the Ba $6p_{1/2}\varepsilon d$ channel with approximately zero total energy its kinetic energy is far larger, and the energy transfer from the first microwave field cycle can be very

large, due to the high momentum the electron has when it is created near the core. This mechanism is also responsible for ATI at energies of up to ten times the ponderomotive energy.[10]

We have made microwave resonance measurements of the Sr $5sn\ell$ energies for $3 \le \ell \le 6$, using a delayed field ionization detection technique, and we have determined both the $\Delta\ell$ intervals and the indirect spin orbit K splittings. We have completed the analysis using a non adiabatic core polarization model which can in principle allow the determination of the dipole and quadrupole polarizabilities and the $< 5s|r|5p >$ and $< 5s|r^2|4d >$ matrix elements of the Sr^+ core.[11,12] Although we were able to obtain excellent values for the indirect spin orbit K splittings of the $4 \le \ell \le 6$ states we were not able to use the values from the $\ell = 4$ states in the analysis since they are coupled by the quadrupole interaction to the $4dnd$ states, which are core penetrating states. Nonetheless, we were able to extract good values for the Sr^+ $< 5s|r|5p >$ and $< 5s|r^2|4d >$ matrix elements.

We have been working to test a proposed approach to identifying the contributing ℓ states in DR. In , It is often the case that a substantial fraction of DR passes through energetically unresolved high ℓ states.[13] Although theses states are energetically unresolved, it should be possible to identify which ℓ states contribute to DR using the Stark effect. The idea is straightforward. In zero field the contribution of an $n\ell$ Rydberg state to the DR rate is proportional to $A_I(n\ell) / A_I(n\ell) + A_R$, where $A_I(n\ell)$ and A_R are the autoionization and radiative decay rates of the $n\ell$ state. For high ℓ states $A_I(n\ell) << A_R$, and the contribution is negligibly small. An electric field E converts the ℓ states to Stark states, and more states contribute to DR. The magnitude of the quantum defect for an isotropic core decreases with low ℓ, and for any value of E there is a value of ℓ, ℓ_E, such that $\ell \ge \ell_E$ states are converted to Stark states. When the E field becomes large enough that $A_I(n\ell_E) \ge A_R$ the DR rate will begin to rise. Since both the quantum defects and the autoionization rates are readily calculable,[14] this technique appears to a be a powerful way of determining which of the energetically unresolved high ℓ states contribute to DR.

It is straightforward to apply this idea to atoms with isotropic ionic cores, with one quantum defect for each ℓ state. Does it work for anisotropic cores, which lead to quadrupole splittings of the Rydberg states?[15] The quadrupole splittings can be characterized by $\bar{K}$, the sum of the angular momentum of the ion core, $\bar{j}_c$, and the orbital angular momentum of the Rydberg electron, $\bar{\ell}$. For a $j_c = 3/2$ core there are four values of the quantum number K, and there is not one quantum defect for each ℓ state, but four. In spite of this complication, due to a $\Delta K = \Delta\ell$ propensity of electric dipole transitions, we think the proposed method will work.

To test this notion we are comparing autoionization of the Ba Ba $6p_{1/2}nk$ and $6p_{3/2}nk$ Stark states. Specifically, we are preparing Ba atoms in $6snk$ Stark states of an incomplete Stark manifold composed of high ℓ states. These atoms are excited to the $6p_{1/2}nk$ or $6p_{3/2}nk$ Stark states using a 493 or 455nm laser pulse which saturates the $6snk \rightarrow 6p_jnk$ transition. In a low E field, one in which ℓ_E is large enough that in the incomplete $6p_jnk$ Stark manifold $A_I(nk) < A_R$, the atoms decay radiatively to the $6snk$ and $5dnk$ Stark states, where they

can be detected by field ionization. On the other hand, if the E field is high enough, and ℓ_S low enough that $A_I(nk) > A_R$ in the incomplete $6p_j nk$ Stark manifold, the atoms autoionize from the $6p_j nk$ Stark state and an autoionization signal is recorded instead of a field ionization signal.

The measurement consists of measuring the autoionization yield of a $6p_j nk$ state, composed principally of high ℓ states, as a function of E. As the field is raised, the Stark state acquires progressively more low ℓ character, and the autoionization increases. To prepare the $6snk$ Stark states in well controlled but small, 1 V/cm, fields we excite the Ba $6s(n+3)d$ state with the laser, and then drive the microwave transition to the Ba $6snk$ state in a field of approximately 10 V/cm. The field is then reduced to the desired lower field by a 1 μs field ramp. We have obtained preliminary data which indicate that the proposed method should work, and a full anlysis is underway.

In the coming year we plan to finish the above project on the field dependence of the autoionization and DR rates. In addition, we plan to do further experiments to test the model we have proposed for above threshold recombination. In our classical model the energy transfer from the microwave field to the electron depends critically on the phase of the microwave field at which the excitation occurs, but with our 5 ns long laser pulses we can not probe the phase dependence. However, if we replace our 5 ns long laser pulse with a 1 ps laser pulse which is phase locked to the microwave field, we can test our classical picture in a direct way. We propose to see if recombination occurs only if the excitation occurs at the correct phase of the microwave pulse. More generally, it should be possible to analyze the energy distribution of the bound states which are formed by the recombination.

References

1. A. Burgess, Astrophys. J. 139, 776 (1964).
2. A.L. Merts, R.D. Cowan, and N.H. Magee, Jr., Los Alamos Report No. LA-62200-MS (1976).
3. S. B. Kraemer, G. J. Ferland, and J. R. Gabel, ApJ. 604 556 (2004).
4. V. L. Jacobs, J. L. Davis, and P. C. Kepple, Phys. Rev. Lett. 37, 1390 (1976).
5. E. W. Schlag, *ZEKE Spectroscopy* (Cambridge University Press, Cambridge, 1998).
6. C. Sathe, M. Strom, M. Agaker, J. Soderstrom,J. E. Rubenson, R. Richter, M. Alagia, S. Stranges, T. W. Gorczyca, and F. Robicheaux, Phys. Rev. Lett. 96, 043002 (2006).
7.. E. S. Shuman, R. R. Jones, and T. F. Gallagher, Phys. Rev. Lett. **101**, 263001 (2008).
8. J.P. Connerade, Proc. R. Soc. London, Ser. A, 362, 361 (1978).
9. H.. B. van Linden van den Heuvell and H. G. Muller, in *Multiphoton Processes,* edited by S. J. Smith and P. L. Knight (Cambridge University Press, Cambridge, 1988).
10. K. J. Schafer, B. Yang, L. F. DiMauro, and K. C. Kulander, Phys. Rev. Lett. **70**, 1599 (1994).
11. T. F. Gallagher, R. Kachru, and N. H. Tran, Phys. Rev. A **43**, 605 (1933).
12. E. S. Shuman and T. F. Gallagher, Phys. Rev. A 75, 044501 (2007).
13. C. Brandau T. Bartsch,A. Hoffnecht,H. Knopp, S. Schippers, W. Shi, A. Muller, N. Grun, W. Scheid, T. Steih, F. Bosch, B. Franzke, C. Kozhuharov, P. H. mokler, F. nolden, M. Steck, T. Stohler, and Z. Stachura, Phys. Rev. Lett. **89**, 053201 (2002).
14. R. R. Jones and T. F. Gallagher, Phys. Rev. A 38, 2846 (1988).
15. C. H. Greene, unpublished.

Publications 2007-2009

1. W. Yang, E. S. Shuman, and T. F. Gallagher, "Spectral hole burning in the dielectronic recombination from a continuum of finite bandwidth," Phys. Rev. A 75, 023411 (2007).
2. E. S. Shuman, J. Nunkaew, and T. F. Gallagher, "Two-photon spectroscopy of Ba 6snℓ states," Phys. Rev. A 75, 044501 (2007).
3. E. S. Shuman, R. R. Jones, and T. F. Gallagher, Phys. Rev. Lett. **101**, 263001 (2008).
4. J. Nunkaew, E. S. Shuman, and T. F. Gallagher, "Indirect spin-orbit K splittings in strontium," Phys. Rev. A 79, 054501 (2009).

Experiments in Ultracold Collisions and Ultracold Molecules

Phillip L. Gould
Department of Physics U-3046
University of Connecticut
2152 Hillside Road
Storrs, CT 06269-3046
<phillip.gould@uconn.edu>

Program Scope:

Ultracold physics continues to play an important role within modern atomic, molecular and optical (AMO) physics. Atoms have traditionally been the main subjects of investigation in this field, but significant progress has recently been made in the production and manipulation of ultracold molecules. A number of techniques for generating ultracold samples of atoms and molecules have emerged, such as laser cooling, evaporative cooling, buffer gas cooling, electrostatic slowing, photoassociation, and Feshbach-resonance magnetoassociation. Various schemes for trapping these cold atoms and molecules have also been developed, including magneto-optical traps, optical traps, magnetic traps, and electrostatic traps. This combination of cooling and trapping techniques has enabled numerous applications such as: quantum degenerate gases (bosons, fermions, and mixtures); optical lattices and simulations of condensed-matter systems; quantum computation; precision measurements and atomic clocks; atom optics and interferometry; targets for ionization studies; ultracold plasmas; ultracold chemistry; and ultracold collisions. At the high densities and low temperatures typically required for these applications, various interactions between the particles can occur. These are important to understand and, hopefully, control. For example, inelastic collisions can cause undesirable heating and/or loss in high-density samples. On the other hand, processes such photoassociation and magnetoassociation allow the formation of ultracold molecules from the constituent atoms. The main goal of our experimental program is to use frequency-chirped laser light to coherently control ultracold collision dynamics, including the process of photoassociative formation of ultracold molecules.

Our experiments start with a Rb magneto-optical trap (MOT). Rb is ideally suited to our experiments for a number of reasons: 1) its 780 nm resonance line nicely matches commercially available diodes lasers; 2) the two stable isotopes (^{85}Rb and ^{87}Rb) allow for interesting comparisons; 3) Rb photoassociation has been extensively investigated by us and others; and 4) ^{87}Rb is the most widely-used atom for BEC studies. Our experiments utilize a phase-stable MOT loaded from a separate “source” MOT. Inelastic collisional rate constants are determined via the density-dependent loss rate of atoms from the trap.

Recent Progress:

We have made recent progress in two main areas: the influence of chirp nonlinearity on the rate of ultracold trap-loss collisions induced by frequency-chirped light; and improved production of chirped pulses on the nanosecond timescale.

The dominant long-range interaction between two atoms colliding in the presence of laser light is the $1/R^3$ dipole-dipole potential (R is the atomic separation). The detuning of the light relative to the atomic resonance determines the Condon radius R_c, the separation at which the atom pair is excited to this potential. Following their excitation, the atoms accelerate toward each other by rolling down the attractive potential. If the kinetic energy gain is sufficient (e.g., >1 K), the atoms will be lost from the trap. By "chirping" the light, i.e., changing its frequency as a function of time, atom pairs spanning a wide range of R can be excited and caused to undergo inelastic trap-loss collisions. Chirped light has the advantage that for sufficiently high intensities, the population transfer to the excited state can be adiabatic, and therefore efficient and robust. Also, the time scale of the chirp can be comparable to that of the atomic motion, allowing the collisions to be controlled by the details of the chirp.

We have examined how the rate of trap-loss collision rate depends on the direction of the chirp. For a certain range of center detunings of the chirp, interesting differences emerge. In the vicinity of –600 MHz (below the atomic resonance), the negative (blue-to-red) chirp results in a significantly smaller collision rate than the positive (red-to-blue) chirp. We attribute this difference to the fact that the attractive potential causes the excited atom pair to always accelerate *inward*, while the Condon radius R_c can move either *inward* (negative chirp) or *outward* (positive chirp), depending on the sign of the chirp. For the positive chirp, the atom pair can only be excited once, since the atom separation and the Condon radius move in opposite directions following the initial excitation. For the negative chirp, however, the Condon radius and the trajectory of the excited atom pair both proceed inward and further interactions between the light and the atom pair can occur. These multiple interactions can interfere destructively, a process we call "coherent collision blocking". This reduces the collisional flux reaching short range in the excited state, and thus the rate of trap-loss collisions. The smaller collisional rate for negative versus positive chirps observed in the experiment is also seen in classical Monte-Carlo simulations as well as in quantum mechanical ones.

We have also used nonlinear frequency chirps to examine the dependence of the trap-loss collision rate on the shape of the chirp. We have focused on the negative chirp case, since the possibility of multiple interactions allows for more control over the collisions. For comparison purposes, we fix the beginning and ending frequencies of the chirp, as well as the total time duration, but vary the shape of the chirp. Starting with a linear chirp, we superimpose a nonlinear variation with either positive curvature (concave-up) or negative curvature (concave-down). For negative chirps, we find a small but significant difference in collision rates for the concave-up versus concave-down shapes. We believe that this is due to details of the matching of the temporal evolution of the Condon radius to the atom-pair trajectories. For the positive chirp, we see no significant difference. This is expected because after the initial excitation, there are no further interactions between the light and the atom pair.

We have devised a novel scheme for generating the frequency-chirped light used in our experiments. Our original method utilized a current ramp applied to an external-cavity diode laser, with the output light amplified by a separate "slave" laser. This worked well for generating chirps up to 1 GHz in 100 ns. Our new technique is based on a fiber-based electro-optic phase modulator driven by an arbitrary waveform generator. In this scheme, a pulse of light from a diode laser is sent through the modulator multiple

times, acquiring the prescribed phase shift during each pass. Each time it emerges from the fiber loop, the light is re-injected into the initial laser to boost the power. We realize much higher chirp rates (>1 GHz in 10 ns) and have the ability to produce chirps of arbitrary shape. In order to control the intensity and produce arbitrary pulses on the nanosecond time scale, we employ a fiber-based electro-optic intensity modulator. This device also causes some residual phase modulation, which we are currently characterizing and attempting to compensate with the phase modulator. Our combined system of phase and intensity modulation is an interesting contrast to pulse shaping with ultrafast lasers. Our scheme operates in the time domain on the nanosecond time scale, while ultrafast pulse shaping takes place in the frequency domain and on the femtosecond time scale.

Future Plans:

Our new method of producing arbitrary chirps and pulses will be applied to study and control interactions between ultracold atoms. In particular we will use chirped pulses to coherently control the formation of ultracold molecules by photoassociation. We are developing pulsed-laser ionization detection of ultracold molecules, which will be employed to detect the products of chirped photoassociation, as well as photoassociation enhanced by chirped long-range excitation. One goal is to optimize the production of ground-state molecules in various states. In general, we anticipate that our ability to control the temporal variation of both the laser frequency (by chirping) and amplitude (by pulsing) will open up new opportunities in the manipulation of ultracold collisions and molecule formation.

Recent Publications:

"Probing Ultracold Collisional Dynamics with Frequency-Chirped Pulses", M.J. Wright, J.A. Pechkis, J.L. Carini, and P.L. Gould, Phys. Rev. A **74**, 063402 (2006).

"Coherent Control of Ultracold Collisions with Chirped Light: Direction Matters", M.J. Wright, J.A. Pechkis, J.L. Carini, S. Kallush, R. Kosloff, and P.L. Gould, Phys. Rev. A **75**, 051401(R), (2007).

"Generation of Arbitrary Frequency Chirps with a Fiber-Based Phase Modulator and Self-Injection-Locked Diode Laser", C.E. Rogers III, M.J. Wright, J.L. Carini, J.A. Pechkis, and P.L. Gould, J. Opt. Soc. Am. B **24**, 1249 (2007).

"Cold Molecules Beat the Shakes", P.L. Gould, Science **322**, 203 (2008) (invited "Perspective" article).

Physics of Correlated Systems

Chris H. Greene
Department of Physics and JILA, University of Colorado, Boulder, CO 80309
chris.greene@colorado.edu

Program Scope

The underlying theme of this project is to develop an improved theoretical understanding of many basic atomic and molecular phenomena of potential relevance to energy transfer, control, or productions. This is a project in basic science, which attempts to understand correlated dynamics, interpreted broadly. Correlations arise whenever two or more degrees of freedom are tightly coupled. They pose a severe challenge to our theoretical understanding because much theory in atomic, molecular, and chemical physics is constrained by the sheer dimensionality of many-particle quantum physics to begin from an uncorrelated independent-particle zeroth-order approximation. Yet in some cases the identification of a key collective coordinate leads to insights that can provide both deeper qualitative insight as well as an enhanced ability to perform detailed theoretical description of such reactive processes. In some cases photon interactions also play a role, and with high-intensity laser interactions these can usually be handled by treating the electromagnetic field classically. This research aims to be as relevant as possible to cutting-edge experimental work across a range of problems being studied in the field of atomic, molecular, and optical physics. This project brings a number of different techniques to bear on problems, in some cases stressing new algorithmic or theoretical lines of attack, sometimes implementing new mechanisms that have not been incorporated into realistic theoretical studies previously, and sometimes pressing forward with more concentrated computational projects when appropriate. The work during the past year has primarily concentrated on the following areas: (i) dissociation initiated by an electron when it collides with a diatomic or triatomic molecule; an efficient energy-transfer process involving Rb + NH. (ii) collisions between an electron and a biological molecule. (iii) ionization and harmonic generation from intense short-pulsed laser light interacting with matter.

Recent Progress (i) Reactive chemical physics

One major project completed within the past year was the theoretical description of a reactive collision between a ground state Rb($5s$) atom and the electronically-excited dimer NH($^1\Delta$) which, remarkably, is very nearly degenerate with the final state channels whose character is Rb($5p$)+NH($^3\Sigma^-$) This energy transfer reaction is complex, in part because the imidogen radical NH and the Rb atom are both highly reactive. Moreover, because one atom in the reaction, Rb, is quite heavy, it challenges the capabilities of quantum chemistry to describe it at a sufficiently realistic level that includes the strong spin-orbit interactions. In this collaborative project, spearheaded by postdoc D. Haxton, we found it difficult to get sufficiently accurate results for the Born-Oppenheimer potential surfaces using the popular quantum chemistry package MOLPRO, but the COLUMBUS package was ultimately able to handle it. For this pilot study, the calculations have been carried out with the NH bond length fixed at 1.925 a_0, whereby the 32 coupled electronic surfaces (including the Kramers degeneracy of this odd-electron number system) are two-dimensional. Following a nontrivial diabatization procedure, the scattering calculation can then be conducted in a relatively straightforward manner, using a DVR-implementation of the R-matrix propagator. The results are reported in Ref.[1], and the main conclusion is that the cross sections for this quenching reaction are quite large, in fact approaching a substantial fraction of the unitarity limit at low collision energies.

We have continued to study the dissociative recombination (DR) process. DR involves an

exchange of energy between the electronic and the nuclear degrees of freedom. This project has continued to study the dissociative recombination of triatomic molecules. We have developed new theoretical tools needed to predict for the first time the low-energy dissociative recombination rate coefficient for electrons that collide with the NO_2^+ molecule. This has required an extension of our techniques so they can treat the direct surface-crossing pathways as well as the indirect Rydberg-mediated pathways. The computations by postdoctoral associate D. Haxton have suggested that the direct pathways will probably be dominant, and the required scattering calculations have determined quantum defect matrices.

In the past year we completed the first theoretical treatment of LiH_2^+ dissociative recombination.[2] This molecule is so weakly bound that it does not fit readily into the rubric of conventional DR theory. Indirect DR via Rydberg state captures have been found to dominate the cross section for this process, and at 300K a relatively fast DR rate coefficient is predicted, in the vicinity of $10^{-7}\mathrm{cm}^3/s$. No theoretical or experimental total DR rate has previously been published for LiH_2^+, which can be compared with this result, although at least one experiment on this molecular target ion was carried out in Stockholm.

Two different mechanisms are believed to control the dissociative recombination of most molecules, the direct pathway in which a neutral potential surface cuts through the Franck-Condon range of the target ion, and the indirect Rydberg pathways for which the rate-limiting step is normally the capture of an incident electron into a vibrationally- or rotationally-excited Rydberg bound state. Comparatively little has thus far been addressed to the problem of treating both direct and indirect pathways for the same molecule. We have taken one step in that direction in the past year in a study of the dissociative recombination of the HeH^+ molecular ion.[3] This project was motivated in part by the desire to see whether the frame transformation methodology, which has been successful in treating examples of purely indirect Rydberg-dominated DR, can be extended to treat direct capture processes involving doubly-excited electronic states as well.

(ii) Electron Collisions with DNA and RNA

The experimental efforts of L. Sanche and his group in Sherbrooke, Quebec have been able to observed correlations between the rates of single and double strand breaks induced by electrons that collide with DNA, with the electron resonances associated with the DNA subunits. The DNA and RNA bases, adenine, guanine, thymine, cytosine, and uracil have now all been studied individually, and they appear to exhibit low energy electron scattering resonances that appear to connect with the experiments. The calculation of electron scattering from molecules as large as the DNA and RNA bases is highly challenging. These bases are of course the two purines adenine ($C_5H_5N_5$), guanine ($C_5H_5N_5O$), and the pyrimidines thymine($C_5H_6N_2O_2$), cytosine($C_4H_5N_3O$), and uracil($C_4H_4N_2O_2$).

One key advance in our theoretical capabilities was developed by a PhD student funded by this project, S. Tonzani, who completed his doctoral degree in 2006. In the course of that work, we developed a three-dimensional finite-element R-matrix scattering program[4] capable of treating molecules as large as the DNA and RNA bases, individually.

During the past year, we have made further progress in a collaborative effort with (former PhD student) S. Tonzani, L. Sanche and L. Caron towards the development of a multiple scattering treatment of resonant electron scattering by a segment of DNA. Specifically, we have combined the individual scattering matrices for an incident electron from the various major DNA components, and then assembled them to treat scattering from a full twist of the DNA double helix. This has helped to assess the possible importance of further resonance-enhancing

or - diminishing effects associated with the global structure of DNA, which can modify the resonant scattering by individual component subunits. This has been the first full multiple scattering description, using quality scattering matrices from the individual subunits, and it represents a significant step towards understanding how secondary electrons in the 0-20 eV range interact with DNA. The initial multiple scattering model and its results were reported last year in [5]. A second study, more realistic because it includes the effect of structural irregularities, notably scattering from the structural water components of DNA and base-pair mis-match, recently appeared in [6]. One conclusion from this study is that amplitude decoherence tends to promote stronger correlations between nearer neighboring bases, owing to a decreased importance of more distant bases. The resulting resonances that have been calculated in this model, e.g. around 3 eV in particular, appear to be likely candidates to play an enhanced role in DNA strand breakage. Another interesting conclusion is that the main scattering features are largely the same, regardless of whether the structural water is included, suggesting that it is the resonances involving the bases that play a dominant role.

(iii) Intense light pulse interactions with an atom, molecule, or cluster.

An earlier study coauthored with graduate student Z. Walters concerned the treatment of vibrational effects in high harmonic generation in SF_6 following molecular excitation by a weaker Raman pulse.[7] Last year, in the course of completing his doctoral degree supported in part by this project, he extended that treatment to higher order. In addition, Walters considered the theoretical description of molecular imaging through either high-harmonic generation or photoelectron angular distributions from aligned molecules. In that study, he made some headway in understanding the limitations of the frequently-employed plane-wave approximation, which are in fact highly problematic for imaging studies that have been carried out to date.[8]

Another topic of recent interest relates to the control of X-ray or XUV radiation transmission through a gas by applying infrared control fields. Interest in that area is partly being stimulated by the new X-ray free-electron lasers under construction around the world, notably in Stanford and Hamburg. Our collaborative study with the Leone group at Berkeley explored the modified XUV absorption spectrum of atomic helium in the vicinity of the n=2 doubly-excited autoionizing states, when they are dressed by a strong infrared laser field. We were able to demonstrate how three-level physics closely related to electromagnetically-induced transparency arises in the physics of enhanced XUV absorption, in addition to some regimes of diminished absorption caused by the infrared field coupling.[9]

In collaboration with D. Elliott's experimental group we are exploring a class of single-photon and two-photon ionization processes in atomic barium. Our calculated results for the separate one-photon and two-photon ionization spectra show encouraging agreement with experiment. But the coherent control aspects, which arise when both lasers simultaneously and coherently ionize the barium atom with a controllable phase difference, have not yet been considered. A study of these coherence phenomena represents a major motivation of this study, namely to give a quantitative theoretical description of phase-controlled directional electron ejection in the presence of two such coherent fields.

Also, a study of alignment and orientation of photofragments produced by photoionization of atomic argon has produced insights into the nature of the angular momentum transferred by the one-photon ionization process.[10] Some other studies supported in part by this project are also included in the reference list.[11, 12]

Immediate Plans

The coherent control study of phase-controlled photoionization of barium, using interference

between single-photon and two-photon ionization, will enter the next and more interesting phase. Specifically, the two separate amplitudes will be combined and the results compared with experimental observations of the phase-dependent photoelectron angular distribution.. This system shows promise to be the first for which first-principles theory can potentially give a quantitative description of the experimental observations of this phenomenon.

The strong-field ionization of molecules and the theoretical description of high-harmonic generation will receive continuing attention, as a part of the whole discipline's thrust to increasingly describe the molecular physics at a plausible, realistic level. A doubly-adiabatic formulation of the helium absorption problem discussed in [9] will also be pursued, to explore the feasibility of an ab initio description of XUV absorption near laser-dressed autoionizing states.

Electron scattering from polyatomic molecules continues to be a long-term project, and eventually we plan to build on the progress we have made in recent years on the description of dissociative recombination in polyatomic molecules, including the role of the Jahn-Teller and Renner-Teller effects. For such studies, we anticipate that our improved understanding of Siegert pseudostates, achieved in the course of the paper below by Santra, Shainline, and the P.I., should prove to be illuminating and practically useful.

Papers published since 2007 that were supported at least in part by this DOE project

---

[1] Theoretical study of the quenching of NH($^1\Delta$) molecules via collisions with Rb atoms, D. J. Haxton, S. A. Wrathmall, H. J. Lewandowski, and C. H. Greene, Phys. Rev. A 80, (2009, in press); see also the preprint at arXiv:0903.3909. (This study and some of the others in this list received partial support from NSF in addition to DOE.)

[2] Indirect dissociative recombination of LiH_2^+ + e, D. J. Haxton and C. H. Greene, Phys. Rev. A **78**, 052704-1 to -10 (2008).

[3] *ab initio* frame transformation calculations of direct and indirect dissociative recombination rates of HeH^+ + e^-, D. J. Haxton and C. H. Greene, Phys. Rev. A **79**, 022701-1 to -7 (2009).

[4] FERM3D: A finite element R-matrix general electron molecule scattering code, S. Tonzani, Comp. Phys. Commun. 176, 146-156 (2007).

[5] Diffraction in low-energy electron scattering from DNA: bridging gas-phase and solid-state theory, L. Caron, L. Sanche, S. Tonzani, and C. H. Greene, Phys. Rev. A 78, 042710-1 to -13 (2008).

[6] Low-energy electron scattering from DNA including structural water and base-pair irregularities, L. Caron, L. Sanche, S. Tonzani, and C. H. Greene, Phys. Rev. A 80, 012705-1 to -6 (2009).

[7] High harmonic generation in SF_6: Raman-excited vibrational quantum beats, Z. B. Walters, S. Tonzani, and C. H. Greene, J. Phys. B **40**, F277-F283 (2007).

[8] Limits of the plane wave approximation in the measurement of molecular properties, Z. B. Walters, S. Tonzani, and C. H. Greene, J. Phys. Chem. A **112**, 9439-9447 (2008).

[9] Femtosecond induced transparency and absorption in the extreme ultraviolet by coherent coupling of the He 2s2p ($^1P^o$) and $2p^2$ ($^1S^e$) double excitation states with 800 nm light, Zhi-Heng Loh, C. H. Greene, and S. R. Leone, Chem. Phys. **350**, 7-13 (2008).

[10] Use of partial-wave decomposition to identify resonant interference e ffects in the photoionization-excitation of argon, T. J. Gay, C. H. Greene, J. R. Machacek, K. W. McLaughlin, H. W. van der Hart, O. Yenen, and D. H. Jaecks, J. Phys. B **42**, 042008-1 to -17 (2009).

[11] Lebedev discrete variable representation, D. Haxton, J. Phys. B 40, 4443-4451 (2007).

[12] Three-body breakup in dissociative electron attachment to the water molecule, D. Haxton, T. N. Rescigno, and C. W. McCurdy, Phys. Rev. A 78, 040702(R)-1 to -4 (2008).

Strongly-Interacting Quantum Gases

Principal Investigator: Murray Holland

murray.holland@colorado.edu

440 UCB, JILA, University of Colorado, Boulder, CO 80309-0440

Research Program

With the use of scattering resonances, such as the Fano-Feshbach resonances, the dilute quantum gas has become an important system for the investigation of strongly-interacting many-body phenomena. This is true for both for the equilibrium state, and the non-equilibrium or dynamic situation. Our theoretical research program aims to explore and analyse strongly-interacting phenomena in these systems. It is generally our plan to be closely connected with experiments so that a pertinent question is always the feasibility of implementing any proposal. The importance of this topic is partly that it connects broadly with other areas of physics, since strongly-interacting phemomena manifests itself in many physical systems; in nuclear physics, particle physics, AMO physics, and condensed matter physics.

Our previous research has involved quantum gases in which strong interactions are induced by Fano-Feshbach resonances, giving for example the well known BCS-BEC crossover systems. Alternatively, strong-correlations may be induced by rapid rotation, where rotation plays the role of a pseudo-magnetic field. In such a situation Hall-effect physics may emerge. We have reported on both of these two projects in the past. During this last year, however, we discovered that a strongly-correlated gas can also be established by placing the atoms in a high quality cavity, as shown in Figure 1.

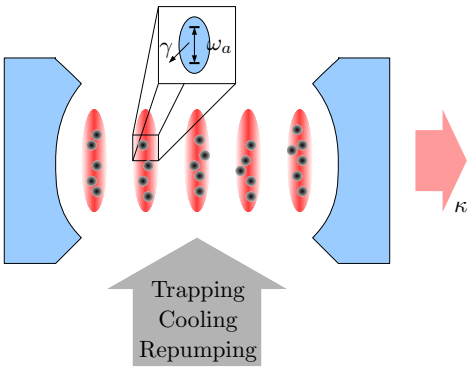

Figure 1: Schematic of the model. N two level atoms are held at the antinodes of a cavity field with an external trapping potential. The atoms have a much narrower linewidth than the cavity, leading to the extreme bad cavity limit and the possibility for steady-state superradiance.

This topic melds together the physics of ultracold gases with quantum optics in order to develop a new kind of complex and collective system that promises to have many applications. Recent progress in experimental techniques has made it possible to trap microscopic as well as mesoscopic ensembles of ultra-cold atoms in high-quality optical cavities. The interaction between atoms and just one quantized field mode is automatically of a very collective nature. In this context the field mode can be thought of as a "bus", shuttling information and mediating long-range interactions between distant atoms.

An initial motivation for this research was to understand the processes underlying novel bright light sources that are based on collective emission from a system of many quantum radiators. The collective emission processes that can occur in these devices are based on purely quantum mechanical interference. They could provide an alternative amplification mechanism for the emission of light to that of a conventional laser. This could open up the possibility to develop light sources with gain materials that cannot be used today, such as atoms with an extremely narrow linewidth and therefore weak oscillator strength. The huge impact that lasers have had on many areas of research and technology makes it an important goal to explore novel laser and light amplification processes.

The systems we consider are cavity quantum electrodynamic (QED) systems where the atomic relaxation rates are much smaller than the relaxation rates of the cavity. This means that the atomic linewidth is much narrower than the linewidth of the cavity. As is illustrated in Figure 2, the bulk of cavity QED research to date has been focused on the opposite limit. In particular, lasers are almost always exclusively in the "good cavity" limit (right edge in Figure 2) where the cavity linewidth is much narrower than the gain bandwidth of the atoms.

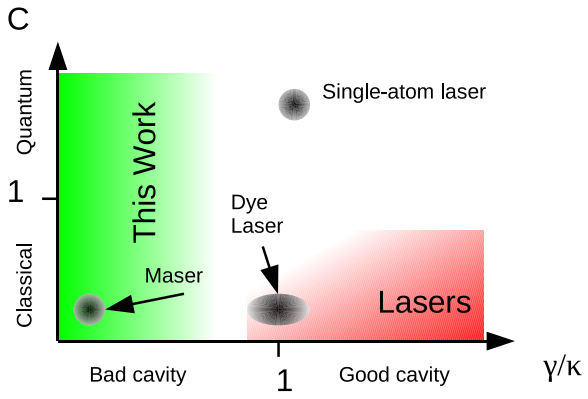

Figure 2: Parameter space of cavity QED systems. On the horizontal axis is the ratio of atomic relaxation rates (represented by γ) to the cavity field relaxation rates (represented by κ). On the vertical axis is the single atom cooperativity parameter $\mathcal{C}$ that quantifies the importance of quantum effects in the light matter interaction. Small $\mathcal{C}$ corresponds to classical systems while large $\mathcal{C}$ corresponds to systems where quantum effects at the single atom and single photon level are important. The green area (left; labelled this work), which is largely unexplored, is the topic of interest here.

Some atomic species have extremely narrow optical transitions due to dipole selection rules. These transitions can be used to make very stable light sources because the atoms are subject to much weaker fluctuations than ordinary optical dipole-allowed transitions. The light emitted on these transitions naturally has a very long coherence time. Unfortunately, the emitted light also has an extremely low intensity and can therefore not be used for applications. In normal

lasers this problem of low out-coupled power could be solved by simply using more atoms, *i.e.* by providing more energy to the system. This is not an option in this case because, in order to see the very narrow linewidth, it is necessary to hold the atoms in a very controlled environment in an atom trap at ultracold temperatures in the μK range. Technologically it is not possible to significantly increase the number of atoms much above 10^6. We must make smarter use of the number of atoms available.

A solution is suggested by the following observation. If we could make the atoms emit photons collectively rather than independently, the emitted power would be increased by an extra factor of N. Collective emission of this kind has been studied extensively both theoretically and experimentally in the form of Dicke superradiance. However, in almost all of these systems, light was emitted as a pulse with a duration that is shorter than the ordinary decay time of the atoms by a factor of $1/N$. This pulse shortening gives rise to a broadening of the spectrum in the frequency domain by a corresponding factor of N. That broadening would more than revoke the potential benefit of using narrow linewidth atoms and is thus not a possible route in this case.

Our principal observation was that it is in fact possible to have superradiant emission in steady state. Furthermore we have confirmed that the resulting radiation has a narrow linewidth similar to that of the underlying atoms and possibly even narrower due to collective effects. A point worth mentioning is that the working principle of this light source is in some sense reversed from that of an ordinary laser. In a normal laser the dipoles of the atoms get out of phase with each other very rapidly so that correlations between the atoms can be completely neglected. Enhanced emission into the laser mode is achieved by having a macroscopic number of photons already present in that mode. Here, on the other hand, the "laser mode" is virtually empty (possibly no more than a single photon) and collective enhancement of the emission is achieved through the presence of a dynamical macroscopic atomic dipole state.

We have developed a detailed theoretical model of this system, the details of which can be found in Ref [3].

Future outlook

Several questions need to be addressed in the future. To have a complete understanding of the requirements for operation of this device, it is necessary to fully understand the recoil effects induced by pumping, the optical lattice, cooling, and interaction with the laser field. The detailed nature of the joint atomic and field state, as well as the higher order correlations between atom and field, also deserves further investigations.

We also plan to examine the applications of this novel light source as a source for interferometry, as an active laser gyroscope, and other similar applications where an ultrastable phase would be beneficial.

Publications in peer-reviewed journals on DOE supported research 2007-present

[1] B. T. Seaman and M. J. Holland, *Evaporative Cooling of a Photon Fluid to Quantum Degeneracy* , arXiv:0807.1356 (under review).

[2] R. A. Pepino, J. Cooper, D. Z. Anderson, and M. J. Holland, *Atomtronic circuits of diodes and transistors*, arXiv:0705.3268 (under review).

[3] D. Meiser, Jun Ye, D. R. Carlson, and M. J. Holland, *Prospects for a millihertz-linewidth laser*, Phys. Rev. Lett. **102**, 163601 (2009).

[4] D. Meiser and M. J. Holland, *Robustness of Heisenberg-limited interferometry with balanced Fock states*, New J. Phys. **11**, 033002 (2009).

[5] J. J. Kinnunen and M. J. Holland, *Bragg spectroscopy of a strongly interacting Bose-Einstein condensate*, New J. Phys. **11**, 013030 (2009).

[6] D. Meiser, Jun Ye, and M. J. Holland, *Spin squeezing in optical lattice clocks via lattice-based QND measurements*, New J. Phys. **10**, 073014 (2008).

[7] R. Bhat, M. Krämer, J. Cooper, and M. J. Holland, *Hall effects in Bose-Einstein condensates in a rotating optical lattice*, Phys. Rev. A **76**, 043601 (2007).

[8] B. T. Seaman, L. D. Carr, and M. J. Holland, *Reply to comment on 'Nonlinear band structure in Bose-Einstein condensates: Nonlinear Schrödinger equation with a Kronig-Penney potential'* , Phys. Rev. A **76**, 017602 (2007).

[9] B. T. Seaman, M. Krämer, D. Z. Anderson, and M. J. Holland, *Atomtronics: Ultracold-atom analogs of electronic devices*, Phys. Rev. A **75**, 023615 (2007).

[10] B. M. Peden, R. Bhat, M. Krämer, and M. J. Holland, *Quasi-angular momentum of Bose and Fermi gases in rotating optical lattices*, J. Phys. B: At. Mol. Opt. Phys. **40** 3725 (2007).

Other Publications on DOE supported research 2007-present

[11] R. A. Pepino, J. Cooper, D. Z. Anderson, and M. J. Holland, *Atom-Optical Analogs of Electronic Components and Devices*, Proceedings of the Dalgarno Celebratory Symposium, Cambridge, Massachusetts 10–12 September 2008, edited by James F Babb, Kate Kirby & Hossein Sadeghpour.

[12] M. Holland and J. Wachter, *Two-channel models of the BCS/BEC crossover*, Proceedings of the Enrico Fermi Summer School Course CLXIV on 'Ultracold Fermi Gases', Nuovo Cimento B & C,Rivista del Nuovo Cimento, Giornale di Fisica (2007).

[13] Jochen Wachter, *Resonant and nonresonant interactions in cold quantum gases*, PhD Thesis, University of Colorado at Boulder (2007).

[14] Brian Seaman, *Quantum dynamics of condensates, atomtronic systems, and photon fluids*, PhD Thesis, University of Colorado at Boulder (2008).

[15] Rajiv Bhat, *Bosons in rotating optical lattices*, PhD Thesis, University of Colorado at Boulder (2008).

Using Intense Short Laser Pulses to Manipulate and View Molecular Dynamics

Robert R. Jones, Physics Department, University of Virginia
382 McCormick Road, P.O. Box 400714, Charlottesville, VA 22904-4714
rrj3c@virginia.edu

I. Program Scope

This project focuses on the exploration and control of non-perturbative dynamics in small molecules driven by strong laser fields. Intense non-resonant laser pulses can radically affect molecules, both in internal and external degrees of freedom. The energy and angular distributions of electrons, ions, and/or photons that are emitted from irradiated molecules contain a wealth of information regarding molecular structure and field-driven dynamics. Not surprisingly, a molecule's alignment with respect to the laser polarization is a critical parameter in determining the effect of the field, and information encoded in photo-fragment distributions may only be interpretable if the molecular axis has a well-defined direction in the laboratory frame. Moreover, even molecules which possess a symmetry axis that can be aligned at a well-defined angle relative to the laser polarization are typically not symmetric with respect to inversion along that axis. Such asymmetric molecules may respond very differently to the alternating positive and negative half-cycles of the electric field in an intense laser pulse. The ability to identify or optically control the head vs. tail orientation of molecules in the laboratory frame is, therefore, critical for observing and characterizing an asymmetric response to standard, symmetric laser fields.

Asymmetric fields afford additional flexibility and control options. Using 2-color ($1\omega+2\omega$) fields with well-defined relative phases, or few-cycle laser pulses with well- defined carrier-envelope (CE) phase, molecules can be exposed to intense oscillating fields in which there is a pronounced difference in the peak amplitude in one direction over another. Such fields break the up/down symmetry in the laboratory frame making it possible to induce and/or exploit asymmetries within a target atom or molecule. For example, when atoms and symmetric molecules are exposed to an asymmetric field, the tunneling ionization amplitude and electron wavepacket trajectories are different for electron emission in the up and down directions. By controlling this difference, one can reduce/eliminate destructive interference between the harmonic emission from these trajectories, enabling the generation of even-order harmonics [1]. In addition, charge-localization induced by an asymmetric field can be used to control directional dissociative ionization (i.e. ion ejection up or down) from symmetric molecules [2]. Ultimately, strong well-controlled asymmetric fields used in combination with preferentially oriented targets will enable experiments seeking to drive electrons in specific directions within and molecules to probe molecular structure/dynamics or to control molecular photoprocesses.

II. Recent Progress

Our work during the current funding period has focused on: (i) achieving and optimizing field-free laser alignment and orientation of molecular targets; (ii) characterizing the alignment dependence of molecular tunneling ionization high-harmonic generation (HHG); (iii) controlling charge localization and directional Coulomb explosion in asymmetric 2-color laser fields, and (iv) exploring the influence of the (often neglected) atomic/molecular potential on laser-driven continuum electron dynamics. During the past year we have made progress and obtained new results on several fronts. First, we have extended our investigation of directional Coulomb

explosion to include triatomic and homonuclear diatomics with HOMOs of π- rather than σ-symmetry. We find that in spite of the fact that the enhanced ionization is expected to proceed differently in these systems, extremely strong directional fragmentation can still be achieved. Second, we have demonstrated that macroscopic propagation effects can result in intensity- and order-dependent reversals in the molecular orientation (parallel/perpendicular) which optimizes the HHG yield. Thus, such effects do not necessarily reflect single molecule structure or dynamics. Third, in collaboration with Tom Gallagher, we are developing a new approach for describing intense laser ionization in high frequency fields. The method involves the application of multi-channel quantum defect theory to dressed-states, providing a convenient framework for treating strongly coupled continua at arbitrarily large photon-orders. Fourth, we have begun an upgrade of our laser system to enable the generation of intense few-cycle phase-stabilized laser pulses. We are now amplifying CE-phase stabilized seed laser pulses and are constructing a second f-2f interferometer to lock the phase of the amplified pulses. In the following paragraphs we describe our results on directional Coulomb explosion and phase-matching effects in HHG from aligned molecules.

A. Controlled Directional Coulomb Explosion in an Asymmetric 2-Color Laser Field

We have studied dissociative ionization of N_2, O_2, CO_2, CO, and HBr in the presence of strong, asymmetric laser fields. Rather than use few-cycle CE-phase stabilized pulses [2], we employ a 2-color field consisting of temporally overlapped 35 fs laser pulses with wavelengths of 400 nm and 800 nm, respectively, and tunable relative carrier phase, φ. A time-of-flight mass spectrometer is used to measure the kinetic energy spectra of atomic and molecular ion fragments as a function of φ for different polarizations of the two pump pulses, different pulse durations, different relative intensities of the 400 nm and 800 nm pulses, and different pump/probe delays.

For all molecules studied, the yields of atomic ion fragments, A^{+m} and B^{+n} with total charge $(m+n)\geq 3$ and $A^{+m} \neq B^{+n}$, show a pronounced, φ-dependent forward/backward asymmetry along the detector axis. For a given ion species, we define an asymmetry parameter, $\beta = (N_+ - N_-)/(N_+ + N_-)$ where N_+ and N_- are the number of ions produced with velocities toward and away from the detector, respectively. At combined laser intensities $I\sim 5 \times 10^{14}$ W/cm^2, large asymmetries, $\beta \sim \pm 0.8$ are observed for $N_2^{3+} \longrightarrow N^{2+} + N^+$ and $O_2^{3+} \longrightarrow O^{2+} + O^+$, with comparable asymmetries in several CO channels, e.g. $CO^{4+} \longrightarrow C^{2+} + O^{2+}$ or $CO^{3+} \longrightarrow C^{2+} + O^+$. Somewhat smaller asymmetries are found in HBr and CO_2. The largest asymmetries are observed when the intensity of the 400 nm beam is one-quarter to one-eighth that of the 800nm pulse. In addition, for all fragments, the maximum β values are obtained at φ_{max}, where the field has the greatest asymmetry. Moreover, in all fragment pairs, the forward/backward asymmetry has the same sign for those ions which require the largest optical fields to produce via tunneling ionization. Since no asymmetry is detected for low charge states, even in CO and HBr, we conclude that selective ionization of molecules with specific orientations, due to native charge localization, is not primarily responsible for our observations. Rather, the directional Coulomb explosion is the result of strong-field dynamics.

Several auxiliary measurements have been performed in an attempt to identify the mechanism for the directional Coulomb explosion. For example, by using circularly polarized pulses, electron recollisions can be suppressed while maintaining a phase-dependent directional

asymmetry in the 2-color field. We find comparable β values with such pulses, indicating that field-driven electron rescattering does not play a dominant role in the process. In addition, using a 2-color pump field with reduced intensity ($I \sim 10^{14}$ W/cm^2) in conjunction with a more intense 800 nm probe, we have confirmed that transient orientation of the heteronuclear species is also not responsible for the asymmetries we observe.

Instead, our measurements are consistent with the notion that enhanced sequential ionization occurs as the molecule dissociates [3,4]. Charge-localization near one atomic ion, induced dynamically by the asymmetric field, makes further ionization much more likely from one ion center than from the other. Through enhanced ionization, higher charged states are most likely produced when the dissociating molecule has expanded to (for molecules with HOMOs of σ-symmetry) or beyond (non-σ HOMOs) a critical internuclear distance, R_c [4,5]. There the most weakly bound electrons can be localized on the uphill side of the combined molecular and optical potential and are more easily ionized in the direction of the maximum field. Following ionization, the atomic ions move apart rapidly under their mutual Coulomb repulsion such that the ion angular distributions at the detector reflect the orientation of the ions at the instant of ionization. Thus, the direction of the asymmetric field maximum determines the preferred emission direction for each atomic ion species. Our measurements indicate that 2-color asymmetric fields can effectively control field-induced charge localization for σ and π orbitals in spite of the fact that the dissociation dynamics are different.

B. Effects of Phase-Matching on HHG from Aligned N_2 in a Hollow Core Waveguide

In the standard model of HHG, an electron tunnel-ionizes in a strong low-frequency laser field, is accelerated to high energies by the field, is driven back toward its parent ion, and recombines by releasing the energy gained from the field as a high-energy photon. For a given laser intensity, the ionization and recombination rate as well as the spatial extent of the returning electron wavepacket depend on the electronic orbital structure and the orientation of the molecule relative to the (linear) laser polarization axis [6]. The recombination amplitude is also a function of the energy of the returning electron. If one assumes that the measured harmonic yield reflects the single molecule response, then comparisons of the harmonic spectrum at different alignment angles and/or between different species can reveal structural or dynamical information [6-9]. Accordingly, recent observations of intensity- and/or order-dependent changes in the preferred alignment direction for maximal harmonic emission from aligned N_2 and CO_2 molecules have been attributed to various aspects of the single molecule response [7,9].

We have observed changes in the preferred alignment direction in N_2 which are due solely to the phase-matching conditions within the target gas. We have used two time-delayed laser pulses to examine HHG from transiently aligned N_2 molecules in a hollow-core waveguide. The extended interaction length in the waveguide allows us to identify alignment-dependent propagation effects which mimic or mask various aspects of the single molecule response.

At low intensities, we find that the harmonic emission in all orders is enhanced for molecules preferentially aligned parallel, rather than perpendicular, to the laser polarization. However, depending on the target gas pressure, at higher intensities the higher order harmonics may, or may not, exhibit a reversal in this orientation preference. The pressure dependence of the reversal provides clear evidence that the phenomenon we observe is due, at least in part, to macroscopic

propagation effects. Simulations that include the alignment-dependence of the tunneling ionization rate and the concomitant changes in phase-matching due to the alignment-dependent free electron density are in qualitative agreement with our observations, indicating that the reversals we observe can be attributed solely to macroscopic propagation effects. While the propagation effects are perhaps more pronounced given the extended interaction length in our waveguide, they should also play a role in gas jet experiments where phase-matching is still important and the degree of alignment can be considerably greater. Clearly, extracting molecular structure or dynamical information from HHG measurements requires a detailed understanding of the phase-matching contribution from different molecular configurations. A manuscript describing our results has been submitted to Physical Review Letters.

III. Future Plans

We plan to continue our efforts to observe transient field-free orientation of polar and non-polar molecules using unipolar electric field pulses and two-color laser fields. We are awaiting the delivery of an Even-Lavie valve which should enable us to achieve sufficient rotational cooling (~ 1K) to produce and study transiently oriented molecules. We also plan to utilize a fiber compressor in conjunction with our CE-phase stabilized amplifier to generate intense few-cycle, CE-phase controlled pulses which will be used to explore directional Coulomb explosion in few-cycle asymmetric fields. In particular, we hope to determine whether the fragment directionality depends on the field asymmetry during the initial ionization step which leads to the expansion of the molecule to R_c, and if directional Coulomb explosion might be employed as a robust single-shot CE-phase detector. In addition, we plan to utilize attosecond pulse trains to photoionize molecules, near threshold, in the presence of a phase-locked laser field. We seek to characterize the effects of the ionic core on the electron energy spectrum to determine if such measurements might be useful for probing changes in molecular potentials with sub-femtosecond resolution.

IV. Publications from Last 3 Years of DOE Sponsored Research (July 2006- July 2009)

i) E. S. Shuman, R. R. Jones, and T. F. Gallagher, "Multiphoton Assisted Recombination," Phys. Rev. Lett. **101**, 263001 (2008).

ii) D. Pinkham, T. Vogt, and R.R. Jones, "Extracting the Polarizability Anisotropy from the Transient Alignment of HBr," J. Chem. Phys. 129, 064307 (2008).

iii) D. Pinkham, K. E. Mooney, and R.R. Jones, "Optimizing Dynamic Alignment in Room Temperature CO," Physical Review A **75**, 013422 (2007).

References

1. N. Dudovich, Nature Phys. **2**, 781 (2006).
2. M.F. Kling *et al.*, Science **312**, 246 (2006); V. Roudnev, B.D. Esry, and I. Ben-Itzhak, Phys. Rev. Lett. **93**, 163601 (2004).
3. T. Seideman, M.Yu. Ivanov, and P.B. Corkum, Phys. Rev. Lett. **75**, 2819 (1995); T. Zuo and A.D. Bandrauk, PRA **52**, R2511 (1995).
4. G. L. Kamta and A.D. Bandrauk, Phys. Rev. A **76**, 053409 (2007).
5. G. L. Kamta and A.D. Bandrauk, Phys. Rev. A **75**, 041401(R) (2007).
6. Itatani *et al*., Nature **432**, 867 (2004).
7. Tsuneto Kanai *et al.*, Nature 435, 470 (2005); C. Vozzi *et al.,* Phys. Rev. Lett. **95**, 153902 (2005); Anh-Thu Le, X.-M. Tong, and C. D. Lin, Phys. Rev. A **73**, 041402(R) (2006).
8. R. Torres *et al.*, Phys. Rev. Lett. **98**, 203007 (2007).

Molecular Dynamics Probed by Coherent Electrons and X-Rays

P.I.s: Henry C. Kapteyn and Margaret M. Murnane
University of Colorado at Boulder, Boulder, CO 80309-0440
Phone: (303) 492-8198; E-mail: kapteyn@jila.colorado.edu

The goal of this work is to develop novel short wavelength probes of materials and of molecules. We have made exciting advances in several experiments that probe complex molecular and materials dynamics using ultrafast, coherent, x-rays and electrons emitted during the high harmonic generation process. There were several highlights as a result of our prior support –

Probing coupled electron and nuclear dynamics in polyatomic molecules [17]
X-ray, electron, or laser beam scattering are common techniques used to probe crystalline or molecular structure and dynamics. To understand how complex reactions happen, the positions of atoms within a solid or a molecule must be monitored as the reaction occurs. Usually an external source of electrons or x-rays is used to monitor a fast process. In this work, we used ultrafast soft x-rays generated by the ionization and recollision of electrons from the molecule itself to probe the internal dynamics of a molecule. This is the first work to explore these effects.

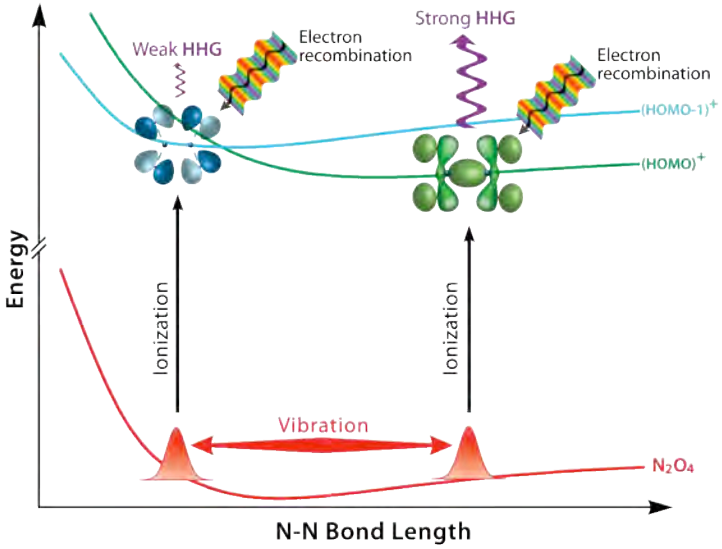

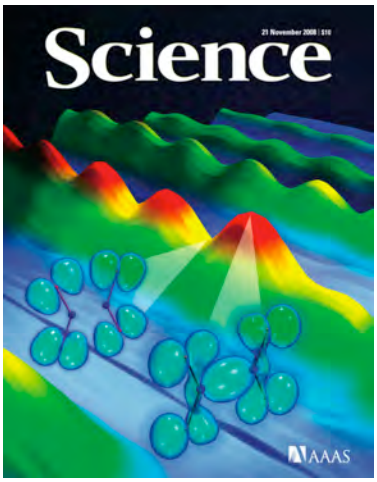

Figure 1. (Left) Time-resolved dynamics in N_2O_4 probed using high harmonic generation. At the inner turning point of N_2O_4 vibration, the ionization favors the "dark" state cation $(HOMO-1)^+$ and the harmonic yield is strongly suppressed At the outer turning point, the ground state cation$(HOMO)^+$ produces bright harmonics. (Right) Cover of *Science*, Nov. 21 issue, 2008.

In an earlier work published in PNAS, we performed the first experiment that used harmonic generation from a molecule to monitor coherent vibrations and discovered that high harmonic generation is very sensitive to small nuclear motions in molecules. In recent exciting work in collaboration with Albert Stolow at NRC Canada, we observed complex multi-state coupled electron and nuclear dynamics by studying HHG emitted from N_2O_4. By exciting large-amplitude vibrations in the ground state of an N_2O_4 dimer, and then irradiating the molecule with a strong laser field, we observe very large modulations in the resultant high harmonic yield. Our observations indicate that harmonics are emitted predominantly at the outer turning point of the vibrational motion. Detailed theoretical calculations reveal that at the outer turning point, the ground state cation is produced predominantly and contributes to the harmonic yield. However,

at the inner turning point, strong field ionization favors the first excited state cation instead of the ground state cation. Due to the symmetry of the cation first excited state, its recombination dipole is approaching zero. This dark state leads to a strong suppression of the harmonic yield at the inner turning point. This work was the first experiment in time-resolved molecular dynamics probed using high harmonic generation, and demonstrated that strong field ionization in HHG can access multiple molecular orbitals.

Radiation femtochemistry [10, 14, 18]

In a series of experiments in collaboration with Robin Santra from Argonne National Laboratory and Lew Cocke from Kansas State University, we made the first use of high-brightness, high repetition-rate high-order harmonic light in conjunction with a COLTRIMS momentum imaging apparatus. In this work, we were able for the first time to observe directly the chemical dynamics initiated by ionizing radiation i.e. *radiation femtochemistry.* This work immediately yielded new and unanticipated findings, exploring dissociation dynamics in highly excited states of N_2 and O_2 molecules. These experiments are uniquely suited to the use of HHG light sources, and explore new science that cannot be accessed using other approaches.

In an earlier experiment, we used soft-x-ray beams generated by high harmonic upconversion to photoionize an N_2 molecule, creating highly excited N_2^+ ions. A strong infrared pulse was then used to probe the ultrafast electronic and nuclear dynamics as the molecule explodes. We found that significant fragmentation occurs through an electron shakeup process, in which a second electron is simultaneously excited during the soft-x-ray photoionization process. During fragmentation, the molecular potential seen by the electron changes rapidly from nearly spherically symmetric, to a two-center molecular potential. Our approach can capture in real time and with Å resolution the influence of ionizing radiation on a range of molecular systems, probing dynamics that are inaccessible using other techniques. The direct observation of molecular dynamics initiated by x-rays had been hindered to date by the lack of bright femtosecond sources of short wavelength light.

More recently, we performed a similar experiment on oxygen molecules with dramatically different results. In this case, the 43eV EUV photon ionizes the molecule and also super-excites O_2^+ to a shake-up state that lies above the double ionization threshold. In past work however, Eland had observed a delayed ejection of the second electron - but the reason for the delay was not understood.

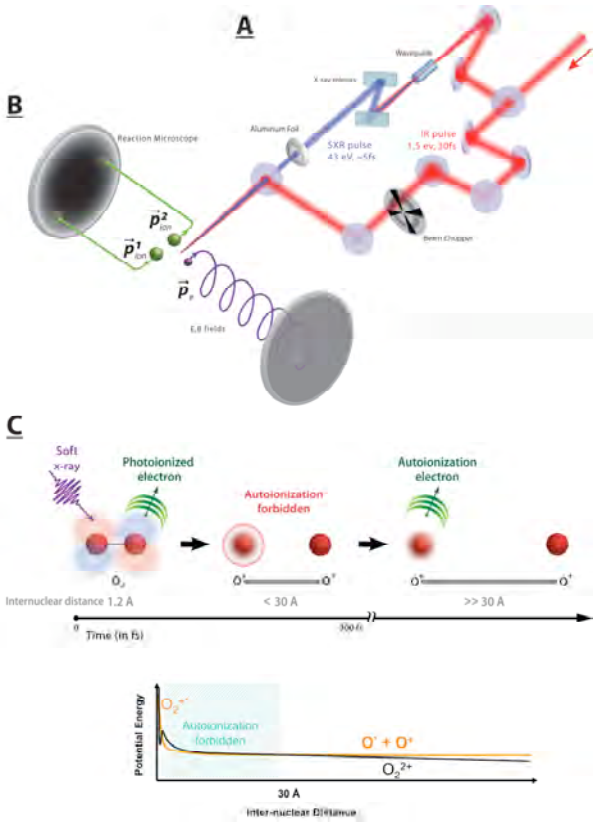

Figure 2: (A) Experimental setup in which a soft x-ray beam photoionizes the O_2 molecule while an IR probe beam ionizes the second electron before it is ejected by the ion. (B) COLTRIMS reaction microscope setup. (C) Schematic of the multistep photoionization, excitation and autoionization of O_2. Autoionization is forbidden until the autoionizing state emerges as a negative-binding energy Feshbach resonance at the internuclear separations of 30 angstroms or greater. *(Science **322**, 1081 (2008).)*

We therefore monitored the breakup of the Coulomb-exploding O^+ fragments in coincidence with the ejected electron. We found that the autoionization of the (O_2^+)* takes place only around the Frank-Condon region and quickly becomes energetically forbidden during the dissociation. Once the internuclear distance reaches 30 Å or greater, ionization is again energetically allowed and the ionized molecule can fall apart. In addition to uncovering a complex and surprising molecular fragmentation mechanism, our results were also the first to detect the birth of a negative binding energy Feshbach resonance in an atom. Prior to this work, negative binding energy states were thought to exist only in ions.

Understanding high harmonic generation from molecules [3, 6, 12, 13, 19]
Recent advances in experiment and theory now make it possible to monitor the amplitude, phase, and polarization state of HHG emission from molecules, over a broad range of harmonic orders. This leads to the intriguing possibility that HHG might have potential as a broadband attosecond-resolution probe of molecular dynamics. However, to achieve this, significant refining and benchmarking of both theory and experiment will be needed. In past work we made the first direct observation of the phase shift in high harmonic emission from molecules that results from the orbital structure. Our work confirmed very directly, through observation of an orientation-dependent π phase shift in the emission, that a simple two-charge center model for molecules with antisymmetric orbitals such as CO_2 does correctly predict the HHG emission phase. However, we observed no phase shift in the HHG emission from molecules with symmetric orbitals such as N_2. We also observed for the first time an effect that goes beyond the simplified model of molecular recollisions – the dispersion of a recolliding electron wavepacket as it returns to a molecular ion following strong field ionization. The influence of the molecular potential can clearly be observed in our data, indicating that a plane wave approximation for the returning electron wavepacket is not sufficient to describe HHG from molecules.

In very recent work, we made the first observation of elliptically polarized harmonic emission from molecules driven by linearly-polarized light. This change in polarization of the HHG field compared with the driving laser field can only occur if there is emission from more than one dipole, so that multi-electron effects (including contributions from more than the HOMO orbital) are important when considering harmonic generation from molecules. This result also provides a means for generating elliptically polarized harmonic beams.

Direct Measurement of the angular dependent ionization cross-section for single photon ionization of N_2 and CO_2 [15]
In work done in collaboration with Steve Pratt from ANL, we combined the use of a state-of-the-art high-harmonic ultrafast soft x-ray source with field-free dynamic alignment, allowing us for the first time to map the angular dependence of molecular photoionization yields for a non-dissociative molecule. The observed modulation in ion yield as a function of molecular alignment was attributed to the molecular-frame transition dipole moment of single photon ionization to the X, A and B states of N_2^+ and CO_2^+. We found that that the transition dipoles for single photon ionization of N_2 and CO_2 at 43eV have larger perpendicular components than parallel ones. A direct comparison with published theoretical partial wave ionization cross-sections confirm these experimental observations—our results were the first experimental data to allow such comparison with theory for bound cation states. The results provide the first step towards a novel method for measuring molecular frame transition dipole matrix elements.

Progress in other DOE-funded collaborations [1, 2, 4, 5, 7 - 9, 16, 20 – 22]
In work done in collaboration with Keith Nelson at MIT, we probed thin film thermoacoustic responses and nano-scale thermal transport using spatially coherent EUV beams. In work done in collaboration with Jorge Rocca at Colorado State University, we significantly extended the energy range of high harmonic generation from Ar ions to 550eV. We also demonstrated *full phase matching* in Ar, Ne and He at energies of 100eV, 200eV and 330eV for the first time. We also developed new phase matching schemes for the hard-x-ray region.

Publications as a result of DOE support since 2006

1. A. Paul, E. Gibson, X. Zhang, A. Lytle, T. Popmintchev, X. Zhou, M. Murnane, I. Christov, H. Kapteyn, "Phase matching techniques for coherent soft-x-ray generation", ***invited paper***, IEEE J. Quant. Electron. **42**, 14 (2006).
2. D. Gaudiosi, E. Gagnon, A. Lytle, J. Fiore, M. Murnane, H. Kapteyn, R. Jimenez, S. Backus, "Scalable multi-kHz Ti:sapphire amplifier based on down-chirped pulse amplification", Opt. Express **14**, 9277 (2006).
3. N. Wagner, A. Wüest, I. Christov, T. Popmintchev, X. Zhou, M. Murnane, H. Kapteyn, "Monitoring Molecular Dynamics using Coherent Electrons from High-Harmonic Generation", *PNAS* **103**, 13279 (2006).
4. D. Gaudiosi, B. Reagan, T. Popmintchev, M. Grisham, M. Berril, O. Cohen, B. Walker, M. Murnane, H. Kapteyn, J. Rocca, "HHG from ions in a capillary discharge", Phys. Rev. Lett. **96**, 203001 (2006).
5. R. Tobey, M. Siemens, M. Murnane, H. Kapteyn, K. Nelson, "Ultrasensitive Transient Grating Measurement of Surface Acoustic Waves in Thin Metal Films with EUV Radiation ", Appl. Phys. Lett. **89**, 091108 (2006).
6. N. Wagner et al., "High-Order X-Ray Raman Scattering using Coherent Electrons from High Harmonic Generation", "Optics in 2006", Optics and Photonics News pp 43 (Dec. 2006). *Also featured on cover*.
7. D. Gaudiosi et al., "HHG from ions in a capillary discharge", "Optics in 2006", Optics & Photonics News, pp 44 (Dec. 2006).
8. Ra'anan I. Tobey, Mark E. Siemens, Oren Cohen, Margaret. M. Murnane, and Henry C. Kapteyn "Ultrafast Extreme Ultraviolet Holography: Dynamic Monitoring of Surface Deformation", Optics Letters **32**, 286 (2007).
9. B.A. Reagan et al., "Enhanced High Harmonic Generation from Xe, Kr, and Ar in a Capillary Discharge", Physical Review A **76**, 013816 (2007).
10. Etienne Gagnon, Predrag Ranitovic, Ariel Paul, C. Lewis Cocke, Margaret M. Murnane, Henry C. Kapteyn, and Arvinder S. Sandhu, "Soft X-ray driven femtosecond molecular dynamics," *Science* **317**, 1374 (2007).
11. Henry C. Kapteyn, Oren Cohen, Ivan Christov, Margaret M. Murnane, "Harnessing Attosecond Science in the Quest for Coherent X-Rays," *Science* **317**, 775 (2007).
12. N. Wagner et al."Extracting the Phase of High Harmonic Emission from a Molecule using Transient Alignment in Mixed Samples," Phys. Rev. A **76**, 061403(R) (2007).
13. Xibin Zhou, Robynne Lock, Wen Li, Nick Wagner, Margaret. M. Murnane, Henry C. Kapteyn, "Molecular Recollision Interferometry in High Harmonic Generation," Physical Review Letters **100**, 073902 (2008).
14. E. Gagnon et al., "Time-resolved momentum imaging system for molecular dynamics studies using a tabletop ultrafast extreme-ultraviolet light source," Rev. Sci. Instrum. **79**, 063102 (2008).
15. I. Thomann, R. Lock, V. Sharma, E. Gagnon, S. Pratt, H. Kapteyn, M. Murnane, W. Li, "Direct Measurement of the Transition Dipole for Single-Photon Photoionization of N2 & CO2," J. Phys. Chem. A **112**, 9382 (2008).
16. T. Tenio Popmintchev, M.C. Chen, O. Cohen, M.E. Grisham, J.J. Rocca, M.M. Murnane, H.C. Kapteyn, "Phase-Matching of High Harmonics Driven by Mid-Infrared Light," Optics Letters **33**, 2128 (2008).
17. W. Li, X. Zhou, R. Lock, S. Patchkovskii, A. Stolow, H. Kapteyn, M. Murnane, "Time-resolved Probing of Dynamics in Polyatomic Molecules using High Harmonic Generation", Science **322**, 1207 (2008). (*on cover)*
18. A. S. Sandhu, E. Gagnon, R. Santra, V. Sharma, W. Li, P. Ho, P. Ranitovic, C. L. Cocke, M. M. Murnane, and H. C. Kapteyn, "Observing the Creation of Electronic Feshbach Resonances in Soft X-ray-Induced O-2 Dissociation," Science **322**, 1081 (2008).
19. X. Zhou, R. Lock, W. Li, N. Wagner, M. Murnane, H. Kapteyn, "Observation of Elliptically Polarized High Harmonic Emission from Molecules Driven by Linearly Polarized Light," Phys. Rev. Lett. **102**, 073902 (2009).
20. M. Siemens, Q. Li, M. Murnane, H. Kapteyn, R. Yang, E. Anderson, K. Nelson, "High-Frequency Acoustic Propagation in Nanostructures Characterized by Coherent EUV Beams", Appl. Phys. Lett. **94**, 093103 (2009).
21. T. Popmintchev, M.-C. Chen, A. Bahabad, M. Gerrity, P. Sidorenko, O. Cohen, I. P. Christov, M. M. Murnane, and H. C. Kapteyn, "Phase matching of high harmonic generation in the soft and hard X-ray regions of the spectrum," Proceedings of the National Academy of Sciences, p. 10.1073/pnas.0903748106, 2009.
22. T. Popmintchev, M. Murnane, H. Kapteyn, to be published, Nature Photonics (2009).

Detailed Investigations of Interactions between Ionizing Radiation and Neutral Gases

Allen Landers landers@physics.auburn.edu
Department of Physics
Auburn University
Auburn, AL 36849

Program Scope

We are investigating phenomena that stem from the many body dynamics associated with ionization of an atom or molecule by photon or charged particle. Our program is funded through the Department of Energy EPSCoR Laboratory Partnership Award in collaboration with Lawrence Berkeley National Laboratory. We are using variations on the well established COLTRIMS technique to measure ions and electrons ejected during these interactions. Photoionization measurements take place at the Advanced Light Source at LBNL as part of the ALS-COLTRIMS collaboration with the groups of Reinhard Dörner at Frankfurt and Ali Belkacem at LBNL. Additional experiments on charged particle impact are conducted locally at Auburn University where we are studying the dissociative molecular dynamics following interactions with either ions or electrons over a velocity range of 1 to 12 atomic units.

Recent Results

1. Breakdown of the Two-step Model in Core-level Photoionization of Neon.

We recently published results in Physical Review Letters [pub 2] that demonstrate for the first time the ability to simultaneously measure the full momentum vectors of both a low energy (~ 1 eV) photoelectron and an energetic (~ 800 eV) Auger electron over 4π solid angle following core-level photoionization by a single photon. This ability to directly measure the angular relationship between the two particles in the Ne^{2+} continuum revealed an interesting effect. Specifically, the photoelectron flux along the direction of the subsequent Auger electron is not diverted, as one might expect in a two-step description of photoionization followed by Auger decay. Rather, the photoelectron flux appears to simply be lost along the small fraction of solid angle near the Auger emission direction.

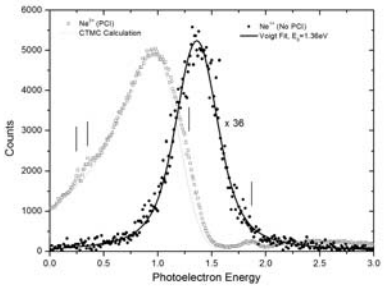

Figure 1: Photoelectron energies. The closed circles (•) of the right hand peak are photoelectrons measured in coincidence with Ne^+ ions and corresponding to direct photoionization with no PCI. The solid line is a Voigt fit. The open squares (□) of the left hand peak are photoelectrons measured in coincidence with Ne^{2+} ions and corresponding to photoionization followed by an Auger decay. The dashed line is the CTMC calculation by Robicheaux. The short vertical markers indicate recapture-remission lines.

Presented here are two figures from the article that demonstrate the power of the technique as well as the effect described above. Figure 1 shows the distribution of electrons for two final charge states of Ne. In the case of Ne+, the photoelectrons emerge with energies given by the photon energy minus the ionization potential, and are spread by the width of the Ne(1s) hole and the experimental resolution. The electrons that correspond to the doubly charged final state of the ion have been shifted in energy by the potential change from 1/r to 2/r upon Auger decay. One can also see the small bumps and shoulders (marked with vertical lines) that arise from recapture of the photoelectron when the potential changes followed by re-emission at discreet energies.

The primary result from this work is shown in Figure 2, which shows the relative angle between Auger and photo electrons. Within the two step model, the initial photoelectron flux is diverted away from the Auger emission direction, as is demonstrated in the calculation by Robicheaux. However, in the measurement, we find that the photoelectrons emitted along the Auger direction are not diverted, but rather, they don't come out at all. This is a strong indication that initial state correlation plays a critical role in this photoionization/Auger process and the 2-step picture of the emission of one electron preceding that of the other doesn't fit for the small amount of phase space where the two are emitted in the same direction.

Additional curves include the calculation folded with multiple factors of the experimental resolution to test if the difference is an instrumental effect.

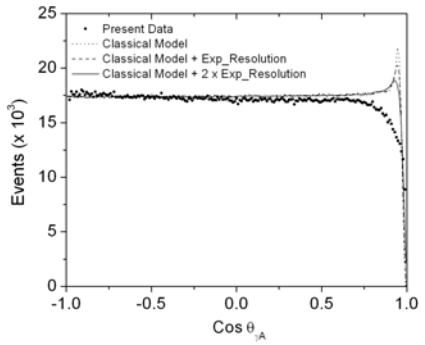

Figure 2: Distribution in cosine of the angle between the Auger electron and photoelectron. Closed circles (•) represent experiment data. Dashed and solid lines correspond to a two-step CTMC calculation (Robicheaux), including cases where the experiment resolution and twice the experiment resolution have been folded into the calculation. The calculation clearly shows a redistribution of photoelectron flux, while it can be seen from the data the flux is actually lost.

2. Double Auger Decay of Neon Following by Core-level Photoionization

There is a small probability (~6 %) that the $Ne(1s^{-1})^+$ hole state will decay via double Auger electron emission. In this decay channel, the final state includes the photoelectron, two Auger electrons and the residual Ne^{3+} ion. We have recently performed an experiment to measure the angular correlation between the three continuum electrons. This measurement might allow, for example, a study of how the relationship between the photoelectron momentum and the momentum sum of the two Augers as function of the energy sharing between the two electrons, which would lead to significant further insight into the roles of initial- and final-state correlation in core-photoionization. Data are currently being analyzed and we anticipate results soon.

Specifically, we have measured three electrons e^- and a recoiling Ne^{3+} ion in coincidence following the core-photoionization of neon. Recognizing that the two-step interpretation is at heart of this investigation, we still use this model to describe the process:

$$Ne + h\nu(870\text{-}890eV) \rightarrow Ne(1s^{-1})^+ + e^-_{photo} \text{ (photoelectron emission)}$$

$$Ne(1s^{-1})^+ + e^-_{photo} \rightarrow Ne(1s^{-1})^{3+} + e^-_{photo} + e^-_{Auger} + e^-_{Auger} \text{ (Double Auger decay)}$$

The aim is to explore the entangled angular distribution of the three emitted electrons with respect to one another. Such a simultaneous vector momentum measurement of three continuum electrons will likely enable a deeper understanding of the relaxation processes in excited atoms. Described below is the physics we plan to investigate as analysis of the data progresses.

Goal 1: Investigation of the correlated Auger-electron emission. We are exploring, for example, the simultaneous angular and energy correlation between the two Auger electrons to deepen our understanding of this highly-correlated decay pathway. We suspect that the double-Auger decay is in many ways similar to the well documented direct double photoionization (one photon in, two electrons out) of say, helium. For roughly equal energy sharing, there might a strong correlation between the two Auger electrons as in a knock-out type mechanism; and for strongly asymmetric energy sharing, there might be little or no correlation between the two electrons as in a shake-off type mechanism.

Goal 2: Understanding the role of initial and final state correlation in core-level photoionization. As discussed above, one primary motivation of the experiment is to shed further light on the breakdown of the two-step model in describing photo-ionization and (possibly) successive Auger-decay. A strong initial-state effect might be observed in the correlation between the sum momentum of the two Augers and the photoelectron. It might be that such an effect is observed to vary with different energy sharing between the Augers.

3. Investigating Asymmetries in the $HD^+(1s\sigma)$ Branching Ratio through Collisions with Electrons

We have built an electron-molecule collision experiment that uses a pulsed COLTRIMS technique that allows for momentum imaging of molecule fragments after dissociative ionization by electrons with energies from 10eV to 2000 eV. Preliminary experiments focus on isotope effects in the dissociative ionization of HD based on prior work by Ben-Itzhak and coworkers for ion impact [ref 1]. A beam from a

pulsed electron gun passes through a diffuse target, followed by a synchronized electric field pulse which extracts the ions to a multi-channel plate detector with delay-line anode.

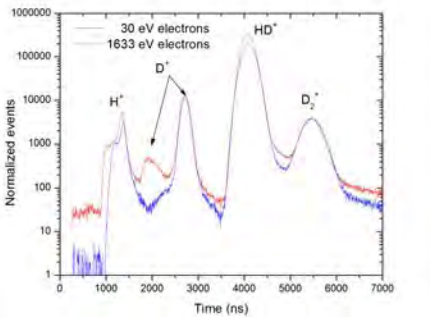

Figure 3: Typical time of flight spectrum showing flight times for ions created by electron impact on HD. The blue and red curves correspond to 30 eV and 1633 eV electron impact energies respectively.

Figure 3 shows data from initial measurements. The shoulder to the left of the H^+ peak arises from fast protons from H_2O contaminant as well as dissociation of HD^{2+} and D_2^{2+}. The secondary D^+ peak arises from energetic dissocation events that are inaccessible for the low energy impact case. Currently we are unable to clearly isolate the dissociative channel of interest due to background effects from water and contaminant H_2 and D_2 in the target gas. We have begun work on a new apparatus that incorporates a localized gas jet for a target, which will allow for full momentum imaging of the molecule fragments and a substantially better separation from background. In the meantime the present apparatus is being rebuilt to accommodate a larger detector and a spectrometer designed for fragment-fragment coincidences in multiply ionizing electron-molecule collitions.

4. Orientation Dependence in the Double Ionization of HD Molecules by Fast Ions

We are currently studying the level of orientation isotropy in the dissociative double ionization of HD molecules by fast ions as a function of projectile velocity. The light ions used to doubly ionize ground state HD molecules originate at the Auburn University Accelerator, which is capable of producing ions with velocities ranging from 1 to 13 atomic units.

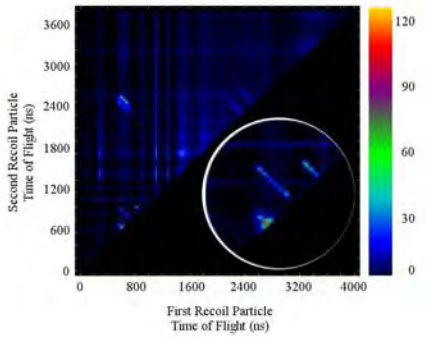

Figure 4: Fragment coincidence spectrum. The enlarged view shows the three species in the equilibrium target gas: HD, H_2 and D_2. This spectrum also shows coincidences from background gases H_2O, N_2 and O_2.

Previous studies have shown that the fragmentation of neutral hydrogen molecules by ion impact sometimes exhibit angular dependencies akin to Young's double slit experiment. These quantum mechanical effects have been observed in capture or transfer ionization [ref 2] as well as in double ionization [ref 3]. A similar experiment on the ground-state dissociation following single ionization [ref 4] showed no such angular dependence. In each case, results were consistent with a simple two-center model that predicts the angular distribution:

$$d\sigma(\theta) = d\sigma_a\left[1+\cos\left(q_z R\cos(\theta)\right)\right]$$

Where R is the internuclear position vector, θ is the angle between the molecular axis and the ion beam direction, and qz is the longitudinal momentum transfer. The latter is well approximated by the energy transfer divided by the incident projectile velocity $q_Z \cong Q/v_p$. Because of the velocity dependence of this model, we are investigating the molecule orientation isotropy for a variety of ion velocities. Preliminary results presented here are for 3 MeV He^{2+} ions with a velocity of 5.5 au. This initial projectile was chosen for convenience and because the results from [ref 3] are for F^{8+} ions with a similar velocity (6.3 au).

Figure 4 shows a typical time of flight correlation plot which demonstrates our success in producing our own HD by mixing H_2 and D_2 with a catalyst. Current results are statistics limited, but we anticipate momentum spectra and molecule angular distributions soon.

References:

1. I. Ben-Itzhak, E. Wells, K. D. Carnes, Vidhya Krishnamurthi, O. L. Weaver, and B. D. Esry *Phys. Rev. Lett* **85**, 58 (2000).
2. D. Cheng, C.L. Cocke, V. Frohne, E.Y. Kamber, J.H. McGuire, and Y. Wang, *Phys. Rev.* A **47** 3923 (1993).
3. A.L. Landers, E. Wells, T. Osipov, et. al. *Phys. Rev.* A **70** 042702 (2004).
4. Nora G. Johnson, R. N. Mello, Michael E. Lundy, J. Kapplinger, Eli Parke, K. D. Carnes, I. Ben-Itzhak, and E. Wells *Phys. Rev*. A **72** 0527711 (2005).

Supported Publications

1. **Photo and Auger Electron Angular Distributions of Fixed-in-Space CO_2** F.P. Sturm, M. Schöffler, S. Lee, T. Osipov, N. Neumann, H.-K. Kim, S. Kirschner, B. Rudek, J.B. Williams, J.D. Daughhetee, C.L. Cocke, K. Ueda, A.L. Landers, Th. Weber, M.H. Prior, A. Belkacem, and R. Dörner, Phys. Rev. A (*accepted for publication* 2009).
2. **Angular Correlation between Photo- and Auger electrons from K-Shell Ionization of Neon** A.L. Landers, F. Robicheaux, T. Jahnke, M. Schöffler, T. Osipov, J. Titze, S.Y. Lee, H. Adaniya, M. Hertlein, P. Ranitovic, I. Bocharova, D. Akoury, A. Bhandary, Th. Weber, M.H. Prior, C.L. Cocke, R. Dörner, and A. Belkacem, Phys. Rev. Lett. **102**, 223001 (2009).
3. **Fragmentation pathways for selected electronic states of the acetylene dication** T Osipov, T N Rescigno, T Weber, S Miyabe, T Jahnke, A S Alnaser, M P Hertlein1, O Jagutzki, L Ph H Schmidt, M Schöffler, L Foucar, S Schössler, T Havermeier, M Odenweller, S Voss, B Feinberg, A L Landers, M H Prior, R Dörner, C L Cocke and A Belkacem, J. Phys. B, **41** 091001 (2008).
4. **Ultrafast Probing of Core Hole Localization in N_2** M. S. Schöffler, J. Titze, N. Petridis, T. Jahnke, K. Cole, L. Ph. H. Schmidt, A. Czasch, D. Akoury, O. Jagutzki, J. B. Williams, N. A. Cherepkov, S. K. Semenov, C. W. McCurdy, T. N. Rescigno, C. L. Cocke, T. Osipov, S. Lee, M. H. Prior, A. Belkacem, A. L. Landers, H. Schmidt-Böcking, Th. Weber, and R. Dörner, Science, **320**, 920 (2008).
5. **Interference in the collective electron momentum in double photoionization of H_2** Kreidi K, Akoury D, Jahnke T, Weber T, Staudte A, Schoffler M, Neumann N, Titze J, Schmidt LPH, Czasch A, Jagutzki O, Costa Fraga RA, Grisenti RE, Smolarski M, Ranitovic P, Cocke CL, Osipov T, Adaniya H, Thompson JC, Prior MH, Belkacem A, Landers AL, Schmidt-Bocking H, and Dorner R., Phys. Rev. Lett., **100**, 133005 (2008).
6. **A two-electron double slit experiment: interference and entanglement in photo double ionization of H_2** D. Akoury, K. Kreidi, T. Jahnke, Th. Weber, A. Staudte, M. Schöffler, N. Neumann, J. Titze, L. Ph. H. Schmidt, A. Czasch, O. Jagutzki1, R.A. Costa Fraga1, R. Grisenti, R. Diez Muino, N. Cherepkov, S. Semenov, P. Ranitovic, C.L. Cocke, T. Osipov, H. Adaniya, M.H. Prior, A. Belkacem, A. Landers, H. Schmidt-B¨ Böcking, and R. Dörner, Science, **318**, 949 (2007).
7. **Single Photon-Induced Symmetry Breaking of H_2 Dissociation** F. Martín, J. Fernández, T. Havermeier, L. Foucar, Th. Weber, K. Kreidi, M. Schöffler, L. Schmidt, T. Jahnke, O. Jagutzki, A. Czasch, E. P. Benis, T. Osipov, A. L. Landers, A. Belkacem, M. H. Prior, H. Schmidt-Böcking, C. L. Cocke, R. Dörner, Science **315**, 629 (2007).
8. **Nondipole effects in the angular distribution of photoelectrons from the C K shell of the CO molecule** K. Hosaka, J. Adachi, A. V. Golovin, M. Takahashi, T. Teramoto, N. Watanabe, T. Jahnke, Th. Weber, M. Schöffler, L. Schmidt, T. Osipov, O. Jagutzki, A. L. Landers, M. H. Prior, H. Schmidt-Böcking, R. Dörner, A. Yagishita, S. K. Semenov, and N. A. Cherepkov, Phys. Rev. A **73**, 022716 (2006).
9. **Momentum-imaging investigations of the dissociation of D_2^+ and the isomerization of acetylene to vinylidene by intense short laser pulses** Alnaser AS, Litvinyuk I, Osipov T, Ulrich B, Landers A, Wells E, Maharjan CM, Ranitovic P, Bochareva I, Ray D, Cocke CL. J. Phys. B 39, 485 (2006).

Program Title:

"Properties of actinide ions from measurements of Rydberg ion fine structure"

Principal Investigator:

Stephen R. Lundeen
Dept. of Physics
Colorado State University
Ft. Collins, CO 80523-1875
lundeen@lamar.colostate.edu

Program Scope:

This project will determine certain properties of chemically significant Uranium and Thorium ions through measurements of fine structure patterns in high-L Rydberg ions consisting of a single weakly bound electron attached to the actinide ion of interest. The measured properties, such as polarizabilities and permanent moments, control the long-range interactions of the ion with the Rydberg electron or other ligands. The ions selected for initial study in this project, U^{6+},U^{5+}. U^{4+}, Th^{4+}, and Th^{3+}, all play significant roles in actinide chemistry, and are all sufficiently complex that *a-priori* calculations of their properties are suspect until tested. The measurements planned under this project should serve the dual purpose of providing data that is directly useful to actinide chemists and providing benchmark tests of relativistic atomic structure calculations. In addition to the work with U and Th ions, which takes place at the J.R. Macdonald Laboratory at Kansas State University, a parallel program of studies with stable singly-charged ions takes place at Colorado State University. These studies are aimed at clarifying theoretical questions connecting the Rydberg fine structure patterns to the properties of the free ion cores, thus directly supporting the actinide ion studies. In addition, they provide training for students who can later participate directly in the actinide work.

Recent Progress:

New ECR Source:

Our first priority this year has been completing the installation of the new 14 GHz permanent magnet ECR ion source at KSU, and of the RESIS beamline where the actinide ion studies will take place. The source was delivered to KSU in January 2008, and planning for its installation began. The old ECR was decommissioned in May 2008, and installation of the new source began in the summer of 2008. The RESIS beamline was completed in October 2008 and the first RESIS signals were observed in early November 2008. Uranium ion beams were first obtained in March, 2009. Over the course of 2009, obtaining source operation at the level specified in the purchase agreement has been a continuing issue. At issue is the intensity of U^{6+} beams. These were specified to be 600 particle nA at a terminal potential of 15 keV, but the maximum intensities obtained to date are about two orders of magnitude smaller. Since the beam intensity is crucial to the S/N in the proposed experiments, we are aggressively pursuing possible improvements.

Pb^{2+} Study:

As an initial test of the new RESIS beamline and ECR source, graduate student Mark Hanni carried out a study of Rydberg states bound to the Pb^{2+} and Pb^{4+} ions. This was motivated in part by discrepant reports of the polarizability of the Pb^{2+} ion in the literature, both based on experiment. One report, based on spectroscopy of $(6s)^2$nd levels concluded that α_d=13.38(2) [1], while another based on the 6s6p lifetime said α_d =7.8(6) [2]. Hanni's data showed clearly that the larger result was correct and that the difference was due to the relatively large polarizability (~6 a.u.) of the closed shell $(5d)^{10}$ Pb^{4+} ion.. The resolved RESIS excitation lines showed structure due to Stark mixing in the upper state of the transition, caused by the presence of a small stray electric field (~0.08 V/cm) in the laser excitation region. This is one of the primary systematic difficulties that will be encountered in the actinide studies, so this warm-up experiment presents a good opportunity to attack this problem on a signal that is relatively easy to observe. Hanni has constructed an electrode structure to be installed in the laser interaction region that we hope will be able to null out fields of this magnitude.

U^{6+} Study:

Despite the unsatisfactory U^{6+} beam intensity, we are pushing ahead with a study of Rydberg levels built on this ion, and trying to optimize all other aspects of the experiment. We're focusing initially on the n=55 to n=109 transition, since it is similar to the transition we used to measure properties of the Kr^{6+} ion [3]. The main difficulty in this experiment is the small size of the signals representing excitation of individual L levels in n=55 of U^{5+}, expected to be less than 1% of the size of the signal representing excitation of the highest L levels in n=55. Aside from the initial U^{6+} beam intensity, the most important factor limiting signal to noise is the size of background count-rates that compete with the expected small signal. In comparison with the high-L signal, we have found the background to be about a factor of 10 larger with a U^{6+} beam, than with the Kr^{6+} beam. The primary source of background appears to be auto-ionizing Rydberg levels, presumably created when metastable excited levels of U^{6+} capture a Rydberg electron in our Rydberg target. Finding a way to reduce this background promises to be a long-term problem. We have recently obtained preliminary evidence of resolved structure in the 55-109 transition in U^{5+} showing evidence of resolved signals that are approximately 0.7% the size of the high-L peak. Additional improvements in S/N will be required before this study can be completed.

Ni Rydberg states:

Many of the actinide studies which we plan involved ions with relatively large angular momentum. The Fr-like U^{5+} and Th^{3+} ions, for example, have $^2F_{5/2}$ ground states. This results in a Rydberg fine structure consisting of six eigenstates for each value of L, more complex than any structure we have studied in the past. In order to explore the physics of such complex structures, we began a study of Rydberg states of Ni. Since the Ni^+ ion has a $^2D_{5/2}$ ground state, it's Rydberg fine structure is analogous to that expected in the U^{5+} and Th^{3+} studies. Graduate student Julie Keele has headed up this study, and has nearly completed its initial phase studying the RESIS excitation spectrum from n=9 to n=19 and n=20. Keele has determined the fine structure energies corresponding to 23

of the 24 n=9 levels with $5 \le L \le 8$. Comparing these energies with the polarization model, she determined the three primary core parameters, scalar and tensor dipole polarizability and quadrupole moment.

$$\alpha_0 = 7.90(6)\ a.u. \qquad \alpha_2 = 1.10(8)\ a.u. \qquad Q = -0.4739(15)\ a.u.$$

The spectra also hints at a fourth order tensor structure due to the permanent hexadecapole moment of the Ni^+ ion, something that is only possible in ions with $J \ge 2$.

Ba Rydberg K-splittings:

One puzzling aspect of our measurements of Ba Rydberg structure obtained in 2007 [4] was the interpretation of the indirect spin-orbit splittings between 6snL Rydberg levels with $K=L \pm 1/2$. Others had suggested that these measurements could be used to determine dipole and quadrupole transition probabilities in Ba^+, but the resulting estimates of quadrupole transition probabilities were badly discrepant with theoretical calculations and with other experimental measurements.[5] This suggested that the theoretical framework that had been used to interpret the measurements was incomplete. Graduate student Shannon Woods looked into this and was able to show that higher-order terms in the perturbation description of Ba Rydberg levels must be included to extract reliable estimates of the matrix elements. She calculated the most significant third and fourth-order contributions to the K-splittings and found that they eliminated the discrepancy between measurements and the best theoretical matrix elements[6].

References

[1] "Series Limit on hydrogenlike series in PbII" C.B. Ross, D.R. Wood, P.S. Scholl, J. Opt. Soc. Am. 66, 36 (1976)

[2] "Determination of polarizabilities and lifetimes for the Mg, Zn, Cd, and Hg isoelectronic sequences", N Reshetnikov, L.J. Curtis, M.S. Brown, and R.E. Irving, Physica Scripta 77, 015301 (2008)

[3] "Polarizability of Kr^{6+} from High-L Kr^{5+} Fine Structure Measurements", S.R. Lundeen and C.W. Fehrenbach, Phys. Rev. A 75, 032523 (2007)

[4] "Fine Structure Measurements in high-L n=17 and n=20 Rydberg states of Barium", E.L. Snow and S.R. LundeenPhys. Rev. A 75, 062512 (2007)

[5] "Ionic dipole and quadrupole matrix elements from nonadiabatic core polarization", E.S. Shuman and T.F. Gallagher, Phys. Rev. A 74, 022502 (2006)

[6] "Theoretical study of lifetimes and polarizabilities in Ba^+", E. Iskrenova-Tchoukova and M.S. Safronova, Phys. Rev. A 78, 012508 (2008)

Immediate Plans:

We are continuing to work towards improvements in S/N in the U^{6+} experiment. This involves improvements in ECR output, reductions in background levels, and improved control of the electric environment at the location of CO_2 laser excitation. Our initial goal is to obtain a solid measurement of the polarizability of U^{6+}. This first actinide experiment is somewhat more difficult than the Th^{4+} experiment, which will be our second experiment, but considerably less difficult than the planned studies of Fr-like ions Th^{3+} and U^{5+}. Our progress in the U^{6+} study will be a good indicator of the future scope of these studies.

The next phase of the Ni study will involve use of microwave spectroscopy to improve the precision of the results. In addition, we will be investigating possible complications in the long-range model of Rydberg fine structure that occur for an ion of this high angular momentum. This will include application of these models to Rydberg levels built on the Fr-like ions Th^{3+} and U^{5+}.

Recent Publications:

"Optical spectroscopy of high-L Rydberg states of Argon" L.E. Wright, E.L. Snow, S.R. Lundeen, and W.G. Sturrus, Phys. Rev. A 75, 022503 (2007)

"Higher-order contributions to fine structure in high-L Rydberg states of Si^{3+}", E.L. Snow and S.R. Lundeen, Phys. Rev. A 75, 062512 (2007)

"Polarizability of Kr^{6+} from High-L Kr^{5+} Fine Structure Measurements", S.R. Lundeen and C.W. Fehrenbach, Phys. Rev. A 75, 032523 (2007)

"Fine Structure Measurements in high-L, n=17 and n=20 Rydberg states of Barium", E.L. Snow and S.R. Lundeen , Phys. Rev. A, 76, 052505 (2007)

"Determination of dipole and quadrupole polarizabilities of Mg^{+} by fine structure measurements in high-L, n=17 Rydberg states of Mg", E.L. Snow and S.R. Lundeen, Phys. Rev. A 77, 052501 (2008)

"Microwave spectroscopy of high-L n=10 Rydberg states of argon", M.E. Hanni, Julie A. Keele, and S.R. Lundeen, Phys. Rev. A 78, 062510 (2008)

"Dipole and Quadrupole transition strengths in Ba^{+} from measurements of K-splittings in high-L Barium Rydberg levels", Shannon L. Woods, S.R. Lundeen, and Erica L Snow (Submitted to Phys. Rev. A, July 2009)

Theory of threshold effects in low-energy atomic collisions

J. H. Macek

Department of Physics and Astronomy,
University of Tennessee, Knoxville, Tennessee and
Oak Ridge National Laboratory, Oak Ridge, Tennessee
email:jmacek@utk.edu

1 Program scope

Our project is predicated upon the view [1,2,7] that developing methods for highly accurate calculations of ion-atom collisions is a timely task for atomic theory. The interactions are known, they are relatively simple, numerical methods such as the Lattice-Time-Dependent-Schrödigner equation are approaching high accuracy, and cross sections accurate at the 1% level are needed to characterize hydrogen atom beams used in plasma diagnostics.

To achieve high accuracy in numerical calculations it is essential to understand all of the physical processes that occur in time-dependent quantum processes. A second goal of our work is to interpret structure in the electron momentum distribution $P(\boldsymbol{k})$ and identify essential physical processes involved in ionization. To do this we have developed a method to extract $P(\boldsymbol{k})$ from time-dependent wave functions that allow us to trace structure in $P(\boldsymbol{k})$ to structure in atomic wave functions when target and projectile are strongly interacting. In this way, we have found that free vortices are formed in one-electron wave functions. Calculations have shown that these vortices may be observed [2].

We also continue our research into structure related to threshold phenomena. The projects listed in this abstract are sponsored by the Department of Energy, Division of Chemical Sciences, through a grant to the University of Tennessee. The research is is carried out in cooperation with Oak Ridge National Laboratory under the ORNL-UT Distinguished Scientist program.

2 Recent progress

Previous work with the Regularized Lattice-Time-Dependent-Schrödinger equation (RLTDSE) method [7] has shown that measured momentum distributions $P(\boldsymbol{k})$ image *coordinate* space wave functions according to

$$P(\boldsymbol{k}) = \lim_{t\to\infty} \left[\left| t^3 \psi(\boldsymbol{r}, t) \right|^2 \right]_{\boldsymbol{r}=\boldsymbol{k}t} \tag{1}$$

where it is understood that $\boldsymbol{r} \neq \boldsymbol{r}_Q$ and $\boldsymbol{r}_Q$ is any potential center. This equation, called the "imaging theorem" allows structure in $P(\boldsymbol{k})$ to be traced to structure in $\psi(\boldsymbol{r}, t)$ at earlier times. Using the RLTDSE method and the imaging theorem we have shown that "holes" in highly accurate momentum distributions are due to free vortices [2]. It was also shown that the vortices are observable, in principle. We have further shown that an exact zero at any point other that at potential centers must be a vortex. Computation of the probability current $\boldsymbol{w}$ near the zero shows that it circulates around the zero and is quantized according to

$$\oint \boldsymbol{w} \cdot d\boldsymbol{l} = 2\pi \tag{2}$$

confirming that the zeros are actually vortices.

Professor J. S. Briggs has pointed out to us that unexplained minima appear in quite different realms, namely, triply differential cross sections (TDCS) in (e,2e) measurements of electron impact on atomic helium. His theoretical work has shown that there is an exact zero near a measured minima. To analyze this minima for vortex structure we have shown that the imaging theorem can be applied to electron impact ionization of multi-electron targets. For two electrons in the final state and the He^+ ion in the ground state we show that

$$\lim_{t\to\infty} t^3 \psi(\boldsymbol{r}_a = \boldsymbol{k}_a t, \boldsymbol{r}_b = \boldsymbol{k}_b t, t) = A(\boldsymbol{k}_a, \boldsymbol{k}_b) \tag{3}$$

$$P(\boldsymbol{k}_a, \boldsymbol{k}_b) \propto |A(\boldsymbol{k}_a, \boldsymbol{k}_b)|^2 \tag{4}$$

where a and b label two unbound electrons in the final state, and energy conservation is understood. The equality holds up to an overall multiplicative constant. To get this result one must suppose that the incident electron is

represented by a wave packet and the $t \to \infty$ limit is taken before the limit of an arbitrarily narrow initial wave packet.

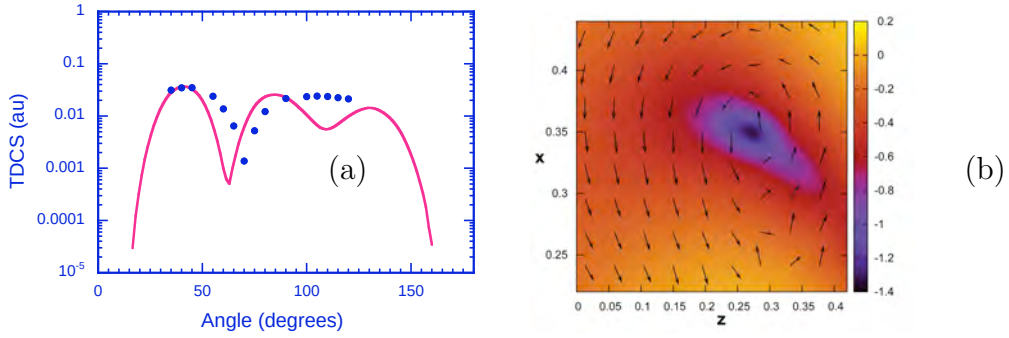

Fig. 1. TDCS for the process $e^- + He \to e^- + e^- + He^+$. (a) TDCS *vs* one-half the angle between the outgoing electron momenta for equal electron energies of 20 eV in the symmetric geometry. The angle between $\boldsymbol{k}_+$ and the incident momentum $\boldsymbol{K}_i$ is 157.5^o. The dots are experimental data of Murray and Read, normalized to theory at 45^o. (b) Contour plot of the computed $\log[|A(\boldsymbol{k}_+, \boldsymbol{k}_{ab})|]$ where the x and z labels refer to the components of $\boldsymbol{k}_+$. The arrows show the direction of $\boldsymbol{w}$.

In general, exact minima for (e,2e) are not expected since measured TCS are incoherent superpositions of singlet and triplet couplings of the two electrons a and b in the final state. For the special case of symmetric geometry with equal energies for the outgoing electrons, only the singlet couplings contributes. Then, there may be exact zeros in the TDCS. Using a 3C correlated final state, as in the previous calculations that found the minimum, we have computed the (e,2e) TDCS for helium targets compared with experimental data in Fig. 1a. The calculations show a minimum similar to the observed minimum.

To check whether this minimum correlates with a vortex we employ momentum variables $\boldsymbol{k}_+ = (\boldsymbol{k}_a + \boldsymbol{k}_b)/2$ and $\boldsymbol{k}_{ab} = (\boldsymbol{k}_a - \boldsymbol{k}_b)/2$ appropriate to the symmetric geometry. A contour plot of the ionization amplitude on a grid in the plane defined by $\boldsymbol{k}_+$ and the incident momentum $\boldsymbol{K}_i$, with the $z-$axis along the incident momentum and the $x-$axis in this plane, is shown in Fig. 1b. The plot shows a zero at $k_{+x} = 0.35$ au, $k_{+z} = 0.27$ au whereas the experimental minimum is at $k_{+x} = 0.38$ au, $k_{+z} = 0.16$ au, thus we conclude that the minimum lies close to a zero and is therefore due to a vortex. This is further confirmed by plotting the direction of the velocity $\boldsymbol{w} = \Im[\nabla_{\boldsymbol{k}_+} \log A]$ which is seen to circulate around the zero. Integration of the current around

the zero gives 2π as is should for a first order zero.

Other projects investigate structure that appears in elastic scattering [4,8], charge exchange reactions [3], low energy three-body interactions [3,6] and ionization by positron impact [5]. The threshold ionization cross section obeys the extended threshold law proposed earlier by us and verified by convergent close coupling model calculations. We find some unanticipated structure owing to hidden crossings of hyperspherical adiabatic potential energy curves.

3 References to DOE sponsored research that appeared in 2007-2009

1. Evolution of Quantum Systems from Microscopic to Macroscopic Scales, Sergey Y. Ovchinnikov, Joseph H. Macek, James S. Sternberg, Teck-Ghee Lee, and David R. Schultz, CAARI 2008 Proceedings AIP Conference Proceedings, **1099**, 164 (2009).
2. Origin, evolution, and imaging of vortices in atomic processes, J.H. Macek J.S. Sternberg and S.Y. Ovchinnikov, T-G. Lee and D.R. Schultz, Phys. Rev. Lett, **102**, 143201(2009).
3. Multiparticle interactions of zero-range potentials, J. H. Macek, Few-Body Syst, **45**,207 (2009).
4. Feshbach resonances in atomic structure and dynamics, J. H. Macek, Proceedings of the JointPhysics/Mathematics Workshop on Quantum Few-Body Systems, AIP Conf. Proc. **998**, 59 (2008).
5. Near-threshold positron impact ionization of hydrogen, S. J. Ward, Krista Jansen, J. Shertzer, and J. H. Macek, Nuc. Inst. Meth. B, **266**, 410 (2008).
6. Efimov states: what are they and why are they important?, J. H. Macek, Phys. Scr. **76**, C3 (2007).
7. Quantum treatment of continuum electrons in the fields of moving charges, Teck-Ghee Lee, S. Yu. Ovchinnikov, J. Sternberg, V. Chupryna,3 D. R. Schultz, and J. H. Macek, A **76**, 050701R (2007).
8. Regge oscillations in electron-atom elastic cross sections, D. Sokolovski, Z. Felfli, S. Yu. Ovchinnikov, J. H. Macek, and A. Z. Msezane, Phys Rev. A **76**, 012705 (2007).

Photoabsorption by Free and Confined Atoms and Ions

Steven T. Manson, Principal Investigator
Department of Physics and Astronomy, Georgia State University, Atlanta, Georgia 30303
(smanson@gsu.edu)

Program Scope

The goals of this research program are: to provide a theoretical adjunct to, and collaboration with, the various atomic and molecular experimental programs that employ third generation light sources, particularly ALS and APS; to generally enhance our understanding of the photoabsorption process; and to study the properties (especially photoabsorption) of confined atoms and ions. To these ends, calculations are performed employing and enhancing cutting-edge methodologies to provide deeper insight into the physics of the experimental results; to provide guidance for future experimental investigations; and seek out new phenomenology, especially in the realm of confined systems. The general areas of programmatic focus are: manifestations of nondipole effects in photoionization; photodetachment of inner and outer shells of atoms and atomic ions (positive and negative); studies of atoms endrohedrally confined in buckyballs, C_{60}, particularly dynamical properties. Flexibility is maintained to respond to opportunities that present themselves as well.

Highlights of Recent Progress

1. Confined Atoms

The study of confined atoms is only beginning. There are a handful of theoretical investigations of various atoms endohedrally confined in C_{60}, but not much in the way of experiment as yet [1,2]. Thus, we are conducting a program of calculations at various levels of approximation, aimed at delineating the properties of such systems, especially photoionization, to provide guidance for the experimental community. Among our recent results, we have found that a huge transfer of oscillator strength from the C_{60} shell, in the neighborhood of the giant plasmon resonance, to the encapsulated atom for both $Ar@C_{60}$ [3] and $Mg@C_{60}$ [4]. In addition, a new type a resonance has been discovered, termed a correlation confinement resonance [5]. Confinement resonances occur in the photoionization of an endohedral atom owing to the interferences of the photoelectron wave function for direct emission with those scattered from the surrounding carbon shell. We have found that the confinement resonances in the dominant subshell cross section can be transferred to other subshell cross sections *via* interchannel coupling. And the photoionization of endohedral atoms within nested fullerenes, called buckyonions, has also been investigated [6]. It is found that, as a result of the multi-walled confining structures, the confinement resonances become considerably more complicated.

Considering a Xe atom endohedrally confined in C_{60}, the formation of a new type of atom-fullerene hybrid state was discovered [7]. These dimer-type states arise from the near-degeneracy of inner levels of the confined atom and the confining shell, in contrast to the known overlap-induced hybrid states around the Fermi level of smaller compounds. The wave functions of these hybrid bound states are essentially a linear

conbination of a localized atomic state and a delocalized shell state which endows these states with rather different properties from (energetically) nearby states of the system. Specifically, we have found that the photoionization cross sections of these hybrid states exhibit rich structures and are radically different from the cross sections of nearby free atomic or fullerene states.

We have made an initial attempt to consider fast charged-particle impact ionization of atoms, looking at the He@C_{60} system [8]. The motivation here is that there are experimental results in this area, along with a search for the possible existence of nondipole plasmon resonances. Our first results indicate that confinement resonances appear in the ionization of endohedrals by charged particle impact as well as in photoionization.

While these various effects have been calculationally demonstrated in particular cases, their importance in that they are, in fact, quite general and it is expected that they will arise in many confined atom systems.

2. Atomic Photoionization

The study of photoionization of atoms at high resolution leads to results of great complexity. Our effort is to perform state-of-the-art calculations, in concert with high-resolution synchrotron experiments, to understand this complexity. Using our upgraded relativistic Breit-Pauli R-matrix methodology we have completed a study of the four-electron Be isoelectronic sequence [9]. Aside from showing that the calculations produce excellent agreement with experiment for the five different members of the sequence where experiment is available, we have found that relativistic interactions are crucial for quantitative accuracy, even for the lowest member of the sequence; quite surprising for Z=4! In addition, it was found that the calculation must be done with a very fine energy grid, or a significant amount of oscillator strength is omitted owing to the existence a very narrow resonances; our energy grid used steps of about 1 μeV to insure that nothing was missed.

3. Nondipole Effects in Atoms

Up until relatively recently, the conventional wisdom was that nondipole effects in photoionization were of importance only at photon energies of tens of keV or higher, despite indications to the contrary more than 35 years ago [10]. The last decade has seen an upsurge in experimental and theoretical results [11] showing that nondipole effects in photoelectron angular distributions could be important down to hundreds [12] and even tens [13] of eV. Our recent work included a study of Cl^- [14] which revealed that there are strong correlation effects in quadrupole channels, and these effects show up in the nondipole contribution to the photoelectron angular distribution at a level predicted to be measurable at rather low energies. We have also found that spin-orbit-activated interchannel coupling (SOAIC) that was found for to be important in dipole photoionization in the vicinity of the thresholds for inner-shell spin-orbit doublets [15], is also present in quadrupole channels, and this SOAIC causes significant alteration of the quadrupole matrix elements which translates to a major effect upon the nondipole angular distribution parameters.

Future Plans

Fundamentally our future plans are to continue on the paths set out above. In the area of confined atoms, we will perform many-body calculation on charged particle impact ionization of endohedral atoms and free fullerene molecules in an effort to elucidate any new insights inherent in the nondipole channels thus produced. In addition, we shall upgrade our theory to include relativistic interactions to be able to deal with heavy endohedrals with quantitative accuracy. The study of the photodetachment of C^- shall move on to the photoabsorption in the vicinity of the K-shell edge of both the ground ^4S and exited ^2D states in order to understand how the slight excitation of the outer shell affects the inner-shell photoabsorption and to pave the way for experiment, in addition to further study of Na^- and K^- where experiment exists. Further, building upon our previous work, we shall attack the problem of inner-shell photoionization of the Sc atom. Additionally, nondipole effects the inner subshells of Hg will be investigated to try to unravel the combined effects of many-body correlation effects and relativistic interactions. In addition, the search for cases where nondipole effects are likely to be significant, as a guide for experiment, and quadrupole Cooper minima, will continue.

Publications Citing DOE Support Since November, 2006

- "Anomalous Behavior of Auger and Radiative Rates and Fluorescence Yields," M. F. Hasoglu, D. Nikolic, T. W. Gorczyca, S. T. Manson, M. H. Chen and N. R. Badnell, Phys. Rev. A **78**, 032509-1-6 (2008).
- "Theoretical Studies of Photoabsorption by Atomic Systems," S. T. Manson, W.-C. Chu, A. M. Sossah and H.-L. Zhou, *Advances in Atomic Molecular and Optical Sciences*, edited by E. Krishnakumar (Allied Publishers, New Delhi, India, 2008), pp. 89-98.
- "Photoionization of C_{60}^-: A Model Study," M. E. Madjet, H. S. Chakraborty, J. M. Rost and S. T. Manson, J. Phys. B **41**, 105101-1-8 (2008).

"Dynamical Effects of Confinement on Atomic Valence Photoionization in $Mg@C_{60}$," M. E. Madjet, H. S. Chakraborty, J. M. Rost and S. T. Manson, Phys. Rev. A **78**, 013201-1-4 (2008).

- "Photoionization of atoms confined in giant single-walled and multiwalled fullerenes," V. K. Dolmatov, P. Brewer and S. T. Manson, Phys. Rev. A **78**, 013415 (2008).
- "Relativistic-Random-Phase Approximation Calculations of Atomic Photoionization: What We Have Learned," S. T. Manson, Can. J. Phys. **87**, 5-8 (2009).
- "Relaxation Effects in Photodetachment of Intermediate p shells of the Chlorine and Bromine Negative Ions," V. Radojevic, J. Jose, G. B. Pradhan, P. C. Deshmukh and S. T. Manson, Can. J. Phys. **87**, 49-54 (2009).
- "Correlation confinement resonances in photoionization of endohedral atoms: Xe@C60," V. K. Dolmatov and S. T. Manson, J. Phys. B **41**, 165001-1-4 (2008).
- "Fast charged-particle impact ionization of endohedral atoms," A. S. Baltenkov, V. K. Dolmatov, S. T. Manson, and A. Z. Msezane, Phys. Rev. A **79**, 043201-1-9 (2009).
- "Photoionization of Doubly-Charged Scandium Ions," A. M. Sossah, H.-L. Zhou, S. T. Manson, Phys. Rev. A **78**, 053405-1-10 (2008).

- "Spin-Orbit interaction Activated Interchannel Coupling in dipole and Quadrupole Photoionization," S. Sunil Kumar, T. Banerjee,P. C. Deshmukh and S. T. Manson, Phys. Rev A **79**, 043401-1-8 (2009).
- "Photoionization of novel hybrid states in endohedral fullerenes," H. S. Chakraborty, M. E. Madjet, T. Rebger, J.-M. Rost and S. T. Manson, Phys. Rev. A **79**, 061201(R)-1-4 (2009).
- "Nondipole and interchannel coupling effects in the photodetachment of Cl-," J. Jose, G. B. Pradhan, P. C. Deshmukh, V. Radojevic and S. T. Manson, Phys. Rev. A. (in press).
- "Comparison of Nondipole Effects in the Ionization of Atoms by Fast Charged Particles and Photons: Ejected Electron Angular Distributions and Drag Currents," A. S. Baltenkov, S. T. Manson and A. Z. Msezane, Phys. Rev. A (submitted).
- "Photoionization of the Be Isoelectronic Sequence: Total Cross Sections," W.-C. Chu, H.-L. Zhou, A. Hibbert and S. T. Manson, J. Phys. B (submitted).

References

[1] V. K. Dolmatov, A. S. Baltenkov, J.-P. Connerade and S. T. Manson, Radiation Phys. Chem. **70**, 417 (2004).
[2] V. K. Dolmatov, Advances in Quantum Chemistry, **58**, 13 (2009).
[3] M. E. Madjet, H. S. Chakraborty and S. T. Manson, Phys. Rev. Letters **99**, 243003 (2007).
[4] M. E. Madjet, H. S. Chakraborty, J. M. Rost and S. T. Manson, Phys. Rev. A **78**, 013201-1-4 (2008).
[5] V. K. Dolmatov and S. T. Manson, J. Phys. B **41**, 165001-1-4 (2008).
[6] V. K. Dolmatov and S. T. Manson, J. Phys. Rev. A **78**, 013415 (2008).
[7] H. S. Chakraborty, M. E. Madjet, T. Renger, J.-M. Rost and S. T. Manson, Phys. Rev. A **79**, 061201(R) (2009).
[8] A. S. Baltenkov, V. K. Dolmatov, S. T. Manson, and A. Z. Msezane, Phys. Rev. A **79**, 043201 (2009).
[9] W.-C. Chu, H.-L. Zhou, A. Hibbert and S. T. Manson, J. Phys B (submitted).
[10] M. O. Krause, Phys. Rev. 177, 151 (1969).
[11] O. Hemmers, R. Guillemin and D. W. Lindle, Radiation Phys. and Chem. **70**, 123 (2004) and references therein.
[12] O. Hemmers, R. Guillemin, E. P. Kanter, B. Kraessig, D. W. Lindle, S. H. Southworth, R. Wehlitz, J. Baker, A. Hudson, M. Lotrakul, D. Rolles, W. C. Stolte, I. C. Tran, A. Wolska, S. W. Yu, M. Ya. Amusia, K. T. Cheng, L. V. Chernysheva, W. R. Johnson and S. T. Manson, Phys. Rev. Letters **91**, 053002 (2003).
[13] V. K. Dolmatov and S. T. Manson, Phys. Rev. Letters **83**, 939 (1999).
[14] J. Jose, G. B. Pradhan, P. C. Deshmukh, V. Radojevic and S. T. Manson, Phys. Rev. A. (in press).
[15] S. Sunil Kumar, T. Banerjee,P. C. Deshmukh and S. T. Manson, Phys. Rev A **79**, 043401 (2009).

PROGRESS REPORT

ELECTRON-DRIVEN PROCESSES IN POLYATOMIC MOLECULES

Investigator: Vincent McKoy

A. A. Noyes Laboratory of Chemical Physics
California Institute of Technology
Pasadena, California 91125

email: mckoy@caltech.edu

PROJECT DESCRIPTION

The focus of this project is the continued development, extension, and application of accurate, scalable methods for computational studies of low-energy electron–molecule collisions, with emphasis on larger polyatomics relevant to biological and materials-processing systems. Because the required calculations are highly numerically intensive, efficient use of large-scale parallel computers is essential, and the computer codes developed for the project are designed to run both on tightly-coupled parallel supercomputers and on workstation clusters.

HIGHLIGHTS

Over the past year we have continued to pursue code development and applications related to electron interactions with biological molecules while continuing productive collaborations with experimental groups. Principal developments include:

- A joint experimental/theoretical study of elastic electron collisions with two alcohols, n-propanol and n-butanol
- A joint experimental/theoretical study of elastic and vibrationally inelastic collisions of electrons with gas-phase water
- A joint experimental/theoretical study of dissociative attachment to HCl

ACCOMPLISHMENTS

During 2009, we continued our studies of slow electron interactions with biomolecules by completing work on the straight-chain alcohols from methanol (CH_3OH) to *n*-butanol (C_4H_9OH). In particular, we wrapped up a combined experimental and theoretical study of *n*-propanol (C_3H_7OH) and *n*-butanol [1], following up on our earlier study of methanol and ethanol [2]. This study was a collaborative effort with the experimental group of Murtadha Khakoo at Cal State Fullerton, who measured differential elastic cross sections, and with experimental and theoretical groups in Brazil, who participated in the measurements and carried out complementary calculations. One interesting result was the observation of f-wave resonances in *n*-propanol and *n*-butanol analogous to those previously seen in the corresponding alkanes, propane and butane [3–6]. Similar structures are weakly visible in ethanol [2] and ethane [7–10] but absent in methanol [2] and methane [8,11]. This "family resemblance" between scattering by the alkanes and the alkyl alcohols is somewhat surprising, since replacing an H atom with a polar OH group significantly changes the structure of the target. This work on alcohols is in part driven by a need for basic data relevant to spark ignition of biofuels. Our collaborators at the Brazilian Bioethanol Science and Technology Center are inaugurating experimental and modeling efforts that will make use of such data.

We also carried out calculations on elastic [12] and vibrationally inelastic [13] electron collisions with the most fundamental biomolecule, H_2O, again in collaboration with the Khakoo group. Our study of the elastic cross section was motivated by intriguing preliminary results of Khakoo *et al.* [14]. Using a new experimental technique designed to reduce the normalization uncertainty in the cross section, they measured significantly larger values of the H_2O elastic cross section in the $\sim$6–10 eV range than found in earlier experimental [15–18] and theoretical [19–22] work, with significant implications for modeling of electron transport in aqueous media, including living tissue. We carried out our calculations in a very

large one-electron basis set, including many functions distributed on centers surrounding the molecule, and incorporated both an extensive treatment of polarization effects and corrections for scattering by the permanent dipole. However, our calculations did not lead to an increased H_2O cross section compared to earlier work; in fact, they are in superb agreement with the most recent and sophisticated prior calculations [21,22]. The true magnitude of the low-energy electron cross section for H_2O thus remains unsettled. We followed up this study of elastic H_2O cross sections with a combined computational and experimental examination of the cross sections for vibrational excitation [13]. The calculations were done in the adiabatic-nuclei approximation and used a simple two-point quadrature scheme in each normal mode. Despite their simplicity, they produced results in generally good agreement with the measurements in the energy range ($\sim$2–10 eV) where the approximations made were most reliable.

For HCl, we carried out high-level (static–exchange plus polarization in a large basis set) calculations to track the energy and lifetime of the σ^* temporary anion as a function of H–Cl bond length. Collaborators at the Charles University (Prague) and the University of Fribourg used our results in a nonlocal model of dissociative attachment to obtain greatly improved agreement with measured values [23].

PLANS FOR COMING YEAR

In the coming year, we plan to complete studies now under way of the RNA base uracil, in which we are studying the effect of coupling between the elastic channel and low-lying triplet states on the third π^* resonance. This calculation has proven quite challenging, but we expect to obtain satisfactory results once certain code improvements are in hand. Those improvements, begun last year and continuing, involve writing scalable parallel replacements for the remaining sequential programs in our main code suite. In the past year we implemented a parallel solver for our linear equations, leaving one remaining step to parallelize. We will also explore using graphics processors (GPGPUs) to accelerate key computational kernels in our parallel scattering code.

We also plan to study resonant electron scattering by ethyl vinyl ether, looking at the effect of internal rotation on the mixing between C–C π^* and C–O or O–H σ^* orbitals and thus on the dissociative attachment process. Ethyl vinyl ether was chosen as a convenient model system for such indirect DA processes, which may play a role in electron-induced damage to biomoleules. The Khakoo group will carry out supporting measurements of the elastic and DA cross sections.

REFERENCES

[1] M. A. Khakoo, J. Muse, H. Silva, M. C. A. Lopes, C. Winstead, V. McKoy, E. M. de Oliveira, R. F. da Costa, M. T. do N. Varella, M. H. F. Bettega, and M. A. P. Lima, Phys. Rev. A **78**, 062714 (2008).

[2] M. A. Khakoo, J. Blumer, K. Keane, C. Campbell, H. Silva, M. C. A. Lopes, C. Winstead, V. McKoy, R. F. da Costa, L. G. Ferreira, M. A. P. Lima, and M. H. F. Bettega, Phys. Rev. A **77**, 042705 (2008).

[3] L. Boesten, M. A. Dillon, H. Tanaka, M. Kimura, and H. Sato, J. Phys. B **27**, 1845 (1994).

[4] M. H. F. Bettega, R. F. da Costa, and M. A. P. Lima, Phys. Rev. A **77**, 052706 (2008).

[5] A. R. Lopes, M. H. F. Bettega, M. A. P. Lima, and L. G. Ferreira, J. Phys. B **37**, 997 (2004).

[6] M. H. F. Bettega, M. A. P. Lima, and L. G. Ferreira, J. Phys. B **40**, 3015 (2007).

[7] D. Matsunaga, M. Kubo, and H. Tanaka, in *Proceedings of the 12th International Conference on the Physics of Electronic and Atomic Collisions*, S. Datz, editor (North-Holland, Amsterdam, 1981), p. 358.

[8] P. J. Curry, W. R. Newell, and A. C. H. Smith, J. Phys. B **18**, 2303 (1985).

[9] H. Tanaka, L. Boesten, D. Matsunaga, and T. Kudo, J. Phys. B **21**, 1255 (1988).

[10] W. Sun, C. W. McCurdy, and B. H. Lengsfield III, J. Chem. Phys. **97**, 5480 (1992).

[11] H. Tanaka, T. Okada, L. Boesten, T. Suzuki, T. Yamamoto, and M. Kubo, J. Phys. B **15**, 3305 (1982).

[12] M. A. Khakoo, H. Silva, J. Muse, M. C. A. Lopes, C. Winstead, and V. McKoy, Phys. Rev. A **78,** 052710 (2008).

[13] M. A. Khakoo, C. Winstead, and V. McKoy, Phys. Rev. A **79**, 052711 (2009).
[14] H. Silva, J. Muse, M. C. A. Lopes, and M. A. Khakoo, Phys. Rev. Lett. **101**, 033201 (2008).
[15] A. Danjo and H. Nishimura, J. Phys. Soc. Jpn. **54**, 1224 (1985).
[16] T.W. Shyn and S.Y. Cho, Phys. Rev. A **36**, 5138 (1987).
[17] W. M. Johnstone and W. R. Newell, J. Phys. B **24**, 3633 (1991).
[18] H. Cho, Y. S. Park, H. Tanaka, and S. J. Buckman, J. Phys. B **37**, 625 (2004).
[19] T. N. Rescigno and B. H. Lengsfield, Z. Phys. D: At., Mol. Clusters **24**, 117 (1992).
[20] M. T. do N. Varella, M. H. F. Bettega, M. A. P. Lima, and L. G. Ferreira, J. Chem. Phys. **111**, 6396 (1999).
[21] A. Faure, J. D. Gorfinkiel, and J. Tennyson, J. Phys. B **37**, 801 (2004)
[22] A. Faure, J. D. Gorfinkiel, and J. Tennyson, Mon. Not. R. Astron. Soc. **347**, 323 (2004).
[23] J. Fedor, P. Kolorenč, M. Čížek, J. Horáček, C. Winstead, and V. McKoy, XXVI International Conference on Photonic, Electronic, and Atomic Collisions, Kalamazoo, Michigan, 22–28 July, 2009.

PROJECT PUBLICATIONS AND PRESENTATIONS, 2007–2009

1. "Electron-Driven Processes in Polyatomic Molecules," V. McKoy, XVI National Conference on Atomic and Molecular Physics, Tata Institute of Fundamental Research, Mumbai, India, 8–11 January, 2007 *(invited talk).*

2. "Resonant Channel Coupling in Electron Scattering by Pyrazine," C. Winstead and V. McKoy, Phys. Rev. Lett. **98**, 113201 (2007).

3. "Interactions of Slow Electrons with Biomolecules," V. McKoy, Molecular Theory for Real Systems Program, University of Tokyo, Japan, 18–19 March, 2007 *(invited talk).*

4. "Recent Computations of Electron Collisions with Large Molecules," V. McKoy, EIPAM 07 (Electron Induced Processes at the Molecular Level), Hveragerđi, Iceland, 25–29 May, 2007 *(invited talk).*

5. "Interactions of Slow Electrons with Biomolecules," V. McKoy, XXV International Conference on Photonic, Electronic, and Atomic Collisions, Freiburg, Germany, 25–30 July, 2007 *(invited talk).*

6. "Electron Collisions with Biomolecules," V. McKoy, Fifteenth International Symposium on Electron–Molecule Collisions and Swarms, Reading, United Kingdom, 1–4 August, 2007 *(invited talk).*

7. "Low-Energy Electron Scattering by Pyrazine," C. Winstead and V. McKoy, Phys. Rev. A **76**, 012712 (2007).

8. "Interaction of Low-Energy Electrons with the Pyrimidine Bases and Nucleosides of DNA," C. Winstead, V. McKoy, and S. d'A. Sanchez, J. Chem. Phys. **127**, 085105 (2007).

9. "Resonant Interactions of Slow Electrons with DNA Constituents," C. Winstead, ASR 2007 (International Symposium on Charged Particle and Photon Interactions with Matter), JAEA Advanced Science Research Center, Tokaimura, Japan, 6–9 November, 2007 *(invited talk).*

10. "Interactions of Slow Electrons with Biomolecules," V. McKoy and C. Winstead, J. Phys. Conf. Ser. **88**, 012072 (2007).

11. "Absolute Elastic Differential and Integral Cross Sections for Electron Scattering from the CF_2 Radical," T. M. Maddern, L. R. Hargreaves, J. R. Francis-Staite, M. J. Brunger, S. J. Buckman, C. Winstead, and V. McKoy, Phys. Rev. Lett. **100**, 063202 (2008).

12. "Interactions of Slow Electrons with DNA," V. McKoy, Chemistry Department Seminar, University of Alabama, Tuscaloosa, Alabama, February 28, 2008.

13. "Low Energy Elastic Electron Scattering from Methanol and Ethanol," M. A. Khakoo, J. Blumer, K. Keane, C. Campbell, H. Silva, M. C. A. Lopes, C. Winstead, V. McKoy, R. F. da Costa, L. G. Ferreira, M. A. P. Lima, and M. H. F. Bettega, Phys. Rev. A **77**, 042705 (2008).

14. "Electron Scattering in Ethene: Excitation of the $\tilde{a}\ ^3B_{1u}$ State, Elastic Scattering and Vibrational Excitation," M. Allan, C. Winstead, and V. McKoy, Phys. Rev. A **77**, 042715 (2008).

15. "Elastic Electron Scattering from 3-Hydroxytetrahydrofuran: Experimental and Theoretical Studies," V. Vizcaino, J. Roberts, J. P. Sullivan, M. J. Brunger, S. J. Buckman, C. Winstead, and V. Mckoy, New J. Phys. **10**, 053002 (2008).

16. "Interactions of Slow Electrons with DNA," V. McKoy, Physics Department Seminar, Federal University of Juiz de Fora, Juiz de Fora, Brazil, June 11, 2008.

17. "Interaction of Slow Electrons with Methyl Phosphate Esters," C. Winstead and V. McKoy, Int. J. Mass Spectrom. **277**, 279 (2008).

18. "Resonant Interactions of Slow Electrons with DNA Constituents," C. Winstead and V. McKoy, Radiat. Phys. Chem. **77**, 1258 (2008).

19. "Electron Collisions with Biomolecules," V. McKoy and C. Winstead, J. Phys. Conf. Ser. **115**, 012020 (2008).

20. "Electron-Impact Dissociation of Oxygen-Containing Molecules—A Critical Review," J. W. McConkey, C. P. Malone, P. V. Johnson, C. Winstead, V. McKoy, and I. Kanik, Phys. Rep. **466**, 1 (2008).

21. "Comment on 'Ring-breaking electron attachment to uracil: Following bond dissociations via evolving resonances' [J. Chem. Phys. **128**, 174302 (2008)]," C. Winstead and V. McKoy, J. Chem. Phys. **129**, 077101 (2008).

22. "Interactions of Slow Electrons with DNA Constituents," V. McKoy and C. Winstead, in *Advances in Atomic, Molecular and Optical Science* (Proceedings of the XVI National Conference on Atomic and Molecular Physics, Mumbai, January 8–11, 2007), E. Krishnakumar, editor (Allied Publishers, New Delhi, 2008), p. 146.

23. "Electron Scattering from H_2O: Elastic Scattering," M. A. Khakoo, H. Silva, J. Muse, M. C. A. Lopes, C. Winstead, and V. McKoy, Phys. Rev. A **78,** 052710 (2008).

24. "Elastic Scattering of Slow Electrons by *n*-Propanol and *n*-Butanol," M. A. Khakoo, J. Muse, H. Silva, M. C. A. Lopes, C. Winstead, V. McKoy, E. M. de Oliveira, R. F. da Costa, M. T. do N. Varella, M. H. F. Bettega, and M. A. P. Lima, Phys. Rev. A **78**, 062714 (2008).

25. "Differential and Integral Cross Sections for Elastic Electron Scattering from CF_2," J. R. Francis-Staite, T. M. Maddern, M. J. Brunger, S. J. Buckman, C. Winstead, V. McKoy, M. A. Bolorizadeh, and H. Cho, Phys. Rev. A **79**, 052705 (2009).

26. "Vibrational Excitation of Water by Electron Impact," M. A. Khakoo, C. Winstead, and V. McKoy, Phys. Rev. A **79**, 052711 (2009).

27. "Low-Energy Electron Collisions with Biomolecules," C. Winstead, Fortieth Annual Meeting the Division of Atomic, Molecular, and Optical Physics of the American Physical Society (DAMOP 2009), Charlottesville, Virginia, 20–23 May, 2009 *(invited talk).*

28. "Improved Nonlocal Resonance Model for Electron–HCl Collisions," J. Fedor, P. Kolorenč, M. Čížek, J. Horáček, C. Winstead, and V. McKoy, XXVI International Conference on Photonic, Electronic, and Atomic Collisions, Kalamazoo, Michigan, 22–28 July, 2009.

ELECTRON/PHOTON INTERACTIONS WITH ATOMS/IONS

Alfred Z. Msezane (email: amsezane@cau.edu)

Clark Atlanta University, Department of Physics and CTSPS
223 James P. Brawley Drive, SW, Atlanta, Georgia 30314

PROGRAM SCOPE

We have developed the unprecedented novel Regge-pole methodology and used it for the fundamental understanding of the mechanism of near-threshold electron attachment in electron-atom elastic scattering as Regge resonances through the calculation of the total cross sections (TCSs) and the Mulholland partial cross sections. Dramatically sharp resonances are found to characterize the near-threshold electron-atom collisions, whose energy positions are identified with the binding energies (BEs) of the anions (ground and excited) formed during the collisions. From the near-threshold elastic TCSs accurate BEs of tenuously bound (BE < 0.1 eV), weakly bound (BE < 1 eV) and complicated open d- and f-sub-shell as well as strongly bound (BE > 1 eV) negative ions can be extracted, requiring no *a priori* knowledge of their values whatsoever.

The development and application of the Random Phase Approximation with Exchange (RPAE) method to atoms (ions) with unfilled sub-shells continue. The theory has also been extended to open outer-shell and inner open-shell atoms (ions) and applied to photoionization, including of A@C60. Methods are developed for calculating the generalized oscillator strength, useful in probing the intricate nature of the valence- and open-shell as well as inner-shell electron transitions. Standard codes are used to generate sophisticated wave functions for investigating CI mixing and relativistic effects in atomic ions. The wave functions are also used to explore correlation effects in dipole and non-dipole studies.

SUMMARY OF RECENT ACCOMPLISHMENTS

Sub-Project 1: Regge Resonances in Low-Energy Electron Elastic Cross Sections for Complex Atoms: Manifestations of Stable Ground and Excited Anions

The knowledge of low-energy collisions of atoms and ions is essential for the exploration of the physics of the cooling and trapping of gaseous atomic ensembles and in the investigation of cold plasmas [1]. Electron-electron correlations and core-polarization interactions are the physical mechanisms that are responsible for the existence and stability of most negative ions. The formation of temporary negative ionic states as resonances and their properties define the mechanism through which low-energy electron scattering deposits energy and induces chemical transitions [2]. Shape resonances are useful for interpreting electron-induced chemical processes resulting in negative ion production [2, 3], and the Ramsauer-Townsend (RT) minima are important *inter alia* in understanding sympathetic cooling and the production of cold molecules from natural fermions [4]. The understanding of chemical reactions involving negative ions requires the knowledge of accurate binding energies (BEs) [5] which in turn influence the fine-structure of weakly bound anions [6].

A.1 Differential Cross Sections for Low-Energy Electron Elastic Scattering by Lanthanide Atoms: La, Ce, Pr, Nd, Eu, Gd, Dy and Tm

Elastic differential cross sections (DCSs) in angle of electron scattering by the representative lanthanide atoms La, Ce, Pr, Nd, Eu, Gd, Dy and Tm have been calculated in the electron impact energy range $0 \leq E \leq 1$ eV [7]. Additionally, the DCSs in electron impact energy are also presented at scattering angles $\theta = 0°$, $90°$ and $180°$ for unambiguous identification of the binding energies (BEs) of the negative ions formed during the collisions as resonances. The shape resonances and the DCSs critical minima are

identified as well. A Thomas-Fermi type potential incorporating the vital core-polarization interaction is used for the calculations. Dramatically sharp resonances are found to characterize the near-threshold electron elastic DCSs, whose energy positions are identified with the BEs of the resultant negative ions. A new procedure is suggested for measuring reliably the BEs of tenuously bound (BE < 0.1 eV), weakly bound (BE < 1 eV) and complicated open d- and f-sub-shell negative ions through the elastic DCSs both in scattering angle and electron impact energy.

A.2 Formation of Excited Anion Bound States in Low-energy Electron Elastic Scattering from Ge, Sn and Pb Atoms: Benchmarking Regge-pole Analysis

Here the recent Regge-pole methodology [8], used with a Thomas-Fermi type potential incorporating the crucial core-polarization interaction, is first benchmarked on the accurately measured BEs of the excited bound states of the Ge^- and Sn^- anions [9] through the BEs of these anions that are extracted from the Regge-pole calculated TCSs. Then we extract the BE of the excited bound state of the Pb^- negative ion from the resonances in the calculated TCS using the Regge pole methodology. The obtained BEs for the excited states of the Ge^- and Sn^- anions [10] agree excellently with those of the measurements [9]; the BE for the excited Pb^- anion requires experimental verification. It is further demonstrated that these BEs can also be extracted directly from the DCSs at the scattering angles $\theta = 0°$, 90° and 180°, giving experimentalists a new simple and direct approach to measuring the BEs of excited bound anion states.

A.3 Excited Anions in Low-energy Electron Collisions with Lanthanide Atoms

The recent Regge-pole methodology [8] has been benchmarked on the accurate BEs of the excited Ge^- and Sn^- anions [9] through the BEs extracted from the Regge-pole calculated elastic TCSs. The method is then used to explore in the near-threshold energy region, $E < 0.20$ eV possible electron attachment to the lanthanide atoms resulting in the formation of weakly bound excited anions as Regge resonances. The resultant elastic TCSs are found to be characterized by extremely narrow resonances whose energy positions are identified with the BEs of the excited anions formed during the collision. The obtained BEs for the excited lanthanide anions are contrasted with the most recently calculated electron affinities (EAs) (ground state BEs), concluding that the EAs for the Pr^-, Sm^-, Tb^-, Dy^-, Ho^-, Er^-, and Tm^- anions [11] may in fact correspond to BEs and definitely not to EAs as claimed [11]. Formation of excited anions is identified in the elastic TCSs of all the lanthanide atoms including Hf, except Eu. The results challenge experimentalists and theoreticians alike since these anions are mostly tenuously bound.

A.4 Low-energy Electron Elastic Collisions with Au and Pt Atoms: Creation of Excited Anions

Low-energy $E < 1$ eV electron elastic scattering from Au and Pt atoms is investigated using the recent Regge pole methodology, first benchmarked on the accurately measured BEs of the excited bound states of the Ge^- and Sn^- anions [9] through the BEs of these anions that are extracted from the Regge-pole calculated TCSs, to search for the possibility of forming and observing stable excited anions as Regge resonances manifesting stable bound excited Au^- and Pt^- anions. The crucial core-polarization interaction essential for the existence and stability of most negative ions is accounted for through the Thomas-Fermi type potential. From the characteristic extremely narrow resonances in the elastic total and Mulholland partial cross sections we identify for the first time ever two excited anion states for each of Au^- and Pt^- anions and extract their BEs [12]. Ramsauer-Townsend minima and shape resonances are determined as well. The calculated DCSs using a partial wave expansion also yield the binding energies.

Sub-Project 2: RPAE Photoionization of I^+ and Ce^{3+} Ions

The RPAE method, which allows for the inclusion of both intra-shell and inter-shell correlations has been developed by our group for atoms (ions) with an outer open-shell or with an inner open-shell. For Ce^{3+} it includes inter-shell coupling between the Ce^{3+} and the various discrete-continuum transitions. The photoionization of the I^+ ion in the energy range of the 4d giant resonance has been studied using our

recently developed RPAE method. Photoionization cross sections for the I^+ 4d-epsilon f, epsilon p, 5s-epsilon p and 5p-epsilon s, epsilon d have been obtained for each term of the ground state [13]. Calculations include all the intra-shell and inter-shell coupling among the 4d, 5s, and 5p sub-shells. Our calculated cross section maximum of 23.12 MB at 90.24 eV for the I^+ 4d giant resonance agrees excellently with the recently measured value of 23(3) at 90 eV.

The photoionization of the Ce^{3+} - Ce^{4+} process has been studied using the RPAE method in the energy region 100-150 eV [14]. Comparison of our results with the recently measured data [15] confirms the suppression effect of the carbon cage in the endohedral fullerene $Ce@C_{82}^+$ photoionization. The reasons for the cause of the confinement resonance and the suppression effect have been discussed.

Sub-Project 3: Fine-structure energy levels, oscillator strengths and lifetimes in Positive Ions

A.1 Fine-structure energy levels and radiative rates in Al-like Copper

We have performed large scale CIV3 calculations of excitation energies from ground state for 97 fine-structure levels as well as of oscillator strengths and radiative decay rates for all electric-dipole-allowed and intercombination transitions among the fine-structure levels of the terms belonging to the lowest configurations of Cu XVII [16]. These states are represented by very extensive CI wave functions obtained with Program CIV3. The important relativistic effects in intermediate coupling are incorporated by means of the Breit-Pauli Hamiltonian. The mixing among several fine-structure levels is found to be so strong that the correct identification of these levels becomes very difficult. The results are expected to be useful to experimentalists in identifying the fine-structure levels. We also predict new data for many fine-structure levels.

A.2 [Ti II] lines observed in η Carinae Sr-filament and lifetimes of the metastable states of Ti^+

Forbidden (E2 and M1) transitions among the lowest 37 fine-structure even parity levels of Ti II have been evaluated using Program CIV3 in a CI calculation in which relativistic effects are accounted for through the full Breit–Pauli interaction in the Hamiltonian matrix. Our *gA* values have been compared with those observed in the η Carinae Sr-filament and good agreements among the calculated and observed lifetimes of a few metastable states have been obtained [17]. It is found that single and double core–valence correlation between the $n = 3$ and 4 complexes are needed for well-converged results. The significance of the results is in the context of the recent experimental discovery of the impact of collisional repopulation and quenching of metastable states on their lifetime measurements.

FUTURE PLANS

The development and application of the CAM theory continue, particularly in chemical reactions and electron-atom/ion collisions. From the sharp resonances in the near-threshold electron elastic scattering TCS's, reliable BEs for tenuously bound and complicated atoms can be extracted through the close scrutiny of the imaginary part of the CAM value. Other research activities, such as GOS and photoionization of inner-shell of open-shell atoms (ions) investigations continue, including the probing of correlations. Extension of the Regge pole approach to the interesting and challenging multichannel case is advancing, including applications to cold collisions and Feshbach resonances.

References and Project Publications 2007-2009

1. M.S. Jamieson, A. Dalgarno, M. Aymar and J. Tharamel, J. Phys. B **42**, 095203 (2009)
2. H. Hotop, M. –W. Rul and I. I. Fabrikant, Physica Scripta T**110**, 22 (2004)
3. S. Zivanov, B. C. Ibanescu, M. Paech *et a*l, J. Phys. B **40,** 101 (2007)
4. S. Aubin, S. Myrskog, M. H. T. Extavour *et al*, Nature Physics **2,** 384 (2004)

5. K. Kasdan and W.C. Lineberger, Phys. Rev. A **10**, 1658 (1974)
6. V.A. Dzuba and G.F. Gribakin, Phys. Rev. A **55**, 2443 (1997)
7. Z. Felfli, A.Z. Msezane and D. Sokolovski, Phys. Rev. A **79**, 062709 (2009)
8. D. Sokolovski, Z. Felfli, S. Ovchinnikov, J. H. Macek and A. Msezane, Phys. Rev. A **76**, 012705 (2007)
9. M. Scheer, R.C. Bilodeau, C.A. Brodie and H.K. Haugen, Phys. Rev. A **58**, 2844 (1998)
10. Z. Felfli, A.Z. Msezane and D. Sokolovski, Phys. Rev. A, Submitted (R) (2009)---being revised
11. M. O' Malley and D.R. Beck, Phys. Rev. A **77**, 012505 (2008); ------, Phys. Rev. A **79**, 012511 (2009)
12. Z. Felfli, A.Z. Msezane and D. Sokolovski, Phys. Rev. A, to be Submitted (2009)
13. Z. Chen and A.Z. Msezane, J. Phys. B, At Press (2009)
14. Z. Chen and A.Z. Msezane, J. Phys. B, At Press (2009)
15. A. Müller *et al,* Phys. Rev. Lett. **101**, 133001 (2008)
16. G. P. Gupta and A. Z. Msezane, Can. J. Phys. At Press (2009)
17. N.C. Deb, A. H. Hibbert, Z. Felfli and A. Z. Msezane, J. Phys. B 42, 015701 (2009)

Project Publications 2007-2009

1. "What can one do with Regge Poles?" D. Sokolovski, A.Z. Msezane, Z. Felfli, S.Yu. Ovchinnikov and J.H. Macek, Nucl. Instr. and Meth. B **261**, 133 (2007)
2. "Energy Levels and Radiative Rates for Transitions in Co XI", F. P. Keenan, K.M. Aggarwal and A.Z. Msezane, Astronomy & Astrophysics **473**, 995 (2007)
3. "Photoionization of Hydrogen-Like Ions Surrounded by Charged Spherical Shell", A. S. Baltenkov, S. T. Manson and A. Z. Msezane, Phys. Rev. A **76**, 042707 (2007)
4. "Octupole Contributions to the Generalized Oscillator Strengths of Discrete Dipole Transitions in Noble Gas Atoms", M. Ya. Amusia, L.V. Chernysheva, Z. Felfli and A.Z. Msezane, Phys. Rev. A**75**, 062703 (2007)
5. "Elastic Electron Scattering From Multicenter Potentials", A. S. Baltenkov, S. T. Manson and A. Z. Msezane, J. Phys. B **40**, 769 (2007)
6. "Simple Method for Electron Affinity Determination: Results for Ca, Sr and Ce", Z. Felfli, A.Z. Msezane, and D. Sokolovski, J. Phys. B **41**, 041001 (2008) (FAST TRACK)
7. "Dramatic Resonances in Low- Energy Electron Scattering from Rb, Cs and Fr", A.Z. Msezane, Z. Felfli, and D. Sokolovski, Chem. Phys. Lett. **456**, 96 (2008)
8. "Near-Threshold Resonances in Electron Elastic Scattering Cross Sections for Au and Pt Atoms", A.Z. Msezane, Z. Felfli and D. Sokolovski, J. Phys. **B 41**,105201 (2008)
9. "Near-Threshold Electron Attachment as Regge Resonances: Cross Sections for K, Rb and Cs Atoms", A.Z. Msezane, Z. Felfli and D. Sokolovski, J. Phys. Chem. A **112,** 10, 199 (2008)
10. "Strong resonances in low-energy electron elastic total and differential cross sections for Hf and Lu atoms", Z. Felfli, A.Z. Msezane and D. Sokolovski, Phys. Rev. A **78**, 030703 (R) (2008)
11. "Low-Energy Electron Elastic Scattering from Complex Atoms: Nd, Eu and Tm", Z. Felfli, A.Z. Msezane and D. Sokolovski, Can. J. Phys. At Press (2009)
12. "Fine-Structure Energy Levels, Oscillator Strengths and Lifetimes in Mn XIII", G. P. Gupta and A. Z. Msezane, Physica Scripta **76**, 225 (2007).
13. "Main Universal Features of the ^{3}He Experimental Temperature–Density Phase Diagram", V.R. Shaginyan, A.Z. Msezane. K.G. Popov and V.A. Stephanovich, Phys. Rev. Lett. **100**, 096406 (2008)
15. "Resonances in Low-Energy Electron Elastic Cross Sections for Lanthanide Atoms", Z. Felfli, A.Z. Msezane and D. Sokolovski, Phys. Rev. A **79**, 012714 (2009)
16. "Energy Scales and Magnetoresistance at a Quantum Critical Point", V.R. Shaginyan, M. Ya. Amusia, A.Z. Msezane, K.G. Popov and V.A. Stephanovich, Physics Letters A **373**, 986 (2009)
17. "Fast charged-particle impact ionization of endohedral atoms: e + He@C_{60}", A. S. Baltenkov, V. K. Dolmatov, S. T. Manson, and A. Z. Msezane, Phys. Rev. A **79**, 043201 (2009)
18. "Fine-structure energy levels, oscillator strengths and lifetimes in Al-like Vanadium", G.P. Gupta and A.Z. Msezane, Europ. J. Phys., Submitted (2009)
19. "Fine-Structure Energy Levels, Oscillator Strengths and Lifetimes in Mn XIII", G. P. Gupta and A. Z. Msezane, Physica Scripta **76**, 225 (2007).
20. "Oscillator Strengths and Lifetimes in Ge XXI", G. P. Gupta and A. Z. Msezane, Phys. Scr.**77**, 035303 (2008)
21. "Ionization of Sodium by the Impact of Alpha Particles", S. Bhattacharya, K.B. Choudhury, N.C. Deb, C. Sinha, K. Roy and A.Z. Msezane, Eur. Phys. J. D **47**, 335 (2008)

Theory and Simulations of Nonlinear X-ray Spectroscopy of Molecules

Shaul Mukamel
University of California, Irvine, CA 92697

Progress Report 2009 DOE DE-FG02-04ER15571

Program Scope

Computational tools are developed for the design and analysis of time-domain experiments that employ sequences of femtosecond to attosecond x-ray pulses in order to probe electronic and nuclear dynamics in molecules. Such experiments will be made possible by the new bright coherent ultrafast sources for soft and hard x-rays. The nonlinear response formalism of optical spectroscopy is extended to predict these new resonant measurements. By creating multiple core holes at selected atoms and controlled times it is possible to study the dynamics and correlations of valence electrons as they respond to these perturbations. Electron motions can thus be directly probed with sub femtosecond time scale and atomic spatial resolution.

Two-dimensional x-ray coherent correlation spectra (2DXCS) obtained by varying two delay periods between pulses show off-diagonal crosspeaks induced by coupling of core transitions of two different types. A unified approach for predicting coherent multidimensional optical and x-ray probes for electron correlations and exciton dynamics was developed. The quasiparticle equation of motion approach that has been tested for vibrational excitons in the infrared and valence excitons in the visible has been extended to describe core excitons. This method offers numerous computational advantages compared with the sum over states techniques. Many-body effects in strongly correlated systems are studied by signals that are induced by electron correlations. Coherent nonlinear optical spectra of Wannier excitons in semiconductor nanostructures are used to test the simulation algorithms and laser pulse sequences and gain insights on their x-ray counterparts.

Recent Progress

The coherent multidimensional techniques which originated with NMR in the 1970s have been extended over the past 15 years to the infrared and visible regimes. These advances have dramatically enhanced the temporal resolution from the millisecond to the femtosecond. NMR spectroscopists have developed principles for the design of pulse sequences that enhance selected spectral features and reveal desired dynamical events. Extending these principles to the optical and X ray regimes offers numerous opportunities for narrowing the line shapes in specific directions, unraveling weak cross-peaks from otherwise congested spectra, and controlling the interferences between quantum pathways. These measurements may be further refined by shaping the spectral and temporal profiles of the pulses. Pulse polarization shaping may lead to unique probes of time-dependent chirality. Common principles which underlie these techniques for coherent spectroscopy of spins, valence electrons, and core electronic excitations, spanning frequencies from radiowaves to hard x-rays have been developed. The novel information extracted from these signals for three physical systems is illustrated in Fig.1. The first application demonstrates how attosecond resonant core spectroscopy may be used to generate core excitations that are highly localized at selected atoms. Such signals can monitor the motions of valence electron wavepackets in real space. In the second system, spectra of GaAs semiconductor quantum wells provide a direct look at many-body electron correlation effects. We directly observe specific projections of the many electron wave function, which can be used to test the quality of various levels of computational techniques for electronic structure. The third application is to photosynthetic light harvesting complexes where 2D signals reveal couplings between chromophores, quantum coherence signatures of chromophore entanglement, and energy-transfer pathways.

A new double-quantum-coherence attosecond x-ray technique was proposed for probing spatially-separated, spectrally-overlapping core-electron transitions. X-ray four-wave mixing signals generated in the $\mathbf{k}_1+\mathbf{k}_2-\mathbf{k}_3$ phase-matching direction were simulated for N 1*s* transitions in paranitroaniline and two-ring hydrocarbons substituted with an amine and a nitroso groups. Here $\mathbf{k}_1$, $\mathbf{k}_2$, and $\mathbf{k}_3$ are the wave vectors of the three incoming pulses in chronological order. This 2DXCS technique provides a background-free probe of couplings between core-electron transitions even for multiple core shells of the same type. This is analogous to homonuclear NMR. Features attributed to couplings between spatially separated core transitions connected by delocalized valence excitations provide information about molecular geometry and electronic structure, unavailable from linear near-edge x-ray absorption (XANES).

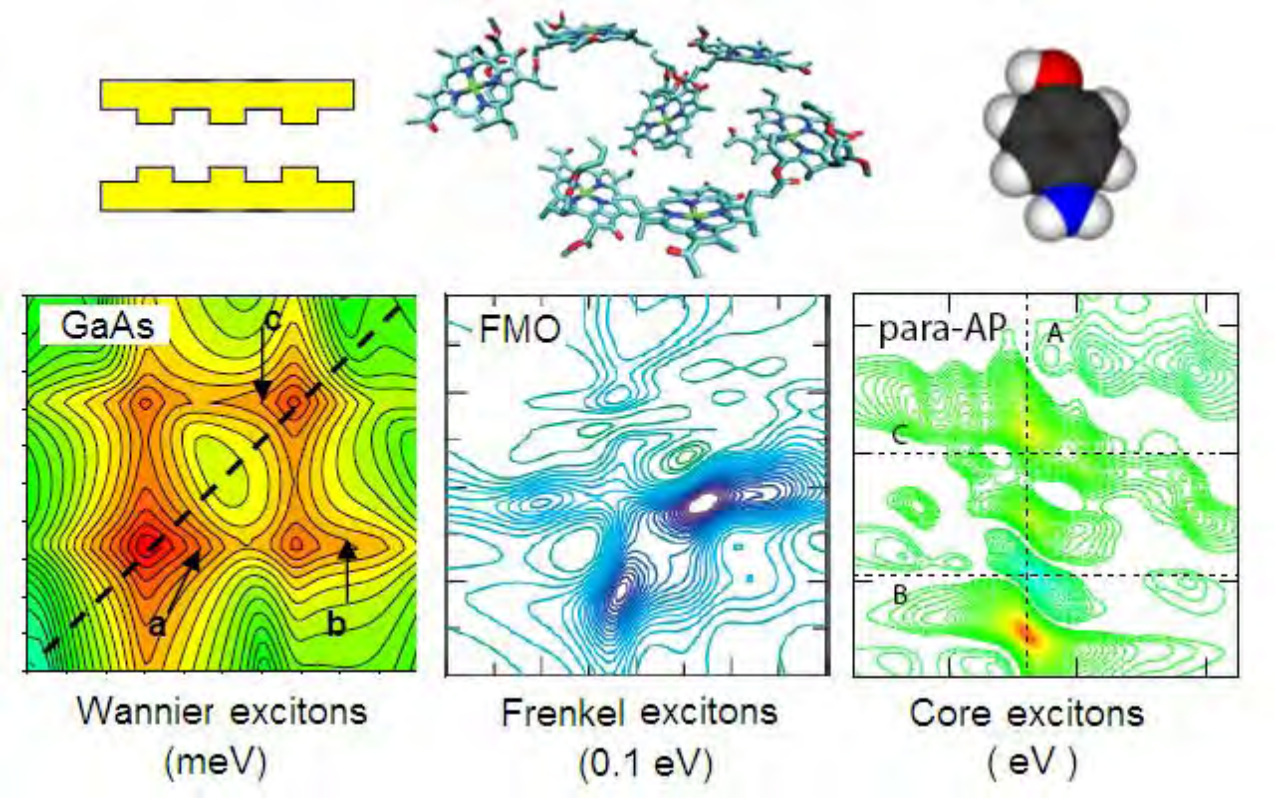

Figure 1: 2D photon echo spectra of core, Wannier and Frenkel excitons in molecules [P20]

Spontaneous and coherent (stimulated) resonant inelastic x-ray Raman-scattering signals were calculated using the Keldysh-Schwinger closed-time path loop and expressed as overlaps of electron-hole wave packets. This attosecond extension of resonant inelastic x-ray spectra (RIXS) was recast in terms of the one-particle Green's functions and configuration-interaction singles wavefunctions of valence excitations. The latter can be readily obtained from standard electronic structure codes. A many-body Green's function approach was developed for computing nonlinear x-ray spectra of strongly correlated systems. The response is described in terms of quasiparticles (QP), thereby avoiding the expensive computation of many-electron eigenstates. Instead, signals are calculated by solving equations of motion for a proper hierarchy of dynamical variables. A Bethe-Salpeter approach for two-excitons provides an efficient computational tool. This formalism was applied to predict coherent signals that probe single and two-core-hole states. The one- and two-particle Green's functions can be obtained from the solution of Hedin-type equations at the *GW* level. The simulated resonant x-ray pump probe signal of cystein is shown in Fig.2.

2D spectroscopy was applied for isolating excitonic Raman coherences in semiconductors. Experimental and simulation results of 2D optical signals in GaAs quantum wells demonstrate how otherwise overlapping Raman coherences may be clearly resolved.

Future Plans

Current Effort focuses on developing higher-level electronic-structure methods for multiple core transitions and identifying 2DXCS signatures of nuclear dynamics and core migration. Pulse shaping strategies for simplifying 2D spectra will be explored. In our previous studies 2DXCS were simulated by summations over the many-electron states of the valence system with *N, N+1,* and *N+2* electrons in the presence of zero, one and two core holes, respectively. The valence and core-excited states were calculated using singly and doubly substituted determinants formed from Hartree-Fock/density functional Kohn-Sham orbitals. The equivalent-core approximation (ECA) was used where the core transitions are described by the valence transitions of the equivalent-core molecule, which has a modified nuclear configuration and an additional electron.

Future applications will employ the Hartree-Fock static exchange approximation (HF-STEX) which has been successfully utilized to predict XANES spectra of molecules. Compared with the ECA, the HF-STEX provides a considerably improved description of the virtual orbitals to which the core electrons are excited,

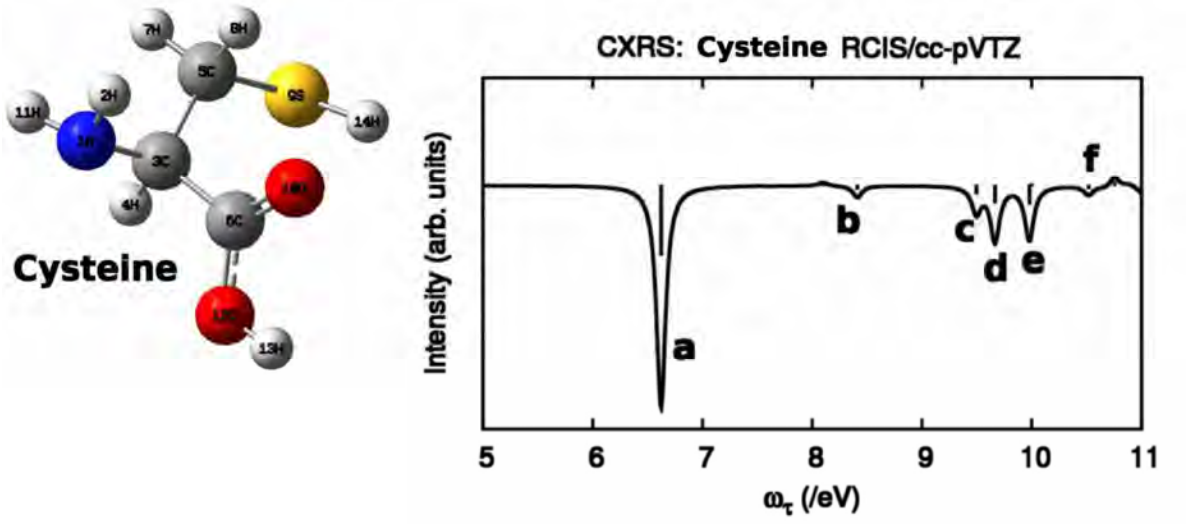

Figure 2: The Fourier transform of the time dependent S1s/S1s x-ray pump-probe (coherent Raman) signal obtained with 4.14fs Gaussian pulses tuned to the sulfur K-edge (2473.5eV) for the amino acid cysteine. A Restricted CI-Singles calculation with the cc-pVTZ basis set is used for the valence excitations.

and a better description of the orbital relaxation effects upon core excitations. In our previous calculations of the 2DXCS signals, the excited-state manifolds with one/two core holes only included the doubly-excited configurations, where one electron is excited from core orbital space to valence orbital space, and one within the valence orbital space. The HF-STEX includes a new class of singly-excited configurations. Such configurations have close energies to the doubly-excited ECA configurations and will result in new peaks in 2DXCS signals. The HF-STEX further allows a low cost study intramolecular charge migration. As pointed out by Cederbaum et al[1], charge migration in large conjugated systems such as peptides are due to orbital relaxation and the electron correlation effect. The former are well described by the HF-STEX. Electron correlation effects will requires a higher level of theory.

The response formalism will be further extended to time resolved photoelectron spectroscopy (TRPES) which is a powerful tool for probing orbital energies in molecules and crystals. The system is prepared in a nonequilibrium state by a laser pulse, and its subsequent time evolution is probed by detecting the electrons generated by a second ionizing pulse. The distribution of the electron kinetic energy (ε) reveals the underlying dynamics through its parametric dependence on the time delay. Relaxation of electrons in metals, and nuclear motions of molecules have been measured by TRPES. This technique can be viewed as a two dimensional (2D) spectroscopy since the signals depend on two parameters $S(\varepsilon,t)$. It is possible to extend this to higher dimensions by subjecting the system to sequences of multiple pulses prior to the ionization. Using two pump pulses, for example, we get a 3D signal $S(\varepsilon,t_1,t_2)$. The correlation function formalism of nonlinear spectroscopy will be extended to account for electron rather than photon detection. TRPES signals will be recast as the modulus square of transition amplitudes whereas heterodyne detected optical signals are given by nonlinear susceptibilities. The two types of signals will be compared and semi classical expressions for the vibrational dynamics underlying these signals will be derived.

The technique will be further extended to atto second electron dynamics. Here the pump ionizes the molecule to create one or several holes (core or valence type). The hole migration can then be probed by a second pulse and detected by either the generated photoelectrons or by directly looking at its absorption. Hole motion is very slow and negligible for deep core states and becomes faster for more shallow holes. While the detection of photoelectrons is more sensitive compared to photons, the two signals are not identical and photon in/photon out measurements are generally complementary to photon in/electron out.

Publications Resulting from the Project

[P1] Quantum Master Equation for Electron Transport Through Quantum Dots and Single Molecules", U. Harbola, M. Esposito and S.Mukamel. Phys. Rev. B. 74,235309 (2007)

[P2] "Manipulating Multidimensional Electronic Spectra of Excitons by Polarization Pulse-Shaping," D. Voronine, D. Abramavicius, S. Mukamel, J.Chem. Phys. 126,044508(2007)

1 J. Breidbach and L. S. Cederbaum, J. Chem. Phys. **118** (2003) 3983, **126** (2007) 034101.

[P3] “Manipulating Multidimensional Nonlinear Spectra of Excitons by Coherent Control with Polarization Pulse Shaping," D. Voronine, D. Abramavicius and S. Mukamel. In Ultrafast Phenomena XV, R.J.D. Miller, A.M. Weiner, P. Cornum and D.M. Jonas (editors) Springer Verlag (2006)
[P4] “Multipoint Correlation Functions for Photon Statistics in Single Molecule Spectroscopy;Stochastic Dynamics in Liouville Space," F. Sanda and S. Mukamel. In "Theory, Modeling and Evaluation of Single -Molecule Measurements", Editors E. Barkai, F. Brown, M. Orrit and H. Yang, World Scientific, (2007).
[P5] “Simulation of X-ray Absorption Near Edge of Organ Metallic Compounds in the Ground and Optically Excited States," R. Pandey and S. Mukamel., J.Phys.Chem.A. 111,805-816 (2007).
[P6] “Two-Dimensional Optical Spectroscopy of Excitons in Semiconductor Quantum Wells: Liouville-Space Pathways Analysis," L. Yang, I.V. Schweigert, S. Cundiff and
S. Mukamel, Phys.Rev.B., 75,125302(2007).
[P7] Comment on “Failure of the Jarzynski Identify for a Simple Quantum System," S.Mukamel. Cond-mat/0701003vl, Dec. 30, 2006.
[P8] “Two-Dimensional Infrared Surface Spectroscopy for CO on Cu(100):Detection of Intermolecular Coupling of Adsorbates," Y. Nagata, Y. Tanimura and S. Mukamel J.Chem.Phys. 126, 204703 (2007).
[P9] “Probing Valence ElectronicWavepacket Dynamics by all X-ray Stimulated Raman Spectroscopy; A Simulation Study," I.V. Schweigert and S. Mukamel Phys. Rev. A.76, 0125041 (2007).
[P10] “Partially-Time-Ordered Keldysh-Loop expansion of Coherent Nonlinear Susceptibilities," S. Mukamel, Phys. Rev.A., 77, 023801, 2008.
[P11] “Two-Dimensional Correlation Spectroscopy of Two-Exciton Resonances in Semi-conductor Quantum Wells," L. Yang and S. Mukamel, Phys. Rev. Lett, 100, 057402, 2008.
[P12] “ Ultrafast Optical Spectroscopy of Spectral Fluctuations in a Dense Atomic Vapor," V.O. Lorenz, S. Mukamel, W. Zhuang and S.T. Cundiff, Phys. Rev. Lett., 100, 013603, 2008.
[P13] “Coherent Ultrafast Core-hole Correlation Spectroscopy: X-ray Analogues of Multidimensional NMR," I. Schweigert and S. Mukamel, Phys. Rev. Lett , 99, 163001, 2007.
[P14] “Simulating Multidimensional Wave Optical Mixing Signals with Finite Pulse Envelopes”, I. Schweigert and S. Mukamel, Phys. Rev. A., 77, 33802, 2008.
[P15] “Probing Interactions Between Core-Electron Transitions by Ultrafast Two Dimensional X-Ray Coherent Correlation Spectroscopy”, I.V. Schweigert and S. Mukamel, J.Chem.Phys. 128, 184307 (2008).
[P16] “Revealing Exciton-Exciton Couplings in Semiconductors by Multidimensional Four Wave Mixing Signals”, L. Yang and S. Mukamel, Phys. Rev. B., 77, 075335 (2008).
[P17] “Many-body Effects in 2-D Optical Spectra of Semiconductor Quantum-Dot Pairs; TDHF approximation and Beyond”, R. Oszwaldowski, D. Abramavicius and S. Mukamel, J. Phys. Cond. Matt. 20, 045206 (2008).
*[P18] “Probing Multiple Core-hole Interactions in the Nitrogen K-edge of DNA Basepairs by multidimensional X-ray Spectroscopy; A Simulation Study”, D. Healion, I. Schweigert and S. Mukamel, J. Phys. Chem.A., 112, 11449-11461 (2008).
*[P19]“Dissecting Quantum Pathways in Two-dimensional Correlation Spectroscopy of Semiconductors”, L. Yang and S. Mukamel, J. of Physics Condensed Matter, 20, 395202 (2008).
*[P20]“Coherent Multidimensional Optical Probes for Electron Correlations and Exciton Dynamics; from NMR to X-rays”, S. Mukamel, D. Abramavicius, L. Yang, W.Zhuang, I.V. Schweigert and D. Voronine. Acct.Chem.Res. 42, 553-562 (2009).
*[P21]“Coherent Multidimensional Optical Spectroscopy Excitons in Molecular Aggregates; Quasiparticle vs. Supermolecule Perspectives”, D. Abramavicius, B. Palmieri, D. Voronine, F. Sanda and S. Mukamel, Chem. Rev. 109, 2350-2408 (2009).
[P22]“Double-quantum Coherence Attosecond X-ray Spectroscopy of Spatially-separated, spectrally-overlaping core-election transitions,” I.V. Schweigert and S. Mukamel. Phys. Rev. A. 78, 052509(2008).
[P23]“Isolating Excitonic Raman Coherence in Semiconductors Using 2D Correlation Spectroscopy”, L.Yang, T. Zhang, A. Bristov, S. Cundiff and S. Mukamel, J.Chem. Phys. 129, 234711 (2008).
[P24] “Coherent Stimulated X-ray Raman Spectroscopy;Attosecond Extension of RIXS”, U. Harbola and S. Mukamel, Phys. Rev. B. 79, 085108 (2009).\
[P25]“Investigation of Electronic Coupling in Semiconductor Double Quantum Wells Using Coherent Optical Two-Dimensional Fourier Transform Spectroscopy”, X. Li, T. Zhang, S. Mukamel, R. P. Mirin, S.T. Cundiff, Solid State Comm., 149, 361-366 (2009).
*[P26] “Many-body Green’s Function Approach to Attosecond Nonlinear X-ray Spectroscopy”, U. Harbola and S. Mukamel, Phys. Rev. B. 79, 235129 (2009).

Nonlinear Photoacoustic Spectroscopies Probed by Ultrafast EUV Light

Keith A. Nelson
Department of Chemistry
Massachusetts Institute of Technology
Cambridge, MA 02139
Email: kanelson@mit.edu

Henry C. Kapteyn, Margaret M. Murnane
JILA
University of Colorado and National Institutes of Technology
Boulder, CO 80309
E-mail: kapteyn@jila.colorado.edu, murnane@jila.colorado.edu

Program Scope

This project is aimed at direct spectroscopic characterization of phenomena that occur on mesoscopic (nanometer) length scales and ultrafast time scales in condensed matter, including non-diffusive thermal transport and the high-wavevector acoustic phonon propagation that mediates it, complex structural relaxation and the density and shear dynamics that mediate it, and nanostructure thermoelastic responses. The primary effort in the project is directed toward nonlinear time-resolved spectroscopy with coherent soft x-ray, or extreme ultraviolet (EUV), wavelengths. Time-resolved four-wave mixing, or transient grating (TG), measurements are conducted in order to directly define an experimental length scale as the interference fringe spacing Λ (or wavevector magnitude $q = 2\pi/\Lambda$) formed by two crossed excitation pulses. [1] The dynamics of material responses at the selected wavevector, including thermoelastically induced surface acoustic waves and thermal diffusion or non-diffusive thermal transport, are recorded through time-resolved measurement of coherent scattering, i.e. diffraction, of variably delayed probe pulses from the transient grating pattern. Progress in high harmonic generation [2] has yielded femtosecond EUV pulses with sufficient energy and focusability for use in TG experiments. EUV probe pulses provide far greater sensitivity than optical pulses to surface acoustic and thermal responses, since the surface modulations change the EUV phase by far more than the optical phase and thereby yield far higher EUV diffraction efficiencies [3]. Crossed EUV excitation pulses will produce interference fringe spacings of tens of nanometers, far smaller than is possible with crossed optical pulses, providing access to mesoscopic length scales, very high acoustic frequencies, and non-ballistic thermal transport [4].

In complementary measurements [5], the frequency rather than the wavevector of an acoustic response is specified by using a sequence of femtosecond excitation pulses at a specified repetition rate, with each pulse thermoelastically driving a single acoustic cycle. In this case the acoustic wave propagates through the sample rather than along the surface, and detection is carried out at the opposite sample surface, i.e. multiple-pulsed excitation is at the front and detection is at the back of the sample. This approach provides access to high-frequency bulk acoustic waves, while the EUV measurements are used to examine surface acoustic waves.

Recent Progress

Several experiments have been pursued recently as a collaboration between MIT, JILA and Erik Anderson at LBL. The first implemented a visible-pump EUV-probe transient grating experiment [6]. Visible light was used to create the excitation grating from the backside of a nickel film that was on a transparent substrate, and the response was probed from the front using EUV light. From the resultant data, we extracted the acoustic dispersion of thin nickel films of varying thickness. This information is of interest for basic science, but we have also shown that it is a very accurate measure of thicknesses of films of 10 nm or less.

In a second set of experiments, a new geometry for time-resolved photoacoustic experiments was demonstrated that promises to provide 2-D images of energy absorption and dissipation in nano-

structured materials [7,8]. This geometry is a form of Gabor holography—the first demonstration of time-resolved holographic imaging using EUV light. The experimental data showed the time-dependent response of a thin film excited by a simple line-focused laser pulse, and a 2-D image of the surface at a fixed time after the excitation pulse. This technique is being investigated as a general method for measuring dynamic processes in nanostructures.

In very recent experiments, we studied ultrahigh-frequency surface acoustic wave propagation in a series of nickel-on-sapphire nanostructures [9]. A surface acoustic wave was generated by optical irradiation of a periodic pattern of thin nickel lines and monitored through time-resolved diffraction of an EUV probe beam. We extended optical measurements of SAW propagation dynamics to frequencies of nearly 50 GHz – the highest SAW frequencies probed using any optical measurements to date – corresponding to wavelengths (determined by the nickel period) as short as 125 nm. We also implemented the first measurement of SAW dispersion in a nanostructure/bulk system. For long acoustic wavelengths, the propagation speed of the SAW is determined predominantly by the substrate properties. However, for shorter acoustic wavelengths, the penetration depth decreases and the SAW is increasingly localized in the nickel, slowing down the propagation speed. The experimental geometry and data are shown in Figure 1. Our results are in excellent agreement with an effective mass model for thin films, modified to account for the presence of the nanostructure.

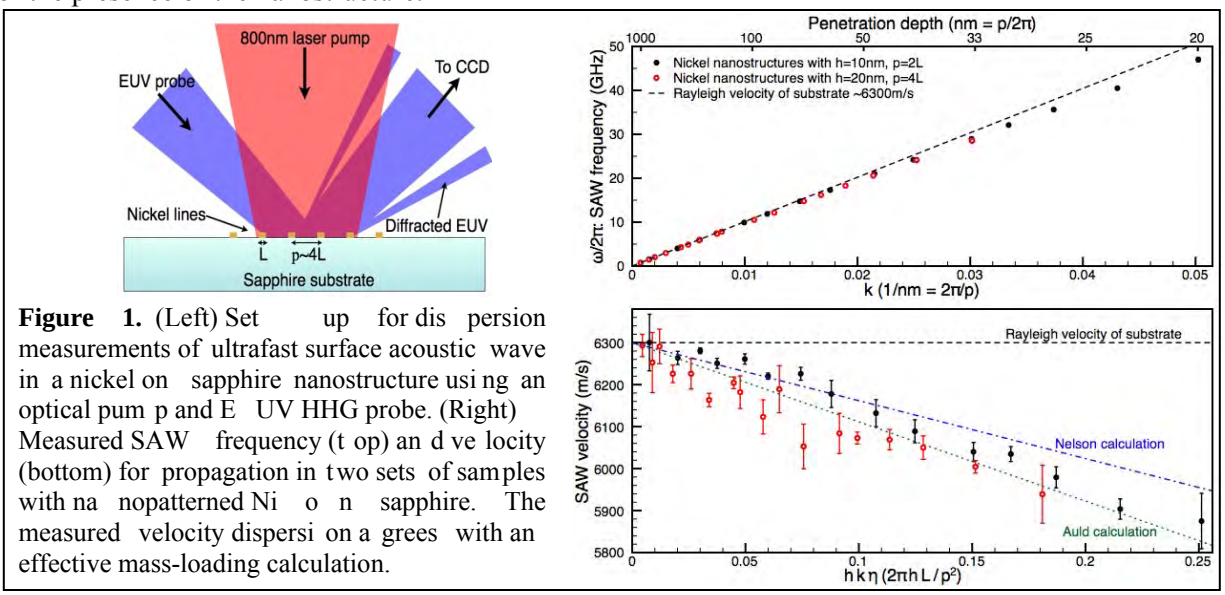

Figure 1. (Left) Set up for dispersion measurements of ultrafast surface acoustic wave in a nickel on sapphire nanostructure using an optical pump and EUV HHG probe. (Right) Measured SAW frequency (top) and velocity (bottom) for propagation in two sets of samples with nanopatterned Ni on sapphire. The measured velocity dispersion agrees with an effective mass-loading calculation.

Fourier theory of thermal transport considers heat transport as a diffusive process where energy flow is driven by a temperature gradient $q \propto -\nabla T$. However, this expression is not valid at length scales smaller than the mean free path for the energy carriers in a material, i.e. the phonon mean free path in an insulator. In this case, heat flow will become "ballistic" - driven by direct point-to-point transport of energy quanta. Past experiments have demonstrated size-dependent ballistic thermal transport *through* nanostructures such as thin films, superlattices, nanowires, and carbon nanotubes. The Fourier law also breaks down in the case of heat dissipation from a nanoscale heat source. However, despite considerable theoretical discussion and practical importance, , non-Fourier heat transport away from a nanoscale heat source has not been experimentally observed to date. Our EUV probing of nickel/sapphire samples has yielded the first observation and quantitative measurements of the transition from diffusive to ballistic thermal transport from a nanoscale hotspot. We measure a significant (as much as 3 times) decrease in energy transport away from the nanoscale heat source compared with Fourier law predictions [10-12]. This finding could have significant impact on the thermal management and reliability of emerging nanoscale devices. Essentially, heat flowing from a nanoscale source should be thought of as emerging from a larger region, with a size corresponding to the phonon mean free path in the substrate. Our results show that the Fourier law can be corrected to describe energy dissipation from nanostructures into bulk through a size-dependent ballistic thermal resistance.

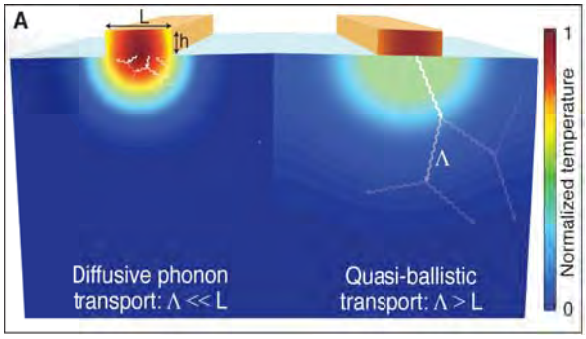

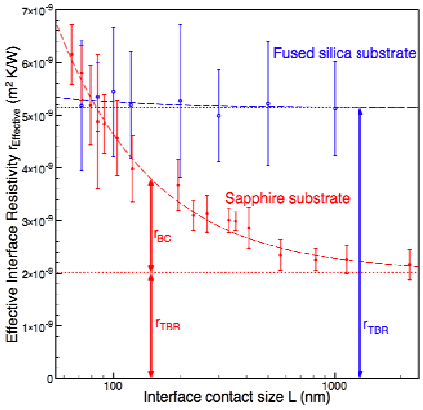

Figure 2. (left) Thermal transport across a nanoscale interface. Schematic illustrating the difference between diffusive and quasi-ballistic thermal transport across an interface. When the lateral dimension of the interface is smaller than the phonon mean path in the substrate, the Fourier diffusive heat equation breaks down. (right) Measured effective thermal resistivity for nickel nanostructures of width L deposited on fused silica (blue hollow dots) and sapphire (red solid dots) substrates. The blue and red dotted horizontal lines show the bulk resistivity r_{TBR} for data from the fused silica and sapphire substrates. The blue and red dashed curves show model predictions for the ballistic resistivity correction $r_{BC} \sim \Lambda/L$, with $\Lambda_{FS} = 2$ nm and $\Lambda_{Sa} = 120$ nm.

We have developed novel methods for measurement of bulk acoustic waves at high frequencies, recently including shear as well as longitudinal waves [13-15]. Acoustic waves at GHz frequencies play key roles in thermal transport. They also mediate structural relaxation in partially ordered and disordered materials including supercooled liquids. We have made the first measurements of GHz shear waves in glass-forming liquids including glycerol, using femtosecond pulse sequences to excite the waves and single femtosecond pulses to monitor them after propagation through the sample. Figure 3 shows the experimental approach and temperature-dependent results for glycerol at selected frequencies. This frequency range has eluded measurements for shear waves until now, and even longitudinal wave data are available for only a few liquids.

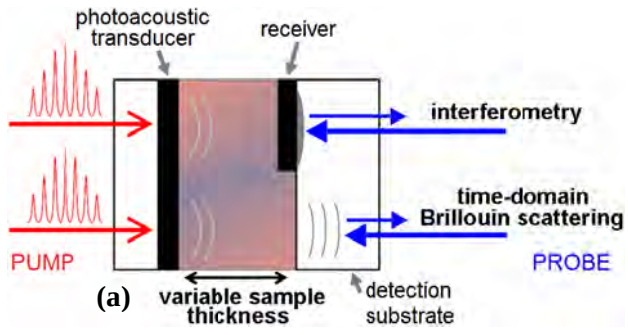

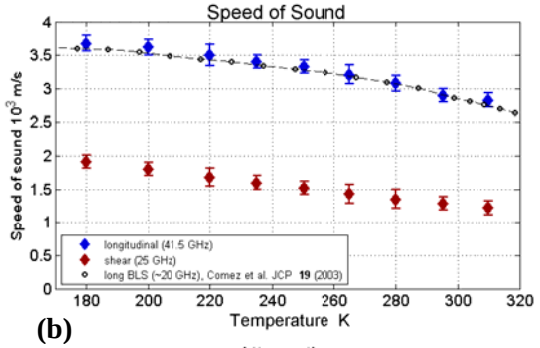

Figure 3. (a) Multiple-pulse generation of acoustic waves that propagate through a liquid sample and are detected on the other side. Shear waves are generated using a crystallographically canted FeT ransducer film. Measurements are made at different liquid thicknesses to extract the acoustic speed and damping rate. (b) *T*-dependent results for 41.5 GHz longitudinal waves and 25.0 GHz shear waves in glycerol, detected in a glass substrate by depolarized coherent Brillouin scattering after propagation through the liquid.

Future Plans

We plan to extend EUV study of quasi-ballistic heat transport to a range of complex nanoscale structures, to combine dynamic photoacoustic and photothermal techniques with coherent EUV imaging techniques that we have recently demonstrated [16,17], and to work toward EUV TG excitation as well as probing. Optical multiple-pulse measurements of GHz shear and longitudinal waves will be used for detailed characterization of the acoustic contributions to thermal transport in insulating materials. These experiments will further our understanding of heat transport fundamentals and thermal management at nanoscale dimensions. Shear and longitudinal waves also will be used to elucidate structural relaxation dynamics in supercooled liquids in order to test fundamental theories of the liquid-glass transition [1].

References

1. "Impulsive stimulated light scattering from glass-forming liquids: I. Generalized hydrodynamics approach; II. Salol relaxation dynamics, nonergodicity parameter, and testing of mode coupling theory," Y. Yang and K.A. Nelson, *J. Chem. Phys*. **103**, 7722-7731; 7732-7739 (1995).
2. "Phase-matched generation of coherent soft-x-rays," A. Rundquist, C. Durfee, Z. Chang, S. Backus, C. Herne, M. M. Murnane and H. C. Kapteyn, *Science* **280**, 1412 – 1415 (1998).
3. "Nanoscale photothermal and photoacoustic transients probed with extreme ultraviolet radiation," R. I. Tobey, E. H. Gershgoren, M. E. Siemens, M. M. Murnane, H. C. Kapteyn, T. Feurer, and K. A. Nelson, *Appl. Phys. Lett.* **85**, 564-566 (2004).
4. G. Chen, *Nanoscale Energy Transport and Conversion*. Oxford: Oxford University Press, 2005.
5. "Generation of ultrahigh frequency tunable acoustic waves," J. D. Choi, T. Feurer, M. Yamaguchi, B. Paxton, and K. A. Nelson, *Appl. Phys. Lett.* **87**, 081907 (2005).
6. "Transient grating measurement of surface acoustic waves in thin metal films with extreme ultraviolet radiation," R.I. Tobey, M.E. Siemens, M.M. Murnane, H.C. Kapteyn, D.H. Torchinsky, and K.A. Nelson, *Appl. Phys. Lett*. **89**, 091108-1 – 091108-3 (2006).
7. "Ultrafast Extreme Ultraviolet Holography: Dynamic Monitoring of Surface Deformation," R.I. Tobey, M.E. Siemens, O. Cohen, M.M. Murnane, H.C. Kapteyn, and K.A. Nelson, *Opt. Lett.* **32**, 286-288 (2007).
8. "Ultrafast extreme ultraviolet holography: Dynamic monitoring of surface deformation," R.I. Tobey, M.E. Siemens, O. Cohen, Q. Li, M.M. Murnane, H.C. Kapteyn, and K.A. Nelson, in *Ultrafast Phenomena XV*, P. Corkum, D. Jonas, R.J.D. Miller, and A.M. Weiner, eds. (Springer-Verlag 2007), pp. 42-44.
9. "High-frequency surface acoustic wave propagation in nanostructures characterized by coherent extreme ultraviolet beam," M.E. Siemens, Q. Li, M.M. Murnane, H.C. Kapteyn, R. Yang, E.H. Anderson, and K.A. Nelson, *Appl. Phys. Lett*. **94**, 093103 (2009).
10. "Nanoscale Heat Transport Probed with Ultrafast Soft X-Rays," M. Siemens, Q. Li, M. Murnane, H. Kapteyn, R. Yang, and K. Nelson, in *Ultrafast Phenomena XVI*, Stresa, Italy, 2008, p. TBP.
11. "Measurement of quasi-ballistic thermal transport from nanoscale interfaces using ultrafast coherent soft x-ray beams," M. Siemens et al., submitted (2009).
12. M. Siemens, et al., invited talk, CLEO/QELS 2008, highlighted in Physics Today, July 2008.
13. "Picosecond photoexcitation of acoustic waves in locally canted gold films," T. Pezeril, F. Leon, D. Chateigner, S.Kooi, and K.A. Nelson, *Appl. Phys. Lett*. **92**, 061908 (2008).
14. "Picosecond shear waves in nano-sized solids and liquids," T. Pezeril, C. Klieber, S. Andrieu, D. Chateigner, and K. A. Nelson, *Proc. SPIE*, **7214**, 721408 (2009).
15. "Optical generation of gigahertz-frequency shear acoustic waves in liquid glycerol," T. Pezeril, C. Klieber, S. Andrieu, and K. A. Nelson, *Phys. Rev. Lett*. **102**, 107402 (2009).
16. "Lensless diffractive imaging using tabletop coherent high-harmonic soft-x-ray beams," R. L. Sandberg, A. Paul, D. A. Raymondson, S. Hadrich, D. M. Gaudiosi, J. Holtsnider, R. I. Tobey, O. Cohen, M. M. Murnane, and H. C. Kapteyn, *Phys. Rev. Lett.* **99**, 098103 (2007).
17. "High numerical aperture tabletop soft x-ray diffraction microscopy with 70-nm resolution," R. L. Sandberg, C. Y. Song, P. W. Wachulak, D. A. Raymondson, A. Paul, B. Amirbekian, E. Lee, A. E. Sakdinawat, C. La-O-Vorakiat, M. C. Marconi, C. S. Menoni, M. M. Murnane, J. J. Rocca, H. C. Kapteyn, and J. W. Miao, *Proc. Nat'l. Acad. Sci. USA* **105**, 24-27 (2008).

Near-field Imaging with a Localized Nonlinear Photon Source

Lukas Novotny (novotny@optics.rochester.edu)
University of Rochester, The Institute of Optics, Rochester, NY, 14627.

1 Program Scope

The goal of this project is the control of a single quantum emitter by use of an optical antenna. More specifically, we are developing and studying optical antennas to selectively influence the stimulated emission rate and the excited state lifetime of an electronic multilevel system (atom, ion, molecule, defect center). In the past project period we made use of the high intrinsic optical nonlinearities of metal nanostructures [4] to create a localized photon source [7]. This source was used to locally excite different molecular systems [2].

2 Recent Progress

We demonstrated high-resolution near-field imaging and spectroscopy using the nonlinear optical response of a gold nanoparticle pair as an excitation photon source. Femtosecond pulses of frequencies ω_1 and ω_2 were used to induce a nonlinear polarization at the four wave mixing (4WM) frequency $2\,\omega_1 - \omega_2$ in the junction of the nanoparticle dimer. The nonlinear response leads to localized photon emission, which is employed as an excitation source for fluorescence and extinction imaging. The principle of this novel imaging technique was demonstrated for samples of fluorescent nanospheres and tubular J-aggregates.

As illustrated in Fig. 1a we attached a gold nanoparticle dimer to the end of a pointed optical fiber. We then irradiated the fabricated dimer antenna with laser pulses of center frequency ω_1 and ω_2, respectively, and monitored the spectrum of the emitted radiation. This procedure helped us to identify suitable dimer antennas for subsequent near-field optical imaging; we retained only antennas that yield a strong third-order response at $\omega_{4WM} = 2\omega_1 - \omega_2$ and a negligible second-order response at $2\omega_1$, $2\omega_2$, and $\omega_1 + \omega_2$. A weak second-order response is indicative for a symmetric dimer antenna, because of its point-symmetry. Representative spectra of the emitted radiation are shown in Fig. 1b,c for two different dimer antennas. In (b) the second-order nonlinear response is clearly recognizable, whereas in (c) it is greatly suppressed.

The laser pulses are generated by a Ti:Sapphire laser providing pulses of duration $\sim 200\,\mathrm{fs}$, repetition rate of $\sim 76\,\mathrm{MHz}$, and tunable wavelength of $\lambda_1 = 740 - 821\,\mathrm{nm}$. This laser also pumps an optical parametric oscillator (OPO) providing pulses of the same duration, and tunable wavelength of $\lambda_2 = 1078 - 1170\,\mathrm{nm}$. A delay line is used to adjust the time difference between the two excitation pulses. Nonlinear four-wave mixing can be generated only when the two exciting laser pulses are overlapping in time and space.
As illustrated in Fig. 1, an objective with numerical aperture NA=1.3 is used to focus both laser beams on the surface of a quartz slide, which supports the sample to be imaged. The average input powers for Ti:Sapphire laser and OPO are $\sim 10 - 20\mu\,\mathrm{W}$ and $\sim 0.5\,\mathrm{mW}$, respectively.

To determine the required excitation power levels we used a sample with monodispersed red fluorescent nanospheres of 40 nm diameter. The absorption spectrum of the nanospheres has a maximum at $\sim 660\,\mathrm{nm}$ and the corresponding fluorescence spectrum peaks at $\sim 680\,\mathrm{nm}$. To excite the nanospheres we tune the four-wave mixing frequency to $\lambda_{4WM} = 630\,\mathrm{nm}$ (c.f. Fig. 1c). The dimer antenna is positioned into the focii of the stationary excitation beams, and the sample with the nanospheres is raster scanned underneath the dimer antenna while detecting the fluorescence in the wavelength range of [694-738] nm. Simultaneously, we record the topography of the sample by monitoring the vertical motion of the particle dimer antenna during shear-force feedback.

Fig. 2 shows a sequence of images of the same sample area. (a-d) are optical images that have been recorded sequentially. (e) is the corresponding topography demonstrating that each fluorescent nanosphere

traces out the characteristic profile of the dimer antenna. The excitation intensity of the laser beams ω_1 and ω_2 was gradually increased from (a) to (d). For low excitation intensities the optical contrast is dominated by extinction of the two-photon luminescence (TPL) continuum emitted from the laser-irradiated dimer antenna. This continuum is very weak in the spectra shown in Fig. 1b,c because high excitation intensities have been used.

For weak intensities the ratio of 4WM to TPL becomes small, which explains the dominance of extinction due to the continuum. The TPL contribution span over the entire detection window giving rise to the observed extinction images.

We gradually increase the excitation power until the emitted fluorescence overcomes the TPL background generated by the dimer antenna. It is evident from Fig. 2d that the fluorescence is strongest when the dimer junction is centered over a nanosphere. The excitation fields and the 4WM intensity are strongest at the junction. Furthermore, it can be expected that fluorescence quenching is weakest near the junction of the dimer. Our results demonstrate that 4WM at the junction of a dimer antenna defines a highly localized and effective fluorescence excitation source. The fluorescence excitation can also be temporally controlled by varying the temporal overlap between the excitation pulses. Introducing a small time delay makes the fluorescence emission disappear.

In conclusion, we have demonstrated that the nonlinear response at a gold nanoparticle junction defines a localized, tunable, and narrow-band photon source, which can be employed for high-resolution fluorescence

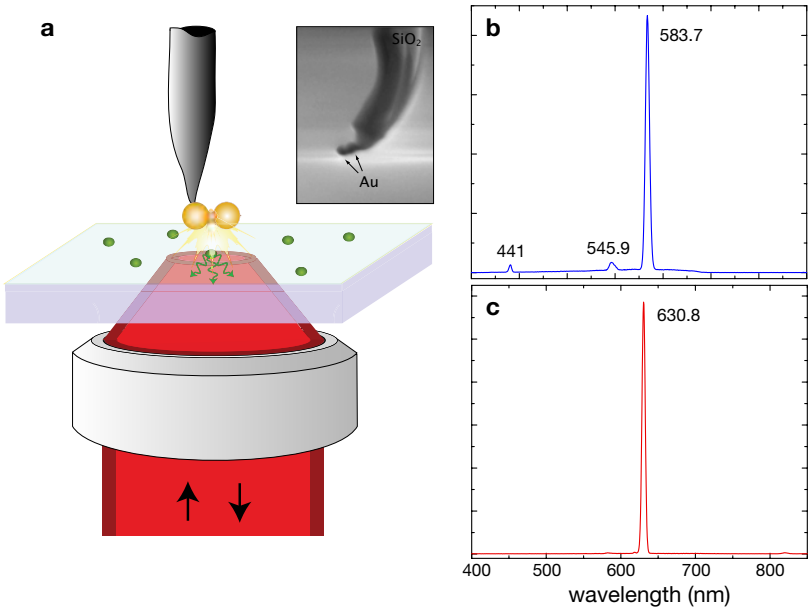

Figure 1: (a) Illustration of the experiment. A gold nanoparticle dimer attached to a sharply pointed optical fiber serves as a nonlinear photon source. The nanoparticle dimer is excited by two incident laser beams of frequencies ω_1 and ω_2, giving rise to four-wave mixing (4WM) at frequency $\omega_{4WM} = 2\omega_1$ - ω_2 generated at the nanoparticle junction. This localized source of radiation is used as a fluorescence excitation source for the sample placed underneath. A near-field fluorescence image is generated by raster scanning the sample and detecting pixel by pixel the emitted fluorescence. Inset: Electron micrograph of a nanoparticle dimer probe. (b,c) Spectra of photons emitted from a ~ 80 nm symmetrical particle dimer excited by laser pulses of center frequency ω_1 and ω_2. (b) Spectrum corresponding to $\lambda_1 = 765$ nm and $\lambda_2 = 1105$ nm, respectively. Four-wave mixing at the dimer junction gives rise to photon emission at $\lambda_{4WM} = 584$ nm. The smaller peaks correspond to residual second-order processes. (c) Spectrum from a highly symmetric nanoparticle dimer recorded for $\lambda_1 = 821$ nm and $\lambda_2 = 1170$ nm. The second-order response is completely suppressed.

imaging. Since the wavelength of the 4WM signal can be tuned over a wide spectral range, the plasmonic dimer is also ideally suited for local extinction measurements. Because of broadband TPL we are able to observe fluorescence only for excitation intensities above a certain threshold. Additionally, the emitted fluorescence can be turned on and off by controlling the temporal overlap between the excitation pulses. Moreover, the 4WM can be tuned into the absorption band of fluorescent molecules. We anticipate that the ability of switching on and off localized photon sources will find applications in nanophotonics and in active plasmonics.

3 Future Plans

In our future work we will study the possibility of exciting surface plasmon polaritons on bulk metal surface by means of four-wave mixing. This process involves the vectorial addition of the momenta of three incident photons, making it possible to penetrate the light cone and directly couple to the SPP dispersion curve. In parallel, we will develop optimized antenna geometries to independently enhance the stimulated and spontaneous emission rate of single quantum emitters.

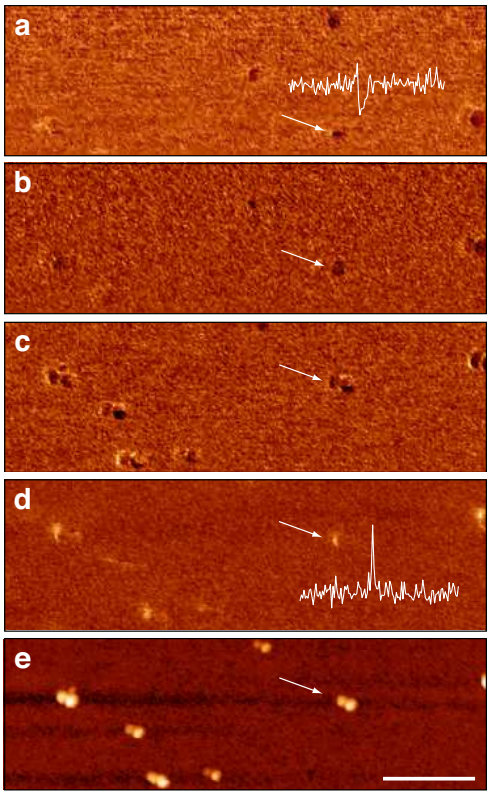

Figure 2: Contrast from 40nm fluorescent nanospheres as a function of excitation intensity. All images show the same sample region. The powers of the laser ω_1 and ω_2 has been continuously increased from (a) to (d). The topographic image (e) shows that each nanosphere traces out the characteristic shape of the dimer antenna. At low excitation powers the contrast is dominated by extinction of two-photon luminescence originating from the dimer antenna. At higher excitation powers the contrast is defined by fluorescence emission from the nanospheres. The fluorescence is at a maximum when the nanosphere faces the junction of the dimer antenna. The insets show cross-sections through the nanosphere indicated by the arrows. Scale bar: 600nm.

DOE Sponsored Publications (2006-2009)

[1] P. Bharadwaj, B. Deutsch, and L. Novotny, "Optical antennas," *Adv. Opt. Phot.*, in print (2009).

[2] S. Palomba, M. Danckwerts, and L. Novotny, "Nonlinear plasmonics with gold nanoparticle antennas," *J. Opt. A: Pure and Appl. Opt.*, in print (2009).

[3] L. Novotny, "Optical antennas tuned to pitch," *Nature* **455**, 879 (2008).

[4] S. Palomba and L. Novotny, "Nonlinear excitation of surface plasmon polaritons by four-wave mixing," *Phys. Rev. Lett.* **101**, 056802 (2008).

[5] L. Novotny and C. Henkel, "Van der Waals versus optical interaction between metal nanoparticles," *Opt. Lett.* **33**, 1029 (2008).

[6] R. J. Moerland, T. H. Taminiau, L. Novotny, N. F. van Hulst, and L. Kuipers, "Reversible polarization control of single molecule emission," *Nano Lett.* **8**, 606 (2008).

[7] M. Danckwerts and L. Novotny, "Optical frequency mixing at coupled gold nanoparticles," *Phys. Rev. Lett.* **98**, 026104 (2007).

[8] P. Anger, P. Bharadwaj, and L. Novotny, "Nanoplasmonic enhancement of single molecule fluorescence," *Nanotechnology* **18**, 044017 (2007).

[9] L. Novotny, "The history of near-field optics," *Progress in Optics* **50**, 137-180, E. Wolf (ed.), Elsevier, Amsterdam (2007).

[10] H. Gersen, L. Novotny, L. Kuipers, and N. F. van Hulst, "On the concept of imaging nanoscale vector fields," *Nature Photonics* **1**, 242 (2007).

[11] L. Novotny and A. Bouhelier, "Near-field optical excitation and detection of surface plasmons," in *Surface Plasmon Nanophotonics*, M. Brongersma (ed.), Kluwer Academic (2007).

[12] P. Bharadwaj and L. Novotny, "Spectral dependence of single molecule fluorescence enhancement," *Opt. Express* **15**, 14266 (2007).

[13] R. Kappeler, D. Erni, C. Xudong, and L. Novotny, "Field computations of optical antennas," *J. Comp. Theor. Nanosc.* **4**, 686 (2007).

[14] P. Anger, P. Bharadwaj, and L. Novotny, "Enhancement and quenching of single molecule fluorescence," *Phys. Rev. Lett.* **96**, 113002 (2006).

[15] N. Anderson, A. Bouhelier and L. Novotny, "Near-field photonics: tip-enhanced microscopy and spectroscopy on the nanoscale," *J. Opt. A: Pure Appl. Opt.* **8**, S227 (2006).

[16] M. R. Beversluis, L. Novotny, and S. J. Stranick, "Programmable vector point-spread function engineering," *Opt. Express* **14**, 2650 (2006).

[17] L. Novotny and S. J. Stranick, "Near-field optical microscopy and spectroscopy with pointed probes," *Ann. Rev. Phys. Chem.* **57**, 303 (2006).

[18] A. Hartschuh, H. Qian, A. J. Meixner, N. Anderson, and L. Novotny "Tip-enhanced optical spectroscopy for surface analysis in biosciences," *Surface and Interface Analysis* **38**, 1472 (2006).

[19] H. Qian, T. Gokus, N. Anderson, L. Novotny, A. J. Meixner, and A. Hartschuh, "Near-field imaging and spectroscopy of electronic states in single-walled carbon nanotubes," *Phys. Stat. Sol. (b)* **243**, 1 (2006).

Electron-Driven Excitation and Dissociation of Molecules

A. E. Orel
Department of Applied Science
University of California, Davis
Davis, CA 95616
aeorel@ucdavis.edu

Program Scope

This program will study how energy is interchanged in electron-polyatomic collisions leading to excitation and dissociation of the molecule. Modern *ab initio* techniques, both for the electron scattering and the subsequent nuclear dynamics studies, are used to accurately treat these problems. This work addresses vibrational excitation, dissociative attachment, and dissociative recombination problems in which a full multi-dimensional treatment of the nuclear dynamics is essential and where non-adiabatic effects are expected to be important.

Recent Progress

We have carried out a number of calculations studying low-energy electron scattering from polyatomic systems leading to vibrational excitation and dissociative attachment, and studies of photoionization of diatomic and triatomic molecules. Much of this work has been done in collaboration with the AMO theory group at Lawrence Berkeley Laboratory headed by T. N. Rescigno and C. W. McCurdy. As a result of this collaboration one of my students is doing his thesis work with the AMO experimental group headed by A. Belkacen. He is currently carrying out experiments on dissociative attachment of systems where we have carried out calculations, both on H_2O and C_2H_2.

Dissociative Attachment of Acetylene

In the previous year we studied dissociative electron attachment (DEA) of the acetylene molecule, with the mechanism:

$$C_2H_2\ (X^1\Sigma_g^+) + e^-(E) \rightarrow (C_2H_2^-)^*(^2\Pi_g) \rightarrow C_2H^-(^1\Sigma^+) + H(^2S)$$

We carried out *ab initio* calculations for elastic electron scattering from acetylene using the complex Kohn variational method and additional quantum chemistry calculations to map out the resonance surface and autoionization width keeping on C-H distance fixed, reducing the problem to three dimensions, the C-CH distance (r), the distance from the other hydrogen atom to the center of mass (R) and the angle in-between them (θ). We then carried out MultiConfiguration Time-Dependent Hartree (MCTDH) calculations [1] to track the dissociation dynamics and obtain the dissociative attachment cross sections. The results of the calculation were described in a paper published in Physical Review A (Publication 6).

More recently, we have performed nuclear dynamics calculations on C_2H_2 and C_2D_2 to study the isotope effect in DEA. Our previous calculations at 0K led to an isotopic ratio of the cross section for C_2H_2 compared to the cross section for C_2D_2 of ~28.9, a factor of 2 higher than recent measurements [2]. Since this reaction proceeds by bending, and this mode is populated at room temperature at which the experiments were performed, the discrepancy was attributed to the contribution of higher vibrational modes. We included the four lowest bending vibrational states that had non-vanishing populations at the experiment temperature of T = 333 K. The resulting

ratio is found to be 17.9 in closer agreement to the experimental value. The results of the calculation were described in a paper submitted to Physical Review A (Publication 8)

Molecular-frame photoelectron angular distributions following k-shell photoionization
We report the results of *ab initio* calculations of cross sections and molecular-frame photoelectron angular distributions for C 1s ionization of CO_2 and propose a mechanism for the recently observed asymmetry of those angular distributions with respect to the CO^+ and O^+ ions produced by subsequent Auger decay. The fixed-nuclei, photoionization amplitudes were constructed using variationally obtained electron-molecular ion scattering wave functions. We have also carried out electronic structure calculations which identify a dissociative state of the CO_2^{2+} dication that is likely populated following Auger decay and which leads to O^++CO^+ fragment ions. We show that a proper accounting of vibrational motion in the computation of the photoelectron angular distributions, along with reasonable assumptions about the nuclear dissociation dynamics, gives results in good agreement with recent experimental observations. We also demonstrate that destructive interference between different partial waves accounts for sudden changes with photon energy in the observed angular distributions. The results of the calculation were described in a paper published in Physical Review A (Publication 7).

Dissociative Electron Attachment to HCN and HNC
Previously we have carried out studies on DEA of ClCN and BrCN (Publication 3). We have extended these calculations to HCN and its isomer HNC. These molecules are known to be among the initial species that drive synthesis of amino acids in the interstellar media. Previous experimental and theoretical studies have indicated low-lying Σ and Π resonances. These resonant states are expected to depend on stretching and bending of the molecule and lead to competition (CN^- + H) and (CN + H^-) products. We have carried out electron scattering calculation using the complex Kohn variational method as a function of the three internal degrees of freedom to obtain the resonance energy surface and autoionization widths. We used this as input to a dynamics calculation using the MCTDH approach [1]. In contrast to acetylene, instead of bending, the H atom tunnels through the barrier to dissociation. The DEA cross section and branching ratios were compared to available experiment and theory. The results of the calculation are described in a paper submitted to Physical Review A (Publication 9).

Formation of inner shell autoionizing CO^+ states below the CO^{++} threshold
Because of the long-range repulsive Coulomb interaction between singly charged ions, the vertical double ionization thresholds of small molecules generally lie above the dissociation limits corresponding to formation of singly charged fragments. This leads to the possibility of forming singly charged molecular ions by photoabsorption in the Franck-Condon region at energies below the lowest dication state, but above the dissociation limit for two singly charged fragment ions. These singly charged molecular ions can emit a second electron by autoionization, but only at larger internuclear separations where the ion falls into the electron+dication continuum. This process has been termed indirect double photoionization. Since these states are characterized by strong conf guration mixing and numerous curve crossings, the inner valence regions of molecular ions continues to be a challenging subject both experimentally and theoretically. The AMO experimental group headed by A. Belkacen has carried a kinetically complete experiment on the production of CO^+ autoionizing states following inner-valence photoionization of carbon monoxide below its double ionization threshold. Momentum imaging spectroscopy was used to

measure the energies and body-frame angular distributions of both photo- and ejected electrons, as well as the kinetic energy release of the atomic ions. We have carried out *ab initio* theoretical calculations, calculating both the potential energy curves of the superexcited states and well as cross sections and molecular-frame photoelectron angular distributions in order to compare with experiment. This has provided insight into the nature of the molecular ion states produced and their subsequent dissociation into autoionizing atomic (O^*) fragments. A paper on this work will be submitted soon to Physical Review Letters. In addition we plan to extend these studies to a similar process observed in water.

FUTURE PLANS

Electron interactions with CF_x radicals

Previously, we have studied the dissociative attachment of CF, the process, $e^- + CF \rightarrow F^- + C$. It was found not to produce significant F^-. The dissociative recombination of the cation CF^+ is interesting since ion-pair formation, the process, $e^- + CF^+ \rightarrow F^- + C^+$ is possible. This has been suggested as a possible source of F^- in these fluorocarbon plasmas. Experiments on the dissociative recombination have been carried out on both the ASTRID and CRYRING storage rings [3]. We have performed extensive structure calculations coupled with electron scattering calculations to characterize both the Rydberg states converging to the ground and low-lying excited states of the ion, as well as the resonant states and their autoionization widths as a function of internuclear separation. This data was used in both an MQDT and wave packet study of the dissociative. The results have be compared to the recent experiments and used to explain the experimental results. Our results are in good agreement with the most recent experimental results [4]. A paper on this work will be submitted soon to Physical Review A.

In collaboration with T.N. Rescigno, LBL, we have begun a study of the radical CF_2. We have performed fixed-nuclei scattering calculations using the Complex Kohn variational method and extracted the resonance parameters, for each geometry of interest, by analyzing the energy dependence of the eigenphase sums. These preliminary calculations have showed a single resonance at low energy that at the static exchange level is unbound at the equilibrium geometry of the ground state. However, at the relaxed SCF level of calculation, which correctly balances the anion and target correlation and has been used previously with great success to study similar resonances, the anion is bound at the equilibrium geometry. This is in contrast to the R-matrix calculations [5] that show the anion to be unbound at the equilibrium geometry. Studies of the resonance surface and autoionization widths have shown that these change little with changes in the bond angle. Therefore we have treated this system at fixed angle constructing two-dimensional surfaces at both the static-exchange and relaxed SCF level. We are currently using this data as input to a dynamics calculation using the MCTDH approach [1].

Dissociative Electron Attachment to HCCCN

Experiments on dissociative electron attachment (DEA) to HCCCN below 12 eV have led predominantly to formation of $CCCN^-$, CN^-, HCC^- and CC^- negative ions. It has been concluded that these fragments result mainly from the decay of π^*-shape resonant state upon electron attachment that involves distortion of the symmetry of the linear neutral molecule. In order to study the dynamics of dissociation in these channels, we subdivided the molecule into three fragments (H), (CC) and (CN); therefore, four internal coordinates consisting in the distances between the center of masses of (H) and (CC) fragments, (CC) and (CN) fragments, the (H)-(CC) angle and the (CC)-(CN) angle are included in the calculation. We have performed electron scattering calculations

using Complex Kohn Variational method to determine the resonance energies and autoionization width for various geometries of the system and construct the complex potential energy surfaces relevant to the metastable $HCCCN^-$ ion. The nuclear dynamics is treated using the Multiconfiguration Time-Dependent Hartree (MCTDH) formalism and the flux of the propagating wavepacket is used to compute the DEA cross section relevant to 4 channels in question. There are some limited experimental studies available on this system.

Dissociative Attachment of Acetylene

Recent experimental work shows that at a higher energy (>7 eV) the channel, which fragments into C_2^- and H_2, becomes open. This reaction proceeds through a higher-lying Feshbach resonance, and involves a dramatic change in geometry to proceed to products. We have begun a series of *ab initio* calculations, with a number of open electronic channels for electron scattering from acetylene using the Complex Kohn variational method. These calculations have shown, not only a series of Feshbach resonances, but also the higher lying shape resonances in the system. More work is needed to study the potential energy surfaces for these states and identify which of these states are involved in the dissociation process. It is possible that more than one state is involved and that interaction between the states must be included. We propose to study this and calculate the multi-dimensional dynamics leading to dissociation.

REFERENCES

1. M. H.Beck, A. Jackle, G.A. Worth and H. –D. Meyer, Phys. Rep., 324 (2000).
2. O. May, J. Fedor, B. C. Ibanescu and M. Allan, Phys. Rev. A. **77**, 040701 (2008).
3. O. Novotny et al, J. Phys. B, **38**, 1471 (2005)
4. O. Novotny et al, J. Phys. Conf. Series, **XX**, XX (2008).
5. I. Rozum, N. J. Mason and Jonathan Tennyson, *J. Phys. B*, **35**, 1583 (2002).

PUBLICATIONS

1. Dynamics of Low-Energy Electron Attachment to Formic Acid, T. N. Rescigno, C. S. Trevisan and A. E. Orel, Phys. Rev. Lett. **96** 213201 (2006).
2. Elastic Scattering of Low-energy Electrons by Tetrahydrofuran, C. S. Trevisan, A. E. Orel and T. N. Rescigno, J. of Phys. B **39** L255 (2006).
3. Dissociative Attachment of ClCN and BrCN, J. Royal and A. E. Orel, J. Chem. Phys, **125** 214307 (2006).
4. Low-Energy Electron Scattering by Formic Acid, C. S. Trevisan, A. E. Orel and T. N. Rescigno, Phys. Rev. A **74** 042716 (2006).
5. Electron-induced resonant dissociation and excitation of NeH^+ and NeD^+, V.Ngassam, A. I. Florescu-Mitchell, and A. E. Orel, Phys.Rev. A, **77**, 042706 (2008)
6. Dissociative Electron Attachment of Acetylene, S. Chourou and A. E. Orel, Phys.Rev. A, **77**, 042709 (2008)
7. Theoretical study of asymmetric molecular-frame photoelectron angular distributions for C 1s photoejection from CO_2 , S. Miyabe, C. W. McCurdy, A. E. Orel, and T. N. Rescigno, Phys. Rev. A **79**, 053401 (2009)
8. Isotope Effect in the Electron Attachment of Acetylene, S. Chourou and A. E. Orel, (submitted Phys.Rev. A).
9. Dissociative Electron Attachment of HCN and HNC, S. Chourou and A. E. Orel, submitted Phys.Rev. A

"Low-Energy Electron Interactions with Liquid Interfaces and Biological Targets"

Thomas M. Orlando
School of Chemistry and Biochemistry and School of Physics,
Georgia Institute of Technology, Atlanta, GA 30332-0400
Thomas.Orlando@chemistry.gatech.edu, Phone: (404) 894-4012, FAX: (404) 894-7452

Project Scope: The primary objectives of this program are to investigate the fundamental physics and chemistry involved in low-energy (1-250 eV) electron interactions with i) condensed films of water co-adsorbed with solvated ions and biologically relevant molecules (i.e. simple nucleic acids, nucleosides and nucleotides), ii) condensed samples of complex biological targets such as deoxyribonucleic acids (DNA) and iii) aqueous solution surfaces and interfaces containing solvated ions and biomolecules. The program concentrates on the important issues dealing with electron initiated damage and energy exchange in the deep valence and shallow core regions of the collision targets. These types of excitations are extremely sensitive to many body interactions and changes in local potentials. The targets we will examine range in complexity from very controlled molecular thin films to realistic biological targets and complicated aqueous solution interfaces. Thus, our proposed investigations should be particularly fruitful in extracting important details regarding the roles of counter ions, interfacial energy exchange, and molecular structure in non-thermal damage of hydrated biological interfaces.

Recent Progress:

Project 1. The role of resonances in the low-energy electron induced damage of DNA.

We have continued to examined theoretically the elastic scattering of 5-30 eV electrons within the B-DNA 5'-CCGGCGCCGG-3' and A-tract DNA 5'-CGCGAATTCGCG-3' sequences using the separable representation of a free-space electron propagator and a curved wave multiple scattering formalism. We have also extended these studies to smaller oligonucleotides. In our plasmid work, we found that the disorder brought about by the surrounding water and helical base stacking lead to featureless amplitude build-up of elastically scattered electrons on the sugars and phosphate groups for all energies between 5-30 eV. Some constructive interference features arising from diffraction were also revealed when examining the structural waters within the major groove. These appeared at 5-10, 12-18 and 22-28 eV for the B-DNA target and at 7-11, 12-18 and 18-25 eV for the A-tract DNA target. Though the diffraction depends upon the base-pair sequence, the energy dependent elastic scattering features are primarily associated with the structural water molecules localized within 8-10 Å spheres surrounding the bases and/or the sugar-phosphate backbone.

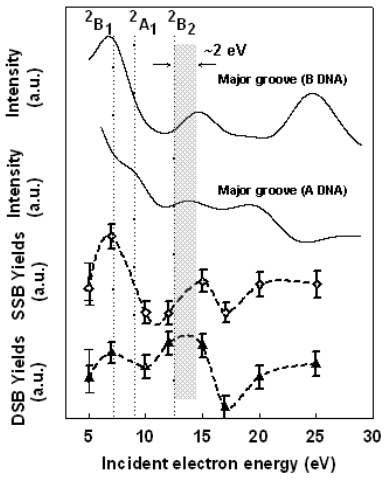

Figure 1. Upper sold lines: Calculated electron intensity at major groove waters for B and A-tract DNA. Experimentally measured single-strand breaks (open diamonds) and double strand breaks (filled circles).

The electron density build-up occurred in energy regimes associated with dissociative electron attachment resonances involving the bases, sugars, phosphate groups and inner shell water. The energy also corresponds to direct electronic excitation and dissociative ionization. As shown above in Figure 1, comparison of our experimental data on the number of single and double strand breaks with the scattering calculation implies that compound H_2O:DNA states may contribute to the energy dependent low-energy electron induced break probability. These resonances are likely to have significant contributions from the perturbed $^2B_1$ and $^2B_2$ DEA states of water.

Project 2. VUV detection of neutral molecules produced during low-energy electron scattering with DNA films.

We have utilized a vacuum ultraviolet (VUV) photon source produced using third-harmonic generation in rare gases to detect the neutral fragments released during the low-energy electron beam induced damage of DNA plasmids physisorbed on graphite substrates. The results generally support the contention that dissociative electron attachment (DEA) resonances localized on DNA sub-units can lead to damage, especially at energies below the ionization threshold. Damage also occurs due to direct dissociative excitation and dissociative ionization.

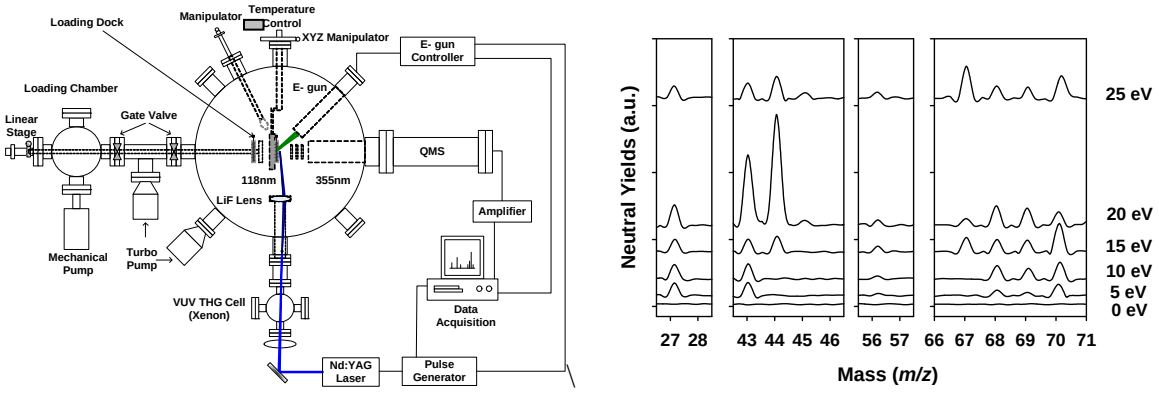

Figure 2. Schematic of the ultrahigh vacuum system constructed for studies of low-energy electron-induced damage of DNA and biologically relevant molecules. The novel aspects of this apparatus involve the Vacuum Ultraviolet (VUV) light source, a cryogenically cooled sample chamber and a liquid dosing capability. The sample transfer stage can be retracted so that ex-situ gel electrophoresis of the DNA deposit can be carried out. The right-hand side of the Figure shows data on VUV detection of the neutral products desorbed from the surface during pulsed electron-irradiation. The incident electron energy is indicated on the right-hand axis.

Most studies of low-energy electron induced damage of DNA concentrate on DEA channels. These are typically examined by monitoring the negative ion desorption products. Though these are very useful studies, complimentary data on the quantum-state distributions of the neutral yields can assist in the assignments of the resonances and primary pathways involved in DNA damage.

Project 3. Coulomb explosions at ice and aqueous surfaces. We have continued our studies of cluster ion production at ice surfaces and have extended these to aqueous

interfaces. Specifically, we have employed a liquid microjet to examine the gas/liquid interface of aqueous salt solutions. Laser excitation at 193 nm produced and removed cations of the form $H^+(H_2O)_n$ and $Na^+(H_2O)_m$ from liquid jet surfaces containing either NaCl, NaBr or NaI. The protonated water cluster yield varied inversely with increasing salt concentration, while the solvated sodium ion cluster yield varied by anion type. The distribution of $H^+(H_2O)_n$ at low salt concentration is identical to that observed from low-energy electron irradiated amorphous ice and the production of these clusters can be accounted for using a localized ionization/Coulomb expulsion model. Production of $Na^+(H_2O)_m$ is not accounted for by this model but required ionization of solvation shell waters and a contact ion/Coulomb expulsion mechanism. The reduced yields of $Na^+(H_2O)_m$ from high concentration (10^{-2} and 10^{-1} M) NaBr and NaI solutions indicate a propensity for Br^- and I^- at the solution surfaces and interfaces.

We have extended these studies of to solutions containing multiply charged ions such as $MgCl_2$. A careful analysis of the spectra shows a similar trend of decreasing protonated water clusters and increasing concentration of cluster ions containing both Mg^+ and $MgOH^+$. The $MgOH^+(H_2O)_m$ and $Mg^+(H_2O)_x$ cluster ions are likely formed when the Coulomb energy generated at the electron depleted surface during laser irradiation surpasses the solvation energy of the magnesium ion. We have also begun to investigate the complexity associated with hydronium ion formation during photoionization of pure water and the controversy surrounding the behavior of the water/vapor interface. Our investigation involves probing the effect of OH^- and H_3O^+ bulk concentrations on the surface enhancement/depletion of photoionization species.

Future Work

The program will continue to focus on the electron interactions with biologically relevant collision partners such as DNA oligomers as well as the building blocks of DNA such as the nucleobases, nucleotides, nucleosides, sugars and phosphates. The program will also continue to focus on how the presence of solvated ions affect scattering resonances and Coulomb processes in the condensed phase. The theoretical work will be extended by using more realistic scattering potentials.

Presentations acknowledging support from this program during 2006-2009

1. T. M. Orlando, "Low-energy Electron-interactions with Complex Biological Targets", American Physical Society, Division of Atomic, Molecular and Optical Physics National meeting, Knoxville, TN, May, 2006.
2. T. M. Orlando, "Low-energy Electron-induced Damage of DNA: The Role of Resonances and Diffraction", Malta, Sept. 15-19, 2006.
3. T. M. Orlando, "Low-energy Electron-induced Damage of DNA: The Role of Resonances and Diffraction", Chemical Physics Symposium Series, California Institute of Technology, Pasadena, CA, Oct. 24, 2006.
4. T. M. Orlando, "Analysis of Organoselenium and Organic Acid Metabolites by Laser Desorption Single Photon Ionization Mass Spectrometry", PITTCON07, Chicago, IL. Feb. 25-Mar. 2, 2007.
5. T. M. Orlando, "Low-Energy Electron Interactions with Hydrated DNA and Complex Biological Interfaces", National American Chemical Society Meeting, Boston, MA August, 2007.
6. T. M. Orlando, "Low-Energy Electron Interactions with Hydrated DNA and Complex Biological Interfaces", Gaseous Electronics Conference, Crystal City, VA, Oct. 2007.
7. T. M. Orlando, "Low-Energy Electron Interactions with Hydrated DNA and Complex Biological Interfaces", Dept. of Physics, Tulane Univ., New Orleans, LA Oct. 30, 2007.

8. T. M. Orlando, "Low-Energy Electron Interactions with Hydrated DNA and Complex Biological Interfaces", Department of Physics, University of Alabama, Al, Jan. 25, 2008.
9. T. M. Orlando, "Probing the interfacial ion composition of low-temperature ice and aqueous salt solution interfaces using Coulomb ejection of cluster ions", Liquid and Solid Aqueous Surfaces and Interfaces Workshop, Telluride, CO, Aug. 10-16, 2008.
10. T. M. Orlando, "Nonthermal Surface Processes and Electron Collisions with Complex Targets", Dept. of Chemistry, University of Alabama, Tuscaloosa, Al, Feb. 3, 2009.
11. T. M. Orlando, "Nonthermal Surface Processes and Electron Collisions with Complex Targets", Dept. of Chemistry, Louisiana State University, Baton Rouge, LA, Feb. 13, 2009.

Publications acknowledging support from this program during 2006-2009

1. Y. Chen, C. Sullards, T. Huang, S. May and T. M. Orlando, "Analysis of Organoselenium and Organic Acid Metabolites by Laser Desorption Single Photon Ionization Mass Spectrometry", *Anal. Chem.* **78** (24), 8386 (2006).
2. D. Oh, M. T. sieger and T. M. Orlando, "Zone Specificity in Low-Energy Electron Stimulated Desorption of Cl^+ from Reconstructed Si(111)-7x7:Cl Surfaces", *Surf. Sci.* **600**, L245-L249 (2006).
3. C. D. Lane, N. G. Petrik, T. M. Orlando and G. A. Kimmel, "Electron-Stimulated Oxidation of Thin Films of Water Adsorbed on TiO_2(110)", *J. Phys. Chem. C*, **111**, 16319 (2007).
4. C. D. Lane, N. G. Petrik, T. M. Orlando and G. A. Kimmel, "Site-Dependent Electron-Stimulated Reactions in Water Films on TiO_2(110)", *J. Chem. Phys.*, **127,** 224706, (2007).
5. Y. Chen, H. Chen, A. Aleksandrov, and T. M. Orlando, "The Roles of Water, Acidity and Surface Morphology on Surface Assisted Laser Desorption", *J. Phys. Chem. C*. **112**, 6953 (2008).
6. G. A. Grieves, N. Petrik, J. Herring-Captain, B. Olanrewaju, A. Aleksandrov, R. G. Tonkyn, S. A. Barlow, G. A. Kimmel, and T. M. Orlando, "Photoionization of Sodium Salt Solutions in a Liquid Jet", *J. Phys. Chem. C.* **112**, 8359, (2008).
7. T. M. Orlando, D. Oh, Y. Chen and A. Aleksandrov, "Low-energy Electron Diffraction and Induced Damage in Hydrated DNA", *J. Chem. Phys.* **128**, 195102 (2008).
8. Y. Chen, A. Aleksandrov and T. M. Orlando, "Probing low-energy electron induced damage of DNA using single-photon ionization mass spectrometry", *Int. J. of Mass Spec. and Ion Physics. Spectr* **277**, 314 (2008).
9. G. A. Grieves, C. D. Lane and T. M. Orlando, "Direct Observation of Intermolecular Coulomb Decay in a Complex Condensed Phase Targets", *Phys. Rev. Lett. (submitted)*.

Energetic Photon and Electron Interactions with Positive Ions

Ronald A. Phaneuf,
Department of Physics /220
University of Nevada
Reno NV 89557-0058
phaneuf@physics.unr.edu

Program Scope

This experimental program investigates photon and electron initiated processes leading to ionization of positively charged atomic and molecular ions. The objective is a quantitative understanding of ionization mechanisms and of the collective dynamic response of bound electrons in atomic and molecular ions to incident EUV photons and electrons. Monoenergetic beams of photons and electrons are merged or crossed with mass/charge analyzed ion beams to probe their internal electronic structure and the dynamics of their interaction. Of particular interest are highly-correlated processes that are manifested as giant dipole resonances in the ionization of atomic ions and also of fullerene ions, whose unique cage structures characterize them as structural intermediates between individual molecules and solids. In addition to precision spectroscopic data for understanding electronic structure and interactions, high-resolution measurements of absolute cross sections for photoionization and electron-impact ionization provide critical benchmarks for testing theoretical approximations such as those used to generate photon opacity databases. Their accuracy is critical to modeling and diagnostics of astrophysical, fusion-energy and laboratory plasmas. Of particular relevance to DOE are those produced by the Z pulsed-power facility at Sandia National Laboratories which is the world's brightest and most efficient x-ray source, and the National Ignition Facility at Lawrence Livermore National Laboratory which is the world's most powerful laser system. Both facilities are dedicated to high-energy-density science and to fusion-energy research.

Recent Progress

The major research thrust has been the application of an ion-photon-beam (IPB) research endstation to experimental studies of photoionization of singly and multiply charged positive ions using monochromatized synchrotron radiation at the Advanced Light Source (ALS). Coupled with the high photon beam intensity and energy resolution available at ALS undulator beamline 10.0, photoion spectroscopy becomes a powerful probe of the internal electronic structure of atomic and molecular ions, permitting tests of sophisticated structure and dynamics computer codes at unprecedented levels of detail and precision. Measurements using the ALS IPB endstation define the state of the art in energy resolution available to studies of photon-ion interactions in the 20 – 300 eV energy range. This program led the development and continues to have primary responsibility for operation of this permanently installed multi-user research endstation.

Due to their large number of atoms, size and hollow cage structure, fullerene molecular ions are of interest as structural intermediates between individual molecules and solids, and exhibit some of the properties of each. As is the case for conducting solids, their large number of valence electrons may be collectively excited in plasmon modes, whereas the excitation of core electrons is localized and of molecular character.

Unusual physical properties of fullerene molecules containing trapped atoms within their hollow carbon cage structures have been predicted by several recent theoretical studies. Phenomena related to resonant interactions of these so-called endohedral fullerenes with EUV light are just beginning to be tested by experiments. A program of photoionization measurements with endohedral fullerene molecular ion beams was initiated with German collaborators from Giessen (A. Müller and S. Schippers) and Dresden (L. Dunsch). The availability of solid samples in milligram quantities permitted proof-of-principle measurements to be made of photoionization of $Sc_3N@C_{80}^+$ and $Ce@C_{82}^+$ with ion beam currents of only a few picoamperes. Both sets of measurements indicated clear signatures of the encaged molecule or atom [5]. Subsequent measurements on $Ce@C_{82}^+$ were successful in quantifying the Ce 4d inner-shell excitation contributions (Figure 1). They suggested a redistribution of the 4d oscillator strength to additional decay channels, and on the basis of accompanying measurements on Ce atomic ions (below), determined the valency of the encaged Ce atom to be +3. A report on this work was published recently in Physical Review Letters [7].

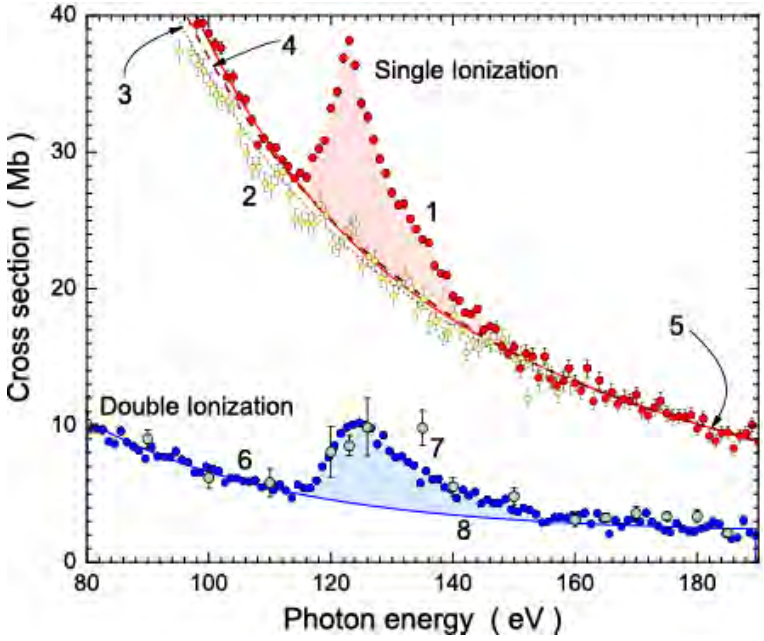

Figure 1. Measured cross sections for single and double photoionization of C_{82}^+ (dashed and solid curves) and $Ce@C_{82}^+$ (solid circles) in the energy range of Ce

- As a reference for the experiments on $Ce@C_{82}^+$, a series of absolute photoionization measurements for atomic ions of the Ce isonuclear sequence (Ce^+ through Ce^{9+}) was completed in the energy range of the 4d giant dipole resonance (110 – 150 eV). The measurements included single, double and triple photoionization of Ce^+, single and double photoionization of Ce^{2+} and Ce^{3+}, and single photoionization of Ce^{4+} – Ce^{9+}. As the initial ion charge state increases, the transition of 4d excitations from continuum to discrete final 4f states is evident in the measured widths and shapes of the resonance features. This investigation and the measurements on $Ce@C_{82}^+$ constituted the Ph.D. dissertation research of M. Habibi [9], and the results on the Ce sequence have been submitted to Physical Review A for publication [10].

- As part of the Ph.D. dissertation research of D. Esteves, an investigation of the n-dependence of photoionization cross sections of fullerene ions C_n^+ in the range $30 < n < 90$ was initiated. The objective was to explore the effects of size, symmetry and shape of the fullerene cage on the strengths and widths of the collective plasmon modes.

Future Plans

The emphasis of future research will be photoionization and photofragmentation of fullerene molecular ions, and of so-called endohedral fullerene ions, which contain an atom or molecule trapped within their closed carbon cages. The latter enable studies of the structure and dynamics of atoms under unique boundary conditions, i.e. of an atom confined within a charged spherical shell. A giant resonance near 22 eV results from the collective photoexcitation of a surface plasmon oscillation of the several hundred electrons in the valence electron shells of fullerene molecules and molecular ions, which also exhibit a volume plasmon resonance centered at 38 eV. Decay of these collective excitations is manifested in photoionization of both empty and endohedral fullerene ions, and also in photofragmentation.

- The *in situ* production of an endohedral fullerene ion beam was demonstrated recently at ALS by passing a 6.22 keV C_{60}^+ ion beam through a gas cell containing Ne, yielding a mass-analyzed beam of 6.0 keV $Ne@C_{60}^+$. These developments set the stage for proposed photoionization measurements with endohedral fullerene ions $A@C_{60}^+$ (A = He, Ne, Ar, Kr, Xe). These experiments will probe the influence of the carbon cage on atomic and molecular resonances associated with the caged atom or molecule, as well as the influence of a caged atom or molecule on the properties of collective plasmon oscillations of the valence-shell electrons of the fullerene molecular ion. Topics of investigation will be theoretically predicted shifts of oscillator strength between the carbon cage and the caged atom due to confinement resonances and the interaction of atomic photoelectrons with the polarized fullerene cage. Other predictions to be explored are so-called *giant endohedral resonances* in the outer-shell photoionization of caged noble gas atoms, and a splitting of the giant Xe 4d resonance in $Xe@C_{60}$ into multiple components due to interference effects.

- Systematic studies are proposed of the relaxation of plasmon oscillations in C_{60}^+ by ejection of an electron, resulting in photoionization, and also by fragmentation, releasing pairs of carbon atoms. Measurements of relative oscillator strengths associated with the surface and volume plasmon oscillations as functions of the number n of carbon atoms comprising the fullerene molecular ion C_n^+ are proposed over the range $30 < n < 90$. The objective of this study is to explore the effects of symmetry and shape of the fullerene cage on the strengths and widths of the collective plasmon modes. This investigation will constitute part of the Ph.D. dissertation research of D. Esteves.

- In selected cases where indicated by the results, the photoionization and photofragmentation measurements conducted at ALS will be complemented by measurements of electron-impact ionization and fragmentation at UNR. Both the fullerene molecular ions and ions of caged species are prime candidates for such

investigations. The UNR facility provides valuable hands-on experience with ion beams to students as well as opportunities for off-line development and testing.

References to Publications of DOE-Sponsored Research (2007-2009)

1. *Photoionization and electron-impact ionization of Ar^{5+},* Jing Cheng Wang, M. Lu, D. Esteves, M. Habibi, G. Alna'Washi, R.A. Phaneuf and A.L.D. Kilcoyne, Phys. Rev. A 75, 062712 (2007).
2. *Colliding-beams Experiments for Studying Fundamental Atomic Processes,* 13th International Conference on the Physics of Highly Charged Ions, Belfast, Northern Ireland, August 28, 2006; J. Phys. Conf. Ser. 58, 1 (2007).
3. *Photoionization of Cl-like K^{2+} and Ca^{3+},* Ghassan Alna'Washi, Ph.D. Dissertation, University of Nevada, Reno (2007)
4. *Reply to Comment on photoexcitation of a volume plasmon in C_{60} ions,* S.W.J. Scully, E.D. Emmons, M.F. Gharaibeh, R.A. Phaneuf, A.L.D. Kilcoyne, A.S. Schlachter, S. Schippers, A. Müller, H.S. Chakraborty, M.E. Madjet and J.M. Rost, Phys. Rev. Lett. 98, 179602 (2007).
5. *Photoionization of the endohedral fullerene ions $Sc_3N@C_{80}^+$ and $Ce@C_{82}^+$ by synchrotron radiation,* A. Müller, S. Schippers, R.A. Phaneuf, M. Habibi, D. Esteves, J.C. Wang, A.L.D. Kilcoyne, A. Aguilar, S. Yang and L. Dunsch, XXV International Conference on Photonic, Electronic and Atomic Collisions, Freiburg, Germany, July 25-31, 2007; J. Phys. Conf. Ser. 88, 02138 (2007).
6. *Colliding-beams Experiments for Studying Fundamental Atomic Processes,* 13th International Conference on the Physics of Highly Charged Ions, Belfast, Northern Ireland, August 28, 2006; J. Phys. Conf. Ser. 58, 1 (2007).
7. *Significant redistribution of Ce 4d oscillator strength observed in photoionization of endohedral $Ce@C_{82}^+$ ions,* A. Müller, S. Schippers, M. Habibi, D. Esteves, J.C. Wang, R.A. Phaneuf, A.L.D. Kilcoyne, A. Aguilar and L. Dunsch, Phys. Rev. Lett. 101, 133001 (2008).
8. *Plasmons in Fullerene Molecules,* R.A. Phaneuf, chapter in "Handbook of Nanophysics," K. Sattler ed. (submitted March, 2009; Taylor & Francis, in press).
9. *Photoionization of the cerium isonuclear sequence and cerium endohedral fullerene*, M. Habibi, Ph.D. Dissertation, University of Nevada, May, 2009.
10. *Photoionization cross sections for the isonuclear sequence of cerium ions,* M. Habibi, D.A. Esteves, R.A. Phaneuf, A.L. D. Kilcoyne, A. Aguilar and C. Cisneros, Phys. Rev. A (submitted June, 2009).
11. *K-shell photoionization of ground-state Li-like carbon ions [C^{3+}]: experiment, theory and comparison with time-reversed photorecombination* A. Müller, S. Schippers, R.A. Phaneuf, S.W.J. Scully, A. Aguilar, I Alvarez, C. Cisneros, E.D. Emmons, M.F. Gharaibeh, G. Hinojosa, A.S. Schlachter and B.M. McLaughlin, J. Phys. B (submitted June, 2009).

Resonant and Nonresonant Photoelectron-Vibrational Coupling

Erwin Poliakoff, Department of Chemistry, Louisiana State University, Baton Rouge, LA 70803, epoliak@lsu.edu

Robert R. Lucchese, Department of Chemistry, Texas A&M University, College Station, TX, 77843, lucchese@mail.chem.tamu.edu

Program Scope

We investigate how photoelectrons exiting from molecular systems interact with vibrational degrees of freedom. Both resonant and nonresonant photoionization phenomena are studied for systems ranging from diatomics to large polyatomics. High resolution gas-phase photoelectron spectroscopy at the Advanced Light Source generate experimental data, and we employ frozen-core Hartree-Fock single-center expansion calculations to provide a theoretical foundation. The goal is to understand how photoelectrons traverse anisotropic molecular frameworks and exchange energy with vibrations. This research benefits the Department of Energy because the results elucidate structure/spectra correlations that will be indispensable for probing complex and disordered systems of DOE interest such as clusters, catalysts, reactive intermediates, transient species, and related species.

Recent Progress

One normally assumes that vibrational and photoelectron motion are decoupled, which leads to the Franck-Condon approximation. There are two salient predictions of the Franck-Condon principle for our present purposes: (1) vibrational branching ratios – i.e., relative rates of production of alternative vibrational levels within an electronic manifold – are independent of photon energy, and (2) single quantum excitations of nontotally symmetric modes are identically zero. Nonresonant and resonant processes can result in coupling molecular vibration and photo electron motion, with the result that vibrational branching ratios become dependent on photon energy, and that forbidden vibrations can be excited. However, almost all of the previous work that has been performed on this topic has focused on extremely simple systems (e.g., diatomics), or highly symmetrical systems. We are currently extending these studies to more complex asymmetric systems. We have studied a number of systems, and there are different classes of Franck-Condon breakdown. For example, one case is when the geometry dependence of the transition amplitude is large because there is a resonance whose energy and or width is sensitive to the value of the coordinate, q. Another instance of deviation from the Frank-Condon approximation occurs when one of the larger transition matrix elements contributing to a process has a zero as a function of energy, i.e., when there is a Cooper minimum, and when the location of the Cooper minimum varies with q. Finally, there can be other q dependent variations of the cross section with energy at high photon energy that can also lead to deviations from the Franck-Condon approximation. Some recent examples of systems we have studied with these different Franck-Condon breakdown modes are considered here.

Branching ratios in the $(8\sigma)^{-1}$ ionization of OCS: A resonant case

It is instructive to consider Franck-Condon breakdown for a relatively simple asymmetric system. This helps to illuminate the new scientific insights that might emerge as we shift to the more complex targets. Figure 1 shows theoretical cross section curves for such a system, OCS.

Note that the cross section curves change dramatically with vibrational coordinate ν_3 (primarily the C–O stretch), but not ν_1 (C–S stretch).

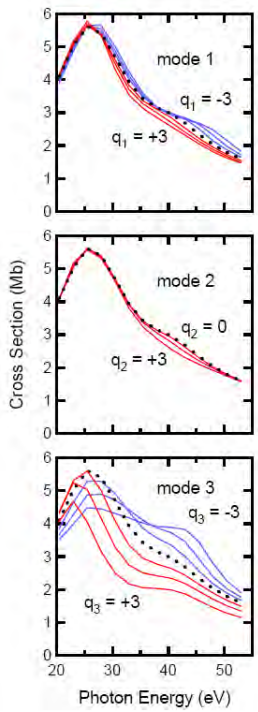

Figure 1. Calculated cross-section curves for the molecule in the equilibrium vs. distorted geometries for all three normal coordinates. These curves were averaged over all orientations of the molecule relative to the incident light.

Modes 1 and 3 and are primarily the C–S and C–O stretches, respectively. (ν_2 is the bending coordinate.) Note the strong dependence of resonance behavior on the C–O bond length (bottom frame), but not on the C–S distance (top frame). This is a simple example showing how the resonant quasi-binding of the photoelectron can have localized effects, and illustrates the rationale of probing asymmetric systems.

Experimental results were also obtained for OCS, and they agree with the predictions of theory. The key point is that the results shown in Fig. 1 for OCS demonstrate that photoelectron-vibrational coupling *can* be site-specific in polyatomic molecules. On the other hand, our recent results on C_6F_6 show that this is not always the case. In the C_6F_6 case, we showed that the photoelectron becomes quasi-bound as a particle in a delocalized cylindrical well. These contrasting results suggest that it would be useful to study asymmetric targets that will allow tests of how vibrational motions couple to photoelectron motion. More complex molecules provide additional vibrational degrees of freedom, and in this spirit, we suggest that DNA and RNA bases are excellent candidates for such studies. These candidates have the added benefit of being relevant to DNA damage.

Nonresonant coupling in ICN: Initial state effects

While the previous example of OCS photoionization shows that it is useful to focus on resonant processes, it is also true – though much less obvious – that it is necessary to consider nonresonant coupling mechanisms. To illustrate this point consider some very recent unpublished data acquired at the HiRAMES (Scienta) apparatus at beamline 10.0.1 on ICN photoionization. In this study, we found that charge transfer from the iodine atom to the CN moiety was strongly coupled to the C–N bond length. Thus, the initial state wavefunction electronic structure is influenced by C–N vibration, thereby leading to an electronic dipole matrix element that depends primarily on this specific vibration. The result is photoelectron-vibrational coupling, and the spectral extent of this Franck-Condon breakdown is very large. Moreover, the qualitative basis for the Franck-Condon breakdown is different than that presented

for OCS. The experimental data and theoretical results are shown below in Fig. 2, and the agreement is very good.

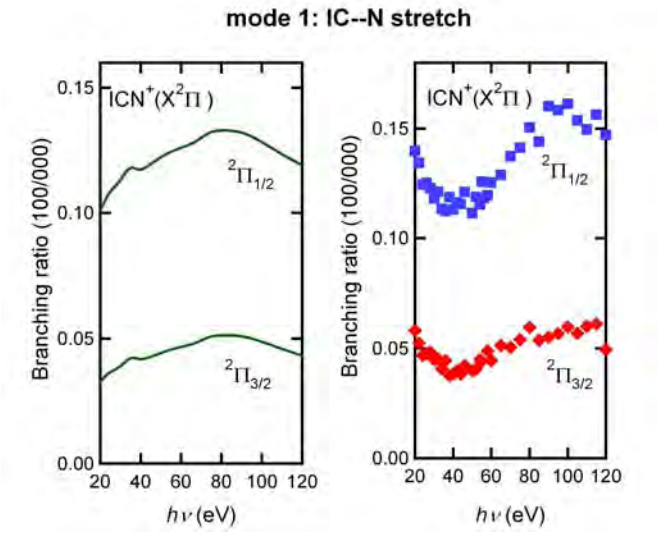

Figure 2. Vibrational branching ratio for $ICN^+(X^2\Pi)$ over a very large energy range. Left hand frame is theory, and right hand frame shows data acquired via photoelectron spectroscopy at the ALS. The different curves correspond to alternative spin-orbit components. Note the wide range of energy spanned by the excursion in the branching ratio (i.e., >60 eV).

The mechanism for the wide-range Franck-Condon breakdown observed for ICN is surprising. It arises from charge transfer between the I-atom and the C–N moiety that is mediated by the C–N bond length. In other words, the initial state wavefunction is changing significantly with C–N distance, and this is verified by examining the cross section for selected high partial waves, as illustrated in Fig. 3.

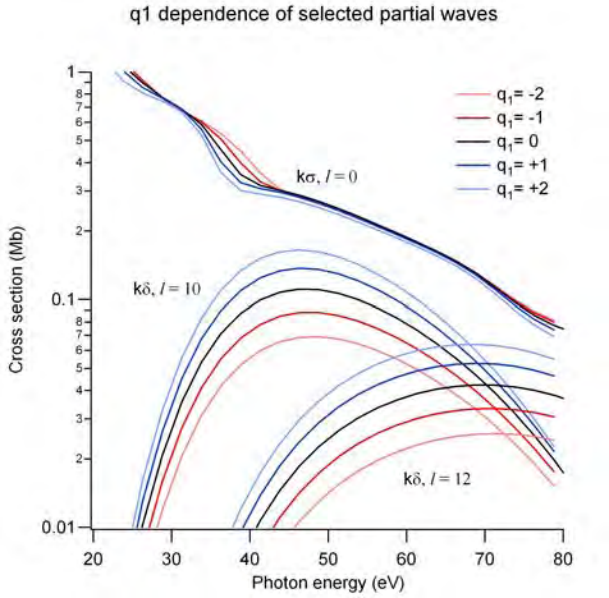

Figure 3. Cross section curves for selected partial waves leading to the production of the $ICN^+(X^2\Pi)$ state.The $k\sigma$ l=0 wave provides a large contribution at low energies, and high very high partial waves in the $k\delta$ channel, e.g., l=10,12, arise primarily from ejection from the I-atom and have an increasing contribution at higher energies. Each of the family of curves shown corresponds to 5 different configurations along the ν_1 vibrational coordinate, q_1. Reduced coordinates are used, and q_1=1 corresponds to the classical turning point in the ground state. Notice that the contributions of the high partial waves depend strongly on the q_1 coordinate (primarily the C-N stretch), and theory shows that this results from the charge transfer from the I-atom to the C-N moiety as the C-N bond length is changed.

Symmetry breaking for degenerate vibrational modes in BF_3

For resonant processes, degenerate vibrational modes are often affected by the trapped photoelectron. We have developed the proper computational framework to treat symmetry

breaking (degenerate) vibrations for such systems, and have recently applied this theory to BF_3. The agreement with experiment is very good, and we will apply these methods will to analogous systems such as C_6F_6, CF_4, and SiF_4.

Future plans

Both the OCS and ICN examples presented above show the utility of probing asymmetric systems. Now that we have demonstrated progress with a simple system, we intend to move on to more complex asymmetric targets, including DNA and RNA bases. We also will use the computational insights generated in the recent BF_3 studies to analyze degenerate symmetry-breaking vibrations for related systems, such as C_6F_6, CF_4, and SiF_4.

References

It the last three years, the following papers have been published based on our DOE funded research, and several more are currently in preparation.

[1] A. Das, E. D. Poliakoff, R. R. Lucchese, and J. D. Bozek, "Launching a particle on a ring: $b_{2u} \rightarrow ke_{2g}$ ionization of C_6F_6," *J. Chem. Phys.* **125**, 164316:1-5 (2006).

[2] E. D. Poliakoff and R. R. Lucchese, "Evolution of photoelectron-vibrational coupling with molecular complexity," *Phys.Scr.* **74**, C71-C79 (2006).

[3] R. Montuoro, R. R. Lucchese, J. D. Bozek, A. Das, and E. D. Poliakoff, "Quasibound continuum states in SiF_4 $\tilde{D}\ ^2A_1$ photoionization: Photoelectron-vibrational coupling," *J. Chem. Phys.* **126**, 244309:1-9 (2007).

[4] A. Das, J. S. Miller, E. D. Poliakoff, R. R. Lucchese, J. Bozek, "Vibrationally resolved photoionization dynamics of CF_4 in the $D\ ^2A_1$ state," *J. Chem. Phys.* **127**, 044312:1-6 (2007).

[5] R. R. Lucchese, J. Söderström, T. Tanaka, M. Hoshino, M. Kitajima, H. Tanaka, A. De Fanis, J.-E. Rubensson, and K. Ueda, "Vibrationally resolved partial cross sections and asymmetry parameters for nitrogen K-shell photoionization of the N_2O molecule," *Phys. Rev. A* **76**, 012506:1-8 (2007).

[6] M. Hoshino, R. Montuoro, R. R. Lucchese, A. De Fanis, U. Hergenhahn, G. Prümper, T. Tanaka, and K. Ueda, "Vibrationally resolved partial cross sections and asymmetry parameters for nitrogen K-shell photoionization of the NO molecule," *J. Phys. B* **41**, 085105:1-7(2008).

[7] G. Prümper, D. Rolles, H. Fukuzawa, X. J. Liu, Z. Pešić, I. Dumitriu, R. R. Lucchese, K. Ueda, and N. Berrah, Measurements of molecular-frame Auger electron angular distributions at the CO C $1s^{-1}$ $2\pi^*$ resonance with high energy resolution, *J. Phys. B* **41**, 215101:1-11 (2008).

[8] Anh-Thu Le, R. R. Lucchese, M. T. Lee, C. D. Lin, Probing molecular frame photoionization via laser generated high-order harmonics from aligned molecules, *Phys. Rev. Lett.* **102**, 203001:1-4 (2009).

[9] Anh-Thu Le, R. R. Lucchese, S. Tonzani, T. Morishita, C. D. Lin, Quantitative rescattering theory for high-order harmonic generation from molecules, *Phys. Rev. A* **80**, 013401:1-23 (2009).

[10] A. Das, E.D. Poliakoff, R.R. Lucchese, and J.D. Bozek, *Mode-specific photoionization dynamics of a simple asymmetric target: OCS*, J. Chem. Phys. **130**, 044302 (2009).

[11] A. Das, J.S. Miller, E.D. Poliakoff, R.R. Lucchese, and J.D. Bozek, *Vibrational Branching Ratios in the $(b_{2u})^{-1}$ Photoionization of C_6F_6*, J. Chem. Phys. (in press).

Control of Molecular Dynamics: Algorithms for Design and Implementation

Herschel Rabitz and Tak-San Ho, Princeton University
Frick Laboratory, Princeton, NJ 08540, hrabitz@princeton.edu, tsho@princeton.edu

A. Program Scope

This research is concerned with the conceptual and algorithmic developments addressing control over quantum dynamics phenomena. The research is theoretical and computational in nature, with a particular focus towards exploring basic principles of importance for laboratory studies, especially in conjunction with the use of optimal control theory and its realization in closed-loop learning experiments. This research program involves a set of interrelated components aiming at developing a deeper understanding of quantum control and providing new algorithms to extend the laboratory control capabilities.

B. Research Progress

In the past year several projects were pursued and the results are summarized below.

1. **Quantum optimal control of isomerization dynamics of a one-dimensional reaction-path model dominated by a competing dissociation channel [1]** We have carried out quantum wave packet optimal control simulations with intense laser pulses for studying molecular isomerization dynamics of a one-dimensional reaction-path model involving a dominant competing dissociation channel. The intrinsic reaction coordinate model mimics the ozone open-to-cyclic ring isomerization along the minimum energy path that successively connects the ozone cyclic ring minimum, the transition state, the global minimum, and the dissociative asymptote on the ozone ground-state potential energy surface. The molecular orientation of the modeled ozone was held constant with respect to the laser-field polarization and several optimal fields were found that all produce nearly perfect isomerization. The optimal control fields were characterized by distinctive high temporal peaks as well as low frequency components, thereby enabling abrupt transfer of the time-dependent wave packet over the transition state from the open minimum to the targeted ring minimum. We also showed that it is possible to obtain weaker optimal laser fields when a reduced level of isomerization is satisfactory.
2. **Landscape of unitary transformations in controlled quantum dynamics[2]** We have considered the control problem of generating unitary transformations, which is especially relevant to current research in quantum information processing and computing. An analysis of optimal control landscapes for unitary transformations has been made from a dynamical perspective in the infinite-dimensional function space of the time-dependent external field. The underlying dynamical landscape has been defined as the Frobenius square

norm of the difference between the control unitary matrix and the target matrix. A nonsingular adaptation matrix was introduced to provide additional freedom for exploring and manipulating key features, specifically the slope and curvature, of the control landscapes. The dynamical analysis reveals many essential geometric features of optimal control landscapes for unitary transformations, including bounds on the local landscape slope and curvature. Close examination of the curvatures at the critical points shows that the unitary transformation control landscapes are free of local traps and proper choices of the adaptation matrix may facilitate the search for optimal control fields producing desired unitary transformations.

3. **Topology of the quantum control landscape for observables[3]** We have made a detailed analysis of the critical topology of the quantum control landscape for observables. The optimization of the expectation value of an observable can be viewed as a directed search over a quantum control landscape. The attainment of the global extrema of this landscape is the goal of quantum control. Local optima will generally exist, and their enumeration is shown to scale factorially with the systems effective Hilbert space dimension. We have found that a Hessian analysis reveals that these local optima have saddlepoint topology and cannot behave as suboptimal extrema traps. The implications of the landscape topology for practical quantum control efforts are discussed, including in the context of nonideal operating conditions.
4. **Laser-pulse photoassociation in a thermal gas of atoms[4,5]** We have presented a nonperturbative treatment for laser-pulse-driven formation of heteronuclear diatomic molecules in a thermal gas of atoms. Based on the assumption of full controllability, the maximum possible photoassociation yield has been obtained. A one-dimensional model was used for calculating the photoassociation probability as a function of the laser parameters as well as for different temperatures. The dependence of the photoassociation yield on the laser frequency and amplitude reveals complex patterns of one- and multiphoton transitions. The photoassociation yield induced by subpicosecond pulses of a priori fixed shape is very low compared to the maximum possible yield.
5. **On the diversity of multiple optimal controls for quantum systems[6]** We have presented simulations of optimal field-free molecular alignment and rotational population transfer, optimized by means of laser pulse shaping guided by evolutionary algorithms. Qualitatively different solutions have been obtained that optimize the alignment and population transfer efficiency to the maximum extent that is possible given the existing constraints on the optimization due to the finite bandwidth and energy of the laser pulse, the finite degrees of freedom in the laser pulse shaping and the evolutionary algorithm employed. The effect of these constraints on the optimization process was discussed at several levels, subject to theoretical as well as experimental considerations. We showed that optimized alignment yields can reach extremely high values, even with severe constraints being present. A correlation was found between the diversity of solutions and the difficulty of the problem. In the pulse shapes that optimize dynamic alignment we have observed a transition between pulse

sequences that maximize the initial population transfer from J = 0 to J = 2 and pulse sequences that optimize the transfer to higher rotational levels.

6. **Incoherent control of locally controllable quantum systems[7]** We have proposed an incoherent control scheme for state control of locally controllable quantum systems. This scheme includes three steps: The first step increases the amplitudes of some desired eigenstates and the corresponding probability of observing these eigenstates, the second step projects, with high probability, the amplified state into a desired eigenstate, and the last step steers this eigenstate into the target state.Within this scheme, two control algorithms are presented for two classes of quantum systems. As an example, the incoherent control scheme was applied to the control of a hydrogen atom by an external field. The results support the suggestion that projective measurements can serve as an effective control and local controllability information can be used to design control laws for quantum systems. Thus, this scheme establishes a subtle connection between control design and controllability analysis of quantum systems and provides an effective engineering approach in controlling quantum systems with partial controllability information.

7. **Principles for determining mechanistic pathways from observable quantum control data[8]** We have used Hamiltonian encoding (HE) methods to understand mechanism in computational studies of laser controlled quantum systems. This work studied the principles for extending such methods to extract control mechanisms from laboratory data. In an experimental setting, observables replace the utilization of wavefunctions in computational HE. With laboratory data, HE gives rise to a set of quadratic equations for the interfering transition amplitudes, and the solution to the equations reveals the mechanistic pathways. The extraction of the mechanism from the system of quadratic equations raises questions of uniqueness and solvability, even in the ideal case without noise. Symmetries were shown to exist in the quadratic system of equations, which is generally overdetermined. Therefore, the mechanism is likely to be unique up to these symmetries. Numerical simulations demonstrated the concepts on simple model systems.

8. **Natural variables for controlling quantum dynamics[9]** We have explored the local geometry of the landscape in state-to-state transitions in the context of natural control variables for the implications upon practical searches for optimal controls. The gradient of the landscape with respect to the control field was shown to always lie in a low-dimensional subspace spanned by basis functions bearing specific knowledge of the system physics, thereby comprising a natural set of variables for the particular optimal control application. The enumeration of these basis functions provides an upper bound on the required number of properly identified control variables. We have suggested a specific experimental protocol to utilize the geometric structure of the landscape for identifying a reduced set of control variables for practical laboratory implementation. Simulations on simple systems were used to illustrate the characteristics of the natural control variables and the prospective experimental protocol.

C. Future Plans

The research in the coming year will mainly focus on the development of efficient, robust machineries for computing desired control fields, aimed at performing large-scale quantum control simulations for atomic and molecular dynamics of current interest. Specifically, we plan to formulate fast iterative schemes for computing high quality control fields from an inverse control problem perspective, with the goal of developing efficient and robust algorithms that are monotonically convergent. In parallel to the algorithmic development, we also plan to study various atomic and molecular dynamics control problems, including laser controlled photo-association processes of atoms in thermal gases and laser controlled isomerization dynamics of the formaldehyde and the corresponding trans- and cis-hydroxycarbene isomers.

D. References

1. Quantum optimal control of isomerization dynamics of a one-dimensional reaction-path model dominated by a competing dissociation channel, Yuzuru Kurosakia, Maxim Artamonov, Tak-San Ho, and Herschel Rabitz, J. Chem. Phys.,(2009), in press.

2. Landscape of unitary transformations in controlled quantum dynamics, T.-S. Ho, J. Dominy, and H. Rabitz, Phys. Rev. A **79**, 013422 (2009).

3. Topology of the quantum control landscape for observables M. Hsieh, R. Wu, and H. Rabitz, J. Chem. Phys. **130**, 104109 (2009).

4. Laser-pulse photoassociation in a thermal gas of atoms, E. F. de Lima, T.-S. Ho, and H. Rabitz, Phys. Rev. A **78**, 063417 (2008).

5. Solution of the Schrodinger equation for the Morse potential with an infinite barrier at long range, E. F. de Lima, T.-S. Ho, and H. Rabitz, J. Phys. A-Math. Theo. **41**, 335303 (2008).

6. On the diversity of multiple optimal controls for quantum systems O M Shir, V Beltrani, Th Back, H Rabitz and M J J Vrakking J. Phys. B: At. Mol. Opt. Phys. **41**, 074021 (2008)

7. Incoherent control of locally controllable quantum systems Daoyi Dong, Chenbin Zhang, Herschel Rabitz, Alexander Pechen, and Tzyh-Jong Tarn, J. Chem. Phys. **129**,154103 (2008).

8. Principles for determining mechanistic pathways from observable quantum control data Richard Sharp Abhra Mitra Herschel Rabitz J. Math. Chem., **44**, 142171 (2008)

9. Natural variables for controlling quantum dynamics Michael Hsieh, Tak-San Ho, Herschel Rabitz Chem. Phys. **352**, 77-84 (2008).

Dual Quantum Gases of Bosons: From Atomic Mixtures to Heteronuclear Molecules

Principal Investigator:

Dr. Chandra Raman
Assistant Professor
School of Physics
Georgia Institute of Technology Atlanta, GA 30332-0430
craman@gatech.edu

Program:

This program centers on creating a dual species atomic Bose-Einstein condensate of ^{23}Na and ^{87}Rb. The eventual goal is to synthesize heteronuclear molecules of the two species. Our approach takes advantage of the large trapped atom number technology available for Na atoms using a Zeeman slower and a dark MOT to sympathetically cool a relatively smaller sample of Rb. Molecules will be created in the vicinity of a Feshbach resonance (see PRA 72, 062505 (2005) for some recent predictions). A future thrust of the molecular effort will be to create a dipolar superfluid, a novel strongly correlated quantum system.

Work completed to date:

- **New apparatus.** A new atomic beam apparatus for the study of trapped ultracold sodium-rubidium mixtures has come online. The machine incorporates a single atomic beam containing both species Na and Rb, dual species Zeeman slowing magnets and a quartz vacuum cell in ultra-high vacuum conditions for good optical access to the two species. In addition, we have implemented a new magnetic trap with separate coils that will allow us to search for Feshbach resonances at magnetic bias fields up to 1 kiloGauss.

- **Dual species magnetic trapping and sympathetic cooling.** We have achieved the first magnetic trapping of Na-Rb atomic mixtures. In addition we have observed the first evidence of sympathetic cooling of Rb by Na. Experiments are ongoing to reduce the Na temperature by microwave evaporation and increase the phase space density.

"Coherent and Incoherent Transitions"

F. Robicheaux
Auburn University, Department of Physics, 206 Allison Lab, Auburn AL 36849
(robicfj@auburn.edu)

Program Scope

This theory project focuses on the time evolution of systems subjected to either coherent or incoherent interactions. This study is divided into three categories: (1) coherent evolution of highly excited quantum states, (2) incoherent evolution of highly excited quantum states, and (3) the interplay between ultra-cold plasmas and Rydberg atoms. Some of the techniques we developed have been used to study collision processes in ions, atoms and molecules. In particular, we have studied the correlation between two (or more) continuum electrons.

Recent Progress 2008-2009

Photon-atom processes in strong magnetic fields: We studied how the radiative recombination changes in a strong magnetic field and how the spin of an electron during a radiative cascade is modified in a strong B-field.[12] The only previous studies of RR in a strong magnetic field relied on classical estimates. We found that this process is equivalent to the radiative decay rate from positive energy states of a confined atom. Using this formulation, we studied the temperature and magnetic field dependence of RR. We found that the rate was changed only if the energy spacing of the Landau levels was larger than k_BT. When this condition is satisfied, the rate tends to increase with increasing magnetic field strength. The enhancement was mainly for recombination into Rydberg states; unlike the B=0 situation, most of the recombination was into weakly bound states. We also found that the magnetic field had a substantial effect on the spin of the electron during the radiative cascade but only for states where the spin-orbit interaction is large enough to compete with the Zeeman splitting.

Fluorescence as a probe of Ultracold plasmas: In a joint study with Bergeson's experimental group, we studied the fluorescence from an ultracold plasma.[11] The experiment was able to measure the time dependence of light emitted by the plasma. This gives a probe of the time dependence of the atom distribution because the light was from deeply bound states which can only be reached after three body recombination and several collisions between free electrons and Rydberg atoms. We found that a peculiarity of the Ca spectrum (a perturbation in the 4snd series) allowed a probe of weakly bound states as well. We were able to use this to study how the three body recombination develops on time scales less than 1 microsecond. For the lowest temperatures studied, we found a different scaling of the recombination rate with density: the fluorescence rate scaled as density^2 instead of the predicted density^3.

Transitions through a chaotic sea: A recent experiment by T. Gallagher's group showed that it is possible to drive a 10 photon transition in Rydberg states without any of the intermediate photons being resonant. We performed classical and quantum calculations of this system to understand how this process works.[16]

Gallagher explained their results as arising from a sequence of avoided crossings. Our quantum calculations were able to reproduce the measurements. Surprisingly, the classical calculations also could reproduce the measurements. The classical mechanism for the transition was an expansion of the chaotic sea to encompass the starting region of phase space; the surprise was that this mechanism could deliver the electron to a small range of n-states which is possible due to the stickiness of the edge the chaotic regions. Also, we found that the development of the angular momenta strongly depended on the duration of the pulse.

Correlation in electron ejection: In a joint study with an experimental project led by A. Landers, we studied the interaction between a pair of electrons ejected from a Ne atom.[18] In this study, a photon is absorbed by a 1s electron giving a free electron with excess energy of order 1 eV. An Auger process occurs a short time later which gives an outgoing electron with approximately 800 eV. We performed a classical Monte Carlo simulation of this process and were able to successfully describe the energy shift of the slow electron due to the Auger process. Also, we could qualitatively reproduce the angular distribution of the ejected electrons, including a lack of electrons going out in the same direction. However, there was a clear feature in the calculation when the electrons have nearly the same outgoing angle that was not present in the experiment. This feature seems to indicate an unexpected (and currently unexplained) correlation in the ejection angle of the two electrons.

Molecules: Some of the techniques we developed for highly excited atoms can be used to investigate processes in molecules. In Ref. [13], we extended the time dependent close coupling method to compute the electron impact ionization of molecules beyond H_2 and obtained results for Li_2 and Li_2^+; this method utilizes a direct time dependent solution of the Schrodinger equation with an incoming electron packet scattering from the molecule. In Ref. [14], we investigated the electron impact ionization of H_2 molecules by computing the differential cross section using the time dependent close coupling method. In particular, we investigated how the orientation of the molecule affects the dependence of the cross section on the angle between the outgoing electrons. New features in the cross sections were found compared with the case where the molecular orientation is averaged.

Three electron continua: Over the past decade we have performed many calculations of processes involving two electron escape from an atom/ion. We directly solve the time dependent Schrodinger equation on a lattice to obtain the relevant wave function. We recently extended the calculations to three electrons escaping an atom, but the method was restricted in energy. By extending this technique, we were able to compute the electron impact double ionization of He for energies up to and beyond the peak of the cross section.[8] During the past year, we extended the method to compute the energy and angle differential cross sections in electron impact double ionization of He.[15] At 106 eV incident energy, the pentuple energy and differential cross sections were in reasonable agreement with experiments.

Attosecond double ionization: We investigated the energy and angle differential probabilities for 2-photon double ionization of He.[17] We used our time dependent

close coupling program to compute how the chirp of the attosecond pulse affected the cross sections. We found interesting effects from the chirp when the energy band width of the pulse becomes comparable to the difference in ionization thresholds of the neutral and positive ion. Different sign of the chirp can produce qualitatively different effects. As an example, the magnitudes and locations of the sequential peaks in the single electron energy distribution varied strongly with the chirp.

Finally, this program has several projects that are strongly numerical but only require knowledge of classical mechanics. This combination is ideal for starting undergraduates on publication quality research. Since 2004, nine undergraduates have participated in this program. Most of these students have completed projects published in peer reviewed journals. One of these students, Michael Wall, was one of 5 undergraduates invited to give a talk on their research at the undergraduate session of the DAMOP 2006 meeting. Two new undergraduates will be hired into the group at the beginning of the Fall 2009 semester and I expect they will continue the successful tradition of undergraduate research.

Future Plans

Transitions through a chaotic sea: Our recent results[16] showing how to transport a system around a classical island has opened the door to studies of interesting systems. We plan to complete investigations into at least two other atomic or molecular systems. There are several promising options: the kicked Hydrogen atom, vibrational transitions in diatomic molecules, the kicked rotor, etc

Ultra-cold plasmas The recent collaboration with Bergeson's group[11] has raised some interesting questions about the early time evolution of ultracold plasmas. In particular, we plan to study the evolution of the components of the plasmas at very early times. In particular, we will study the scattering of electrons and ions from Rydberg atoms. This involves the investigation of how low energy electrons scatter in the presence of ions.

Anti-hydrogen motivated calculations The next generation experiments are aimed at trapping the anti-hydrogen atom. To address possible issues, we will investigate processes that arise from this goal. In particular, we plan to study the three body recombination rate when all of the particles have the same mass.

Coherent evolution Motivated by the collaboration with Landers,[18] we will devote substantial time to the interaction between two free electrons or the interaction between a free electron and a Rydberg atom. This was the most speculative aspect of the proposal and the last major component of the original proposal that hasn't been investigated.

DOE Supported Publications (7/2006-7/2009)

[1] C.L. Taylor, Jingjing Zhang, and F. Robicheaux, J. Phys. B **39**, 4945 (2006).
[2] T. Topcu, M.S. Pindzola, C.P. Balance, D.C. Griffin, and F. Robicheaux, Phys. Rev. A **74**, 062708 (2006).
[3] F. Robicheaux, J. Phys. B **40**, 271 (2007).

[4] M.S. Pindzola, F. Robicheaux, S.D. Loch, J.C. Berengut, T. Topcu, J. Colgan, M. Foster, D.C. Griffin, C.P. Balance, D.R. Schultz, T. Minami, N.R. Badnell, M.C. Witthoeft, D.R. Plante, D. M. Mitnik, J.A. Ludlow, and U. Kleiman, J. Phys. B **40**, R39 (2007).
[5] J. Colgan, M.S. Pindzola, and F. Robicheaux, Phys. Rev. Lett. **98**, 153001 (2007).
[6] T. Topcu and F. Robicheaux, J. Phys. B **40**, 1925 (2007).
[7] M. S. Pindzola, F. Robicheaux, J. Colgan, and C. P. Balance, Phys. Rev. A **76**, 012714 (2007).
[8] M. S. Pindzola, F. Robicheaux, and J. Colgan, Phys. Rev. A **76**, 024704 (2007).
[9] J. Colgan, M. Foster, M. S. Pindzola, and F. Robicheaux, J. Phys. B **40**, 4391 (2007).
[10] J. Colgan, M. S. Pindzola, and F. Robicheaux, J. Phys. B **41**, 121002 (2008).
[11] S.D. Bergeson and F. Robicheaux, Phys. Rev. Lett. **101**, 073202 (2008).
[12] F. Robicheaux, J. Phys. B **41**, 192001 (2008).
[13] M.S. Pindzola, F. Robicheaux, and J. Colgan, J. Phys. B **41**, 235202 (2008).
[14] J. Colgan, M.S. Pindzola, F. Robicheaux, C. Kaiser, A.J. Murray, and D.H. Madison, Phys. Rev. Lett. **101**, 233201 (2008).
[15] M.S. Pindzola, F. Robicheaux, and J. Colgan, J. Phys. B **41**, 235202 (2008).
[16] T. Topcu and F. Robicheaux, J. Phys. B **42**, 044014 (2009).
[17] T.-G. Lee, M.S. Pindzola, and F. Robicheaux, Phys. Rev. A **79**, 053420 (2009).
[18] A.L. Landers, F. Robicheaux, T. Jahnke, M. Schoffler, T. Osipov, J. Titze, S.Y. Lee, H. Adaniya, M. Hertlein, P. Ranitovic, I. Bocharova, D. Akoury, A. Bhandary, Th. Weber, M.H. Prior, C.L. Cocke, R. Dorner, and A. Belkacem, Phys. Rev. Lett. **102**, 223001 (2009).

Phase Matching of High Harmonics in Capillary Discharge Plasmas for Bright, Coherent, Table-top, keV X-rays

Jorge J. Rocca,
Electrical and Computer Eng Department, Colorado State University, Fort Collins, CO 80523-1373
rocca@engr.colostate.edu
Henry C. Kapteyn
JILA/Physics Department, University of Colorado, Boulder, CO 80309-0440
kapteyn@jila.colorado.edu

Program description

This project is exploring the use of a pre-ionized medium created by a compact capillary discharge to guide high intensity laser light in order to - 1) extend the cutoff photon energy for high-order harmonic generation (HHG) using ions, and 2) implement new phase matching schemes in fully-ionized plasmas in order to generate bright, fully coherent, HHG beams. The use of a discharge-created plasma reduces ionization-induced defocusing of the driving laser as well as energy loss. In work to date, we extended high harmonic emission from Xe up to an unprecedented photon energy of 160 eV [1], and observed HHG emission at energies up to 170 eV in Kr and 275 eV in Ar [5]. The discharge plasma also provided means to spectrally tune the harmonics by tailoring the initial level of ionization of the medium. We also employed a complementary technique of using longer wavelength driving light at 1.3 μm to extend full phase matching of high harmonic generation in Ar, Ne and He up to 100, 200, and 330 eV respectively - well beyond the phase-matching limit for 0.8 μm [7]. This opens the possibility of combining these techniques with new phase matching schemes in capillary discharge plasmas to generate significantly increased HHG flux for applications experiments at much higher photon energies than are currently accessible (100 eV- 10 keV)

In related work we have characterized the output from a soft x-ray laser plasma amplifier seeded with high harmonic pulses. We have demonstrated that injection-seeding of soft x-ray amplifiers created by laser heating of solid targets generates intense soft x-ray pulses with essentially full spatial and temporal coherence, low divergence, short pulsewidth, and defined polarization[9]. We have measured that the soft x-ray laser pulses generated by this technique are the shortest soft x-ray pulse duration demonstrated to date from a plasma amplifier. During the past year we have measured and modeled the near-field and far-field characteristics of these new coherent soft x-ray sources. Results show that injection-seeding of soft x-ray laser amplifiers dramatically improve the beam characteristics.

High harmonic generation from ions

The highest photon energy that can be produced through HHG is predicted by the cutoff rule to be $h\nu_{max} = I_p + 3.2U_p$, where I_p is the ionization potential of the gas and $U_p \propto I\lambda^2$ is the quiver energy of the liberated electron. In principle, using long wavelength or high intensity lasers, $h\nu_{max}$ may be as high as 10 keV before relativistic effects suppress rescattering and HHG. To date however, for many experiments the highest harmonic photon energies observed have not been limited by the available laser intensity, but rather by ionization of the nonlinear medium by the driving laser. The resulting free electron plasma refractively defocuses the driving laser, reducing the peak laser intensity and consequently the highest harmonic photon energy observed. Moreover, the loss of the laser energy due to photoionization limits the length in the medium over which a high peak laser intensity can be maintained.

To overcome these limitations, we are investigating the use of a capillary discharge plasma waveguide to create a preformed plasma with a tailored level of ionization. This makes it possible to generate higher photon energies from ionization of ions with correspondingly higher I_p. Additionally, the concave radial electron density profile of the capillary discharge plasma produces an index waveguide that combats additional ionization-induced defocusing of the laser and allows for a decreased laser intensity near the walls of the capillary, making it possible to guide the higher intensities required for shorter wavelength generation without damaging the walls. In past work, by generating harmonics in a

capillary discharge, we have observed photon energies up to ~160 eV in Xe, well above the highest previously observed value of ~70 eV [1]. For Kr and Ar, the observed maximum photon energies were extended further, to 170 eV and 275 eV respectively [5].

The previous experiments were done at repetition rates of 10Hz, limited by both the laser system and the capillary discharge source. To understand the limiting physics for HHG from ions, we recently investigated HHG in gas-filled waveguides driven by kHz lasers. The increased signal-to-noise allowed us to dramatically extend the cutoff photon energy in Ar to above 500 eV for the first time, and also demonstrate HHG from multiply-charged ions for the first time [10]. This dramatic increase in the maximum photon energy was possible by combining laser pulse self-compression and high harmonic generation within a single waveguide, which enhances the laser intensity and counteracts ionization-induced defocusing, This work thus demonstrated a pathway for extending high harmonic emission to very high photon energies using large, multiply-charged, ions with high ionization potentials. Our future plans are to reproduce these results in guiding plasma discharges, at repetition rates >> 100 Hz.

New phase matching schemes for HHG at keV photon energies

In future work, we also plan to implement new phase-matching techniques to further extend the range of bright photon energies that can be generated. In preliminary work, we implemented quasi phase matching (QPM) techniques by counter-propagating an infrared laser beam in a discharge plasma medium. The presence of the counter-propagating field eliminates emission from regions that contribute out-of-phase to the HHG signal. This technique is especially well suited to generation of very high photon energies in a capillary discharge due to the extremely uniform nature of the discharge created plasma column and the reduced ionization-induced refraction. However, fluctuations in our 10 Hz laser/discharge system prevented us from implementing these schemes. Thus, we are embarking on an upgrade project to increase the repetition rate to > 100 Hz in a different system.

In the interim, in exciting recent work, we showed that by using mid-infrared driving lasers of moderate intensity, HHG presents an experimentally feasible and straightforward route for generating bright, fully coherent, beams up to ≈ 10 keV photon energies. Experimentally, using a driving laser wavelength of 1.3μm, we demonstrated macroscopic phase matching over centimeter distances at ~13 nm (100 eV) in Argon, at ~6 nm (200 eV) in Neon, and in the water window region of the spectrum around 4 nm (330 eV) in Helium. Moreover, phase-matched conversion in this weakly ionized regime is quite advantageous because the driving laser beam experiences minimal nonlinear distortion, resulting in an excellent spatial coherence of the HHG beam. Images of the HHG beam in the water window region of

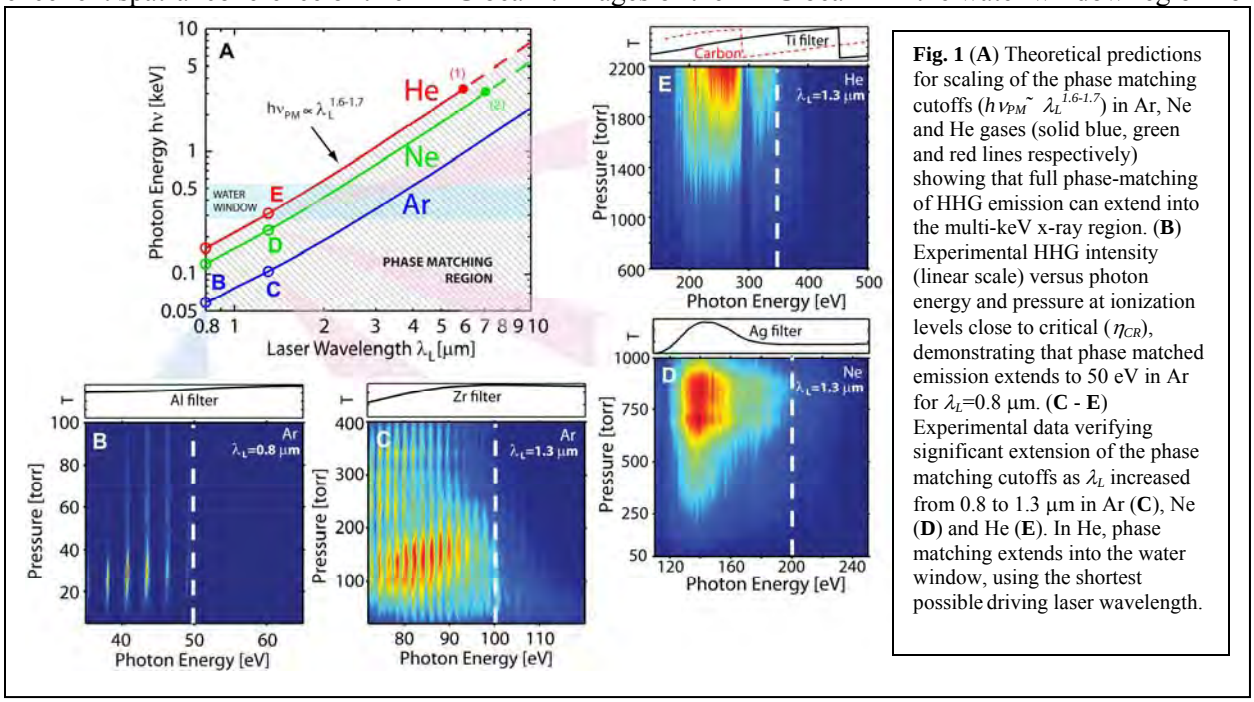

Fig. 1 (**A**) Theoretical predictions for scaling of the phase matching cutoffs ($h\nu_{PM} \sim \lambda_L^{1.6\text{-}1.7}$) in Ar, Ne and He gases (solid blue, green and red lines respectively) showing that full phase-matching of HHG emission can extend into the multi-keV x-ray region. (**B**) Experimental HHG intensity (linear scale) versus photon energy and pressure at ionization levels close to critical (η_{CR}), demonstrating that phase matched emission extends to 50 eV in Ar for λ_L=0.8 μm. (**C** - **E**) Experimental data verifying significant extension of the phase matching cutoffs as λ_L increased from 0.8 to 1.3 μm in Ar (**C**), Ne (**D**) and He (**E**). In He, phase matching extends into the water window, using the shortest possible driving laser wavelength.

the spectrum indicate a well-directed beam, as expected for phase-matched emission. Moreover, through direct comparison between theory and experiment, we quantitatively tested our conceptual understanding of this wavelength scaling of phase matching, verifying that the phase matching mechanism is similar to the case for 0.8 μm driving lasers: namely, full phase matching is achieved through a balance between the neutral atom and plasma dispersions in a weakly ionized gas (including any geometric terms). The increased phase matching pressures and good transparency mitigates the unfavorable $\lambda^{-5.5}$ single atom susceptibility. Finally and most importantly, we show that the optimum phase matching conditions scale very favorably, even well into the multi-keV hard x-ray region of the spectrum, using infrared driving lasers. In the future, we will combine quasi-phase matching, infrared driving lasers, and plasma discharges to implement bright, ultrafast, fully coherent, x-ray beams.

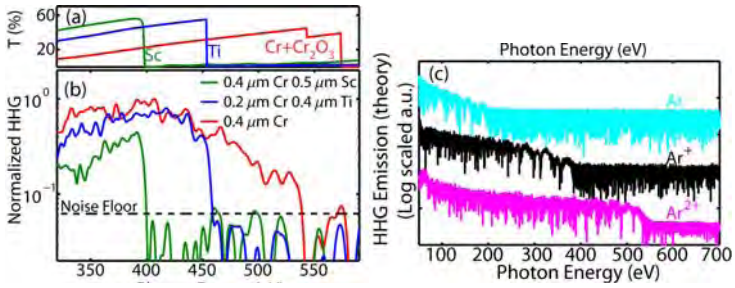

Fig. 2 The spatial and temporal confinement of the driving laser beam at very high levels of ionization results in HHG emission from doubly ionized Ar extending to above 500 eV for the first time. (a) Filters used to block the laser. (b) Experimental HHG emission. (c) Theoretical HHG emission from different ion stages.

Characterization of a Soft X-Ray Laser Amplifier Seeded with High Harmonics

Soft x-ray lasers (SXL) are complementary to HHG as a source of coherent light at short wavelengths for applications, due to their ability to generate pulses with significantly higher pulse energy. By injection-seeding soft x-ray laser plasma amplifiers with high harmonic pulses, we have created a fundamentally new regime for the generation of short soft x-ray laser pulses from plasmas created by laser heating of solid targets. Coherent high harmonic (HH) pulses can be amplified in population inversions created in dense plasmas while preserving many of their properties. Therefore, injection seeding of SXL amplifiers with HH can generate intense soft x-ray pulses with extremely high spatial coherence, low divergence, short pulse width, and defined polarization.

Our group demonstrated the saturated amplification of HH seed pulses in several transitions of Ne-like and Ni-like ions at wavelengths ranging from 32.6 nm to 13.2 nm. The seeding of this type of high density laser-heated solid target SXL amplifier, with its characteristic high saturation intensity and broad laser line width, resulted in phase-coherent laser output with a higher intensity and shorter pulse duration than we obtained previously. The high density of the se SXL plasma amplifiers results in relatively broad laser line bandwidths that in principle can support the generation of sub-ps SXL pulses. Last year, using an streak-camera developed at Kansas State University we realized the first measurement of the duration soft x-ray laser pulses from such an injection-seeded plasma amplifier. The pulse duration of Ne-like Ti laser operating at 32.6 nm was measured to be ~ 1 ps [9] This is the shortest soft x-ray pulse duration demonstrated to date from a plasma amplifier. The results were compared with hydrodynamic/atomic physics model computations that show that injection seeding of denser plasmas with a tailored gain profile will lead to femtosecond SXLs

During the past year we have measured and modeled the near-field characteristics of these new lasers. We have simulated the characteristics of seeded SXLs using a 3D ray-trace post processor to a hydrodynamic/atomic physics code. This code calculates propagation of the signal through the plasma column, including the growth of both the seed pulse and the amplified spontaneous emission (ASE). The gain is computed by a fully transient rate equation model that includes stimulated emission and radiation transport. The ray trace computation is capable of fully resolving the spatial, angular, temporal, and frequency profiles of both the ASE and seeded beams. Temporal broadening of the input seed pulse due to both line narrowing in the amplifier and saturation broadening are included. The computed near field (left) and far field (right) patterns of a 13.9 nm Ni-like Ag seeded x-ray laser are shown in Fig. 3.

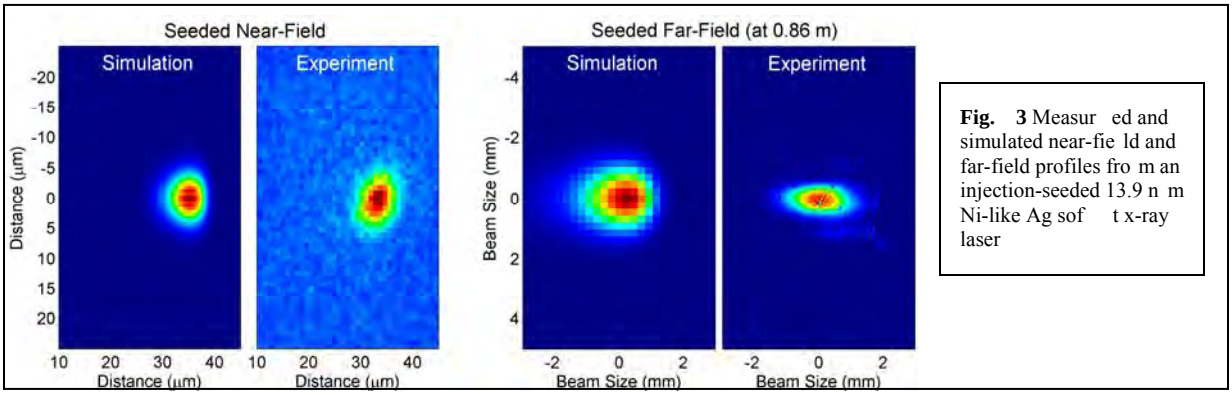

Fig. 3 Measured and simulated near-field and far-field profiles from an injection-seeded 13.9 nm Ni-like Ag soft x-ray laser

Because the input seed has a small divergence that is maintained during amplification, the divergence of the seeded SXL can be up to an order of magnitude smaller than that of the unseeded (ASE) laser. The near field pattern of the seeded laser is also about 2x smaller that the unseeded laser beam. In the future we plan to characterize the temporal coherence properties of this new SXLs.

Future plans

In the future, we will combine quasi-phase matching, infrared driving lasers, and discharges plasmas to implement bright, ultrafast, fully coherent, x-ray beams.

Journal publications from DOE sponsored research 2006-2009

1. D.M. Gaudiosi, B. Reagan, T. Popmintchev, M. Grisham, M. Berrill, O. Cohen, B.C. Walker, M.M. Murnane, H.C. Kapteyn, and J.J. Rocca, "High-Order Harmonic Generation from Ions in a Capillary Discharge", Physical Review Letters, 96, 203001 (2006).
2. J.J. Rocca, H.C Kapteyn, D.T. Attwood, M.M. Murnane, C.S. Menoni, and E. Anderson, "Tabletop Lasers in the Extreme Ultraviolet", (Invited) Optics & Photonics News, 17, No. 11, pg. 30, (2006).
3. D. Gaudiosi, B. Reagan, T. Popmintchev, M. Grisham, M. Berrill, O. Cohen, B.C. Walker, M.M. Murnane, H.C. Kapteyn, and J.J. Rocca, "High Harmonic Generation from Ions in a Capillary Discharge Plasma Waveguide", Optics & Photonics News, 17, No. 12, p. 44, (2006).
4. M.A. Larotonda, Y. Wang, M. Berrill, B.M. Luther, J.J. Rocca, M. Man Shakya, S. Gilbertson, and Z. Chang, "Pulse duration measurements of grazing incidence pumped high repetition rate Ni-like Ag and Cd transient soft x-ray lasers", Optics Letters, 31, 3043, (2006).
5. B.A. Reagan, T. Popmintchev, M.E. Grisham, D.M. Gaudiosi, M. Berrill, O. Cohen, B.C. Walker, M.M. Murnane, J.J. Rocca, and H.C. Kapteyn, "Enhanced High Harmonic Generation from Xe, Kr, and Ar in a Capillary Discharge", Physical Review A, 013816, (2007).
6. O. Cohen, X. Zhang, A. Lytle, T. Popmintchev, M. Murnane, H. Kapteyn, "Optically-induced grating-assisted phase matching in high-harmonic generation", Physical Review Letters 99, 53902 (2007).
7. T. Popmintchev, M.C. Chen, O. Cohen, M. Grisham, J.J. Rocca, M.M. Murnane and H.C. Kapteyn, "Extended Phase Matching of High Harmonics Driven by Mid-Infrared Light", Optics Letters, 2128, 33, (2008).
8. T. Popmintchev, M.-C. Chen, A. Bahabad, M. Gerrity, P. Sidorenko, O. Cohen, I. P. Christov, M.M. Murnane, and H.C. Kapteyn, "Phase matching of high harmonic generation in the soft and hard X-ray regions of the spectrum," Proceedings of the National Academy of Sciences, p. 10.1073/pnas.0903748106, (2009).
9. Y. Wang, M. Berrill, F. Pedaci, M.M. Shakya, S. Gilbertson, Z. Chang, E. Granados, B.M. Luther, M.A. Larotonda, and J.J. Rocca, "Measurement of 1 Picosecond Soft X-Ray Laser Pulses from an Injection-Seeded Plasma amplifier", Phys. Rev. A 79, 023810 (2009).
10. P. Arpin, T. Popmintchev, N.L. Wagner, A.L. Lytle, O. Cohen, H.C. Kapteyn, and M.M. Murnane, "Enhanced high harmonic generation from multiply-ionized argon above 500 eV through laser pulse self compression", submitted to Physical Review Letters, (2009).
11. T. Popmintchev, M.M. Murnane, and H.C. Kapteyn, Nature Photonics, to be published (2009).

Ultrafast holographic x-ray imaging and its application to picosecond ultrasonic wave dynamics in bulk materials

Christoph G. Rose-Petruck
** Department of Chemistry, Box H, Brown University, Providence, RI 02912*
phone: (401) 863-1533, fax: (401) 863-2594, Christoph_Rose-Petruck@brown.edu

1 Program Scope

The focus of this work is to develop ultrafast, holographic x-ray imaging methods suitable for use with laser plasma x-ray sources. The methods will image structural dynamics and motions in materials using phase shifts imparted on the x-ray waves as they propagate though the material. The planned work seeks to directly observe, for instance, phonon wave packets, shock waves, or phonon solitons propagating in the bulk of materials. This work was funded in the spring of 2008.

Imaging of bulk materials relies on Propagation-based Differential Phase Contrast Imaging (PDPCI) which measures the Laplacian of the real part of the index of refraction, n_r, of the material and Talbot Effect imaging (TEI), which measures the 1st spatial derivative of n_r. No x-ray interferometers will be used. The sensitivity to of the measurements to density variations is up to 1000 times larger than that of conventional x-ray absorption based imaging methods.

As an additional component of the program, ultrafast x-ray absorption experiments are setup up at 7ID-C, APS, Argonne National laboratory. First experimental results related to the ultrafast dynamics of iron pentacarbonyl are presented.

2 Recent Progress

Progress has been made in four research topics funded by this DOE grant.

2.1 Theoretical study of PDPCI: Transmission functions separable in cylindrical coordinates

A Fresnel-Kirchhoff integral can be used to calculate PDPC images when the transmission function of the object is known. Expressions for the image intensity have been derived for objects with axial symmetry for an x-ray source with non-vanishing dimensions, such as our laser-driven plasma x-ray source. An expression for the image intensity has been derived for an x-ray source whose intensity distribution is described by a Gaussian function, from which an expression for the limiting case of a point source of radiation is found. The expressions for image intensity are evaluated for cases where the magnification is substantially greater than one, as would be employed in biological imaging. Experiments using a micro-focus x-ray tube and x-ray CCD camera are reported to determine the capability of the method for imaging small spherical objects. A related paper has been accepted in the Journal of Applied Physcis.[1]

2.2 X-ray elastography: modification of x-ray phase contrast images using ultrasonic radiation

The high resolution characteristic of PDPCI can be used in conjunction with directed ultrasound to detect small displacements in soft tissues or soft materials generated by differential acoustic radiation pressure. The imaging method is based on subtraction of two x-ray images, the first image taken with, and the second taken without the presence of ultrasound. The subtraction enhances phase contrast features, and, to a large extent, removes absorption contrast so that differential movement of volumes with different acoustic impedances or relative ultrasonic absorption is highlighted in the image. Interfacial features of objects with differing densities are delineated in the image as a result of both the displacement introduced by the ultrasound and the inherent sensitivity of PDPCI to density variations. Experiments with ex vivo murine tumors, and human tumor phantoms, as well as gas inclusions in soft materials are imaged. While this work addresses primarily bio-medical applications, it also studies the effect of ultrasonic waves on gas bubbles in soft materials. This, in turn will be useful in applications such as the PDPC imaging of photo-acoustic cavitation in liquids, which have been shown to accompany laser-induced water-gas reactions on the surfaces of carbon nanoparticles in optically opaque suspensions. A setup for imaging shockwaves and cavitations in such suspensions using the ultrafast laser-plasma x-ray

source has just been completed. A related paper has been accepted in the Journal of Applied Physcis.[2]

2.3 Simulations of PDPCI of shock waves in beryllium

Experiments will image the ultrasonic wave propagation in liquid and solid materials. In preparation for these experiments, simulations of the PDPC image intensity distribution caused by 1-D ultrasonic waves have been calculated by explicitly solving the Fresnel integral. Thus, no approximations such as the transport of intensity approximation have been made. An example for the results is shown in Figure 1. The upper panel shows the ultrasonic wave typically produced by ultrafast laser-induced lattice expansions. In our case we assumed that 800-nm laser pulses with a pulse length of 200ps are heating a beryllium sample with a fluence of that 160-mJ/cm². 25% absorption was assumed. While the fluence seems high, the value is below the damage threshold of the material and corresponds to and intensity of just 8×10^{8} W/cm². The theoretical description of such a wave has been demonstrated in the literature. The strain amplitude is 0.08%. This wave is PDPC imaged with a 7-keV radiation and a magnification of the setup of 3.3. The thickness of the Be sheet was 500 µm. The resulting intensity pattern is shown in the lower panel of Figure 1. The red line is the pattern for a perfect point source, the blue line is the pattern for our plasma x-ray source (diameter: 13 µm). Note that the contrast modulations for the 13-µm source are about 1% for only 0.08% strain. This is due to the fact that the signal of PDPCI is proportional to the Laplacian of the density profile and the ultrasonic wavelength is short. This "enhances" the signal intensity compared to interferometric measurement of the density. Considering that we are able to pump the sample with 5 times more power and that it might be possible to reduce the reflectivity of the sample by blackening the surface, shockwaves of up to 1% strain should be possible causing a 5% intensity variation. While not directly a goal of this proposal, the reduction of the plasma source diameter would be very valuable as it increases not just the resolution but most importantly the signal that can be detected. Finally, the bi-polar wave created here will not appear in liquid samples, where pure compression waves dominate after liquid ablation off the surface. This, in turn, causes a much stronger PDPC signal because of the absence of the partial cancellation of the signals as for the bipolar strain wave.

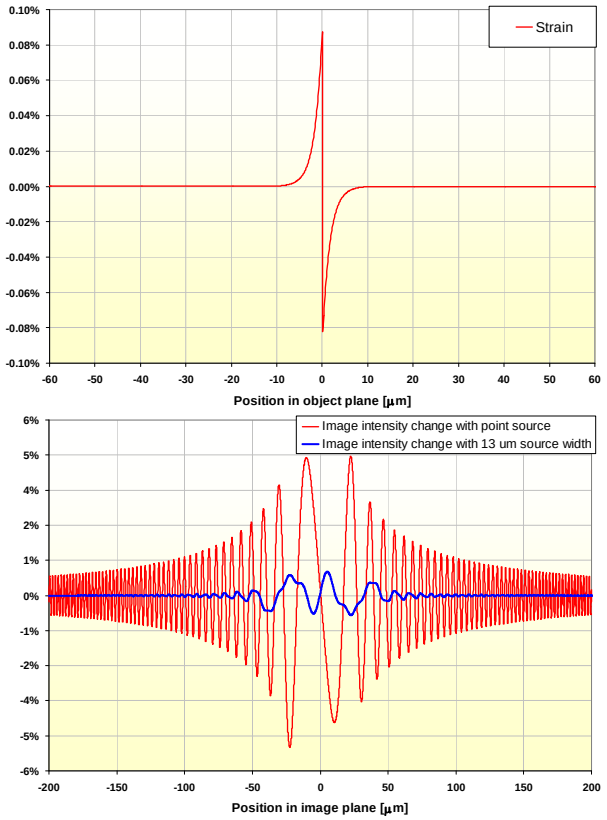

Figure 1: Upper image: Simulated shock wave induced in a 500-µm thick beryllium sheet with a laser fluence of 160mJ/cm². Laser pulse wavelength: 800 nm, pulse length: 200 ps, 25% absorption of laser light;
Lower image: PDPC image of the shockwave for point source and the 13-µm diameter plasma source. Calculations were performed with for realistic experimental conditions with a magnification of 3.3 and a x-ray photon energy of 7 keV.

2.4 Ultrafast XAFS measurements at the Advanced Photon Source, ANL

In collaboration with Dr. Bernhard Adams and Dr. Mathieu Chollet, Argonne National Laboratory, we have set up an UXAFS instrument at 7-ID-C. It consists of a high-speed x-ray chopper, liquid sample jet chamber with laser and x-ray beam diagnostic followed by an x-ray streak camera.

80-ps x-ray pulses are monochromatized in the 4–crystal beamline monochromator. High-harmonic x-rays are suppressed by slightly detuning two of the crystals. The primary x-ray flux is subsequently chopped with a high speed chopper and transmitted through the liquid sample jet. The excitation laser

beam is directed onto the sample co-linearly with the x-ray beam. The x-radiation transmitted though the sample is detected by a x-ray streak camera for ultrafast measurement of the temporal evolution of the x-ray intensity transmitted through a sample solution after UV photo excitation. Since the APS pulses are 150-ps (in hybrid-mode), each streak covers a large time window with a 2-ps resolution. These measurements are carried at various, sequentially selected x-ray energies covering the iron K XANES and EXAFS range.

The first measurements with the new instrument were carried out in August 2009 following preliminary measurements with a prototype in the spring of 2009. The basic performance of the system is illustrated in Figure 2. A read-out image of the streak camera is shown. The time axis is in horizontal direction. The x-ray beam is separated into two sections by inserting a wire into the x-ray beam, thereby clearly separating the laser-pumped form the un-pumped region. The upper part is the pumped area; the lower part serves as a reference area. Additionally, a fiducial is imaged onto the photocathode to serve as a timing reference. The plot in Figure 2 shows the line outs of the image. This streak simply measures the pulse structure of the APS hybrid pulses. Note that the fine structure is primarily caused by the non-uniformity of the multichannelplate at the output of the streak camera.

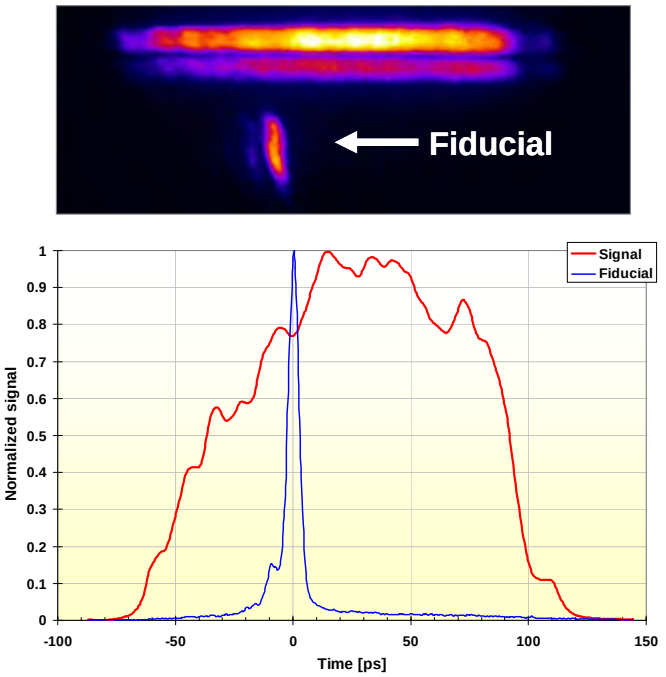

Figure 2: Streak and lineout of an APS pulse operating in hybrid mode. The streak is divided into a pumped and a reference region. The fiducial serves as a timing marker.

Static XANES spectra of $[Fe(CN)_6]^{4-}$ have been measured by acquiring a few hundred streaks at x-ray energies from 7.1 to 7.6 keV.

Time-resolved measurements were done with $Fe(CO)_5$ in ethanol. This chemical system serves as a model for complexes that are electronically saturated but sterically uncrowded. We recently demonstrated that iron pentacarbonyl forms weakly bound complexes with a single solvent molecule in solution. This "pre-assembly" of iron pentacarbonyl with a solvent molecule, in principle permits concerted ligand substitution reactions, i.e. the simultaneous bond-formation with the associated solvent molecule and the simultaneous dissociation of a carbonyl ligand after photo-initiation of a chemical reactions. Thus, this system may permit measurements of the ultrafast structural dynamics of *bi*-molecular reactions under ambient conditions *without* a diffusive reactant encounter after photo excitation.

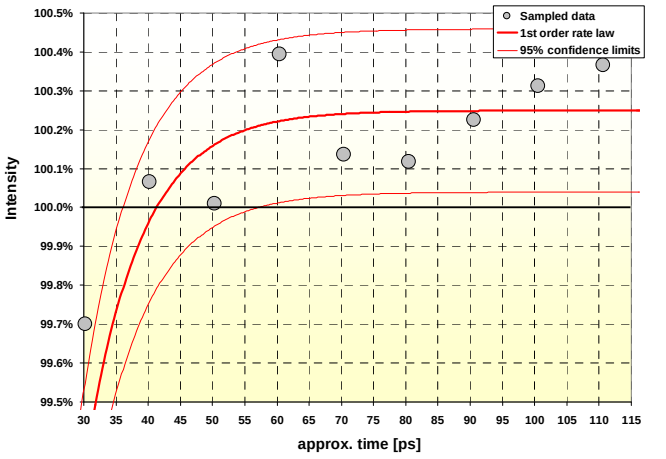

Figure 3: Time-dependent x-ray absorption streak of $Fe(CO)_5$ in ethanol measured at 7.130 keV.

400-nm laser pulse excitation initiated the reaction $Fe(CO)_5 + etOH + h\nu_{400nm} \rightarrow Fe(CO)_4etOH + CO$. A typical laser-pump x-ray probe measurements at a selected x-ray wavelength comprised 1 000 streak images with the pump laser alternately being switch on and off. The approximate pump-probe timing was determined by imaging both, the laser and the x-ray pulses, onto the same photodiode while referencing

the observed pulses to a reference diode. We estimate that this procedure yielded the timing accurate to about 20 ps. The exposure time for each image was 750 ms. The experiment was running at 5 kHz repetition rate. Thus, 500 images with laser on and 500 images with laser off were measured. The un-pumped (laser off) streaks were used to normalize the laser-on streaks. This normalization typically resulted in a signal intensity of 1.000 with a standard deviation of 0.25%. The result of a preliminary data analysis of one of the streaks is shown in Figure 3. The signal is clearly increasing above the 100%-line on a time-scale that is consistent with transient IR measurements by other authors. A 1st order rate law was fitted to the data. Since the details of the chemical dynamics observed here have not been determined, the choice of this rate law is somewhat arbitrary. Nevertheless, it is a helpful visual guide. The 95% confidence interval is also shown. Note that the corresponding plot of normalized data from areas in the same streak images that were not laser excited, yield a flat line at 100% with a 95%-confidence interval of ±0.16%. Thus, the increase shown is statistically significant and does not suffer from systematic errors. The data analysis is still incomplete. For instance, the timing jitter, primarily caused by the absence of relay imaging optics between the laser system and the x-ray hutch is about 10ps. While this will be rectified for the next beamtime, we will use software to "de-jitter" the streaks as well as possible. The jitter is also the reason why the data points in Figure 3 are not shown with full 2-ps resolution. The calibration of the time axis is approximate in this figure but a calibration measurement has been performed.

In summary, the first results from the new UXAFS instrument at ID7-C are encouraging although they are not a complete data set yet and the data analysis is still in progress.

3 Future plans

The imaging work will be applied to clathrate hydrates samples that can be used for the capture of gases such as CO_2. Additionally, we currently manufacture binary x-ray phase gratings based on silicon single crystals. These gratings will be used for time-resolved x-ray Talbot imaging. The UXAFS experiment will be continued. System improvements to the beamline optics, laser beam transport system, and UXAFS instrument will be made before the next beamtime in the winter of 2009.

4 Papers acknowledging this DOE grant

1. "X-ray Phase Contrast Imaging: Transmission Functions Separable in Cylindrical Coordinates," G. Cao, T. Hamilton, C. M. Laperle, C. Rose-Petruck and G. J. Diebold, J. Appl. Phys. 105, 102002 (2009).

2. "X-ray elastography : Modification of x-ray phase contrast images using ultrasonic radiation pressure," T. J. Hamilton, C. Bailat, S. Gehring, C. M. Laperle, J. Wands, C. Rose-Petruck and G. J. Diebold, Journal of Applied Physics 105 (10), 102001 (2009).

Development of continuous REMPI detection of the PbF molecule for measurement of the electron's electric dipole moment

Neil Shafer-Ray*, Gregory Hall**, and Trevor Sears**
*University of Oklahoma Homer L. Dodge Department of Physics and Astronomy (shaferry@physics.ou.edu)
**Brookhaven National Laboratory

1) Program Scope

In 1950 Purcell and Ramsey[1] suggested that the electron might have a CP-violating electric dipole moment (e-EDM) proportional to its spin angular momentum. This possibility initiated an ongoing hunt for the e-EDM that has been spurred on by the recognition of the importance of CP-violation to the formation of a matter-dominated universe[2] as well as a difference in magnitude of the Supersymmetric[3] and Standard Model[4] prediction for its value. The current limit on the e-EDM is 1.6×10^{-27}e·cm as determined in a Ramsey beam resonance study of the Tl atom[5].

The PbF molecule provides a unique opportunity to measure the e-EDM. The molecule's odd electron, heavy mass, and large internal field combine to give it an intrinsic sensitivity to an e-EDM that is over three orders of magnitude bigger than that of the Tl atom[6]. In addition to this increased intrinsic sensitivity, the ground state of the PbF molecule allows for a "magic" electric field at which the magnetic moment vanishes[7]. All of these advantages create an opportunity to significantly lower the current limit on the e-EDM. These advantages can only be realized if an intense source of ground-state PbF molecules can be created and detected with high efficiency. The scope of this project is to (1) create a rotationally cold molecular beam source of PbF, (2) achieve a continuous ionization scheme for sensitive state selective detection of the PbF molecule.

2) Recent Progress

2.1) The Effect of the Geometric Phase on the Possible Measurement of the Electron's Electric Dipole Moment Using Molecules Confined by a Stark-Graviational Trap

It is possible to envision a molecular $e - EDM$ experiment which probes PbF molecules confined to a region in space by a non-uniform electric field. In fact, the original aim of this DOE-funded research was to create a cold source of PbF molecules that could be loaded into such a trap. We soon realized, however, that such an experiment would have a coherence time τ limited not by the lifetime of molecules in the trap, but instead by a geometric phase effect that couples the angular momentum of the center-of-mass motion of a molecule to its internal angular momentum. We used the formalism of Longuett-Higgens[8] to derive an effective Hamiltonian for this effect and determined the coherence time τ . Specifically we find that, for trapped $^{208}Pb^{19}F$ molecules,

$\tau \approx \left[\frac{T}{23mK}\right]^{-2}$ sec. This is an unfortunate result because our proposed cooling techniques do not produce a sub-Kelvin population of PbF molecules. For this reason, a change in direction of the research project was requested and granted by the DOE. Specifically, our effort was shifted to the development of a continuous resonance-enhanced multiphoton ionization detection scheme

2.2) Direct measurement of the lifetime of the D state of PbF

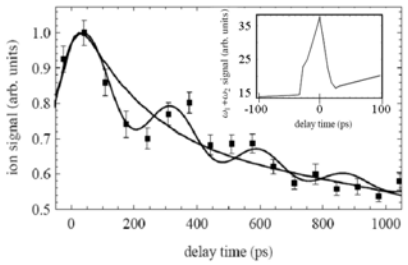

Figure 1: Decay of the D state of PbF

The A state is the only electronically excited state of PbF known to have a lifetime that is sufficiently long to allow for state-selective detection. Unfortunately, direct ionization of this state proves to be impractical: The uv laser radiation required to ionize the A state also directly ionizes the ground state via an efficient $1+1$ ionization process. This non-state-selective one-color process completely swamps any state-selective two-color $1+1$ ionization process that might occur. This fact led us to the $1+1+1$ doubly resonance enhanced ionization scheme

$$X \underset{436\,\mathrm{nm}}{\rightarrow} A \underset{477\,\mathrm{nm}}{\rightarrow} D \underset{532\,\mathrm{nm}}{\rightarrow} PbF^{+}. \tag{1}$$

Knowledge of the $D-$state lifetime is critical to the design of an optimal laser system to implement this ionization scheme. Unfortunately the bandwidth of the Nd:YAG pumped dye laser system used to discover the $A \rightarrow D \rightarrow PbF^{+}$ ionization pathway is not sufficiently narrow to make a conclusive statement about the $D-$state lifetime. For this reason we coaxed our 7-ns Nd:YAG laser system to perform a time domain measurement with picosecond resolution. To accomplish this we took advantage of the temporal mode structure of our unseeded Nd:YAG laser-pumped dye laser system. This structure is observed in an auto-correlation measurement that monitors the 251-nm radiation resulting from sum-frequency generation of 532-nm and 477-nm laser radiation in a BBO crystal as a function of an optical delay between the two input wavelengths (Figure 1, inset.) The lifetime of the D state of PbF is made by observing the PbF^{+} ionization signal as a function of the delay between the 476.6-nm and 532-nm laser radiation. The resulting time-dependent ionization signal (Figure 1) indicates a lifetime of 250 ± 150 ps. The $D-$state lifetime is short enough to dramatically reduce the efficiency of an ionization scheme utilizing continuous wave radiation. For this reason, we employ a pseudo-continuous source of laser

radiation producing (see section 2.4.)

2.3) Characterization of the X_1, A, B, D, E, and F states of PbF

We have completed a detailed spectroscopic study of all known electronic states of the PbF molecule except the C state (which we can not detect with rotational-state resolution.) These states were detected with 2-dimensional resonance-enhanced multiphoton ionization via the process $X_1\,{}^2\Pi_{1/2} \rightarrow A^2\Sigma_{1/2} \rightarrow [B, D, E, \text{or } F] \rightarrow PbF^+$. A typical spectrum is shown in Figure 2. With this REMPI scheme, we have corrected values of T_e by as much as 100 cm^{-1}, we have determined heretofore unknown rotational constants, we have assigned term symbols to the C and D, states, and determined the value of Ω for the E and F states. We have also confirmed the parity of the B state. One interesting finding is that the assumed electronic mixing of the X_1, X_2, and A states is not as simple as once thought. In a simple three-state ${}^2\Pi_{1/2} - {}^2\Pi_{3/2} - {}^2\Sigma_{1/2}$ mixing scheme, the sum of the ratio of omega-doubling constant to rotational constant p/B is ± 2 (see [9, 6].) These ratios are given in the table below for the X_1, A, and D states.

	$X_1(v=0)$	$A(v=7)$	$A(v=0)$	$D(v=0)$
p/β	-0.605	2.60	2.996	-1.04

(2)

This table, as well as the energy levels of the electronic states suggest that the $X_1\,{}^2\Pi_{1/2}$, $X_2\,{}^2\Pi_{3/2} \rightarrow A^2\Sigma_{1/2}(v=7)$ system forms one strongly mixed ${}^2\Pi - {}^2\Sigma$ system whereas the $D\,{}^2\Pi_{1/2}$, $C\,{}^2\Pi_{3/2} \rightarrow A^2\Sigma_{1/2}(v=0)$ forms another. In light of this finding, a re-evaluation of the sensitivity of the molecule's sensitivity to parity violation is needed.

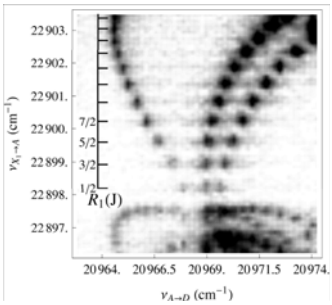

Figure 2: 2-D spectrum of the $X_1 \rightarrow A \rightarrow D$ transition.

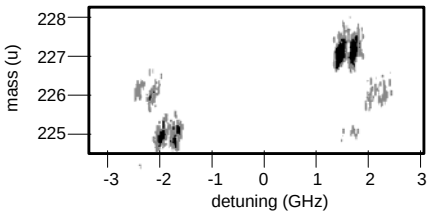

Figure 3: Continuous ionization of the $X_1(v=0, J=67/2) \rightarrow A(v=1, J=69/2)$ transition

2.4) Observation of continuous ionization of the PbF molecule

Up until this year, we detected the PbF molecule using a 10−Hz Nd:YAG pumped dye laser system. Whereas this system allowed for high sensitivity, its duty cycle was low (~10^{-5}) and its resolution limited to approximately 1 GHz. Recently we have achieved continuous ionization detection of the PbF

molecule. Here a diode laser is used to excite the $X_1 \rightarrow A$ transition and a pseudo continuous laser system (76MHz, 6ps, Nd:YVO_4-pumped OPO) is used to drive the A state to ionization. A coincidence detector is then used to detect electrons that arrive in coincidence with PbF^+ molecules. By recording these events,we are able to measure the mass-frequency spectrum of the $X_1 \rightarrow A$ transition. Figure 3 shows such a spectrum. The spectra clearly resolves the $^{206}Pb^{19}F$,$^{207}Pb^{19}F$, and $^{208}Pb^{19}F$ molecules. The small frequency doubling of all peaks is due to the fluorine nucleus whereas the large doubling of the $^{207}Pb^{19}F$ transition is due to the lead nucleus.

3) Future Plans

A new source of PbF molecules has been built and tested. It consists of a Boron Nitride nozzle that cracks PbF_2 when heated to 1400^oC. Unfortunately, the PbF_2 evaporates too quickly to do useful science. Modifications to this new source are being made that allow us to independently control the exit orifice temperature (which controls the degree of cracking of the gas-phase PbF_2) and the temperature of the PbF_2 salt (which controls the vapor pressure and hence lifetime of the source.) It is our hope that this high temperature source will allow us to rotationally cool the beam without clogging the nozzle or quenching the PbF. In addition to the improvement of our source of PbF, we are working to improve our continuous ionization source. The ionization scheme is roughly an order of magnitude less sensitive then our design goal. (We are currently collecting signal at a maximum rate of 100 Hz) To improve the situation, we are both attempting new ionization schemes and increasing the intensity of laser radiation used to drive the three transitions required to ionize the molecule.

4) References

[1] E. Purcell, N. Ramsey, *Phys Rev*, 78 807 (1950).

[2] Sakharov, *JETP Lett*, 5 24 (1967).

[3] R. Arnowitt, B. Dutta, Y. Santoso, *Phys Rev D* 64 113010 (2001).

[4] F. Hoogeveen, *Nuc Phys*, B341 322 (1990).

[5] Regan, Commins, Schmidt, DeMille, *Phys Rev Let* 88 71805 (2002).

[6] Kozlov, Fomichev, Dmitriev, Labzovsky, Titov, *J Phys B* 20 4039 (1987).

[7] N. E. Shafer-Ray, *Phys Rev A* 73 34102 (2006).

[8] Longuet-Higgens, Advances Spec II, (1961)

[9] I. Kopp, J. Hougen, *Can J Phys* 45 2581 (1967).

5) DOE Sponsored Publications

1. State-selective detection of the PbF molecule by double resonant multiphoton ionization, P. Sivakumar, C.P. McRaven, Dustin Combs, N.E. Shafer-Ray, and Victor Ezhov, *Phys. Rev. A* 77, 062508 (2008.)

2. Effect of the geometric phase on the possible measurement of the electron's electric dipole moment using molecules confined by a Stark gravitational trap, Milinda Rupasinghe and N.E. Shafer-Ray, Phys. Rev. A 78, 033427 (2008)

DYNAMICS OF FEW-BODY ATOMIC PROCESSES

Anthony F. Starace

The University of Nebraska
Department of Physics and Astronomy
116 Brace Laboratory
Lincoln, NE 68588-0111

Email: astarace1@unl.edu

PROGRAM SCOPE

The goals of this project are to understand and describe processes involving energy transfers from electromagnetic radiation to matter as well as the dynamics of interacting few-body, quantum systems. Investigations of current interest are in the general areas of strong field physics, attosecond physics, high energy density physics, and multiphoton and double photoionization processes. Nearly all projects under investigation involve large-scale numerical computations for the direct solution of the three-dimensional time-dependent or time-independent Schrödinger equation describing the interaction of atomic systems with electromagnetic radiation. Principal benefits and outcomes of this research are improved understanding of how to control atomic processes with electromagnetic radiation and how to transfer energy from electromagnetic radiation to matter. In some cases our studies are supportive of and/or have been stimulated by experimental work carried out by other investigators funded by the DOE AMO physics program.

RECENT PROGRESS

A. Threshold-Related Enhancements of Rescattering Plateaus in Laser-Assisted Electron-Atom Scattering

Our recently developed time-dependent effective range [TDER] theory for above-threshold ionization processes [see M.V. Frolov et al., *Phys. Rev. Lett.* **91**, 053003 (2003)] has very recently been extended to give an essentially exact account of laser-assisted, electron-atom scattering (LAES) processes. The TDER theory combines the well-known effective range theory (for electrons interacting with a short-range potential) and the equally well-known Floquet theory (for atomic systems interacting with a monochromatic laser field). Our initial focus has been the study of threshold-related enhancements of the strong-field rescattering plateau in LAES spectra. These threshold phenomena are known to occur in above-threshold ionization as well as in high-order harmonic generation at the closing of a multiphoton ionization channel. Such threshold phenomena can also occur in electron–atom scattering in a laser field, because this process is substantially multichannel in nature: the possible transitions of an electron with momentum p and energy $E=p^2/2m$ to states with energies $E_n=E+n\omega$ correspond to absorption ($n>0$), elastic scattering ($n=0$), and induced emission ($n<0$) of laser field photons. In the latter case, the number of emitted photons is limited by the threshold value $n_{\min} = -[E/\omega]$ (where $[x]$ is the integer part of x). In contrast to above-threshold ionization and the generation of high harmonics,

the threshold conditions for laser-assisted electron-atom scattering are independent of the field intensity and are achieved by varying either the electron energy E or the field frequency ω so as to satisfy the relation $E=\mu\omega$, where $\mu=1, 2, \ldots$. (Thus, the multiphoton emission threshold corresponds to $n_{min}= -\mu$.) According to general scattering theory, threshold anomalies can exist in all channels with $n>n_{min}$. However, their character and the region of n values in which the threshold modification of the cross sections is significant depend on both the specific process and on the parameters of the problem and thus cannot be determined without a detailed investigation of the particular process being considered.

Whereas in above threshold ionization and in high-order harmonic generation, threshold-related enhancements of strong field rescattering plateaus occur at the closing of either even or odd multiphoton ionization channels, we have found that in laser-assisted electron-atom scattering the enhancements of the plateaus occur at the opening of both even and odd multiphoton channels. These enhancements have been found to increase the electron scattering cross sections with absorption of n laser photons by several orders of magnitude. Our results also show that threshold phenomena are typical features for the electron rescattering plateau region in the cross sections for all atomic photoprocesses in a strong laser field. Numerical results for e - H and e - F scattering have been investigated thus far. (*See reference [10] in the publication list below*.)

B. Angularly Resolved Electron Spectra of H^- Produced by Few-Cycle Laser Pulses

We have recently investigated the detachment of the H^- negative ion by a linearly-polarized, few cycle laser pulse. The angular distribution of the detached electrons is found to be extremely sensitive to the carrier-envelope phase of the few-cycle laser pulse. Results have been obtained for laser pulses with various pulse widths. The sensitivity of the detached electron momentum distributions thus is shown to provide a measure of the characteristics of the short laser pulse and, in particular, of its carrier-envelope phase. (*See reference [11] in the publication list below*.)

C. Plateau Structure in Resonant Laser-Assisted Electron-Atom Scattering

Nearly constant cross sections (as a function of the number of absorbed photons) have been predicted over a large range of scattered electron energies in laser-assisted electron-atom scattering (LAES) for both linear [N.L. Manakov et al., JETP Lett **76**, 258 (2002)] and circular [A.V. Flegel et al., Phys. Lett. A **334**, 197 (2005)] laser polarizations. Such "plateau" structures have been investigated for over two decades in other intense laser processes, e.g., above threshold ionization/detachment (ATI/ATD) and high-order harmonic generation. Interest in such plateaus centers on the possibility of transferring large amounts of energy from a laser field into either electron kinetic energy or high order harmonics without significant decreases in yields. However, for all processes the absolute values of the n-photon rates in the plateau region are orders of magnitude smaller than in the region of small n. Hence, mechanisms for increasing rates on the plateau are of great interest. For LAES, two such mechanisms exist: threshold-related phenomena at the closing of the stimulated multiphoton emission channel [10] and resonance scattering. These two mechanisms occur under different conditions: the former occur at incident electron energies equal to multiples of the photon energy, while the latter occurs for those electron energies at which the electron is temporarily captured (following stimulated emission of μ laser photons) into a bound state of the potential $U(r)$ of the target atom and then detached by absorbing $n+\mu$ photons.

We have recently predicted significant resonant enhancements of plateau features in LAES for the case of electron scattering from neutral atoms supporting negative ions and show that the shape of the high-energy plateau in resonant LAES spectra coincides with that for ATD [12]. Since resonant phenomena disappear in a perturbative treatment of the potential *U(r)*, both the electron-atom and electron-laser interactions must be treated non-perturbatively. We thus employ time-dependent effective range (TDER) theory [10], which extends effective range theory for low-energy elastic electron scattering from a short-range potential *U(r)* to the case of LAES. Resonance enhancements of the LAES plateau are significant for both electron scattering at fixed angle θ (relative to the incident electron momentum) and the angle-integrated electron spectrum. The magnitudes of resonance enhancements are found to significantly exceed those for threshold-related ones [10].

The remarkable similarity between plateau features in resonant LAES and ATD implies that information about ATD may be obtained from results for resonant LAES and vice versa. These results are useful for better understanding of resonant phenomena in intense laser-atom interactions, as well as for planning of experiments on laser-modified electron-atom scattering. (*See reference [12] in the publication list below*.)

D. Few-Cycle Attosecond Pulse Chirp Effects on Asymmetries in Ionized Electron Momentum Distributions

We have recently analyzed numerically the asymmetries of ionized electron momentum distributions produced by chirped few-cycle attosecond pulses having various fixed carrier-envelope-phases (CEPs). The central frequency of the pulse is chosen to be 25 eV, which is well above the ionization threshold, so that the contribution of excited states is negligible, the atomic structure is unimportant, and we can focus in the effects of the chirp. Our results are based on solutions of the time-dependent Schrödinger equation for the ground state of the hydrogen atom interacting with a chirped, few-cycle attosecond pulse. Our results allow one to make the following conclusions: First, for few-cycle attosecond pulses having even a small chirp, the asymmetry in the ionized electron momentum distribution can be changed significantly and is sensitive to the sign of the chirp. Second, this asymmetry is also quite sensitive to the CEP of the pulse, even for chirped pulses; the maximum asymmetry is very sensitive to both the chirp and the CEP, occurring for non-zero but small values of the chirp. Third, regarding the energy distributions along $\theta = 0$ and $\theta = \pi$ for chirped pulses, the asymmetry can vanish at particular electron energies that are very sensitive to the chirp. Finally, our results demonstrate clearly that asymmetries in the momentum distributions of electrons ionized by few-cycle, chirped attosecond pulses may provide a means for experimentalists to better characterize their pulses. (*See reference [13] in the publication list below*.)

FUTURE PLANS

Our group is currently carrying out research on the following additional projects: (1) Analyzing few-cycle XUV attosecond pulse carrier-envelope-phase effects on ionized electron momentum and energy distributions in the presence of a few-femtosecond IR laser pulse; (2) Modelling XUV attosecond pulse ionization plus excitation processes in He; (3) Developing an analytic theory for few-cycle attosecond pulse ionized electron spectra using perturbation theory.

PUBLICATIONS STEMMING FROM DOE-SPONSORED RESEARCH (2006 – 2009)

[1] A.Y. Istomin, N.L. Manakov, A.V. Meremianin, and A.F. Starace, "Non-Dipole Effects in Double Photoionization of He," in *Ionization, Correlation, and Polarization in Atomic Collisions*, ed. A. Lahmam-Bennani and B. Lohmann (A.I.P., Melville, NY, 2006), pp. 18-23.

[2] A.Y. Istomin, A.F. Starace, N.L. Manakov, A.V. Meremianin, A.S. Kheifets, and I. Bray, "Nondipole Effects in Double Photoionization of He at 450 eV Excess Energy," J. Phys. B **39**, L35 (2006).

[3] S.X. Hu and A.F. Starace, "Laser Acceleration of Electrons to GeV Energies Using Highly Charged Ions," Phys. Rev. E **73**, 066502 (2006).

[4] L.Y. Peng, Q. Wang, and A.F. Starace, "Photodetachment of H^- by a Short Laser Pulse in Crossed Static Electric and Magnetic Fields," Phys. Rev. A **74**, 023402 (2006).

[5] A.Y. Istomin, E.A. Pronin, N.L. Manakov, S.I. Marmo, and A.F. Starace, "Elliptic and Circular Dichroism Effects in Two–Photon Double Ionization of Atoms," Phys. Rev. Lett. **97**, 123002 (2006).

[6] L.Y. Peng and A.F. Starace, "Application of Coulomb Wave Function Discrete Variable Representation to Atomic Systems in Strong Laser Fields," J. Chem. Phys. **125**, 154311 (2006).

[7] G. Lagmago Kamta, A.Y. Istomin, and A.F. Starace, "Thermal Entanglement of Two Interacting Qubits in a Static Magnetic Field," Eur. Phys. J. D **44**, 389 (2007).

[8] L.Y. Peng and A.F. Starace, "Attosecond Pulse Carrier-Envelope Phase Effects on Ionized Electron Momentum and Energy Distributions," Phys. Rev. A **76**, 043401 (2007).

[9] L.Y. Peng, E.A. Pronin, and A.F.Starace, "Attosecond Pulse Carrier-Envelope Phase Effects on Ionized Electron Momentum and Energy Distributions: Roles of Frequency, Intensity, and an Additional IR Pulse," New J. Phys. **10**, 025030 (2008).

[10] N.L. Manakov, A.F. Starace, A.V. Flegel, and M.V. Frolov, "Threshold Phenomena in Electron-Atom Scattering in a Laser Field," JETP Lett. **87**, 92 (2008).

[11] L.-Y. Peng, Q. Gong, and A.F. Starace, "Angularly Resolved Electron Spectra of H^- by Few-Cycle Laser Pulses," Phys. Rev. A **77**, 065403 (2008).

[12] A. V. Flegel, M. V. Frolov, N. L. Manakov, and Anthony F. Starace, "Plateau Structure in Resonant Laser-Assisted Electron-Atom Scattering," Phys. Rev. Lett. **102**, 103201 (2009).

[13] F. Tan, L.Y. Peng, Q. Gong, E.A. Pronin, and A.F. Starace, "Few-Cycle Attosecond Pulse Chirp Effects on Asymmetries in Ionized Electron Momentum Distributions," *Phys. Rev. A* **80**, xxxxxx (2009).

FEMTOSECOND AND ATTOSECOND LASER-PULSE ENERGY TRANSFORMATION AND CONCENTRATION IN NANOSTRUCTURED SYSTEMS

DOE Grant No. DE-FG02-01ER15213

Mark I. Stockman, Pi

Department of Physics and Astronomy, Georgia State University, Atlanta, GA 30303
E-mail: mstockman@gsu.edu, URL: http://www.phy-astr.gsu.edu/stockman

Annual Report for the tree-year Grant Period of 2007-2009 (Publications 2007-2009)

1 Program Scope

The program is aimed at theoretical investigations of a wide range of phenomena induced by ultrafast laser-light excitation of nanostructured or nanosize systems, in particular, metal/semiconductor/dielectric nanocomposites and nanoclusters. Among the primary phenomena are processes of energy transformation, generation, transfer, and localization on the nanoscale and coherent control of such phenomena.

2 Recent Progress and Publications

During the current report period the following papers were supported by this DOE grant. Published in 2009 are: Refs. [1-3], in 2008: Refs. [4-16], and in 2007: Refs. [17-23]. Most of these publications are in top-level refereed journals [1, 2, 5-8, 11-14, 16-19, 21, 22]; there is also a book chapter [4] and advance preprint publications in the ArXiv [3, 9, 10, 15, 20, 23]. Below we highlight the recent publications that we consider most significant.

2.1 Ultrafast Active Plasmonics [1]

Surface plasmon polaritons (SPPs), propagating bound oscillations of electrons and light at a metal surface, have great potential as information carriers for next-generation, highly integrated nanophotonic devices. A number of techniques for controlling the propagation of SPP signals have been demonstrated. However, with sub-microsecond or nanosecond response times at best, these techniques are too slow for future applications. We have reported that femtosecond optical frequency plasmon pulses can be modulated on the femtosecond timescale by direct ultrafast optical excitation of the metal, thereby offering unprecedented terahertz modulation bandwidth-a speed of many orders of magnitude faster than existing technologies. This work was done in collaboration with experimental group of Prof. N. Zheludev (University of Southampton, UK).

2.2 Nanoconcentration of Terahertz (THz) Radiation in Metal Plasmonic Waveguides [8, 9]

We establish the principal limits for the nanoconcentration of the THz radiation in metal/dielectric waveguides and determine their optimum shapes required for this nanoconcentration [8, 9]. We predict that the adiabatic compression of THz radiation from the initial spot size of order of vacuum wavelength (~10-100 micron) to the final size of ~100-250 nm can be achieved, while the THz radiation intensity is increased by a factor of ~ 10 to ~ 250. This THz energy nanoconcentration will not only improve the spatial resolution and increase the signal/noise ratio for the THz imaging and spectroscopy, but in combination with the recently developed sources of powerful THz pulses will allow the observation of nonlinear THz effects and a variety of nonlinear spectroscopies (such as two-dimensional spectroscopy), which are highly informative. This will find a wide spectrum of applications in science, engineering, biomedical research, environmental monitoring, and defense.

2.3 Efficient Nanolens in Full Electrodynamics [16, 24]

As an efficient nanolens, we have proposed a self-similar linear chain of several metal nanospheres with progressively decreasing sizes and separations [25]. The proposed system can be used for nanooptical detection, Raman characterization, nonlinear spectroscopy, nano-manipulation of single molecules or nanoparticles, and other applications. The second harmonic local fields form a very sharp nanofocus between the smallest spheres where these fields are enhanced by more than two orders of magnitude. This effect can be used for diagnostics and nanosensors. We have also obtained the first results on the Surface Enhanced Raman Scattering (SERS) in the nanosphere nanolens [24] where we show the SERS enhancement factor differ significantly from the commonly used fourth power of the local field enhancement. Recently, we have performed full electrodynamic modeling of the nanolenses [16]. We have confirmed the high predicted level of enhancement and found new electrodynamic resonances where the nanosphere aggregate works both as a plasmonic nanoantenna and as electrodynamic metal antenna.

2.4 Plasmonic Renormalization of Coulomb Interactions [14, 15]

A significant field of activity has study of the effects of the proximity to plasmonic systems on Coulomb interactions in electrons in molecules and semiconductors, i.e., plasmonic resonant renormalization of the Coulomb interactions. We have developed a general theory of the plasmonic enhancement of the many-body phenomena resulting in a closed expression for the surface plasmon-dressed Coulomb interaction [14, 15]. We have illustrated this theory by computing the dressed interaction explicitly for an important example of metal–dielectric nanoshells which exhibits a rich resonant behavior in magnitude and phase. This interaction is used to describe the nanoplasmonic-enhanced Förster resonant energy transfer (FR ET) between nanocrystal quantum dots near a metal/dielectric nanoshell. The effects of the nanoplasmonic renormalization of the Coulomb interaction are of great importance for electron-interaction effects such as electron scattering, Auger relaxation and ionization, chemical reactions, and many-electron kinetics. Ref. [14] has been chosen by the Editors of the New J. Phys. for the collection *The NJP Best of 2008*.

2.5 Time-Reversal Solution of the Problem of Spatio-Temporal Coherent Control on the Nanoscale [11, 20]

Our research has significantly focused on problem of controlling localization of the energy of ultrafast (femtosecond) optical excitation on the nanoscale. We have proposed and theoretically developed a distinct approach to solving this fundamental problem [26-32]. This approach, based on the using the relative phase of the light pulse as a functional degree of freedom, allows one to control the spatial-temporal distribution of the excitation energy on the nanometer-femtosecond scale. One of the most fundamental problems in nanoplasmonics and nanooptics generally is the spatio-temporal coherent control of nanoscale localization of optical energy. However, a key element was missing: an efficient and robust method to determine a shape of the controlling femtosecond pulse that would compel the femtosecond evolution of the nanoscale optical fields in a plasmonic system to result in the spatio-temporal concentration of the optical energy at a given nano-site within a required femtosecond interval of time. We have solved this problem by using the idea of the time-reversal [11, 20]. We have shown that by exciting a system at a given spot, recording the produced wave in one direction in the far zone, time reversing it and sending the produced plane wave back to the system leads to the required spatio-temporal energy localization. This method can be used both theoretically and experimentally to determined the required polarization, phase and amplitude modulation of the controlling pulses.

2.6 Optimized Concentration of Optical Energy in Tapered Nanoplasmonic Waveguide [[13]

In collaboration with D. Gramotnev (Queensland University of Technology, Brisbane, Australia), we have established the optimum shape of a tapered-rod plasmonic waveguide for the optimized nanolocalization of optical energy [13]. This, mostly computational, work allows one to eliminate the condition of adiabaticity. The maximum optical energy delivered to the tip of the structure is achieved when the rate of tapering slightly exceeds that imposed by the adiabatic condition.

2.7 Attosecond Nanoplasmonics [2, 17, 18]

In collaboration with M. Kling, U. Kleineberg, and F. Krausz et al. from Max Plank Institute for Quantum Optics (Garching, Germany) and Ludwig Maximilian University (Munich, Germany), we have theoretically developed a novel concept called Attosecond Nanoplasmonic Field Microscope [17]. It is based on the use of attosecond laser pulses synchronized with an intense, waveform-stabilized optical field driving a nanosystem. The attosecond pulses cause photoemission of electrons in a given phase of the optical excitation, which are accelerated in the local nanoplasmonic fields. This work sets the foundation of a novel direction in nanoplasmonics that is attosecond nanoplasmonics that studies that fastest phenomena existing at the nanoscale. There has been a recent progress in experimental work in this direction [2].

In a related development, we have shown that the carrier-envelope phase (CEP) of an excitation pulse significantly defines ultrafast responses of metal nanostructures in the regime of the above-threshold ionization (optical field emission) [18]. This suggests a way to build ultrasensitive detectors of the CEP, which is an important problem of the quantum optics.

2.8 Full Spatio-Temporal Control on Nanoscale [22]

In collaboration with K. Nelson (MIT), we have proposed an approach of full coherent control on the nanoscale [22]. This is a nanoplasmonic counterpart of the active phased array radar. It uses excitation of the plasmon polariton waves by independently exciting a set of nanoparticles on a thin metal layer by shaped laser pulses uses an array of pulse shapers. The surface plasmon polariton waves excited in such a way interfere to form a front converging to an arbitrarily defined nanoscale point. This approach can be used for a wide range of applications from ultramicroscopy to controlling computations on the nanoscale.

2.9 Criterion of Negative Refraction with Low Optical Losses [19]

We have derived a novel criterion that defines a possibility of a negative-index material that would have a negligible loss at a given, working frequency [19]. This criterion is rigorous and general, based on the fundamental principle of causality. It shows that to achieve a negative refraction, a significant loss must be present in the vicinity of the working frequency. This criterion will guide the further quest for the low-loss negative index materials worldwide.

2.10 Surface Enhanced Raman Scattering (SERS) [12, 33]

We have revisited theory of one of the most important phenomena in nanoplasmonics, Surface Enhanced Raman Scattering [12, 33]. This theory shows that the predicted levels of enhancement in the red spectral region are still several orders of magnitude less than the enhancement factors $\sim 10^{13} - 10^{14}$ observed experimentally. The difference may be due to the effects not taken into account by the theory: self-similar enhancement [25] or chemical enhancement [34].

Recently, an important development of SERS has been achieved with our participation. For the first time, the enhancing effect of nanolenses (see Sec. 2.3) have been observed [12]. This opens up a way to produce a reproducible, robust, and efficient substrate for SERS with very low background.

2.11 Plans for the Near Future

We will continue the collaborations with the experimental and theoretical groups that we have developed. Among the future projects, we will develop theory of the attosecond nanoplasmonics (see Sec. 2.6). Another group of projects is related to the time-reversal coherent control on the nanoscale proposed recently by us (see Sec. 2.1). There has been a new Focused Program by German Science Foundation *Ultrafast Nanooptics* recently started with more than 25 groups funded. This Program was to a significant extent induced by our DOE-sponsored work on ultrafast nanoplasmonics. We will continue to work actively in this direction to keep our leading positions. As a result of this collaboration, there a paper [35] submitted and under consideration in Nature Photonics.

Recently, the interest to SPASER, which we introduced in the framework of our first DOE-sponsored project, has tremendously increased. In response to the request by Nature Photonics, we have written a Commentary on SPASER [6]. We intend to revisit and further develop theory of SPASER on the basis of the density matrix approach for quantum dots coupled to the quantized surface plasmon field. We have recently submitted a paper [36] in which theory of SPASER is significantly developed.

A dramatic development in nonlinear nanoplasmonics reported recently has been the discovery of the high-harmonic generation by radiation from an oscillator (without the commonly used amplifiers) on a table top, using plasmonic enhancement in nanoantenna array [37]. We have recently written a News and Views article requested by Nature [5] describing the stunning horizons that this discovery opens up. Currently we are actively collaborating on this subject with the group of Dr. Matthias Kling (MPQ, Garching, Germany) providing theoretical ideas and support for the ongoing experiments.

One of the most promising directions of our work is ultrafast nanooptics in ultrastrong fields. In this research, we are actively collaborating with the Division of Attosecond and Ultrastrong Fields at Max Planck Institute for Quantum Optics (MPQ) (Garching, Germany) headed by Prof. F. Krausz where I have spent the last nine month on a sabbatical leave.

References

1. K. F. MacDonald, Z. L. Samson, M. I. Stockman, and N. I. Zheludev, *Ultrafast Active Plasmonics*, Nat. Phot. **3**, 55-58 (2009) (**Times Cited: 6**).
2. J. Q. Lin, N. Weber, A. Wirth, S. H. Chew, M. Escher, M. Merkel, M. F. Kling, M. I. Stockman, F. Krausz, and U. Kleineberg, *Time of Flight-Photoemission Electron Microscope for Ultrahigh Spatiotemporal Probing of Nanoplasmonic Optical Fields*, J. Phys.: Condens. Mat. **21**, 314005-1-7 (2009).
3. M. Durach, A. Rusina, and M. I. Stockman, *Giant Surface Plasmon Induced Drag Effect (SPIDEr) in Metal Nanowires*, arXiv:0907.1621 1-5 (2009).
4. M. I. Stockman, *Adiabatic Concentration and Coherent Control in Nanoplasmonic Waveguides* in *Plasmonic Nanoguides and Circuits*, edited by S. I. Bozhevolny (World Scientific Publishing, Singapore, 2008), p. 353-404.
5. M. I. Stockman, *Attosecond Physics - an Easier Route to High Harmony*, Nature **453**, 731-733 (2008).
6. M. I. Stockman, *Spasers Explained*, Nat. Phot. **2**, 327-329 (2008) (**Times Cited: 2**).
7. M. I. Stockman, *Ultrafast Nanoplasmonics under Coherent Control*, New J. Phys. **10** 025031-1-20 (2008) (**Times Cited: 2**).
8. A. Rusina, M. Durach, K. A. Nelson, and M. I. Stockman, *Nanoconcentration of Terahertz Radiation in Plasmonic Waveguides*, Opt. Expr. **16**, 18576-18589 (2008).
9. A. Rusina, M. Durach, K. A. Nelson, and M. I. Stockman, *Nanoconcentration of Terahertz Radiation in Plasmonic Waveguides*, arXiv:0808.1324 2008).

10. K. F. MacDonald, Z. L. Samson, M. I. Stockman, and N. I. Zheludev, *Ultrafast Active Plasmonics: Transmission and Control of Femtosecond Plasmon Signals*, arXiv:0807.2542 2008).
11. X. Li and M. I. Stockman, *Highly Efficient Spatiotemporal Coherent Control in Nanoplasmonics on a Nanometer-Femtosecond Scale by Time Reversal*, Phys. Rev. B **77**, 195109-1-10 (2008) (**Times Cited: 3**).
12. J. Kneipp, X. Li, M. Sherwood, U. Panne, H. Kneipp, M. I. Stockman, and K. Kneipp, *Gold Nanolenses Generated by Laser Ablation-Efficient Enhancing Structure for Surface Enhanced Raman Scattering Analytics and Sensing*, Anal. Chem. **80**, 4247-4251 (2008) (**Times Cited: 2**).
13. D. K. Gramotnev, M. W. Vogel, and M. I. Stockman, *Optimized Nonadiabatic Nanofocusing of Plasmons by Tapered Metal Rods*, J. Appl. Phys. **104**, 034311-1-8 (2008) (**Times Cited: 5**).
14. M. Durach, A. Rusina, V. I. Klimov, and M. I. Stockman, *Nanoplasmonic Renormalization and Enhancement of Coulomb Interactions*, New J. Phys. **10**, 105011-1-14 (2008).
15. M. Durach, A. Rusina, V. Klimov, and M. I. Stockman, *Nanoplasmonic Renormalization and Enhancement of Coulomb Interactions*, arXiv:0802.0229 2008).
16. J. Dai, F. Cajko, I. Tsukerman, and M. I. Stockman, *Electrodynamic Effects in Plasmonic Nanolenses*, Phys. Rev. B **77**, 115419-1-5 (2008) (**Times Cited: 6**).
17. M. I. Stockman, M. F. Kling, U. Kleineberg, and F. Krausz, *Attosecond Nanoplasmonic Field Microscope*, Nat. Phot. **1**, 539-544 (2007) (**Times Cited: 17**).
18. M. I. Stockman and P. Hewageegana, *Absolute Phase Effect in Ultrafast Optical Responses of Metal Nanostructures*, Appl. Phys. A **89**, 247-250 (2007).
19. M. I. Stockman, *Criterion for Negative Refraction with Low Optical Losses from a Fundamental Principle of Causality*, Phys. Rev. Lett. **98**, 177404-1-4 (2007) (**Times Cited: 36**).
20. X. Li and M. I. Stockman, *Time-Reversal Coherent Control in Nanoplasmonics*, arXiv:0705.0553 2007).
21. P. Hewageegana and M. I. Stockman, *Plasmonic Enhancing Nanoantennas for Photodetection*, Infrared Phys Techn **50**, 177-181 (2007) (**Times Cited: 3**).
22. M. Durach, A. Rusina, M. I. Stockman, and K. Nelson, *Toward Full Spatiotemporal Control on the Nanoscale*, Nano Lett. **7**, 3145-3149 (2007) (**Times Cited: 5**).
23. M. Durach, A. Rusina, K. Nelson, and M. I. Stockman, *Toward Full Spatio-Temporal Control on the Nanoscale*, arXiv:0705.0725 2007).
24. K. Li, M. I. Stockman, and D. J. Bergman, *Li, Stockman, and Bergman Reply to Comment On "Self-Similar Chain of Metal Nanospheres as an Efficient Nanolens"*, Phys. Rev. Lett. **97**, 079702 (2006).
25. K. Li, M. I. Stockman, and D. J. Bergman, *Self-Similar Chain of Metal Nanospheres as an Efficient Nanolens*, Phys. Rev. Lett. **91**, 227402-1-4 (2003) (**Times Cited: 196**).
26. M. I. Stockman, S. V. Faleev, and D. J. Bergman, *Coherent Control of Femtosecond Energy Localization in Nanosystems*, Phys. Rev. Lett. **88**, 67402-1-4 (2002). (**Times Cited: 70**).
27. M. I. Stockman, S. V. Faleev, and D. J. Bergman, *Coherently Controlled Femtosecond Energy Localization on Nanoscale*, Appl. Phys. B **74**, S63-S67 (2002).
28. M. I. Stockman, S. V. Faleev, and D. J. Bergman, *Coherently-Controlled Femtosecond Energy Localization on Nanoscale*, Appl. Phys. B **74**, 63-67 (2002).
29. M. I. Stockman, D. J. Bergman, and T. Kobayashi, in Proceedings of SPIE: Plasmonics: Metallic Nanostructures and Their Optical Properties, edited by N. J. Halas, *Coherent Control of Ultrafast Nanoscale Localization of Optical Excitation Energy* (SPIE, San Diego, California, 2003), Vol. 5221, p. 182-196
30. M. I. Stockman, S. V. Faleev, and D. J. Bergman, in Ultrafast Phenomena XIII, *Coherently-Controlled Femtosecond Energy Localization on Nanoscale* (Springer, Berlin, Heidelberg, New York, 2003)
31. M. I. Stockman, D. J. Bergman, and T. Kobayashi, *Coherent Control of Nanoscale Localization of Ultrafast Optical Excitation in Nanosystems*, Phys. Rev. B **69**, 054202-10 (2004) (**Times Cited: 25**).
32. M. I. Stockman and P. Hewageegana, *Nanolocalized Nonlinear Electron Photoemission under Coherent Control*, Nano Lett. **5**, 2325-2329 (2005) (**Times Cited: 9**).
33. M. I. Stockman, in Springer Series Topics in Applied Physics, edited by K. Kneipp, M. Moskovits and H. Kneipp, *Surface Enhanced Raman Scattering – Physics and Applications* (Springer-Verlag, Heidelberg New York Tokyo, 2006), p. 47-66
34. J. Jiang, K. Bosnick, M. Maillard, and L. Brus, *Single Molecule Raman Spectroscopy at the Junctions of Large Ag Nanocrystals*, J. Phys. Chem. B **107**, 9964-9972 (2003).
35. T. Utikal, M. I. Stockman, A. P. Heberle, M. Lippitz, and H. Giessen1, *Ultrafast Coherent Control of the Linear and Nonlinear Optical Responses of a Hybrid Plasmonic-Photonic System*, Nature Physics (Submitted: Under Consideration) (2009).
36. M. I. Stockman, *Spaser as Nanoscale Quantum Generator and Ultrafast Amplifier*, Nat. Phot. (Submitted: Under Consideration) (2009).
37. S. Kim, J. H. Jin, Y. J. Kim, I. Y. Park, Y. Kim, and S. W. Kim, *High-Harmonic Generation by Resonant Plasmon Field Enhancement*, Nature **453**, 757-760 (2008).

Laser-Produced Coherent X-Ray Sources

Donald Umstadter, Physics and Astronomy Department, 212 Ferguson Hall, University of Nebraska, Lincoln, NE 68588-0111, dpu@unlserve.unl.edu

Program Scope

In this project, we experimentally and theoretically explore the physics of novel x-ray sources, based on the interactions of ultra-high-intensity laser light with matter. Laser-accelerated electron beams are used to produce x-rays in the energy range 1-100 keV using techniques such as Thomson scattering off a second laser pulse, or betatron oscillations in a laser-produced ion channel. Such photon sources can provide information on the structure of matter with atomic-scale resolution, on both the spatial and temporal scale lengths–simultaneously. Moreover, because the electron beam is accelerated by the ultra-high gradient of a laser-driven wakefield, the combined length of both the accelerator and wiggler regions is only a few millimeters. The x-ray source design parameters are sub-angstrom wavelength, femtosecond pulse duration, and university-laboratory–scale footprint. The required components, laser system (delivering peak power >100 TW at a repetition rate of 10 Hz) and electron accelerator (delivering beams with energy up to 800 MeV and divergence of 2 mrad) have been developed and characterized.

This project involves the physics at the forefront of relativistic plasma physics and beams, as well as relativistic nonlinear optics. Applications include the study of ultrafast chemical, biological and physical processes, such as inner-shell electronic or phase transitions. Industrial applications include non-destructive evaluation, large-standoff–distance imaging of cracks, remote sensing and the detection of shielded nuclear materials.

Recent Results

We have studied x-ray generation from betatron emission, improved the performance of the laser-wakefield accelerator by implementation of the optical injection technique, refined the procedure for overlapping the electron beam with the scattering beam for Thomson scattering, and increased the x-ray detection signal-to-noise ratio.

Generation of betatron x-rays from plasma channels

A high-power laser pulse propagating through plasma expels electrons due to the transverse ponderomotive force. The wakefield driven by the laser pulse accelerates electrons to MeV energies. In the ion channel produced by the laser pulse, the relativistic electrons execute betatron motion and radiate x-rays. Depending on the regime in which the electrons are accelerated, the x-rays may be produced by a Maxwellian electron beam or a quasi-monoenergetic beam. The oscillatory motion of the electrons in the ion channel has an angular frequency $\omega_b = \omega_p / \sqrt{2\gamma}$ where $\omega_p = \sqrt{n_e e^2 / m\varepsilon_0}$ is the electron plasma frequency for an electron density n_e. The period motion of motion of electrons with a period λ_b in a wiggler with strength parameter $K = \gamma k_b r_0$ leads to the production of x-rays. Two regimes are of particular interest (i) $K \ll 1$, the motion is akin to an undulator with radiation being primarily emitted at the fundamental frequency, $\omega_f = \sqrt{2}\omega_p \gamma^{3/2}$ (ii) $K >> 1$ corresponds to the wiggler regime, wherein broadband radiation is emitted with a cutoff frequency $\omega_c = (3/2)\gamma^3 c r_0 k_b^2$. The spectral characteristics of the emitted radiation depend on the initial electron energy as well as the plasma channel including the initial coordinate.

Prior work on betatron emission has been performed in high-density channels with lower energy polychromatic electron beams.[1] We are now able to produce high-quality electron beams and extended plasma channels that will efficiently produce x-rays. Preliminary experiments have been performed to study this process and a forward directed beam of x-rays observed. High-power laser pulses are focused onto a gas jet and produce energetic electron beams by the process of laser wakefield acceleration. These electrons then oscillate in the plasma channel and

[1] A. Rousse, K. Ta Phuoc, R. Shah, A. Pukhov, E. Lefebvre, V. Malka, S. Kiselev, F. Burgy, J.-P. Rousseau, D. Umstadter, and D. Hulin, "Production of a keV X-Ray Beam from Synchrotron Radiation in Relativistic Laser-Plasma Interaction," *Phys. Rev. Lett.* **93**, 135005 (2004).

radiate x-rays. These are detected with sensitive image plate detectors. The x-rays excite metastable states in the detector which can then be read off with a laser. A 2-μm thick aluminum foil is used to protect the plates from infra-red light. The channeling of the laser beam through the plasma is optically imaged. A strong magnetic field is used to measure the energy of the electrons and also ensure that the x-ray detector does not see any electrons. A mesh is placed along the path of the x-rays for source size measurements. Using this setup we have observed x-rays in the forward direction. The results are shown in Figure 1. With a monoenergetic electron beam, a forward cone of x-rays is observed. Simple attenuation measurements with filters indicate a mean energy of 5 keV.

Optical injection of electrons into wakefield plasma waves

The electrons that are accelerated by laser wakefields can be injected either by internal or external means. In the latter case, a separate (external) electron accelerator, such as an RF gun, pre-accelerates electrons that are focused into the wakefield plasma wave. This method, however, suffers from problems such as a mismatch between the lengths of the electron bunch and the accelerator bucket, as well as timing jitter.

In the case of internal injection, the electrons come from the plasma used to support the wakefield. The greatest degree of accelerator stability, control and tunability can be achieved by means of active injection, in which the means of electron injection is separated from that of plasma wave generation.[2] In one such approach, the case of optical injection, a separate laser pulse, synchronized with the wakefield driver laser pulse, acts to kick electrons into the proper phase to become trapped by the wakefield.[2]

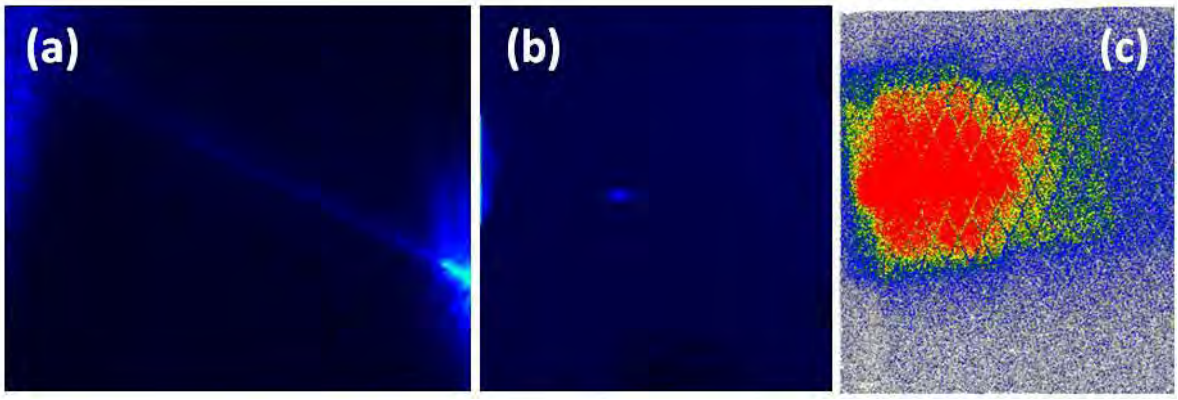

Figure 1: Observation of betatron emission from laser-produced plasma channels. (a) laser channel observed by imaging fundamental light scattered from the channel (b) monoenergetic electron beam with energy of 150 MeV (c) forward directed cone of x-rays superimposed on mesh. The x-ray energy from filtered measurements is ~5 keV.

We have recently demonstrated this technique experimentally using the experimental setup illustrated in Figure 2. A second synchronized high intensity laser pulse (Pulse 2), from the same laser system, was directed in an almost counter-propagating direction (170 degrees) to the direction of the wakefield drive pulse (Pulse 1), and overlapped spatially with the wakefield. In the current experiments a 3 mm supersonic nozzle is used. For initial observation of optical injection the two pulses interact in the center of the nozzle as shown. The plasma density is chosen to be 5×10^{18} cm^{-3} and the laser power used in these experiments is 25 TW. Also, the nozzle is translated by 500 μm from the optimal position for generation of self-injected electron beams to ensure that Pulse 1 by itself does not produce an electron beam. Pulse 3 is a low power beam used for shadowgraphy. A fluorescent screen was placed several centimeters downstream from the interaction point and a magnet used for energy dispersion. An aluminum foil placed in front of the screen prevented the laser beam from reaching the screen.

[2] D. Umstadter, J. K. Kim, and E. Dodd, "Laser Injection of Ultrashort Electron Pulses into Wakefield Plasma Waves," *Phys. Rev. Lett.* **76**, 2073 (1996).

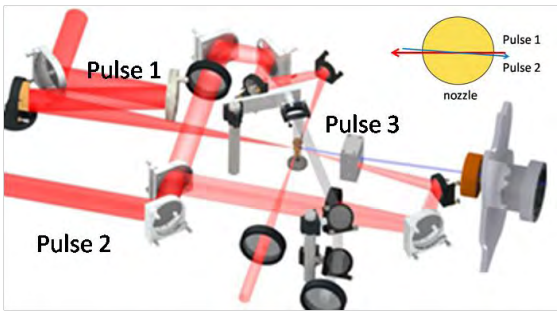

Figure 2: Schematic of the experimental setup to obtain electron beams by optical injection. Pulse 1 drives a wake in the supersonic nozzle while pulse 2 injects electrons into the wake at the correct phase. Pulse 3 is a low power beam used for shadowgraphy in order to overlap Pulses 1 and 2. The inset shows the interaction point where the two pulses interact in a nearly counterpropagating geometry.

Figure 3 shows a series of energy resolved electron spectra, comprised of CCD camera images of the fluorescent screen on different laser shots, which show no presence of electron beam when injection pulse was not present. In Figure 4 is shown a series of CCD camera images of the fluorescent screen on different laser shots showing the presence of an electron beam when the injection pulse was present. For the beams depicted above, the energy is 245 MeV with an angular divergence of 2.8 mrad.

A significant advantage of the injection technique is that it permits tunability of the source by varying the injection point. In our experiments this is done by either changing the temporal delay which alters the point at which injection occurs or by translating the supersonic nozzle. The former is preferable because in the latter case the wake produced by the first pulse gets modified. By varying the delay we could tune the electron energy from 160 MeV to 315 MeV with beam quality comparable to what is shown for 245 MeV.

Figure 3: A series of energy resolved electron spectra, comprised of CCD camera images of the fluorescent screen on different laser shots showing no presence of electron beam when injection pulse was not present.

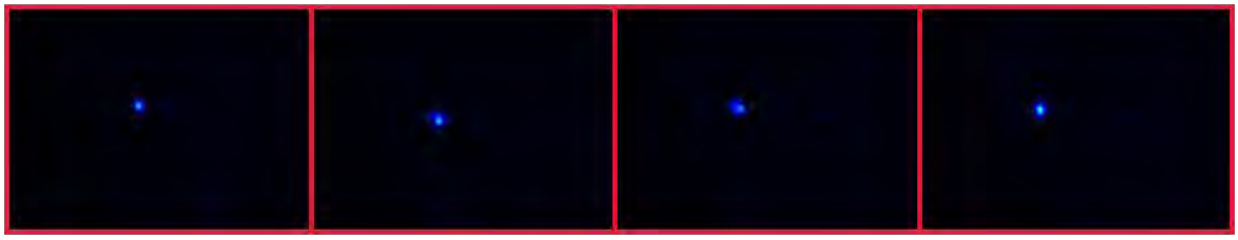

Figure 4: Energy resolved electron spectra, comprised of CCD camera images of the fluorescent screen showing presence of electron beam when injection pulse was present. The electron beam energy was measured to be 245 MeV with a divergence of 2.8 mrad and beam charge of 400 pC.

Passive self-injection occurs when the wakefield is driven to sufficient amplitude to cause wavebreaking, which results in electrons becoming trapped in the wakefield. This method is most successful with use of ultrashort laser pulses in the so-called bubble regime, in which a single acceleration bucket is formed. We have found a set of parameters, in which the laser and plasma wave parameters are matched. Last year we reported the generation of stable high energy (400 MeV), low angular divergence (< 2 mrad) beams by use of a 4-mm long plasma. We have since then obtained electron beams with energy up to 0.8 GeV, by extending the length of the plasma to 1 cm.

These improvements in the performance of the laser wakefield electron accelerator will benefit the generation of monoenergetic hard x-rays.

Current Activities and Future Plans

The study of betatron x-rays from the oscillation of relativistic electrons in plasma channels will be further investigated. In particular, we will seek to identify the characteristics of betatron radiation in the bubble regime of wakefield acceleration. Prior studies indicate that in the self-modulated regime a broadband emission spectrum is observed in the forward direction with an angular spread of 20-50 mrad. We have observed betatron emission with quasi-monoenergetic beam. As described previously, the betatron emission depends on both the plasma characteristics as well as the acceleration of electrons by the laser wakefield. In the regime of quasi-monoenergetic electron acceleration, the electron energies are extremely large (γ = 20-1,600) and tunable, making for a broadband, tunable x-ray source.

Proof-of-principle experiments are currently underway to use the electron beam and laser pulse discussed above to also generate ultrashort pulses of 100-keV energy x-rays by means of Thomson scattering. All optical elements have been aligned to focus the scattering laser pulse (in a counter-propagating direction) to overlap with the electron pulse at the exit of the accelerator. Also, the requisite x-ray detectors and spectrometers have now been tested an integrated into the experiment. Recently, the detection sensitivity has been significantly improved (by a factor of 10^3), and the background noise level has been suppressed.

The Diocles laser system is currently being upgraded in peak power by an order of magnitude, to the PW level. An additional amplifier is being added, which will be pumped with four Nd:Glass pump lasers, each producing 25 J of pump power, to amplify the 800-nm beam from the current 5 J to 50 J per pulse. The amplified pulse will be compressed to 30 fs with output energy of 30 J. The four pump lasers, an additional compressor chamber, and the requisite larger diffraction gratings (60 cm x 50 cm) have already been manufactured and delivered to UNL. Once the PW amplifier upgrade is completed, the system's repetition rate will be 0.1 Hz, the highest of any planned or existing PW laser in the U.S. This increase will enable access to the highly relativistic Thomson scattering regime.

DOE-Sponsored Publications (published within last three years)

1. Donald Umstadter, Sudeep Banerjee, Vidya Ramanathan, Nathan Powers, Nathaniel Cunningham, and Nate Chandler-Smith, "Development of a Source of Quasi-Monochromatic MeV Energy Photons," CP1099, *Application of Accelerators in Research and Industry: 20th International Conference*, edited by F. D. McDaniel and B. L. Doyle (AIP, 2009), p. 606.
2. Scott M. Sepke, Donald P. Umstadter, "Analytical solutions for the electromagnetic fields of flattened and annular Gaussian laser modes. I. Small F-number laser focusing," *JOSA B* **23**, 2157-2165 (2007).
3. D. Umstadter, S.Y. Chen, A. Maksimchuk, K. Flippo, V.Y. Bychenkov, Y. Sentoku, and K. Mima, "Short pulses of energetic electrons and ions produced by high-intensity lasers for laser fusion," *Current Trends in International Fusion Research: Proceedings NRC Research Press*, National Research Council of Canada, Ottawa, ON K1A OR6, Canada (2007), p. 389.
4. S. Chen, M. Rever, P. Zhang, W. Theobald, and D. Umstadter, "Observation of relativistic cross-phase modulation in high-intensity laser-plasma interactions," *Phys. Rev. E* **74**, 046406 (2006).
5. Scott M. Sepke, Donald P. Umstadter, "Exact analytical solution for the vector electromagnetic field of Gaussian, flattened Gaussian, and annular Gaussian laser modes," *Optics Lett.* **31**, 1447-1449 (2006).
6. Scott M. Sepke and Donald P. Umstadter, "Analytical solutions for the electromagnetic fields of tightly focused laser beams of arbitrary pulse length," *Optics Lett.* **31**, 2589-2591 (2006).
7. D. Umstadter, S. Banerjee, S. Chen, S. Sepke, A. Maksimchuk, A., Valenzuela, A. Rousse, R. Shah, and K. Ta Phuoc, "Generation of ultrashort pulses of electrons, X-rays and optical pulses by relativistically strong light," AIP Conference Proceedings, *Superstrong Fields in Plasma: Third International Conference on Superstrong Fields in Plasmas*, vol. 827 (2006), p. 86.
8. Scott M. Sepke, Donald P. Umstadter, "Analytical solutions for the electromagnetic fields of flattened and annular Gaussian laser modes. II. Large F-number laser focusing," *JOSA B* **23**, 2166-2173 (2006).
9. Scott M. Sepke, Donald P. Umstadter, "Analytical solutions for the electromagnetic fields of flattened and annular Gaussian laser modes. III. Arbitrary length pulses and spot sizes," *JOSA B* **23**, 2295-2302 (2006).

Combining High Level *Ab Initio* Calculations with Laser Control of Molecular Dynamics

Thomas Weinacht
Department of Physics and Astronomy
Stony Brook University
Stony Brook, NY
tweinacht@sunysb.edu

and

Spiridoula Matsika
Department of Chemistry
Temple University
Philadelphia, PA
smatsika@temple.edu

1 Program Scope

We use intense, shaped, ultrafast laser pulses to control molecular dynamics and high level *ab initio* calculations to interpret and guide the control. We are applying the techniques and understanding we have developed to molecular wave function imaging and pulse shape spectroscopy.

2 Recent Progress

2.1 Controlling Molecular Isomerization

Isomerization plays a crucial role in fundamental processes such as vision and combustion, and there is substantial interest in controlling isomerization from the perspective of molecular switches. We have used shaped ultrafast laser pulses in the deep ultraviolet to control the ring opening isomerization of 1,3-cyclohexadiene (CHD) to form 1,3,5-hexatriene (HT). The experiments are performed with a gas phase sample, and the isomerization yield is probed with dissociative ionization driven by a time-delayed, intense infrared laser pulse[1]. We find that a shaped pulse yields a ~ 37 % increase in the isomerization over an unshaped laser pulse. Differences in the electronic structure of the ions for the two isomers, as shown by *ab initio* calculations, result in very different fragmentation products following strong-field ionization, and we use this to monitor control over the isomerization of molecules such as CHD in the gas phase. We carried out multireference perturbation theory calculations on the ionic states of CHD as a function of the C-C bond breaking, which is representative of the reaction coordinate for the isomerization. The calculations show how the gap between the excited cationic states changes along the reaction coordinate, giving rise to different fragmentation patterns. As strong field ionization is very sensitive to the effective ionization potential, the smaller energy gap between the ground and first excited states of HT^+ leads to population of excited ionic states during ionization in the strong IR pulse leading to fragmentation, whereas the larger gap in CHD^+ leads primarily to excitation of the ground ionic state. Our measurements and calculations demonstrate how one can use strong-field dissociative ionization as a diagnostic tool for closed-loop control experiments in the gas phase when the different final states have identical atomic composition but different geometries.

2.2 Ionic States of Cytosine as a Tool to Monitor its Excited State Dynamics

The use of dissociative ionization as a probe of molecular configuration seems to be a general tool for molecules with low lying resonances in the cation. Measurements we have performed in phenyl acetylene in analogy to our CHD measurements indicate that there are significant conformational changes occurring on femtosecond timescales following excitation at 260 nm. We are currently working on applying this technique to the DNA bases, for which Matsika has performed detailed calculations of the excited neutral states.[2;3]

All DNA/RNA bases have very short excited state lifetimes which are attributed to relaxation pathways through conical intersections.[4] This has been supported by several theoretical

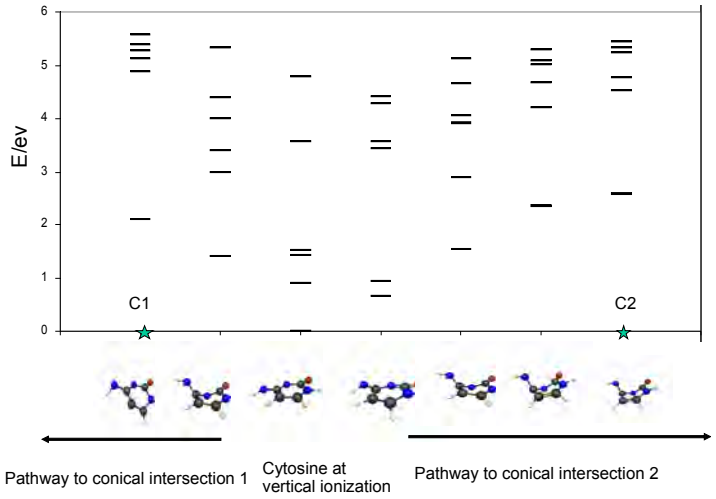

Figure 1: Excited states of the cytosine radical cation, calculated using CASSCF, at various critical points along two relaxation pathways of the neutral. After excitation on the S_1 surface of neutral cytosine, two pathways can lead to conical intersections C1 and C2.

studies, which show the existence of conical intersections in all nucleobases. In cytosine two different pathways have been calculated that can lead to radiationless relaxation through conical intersections. The *ab initio* calculations, however, cannot predict whether both pathways are accessible or whether only one dominates the dynamics. Dissociative ionization after UV excitation can provide very useful information of the excited state dynamics. In order to interpret the measurements, we have performed multiconfigurational calculations (CASSCF) of the ionic spectrum for cytosine at critical points along two relaxation pathways of the neutral. These calculations, shown in Fig. 1, reveal that the gap between ground and excited states in the cation differs significantly along the relaxation pathways, providing great promise for observing dynamics and differentiating between the various pathways. Furthermore, the IP changes significantly along the relaxation pathways, suggesting that the ion yields for both the parent and fragment ions will show dramatic changes as a result of the neutral dynamics.

2.3 Towards Pulse Shape Spectroscopy

Many of our control experiments lead naturally to the development of 'pulse shape spectroscopy', where rather than measuring a molecular fragment yield or emission/absorption as a function of laser frequency, one measures the yield or emission/absorption as a function of laser pulse shape (spectral phase)[5]. While these types of measurements may offer a wealth of information regarding molecular structure and dynamics, an important hurdle to overcome is the interpretation of the measurements for strong field shaped pulses, which typically show a complicated dependence on many pulse shape parameters which are coupled[6]. Our approach is to tackle the problem from both sides of the complexity spectrum, interpreting closed loop learning control experiments with the aid of molecular structure and wave packet calculations, as well as performing simple pulse shape parameter scans, where the interpretation of the measurements can borrow from established techniques. In terms of the second approach, we are currently pursuing two dimensional (2D) Fourier transform electronic spectroscopy experiments[7] in the deep ultraviolet with the aid of our recently developed acousto-optic modulator based deep UV pulse shaper[8]. The pulse shaper can be used to generate the excitation pulse pair, with arbitrary control over the relative phase and delay of the pulse and very high phase stability (measured to be better than $\lambda/200$ at 260 nm, which corresponds to a timing jitter of less than 10 attoseconds). With arbitrary control over

the phase and delay between the pulses, we can work in a rotating frame, sampling at rates much lower than the laser frequency, and we can also implement phase cycling for improved data quality[9;10]. Two dimensional spectroscopy is a natural starting point for pulse shape spectroscopy, as there is an established framework for interpreting the measurements and pulse shaping greatly simplifies the experimental apparatus and allows for increased freedom in the excitation pulse sequence.

Performing 2D spectroscopy in the deep UV allows us to work on the DNA bases, for which excited state dynamics on the S_1 surface is of particular interest as discussed above. Figure 2 shows our recently measured 2D UV spectrum for adenine, with a comparison between data taken with and without phase cycling. Panel (a) shows data taken without phase cycling and panel (b) shows data taken with phase cycling. Both data sets were taken with the same number of laser shots and pulse energies, so they can be compared directly. As is clear from the figure, phase cycling improves the signal to noise in the data.

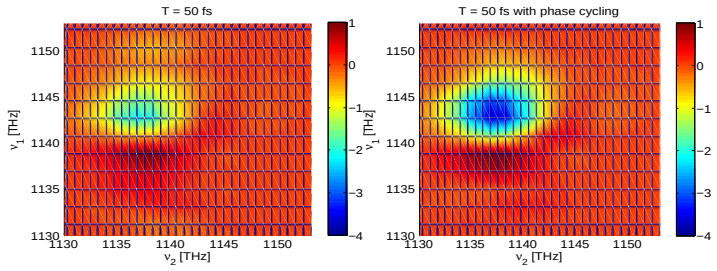

Figure 2: Real component of the 2D spectrum of Adenine in water (a) without phase cycling, (b) with four-phase-cycling.

3 Future Plans

3.1 Developing Pulse Shape Spectroscopy

We are currently working on extending our 2D UV spectroscopy measurements to include probing at different wavelengths. This will allow us to follow wave packet dynamics on the excited state far from the Franck Condon point. Our current experimental apparatus allows us to easily probe at $\sim 390\ nm$ and $\sim 780\ nm$. If we are able to measure interesting dynamics at these colors, we will also pursue measurements throughout the UV and visible, generating a broadband probe via continuum generation[11]. Ultimately, we would like to extend our measurements to more complicated pulse shape parameterizations, including multiple pulses with different relative phases, which are easily programmed onto the laser via our pulse shaper.

3.2 UV Pump IR Probe Experiments in DNA Bases

We have recently upgraded our molecular beam for the UV pump IR probe experiments in order to be able to perform measurements on the DNA bases. The cationic state calculations show promise for being able to track the dynamics in the neutral excited state via dissociative ionization in analogy to the CHD pump-probe measurements. This should allow us to distinguish between the allowed pathways that the electronic structure calculations predict. Furthermore, we are interested in trying to influence the dynamics in the excited state by shaping the UV excitation pulse as we have done in CHD.

3.3 Time-Dependent Nuclear Dynamics

We are also working on extending our *ab initio* calculations to include time-dependent nuclear dynamics. This will enable us to interpret the dynamical behavior of the systems observed experimentally. It will also provide us with the tools to understand the control mechanisms in the future. Standard wave-packet propagation methods are computationally intensive and are usually restricted to a small number of degrees of freedom, so these methods are of limited applicability for studying the polyatomic systems we are interested in. The multiconfigurational time-dependent Hartree method (MCTDH) developed by Manthe, Meyer and Cederbaum is a more appropriate choice since it can be used with more degrees of freedom.[12] In MCTDH the wavefunction is expressed as an expansion of many configurations, where each configuration is built as a Hartree product of time-dependent single-particle functions. We are working on using this method with the potential energy surfaces obtained from our ab initio calculations.

References

[1] W. Fuß, W. E. Schmid, and S. A. Trushin, J. Chem. Phys. **112**, 8347 (2000).

[2] S. Matsika, J. Phys. Chem. A **108**, 7584 (2004).

[3] K. A. Kistler and S. Matsika, J. Phys. Chem. A **111**, 2650 (2007).

[4] C. E. Crespo-Hernandez, B. Cohen, P. M. Hare, and B. Kohler, Chem. Rev. **104**, 1977 (2004).

[5] T. Seideman and R. J. Gordon, Advances in Chemical Physics **140**, 2 (2008).

[6] D. Cardoza, C. Trallero-Herrero, F. Langhojer, H. Rabitz, and T. Weinacht, J. Chem. Phys. **122**, 124306 (2005).

[7] D. Jonas, Annu. Rev. Phys. Chem. **54**, 425 (2003).

[8] B. J. Pearson and T. Weinacht, **15**, 4385 (2007).

[9] P. F. Tian, D. Keusters, Y. Suzaki, and W. S. Warren, Science **300**, 1553 (2003).

[10] S. H. Shim and M. T. Zanni, Physical Chemistry Chemical Physics **11**, 748 (2009).

[11] P. F. Tekavec, J. A. Myers, K. L. M. Lewis, and J. P. Ogilvie, Optics Letters **34**, 1390 (2009).

[12] G. A. Worth, H.-D. Meyer, and L. S. Cederbaum, *Multidimensional Dynamics Involving a Conical Intersection: Wavepacket Calculations Using the MCTDH Method* (World Scientific, Singapore, 2004), p. 583.

4 Publications of DOE Sponsored Research

- "Interpreting Ultrafast Molecular Fragmentation Dynamics with *ab initio* Calculations", C. Trallero, B. J. Pearson, T. Weinacht, K. Gilliard and S. Matsika, *J. Chem. Phys.*, **128**, 124107, (2008)
- "Closed-Loop Learning Control of Isomerization using Shaped Ultrafast Laser Pulses in the Deep Ultraviolet", M. Kotur, T. Weinacht, B. J. Pearson and S. Matsika *J. Chem. Phys.*, **130**, 134311, (2009)

Cold and ultracold polar molecules

Jun Ye

JILA, National Institute of Standards and Technology and University of Colorado

Boulder, Colorado 80309-0440

Ye@jila.colorado.edu

Study of ultracold molecules promises important prospects such as novel control of chemical reactions and molecular collisions, precision measurement of fundamental physical properties, and new methods for quantum information processing and simulations of quantum states of matter. A variety of chemically interesting molecular species can be prepared in a single internal state at temperatures of a few milliKelvins. Located in a magnetic trap and polarized under a uniform electric field, these molecules now allow explorations of low-energy scatterings near the quantum threshold and they will be subject to studies of collision and reaction dynamics that are dominated by long-range, anisotropic dipolar interactions.

A quantum degenerate gas of polar molecules will greatly facilitate these research activities. In collaboration with Deborah Jin, we have achieved a high phase-space-density polar molecular gas in the absolute ro-vibrational ground state. These molecules are confined in an optical trap, with a density of 10^{12} cm^{-3} at a temperature of 300 nK and a measured permanent electric dipole moment of 0.55 Debye. By preparing these molecules in a single quantum state including the nuclear spin, we are now studying state-specific chemical reactions at ultralow temperatures. Novel dipolar collisions between molecules have been discovered. In addition to exploring molecular dynamics and reactions in the quantum regime with manifestly long-range, anisotropic dipolar characters, these highly dense polar molecules will open the door to studies of new quantum phase transitions.

Recent publications:

[1] B. C. Sawyer, B. L. Lev, E. R. Hudson, B. K. Stuhl, M. Lara, J. L. Bohn, and J. Ye, "Magneto-electrostatic trapping of ground state OH molecules," Phys. Rev. Lett. 98, 253002 (2007).

[2] B. C. Sawyer, B. K. Stuhl, B. L. Lev, J. Ye, and E. R. Hudson, "Mitigation of loss within a molecular Stark decelerator," Euro. Phys. J. D 48, 197 – 209 (2008).

[3] E. A. Shapiro, A. Pe'er, J. Ye, and M. Shapiro, "Piecewise adiabatic population transfer in a molecule via a wave packet," Phys. Rev. Lett. 101, 023601 (2008).

[4] B. C. Sawyer, B. K. Stuhl, D. Wang, E. Yeo, and J. Ye, "Molecular beam collisions with a magnetically-trapped target," Phys. Rev. Lett. 101, 203203 (2008).

[5] B. K. Stuhl, B. C. Sawyer, D. Wang, and J. Ye, "A magneto-optical trap for polar molecules," Phys. Rev. Lett. 101, 243002 (2008).
[6] L. D. Carr, D. DeMille, R. Krems, and J. Ye, "Cold and Ultracold Molecules – Science, Technology, and Applications," New. J. Phys. 11, 055049 (2009).
[7] S. Ospelkaus, K.-K. Ni, M. H. G. de Miranda, B. Neyenhuis, D. Wang, S. Kotochigova, P. S. Julienne, D. S. Jin, and J. Ye, "Ultracold polar molecules near quantum degeneracy," Faraday Discussions, DOI: 10.1039/B821298H, Royal Society of Chemistry, UK (2009).

Author Index and List of Participants

Author Index

Author Index

Author Index

Author Index

Author Index

Participants

Mark Bannister
Oak Ridge National Laboratory
PO Box 2008, Bldg 6010, MS-6372
Oak Ridge, TN 37831-6372
Phone: 865-574-4700
E-Mail: bannisterme@ornl.gov

Matt Beard
National Renewable Energy Laboratory
1617 Cole Blvd.
Golden, CO 80401
Phone: 303-384-6781
E-Mail: matt.beard@nrel.gov

Ali Belkacem
Lawrence Berkeley National Laboratory
MS: 2R0100
Berkeley, CA 94720
Phone: 510 486 7778
E-Mail: abelkacem@lbl.gov

Itzhak Ben-Itzhak
J.R. Macdonald Laboratory
Kansas State University
Department of Physics
Manhattan, Kansas 66506
Phone: 785-532-1636
E-Mail: ibi@phys.ksu.edu

Nora Berrah
Western Michigan University
Physics Department
Kalamazoo, MI 49008
Phone: 269 387 4955
E-Mail: nora.berrah@wmich.edu

Mike Bogan
SLAC National Accelerator Laboratory
PULSE
2575 Sand Hill Rd. Mail Stop 59
Menlo Park, CA 94025
Phone: 650 926-2731
E-Mail: mbogan@SLAC.Stanford.EDU

John Bohn
JILA, University of Colorado
UCB 440
Boulder, CO 80305
Phone: 303-492-5426
E-Mail: bohn@murphy.colorado.edu

Philip Bucksbaum
SLAC
2575 Sand Hill Road
Menlo Park, CA 94025
Phone: 650-926-5337
E-Mail: phb@slac.stanford.ed

Michael Casassa
DOE BES
19901 Germantown Road
Germantown, MD 20874
Phone: 301-903-0448
E-Mail: michael.casassa@science.doe.gov

Zenghu Chang Chang
Kansas State University
116 Cardwell Hall
Manhattan, KS 66506
Phone: (785) 5321621
E-Mail: chang@phys.ksu.edu

Shih-I Chu
University of Kansas
Dept. of Chemistry, 2010 Malott Hall
Lawrence, Kansas 66045
Phone: 785-864-4094
E-Mail: sichu@ku.edu

Charles Cocke
Kansas State University
Physics Department
Manhattan, KS 66506
Phone: 785 532 1609
E-Mail: cocke@phys.ksu.edu

Robin Côté
University of Connecticut
2152 Hillside Road, U-3046
Storrs, CT 06269-3046
Phone: (860) 486 4912
E-Mail: rcote@phys.uconn.edu

Steven Cundiff
NIST/JILA
440 UCB
Boulder, CO 80516
Phone: 303-492-7858
E-Mail: cundiffs@jila.colorado.edu

Participants

Alexander Dalgarno
Harvard University
CFA,60 Garden Street
Cambridge, MA 02138
Phone: 617 495 4403
E-Mail: adalgarno@cfa.harvard.edu

David DeMille
Yale University
Physics Department
P.O. Box 208120
New Haven, CT 06520
Phone: 203-432-3833
E-Mail: david.demille@yale.edu

Brett DePaola
J. R. Macdonald Laboratory
Kansas State University
116 Cardwell Hall
Manhattan, KS 66506
Phone: 785-532-6777
E-Mail: depaola@phys.ksu.edu

Louis DiMauro
The Ohio State University
5441 Dublin Road
Dublin, OH 43016
Phone: 614-688-5726
E-Mail: dimauro@mps.ohio-state.edu

Todd Ditmire
University of Texas at Austin
1 University Station #C1600
Austin, tX 78712
Phone: 512-471-3296
E-Mail: tditmire@physics.utexas.edu

John Doyle
Harvard University
17 Oxford Street
Cambridge, MA 02138
Phone: 617-495-3201
E-Mail: john.m.doyle@gmail.com

Robert Dunford
Argonne National Laboratory
991 Huntleigh Dr.
Naperville, IL 60540
Phone: 630-369-4258
E-Mail: dunford@anl.gov

Joseph Eberly
University of Rochester
600 wilson blvd.
rochester, ny 14627
Phone: 585-275-4351
E-Mail: eberly@pas.rochester.edu

Brett Esry
J.R. Macdonald Lab
Kansas State University
116 Cardwell Hall
Manhattan, KS 66506
Phone: 785-532-1620
E-Mail: esry@phys.ksu.edu

Jim Feagin
Cal State Univ Fullerton
Physics Department
Fullerton, CA 92834
Phone: 657-278-4827
E-Mail: jfeagin@fullerton.edu

Kelly Gaffney
Stanford/SLAC
2575 Sand Hill Rd
Menlo Park, CA 94025
Phone: 650-248-8869
E-Mail: kgaffney@slac.Stanford.edu

Thomas Gallagher
University of Virginia
Department of Physics
Charlottesville, VA 22904
Phone: 434 924 6817
E-Mail: tfg@virginia.edu

Oliver Gessner
Lawrence Berkeley National Laboratory
1 Cyclotron Road
Berkeley, CA 94720
Phone: 510-486-6929
E-Mail: ogessner@lbl.gov

Phillip Gould
University of Connecticut
Physics Dept. U-3046, 2152 Hillside Rd.
Storrs, CT 06269-3046
Phone: 860-486-2950
E-Mail: phillip.gould@uconn.edu

Participants

Chris Greene
University of Colorado
JILA
Boulder, CO 80309-0440
Phone: 303-492-4770
E-Mail: chris.greene@colorado.edu

Richard Greene
DOE BES
19901 Germantown Road
Germantown, MD 20874
Phone: (301) 903-6190
E-Mail: Richard.Greene@science.doe.gov

Markus Gühr
Stanford PULSE Institute
SLAC National Accelerator Laboratory, 2575 Sand Hill Rd
Menlo Park, CA 94025
Phone: +1 650 725 3306
E-Mail: mguehr@stanford.edu

Murray Holland
University of Colorado/JILA
440 UCB JILA
Boulder, CO 80309-0440
Phone: 303-5541127
E-Mail: murray.holland@colorado.edu

Robert Jones
University of Virginia
382 McCormick Road
Charlottesville, VA 22904-4714
Phone: (434)924-3088
E-Mail: bjones@virginia.edu

Henry Kapteyn
University of Colorado/JILA
440 UCB
Boulder, CO 80309-0440
Phone: 303-492-6763
E-Mail: kreid@jila.colorado.edu

Helen Kerch
DOE BES
19901 Germantown Road
Germantown, MD 20874-1920
Phone: 301 903 2346
E-Mail: helen.kerch@science.doe.gov

Jeffrey Krause
DOE BES
19901 Germantown Road
Germantown, MD 20874
Phone: 301-903-5827
E-Mail: Jeff.Krause@science.doe.gov

Vinod Kumarappan
Kansas State University
Dept of Physics
116 Cardwell Hall
Manhattan, KS 66506
Phone: 785532-3415
E-Mail: vinod@phys.ksu.edu

Allen Landers
Auburn University
206 Allison Laboratory
Auburn, AL 36849
Phone: 334844-4048
E-Mail: landers@physics.auburn.edu

Stephen Leone
Lawrence Berkeley National Laboratory
1 Cyclotron Road
Berkeley, CA 94720
Phone: 510643-5467
E-Mail: srl@berkeley.edu

Chii Dong Lin
Kansas State University
Dept of Physics
Manhattan, KS 66502
Phone: 785537-9174
E-Mail: cdlin@phys.ksu.edu

Robert Lucchese
Texas A&M University
Department of Chemistry
College Station, TX 77843
Phone: (979) 845-0187
E-Mail: lucchese@mail.chem.tamu.edu

Stephen Lundeen
Colorado State University
Dept. of Physics
Fort Collins, CO 80523-1875
Phone: 970-491-6647
E-Mail: lundeen@lamar.colostate.edu

Participants

Joseph Maceek
Oak Ridge National Laboratory
401 Nielsen Physics Bldg.
1408 Circle Dr.,
Knoxville, TN 37906-1200
Phone: (865) 974-0770
E-Mail: jmacek@utk.edu

Steven Manson
Georgia State University
Deoartment of Physics & Astronomy
Atlanta, GA 30030
Phone: 404-413-6046
E-Mail: smanson@gsu.edu

Diane Marceau
DOE BES
19901 Germantown Road
Germantown, MD 20874
Phone: 301-903-0235
E-Mail: diane.marceau@science.doe.gov

Todd Martinez
SLAC National Accelerator Laboratory
2575 Sand Hill Rd
Menlo Park, CA 94025
Phone: 650-736-8860
E-Mail: Todd.Martinez@stanford.edu

Spiridoula Matsika
Temple University
1901 N.13th Street
Philadelphia, PA 19122
Phone: 215 2047703
E-Mail: smatsika@temple.edu

William McCurdy
Lawrence Berkeley National Laboratory
One Cyclotron Road
Berkeley, CA 94720
Phone: 510 486 4283
E-Mail: cwmccurdy@lbl.gov

Fred Meyer
Oak Ridge National Laboratory
Physics Div., Bldg. 6010
P.O. Box 2008
Oak Ridge, TN 37831-6372
Phone: (865) 574-4705
E-Mail: meyerfw@ornl.gov

Terry Miller
Ohio State University
Dept. of Chemistry
Columbus, OH 43210
Phone: 614292-2569
E-Mail: tamiller@chemistry.ohio-state.edu

John Miller
DOE BES
19901 Germantown Road
Germantown, MD 20874-1920
Phone: 301 903 5806
E-Mail: John.Miller@science.doe.gov

Alfred Z. Msezane
Clark Atlanta University
223 James P. Brawley Drive SW
ATLANTA, GA 30314
Phone: 404 880 8663
E-Mail: amsezane@cau.edu

Shaul Mukamel
University of California, Irvine
1102 Natural Sciences II
Irvine, CA 92697-2025
Phone: 949-824-7600
E-Mail: smukamel@uci.edu

Margaret Murnane
University of Colorado/JILA
440 UCB
Boulder, CO 80309-0440
Phone: 303-492-6763
E-Mail: kreid@jila.colorado.edu

Keith Nelson
MIT
Room 6-235
Cambridge, MA 02139
Phone: 617-253-1423
E-Mail: kanelson@mit.edu

Lukas Novotny
University of Rochester
The Institute of Optics
Rochester, NY 14627
Phone: (585) 385-8533
E-Mail: novotny@optics.rochester.edu

Participants

Ann Orel
University of California, Davis
One Shields Ave.
Davis, CA 95616
Phone: 530-752-6025
E-Mail: aeorel@ucdavis.edu

Thomas Orlando
Georgia Institute of Technology
901 Atlantic Drive
Atlanta, GA 30332-0400
Phone: 404 894 4012
E-Mail:
thomas.orlando@chemistry.gatech.edu

Mark Pederson
DOE BES
1000 Independence Avenue, SW
Washington, DC 20584-1290
Phone: 301-903-9956
E-Mail: mark.pederson@science.doe.gov

Ronald Phaneuf
University of Nevada
Department of Physics /220
Reno, NV 89557
Phone: 775-784-6818
E-Mail: phaneuf@unr.edu

Erwin Poliakoff
Louisiana State University
Chemistry Department
Baton Rouge, LA 70803
Phone: 225.578.2933
E-Mail: epoliak@lsu.edu

Herschel Rabitz
Princeton University
Frick Laboratory
Princeton, NJ 08544
Phone: 609258-3917
E-Mail: hrabitz@princeton.edu

Larry A. Rahn
DOE BES
19901 Germantown Road
Germantown, MD 20874-1920
Phone: 301 903 2508
E-Mail: larry.rahn@science.doe.gov

Chandra Raman
Georgia Tech Physics
837 state st
Atlanta, GA 30332
Phone: 404-894-9062
E-Mail: craman@gatech.edu

Thomas Rescigno
Lawrence Berkeley National Laboratory
1 Cyclotron Rd, MS2-100
Berkeley, CA 94720
Phone: 510 486 8652
E-Mail: TNRescigno@lbl.gov

Francis Robicheaux
Auburn University
206 Allison Lab
Auburn, AL 36849
Phone: 334-844-4366
E-Mail: robicfj@auburn.edu

Jorge Rocca
Colorado State University
1320 Campus Delviery ERC B229
Fort Collins, CO 80523-1320
Phone: 970-491-8847
E-Mail: matilda@colostate.edu

Eric Rohlfing
DOE BES
19901 Germantown Road
Germantown, MD 20874-1920
Phone: 301 903 8165
E-Mail: Eric.Rohlfing@science.doe.gov

Christoph Rose-Petruck
Brown University
324 Brook Street
Providence, RI 02912
Phone: 401 863 1533
E-Mail: crosepet@brown.edu

Robin Santra
Argonne National Laboratory
9700 South Cass Avenue
Argonne, IL 60439
Phone: 630-252-4994
E-Mail: rsantra@anl.gov

Participants

Richard Schaller
Los Alamos National Laboratory
MS-J567
Los Alamos, NM 87545
Phone: 505-664-0338
E-Mail: rdsx@lanl.gov

Robert Schoenlein
Lawrence Berkeley National Laboratory
1 Cyclotron Rd. MS: 2-300
Berkeley, CA 94720
Phone: 510-486-6557
E-Mail: rwschoenlein@lbl.gov

David Schultz
Oak Ridge National Laboratory
Physics Div., Bldg. 6010
P.O. Box 2008
Oak Ridge, TN 37831-6372
Phone: (865) 576-9461
E-Mail: schultzd@ornl.gov

Neil Shafer-Ray
University of Oklahoma
440 West Brooks St
Norman, OK 73019
Phone: 405-325-2890x36123
E-Mail: shaferry@physics.ou.edu

Anthony F Starace
University of Nebraska
116 Brace Laboratory
Lincoln, NE 68588-0111
Phone: 402-472-2795
E-Mail: astarace1@unl.edu

Mark Stockman
Georgia State University
Department of Physics and Astronomy
Atlanta, GA 30303
Phone: 678-457-4739
E-Mail: mstockman@gsu.edu

Donald Umstadter
University of Nebraska-Lincoln
212 Ferguson Hall
Lincoln, NE 68588-0111
Phone: 402-472-8115
E-Mail: dpu@unlserve.unl.edu

Thorsten Weber
Lawrence Berkeley National Laboratory
One Cyclotron Road
Berkeley, CA 94720
Phone: 510-486-5588
E-Mail: TWeber@lbl.gov

Thomsd Weinacht
Stony Brook University
Department of Physics and Astronomy
Stony Brook, NY 11794-3800
Phone: 631 632 8163
E-Mail: tweinacht@sunysb.edu

Jun Ye
JILA/NIST, University of Colorado
440 UCB, University of Colorado
Boulder, Colorado 80309-0440
Phone: 303-735-3171
E-Mail: ye@jila.colorado.edu

Linda Young
Argonne National Laboratory
9700 S. Cass Avenue, 203/F-125
Argonne, IL 60439
Phone: 630-252-8878
E-Mail: young@anl.gov